EVALUATION OF MULTIPLE CORROSION PROTECTION SYSTEMS FOR REINFORCED CONCRETE BRIDGE DECKS

BY

Jason Draper

Submitted to the graduate degree program in Civil, Environmental, and Architectural Engineering and the Graduate Faculty of the University of Kansas School of Engineering in partial fulfillment of the requirements for the degree of Master of Science.

_____
Chairperson

Committee members _____

_____

Date defended: Dec. 1, 2009

The Thesis Committee for Jason Draper certifies
that this is the approved Version of the following thesis:

EVALUATION OF MULTIPLE CORROSION PROTECTION SYSTEMS FOR

REINFORCED CONCRETE BRIDGE DECKS

Committee:

_____
Chairperson

_____

_____

Date approved:_____

ABSTRACT

Chloride-induced corrosion is one of the leading causes of premature serviceability failure in reinforced concrete bridge decks. In an effort to mitigate the effect of corrosion on the longevity of concrete bridge decks, several corrosion protection systems have been developed. The current study evaluates the effectiveness of multiple corrosion protection strategies when used in conjunction with epoxy-coated reinforcement (ECR). The epoxy coating in all test bars is penetrated with either four or ten 3-mm (1/8-in.) diameter holes. The systems evaluated include three corrosion inhibitors (DCI-S, Rheocrete 222+, and Hycrete DSS) in concrete with a *w/c* ratio of 0.45 and 0.35, an ECR containing a primer of microencapsulated calcium nitrite between the epoxy and the steel in concrete with a *w/c* ratio of 0.45 and 0.35, three types of increased adhesion ECR (ECR pretreated with chromate prior to the application of the epoxy coating, and ECR with increased adhesion epoxies developed by DuPont and Valspar) evaluated in concrete with a *w/c* ratio of 0.45, as well as in concrete containing DCI-S corrosion inhibitor, and multiple-coated reinforcement that contains a zinc layer between the steel and the DuPont 8-2739 epoxy coating in concrete with a *w/c* ratio of 0.45. Conventional steel and epoxy-coated reinforcement serve as control specimens; the performance of the epoxy-coated reinforcement is compared to the performance of the conventional steel reinforcement. Each corrosion protection system is evaluated using the Southern Exposure and cracked beam tests. Macrocell and microcell corrosion losses, mat-to-mat resistances, top and bottom mat corrosion potentials, and critical chloride concentrations are measured during the test.

Upon completion of the study, each specimen is autopsied and any disbondment of the epoxy coating from the steel is measured.

Of the systems evaluated in this study, conventional steel exhibits the greatest amount of corrosion. ECR, whether in uncracked or cracked concrete, exhibits low corrosion losses; well below the magnitude required to cause corrosion-induced surface deterioration. A lower *w/c* ratio provides additional protection in uncracked concrete, but affords little to no protection in cracked concrete. Corrosion inhibitors, while effective in uncracked concrete, afford no additional protection against corrosion in cracked concrete. All three improved adhesion ECR systems exhibit corrosion performance that is similar to conventional ECR. Multiple-coated reinforcement exhibits greater corrosion losses than conventional ECR, but the corrosion losses are below the magnitude of corrosion loss required to cause corrosion-induced surface deterioration. The effective critical chloride threshold for epoxy-coated reinforcement is several times higher than that of conventional reinforcement.

A relationship exists between microcell and macrocell corrosion loss, and between both microcell and macrocell corrosion loss and the disbonded area of epoxy observed on the bar. The cathodic disbondment test (ASTM A775) does not appear to be a reliable indicator of corrosion disbondment performance of in-service epoxy-coated reinforcement.

Key words: chlorides, concrete, corrosion, corrosion inhibitor, epoxy-coated reinforcement, linear polarization resistance, multiple corrosion protection systems, potential, epoxy disbondment

ACKNOWLEDGEMENTS

This report is based on a thesis submitted by Jason Draper in partial fulfillment of the requirements of the MSCE degree. Major funding and material support for this research was provided by the United States Department of Transportation Federal Highway Administration under Contract No. DTFH61-03-C-00131, with technical oversight by Yash Paul Virmani, and the Kansas Department of Transportation under Contract Nos. C1121 and C1281, with technical oversight by Dan Scherschligt and Don Whisler. Additional support for this project was provided by the Concrete Reinforcing Steel Institute, DuPont Powder Coatings, 3M Corporation, Valspar Corporation, BASF Construction Chemicals, W. R. Grace & Co., Hycrete Inc., Western Coating, Inc., and LRM Industries.

TABLE OF CONTENTS

LIST OF TABLES

LIST OF FIGURES

CHAPTER 1

INTRODUCTION

1.1 General

Corrosion is a destructive electrochemical process in which metals that are in a purified form revert to a more thermodynamically stable state. Corrosion of steel in reinforced concrete bridge decks first became apparent with the in the late 1960s and early 1970s, when bridge decks with design lives of 50 years began requiring maintenance, in some cases, with less than ten years of service. Corrosion in reinforced concrete bridge decks is typically caused by chloride contamination of the concrete due to the use of deicing salts. Corrosion in highway bridges has an annual direct cost of $8.3 billion. Indirect costs, due to traffic delays and lost productivity, may be ten times this value (Yunovich et al. 2002).

A number of corrosion protection systems have been developed to extend the service life of reinforced concrete bridge decks. Epoxy-coated reinforcement is widely used as a corrosion protection system. The reinforcing steel is coated with a fusion bonded polymer coating that acts as a barrier between the steel and the chlorides, oxygen, and moisture in the surrounding concrete pore solution. Other methods, such as decreased permeability concrete and increased concrete cover, slow the ingress of the chloride ions to the level of the reinforcing steel, thereby increasing the time to corrosion initiation. Another method for minimizing corrosion is the use of corrosion inhibitors in the concrete. Corrosion inhibitors are chemical admixtures

that hinder the corrosion of the reinforcing steel. They are typically added to plastic concrete, but have also been shown to have an effect when applied to the surface of hardened concrete (Civjan 2005). The current study evaluates the effectiveness of several corrosion protection systems when used in conjunction with epoxy-coated reinforcement, and is a continuation of the work reported by Gong (2006) and Guo (2006). Three corrosion inhibitors (DCI, Rheocrete 222+, and Hycrete DSS) are evaluated. The effect of decreased concrete permeability on the effectiveness of these inhibitors is also examined. Epoxy-coated reinforcing bars fabricated using three different enhanced adhesion epoxies (epoxy with chromate pretreatment, DuPont, and Valspar) are evaluated. Multiple-coated bars, which contain a zinc layer between the epoxy coating and the underlying steel are also investigated. A description of each corrosion protection system evaluated in this study is given in Section 1.6.

1.2 Corrosion of Reinforcing Steel in Concrete

Corrosion is a destructive electrochemical process that occurs between a metal and its environment. A corrosion cell consists of four parts: an anode, a cathode, an electrolyte, and an electrical connection between the anode and cathode. All four components must be present for the corrosion reactions to occur. In the case of corrosion in reinforced concrete, the reinforcement serves as both the anode and the cathode. Reinforcing bars become electrically connected through physical contact and through bar supports. The pore solution contained within the concrete serves as

the electrolyte. The anode is the site where iron atoms are oxidized. The oxidation reaction results in the formation of ferrous ions and electrons.

$$Fe \rightarrow Fe^{2+} + 2e^{-} \tag{1.1}$$

The ferrous ions produced in the oxidation reaction remain at the anode, while the electrons travel through the electrical connection from the anode to the cathode, where they combine with oxygen and water in a reduction reaction [Eq. (1.2)] to form hydroxyl ions.

$$½O_2 + H_2O + 2e^{-} \rightarrow 2OH^{-} \tag{1.2}$$

The dissolved ferrous ions react with the hydroxyl ions to produce ferrous hydroxide.

$$Fe^{2+} + 2OH^{-} \rightarrow Fe(OH)_2 \tag{1.3}$$

If oxygen is present in the surrounding solution, the ferrous hydroxide is oxidized into ferric hydroxide [Eq. (1.4)] and subsequently forms hydrated ferric oxide [Eq. (1.5)], commonly known as rust.

$$4Fe(OH)_2 + O_2 + 2H_2O \rightarrow 4Fe(OH)_3 \tag{1.4}$$

$$2Fe(OH)_3 \rightarrow Fe_2O_3 \cdot H_2O + 2H_2O \tag{1.5}$$

The hydrated ferric oxide occupies as much as six times the volume of the original iron atoms (Mehta and Monteiro 2006). This increase in volume, in turn, causes tensile stresses to develop within the concrete and eventually leads to cracking and spalling of the concrete cover.

The oxidation of ferrous hydroxide into ferric hydroxide is prevented if the solution surrounding the steel has a high pH. In this case, ferrous hydroxide is oxidized into γ-ferric oxyhydroxide.

$$2Fe(OH)_2 + \tfrac{1}{2}O_2 \rightarrow 2\gamma\text{-}FeOOH + H_2O \qquad (1.6)$$

The resulting γ-ferric oxyhydroxide forms a tightly adhering protective barrier around the steel, which prevents further corrosion from occurring by limiting access of moisture and oxygen to the underlying steel and by limiting the solubility of the iron. This process is known as passivation and occurs in steel embedded into normal concrete because of the high pH of the concrete pore solution. As long as this passive film remains intact, further corrosion will not occur.

Depassivation, or the destruction of the passive film protecting the reinforcing steel can occur in two ways. First, the passive layer is destroyed if the pH of the pore solution drops below 11.5 (Bernard and Verbeck 1975). Carbonation of the concrete (the ingress of carbon dioxide into the concrete) can lower the pH of the pore solution and, therefore, cause depassivation. In most circumstances, carbonation can be prevented by using a low permeability concrete and by ensuring that adequate cover is provided for reinforcement.

Depassivation can also occur if chloride ions are introduced into the pore solution. Chloride ions can cause the γ-ferric oxyhydroxide protective film to destabilize, even in pore solutions with a pH above 11.5. The chloride ions react with ferrous ions to produce an iron-chloride complex that reacts with hydroxyl ions to form ferrous hydroxide.

$$Fe^{2+} + Cl^- \rightarrow [FeCl\,complex]^+ \quad (1.7)$$

$$[FeCl]^+ + 2OH^- \rightarrow Fe(OH)_2 + Cl^- \quad (1.8)$$

The ferrous hydroxide produced in the reaction shown in Eq. (1.8) can then be converted into ferric oxide as previously described. Because the chloride ions are left unconsumed in Eq. (1.8), they are again available to continue attacking the passive layer protecting the steel (Mindess et al. 2003). In addition to destroying the passive layer that protects the reinforcing steel, chloride ions also have additional negative effects on the corrosion behavior of reinforcement in concrete. Chloride ions reduce the solubility of calcium hydroxide and thereby reduce the pH of the pore solution (Hunkeler 2005). The free chloride ions also increase the electrical conductivity of the concrete (increasing the efficiency of the electrolyte) and result in an increase in the moisture content of the concrete due to the hygroscopic properties of chloride-containing salts.

1.3 Corrosion Threshold

The concentration of chloride ions required to initiate corrosion of reinforcing steel is known as the critical chloride threshold. There have been many studies that have been undertaken to determine the corrosion threshold of reinforcing steel in concrete (see Glass and Buenfeld 1997). The variation in the threshold values observed in these studies suggests that there is not a single value for the corrosion threshold; rather the corrosion threshold appears to depend on a number variables, the most influential of which are the pH of the pore solution, the availability of oxygen

and moisture at the location of the steel, and the presence of voids at the steel/concrete interface (Bertolini et al. 2004). The critical chloride threshold is typically expressed in terms of percent chloride by mass of cement, weight of chloride ions per unit volume of concrete, or as a chloride/hydroxyl ion ratio.

More chlorides are needed to initiate corrosion at higher pH levels. Consequently, corrosion threshold values are sometimes reported as a chloride/hydroxyl ion ratio. Hausmann (1967) tested bare reinforcement in alkaline solutions that contained sodium chloride, and concluded that for a pH between 11.6 and 12.4, the critical Cl^-/OH^- ratio was about 0.60. Chloride threshold results obtained by Gouda (1970) were subsequently converted into Cl^-/OH^- ratios and reported by Diamond (1986), who used the reported solution pH to estimate the OH^- concentration. These Cl^-/OH^- values varied from 0.27 to 0.57 for pH values ranging from 11.8 to 13.3. Gouda's values were also based on bare reinforcement submerged in an alkaline solution contaminated with chlorides. Later studies have shown that tests with steel reinforcement that is embedded in mortar or concrete have higher Cl^-/OH^- ratios at the onset of corrosion than tests with reinforcement placed in solution (Hussain et al. 1996). Glass and Buenfeld (1997) analyzed corrosion threshold data compiled from twenty different studies. The threshold Cl^-/OH^- ratios that were reported ranged from 0.22 to 40, with most values ranging between 0.2 and 0.8. The higher Cl^-/OH^- ratios, ranging from 1 to 40, were measured in the extracted pore solutions of concrete specimens. They stated that measuring critical chloride thresholds in terms of a Cl^-/OH^- ratio held no advantage over expressing threshold

levels in terms of total chloride content. Expressing thresholds in terms of total chloride content may be more convenient than expressing it in terms of a Cl^-/OH^- ratio because it can be difficult to measure the OH^- concentration in concrete or mortar pore solution. Typically, the chloride threshold for conventional steel reinforcement in concrete is within the range of 0.6 to 0.9 kg/m^3 (1.0 to 1.5 lb/yd^3) (Metha and Monteiro 2006).

It is important to note that not all chlorides present in the concrete contribute to the deterioration of the passive layer protecting the reinforcement. The total chloride content of the concrete consists of the water soluble chloride ions dissolved in the pore solution and the chloride ions that are bound to components of the cement paste. For example, tricalcium aluminate in cement can react with some available chloride ions to form calcium chloroaluminate ($3CaO \cdot Al_2O_3 \cdot CaCl_2 \cdot 10H_2O$), also known as Friedel's salt. This process is often referred to as chloride binding. Bound chlorides are normally not available to react with the passive layer of the reinforcement, and therefore, do not promote corrosion. These chlorides, however, can be released if the pH of the concrete drops below 12, and would, therefore, be available to promote corrosion (Bertolini et al. 2004, Glass and Buenfeld 1997). Therefore, even bound chlorides can pose a potential threat to the passive layer protecting the reinforcement.

1.4 Corrosion Monitoring Methods

Several electrochemical methods have been developed to monitor the corrosion of reinforcement in concrete. The most commonly used include measuring the macrocell corrosion rate, corrosion potential, and linear polarization resistance, electrical impedance spectroscopy, and galvanostatic pulse measurements. The first three methods are used in the current study and will be described in detail in the following sections.

1.4.1 Macrocell Corrosion Rate

Within reinforced concrete structures, corrosion often occurs as the result of the formation of a macrocell. In the macrocell, one portion of the reinforcing bars, such as the top mat in a bridge deck, serves as the anode, while another portion, such as the bottom bars in a bridge deck, serves as the cathode. The macrocell corrosion rate is a measure of the quantity of electrons moving from the anode to the cathode. As previously mentioned, when the steel at the anode corrodes, it releases electrons that flow through an electrical connection to the cathode. The rate at which the electrons move from anode to cathode across the electrical connection is the macrocell current. The corrosion rate can be expressed as either the corrosion current density ($\mu A/cm^2$) or as the rate of loss of material in terms of depth of material per unit of time (μm/year). The two are related through Faraday's Law:

$$R = k\frac{ia}{nF\rho} \tag{1.8}$$

where

R = corrosion rate, depth of material lost per unit of time (μm/yr)

i = corrosion current density (μA/cm^2)

k = conversion factor, 31.5·(10^4) amp·μm·sec/μA·cm·year

a = atomic weight of the metal = 55.8 g/gm-mol for iron

n = number of electrons transferred for each ion oxidized = 2 for iron

F = Faraday's constant = 96500 Coulombs/gm-mol

ρ = density of metal (g/cm^3) = 7.87 g/cm^3 for iron

In laboratory specimens, two separate bars (or two separate groups of bars) are connected electrically. One bar (or group of bars) is placed in a corrosive environment, and becomes the anode, while the other bar (or group of bars) becomes the cathode. The electrical connection between the anode and cathode includes a resistor. The macrocell corrosion current density is determined by measuring the voltage drop across the resistor. This voltage can then be converted into a current density using Ohm's Law:

$$i = \frac{V}{\Omega A} \tag{1.9}$$

where

V = voltage drop across the resistor (mV)

Ω = resistance of the resistor (kΩ)

A = surface are of the anode, cm^2

The corrosion current density i gives an instantaneous measurement of the rate of metal loss. If corrosion rate measurements are taken at specific time intervals, they

can be numerically integrated to give an estimated total loss of the metal (μm) due to corrosion. This corrosion loss is only an estimate, however, because corrosion rates can fluctuate between measurements. In addition, macrocell corrosion measurements only account for macrocell corrosion, that is, corrosion that produces electrons flowing through the resistor. Microcell corrosion, or corrosion in which the anode and cathode form on the same bar, cannot be measured in this manner because the electrons formed during the oxidation of the steel flow only within the bar itself as they pass from the anode to the cathode, rather than flowing through the resistor. Microcell corrosion rates, however, can be measured using Linear Polarization Resistance measurements, which are discussed in Section 1.4.3.

Macrocell corrosion is thought to be the primary corrosion mechanism that contributes to the premature deterioration of reinforced concrete bridge decks (Virmani 1990). Pfeifer (2000) included a review of six studies that evaluated the amount of uniform corrosion loss sustained by a reinforcing bar that would cause cracking of the surrounding concrete cover. The corrosion loss values reported ranged from 13 to 38 μm, with an average of 25 μm. It was noted that to provide a service life of 75 years, the corrosion rate of the reinforcement must be kept below 0.3 μm/yr.

The critical corrosion rate of 0.3 μm/yr given by Pfiefer to achieve a service life of 75 years assumes uniform corrosion over the entire surface of the reinforcement. However, in the case of epoxy-coated reinforcement, corrosion is more likely to be limited to small regions on the bar (small damaged areas). Torres-

Acosta and Sagüés (2004) investigated the critical corrosion loss, x_{CRIT}, required to crack concrete in which corrosion occurs over a limited length of the bar. In this study, 16 cylindrical concrete specimens and 22 prismatic beam specimens were tested. The cylindrical specimens consisted of a pipe centrally embedded into a cylindrical concrete section. The pipe, which was mechanically continuous, had a central portion that consisted of a carbon steel pipe (which served as the controlled anodic area) and outer portions that consisted of polyvinyl chloride pipe. The prismatic beam specimens consisted of a concrete prism with dimensions 140 x 140 x 406 mm (5-1/2 x 5-1/2 x 16 in.) containing an embedded dual material reinforcing bar (with a carbon steel center segment and two Type 316 LN stainless steel segments at both ends) centered on one of the cross section sides. Concrete covers ranged from 27.5 to 65.7 mm (1.08 to 2.59 in.) in the cylindrical specimens and from 13 to 45 mm (0.51 to 1.77 in.) for the beam specimens. The pipe used in the cylindrical specimens had a 21-mm (0.83-in.) outside diameter with a 3-mm (0.12-in.) wall thickness. No. 2 and No. 4 (6 and 13 mm diameter, respectively) reinforcement was used in the beam specimens. Anodic lengths (the length of steel exposed to corrosion) varied between 19.1 and 95 mm (0.75 and 3.74 in.) in the cylindrical specimens and between 18.7 and 408.4 mm (0.74 and 16.0 in.) in the beam specimens. The study showed that the amount of corrosion loss required to cause concrete cracking was dependent on the bar diameter, the length of bar exposed to corrosion (anodic length) and the concrete cover. Values of x_{CRIT} between 30 to 272 μm were observed as a function of concrete

cover, reinforcing bar diameter, and anodic length. Torres-Acosta and Sagüés summarized their findings with the expression:

$$x_{CRIT} = 0.011(C/\phi)(C/L+1)^2 \quad (1.10)$$

where

x_{CRIT} = critical amount of steel corrosion penetration to cause concrete cracking (mm)

C = concrete cover (mm)

ϕ = reinforcing bar diameter (mm)

L = length of corroding rebar (anodic length, mm)

Gong et al. (2006) evaluated the accuracy of Eq. (1.10) by using data collected by Balma et al. (2005) and McDonald et al. (1998) on SE specimens and comparing the observed behavior (cracked versus uncracked concrete) with the behavior predicted by Eq. (1.10). Gong et al. noted that, since the corrosion products formed on the top bars of the SE specimens (see Section 1.5), the corrosion products are typically on only one side of a bar. Since the tensile stresses produced by the increased volume of corrosion products forming on only one side of a bar should be, at most, one-half of that caused by corrosion products forming over a ring shaped region along the anodic length, it was reasoned that twice the corrosion loss given by Eq. (1.10) would be needed to crack the concrete in the SE specimens. Gong's evaluation showed that Eq. (1.10) reasonably predicted the amount of corrosion loss required to cause concrete cracking, and that the amount of corrosion loss on the damaged epoxy required to cause concrete cracking is approximately 100 times

higher than that for uncoated reinforcement. This corresponds to a corrosion loss of 2500 μm (0.10 in.).

1.4.2 Corrosion Potential

The corrosion potential of a metal is a measure of its tendency to oxidize. Corrosion potential is measured with respect to a reference corrosion cell. As steel becomes more prone to corrosion, its electrochemical potential versus the reference cell becomes more negative. The standard hydrogen electrode (SHE) has been established as the standard reference electrode, and its electrochemical potential is defined as 0.0 V. The SHE, however, is not convenient for measuring the corrosion potential of laboratory specimens or in-place structures; therefore, other reference electrodes have been developed for use in these situations. The two most common are the saturated calomel electrode (SCE) and the copper-copper sulfate electrode (CSE). The saturated calomel electrode and the copper-copper sulfate electrode have half-cell potentials of 0.241 V and 0.316 V, respectively, versus the SHE.

Corrosion potential measurements give an indication of the probability of corrosion activity in the steel, but give no information on the rate of corrosion. Due to their simplicity, however, corrosion potential measurements are widely used to monitor corrosion within structures in service. ASTM C 876, a standard for measuring the corrosion potential of uncoated reinforcing steel in concrete, gives the probability of the occurrence of active corrosion based on half-cell potential readings. These probabilities are given in Table 1.1.

Table 1.1 – Corrosion probabilities based on corrosion half-cell potentials

Half-cell Potential (V)		Probability of Steel Corrosion
CSE	SCE	
> –0.200	> –0.125	Less than 10%
–0.200 to –0.350	–0.125 to –0.275	Corrosion activity uncertain
< –0.350	< –0.275	Greater than 90%

When using corrosion potential readings to analyze the corrosion behavior of concrete reinforcing bars, it is important to consider the factors that may affect corrosion potential. These factors include the availability of oxygen to the bar, the resistance of the concrete, the presence of corrosion inhibitors, and the presence of chlorides. Furthermore, it may be impossible to obtain stable corrosion potential readings for reinforcement with an undamaged epoxy coating because the epoxy blocks the connection to the measuring circuit (Gu and Beaudoin 1998).

1.4.3 Linear Polarization Resistance

The linear polarization resistance method is a nondestructive electrochemical technique for measuring the corrosion rate of a metal. It is based on the observation that the current-potential curve (the polarization curve) of a metal is nearly linear on the portion of the curve near the equilibrium potential (the open circuit corrosion potential of the half-cell). The slope of the linear portion of the curve is known as the polarization resistance (R_p) and is defined by the following equation (Jones 1996):

$$R_p = \left(\frac{\Delta E}{\Delta i} \right)_{\Delta E \to 0} \tag{1.11}$$

where

ΔE = the difference between the imposed potential and the equilibrium potential

Δi = the difference between the equilibrium corrosion current density and current density required to maintain the imposed potential

Polarization resistance is inversely proportional to the corrosion rate (expressed as corrosion current density) through the Stern-Geary equation (Stern and Geary 1957).

$$i = \frac{B}{R_p} \tag{1.11}$$

where

R_p = polarization resistance ($k\Omega \cdot cm^2$)

B = Stern-Geary constant = $\dfrac{\beta_a \beta_c}{2.303(\beta_a + \beta_c)}$

β_a = anodic Tafel constant (mV/decade)

β_c = cathodic Tafel constant (mV/decade)

Previous studies have shown that for actively corroding reinforcing steel and galvanized reinforcement in concrete, a Stern-Geary constant B of 26 mV is appropriate (Andrade and González 1978, McDonald et al. 1998). This corresponds to using 120 mV/decade for both anodic and cathodic Tafel constants, β_a and β_c.

Linear polarization resistance measurements are most commonly performed using a potentiostat that is connected to the working electrode (the steel reinforcement), a counter-electrode, and a reference electrode (such as a SCE or CSE). After the equilibrium potential is measured, the potentiostat then imposes a potential difference that is predetermined. The current required to achieve the potential

difference is then recorded, and a new potential difference is applied. This is repeated incrementally over a range of potentials (usually –10 to +10 mV versus the equilibrium potential). These values are plotted on a graph of voltage versus current, and the slope of the resulting curve is the polarization resistance, R_p.

1.5 Corrosion Test Methods

A wide variety of laboratory methods have been developed to investigate the corrosion of reinforcement in concrete. The current study utilizes two widely used bench-scale test specimens: the Southern Exposure (SE) test and the Cracked Beam (CB) test. Both tests are designed to simulate the exposure conditions of reinforcement in a concrete bridge deck. The SE test simulates conditions of reinforcement in uncracked concrete, while the CB test simulates reinforcement that lies directly beneath a crack that is oriented parallel to the bar. A thorough history of the development of the SE and CB tests in corrosion research is presented by Guo et al. (2006). These tests are described in detail in Chapter 2.

1.6 Corrosion Protection Systems

A number of methods have been developed to mitigate the problem of corrosion of concrete reinforcement. The corrosion protection systems investigated in the current study can be divided into three groups: use of epoxy-coated reinforcement, use of quality, low permeability concrete, and use of corrosion

inhibitors in the concrete. Each of these methods will be discussed in detail in the subsequent sections.

1.6.1 Epoxy-coated Reinforcement

In the United States, the most common method used to limit the corrosion of reinforcement in concrete bridge decks is to coat the reinforcement with epoxy. Epoxy-coated reinforcement (ECR) was developed in the 1970s. The current study investigates the effectiveness of conventional epoxy-coated reinforcement, along with three types of high adhesion ECR, and a multiple-coated reinforcement that includes a layer of zinc between the steel and the epoxy coating.

The first step in producing epoxy-coated reinforcement is preparing the surface of the steel reinforcement by abrasive blast cleaning to remove millscale, rust, and surface contaminates. The steel is then heated, and passed through a spray of dry epoxy powder. The epoxy powder is electrostatically charged, causing the particles to be attracted to the reinforcement. Upon touching the bar, the epoxy melts and adheres to its surface, after which the bar is quenched with water. When placed in a bridge deck, epoxy-coated reinforcement works in two ways to prevent corrosion. First, the epoxy layer provides a physical barrier that impedes access of oxygen, water, and chloride ions to the surface of the steel. Additionally, the epoxy electrically isolates the steel from both the surrounding concrete and adjacent reinforcement, thus preventing the formation of electrical connections and, in turn, the formation of a macrocell within the bridge deck.

There are limitations to the amount of protection that epoxy-coated reinforcement affords to the underlying steel. The ability of the epoxy coating to prevent corrosion is closely tied to its continuity. Small imperfections in the coating, known as holidays, can allow strongly anodic sites to form on the surface of the underlying steel. The epoxy coating is susceptible to damage during shipment and placement. In-situ epoxy-coated reinforcement can also suffer a loss of adhesion between the epoxy coating and the underlying steel, a process referred to as disbondment.

Many studies have been undertaken to assess the effectiveness of epoxy-coated reinforcement in preventing corrosion. While some studies have shown that epoxy-coated reinforcement is extremely effective, other studies have cast doubt onto its effectiveness. For example, bridges constructed in Florida Keys using first generation epoxy-coated reinforcement began showing signs of corrosion after only six years of service. It was later found that the epoxy had lost its adhesion to the steel surface. Manning (1996) provides several instances in which deteriorating corrosion performance has been accompanied by a loss of coating adhesion, both in the laboratory and in the field.

Pyc et. al (2000) studied the field condition of ECR from 250 cores obtained from 18 bridge decks in the State of Virginia. The age of the decks from which the cores were taken ranged from 2 to 20 years. Each core was evaluated visually for cracking and delamination of the concrete. The level of carbonation in the concrete was also measured. A total length of 0.9 to 1.2 m of ECR was examined for each

bridge deck. The ECR was inspected for visible damage and for holidays. The adhesion of the ECR was tested using the knife-peel test, and the level of disbondment was assigned a number between one and five based on the severity of the disbondment present, five being the most severe. Linear polarization and electrochemical impedance spectroscopy measurements were also taken on three ECR specimens from each bridge deck to determine the corrosion rate of the reinforcement. It was shown that disbondment of the ECR occurred in as little as four years.

In a study related to the work done by Pyc et. al (2000), Brown et. al (2006) studied the corrosion resistance of ECR taken from ten existing bridge decks in the State of Virginia. Two bridges contained conventional steel reinforcement, while the other eight contained ECR. The bridges were built using identical water-cement ratios and concrete cover specifications. The ages of the bridge decks ranged from 4 to 18 years. A total of 141 concrete cores, 101.6 mm (4 in.) in diameter, were taken from the bridge decks for evaluation. Of these, 101 cores were taken from locations of the bridge deck without a surface crack, while the remaining 40 were taken at the location of a surface crack. Each core contained the top-bar reinforcement of the bridge deck. In the laboratory, the top cover of each specimen was removed so that only 0.5 in. (13 mm) of concrete cover remained over the bar. The tops of the specimens were ponded with 3% NaCl solution, using a 2 days ponded, 5 days dried ponding cycling. The corrosion behavior of the specimens was monitored during the test using a combination of corrosion potential measurements and electrical

impedance spectroscopy (EIS) over a 22 month period. At the end of the tests, 27 out of the 28 bare steel specimens exhibited concrete cracking, while only 21 of the 113 ECR specimens had exhibited cracking. The study concluded that the ECR required higher chloride concentrations to cause concrete cracking, but that the critical chloride thresholds for conventional steel and ECR were not statistically different. It was concluded that the use of ECR in bridge decks only affords an additional service life of five years beyond that of conventional steel.

A comprehensive list of studies performed on epoxy-coated reinforcement was presented by Kepler et al. (2000). Despite the controversy surrounding the effectiveness of epoxy-coated reinforcement, it appears to extend the service life of a structure beyond that of a comparable structure fabricated using conventional steel reinforcement.

1.6.2 Low Permeability and Low Cracking Concrete

Low permeability concrete can also provide significant corrosion protection to embedded reinforcement. This is most commonly obtained by using a low water-cement ratio. Low permeability provides corrosion protection in two different ways. First, it increases the amount of time required for the chloride ions and oxygen to reach the reinforcement. Secondly, low permeability concretes have a higher electrical resistivity, which slows the electrochemical reactions of the corrosion cell. Mineral admixtures can also be added to the concrete to decrease its permeability.

Chloride induced corrosion of reinforcement is aggravated by the presence of cracks in the concrete. Cracks in the concrete provide a path of direct access for the

chloride ions to the reinforcing steel, and therefore, low permeability concrete offers little to no corrosion protection when cracks are present. Lindquist et. al (2005, 2006) measured chloride levels on 59 bridge decks in Kansas. Chloride levels taken away from cracks at the level of the top reinforcement were well below the chloride threshold of conventional reinforcement. The chloride levels taken at crack locations, however, showed that the chloride threshold of conventional reinforcement could be exceeded within the first year of service.

1.6.3 Corrosion Inhibitors

Corrosion inhibitors are chemicals that can be added to concrete in relatively small proportions to reduce or prevent the corrosion of embedded steel reinforcement. They are used in both new and existing structures, and have been shown to be a relatively simple and cost-effective way of mitigating corrosion in reinforced concrete structures. Corrosion inhibitors may extend the service life of a structure by either delaying the onset of corrosion or by reducing the corrosion rate of the reinforcement after corrosion initiation has already occurred. The effectiveness of corrosion inhibitors is reduced when cracks are present in the concrete.

Although corrosion inhibitors can be categorized a number of ways, they are most commonly classified as organic and inorganic (depending on chemical composition), or as anodic, cathodic or mixed inhibitors, alluding to the mechanism by which they influence the corrosion process. Anodic corrosion inhibitors act by forming an oxide film barrier on the surface of the anodic steel, thus interfering with metal oxidation. They may also work by stabilizing the passive protective layer on

the steel. Cathodic corrosion inhibitors work by forming an insoluble film on the surface of the cathodic steel, thus reducing the rate of the reduction reaction. Mixed corrosion inhibitors work by blocking the chemical reactions at both the anode and the cathode. This is accomplished by forming a physical barrier on the surface of the steel and/or by chemically competing with the chloride ions that cause corrosion. The current study investigates three corrosion inhibitors: Rheocrete 222+, Hycrete-DSS, and calcium nitrite. A description of these three corrosion inhibitors, followed by a discussion of the recent work that has been undertaken to evaluate the effectiveness of these inhibitors, will occupy the balance of this section. For a more comprehensive review of previous work, the reader is referred to Guo et al. (2006) and Civjan et al. (2003).

Rheocrete 222+ is an organic corrosion inhibiting admixture (OCIA) comprised of an aqueous solution of amines and esters. There are two mechanism by which Rheocrete 222+ provides protection to the reinforcement. First, an amino alcohol forms a protective film over the surface of the reinforcement, acting as a cathodic inhibitor. Secondly, like other organic corrosion inhibitors, it reduces the permeability of the concrete, thus lowering the ingress rate of the chloride ions. This is accomplished by the hydrolysis of the esters and the formation of insoluble calcium salts of fatty acids. These salts, which form within the pore structure of the concrete, are hydrophobic, and therefore decrease the permeability of the concrete (Gaidis 2004).

Hycrete DSS is an organic corrosion inhibitor comprised of disodium tetrapropenyl succinate. According to the manufacturer, Hycrete forms a protective film around the reinforcing steel. It also forms a hydrophobic precipitate that fills the capillaries of the concrete, effectively reducing the rate of chloride diffusion via capillary absorption. Hycrete is a relatively new corrosion inhibitor; consequently, there is only limited data available in the literature concerning its effectiveness or mode of protection.

Calcium nitrite is the most widely established corrosion inhibitor used in reinforced concrete. It has been in use for nearly 30 years, and numerous reports have been published concerning its effectiveness. It is an anodic corrosion inhibitor, and helps suppress corrosion by reacting with ferrous oxide to form gamma-ferric oxyhydroxide, the material that comprises the passive protective layer on steel.

$$Fe^{2+} + OH^{-} + NO_2^{-} \rightarrow NO(g) + \gamma - FeOOH \qquad (1.12)$$

Because nitrite ions are consumed when calcium nitrite protects steel, the corrosion protection offered by the calcium nitrite will diminish over time, if ferrous ions are produced due to corrosion. In the absence of corrosion, however, calcium nitrite does not lose its effectiveness. For calcium nitrite to provide any protection to the steel, the chloride-nitrite ratio must be sufficiently low (Berke and Rosenberg 1989). While it is believed by some that insufficient or excess quantities of an anodic corrosion inhibitor may aggravate corrosion of reinforcing steel in concrete, there is little evidence of this in the literature (Hansson et al. 1998).

Calcium nitrite is commercially available as Darex Corrosion Inhibitor (DCI), as well as in other forms. DCI is an inorganic corrosion inhibitor that contains 30% calcium nitrite and 70% water. Because calcium nitrite also acts as a set accelerator, DCI is available in a version that includes a set retarder (DCI-S).

Nmai et al. (1992) studied the effectiveness of an organic corrosion inhibitor comprised of "amines and esters in a water medium" using a test specimen similar to the Southern Exposure test specimen. It was found that corrosion initiation in the corrosion inhibitor specimens occurred at 36 weeks, compared to a corrosion initiation of nine weeks in the control specimens. In specimens containing cracks, the specimens containing the corrosion inhibitor showed delayed corrosion initiation compared to the control specimens. Other studies have shown a combination of amines and esters to be ineffective in preventing corrosion (Berke et al. 1993, Pyc 1999).

Civjan et al. (2005) used modified ASTM G 109 specimens to evaluate the effectiveness of Hycrete-DSS and calcium nitrite, as well as the mineral admixtures fly ash, silica fume, and granulated blast furnace slag. A total of fourteen mix designs were used, with the two corrosion inhibitors being tested separately, as well as in varying combinations with the other mineral admixtures. Each admixture combination was evaluated in both cracked and uncracked concrete. Corrosion activity was monitored using corrosion half-cell potentials, macrocell corrosion rate readings, visual inspection, and autopsy evaluations. Calcium nitrite provided excellent corrosion protection in uncracked concrete, but offered no advantages in

cracked concrete. Of all the admixtures tested, Hycrete-DSS when used alone or in conjunction with calcium nitrite, was the more effective corrosion inhibitor of the two corrosion inhibitors, both in uncracked and cracked concrete. The exact mechanism providing this protection is not well understood, but it was suggested that it might be due to the hydrophobic properties of Hycrete, which may make chloride ingress more difficult, or to the inhibitive action of the Hycrete at the surface of the steel. It was also noted that the Hycrete greatly reduced the permeability of the concrete.

In 2005, a field evaluation of calcium nitrite's effectiveness in marine structures was undertaken by the Harbors Division of the Hawaii Department of Transportation (Bola and Newtson 2005). Five sites in existing concrete pier structures that were fabricated with varying amounts of admixed calcium nitrite were evaluated using linear polarization resistance and half-cell potentials. Each site consisted of a portion of concrete slab on the pier. The permeability, pH, and chloride ion concentration profiles of the concrete were also measured. The study determined that slabs containing lower dosages of calcium nitrite [12.4 L/m^3 (2.5 gal/yd^3)] showed greater corrosion activity than the slabs with higher dosages of calcium nitrite [19.9 L/m^3 (4.0 gal/yd^3)], despite the fact that the slabs with the higher dosage of calcium nitrite had more permeable concrete and were therefore more susceptible to corrosion. The reduced corrosion activity in these sites was attributed to the higher dosage of calcium nitrite. The site with the highest dosage of calcium nitrite [22.3 L/m^3 (4.5 gal/yd^3)], which was also subjected to the most severe chloride exposure, showed the least amount of corrosion activity.

Ann et al. (2006) investigated the effectiveness of calcium nitrite using steel embedded in mortar. The steel was centrally embedded into a mortar cylinder, which provided a uniform mortar cover of 33 mm. Five dosages of chloride and four dosages of calcium nitrite were introduced into the mixing water. Linear polarization resistance measurements were used to evaluate the corrosion rate of each specimen. It was observed that at all chloride levels, an increase in calcium nitrite concentration produced a decrease in corrosion rate. Calcium nitrite was shown to increase the chloride corrosion threshold from 0.18% to 0.33% Cl^- by weight of cement for specimens without calcium nitrite to 0.22% to 1.95% Cl^- by weight of cement for specimens with calcium nitrite. It was also observed that a nitrite to chloride molar ratio of between 0.34 and 0.66 was needed for the calcium nitrite to effectively reduce corrosion activity. The specimens with calcium nitrite, however, also exhibited increased permeability, as measured using the rapid chloride permeability test (RCPT). The calcium nitrite apparently facilitated faster chloride ion transport, which could potentially offset the beneficial effects of the calcium nitrite in increasing the chloride threshold. It should be noted, however, that the rapid chloride permeability test does not directly measure the diffusion coefficient of the concrete; rather, it measures the conductivity of the concrete. Consequently, the presence of nitrite ions in the concrete due to the addition of calcium nitrite may simply increase the conductivity in the concrete, thereby decreasing the *apparent* permeability of the concrete.

Ormellese et al. (2006) studied the effectiveness of calcium nitrite and three different organic corrosion inhibitors, including an organic inhibitor comprised of amine-esters. They tested the effects of the inhibitors on steel bars submerged in a saturated calcium hydroxide solution, as well as on bars embedded in concrete. Corrosion half-cell potentials were monitored using a saturated calomel electrode, and corrosion rates were measured using linear polarization resistance. The chloride profile in the reinforced concrete specimens, as well as in plain concrete specimens cast with the same mix proportions as used for the reinforced specimens, was measured. The study concluded that the nitrite-based inhibitor and all of the organic corrosion inhibitors delayed the onset of chloride induced corrosion. It was surmised that the main mechanism of corrosion protection from the organic inhibitors was the reduction of the chloride penetration rate by reducing the permeability of the concrete. It was also observed that the organic corrosion inhibitor consisting of amines and esters caused an increase in the critical chloride threshold in both the solution and concrete tests.

1.7 Objective and Scope

The objective of the current study is to evaluate the effectiveness of multiple corrosion protection strategies when used in conjunction with epoxy-coated reinforcement (ECR). The following protection systems are evaluated in this study:

1. Three corrosion inhibitors: DCI-S, Rheocrete 222+, and Hycrete DSS, admixed in concrete with *w/c* ratios of 0.45 and 0.35.

2. ECR containing a primer of microencapsulated calcium nitrite between the epoxy and the steel, embedded into concrete with *w/c* ratios of 0.45 and 0.35. The calcium nitrite primer acts as a corrosion inhibitor in any areas where the epoxy coating may be damaged.
3. Three types of increased adhesion ECR: ECR pretreated with chromate prior to the application of the epoxy coating, ECR reinforcement with an increased adhesion epoxy developed by DuPont, and ECR reinforcement with an increased adhesion epoxy developed by Valspar, embedded in concrete with a *w/c* ratio of 0.45.
4. Multiple-coated reinforcement, with a zinc layer (nominal thickness of 0.05 mm, or 2 mils) between the steel and the epoxy coating, in concrete with a *w/c* ratio of 0.45. The zinc layer is comprised of 98% zinc and 2% aluminum, and the epoxy used is DuPont 8-2739 (flex west blue).
5. The three types of high adhesion ECR listed in item 3 cast into concrete containing admixed DCI-S corrosion inhibitor.

Unless otherwise specified above, the epoxy coating used on the ECR reinforcement is 3M™ Scotchkote™ 413 Fusion Bonded Epoxy.

The corrosion protection afforded by each system is evaluated using the Southern Exposure and Cracked Beam test specimens, as described in Chapter 2. Corrosion activity in each specimen is monitored by measuring the macrocell voltage drop, mat-to-mat resistance and half-cell corrosion potential of both the top and bottom mats of steel. Linear polarization resistance measurements are also performed

on one specimen for each corrosion protection system and specimen type. Conventional steel and conventional ECR specimens are fabricated and monitored as control specimens. For each specimen, chloride concentrations are measured in the concrete at the level of the bar at the time of corrosion initiation, at 48 weeks, and at the end of the test.

CHAPTER 2

EXPERIMENTAL WORK

The Southern Exposure (SE) and the cracked beam (CB) tests are used in the current study to evaluate the corrosion performance of multiple corrosion protection systems. Corrosion activity is monitored using the methods previously discussed in Chapter 1. This chapter provides a comprehensive description of the test procedures and test program used to evaluate the effectiveness of multiple corrosion protection systems when used with epoxy-coated reinforcement (ECR). These systems include three ECR steels with improved adhesion between the epoxy and the steel (ECR with chromate pretreatment, DuPont, Valspar), two organic corrosion inhibitors in the concrete (Rheocrete 222+, Hycrete DSS), one inorganic corrosion inhibitor, calcium nitrite, in the concrete (DCI-S) and in microencapsulated form as a primer, and multiple-coated reinforcement (ECR with a zinc coating between the epoxy coating and the underlying steel). Conventional steel and conventional epoxy-coated reinforcement are evaluated as control specimens for comparison. The specimens containing corrosion inhibitor, the ECR with calcium nitrite primer, and the control specimens are tested with two water-cement (*w/c*) ratios, 0.45 and 0.35. The specimens with increased adhesion ECR are also tested in concrete containing DCI-S.

2.1 Corrosion Protection Systems Evaluated

A description of the corrosion protection systems evaluated is presented in this section.

2.1.1 Reinforcing Bar

Conv. – Conventional steel

ECR – Epoxy-coated reinforcement

ECR(Chromate) – ECR with a chromate pretreatment of the steel prior to the application of epoxy

ECR(DuPont) – ECR with an improved adhesion epoxy coating produced by DuPont

ECR(Valspar) – ECR with an improved adhesion epoxy produced by Valspar

ECR(primer/Ca(NO$_2$)$_2$) – ECR with a primer containing microencapsulated calcium nitrite between the steel and the epoxy

MC – Multiple-coated reinforcement, with a zinc layer (98% zinc, 2% aluminum), with a nominal thickness of 0.05 mm (2 mils), between the steel and the epoxy. The epoxy used to coat the bar is DuPont 8-2739 (flex west blue).

Unless otherwise specified, the epoxy used to coat the ECR specimens is 3M™ Scotchkote™ 413 Fusion Bonded Epoxy.

2.1.2 Corrosion Inhibitors

Rheocrete – Rheocrete 222+, manufactured by BASF Admixtures, Inc. Specific gravity = 0.98-0.99; 10-16% solids. The dosage used in the current study is 5 L/m^3 (1 gal/yd^3).

DCI – Darex Corrosion Inhibitor (DCI-S), a corrosion inhibitor containing 30% calcium nitrite, 70% water, and a set retarder, manufactured by W. R. Grace. Specific gravity = 1.2-1.3; 33% solids. The dosage used in the current study is 15 L/m^3 (3 gal/yd^3).

Hycrete – Hycrete DSS, manufactured by Hycrete, Inc. Specific gravity = 1.04-1.07; 19.5-20.5% solids. The dosage used in the current study is 2.25% by weight of cement.

2.2 Southern Exposure and Cracked Beam Tests

The Southern Exposure (SE) test simulates the exposure conditions in uncracked reinforced concrete. The SE specimen consists of a concrete slab, $305 \times 305 \times 178$ mm ($12 \times 12 \times 7$ in.), with two No. 16 (No. 5) bars in the top mat and four No. 16 (No. 5) bars in the bottom mat. The bars in the top and bottom mat are identical in terms of type of epoxy coating and number of holes through the epoxy. The steel in each mat runs the entire length of the specimen. Both top and bottom mats have a concrete clear cover of 25 mm (1 in.). The steel in the top mat is electrically connected to the steel in the bottom mat through a terminal box containing a switch and a 10-ohm resistor. A concrete dam, 19 mm (3/4 in.) high, is

cast monolithically around the top of the specimen, facilitating the retention of ponded salt solution. Figure 2.1 shows a schematic diagram of the SE test specimen.

The cracked beam (CB) test is similar to the SE test, but simulates the exposure conditions in cracked concrete. The CB specimen is one-half the width of the SE specimen [305×152×178 mm (12×6×7 in.)] and contains one bar in the top mat and two bars in the bottom mat. A stainless steel shim, 0.3 mm (12 mil) thick, is attached to the casting mold to produce a 152 mm (6 in.) long crack, 25 mm (1 in.) deep when the specimen is cast. The crack is centered longitudinally along the length of the bar. The cracked beam specimen is shown in Figure 2.2.

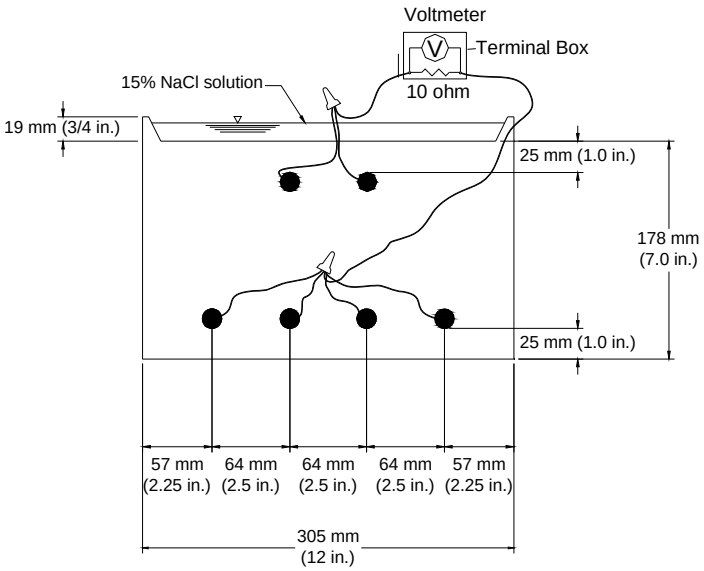

Figure 2.1 – Southern Exposure test specimen

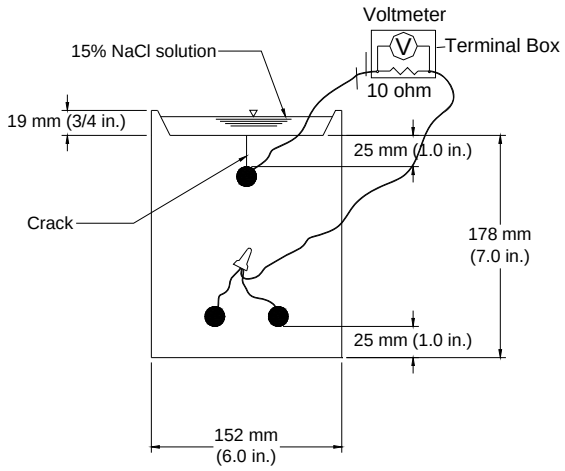

Figure 2.2 – Cracked beam test specimen

2.2.1 Materials and Equipment

The following materials and equipment are used in the SE and CB test programs.

Resistor – A 10-ohm resistor is electrically connected between the top and bottom mats of each specimen.

Wire – 16 AWG wire is used for making all electrical connections.

Terminal Box – For each specimen, the terminal box includes one red and one black binding post, as well as a 10-ohm resistor and a switch. The 10-ohm resistor and switch are wired in series between the red and black posts. The black post is wired to the bottom mat of the specimen and the red post is wired to the top mat of the specimen. The terminal box is used to house the resistor and switch that connects the top and bottom mats. During the test, the switch closes the circuit to allow current to flow through the system. The switch is temporarily opened when mat-to-mat resistance, corrosion potential, and open

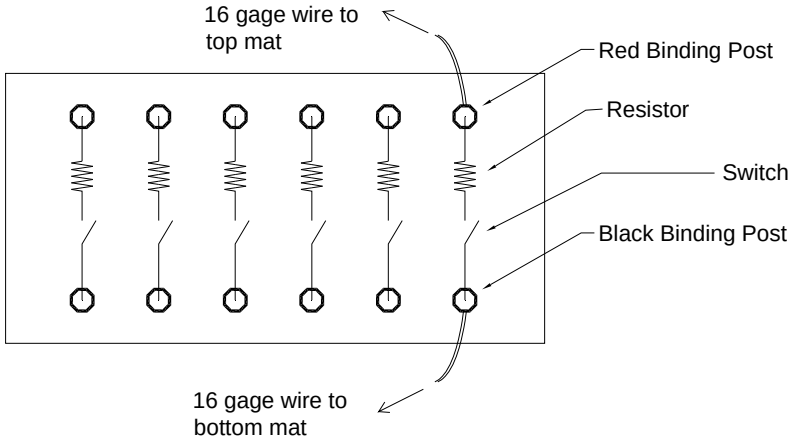

Figure 2.3 – Terminal box diagram

circuit linear polarization resistance measurements are made. The terminal box is illustrated in Figure 2.3.

Salt Solution – 15% NaCl by mass dissolved in deionized water is used to pond the specimens (6.04 m ion concentration).

Epoxy – Sewer Guard HBS 100 Epoxy Liner, manufactured by BASF. This epoxy is used to coat the sides of the specimens.

NaCl – Used to make the salt solution, from Fisher Scientific.

Rheobuild 1000 – High range water reducer, manufactured by BASF.

Concrete – Two water-cement (*w/c*) ratios, 0.45 and 0.35, were used. The concrete had a 76 ± 13 mm (3 ± ½ in.) slump, with 6 ± 1% entrained air. The mix designs for the concrete are shown in Table 2.1. The following constituents were used in the concrete:

Cement – Type I/II portland cement.

Table 2.1 – Concrete mix proportions

w/c	Water	Cement	Coarse Aggregate	Fine Aggregate	Air-entraining Agent	DCI	Hycrete	Rheocrete	Super-plasticizer
	kg/m^3 (lb/yd^3)	kg/m^3 (lb/yd^3)	kg/m^3 (lb/yd^3)	kg/m^3 (lb/yd^3)	mL/m^3 (oz/yd^3)	L/m^3 (gal/yd^3)	kg/m^3 (lb/yd^3)	L/m^3 (gal/yd^3)	L/m^3 (gal/yd^3)
0.45	160 (269)	355 (598)	881 (1484)	852 (1435)	90 (2.33)	-	-	-	-
	147.4 (248.2)	355 (598)	881 (1484)	852 (1435)	140 (3.62)	15 (3.03)	-	-	-
	154.0 (259.4)	355 (598)	881 (1484)	852 (1435)	35 (1.18)	-	8.0 (13.5)	-	-
	155.7 (262.2)	355 (598)	881 (1484)	852 (1435)	300 (7.74)	-	-	5 (1.01)	-
0.35	153 (258)	438 (738)	862 (1452)	764 (1287)	355 (9.16)	-	-	-	2.12 (0.43)
	140.4 (236.4)	438 (738)	862 (1452)	764 (1287)	740 (19.1)	15 (3.03)	-	-	2.12 (0.43)
	145.6 (245.2)	438 (738)	862 (1452)	764 (1287)	330 (8.52)	-	9.9 (16.7)	-	2.25 (0.45)
	148.7 (250.4)	438 (738)	862 (1452)	764 (1287)	1480 (38.2)	-	-	5 (1.01)	2.25 (0.45)

Coarse Aggregate – Crushed limestone from Fogle Quarry with 19 mm (¾ in.) nominal maximum size, bulk specific gravity (SSD) = 2.58, absorption = 2.3%, and unit weight of 1536 kg/m^3 (95.9 lb/ft^3).

Fine Aggregate – Kansas River sand with bulk specific gravity (SSD) = 2.62, absorption = 0.8%, and fineness modulus = 2.51.

Air-entraining Agent – Daravair 1400 from W. R. Grace, Inc.

Water – Tap water. The amount of water used is appropriately adjusted when a corrosion inhibitor is used.

Voltmeter – Agilent Technologies 34401A Digital Multimeter. Used to measure the corrosion half cell potential of the reinforcing steel in conjunction with the SCE electrode.

Nanovoltmeter – Keithley 2182A Nanovoltmeter. Used to measure the macrocell voltage drop across the 10 ohm resistor.

Ohmmeter – Agilent 4338B Milliohmeter. Used to measure mat-to-mat resistance.

Saturated Calomel Electrode (SCE) – Accumet epoxy body calomel reference electrode, Fisher Scientific Catalogue No. 13-620-258 (liquid electrolyte). Used to measure corrosion half cell potentials of the reinforcement.

Shop vacuum cleaner – Used to remove ponded salt solution from the top of the specimens at the beginning of each drying cycle.

Concrete Mixer – Lancaster Counter Current Batch Mixer with a capacity of 0.06 m^3 (2 ft^3), manufactured by Lancaster Iron Works, Inc. The mixer complies with ASTM C 192.

Heat Tent – The tent is 1.2 m (3.5 ft) high, 1.33 m (4 ft) wide, and 2.67 m (8 ft) long. The roof and ends are constructed of 19-mm (3/4-in.) thick plywood. The structure consists of six 2.67 m (8 ft) 2 × 4 studs enclosed using two layers of plastic sheeting that are separated by 25 mm (1 in.). The tent is designed to be movable and can accommodate 12 SE and 12 CB specimens. Three 250-watt heating lamps are attached to the roof of the tent, spaced evenly along the length of the tent. When in place, the lamps are 450 mm (18 in.) above tops of the specimens. A thermostat, installed on the tent, is used to maintain the SE and CB specimens at a temperature of 38 ± 2°C (100 ± 3°F).

2.2.2 Test Specimen Preparation

The following procedure is used to prepare the reinforcing bars used in the Southern Exposure and cracked beam test specimens:

1. Reinforcing bars are cut to a length of 305 mm (12 in.) using a horizontal band saw.

2. Each bar is drilled and tapped at each end to accommodate a 10-24 threaded bolt to a depth of 13 mm (0.5 in.).
3. Conventional steel reinforcement is soaked in acetone for at least two hours and then cleaned vigorously with nylon brush to remove surface oil and debris. Epoxy-coated reinforcement is cleaned with warm, soapy water. Both types of reinforcement are allowed to air dry.
4. The coating on epoxy-coated is penetrated by either 4 or 10 3-mm (1/8-in.) diameter holes. This simulates damage that may occur to epoxy-coated reinforcement during placement in a bridge deck. These holes are created using a 3-mm (1/8-in.) diameter four flute drill bit mounted on a milling machine. The hole is drilled to a depth of 0.4 mm (15 mils). An equal number of holes are made on each side of the reinforcement, and the holes are equally distributed along the length of the bar. Each hole is centered between the longitudinal and transverse ribs that surround it.
5. While some multiple-coated bars have both their epoxy and zinc layers penetrated, others have only their epoxy coating penetrated, leaving the underlying zinc layer intact. This is accomplished by burning a 3-mm (1/8-in.) diameter hole in the epoxy layer with a soldering gun set to 400°C (752°F), which is below the melting point of zinc. Any remaining debris is removed with acetone.

The following procedure is used in fabricating the Southern Exposure and cracked beam specimens:

1. Forms for casting the specimens are made of 19-mm (3/4-in.) thick plywood. Each form consists of two side pieces, two end pieces, and one bottom piece. Small holes are drilled in the end pieces to accommodate screws for securing the reinforcement in place.
2. The forms are constructed so that specimens are cast upside down. The bottom of the form is fabricated so that a 19-mm (3/4-in.) concrete dam is monolithically cast around the perimeter of the specimen. This dam later serves to retain ponding solution on the top of the specimen.
3. After assembly, the interior of the forms is coated with mineral oil, and all joints are sealed with an oil-based clay to prevent leakage from the form.
4. For the CB test, a 0.3-mm (12-mil) thick stainless steel shim is attached to the bottom of the form.
5. The reinforcement is bolted into their proper location. ECR reinforcement is placed so that the holes in the reinforcement face the top and bottom of the specimen.
6. The concrete is mixed in accordance with ASTM C 192. Each specimen is cast in two equal lifts. Each layer is consolidated for 30 seconds by means of a vibrating table with an amplitude of 0.15 mm (0.006 in.) at a frequency of 60 Hz. A wooden float is used to finish the surface.

The Southern Exposure and cracked beam specimens are cured using the following procedure:

1. The SE specimens are cured for 24 hours in the mold at room temperature. CB specimens are removed from the molds between 8 to 12 hours so that the stainless steel shim may be easily removed.
2. Once removed from the mold, the specimens are cured in a closed plastic bag containing distilled water until 72 hours after casting.
3. The specimens are then removed from the plastic bag and are permitted to air cure for 25 days. Specimens are stored such that all surfaces of the specimen are exposed to the air.
4. On day 27 after casting, 16-gage insulated copper electrical wire is attached to the reinforcement on one side of the specimen using 10-24×1/2 (13-mm [0.5-in.] long) stainless steel screws. Screws are also inserted into the other ends of the reinforcement.
5. Immediately after the screws and wire have been attached, the specimen is coated with Sewer Guard HBS 100 Epoxy. The epoxy is mixed according to the manufacturer's recommendations and is applied to the vertical sides of the specimen (including electrical connections and the ends of the reinforcement) with a bristle paint brush.
6. The test begins 28 days after casting the specimen. The top and bottom bars are connected through a switch across a 10-ohm resistor.

2.2.3 Test Procedure

The test duration for both SE and CB tests is 96 weeks. Macrocell voltage drop, mat-to-mat resistance, and open circuit corrosion potentials are measured

weekly. Linear polarization resistance measurements are recorded every four weeks for one SE and one CB test for each type of corrosion protection system evaluated. Ponding-drying cycles are used to accelerate the ingress of the chloride ions.

1. On the first day, specimens are ponded with a 15% (6.04 m ion concentration) NaCl solution. The specimens remain ponded for four days at room temperature [23 ± 2°C (73 ± 3°F)]. Plastic sheeting is placed over the specimens to prevent the evaporation of the solution. During this period, the circuit between top and bottom mats remains connected.
2. On day four, the voltage drop across the resistor is recorded. The circuit is then opened, and the mat-to-mat resistance is recorded. The open circuit is maintained for at least two hours to allow the open circuit potential of the steel to reach equilibrium. A saturated calomel electrode (SCE) is then submerged in the ponding solution and the half-cell potential of the top and bottom mats is recorded.
3. Linear polarization resistance (LPR) readings are taken on the open and closed circuits of one SE and one CB specimen from each testing group. LPR readings are taken on the open circuit every four weeks. LPR readings are taken on the closed circuit every eight weeks. The first LPR reading is usually taken at four weeks, although for some specimens, it was taken as late as 16 weeks. The LPR test procedure is described in Section 2.3.

4. Upon completion of all readings, the ponding solution is removed from the surface of the specimen using a shop vacuum. A heat tent is placed over the specimens to maintain a temperature of 38 ± 2°C (100 ± 3°F). The specimens remain in this environment for three days.
5. After three days, the tent is removed, and the specimens are ponded again, beginning a new weekly cycle.
6. The weekly ponding-drying cycle is repeated for 12 weeks. The specimens are then subjected to a continuous ponding cycle of 12 weeks at room temperature. Plastic sheeting remains in place to limit evaporation of the ponding solution. The specimens are carefully monitored, and where needed, deionized water is added to the specimens to replenish any water that has been lost due to evaporation.
7. After the 12-week continuous ponding cycle, another 12 week ponding-drying cycle begins. The combined 24-week cycle is repeated three times to complete the 96 week test. For some specimens, the test is extended to periods as long as 120 weeks.

2.3 Linear Polarization Resistance (LPR) Test

The linear polarization resistance test is a nondestructive electrochemical technique for measuring the corrosion rate of a metal. The test is used to measure the microcell corrosion rate of the reinforcement. LPR measurements are taken on one SE and one CB test for each corrosion protection system. Separate LPR

measurements are taken on top and bottom mats (open circuit) every four weeks. LPR measurements are taken on connected top and bottom mats (closed circuit) every eight weeks.

LPR measurements are taken using a PC4/750 Potentiostat and DC105 corrosion measurement system from Gamry Instruments. The top and/or bottom mats act as the working electrode. A solid platinum wire, immersed into the ponding solution, is used as the counter electrode. A saturated calomel electrode is immersed in the ponding solution and acts as the reference electrode. The setup window for the LPR test in the DC105 software is shown in Figure 2.4. The DC105 software requires the following user input:

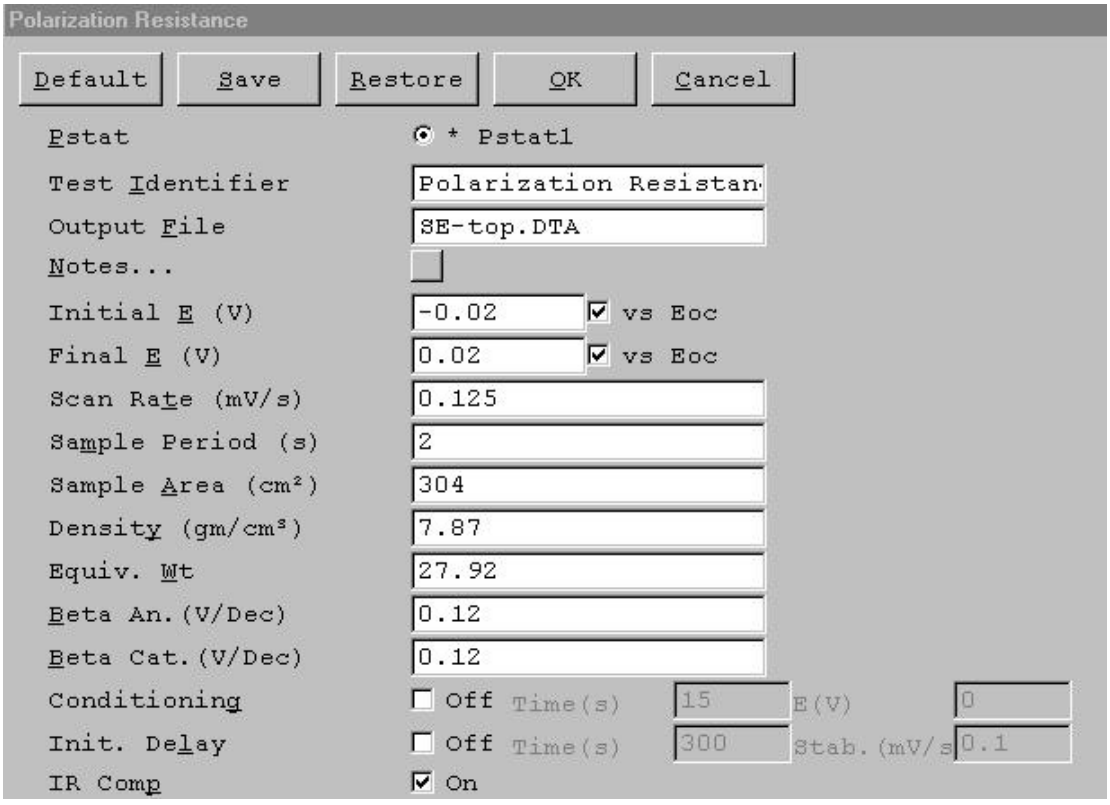

Figure 2.4 – LPR Test setup window for specimen containing steel

Initial E and Final E – These are the starting and ending potential differences with respect to the open circuit potential over which the LPR measurements are made. This is referred to as the potential sweep. A range of -20 mV to +20 mV is used for the current study.

Scan Rate – The scan rate defines the rate that the potential sweep is executed. A scan rate of 0.125 mV/sec is used in the current study.

Sample Period – The sample period sets the spacing between data points. A data point is recorded every two seconds in the current study.

Sample Area – The sample area is the exposed surface area of the reinforcing bar, in cm^2. This value varies, depending on whether SE or CB specimens and top or bottom mats are being measured. The values used are given in Table 2.2.

Density – The density of metal; 7.87 g/cm^3 for steel or 7.14 g/cm^3 for zinc.

Equiv. Wt. – The equivalent weight of the steel or zinc. This is equal to the atomic weight of the metal divided by the number of valence electrons (27.92 for iron and 32.7 for zinc).

Beta An. – The anodic Tafel constant. The current study uses 0.12 V/Decade for both steel and zinc specimens.

Beta Cat. – The cathodic Tafel constant. The current study uses 0.12 V/Decade for both steel and zinc specimens.

Table 2.2 – Exposed steel surface area in cm^2 (in^2) for the linear polarization test

Steel Location	SE	CB
Top Mat	304 (47.1)	152 (23.6)
Bottom Mat	608 (94.2)	304 (47.1)
Connected Mat	912 (141.4)	456 (70.7)

Conditioning – Not used in the current study.

Init. Delay – Not used in the current study.

Upon initiation of a linear polarization measurement, the Gamry PC4 determines the open-circuit potential of the working electrode E_{oc}. The system then imposes a voltage sweep from –20 mV to +20 mV relative to E_{oc}. During this process, a plot of current versus potential is displayed. Upon termination, the data is saved as a file and can be analyzed using the POLRES analysis software included in the DC105 software package. The software is then used to apply a linear best fit line within the range of −10 mV to +10 mV relative to E_{oc}. The slope of this line is the polarization resistance, R_p. The Stern-Geary equation [Eq. (2.1)] is then used to determine the corrosion rate:

$$r = C \times i_{corr} = C \times 1000 \frac{B}{R_p} \tag{2.1}$$

where

r = total corrosion rate (μm/yr)

C = $\frac{ka}{nF\rho}$ = 11.59 for iron; 14.99 for zinc

k = conversion factor, $31.5 \cdot (10^4)$ amp·μm·sec/μA·cm·year

a = atomic weight of the metal = 55.8 g/mol for iron; 65.4 g/mol for zinc

n = number of electrons transferred for each ion oxidized = 2 for iron and zinc

F = Faraday's constant = 96500 Coulombs/mol

ρ = density of metal (g/cm^3) = 7.87 g/cm^3 for iron; 7.14 g/cm^3 for zinc

i_{corr} = corrosion current density (μA/cm^2)

R_p = polarization resistance (Ω·cm^2)

B = Stern-Geary constant (26 mV)

2.4 Chloride Analysis

The current study includes an investigation of the critical chloride threshold of each corrosion protection system. This is accomplished by sampling and testing concrete at the depth of the steel reinforcement to determine its chloride concentration. This section describes the methods of sampling and testing for determining the chloride threshold.

2.4.1 Chloride Sampling

Concrete is sampled from each SE specimen at three different points in time during the testing program, when corrosion initiation is observed in the specimen, at 48 weeks, and at 96 weeks or at the termination of the test if the test period exceeds 96 weeks. In this study, corrosion initiation is defined as occurring when a macrocell corrosion rate of 0.3 μm/yr is observed or when the corrosion potential of the top mat is more negative than –0.275 V versus the saturated calomel electrode (SCE). The following procedure is used to sample concrete:

1. The specimen is disconnected from the circuit and placed on a clean, dry surface. The side of the specimen from which the specimen will be drilled to obtain the sample is thoroughly washed using warm, soapy water. The specimen is then rinsed twice, the first time with tap water and the second time with deionized water. The surface is then dried with paper towels.
2. The specimen is marked at the desired sampling depth from the ponded surface of the concrete. Two different depths are used. Samples taken at corrosion initiation and at the end of the test are drilled so that the top of the drill bit is at the same depth as the top of the reinforcing steel in the top mat, as shown in Figures 2.5 and 2.6. Samples that are taken at 48 weeks are drilled so that the center of the drill bit is at the same depth as the center of the reinforcing steel in the top mat, as shown in Figures 2.7 and 2.8.

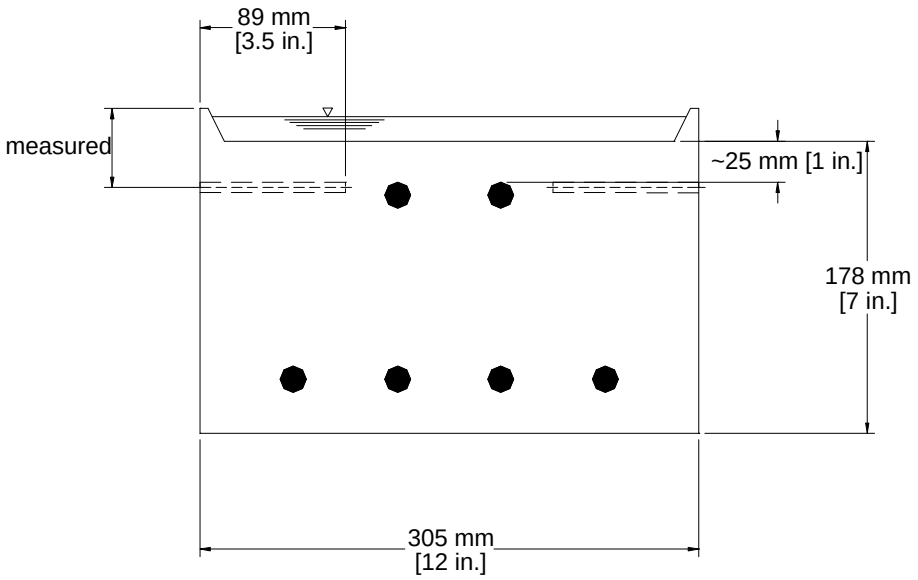

Figure 2.5 – Sampling locations in SE specimen at corrosion initiation, front view

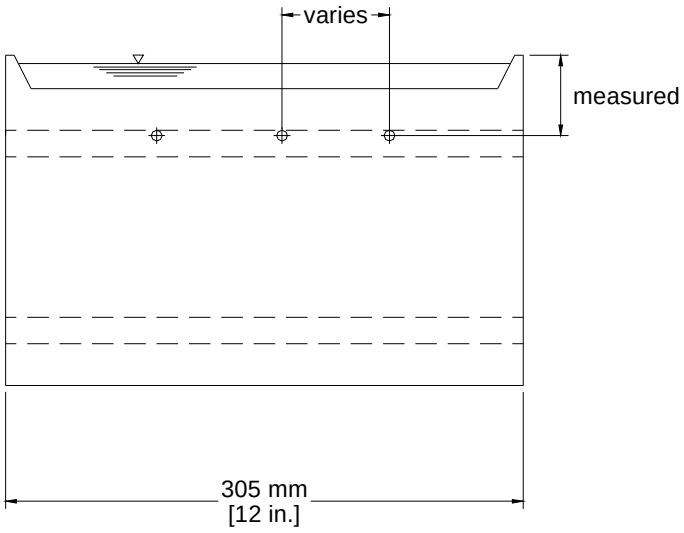

Figure 2.6 – Sampling locations in SE specimen at corrosion initiation, side view

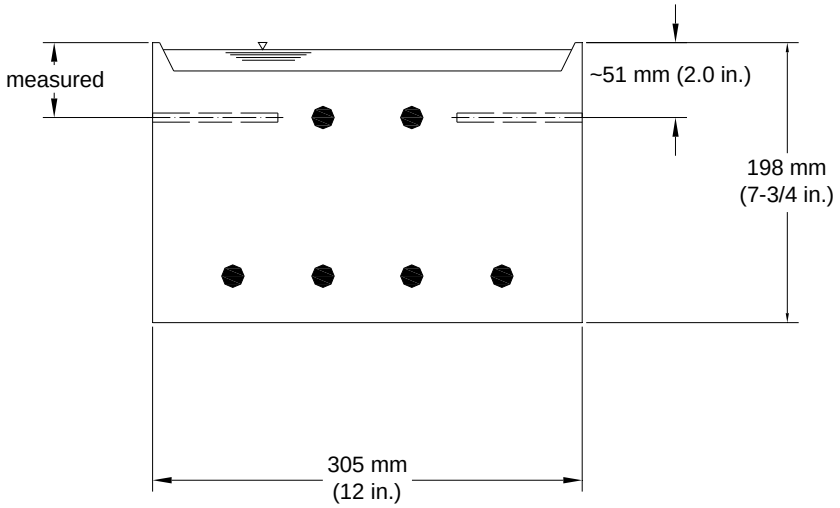

Figure 2.7 – Sampling locations in SE specimen at 48 weeks and end of life, front view

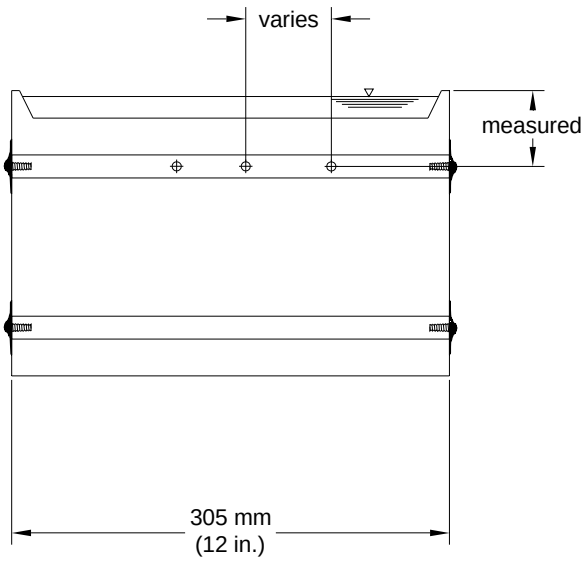

Figure 2.8 – Sampling locations in SE specimen at 48 weeks and end of life, side view

3. The specimen is placed on a drill press. A hole is drilled at the level previously marked in step 2 using a 6.4-mm (0.25-in.) diameter drill bit. The hole is perpendicular to the side of the specimen and is parallel to the ponded surface of the specimen. The hole is initially drilled to a depth of 12.7 mm (0.5 in.). The resulting concrete powder is discarded using a vacuum to clean the area surrounding the hole. The drill bit is then cleaned using deionized water and tissue paper.
4. Drilling recommences, and the hole is drilled to a depth of 89 mm (3.5 in.). The resulting concrete powder is transferred to a zip lock plastic bag with the aid of a 2-inch bristle brush and a piece of printer paper.

5. The drill bit is again rinsed with deionized water and dried with tissue paper, and any remaining concrete sample on the surface of the specimen is removed with a vacuum.
6. A total of three samples are taken from each side of the specimen, resulting in six samples per specimen. Each hole yields approximately six grams of concrete.
7. During the entire sampling process, care is taken to avoid contamination of the sample by outside chlorides.
8. The holes remaining in the SE specimen are filled using an oil-based modeling clay, and the specimen is reconnected to the circuit.

2.4.2 Chloride Analysis

The pulverized concrete samples that are collected from the SE specimens are tested using Procedure A in AASHTO T 260-97 "Standard Method of Test for Sampling and Testing for Chloride Ion in Concrete and Concrete Raw Materials." After the powdered concrete sample is processed in boiling distilled water, the chloride content is measured through potentiometric titration using silver nitrate as a titrant. An ion-selective electrode (Orion Model 96-17 combination ion-selective electrode) connected to a millivoltmeter (Fluke 83 digital multimeter) is used to measure potential differences during the titration. The largest potential increase between two consecutive readings indicates the endpoint of the titration. This procedure gives the chloride concentration in terms of percent Cl^- ion by weight of

concrete. This is converted into kg/m^3 (lb/yd^3) of concrete by multiplying by the unit weight of concrete, 2246 kg/m^3 (3786 lb/yd^3).

2.5 Autopsy Evaluation

Upon completion of an SE or CB test, specimens are autopsied and the embedded reinforcement is inspected. The extraction of the bars from the specimen is facilitated by breaking the specimen with a hydraulic compression testing machine. After extraction, each bar is photographed. The color of any corrosion product present on the surface of the bar is noted. The degree of disbondment in the area surrounding the drilled holes is evaluated using the following procedure, which is adapted from the test used for measuring cathodic disbondment of coatings in ASTM G 8 and ASTM A 775:

1. At the site of the hole, radial cuts in the epoxy are made at 45° from the longitudinal axis of the reinforcing bar with a sharp, thin-bladed knife. Care is taken to ensure that the entire depth of the epoxy is penetrated by the blade.
2. An attempt is made to lift off any disbonded epoxy from the underlying steel surface using the point of the knife. Epoxy is removed along the surface of the bar until it will no longer separate from the steel surface with ease.
3. The radius of disbondment is measured at 0°, 90°, 180°, and 270°, with 0° and 180° representing the longitudinal axis of the bar. If the

average of the four radii is greater than 12 mm (1/2 in.), the epoxy is said to have suffered total disbondment (TD), and the disbonded area is not measured.

4. The area of disbondment is measured using a transparent film upon which has been printed a grid consisting of 2.54 mm (0.1 in.) squares. This film is placed on the disbonded surface, and the shape of the disbonded surface is traced onto the film. The disbonded area is then obtained by counting the number of squares within the traced area.
5. A photograph is taken of the disbonded area, and the color of any corrosion product is noted.

This procedure is performed for two holes on the original upper surface and for one hole on the original lower surface of each bar tested. One top bar and one bottom bar are tested for disbondment for each SE and CB specimen.

2.6 Test Program

A total of 96 Southern Exposure and 87 cracked beam specimens were tested in the current study. Conventional steel and epoxy-coated reinforcement serve as control specimens and are compared to 11 multiple corrosion protection systems. The Southern Exposure and cracked beam test programs are summarized in Tables 2.3 and 2.4, respectively. Linear polarization resistance measurements are taken on one specimen from each test group. The specimen number that is used for the LPR

Table 2.3 – Test program for the Southern Exposure test

Steel Designation[a]	Number of Tests	LPR Specimen No.
Control		
Conv.-45	6	6
Conv.-35	3	3
ECR-4h-45	6	6
ECR-10h-45	3	3
ECR-10h-35	3	3
Corrosion inhibitors		
ECR(DCI)-4h-45	3	3
ECR(DCI)-10h-45	3	3
ECR(DCI)-10h-35	3	3
ECR(RH)-4h-45	3	3
ECR(RH)-10h-45	3	3
ECR(RH)-10h-35	3	3
ECR(HY)-4h-45	3	3
ECR(HY)-10h-45	3	3
ECR(HY)-10h-35	3	3
ECR(primer/$Ca(NO_2)_2$)-4h-45	3	3
ECR(primer/$Ca(NO_2)_2$)-10h-45	3	3
ECR(primer/$Ca(NO_2)_2$)-10h-35	3	3
Multiple Coated Bars		
MC(both layers penetrated)-4h-45	3	3
MC(both layers penetrated)-10h-45	3	3
MC(only epoxy penetrated)-4h-45	3	3
MC(only epoxy penetrated)-10h-45	3	3
Increased Adhesion ECR		
ECR(Chromate)-4h-45	3	1
ECR(Chromate)-10h-45	3	1
ECR(DuPont)-4h-45	3	1
ECR(DuPont)-10h-45	3	1
ECR(Valspar)-4h-45	3	1
ECR(Valspar)-10h-45	3	1
Increased Adhesion ECR with Corrosion Inhibitor DCI		
ECR(Chromate/DCI)-4h-45	3	1
ECR(DuPont/DCI)-4h-45	3	1
ECR(Valspar/DCI)-4h-45	3	1

[a] Conv. = conventional steel. ECR = conventional epoxy-coated reinforcement.
ECR(Chromate) = ECR with the chromate pretreatment.
ECR(DuPont) = ECR with high adhesion DuPont coating.
ECR(Valspar) = ECR with high adhesion Valspar coating.
ECR(DCI) = ECR in concrete with DCI inhibitor.
ECR(Rheocrete) = ECR in concrete with Rheocrete inhibitor.
ECR (Hycrete) = normal ECR with Hycrete inhibitor.
MC(both layers penetrated) = multiple coated bars with both zinc and epoxy layers penetrated.
MC(only epoxy penetrated) = mutiple coated bars with only epoxy layer penetrated.
4h = bar with four holes through epoxy, 10h = bar with 10 holes through epoxy.
45 = concrete with *w/c* =0.45; 35 = concrete with *w/c* =0.45.

Table 2.4 – Test program for the cracked beam test

Steel Designation[a]	Number of Tests	LPR Specimen No.
Control		
Conv.-45	6	6
Conv.-35	3	3
ECR-4h-45	6	6
ECR-10h-45	3	3
ECR-10h-35	3	3
Corrosion inhibitors		
ECR(DCI)-4h-45	3	3
ECR(DCI)-10h-45	3	3
ECR(DCI)-10h-35	3	3
ECR(RH)-4h-45	3	3
ECR(RH)-10h-45	3	3
ECR(RH)-10h-35	3	3
ECR(HY)-4h-45	3	3
ECR(HY)-10h-45	3	3
ECR(HY)-10h-35	3	3
ECR(primer/$Ca(NO_2)_2$)-4h-45	3	3
ECR(primer/$Ca(NO_2)_2$)-10h-45	3	3
ECR(primer/$Ca(NO_2)_2$)-10h-35	3	3
Multiple Coated Bars		
MC(both layers penetrated)-4h-45	3	3
MC(both layers penetrated)-10h-45	3	3
MC(only epoxy penetrated)-4h-45	3	3
MC(only epoxy penetrated)-10h-45	3	3
Increased Adhesion ECR		
ECR(Chromate)-4h-45	3	1
ECR(Chromate)-10h-45	3	1
ECR(DuPont)-4h-45	3	1
ECR(DuPont)-10h-45	3	1
ECR(Valspar)-4h-45	3	1
ECR(Valspar)-10h-45	3	1

[a] Conv. = conventional steel. ECR = conventional epoxy-coated reinforcement.
ECR(Chromate) = ECR with the chromate pretreatment.
ECR(DuPont) = ECR with high adhesion DuPont coating.
ECR(Valspar) = ECR with high adhesion Valspar coating.
ECR(DCI) = ECR in concrete with DCI inhibitor.
ECR(Rheocrete) = ECR in concrete with Rheocrete inhibitor.
ECR (Hycrete) = normal ECR with Hycrete inhibitor.
MC(both layers penetrated) = multiple coated bars with both zinc and epoxy layers penetrated.
MC(only epoxy penetrated) = mutiple coated bars with only epoxy layer penetrated.
4h = bar with four holes through epoxy, 10h = bar with 10 holes through epoxy.
45 = concrete with *w/c* =0.45; 35 = concrete with *w/c* =0.45.

test from each group is specified in Tables 2.3 and 2.4 for Southern Exposure and cracked beam tests, respectively.

CHAPTER 3

RESULTS

The test results of the Southern Exposure and Cracked Beam tests are presented in this chapter. The results include the macrocell corrosion rate, corrosion loss, mat-to-mat resistance, corrosion potential of the top and bottom mats with respect to a copper-copper sulfate electrode (CSE), and the microcell corrosion rate of the top bar, as measured using linear polarization resistance. Disbondment measurements taken on the epoxy-coated reinforcement at the end of the test are also presented. Finally, critical chloride corrosion thresholds for each test group are presented.

To simulate damage that may occur during placement on a bridge deck, the coating on epoxy-coated and multiple-coated reinforcement is penetrated by either four or ten holes through the epoxy. For these specimens, the corrosion rate results are reported based on both the total area of the bar and the area of the steel exposed by the holes drilled into the epoxy. In this chapter, results based on exposed area are indicated by an asterisk (*). Analyzing results based on exposed area is useful when comparing the performance of four and ten-hole specimens. Table 3.1 contains the bar length, total bar area, and the area of steel exposed by the holes through the epoxy, as well as the ratio of corrosion rates and losses based on exposed area to corrosion rates and losses based on total area for the specimens reported in this study. The

areas are expressed in cm^2 because this is the standard unit of area within the field of corrosion technology.

Table 3.1 - Total bar areas, exposed steel areas, and the corrosion rate ratios for Southern Exposure and Cracked Beam specimens with four and ten holes through the epoxy coating

Test Method		SE	CB
Number of Top Bars		2	1
Bar Length mm (in.)		305 (12)	305 (12)
Total Bar Area cm^2 ($in.^2$)		304 (47.1)	152 (23.6)
4 holes	Exposed Area cm^2 ($in.^2$)	0.63 (0.10)	0.32 (0.05)
	Ratio*	480	480
10 holes	Exposed Area cm^2 ($in.^2$)	1.59 (0.25)	0.79 (0.12)
	Ratio*	192	192

* Ratio of total area to exposed area

It was observed that, when measuring the voltage drop across the resistor between the anode and the cathode, the reading on the voltmeter would fluctuate by ±0.003 mV due to background electromagnetic interference, even when no current was flowing at the beginning of the test. Therefore, readings in this range are treated as representing a corrosion rate of zero.

During a portion of the tests, the milliohmeter used to measure the mat-to-mat resistance was inoperative. Consequently, a number of specimens will have periods during which no mat-to-mat resistance is reported. Because specimens within a group were not always cast at the same date, this period may fall within different weeks for specimens of the same group. As a result, the averages presented in the plots for these specimens may at times represent the average of just one or two

specimens. The individual specimens included in the average are shown in the individual mat-to-mat resistance measurements presented in Appendix B.

The analyses and evaluations contained within this report are based on the test results of all specimens at 96 weeks, though testing of some specimens in this study was extended to periods as long as 120 weeks. Sections 3.1 through 3.5 cover the macrocell corrosion rate, total corrosion loss, and top and bottom corrosion potentials for the control specimens, specimens containing corrosion inhibitors, specimens with increased adhesion ECR, specimens with increased adhesion ECR cast in concrete containing DCI corrosion inhibitor, and multiple-coated reinforcement. Section 3.6 presents the linear polarization resistance results. Section 3.7 presents the observations and disbondment data collected upon autopsy of the specimens. The results of the critical chloride corrosion threshold analyses are presented in Section 3.8. The macrocell corrosion rates (based on total area), losses, mat-to-mat resistances, and corrosion potential measurements for individual specimens are provided in Appendix A. The results based on the total area of the ECR specimens can be converted to exposed area by multiplying by the appropriate ratio given in Table 3.1. The macrocell and microcell corrosion losses presented in this chapter will be compared in Chapter 4. Chapter 4 will also compare the disbondment measurements presented in this chapter with corrosion losses and cathodic disbondment test results previously published by Gong et al. (2006), as well as provide a comparison between the performance of each corrosion protection system evaluated in this study.

3.1 Conventional Steel and Conventional Epoxy-Coated Reinforcement

This section presents the test results of the Southern Exposure and cracked beam specimens containing conventional steel and conventional epoxy-coated reinforcement (ECR). These specimens serve as control specimens for comparison with the other corrosion protection systems evaluated in this study, and therefore, the results shown in this section will be repeated in the sections that deal with the other corrosion protection systems included in this study. Six Southern Exposure and six cracked beam tests were performed for both conventional steel and ECR with four holes through the epoxy in concrete with *w/c* = 0.45. Three each Southern Exposure and cracked beam tests were performed for ECR with ten holes through the epoxy in concrete with *w/c* = 0.45 and for conventional steel and ECR with ten holes through the epoxy in concrete with *w/c* = 0.35. The results for one Southern Exposure specimen, conventional steel specimen number one with *w/c* = 0.45 (Conv.-45-1), have been omitted from the analysis because no significant corrosion activity was observed in this specimen during the test, as shown in Figure A.1.

3.1.1 Southern Exposure Test

Figure 3.1 shows the average corrosion rates based on the total area of the top bars in contact with concrete for conventional steel and ECR specimens. The conventional steel specimens with *w/c* = 0.45 (Conv.) and with *w/c* = 0.35 (Conv.-35) show higher corrosion rates than any of the conventional ECR specimens. The Conv.-45 specimens show indications of corrosion beginning at week 15. Between weeks 18 and 22, the Conv.-45 specimens show a negative average corrosion rate.

The reason for the "negative" rate is that before corrosion initiation occurs, the macrocell voltage drop between the top and bottom mats can fluctuate between slightly positive and slightly negative values. A negative rate, does not, in fact, represent negative corrosion; rather, it indicates a flow of electrons from the bottom mat to the top mat. The Conv.-35 specimens show no corrosion activity until week 48. It appears that the lower permeability of the concrete with a lower water-cement ratio delays the corrosion initiation of the reinforcement in uncracked concrete. Once corrosion begins, the Conv.-35 specimens show smaller corrosion rates than the Conv.-45 specimens between weeks 48 and 65. Between weeks 65 and 77, both Conv.-45 and Conv.-35 specimens exhibit corrosion rates of similar magnitude, and

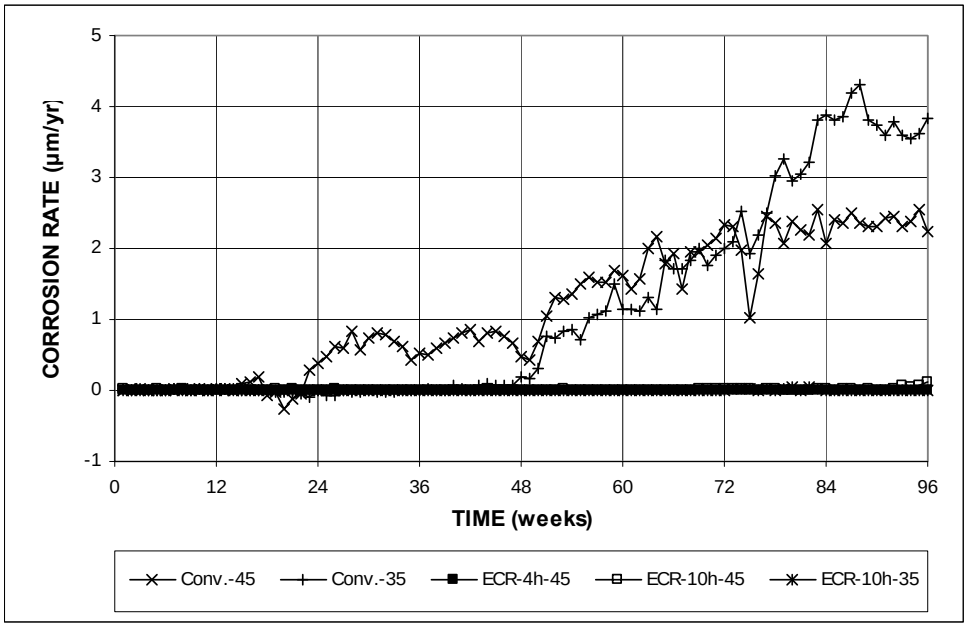

Figure 3.1 – Average corrosion rate, Southern Exposure test for specimens containing conventional steel reinforcement and ECR with four and ten holes through the epoxy, w/c = 0.45 and 0.35.

beyond week 77, the Conv.-35 specimens show higher corrosion rates than the Conv.-45 specimens. The corrosion rates based on total area of ECR-4h-45, ECR-10h-45 and ECR-10h-35 specimens are all less than 0.06 μm/yr, which is negligible when compared to the specimens containing conventional steel.

Figure 3.2 shows the average corrosion rates of the ECR-4h-45, ECR-10h-45 and ECR-10h-35 specimens, based on the area of steel exposed by the four or ten holes through the epoxy. Both ECR-4h-45 and ECR-10h-35 specimens show no corrosion rate above 10 μm/yr during the 96 week test period. Between weeks 92 and 96, the ECR-10h-45 specimens began exhibiting a significant increase in corrosion activity. This increase in corrosion activity was observed in all three individual specimens, as shown in Figure A.13a.

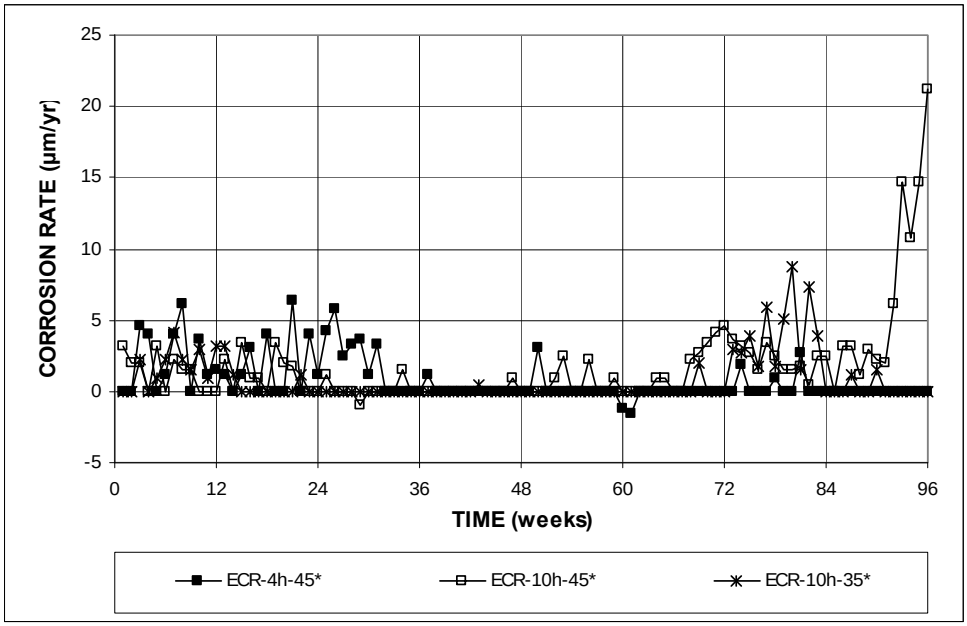

Figure 3.2 – Average corrosion rate based on exposed area, Southern Exposure test for specimens containing ECR with four and ten holes through the epoxy, w/c = 0.45 and 0.35.

Figures 3.3 and 3.4 show the average corrosion loss for specimens containing conventional steel and ECR. In these figures, the slope of the plotted line represents the average corrosion rate. Therefore, a horizontal slope indicates no corrosion activity, whereas a positive slope indicates active corrosion. Steeper slopes represent higher corrosion rates. A discontinuity, where the slope changes from horizontal or nearly horizontal to a positive slope, indicates the point of corrosion initiation. As shown in Figure 3.3, conventional steel specimens exhibit much higher corrosion losses than the ECR control specimens. This is also true for all of the other systems with epoxy-coated reinforcement tested in this study. As described earlier, the Conv.-45 specimens are the first to exhibit corrosion loss. As previously noted, corrosion initiation occurs later in the Conv.-35 specimens than in the Conv.-45 specimens.

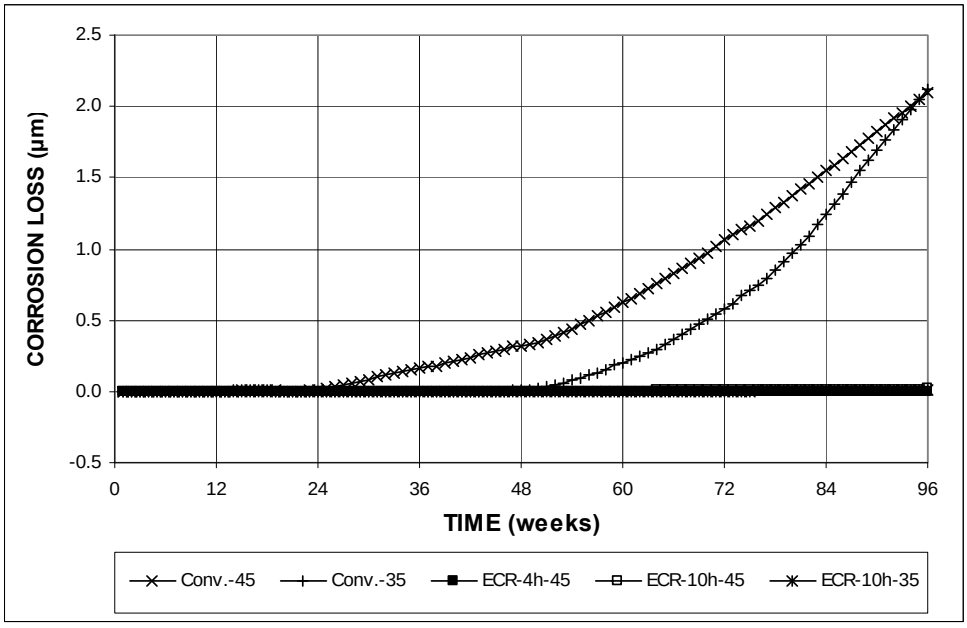

Figure 3.3 – Average corrosion loss, Southern Exposure test for specimens containing conventional steel and ECR with four and ten holes through the epoxy, *w/c* = 0.45 and 0.35.

This is also apparent in Figure 3.3. However, by 96 weeks, the Conv.-35 specimens have suffered as much corrosion loss as the Conv.-45 specimens. Therefore, while the specimens with a lower *w/c* ratio have shown delayed onset of corrosion, the conventional steel specimens with *w/c* = 0.35 ratio ultimately hold no advantage over the conventional steel specimens in concrete with *w/c* = 0.45 in the current tests.

As shown in Figure 3.4, the ECR-10h-45 specimens exhibited the highest corrosion loss based on exposed area of the three epoxy-coated bar series, with a corrosion loss of 3.21 μm at week 96, followed by ECR-4h-45 and ECR-10h-35 with respective corrosion losses of 1.51 and 1.47 μm at week 96. The ECR-10h-45 specimens exhibited a significant increase in corrosion rate at week 68. As shown in Figure A.13, this increase is observed in two out of the three ECR-10h-45 specimens.

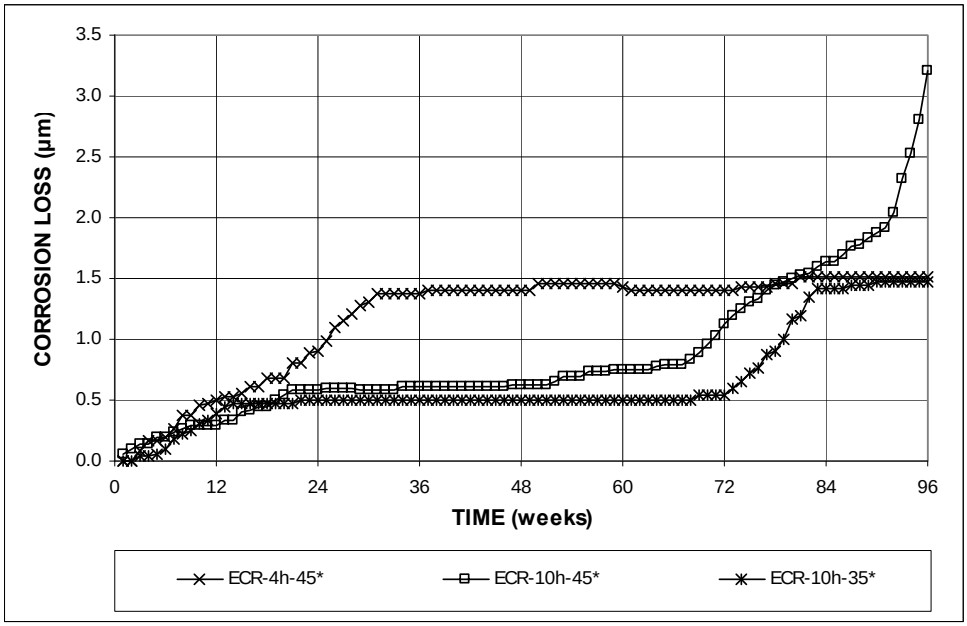

Figure 3.4 – Average corrosion loss based on exposed area, Southern Exposure test for specimens containing ECR with four and ten holes through the epoxy, *w/c* = 0.45 and 0.35.

A comparable increase is not observed in the ECR-10h-35 specimens until week 73, and this increase in corrosion rate is only observed until week 83, after which little increase in corrosion loss is observed. As with the conventional steel specimens, it appears that the lower w/c ratio causes a delay in the corrosion initiation of the reinforcement, although this delay is less pronounced in the specimens with ECR.

As shown in Figure 3.5, the Conv.-35 specimens exhibit the lowest mat-to-mat resistances of the control specimens, with a maximum mat-to-mat resistance of 587 ohms during the test. This is followed by the Conv.-45, ECR-10h-35, ECR-10h-45, and ECR-4h-45 specimens, exhibiting maximum mat-to-mat resistances of 1418, 5989, 6710, and 11,711 ohms, respectively. During the test, the specimens containing the Conv.-45 and Conv.-35 specimens exhibit similar resistances. The ECR-10h-45 and ECR-10h-35 specimens exhibit similar resistances for the first 28 weeks of the test, with growing disparity between the two specimens being observed from weeks 28 to 96. The low resistances observed for the specimens containing conventional steel are attributable to the unprotected surface of the steel being in contact with the surrounding pore solution. The epoxy-coating in the ECR specimens acts as an electrical barrier between the underlying steel and the pore solution, causing greater mat-to-mat resistances. Consequently, ECR specimens with four holes through the epoxy show higher mat-to-mat resistances than ECR specimens with 10 holes through the epoxy. The mat-to-mat resistance of all control specimens gradually increases with time for at least the first 60 weeks. This is probably due to the formation of corrosion products on the surface of the steel that restrict access of the pore solution

to the surface of the steel. After week 60, the mat-to-mat resistances of ECR specimens become more erratic, with no generally observable increase or decrease, while the mat-to-mat resistances of the conventional steel specimens continue to increase slightly with time through 96 weeks.

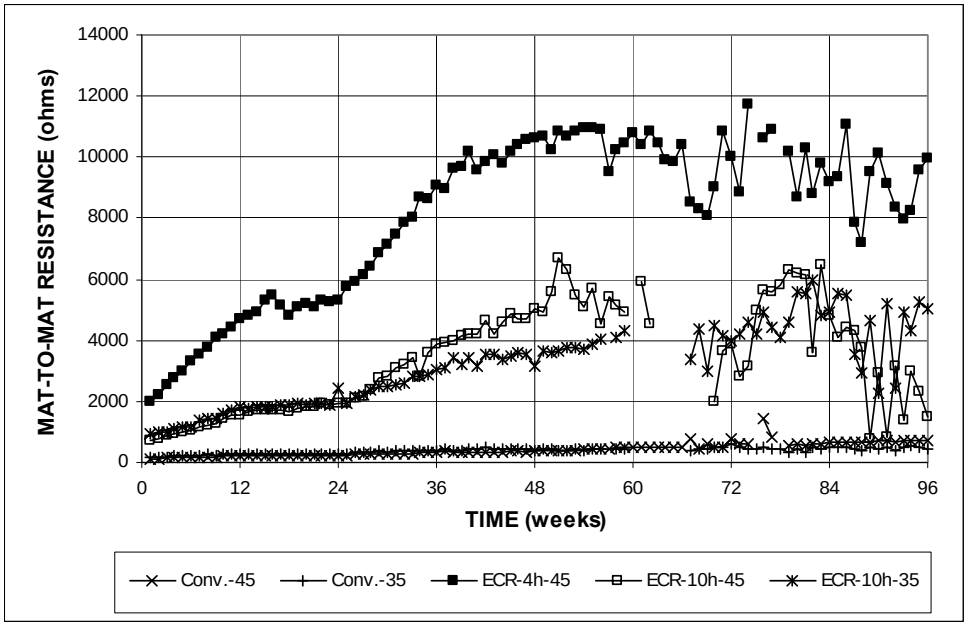

Figure 3.5 – Average mat-to-mat resistance, Southern Exposure test for specimens containing conventional steel and ECR with four and ten holes through the epoxy, *w/c* = 0.45 and 0.35.

For specimens containing conventional steel and ECR, Figures 3.6 and 3.7 show the respective average open circuit corrosion potentials versus a copper-copper sulfate electrode (CSE) for the top and bottom mats of steel. As pointed out in Chapter 1, a corrosion potential more negative than –0.350 V with respect to CSE indicates a probability of steel corrosion of greater than 90 percent. The top mats of the Conv.-45 and Conv.-35 specimens begin exhibiting corrosion potentials lower than –0.350 V at weeks 27 and 52, respectively, and remain more negative than

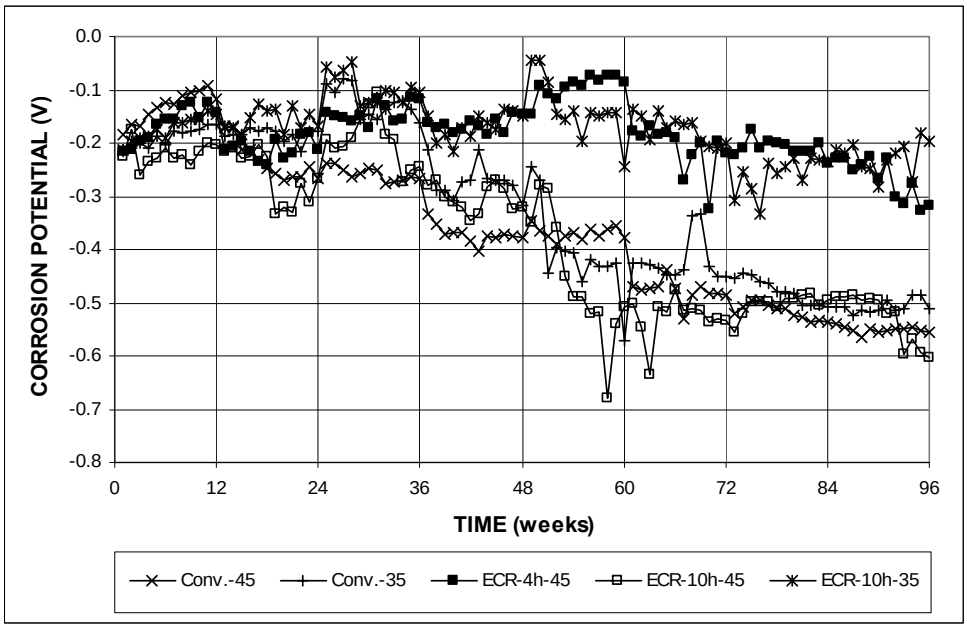

Figure 3.6 – Average top mat corrosion potential, Southern Exposure test for specimens containing conventional steel and ECR with four and ten holes through the epoxy, *w/c* = 0.45 and 0.35.

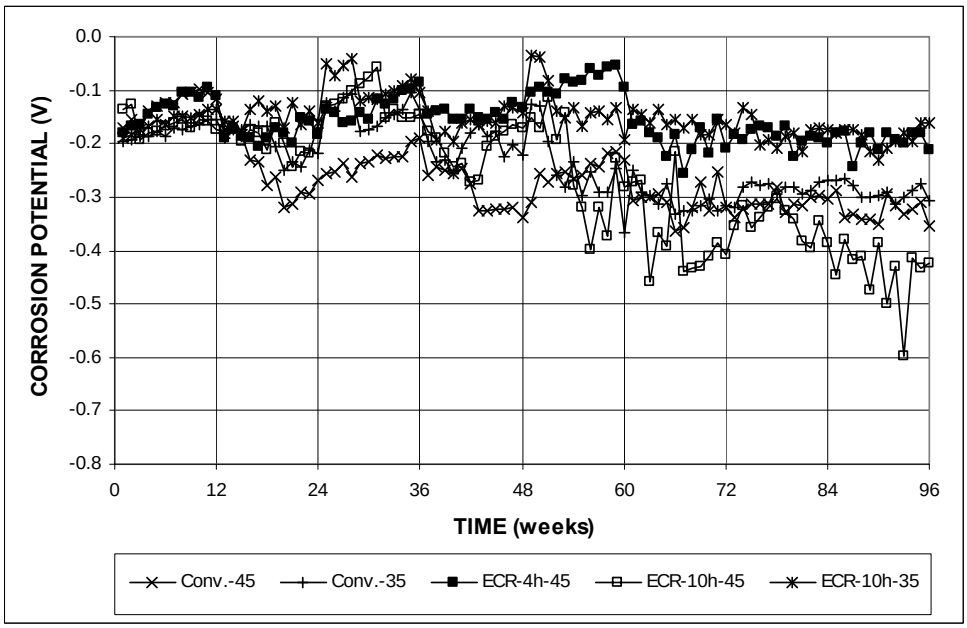

Figure 3.7 – Average bottom mat corrosion potential, Southern Exposure test for specimens containing conventional steel and ECR with four and ten holes through the epoxy, *w/c* = 0.45 and 0.35.

– 0.350 V for the remainder of the test. The ECR-10h-45 specimens are the only ECR specimens to exhibit an average top mat corrosion potential less than –0.350 V, beginning at week 52 with a corrosion potential of –0.358 V and remaining more negative than –0.350 V for the remainder of the test. The most negative corrosion potentials observed in the top mat of the ECR-4h-45 and ECR-10h-35 specimens are –0.328 V and –0.333 V at weeks 95 and 76, respectively. The bottom mats of Conv.-45 specimens were generally more positive than –0.350, except for weeks 66, 67, and 96, with potentials of –0.363, –0.356 V, and –0.355 V, respectfully. Only at week 60 did the Conv.-35 specimens show a potential less than –0.350 V, with a potential of –0.367 V. The only control specimens to exhibit bottom mat corrosion potentials below –0.350 V for a continuous period are the ECR-10h-45 specimens. The first corrosion potential observed in these specimens below –0.350 V occurs at week 56, while the first period with corrosion potentials continuously below –0.350 V occurs between weeks 67 and 73. The corrosion potentials in the top mat are generally more negative than the potentials observed in the bottom mat. Between weeks 18 and 22, the Conv.-45 specimens exhibited an average bottom mat potential more negative than the top mat accompanied by a negative macrocell corrosion rate, indicating that during this period, a small amount of corrosion was occurring in the bottom mat of the specimens. Similar behavior is observed for the Conv.-35 specimens between weeks 19 and 33, excluding weeks 24, 27, and 30.

Table 3.2 summarizes the corrosion losses observed at the end of the test for the Southern Exposure control specimens. The Conv.-35 and Conv.-45 exhibited the

highest corrosion losses of the control specimens, 2.12 and 2.10 μm, respectively. As previously noted, although the lower *w/c* ratio delayed corrosion initiation in the Conv.-35 specimens, by the end of the test, the Conv.-35 specimens exhibited corrosion losses similar to the Conv.-45 specimens. Therefore, the lower *w/c* ratio ultimately provided no additional protection to the conventional steel reinforcement. All specimens containing epoxy-coated reinforcement show very low corrosion losses based on total area, the highest being ECR-10h-45 with 0.017 μm by week 96. Based on exposed area, the ECR-10h-45 specimens also exhibited the highest corrosion loss, 3.21 μm, of the epoxy-coated specimens. The ECR-4h-45 and ECR-10h-35 specimens exhibited corrosion losses of 1.51 and 1.47 μm, respectively.

Table 3.2 – Average corrosion loss (μm) at week 96 as measured in the Southern Exposure test for specimens containing conventional steel and ECR

Steel Designation[a]	Specimen						Average	Standard Deviation
	1	2	3	4	5	6		
Total Area								
Conv.-45	0.048[b]	2.61	1.08	2.97	1.61	2.21	2.10	0.76
Conv.-35	1.05	4.22	1.10				2.12	1.82
ECR-4h-45	0.003	0.002	0.003	0.002	0.004	0.005	0.003	0.001
ECR-10h-45	0.019	0.008	0.023				0.017	0.008
ECR-10h-35	0.011	0.003	0.010				0.008	0.004
Exposed Area								
ECR-4h-45*	1.44	0.950	1.23	0.739	2.08	2.60	1.51	0.708
ECR-10h-45*	3.66	1.58	4.41				3.21	1.47
ECR-10h-35*	2.03	0.549	1.83				1.47	0.803

[a] Conv. = conventional steel. ECR = conventional epoxy-coated reinforcement.
4h = bar with four holes through epoxy, 10h = bar with 10 holes through epoxy.
45 = concrete with *w/c* =0.45, 35 = concrete with *w/c* =0.35.

[b] Excluded from average due to low corrosion activity.

* Corrosion loss calculation based on the exposed area of four or ten 3-mm (1/8-in.) diamter holes.

3.1.2 Cracked Beam Test

As shown in Figure 3.8, cracked beams specimens containing conventional steel show significantly higher corrosion rates than specimens containing ECR. Unlike the uncracked specimens, the cracked beam specimens with conventional steel in concretes with *w/c* = 0.45 and *w/c* = 0.35 begin exhibiting a high corrosion rate during the first week of the test, with average corrosion rates of 10.9 and 10.3 μm/yr for Conv.-45 and Conv.-35, respectively. As mentioned in Chapter 1, chlorides must diffuse through uncracked concrete to the level of the reinforcement and must reach a sufficient concentration (the critical chloride threshold) before they can initiate corrosion in reinforcement. However, as the data indicates, when a crack is present in concrete, it provides the chloride ions with direct access to the reinforcing steel, and corrosion initiation can begin with the first application of chlorides. As shown in Figure A.3a, all six cracked beam specimens exhibit corrosion by the end of the first week of the test. However, by week 9, the corrosion rates observed in these specimens drop to roughly half their initial value. As corrosion products form on the surface of the reinforcement, they can fill the crack in the concrete and can inhibit the access of chloride ions and oxygen to the surface of the steel, thereby limiting the rate of the corrosion reaction. For the remainder of the test, the average corrosion rate of the specimens with conventional steel gradually increases with time, except for a brief period between weeks 60 and 73 for the Conv.-45 specimens. As shown in Figure 3.9, there is little discernable difference between the corrosion rates based on exposed area of the cracked beam specimens containing ECR.

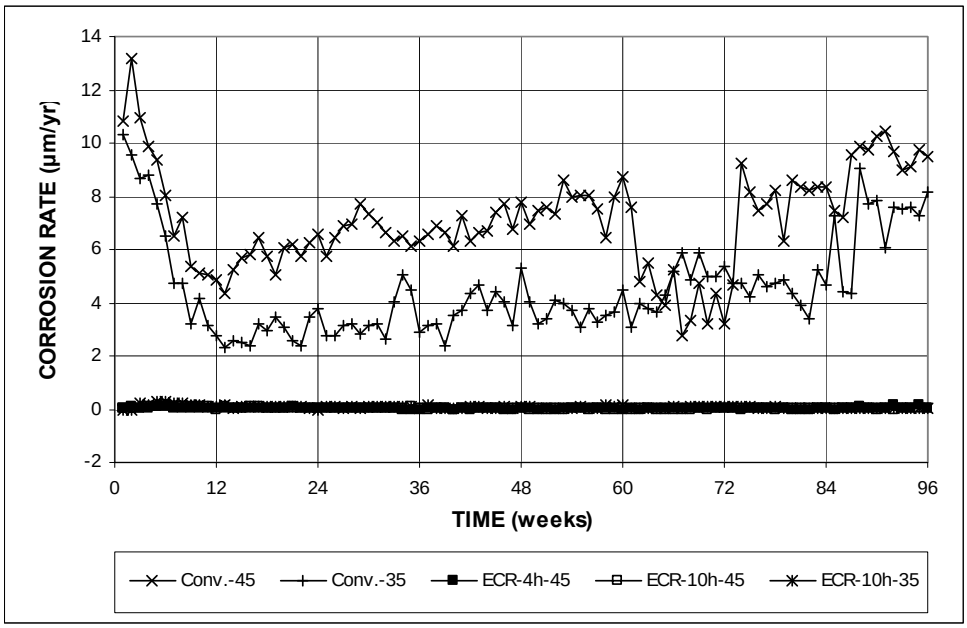

Figure 3.8 – Average corrosion rate, cracked beam test for specimens containing conventional steel and ECR with four and ten holes through the epoxy, *w/c* = 0.45 and 0.35.

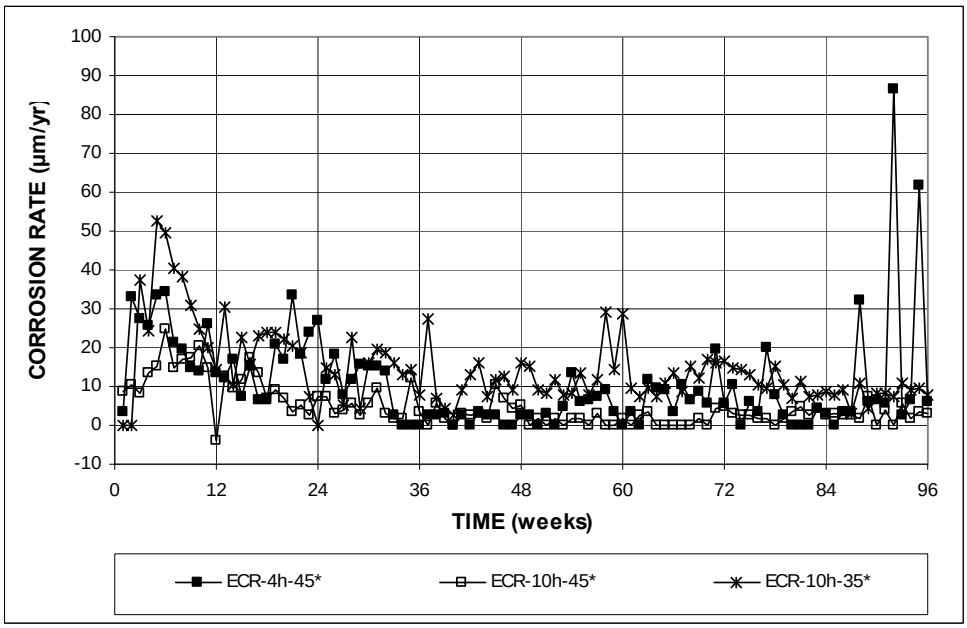

Figure 3.9 – Average corrosion rate based on exposed area, cracked beam test for specimens containing ECR with four and ten holes through the epoxy, *w/c* = 0.45 and 0.35.

The average corrosion losses based on total area for all control specimens are shown in Figure 3.10. The Conv.-45 specimens exhibit the highest corrosion losses, followed by the Conv.-35 specimens. Both are significantly higher than any system containing epoxy-coated steel tested in this study. It appears that the conventional steel was protected to some degree from corrosion by the lower *w/c* ratio, even in the presence of a crack. This may be due to the lower permeability concrete restricting the availability of oxygen to the bottom mat, thereby hindering the cathodic reduction reaction, which in turn inhibits macrocell corrosion. However, the lower permeability concrete provides no advantage for ECR specimens, as demonstrated in Figure 3.11, which shows the average corrosion losses based on exposed area for the ECR specimens. The ECR-10h-35 specimens exhibit the highest corrosion loss, followed

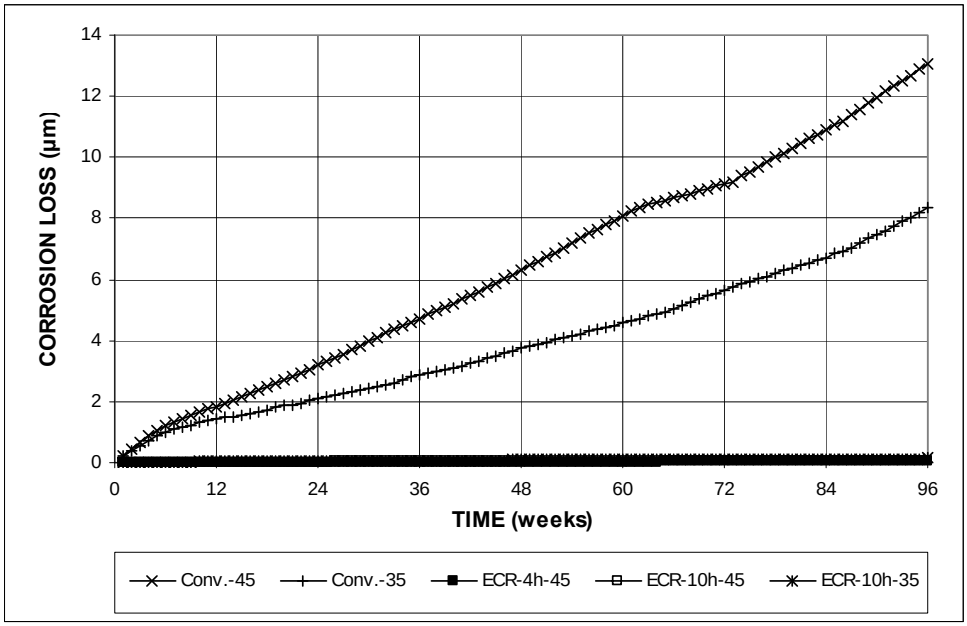

Figure 3.10 – Average corrosion loss, cracked beam test for specimens containing conventional steel and ECR with four and ten holes through the epoxy, *w/c* = 0.45 and 0.35.

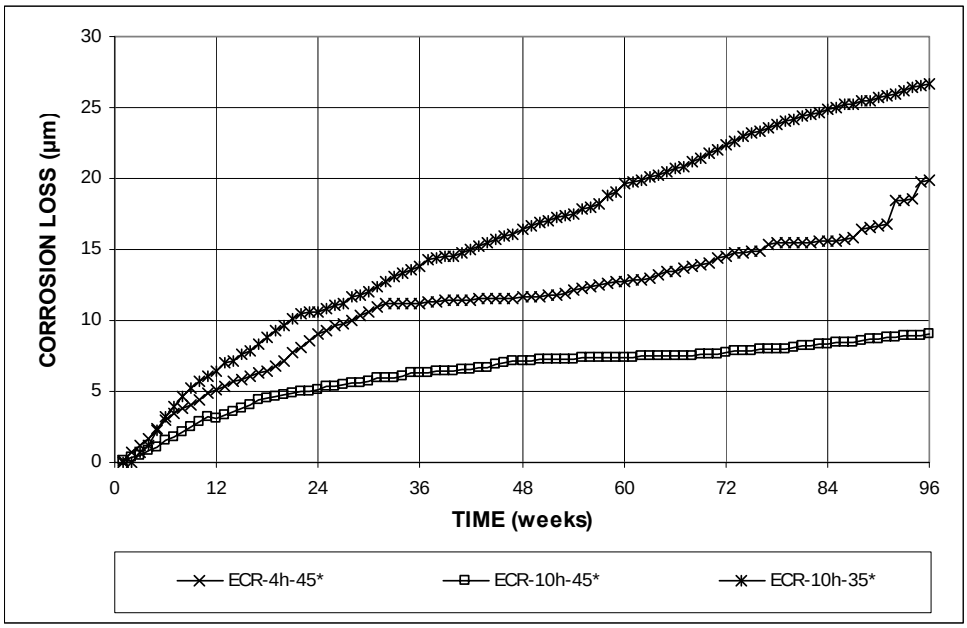

Figure 3.11 – Average corrosion loss based on exposed area, cracked beam test for specimens containing ECR with four and ten holes through the epoxy, *w/c* = 0.45 and 0.35.

by those in ECR-4h-45, and ECR-10h-45. While the Conv.-35 specimens may have benefited from the lower *w/c* ratio, it is clear from Figure 3.11 that the ECR-10h-35 specimens did not. It is worth mentioning, however, that these corrosion losses are based on very low corrosion currents acting over a small area of exposed bar. As such, the differences in corrosion losses shown for each system in Figure 3.11 may not indicate significantly different corrosion performance.

Figure 3.12 shows the average mat-to-mat resistance of the cracked beam tests containing conventional steel and ECR. The largest mat-to-mat resistance observed during the test is 19,081 ohms for the ECR-4h-45 specimens, followed by 17,532 and 14,823 ohms for the ECR-10h-45 and ECR-10h-35 specimens, respectively. The resistance observed in the specimens containing conventional steel never rose above

2000 ohms. During the first 48 weeks, the mat-to-mat resistance of all specimens increases with time, suggesting the formation of corrosion and hydration products within the concrete. After 48 weeks, the mat-to-mat resistance measured in the specimens with ECR becomes unstable, and little information can be drawn from this data. One possibility is that additional cracking in the specimen may periodically alter the resistance due to the formation of corrosion and hydration products.

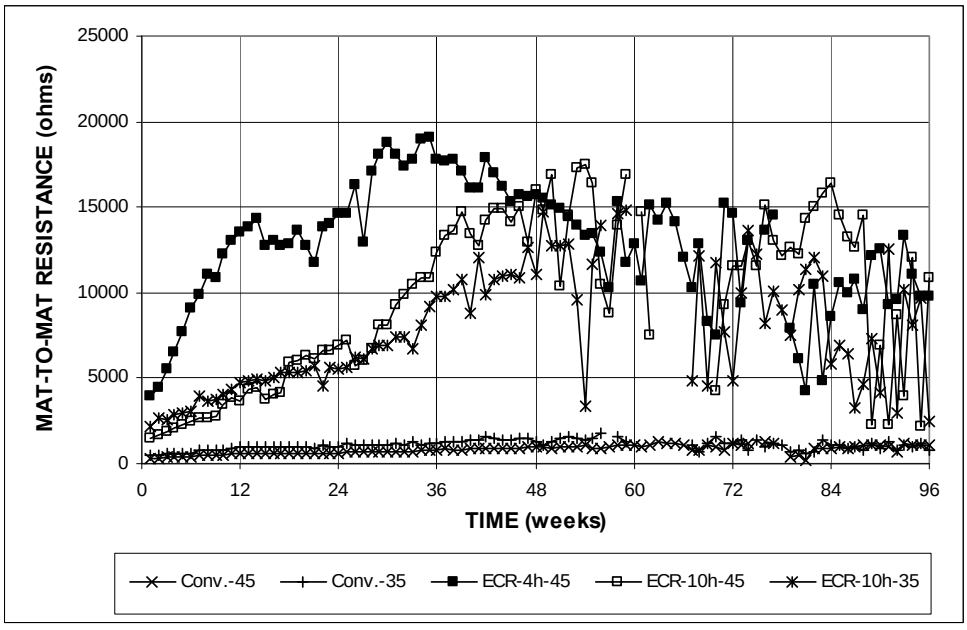

Figure 3.12 – Average mat-to-mat resistance, cracked beam test for specimens containing conventional steel and ECR with four and ten holes through the epoxy, *w/c* = 0.45 and 0.35.

The average corrosion potentials versus a copper-copper sulfate electrode (CSE) for the cracked beam specimens containing conventional steel and ECR are shown for the top and bottom mats in Figures 3.13 and 3.14, respectively. By the first week, the top mat corrosion potentials for the Conv.-45 and Conv.-35 specimens are –0.531 and –0.558 V, respectively, indicating a high probability of corrosion in the

top mats. The ECR-4h-45 specimen group is the third to show a high indication of corrosion, reaching a potential of –0.381 by week 2. The ECR-10h-35 and ECR-10h-45 specimens follow with potentials of –0.609 and –0.474 V at weeks 3 and 4, respectively. The top mat corrosion potentials for all control specimens remain more negative than –0.350 V for the remainder of the test. The corrosion potential of the bottom mat in the Conv.-45 specimens first begins showing strong indications of corrosion between week 17 and week 24. The potential of the bottom mat then remains more positive than –0.350 V until week 61. After week 61, the bottom mat remains more negative than –0.350 V for the remainder of the test. The bottom mat of the Conv.-35 specimens exhibit average potentials that indicate a high probability of corrosion during weeks 37 to 42, 64 to 66, and 88 to 93, inclusive. From weeks 91

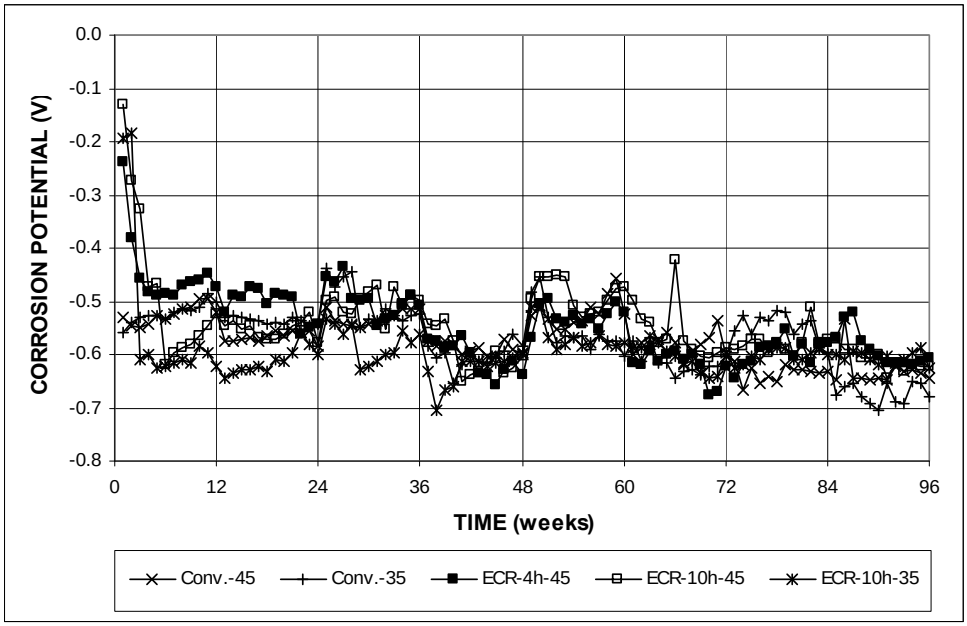

Figure 3.13 – Average top mat corrosion potential, cracked beam test for specimens containing conventional steel and ECR with four and ten holes through the epoxy, *w/c* = 0.45 and 0.35.

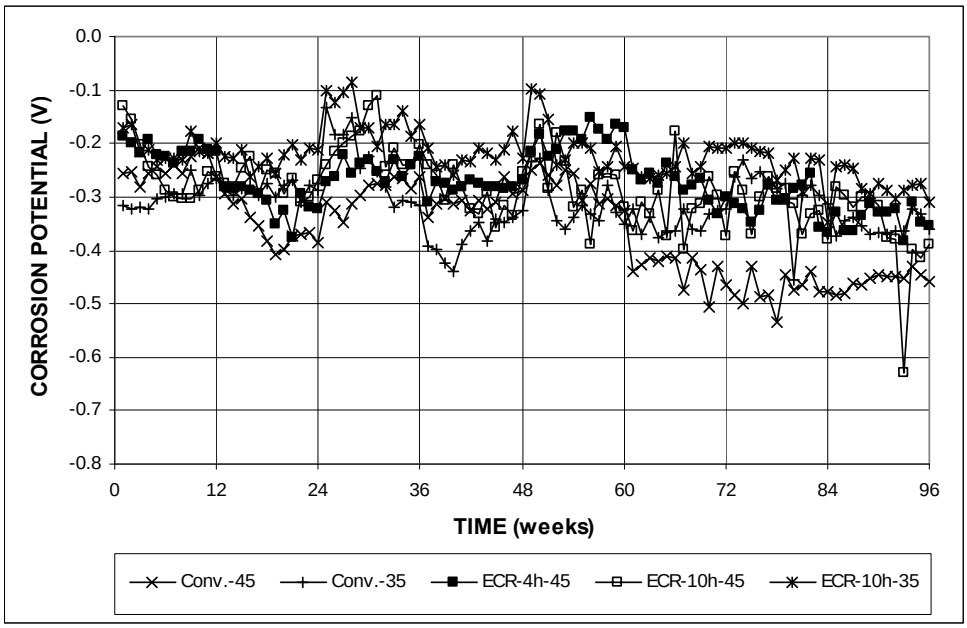

Figure 3.14 – Average bottom mat corrosion potential, cracked beam test for specimens containing conventional steel and ECR with four and ten holes through the epoxy, *w/c* = 0.45 and 0.35.

through 96, the ECR-10h-45 specimens exhibit corrosion potentials more negative than –0.350 V. The ECR-4h-45 specimens occasionally exhibit a high probability of corrosion in the bottom mat, but these occurrences are isolated, and in no case extend longer than two weeks. ECR-10h-35 is the only specimen group not to exhibit an average bottom mat potential more negative than –0.350 V during the test.

Table 3.3 summarizes the average corrosion losses in the cracked beam control specimens observed at the end of 96 weeks. The Conv.-45 specimens had the highest corrosion loss, 13.1 μm, followed by 8.34 μm for Conv.-35. Based on total area, the ECR-10h-35 specimens exhibited an average corrosion loss of 0.139 μm, the highest among the epoxy-coated specimens, followed by the ECR-10h-45 and the ECR-4h-45 specimens with losses of 0.047 and 0.041 μm, respectively. When

analyzed based on exposed area, the ECR-10h-35 specimens still exhibited the highest corrosion loss among the epoxy-coated specimens, 26.7 μm. Based on exposed area, the ECR-4h-45 specimens, with a loss of 19.9 μm, exhibited a higher loss than the ECR-10h-45 specimens, 9.04 μm.

Table 3.3 – Average corrosion loss (μm) at week 96 as measured in the cracked beam test for specimens containing conventional steel and ECR

Steel Designation[a]	Specimen						Average	Standard Deviation
	1	2	3	4	5	6		
Total Area								
Conv.-45	17.6	8.53	7.29	15.4	15.2	14.5	13.1	4.15
Conv.-35	11.5	6.02	7.51				8.34	2.82
ECR-4h-45	0.035	0.071	0.017	0.069	0.042	0.015	0.041	0.024
ECR-10h-45	0.026	0.083	0.032				0.047	0.031
ECR-10h-35	0.132	0.124	0.162				0.139	0.020
Exposed Area								
ECR-4h-45*	17.0	34.1	8.02	33.1	20.3	7.04	19.9	11.8
ECR-10h-45*	4.98	16.0	6.14				9.04	6.05
ECR-10h-35*	25.3	23.8	31.1				26.7	3.84

[a] Conv. = conventional steel. ECR = conventional epoxy-coated reinforcement.
4h = bar with four holes through epoxy, 10h = bar with 10 holes through epoxy.
45 = concrete with *w/c* =0.45; 35 = concrete with *w/c* =0.35.

* Corrosion loss calculation based on the exposed area of four or ten 3-mm (1/8-in.) diamter holes.

3.2 Corrosion Inhibitors

This section presents the results of the Southern Exposure and cracked beam tests for specimens containing ECR and corrosion inhibitors. Three admixed corrosion inhibitors, DCI (calcium nitrite), Rheocrete, and Hycrete, are evaluated, in addition to an epoxy-coated reinforcement with a primer containing microencapsulated calcium nitrite between the epoxy and the steel. The corrosion inhibitors are evaluated with ECR containing four and ten holes through the epoxy cast in concrete with *w/c* = 0.45 and with ECR containing ten holes through the epoxy

cast in concrete with *w/c* = 0.35. Each system is evaluated using three Southern Exposure and three cracked beam specimens, and the results are compared with those for conventional steel and conventional epoxy-coated reinforcement described in Section 3.1.

3.2.1 Southern Exposure Test

Figures 3.15 and 3.16 show the average corrosion rates based on total and exposed area, respectively, for specimens cast using concrete with *w/c* = 0.45 and bars with four holes through the epoxy layer. Figure 3.15(a) compares the high corrosion rate based on total area for conventional steel reinforcement with the corrosion rates of the specimens containing epoxy-coated reinforcement. As shown in Figures 3.15(b) and 3.16, the conventional ECR-4h-45 specimens exhibit the highest corrosion rates among ECR specimens between weeks 10 and 31. At week 45, the specimens with the calcium nitrite primer, ECR(primer/Ca(NO2)2)-4h-45, begin to show average corrosion rates that are noticeably higher than the other ECR specimens. As shown in Figure A.57(a), this increase is observed in one of the three specimens. Between weeks 68 and 96, an increase in the average corrosion rate is again observed in ECR(primer/Ca(NO2)2)-4h-45 specimens, with values between 0.008 and 0.039 μm/yr based on total area and between 3.66 and 18.9 μm/yr based on exposed area. As shown in Figure A.57(a), this increase in corrosion activity is observed in one specimen from weeks 68-86 and in two specimens from weeks 86-96. From weeks 74 to 96, with the exclusion of week 88, the Rheocrete specimens, ECR(RH)-4h-45, also exhibit a noticeable increase in corrosion activity, with an

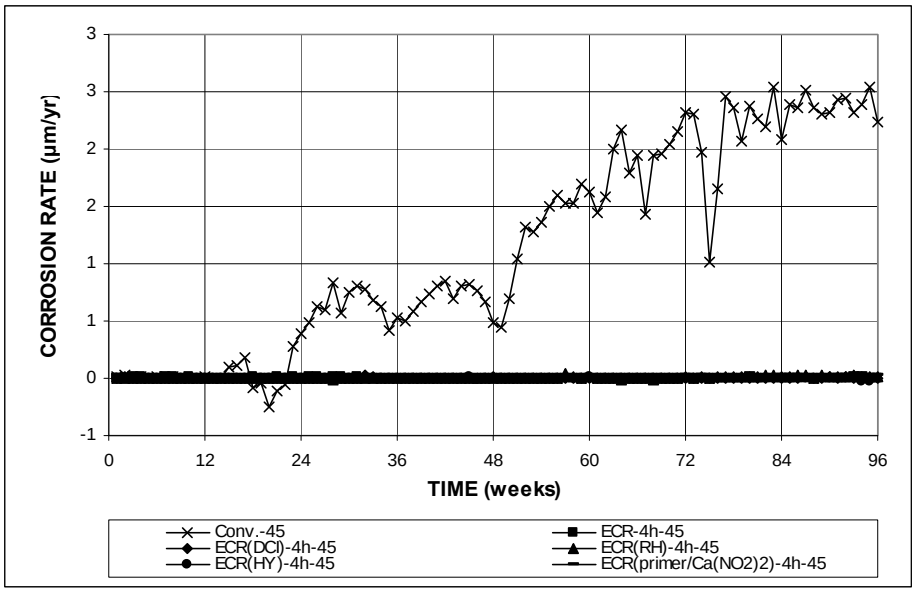

Figure 3.15 (a) – Average corrosion rate, Southern Exposure test for specimens containing conventional steel, ECR, ECR in concrete with corrosion inhibitors, and ECR with a calcium nitrite primer, *w/c* = 0.45. Bars with four holes in epoxy coating.

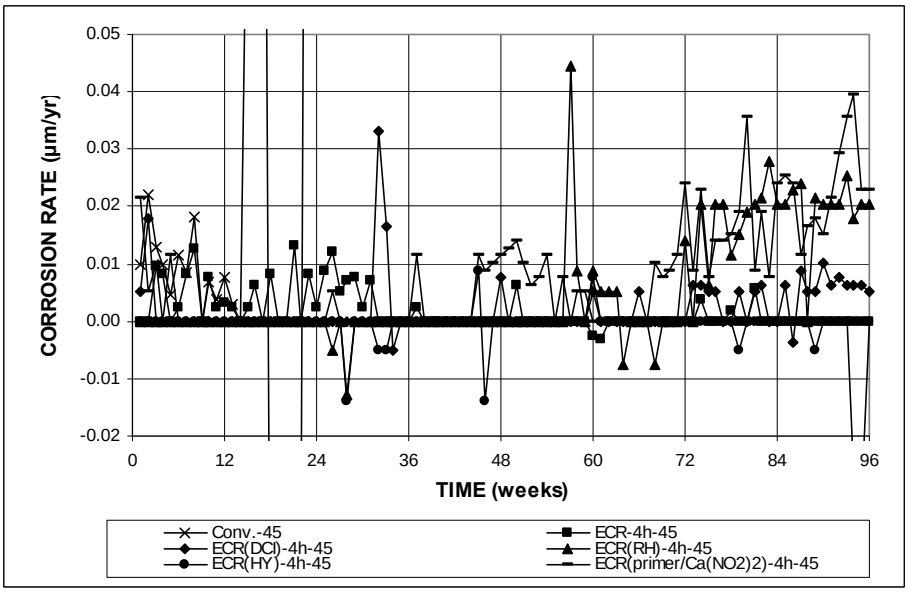

Figure 3.15 (b) – Average corrosion rate, Southern Exposure test for specimens containing conventional steel, ECR, ECR in concrete with corrosion inhibitors, and ECR with a calcium nitrite primer, *w/c* = 0.45. Bars with four holes in epoxy coating. (Different scale)

average corrosion rate ranging between 0.006 and 0.028 μm/yr based on total area and between 3.05 and 13.4 μm/yr based on exposed area. As shown in Figure A.33(a), this corrosion activity is only observed in one specimen, SE-ECR(RH)-4h-45-2. The specimens containing DCI corrosion inhibitor, SE-ECR(DCI)-4h-45, begin exhibiting corrosion at week 72, and continue to corrode for the remainder of the test. No significant corrosion is observed in the specimens containing Hycrete (SE-ECR(HY)-4h-45).

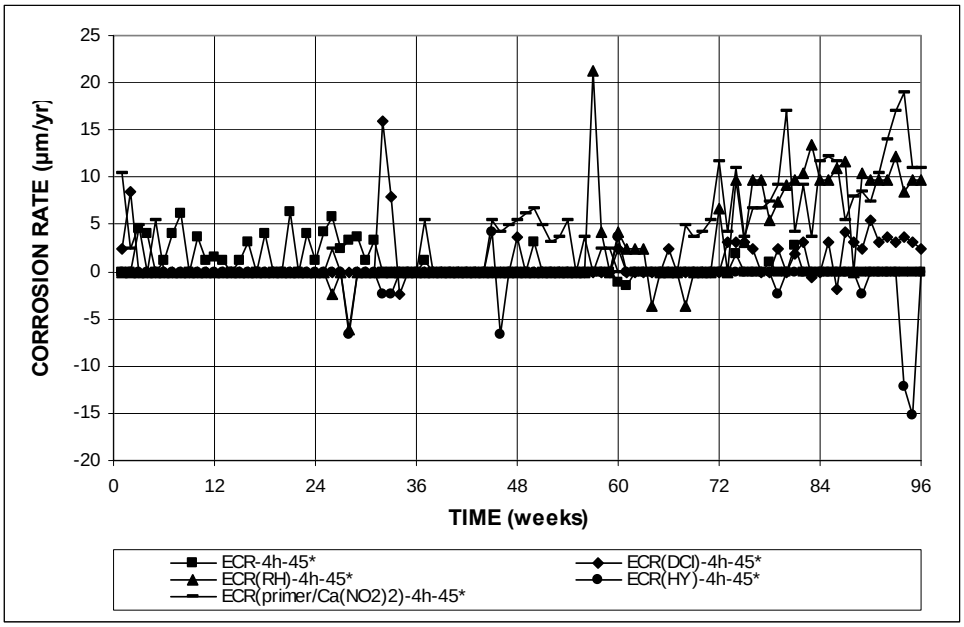

Figure 3.16 – Average corrosion rate based on exposed area, Southern Exposure test for specimens containing ECR, ECR in concrete with corrosion inhibitors, and ECR with a calcium nitrite primer, *w/c* = 0.45. Bars with four holes in epoxy coating.

Figures 3.17 and 3.18 show the average corrosion rates of the Southern Exposure specimens with ECR containing ten holes through the epoxy cast in concrete with *w/*c = 0.45 and corrosion inhibitors. Figure 3.17(a) compares the high corrosion rates based on total area for specimens containing conventional steel

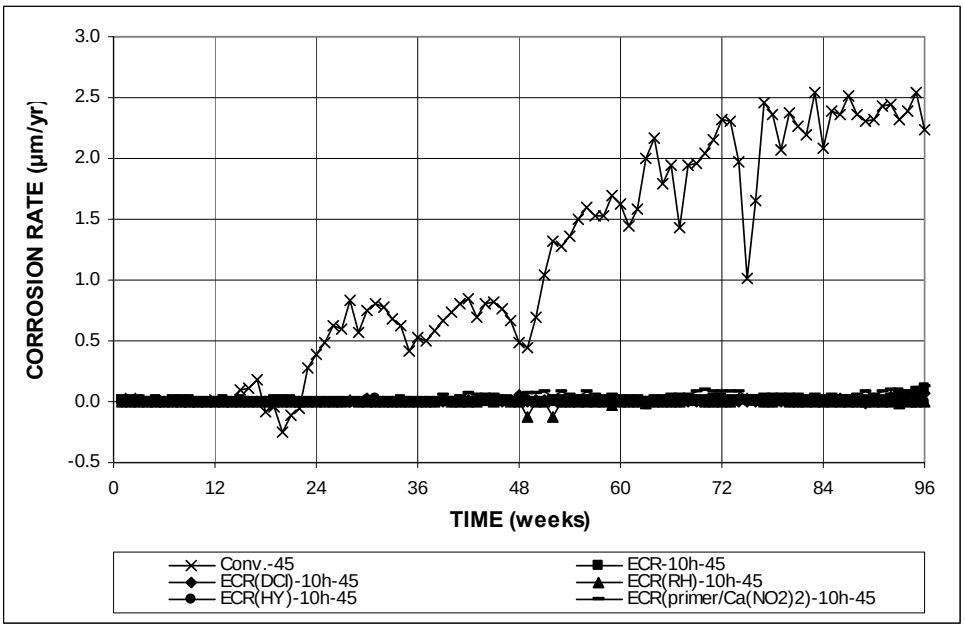

Figure 3.17 (a) – Average corrosion rate, Southern Exposure test for specimens containing conventional steel, ECR, ECR in concrete with corrosion inhibitors, and ECR with a calcium nitrite primer, *w/c* = 0.45. Bars with ten holes in epoxy coating.

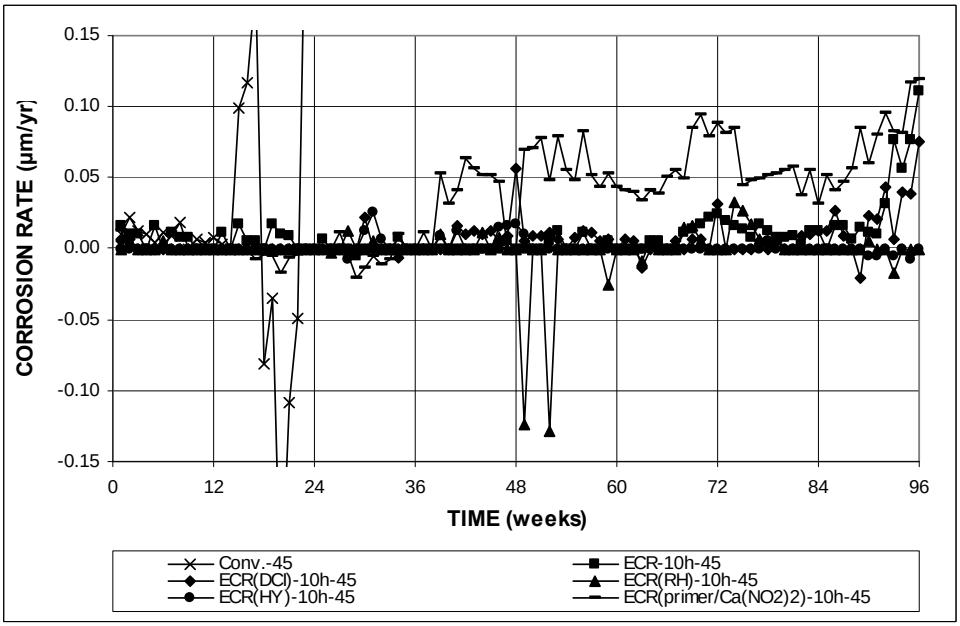

Figure 3.17 (b) – Average corrosion rate, Southern Exposure test for specimens containing conventional steel, ECR, ECR in concrete with corrosion inhibitors, and ECR with a calcium nitrite primer, *w/c* = 0.45. Bars with ten holes in epoxy coating. (Different scale)

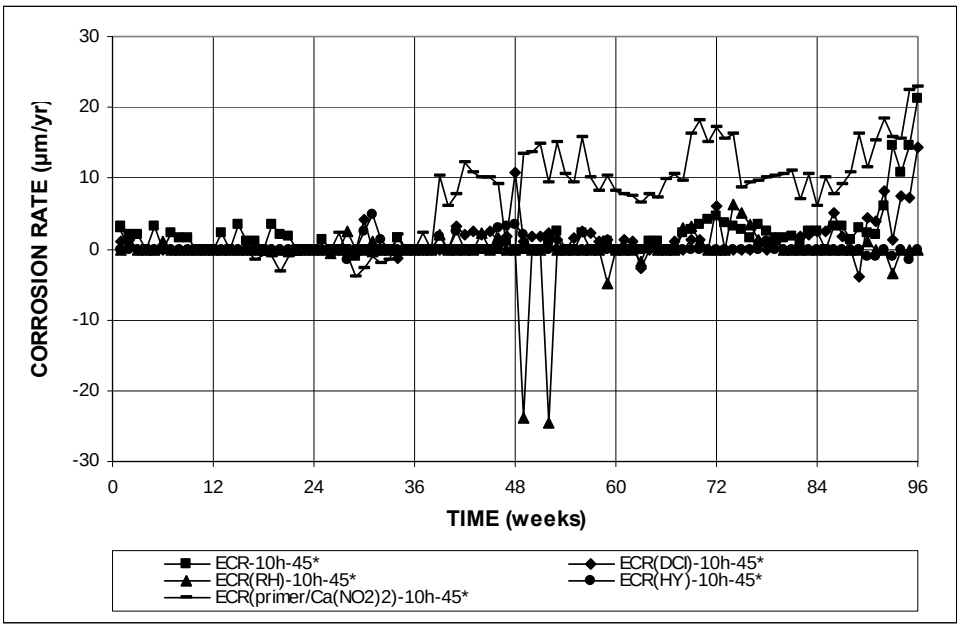

Figure 3.18 – Average corrosion rate based on exposed area, Southern Exposure test for specimens containing ECR, ECR in concrete with corrosion inhibitors, and ECR with a calcium nitrite primer, *w/c* = 0.45. Bars with ten holes in epoxy coating.

reinforcement with the low corrosion rates of specimens containing epoxy-coated reinforcement. As shown in Figures 3.17(b) and 3.18, the ECR(primer/Ca(NO2)2)-10h-45 specimens exhibit significant corrosion activity beginning at week 39 and continuing until the end of the test. During this period, the average corrosion rate ranges between 0.032 to 0.119 µm/yr based on total area and from 6.10 to 22.9 µm/yr based on exposed area, except for weeks 47 and 48, during which no corrosion is detected. As shown in Figure A.61(b), this increase of corrosion activity is observed in one specimen at week 39, in two specimens by week 51, and in all three specimens by week 69. A comparison between the ECR(primer/Ca(NO2)2) specimens with four and ten holes through the epoxy in concrete with *w/c* = 0.45 shows that corrosion

initiated sooner in specimens with 10 holes through the epoxy (week 39) than in specimens with four holes through the epoxy (week 45).

At week 92, one other specimen group, ECR(DCI)-10h-45, along with the ECR control group, exhibited increased corrosion rates, with a final average corrosion rate at 96 weeks of 0.075 and 14.4 μm/yr based on total and exposed area, respectively. Figure A.25(b) shows that this increase in corrosion rate was observed in two out of the three ECR(DCI)-10h-45 specimens. The ECR(RH)-10h-45 specimens show large negative average corrosion rates at weeks 49 and 52. As shown in Figure A.37(a), these negative corrosion rates correspond to a negative corrosion rate observed in one specimen, ECR(RH)-10h-45-2, at week 49 and in all three specimens at week 52. The large negative corrosion rate in specimen ECR(RH)-10h-45-2 is accompanied by a highly negative bottom mat potential, indicating that the bottom mat is actually corroding during this week. However, the negative corrosion rates observed at week 52 are not accompanied by highly negative corrosion potentials, and are, therefore, probably due to an aberrant reading. For the remaining portions of the test, the ECR(RH)-10h-45 and ECR(HY)-10h-45 specimens exhibit no significant corrosion.

Figures 3.19 and 3.20 show the average corrosion rates for Southern Exposure specimens with ECR bars containing ten holes through the epoxy cast in concrete with *w/c* = 0.35 and corrosion inhibitors. Figure 3.19(a) compares the high corrosion rates for the specimens containing conventional steel reinforcement with the low corrosion rates of the specimens containing epoxy-coated reinforcement. Figures

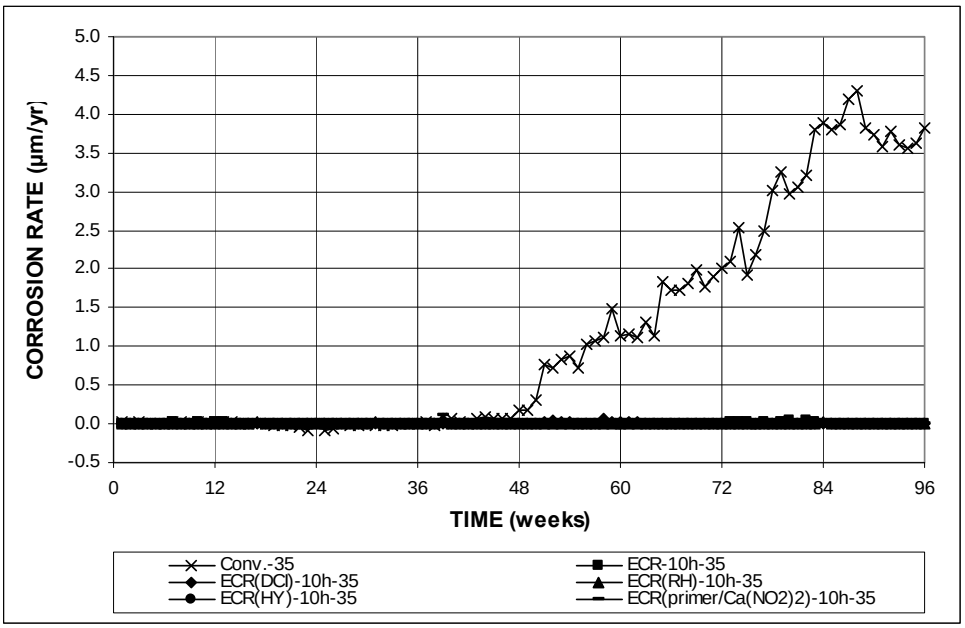

Figure 3.19 (a) – Average corrosion rate, Southern Exposure test for specimens containing conventional steel, ECR, ECR in concrete with corrosion inhibitors, and ECR with a calcium nitrite primer, *w/c* = 0.35. Bars with ten holes in epoxy coating.

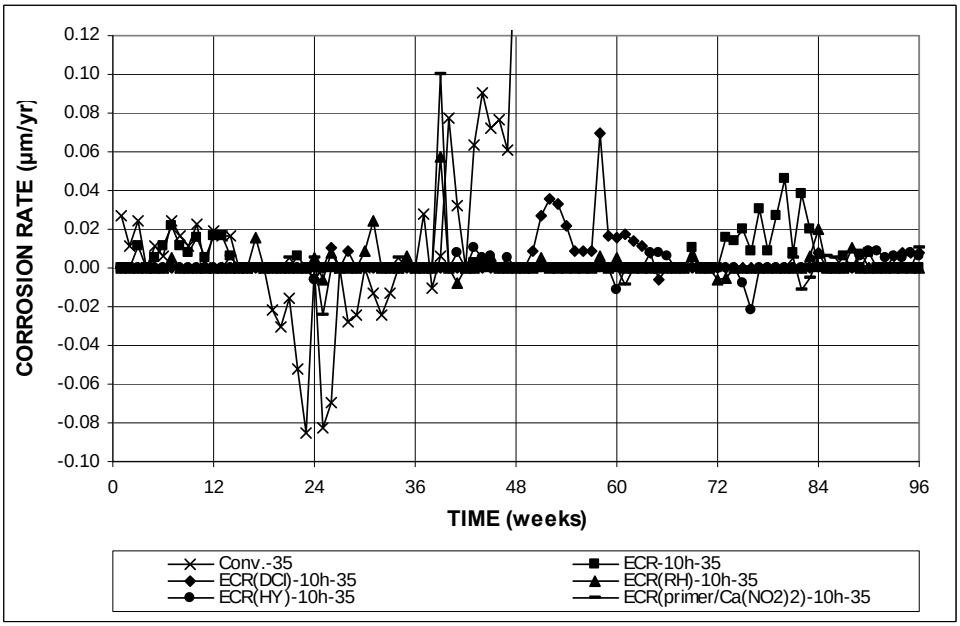

Figure 3.19 (b) – Average corrosion rate, Southern Exposure test for specimens containing conventional steel, ECR, ECR in concrete with corrosion inhibitors, and ECR with a calcium nitrite primer, *w/c* = 0.35. Bars with ten holes in epoxy coating. (Different scale)

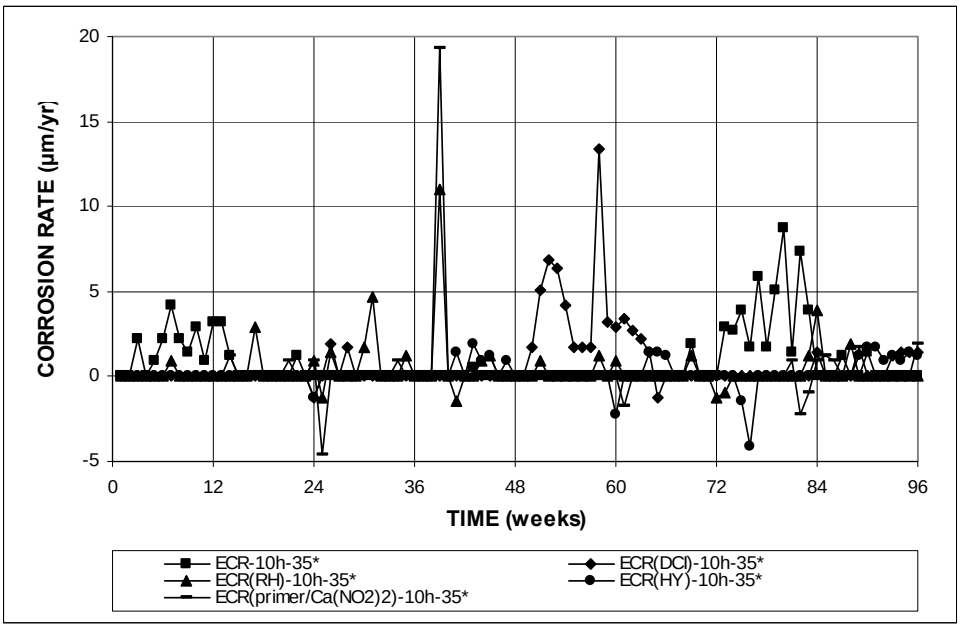

Figure 3.20 – Average corrosion rate based on exposed area, Southern Exposure test for specimens containing ECR, ECR in concrete with corrosion inhibitors, and ECR with a calcium nitrite primer, *w/c* = 0.35. Bars with ten holes in epoxy coating.

3.19(b) and 3.20 show that the ECR(DCI)-10h-35 specimens exhibit slightly elevated average corrosion rates between weeks 50 and 64. During this period, the highest average corrosion rate observed in these specimens is 0.070 and 13.4 µm/yr based on total and exposed area, respectively, at week 58. As shown in Figure A.29(a), this increase in the average corrosion rate is caused by an increase in the corrosion rate in one specimen at any given time (specimen 1 shows increased corrosion rates between weeks 50 and 58, while specimen 3 shows increased corrosion rates between weeks 58 and 64). The ECR(RH)-10h-35 and ECR(primer/Ca(NO2)2)-10h-35 specimens show high average corrosion rates at week 39. This increase occurs in two out of the three ECR(RH)-10h-35 specimens and in all three of the ECR(primer/Ca(NO2)2)-10h-35 specimens. In all likelihood, these high corrosion rates are due to aberrant

readings. The ECR(HY)-10h-35 specimens begin exhibiting corrosion beginning at week 89, which continues for the remainder of the test.

Figures 3.21 and 3.22 show the average corrosion loss of the Southern Exposure specimens containing ECR with four holes through the epoxy cast with corrosion inhibitors in the concrete, along with the losses for the control specimens, based on total and exposed area, respectively. As shown in Figure 3.21, the conventional steel specimens exhibit a higher corrosion loss than any of the ECR specimens cast in concrete with corrosion inhibitors. Figure 3.22 shows that two of the systems have undergone corrosion initiation, ECR(primer/Ca(NO2)2)-4h-45 and ECR(RH)-4h-45. As previously observed, the ECR(primer/Ca(NO2)2)-4h-45 specimens begin corroding at week 45, and, by week 60, appear to passivate,

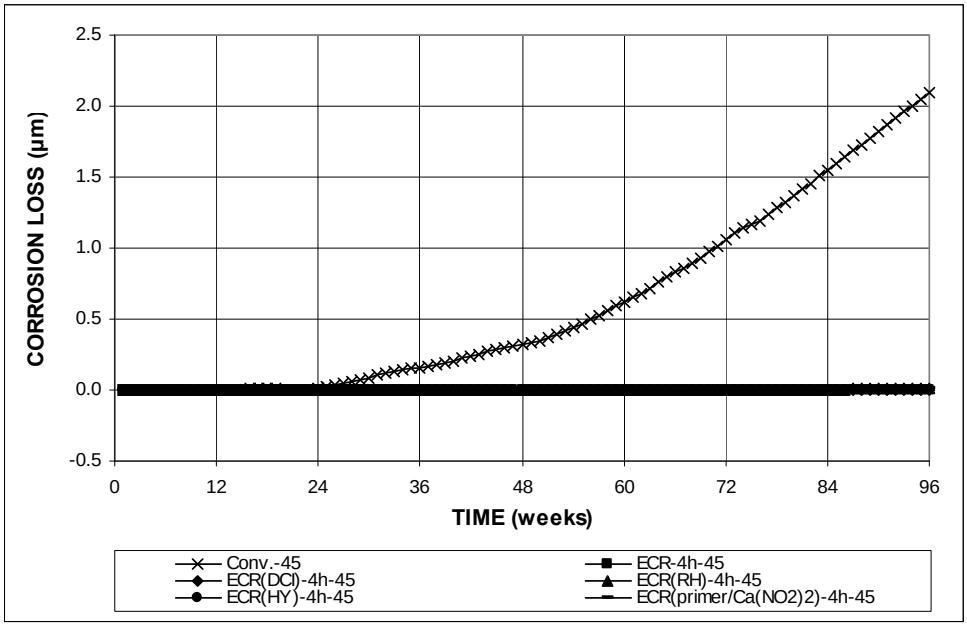

Figure 3.21 – Average corrosion loss, Southern Exposure test for specimens containing conventional steel, ECR, ECR in concrete with corrosion inhibitors, and ECR with a calcium nitrite primer, *w/c* = 0.45. Bars with four holes in epoxy coating.

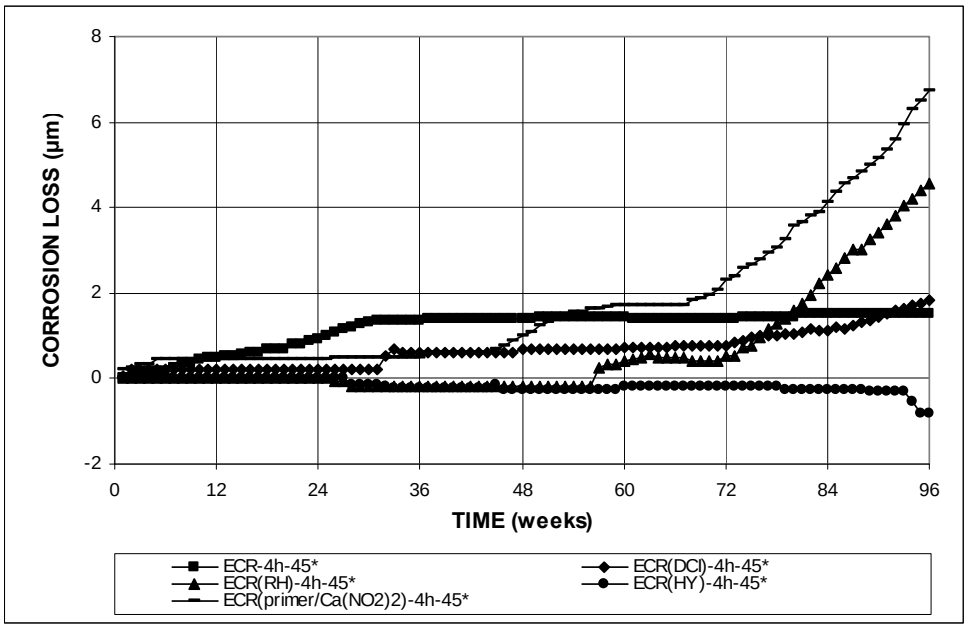

Figure 3.22 – Average corrosion loss based on exposed area, Southern Exposure test for specimens containing ECR, ECR in concrete with corrosion inhibitors, and ECR with a calcium nitrite primer, *w/c* = 0.45. Bars with four holes in epoxy coating.

followed by another period of active corrosion between weeks 68 and 96. The ECR(RH)-4h-45 specimens begin showing increasing corrosion losses beginning at week 74, and continue to exhibit nearly steady-state corrosion for the remainder of the test. The remaining specimens, ECR-(DCI)-4h-45 and ECR(HY)-4h-45, show little significant corrosion activity.

Figures 3.23 and 3.24 show the average corrosion losses of Southern Exposure specimens with ECR containing 10 holes through the epoxy cast in concrete with *w*/c = 0.45 and corrosion inhibitors, based on total and exposed area, respectively. As shown in Figure 3.23 and observed in earlier comparisons, conventional steel exhibits higher corrosion losses than all of the ECR specimens. Figure 3.24 shows that the ECR(primer/Ca(NO2)2)-10h-45 specimens exhibit the

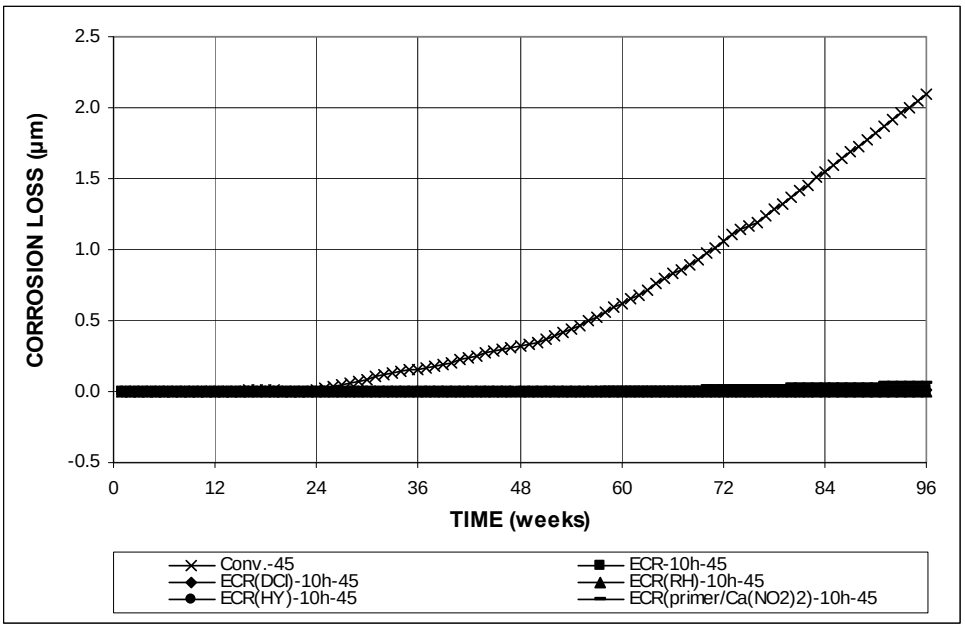

Figure 3.23 – Average corrosion loss, Southern Exposure test for specimens containing conventional steel, ECR, ECR in concrete with corrosion inhibitors, and ECR with a calcium nitrite primer, *w/c* = 0.45. Bars with ten holes in epoxy coating.

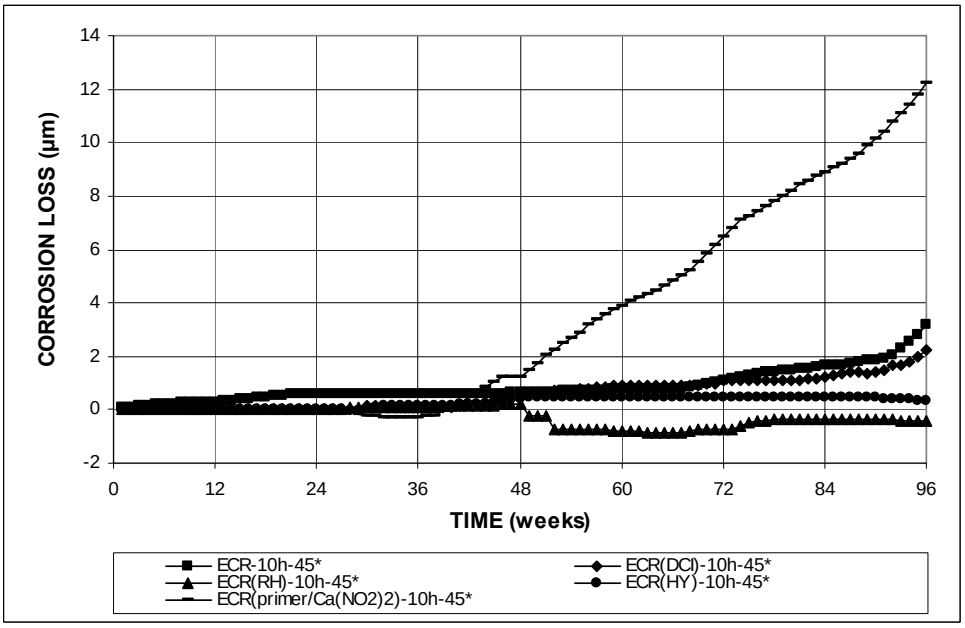

Figure 3.24 – Average corrosion loss based on exposed area, Southern Exposure test for specimens containing ECR, ECR in concrete with corrosion inhibitors, and ECR with a calcium nitrite primer, *w/c* = 0.45. Bars with ten holes in epoxy coating.

highest corrosion losses among the ECR specimens beginning at week 43 and continuing for the remainder of the test. As mentioned previously, corrosion initiation occurred in one ECR(primer/Ca(NO2)2)-10h-45 specimen at week 39, followed by initiation in the other two specimens at weeks 51 and 69 [Figure A.61(b)]. All other ECR specimens with corrosion inhibitors [ECR(RH)-10h-45, ECR(DCI)-10h-45, and ECR(HY)-10h-45] exhibit lower average corrosion losses than the control ECR specimens for the duration of the test. From week 49 to the end of the test, the ECR(RH)-10h-45 specimens have a negative average corrosion loss. These losses are due to the large negative corrosion rates measured at weeks 49 and 52. As mentioned previously, the large negative corrosion loss observed at week 52 is probably due to an aberrant reading. Therefore, the negative average corrosion loss exhibited by the ECR(RH)-10h-45 specimens is insignificant.

Figures 3.25 and 3.26 show the average corrosion losses based on total and exposed area, respectively, of the Southern Exposure specimens with ECR containing 10 holes through the epoxy cast in concrete with *w*/c = 0.35 and corrosion inhibitors. As shown in Figure 3.25, conventional steel specimens exhibit higher corrosion losses than all of the ECR specimens. During the first 53 weeks, all ECR specimens with corrosion inhibitors exhibit lower average corrosion losses than the ECR control specimens. At week 54, the average corrosion loss observed in the ECR(DCI)-10h-35 specimens surpasses the loss observed in the ECR control specimens. By week 64, ECR(DCI)-10h-35 specimens appear to passivate, and at week 80, the ECR control specimens again exhibit the highest corrosion losses among the ECR specimens. The

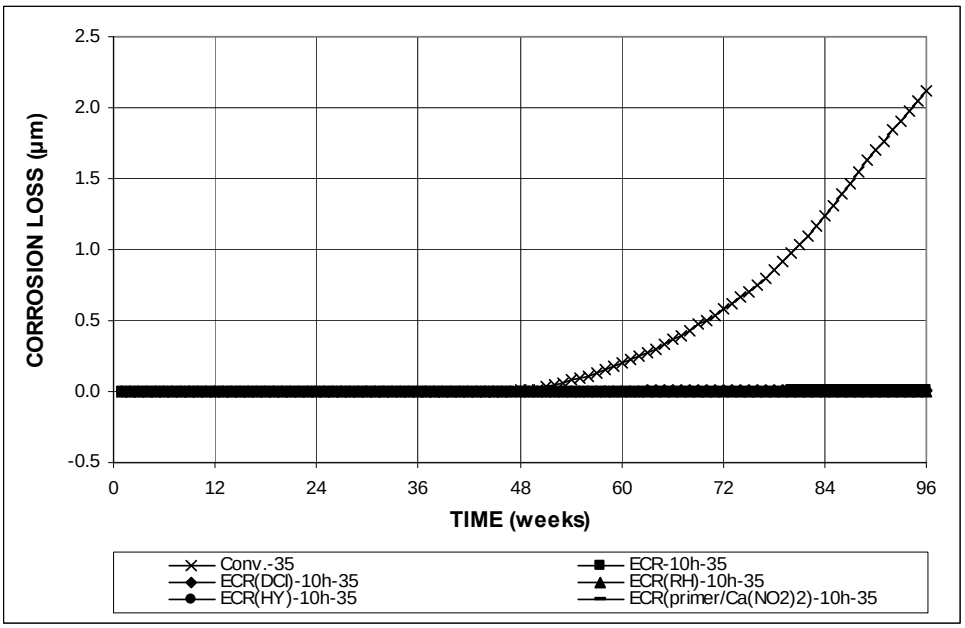

Figure 3.25 – Average corrosion loss, Southern Exposure test for specimens containing conventional steel, ECR, ECR in concrete with corrosion inhibitors, and ECR with a calcium nitrite primer, *w/c* = 0.35. Bars with ten holes in epoxy coating.

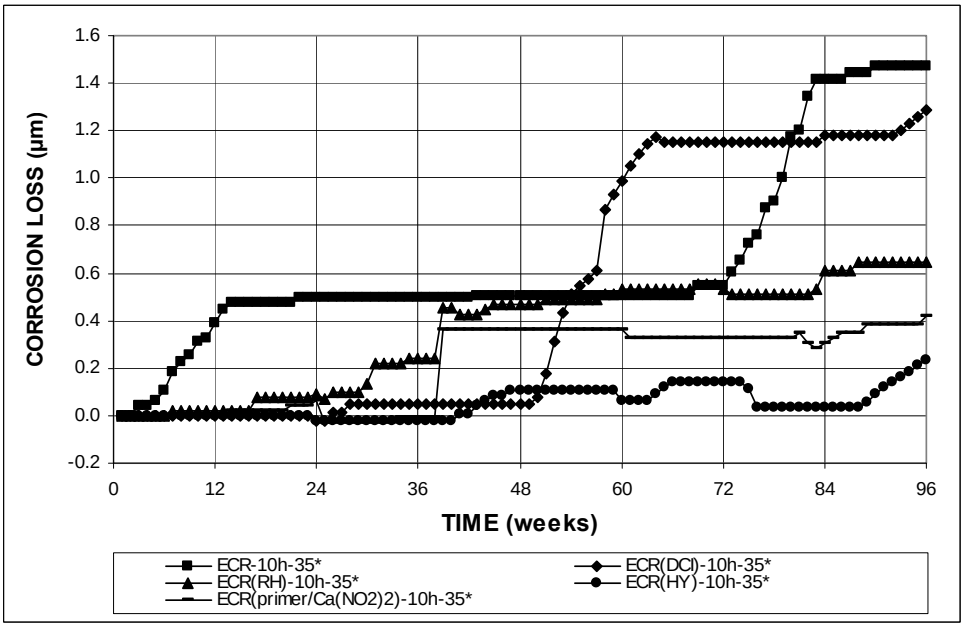

Figure 3.26 – Average corrosion loss based on exposed area, Southern Exposure test for specimens containing ECR, ECR in concrete with corrosion inhibitors, and ECR with a calcium nitrite primer, *w/c* = 0.35. Bars with ten holes in epoxy coating.

remaining ECR specimens do not exhibit average corrosion losses above 0.7 μm based on exposed area.

Table 3.4 summarizes the total average corrosion losses at 96 weeks for Southern Exposure ECR specimens cast in concrete with corrosion inhibitors. Based on total area, the ECR(primer/Ca(NO2)2)-10h-45 and ECR(primer/Ca(NO2)2)-4h-45 specimens exhibit the highest corrosion losses among the ECR specimens shown in the table, with values of 0.064 and 0.014 μm, respectively. The ECR(DCI)-10h-45 specimens exhibit an average total corrosion loss of 0.012 μm. All other specimens exhibit total corrosion loss based on total area of 0.010 μm or less. Based on exposed area, the ECR(primer/Ca(NO2)2)-10h-45 and ECR(primer/Ca(NO2)2)-4h-45 specimens exhibit the highest corrosion losses among the ECR specimens, with values of 12.3 and 6.72 μm, respectively. Rheocrete specimens with four holes through the epoxy exhibit the third highest corrosion loss, 4.58 μm, but this is due to corrosion observed in only one of three specimens. DCI specimens with four and ten holes through the epoxy in concrete with *w/c* = 0.45 have corrosion losses based on the exposed area of 2.23 and 1.82 μm, respectively. The ECR(DCI)-10h-35 specimens exhibit a total average corrosion loss of 1.29 μm, based on exposed area. All other specimens show corrosion losses less than 1 μm based on exposed area. As previously mentioned, the negative corrosion losses are due to the numerical integration of negative corrosion rate measurements, which indicate electrons flowing from the bottom mat to the top mat. In this case, negative corrosion losses can be considered as “no significant corrosion activity occurring” in the specimen.

Table 3.4 – Average corrosion loss (μm) at week 96 as measured in the Southern Exposure test for specimens containing ECR in concrete with corrosion inhibitors and ECR with a calcium nitrite primer

Steel Designation[a]	Specimen			Average	Standard Deviation
	1	2	3		
Total Area					
ECR(DCI)-4h-45	0.002	0.008	0.002	0.004	0.003
ECR(DCI)-10h-45	-0.002	0.020	0.016	0.012	0.012
ECR(DCI)-10h-35	0.012	0.001	0.008	0.007	0.006
ECR(RH)-4h-45	0.000	0.030	-0.002	0.010	0.018
ECR(RH)-10h-45	0.001	-0.009	-0.001	-0.003	0.005
ECR(RH)-10h-35	0.002	0.005	0.003	0.003	0.001
ECR(HY)-4h-45	-0.001	-0.002	-0.002	-0.002	0.001
ECR(HY)-10h-45	0.003	-0.001	0.003	0.002	0.003
ECR(HY)-10h-35	0.006	-0.002	-0.001	0.001	0.004
ECR(primer/$Ca(NO_2)_2$)-4h-45	0.005	0.012	0.026	0.014	0.011
ECR(primer/$Ca(NO_2)_2$)-10h-45	0.031	0.137	0.022	0.064	0.064
ECR(primer/$Ca(NO_2)_2$)-10h-35	0.003	0.002	0.001	0.002	0.001
Exposed Area					
ECR(DCI)-4h-45*	0.985	3.62	0.845	1.82	1.57
ECR(DCI)-10h-45*	-0.366	3.90	3.17	2.23	2.28
ECR(DCI)-10h-35*	2.25	0.113	1.49	1.29	1.08
ECR(RH)-4h-45*	0.000	14.5	-0.739	4.58	8.57
ECR(RH)-10h-45*	0.267	-2.08	0.633	-0.394	1.47
ECR(RH)-10h-35*	0.479	0.943	0.521	0.648	0.257
ECR(HY)-4h-45*	-0.387	-0.950	-1.13	-0.821	0.386
ECR(HY)-10h-45*	0.648	-0.197	0.662	0.371	0.492
ECR(HY)-10h-35*	1.17	-0.296	-0.169	0.235	0.811
ECR(primer/$Ca(NO_2)_2$)-4h-45*	2.18	5.63	12.4	6.72	5.17
ECR(primer/$Ca(NO_2)_2$)-10h-45*	6.02	26.4	4.32	12.3	12.3
ECR(primer/$Ca(NO_2)_2$)-10h-35*	0.605	0.479	0.169	0.418	0.224

[a] ECR(DCI) = ECR in concrete with DCI inhibitor.
ECR(Rheocrete) = ECR in concrete with Rheocrete inhibitor.
ECR (Hycrete) = normal ECR with Hycrete inhibitor.
4h = bar with four holes through epoxy, 10h = bar with 10 holes through epoxy.
45 = concrete with *w/c* =0.45; 35 = concrete with *w/c* =0.35.

* Corrosion loss calculation based on the exposed area of four or ten 3-mm (1/8-in.) diamter holes.

Figures 3.27 and 3.28 show the average mat-to-mat resistances for ECR specimens containing four and ten holes through the epoxy in concrete with *w/c* = 0.45, respectively. Figure 3.29 shows the average mat-to-mat resistance for ECR specimens with ten holes through the epoxy in concrete with *w/c* = 0.35. As shown in

all three figures, the mat-to-mat resistances in all specimens generally increase with time for the first 48 weeks of the test. During the first 48 weeks, specimens with ten holes through the epoxy generally show lower resistances than specimens with four holes through the epoxy. The greater area of exposed steel in the ten-hole specimens causes their resistance to be lower than that of four-hole specimens. Specimens with ten holes through the epoxy in concrete with *w/c* = 0.35 show the lowest resistances among the ECR specimens. All ECR specimens have higher mat-to-mat resistances than the conventional steel control specimens. As previously mentioned, this is due to the epoxy coating, which limits the access of the electrolyte to the surface of the bar. After week 48, the mat-to-mat resistances become increasingly sporadic, and no conclusions can be made from this data.

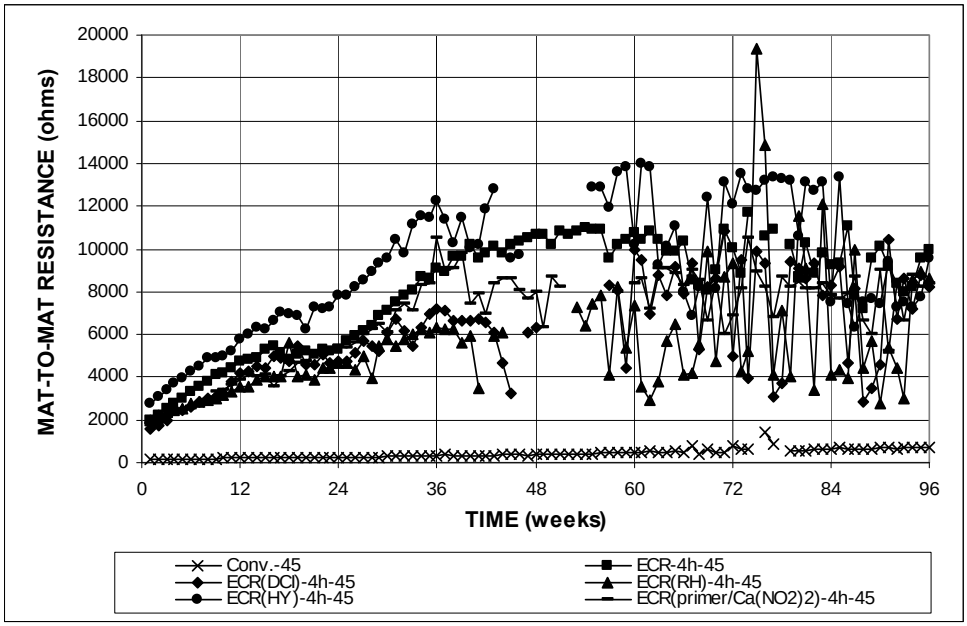

Figure 3.27 – Average mat-to-mat resistance, Southern Exposure test for specimens containing conventional steel, ECR, ECR in concrete with corrosion inhibitors, and ECR with a calcium nitrite primer, *w/c* = 0.45. Bars with four holes in epoxy coating.

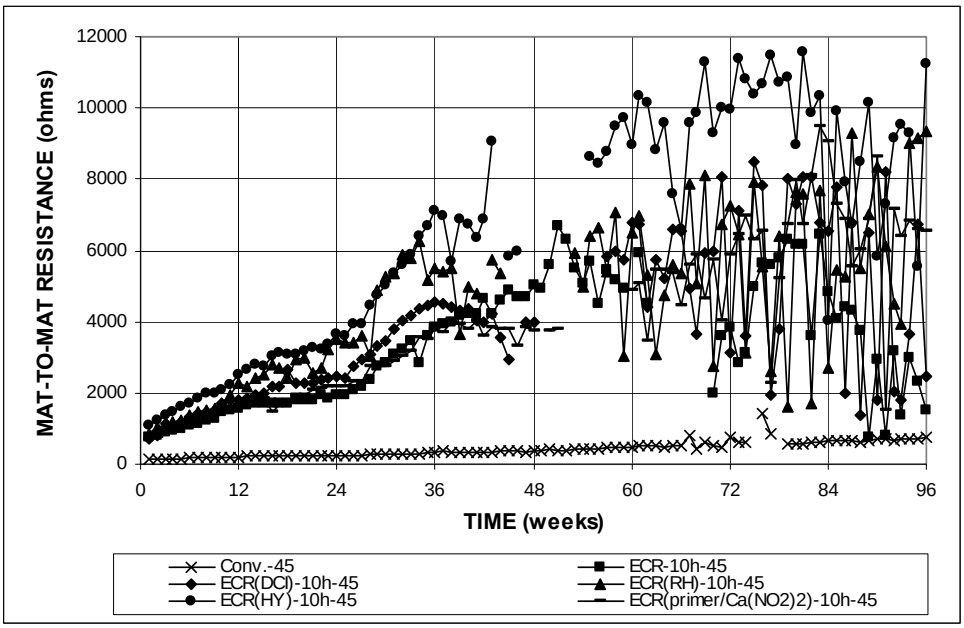

Figure 3.28 – Average mat-to-mat resistance, Southern Exposure test for specimens containing conventional steel, ECR, ECR in concrete with corrosion inhibitors, and ECR with a calcium nitrite primer, *w/c* = 0.45. Bars with ten holes in epoxy coating.

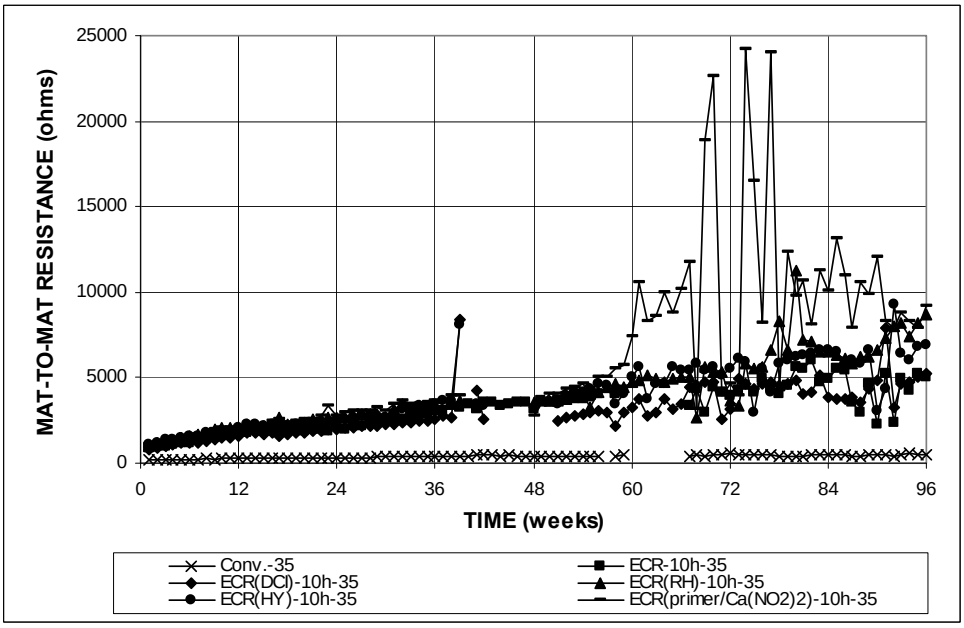

Figure 3.29 – Average mat-to-mat resistance, Southern Exposure test for specimens containing conventional steel, ECR, ECR in concrete with corrosion inhibitors, and ECR with a calcium nitrite primer, *w/c* = 0.35. Bars with ten holes in epoxy coating.

Figures 3.30 through 3.32 show the average top and bottom mat corrosion potentials with respect to a copper-copper sulfate electrode. Active corrosion is indicated by corrosion potentials that are more negative than –0.350 V. As shown in Figure 3.30(a), the top mat in the conventional steel specimens begins corroding at week 38, earlier than any of the ECR specimens with four holes through the epoxy. The first epoxy-coated specimens to show indications of corrosion in the top mat are the ECR(primer/Ca(NO2)2)-4h-45 specimens, at week 45, continuing to indicate corrosion until week 53, after which the top mat appears to passivate. After week 67, the top mats in the ECR(primer/Ca(NO2)2)-4h-45 specimens again exhibit active corrosion and continue to corrode for the remainder of the test. The ECR(DCI)-4h-45 specimens have top mat potentials that indicate active corrosion at weeks 60 and 61,

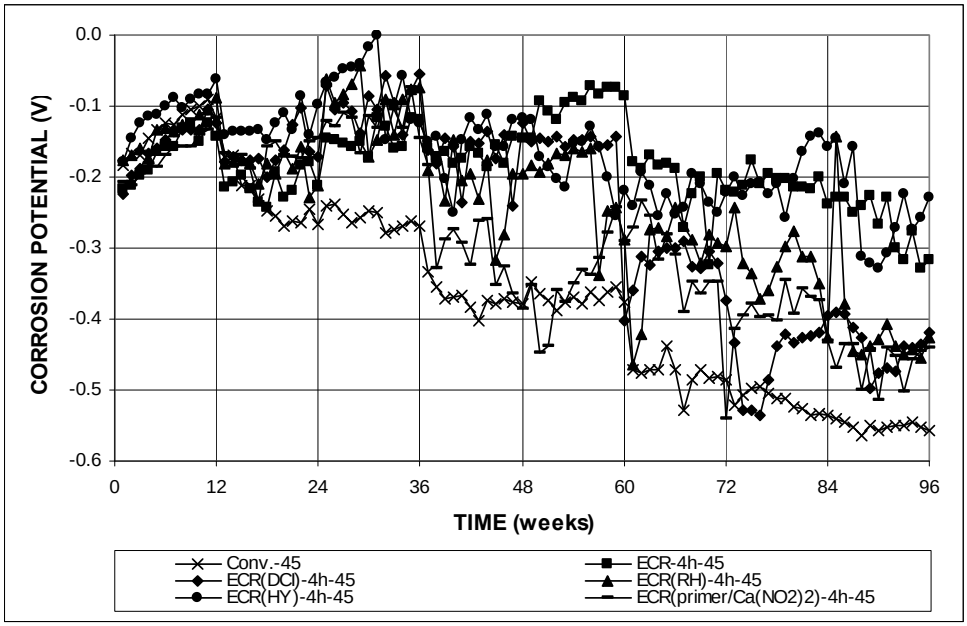

Figure 3.30 (a) – Average top mat corrosion potential, Southern Exposure test for specimens containing conventional steel, ECR, ECR in concrete with corrosion inhibitors, and ECR with a calcium nitrite primer, *w/c* = 0.45. Bars with four holes in epoxy coating.

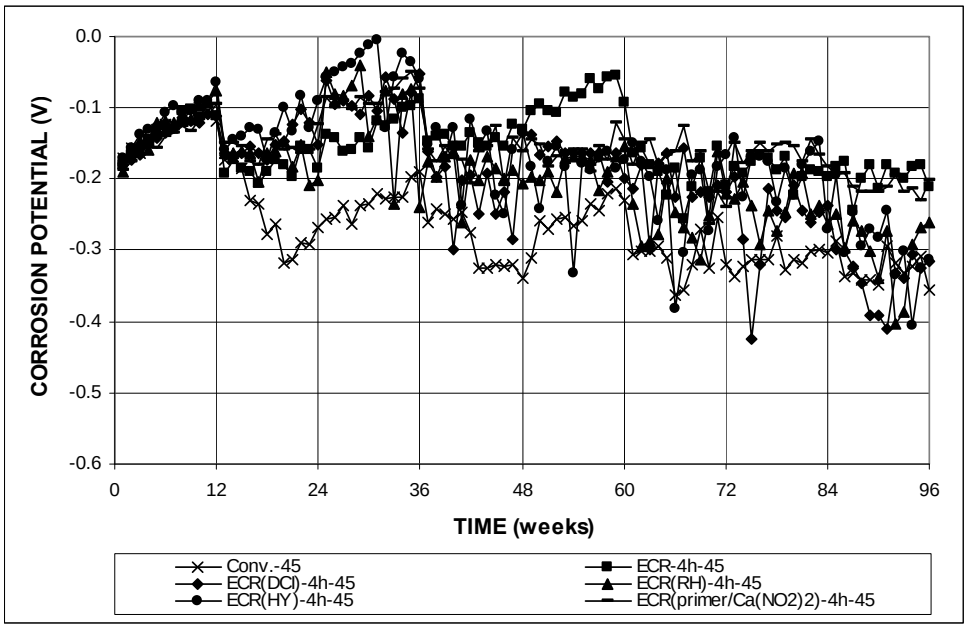

Figure 3.30 (b) – Average bottom mat corrosion potential, Southern Exposure test for specimens containing conventional steel, ECR, ECR in concrete with corrosion inhibitors, and ECR with a calcium nitrite primer, *w/c* = 0.45. Bars with four holes in epoxy coating.

and again from week 72 to the end of the test. After week 83, the top mat potentials of the ECR(RH)-4h-45 specimens remain below –0.350 V , except for week 85. The ECR control specimens and the Hycrete specimens are the only specimens in the group that do not exhibit any active corrosion in the top mat based on corrosion potential during the test period. As shown in Figure 3.30(b), the bottom mat potentials of all ECR specimens generally indicate a low probability of corrosion during the course of the test. In no instance does the average corrosion potential in any specimen remain more negative than –0.350 V for more than three consecutive weeks.

As shown in Figure 3.31(a), the first ECR specimens with ten holes through the epoxy to show corrosion activity in the top mat are the ECR(primer/Ca(NO2)2)-

10h-45 specimens, beginning at week 47 and continuing for the remainder of the test, with the exception of weeks 48 and 59. The ECR(DCI)-10h-45 specimens also exhibit a top mat potential more negative than –0.350 V, but appear to passivate by the next week, and do not show additional indications of active corrosion until week 56. At week 52, the ECR control specimens with ten holes through the epoxy begin exhibiting active corrosion, and average top mat potentials for these specimens generally remain more negative than –0.350 V for the remainder of the test. Only twice, at week 68 and between weeks 74 and 76, do the ECR(RH)-10h-45 specimens exhibit active corrosion in the top mat, and not once during the 96 week test period do the ECR(HY)-10h-45 specimens exhibit corrosion in the top mat based on corrosion potential.

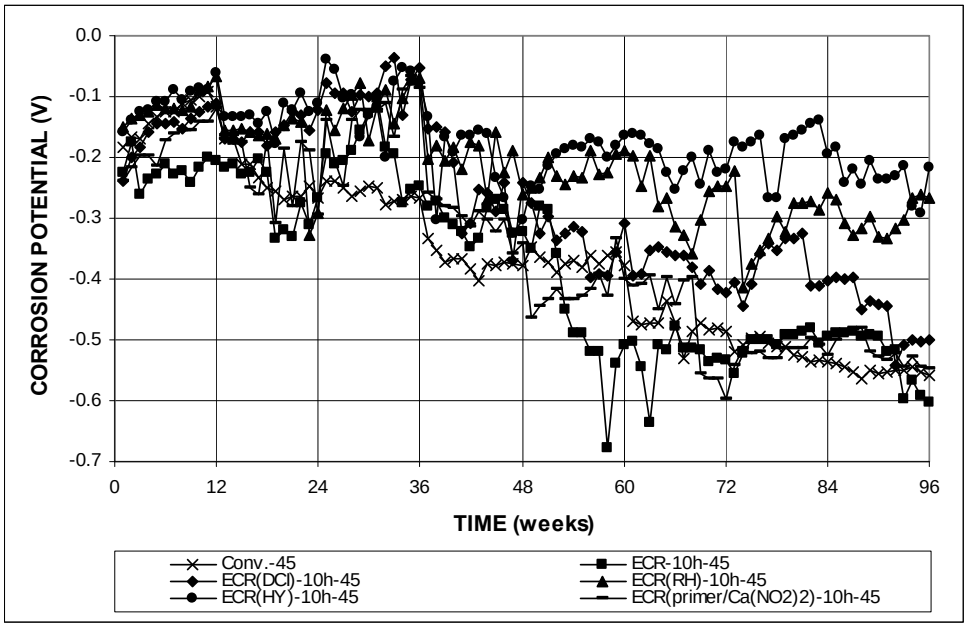

Figure 3.31 (a) – Average top mat corrosion potential, Southern Exposure test for specimens containing conventional steel, ECR, ECR in concrete with corrosion inhibitors, and ECR with a calcium nitrite primer, *w/c* = 0.45. Bars with ten holes in epoxy coating.

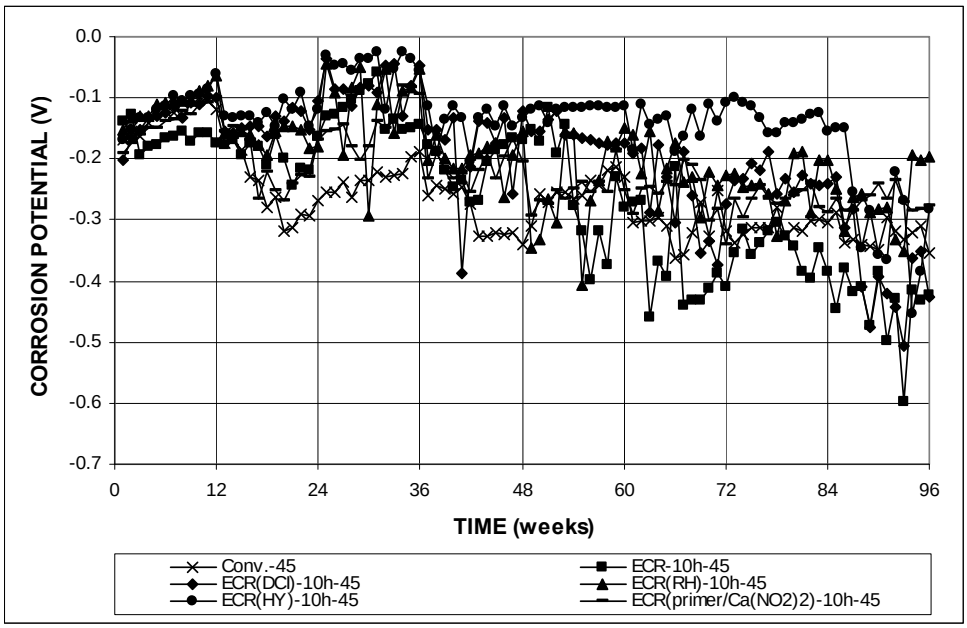

Figure 3.31 (b) – Average bottom mat corrosion potential, Southern Exposure test for specimens containing conventional steel, ECR, ECR in concrete with corrosion inhibitors, and ECR with a calcium nitrite primer, *w/c* = 0.45. Bars with ten holes in epoxy coating.

As shown in Figure 3.31(b), active corrosion in the bottom mat in ECR specimens is first exhibited by the ECR(RH)-10h-45 specimens, which contain the corrosion inhibitor Rheocrete 222+, at week 55, although by the next week, the bottom mat appears to again be passive. The bottom mat in the Rheocrete specimens stays passive for the remainder of the test, with the exception of week 93. The ECR control specimens with ten holes through the epoxy show the most corrosion activity in the bottom mat among all ECR specimens and conventional steel specimens, with sustained periods of active corrosion observed between weeks 67 and 73 and between weeks 84 and 96. The ECR(DCI)-10h-45 specimens also begin exhibiting sustained active corrosion in the bottom mat at week 88 and continuing for the remainder of the

test. The ECR(HY)-10h-45 and conventional steel control specimens show little corrosion activity in the bottom mat during the 96 week test period.

As shown in Figure 3.32(a), the Conv.-35 specimens begin showing signs of active corrosion in the top mat before any of the ECR specimens cast in concrete with *w/c* = 0.35. The only other specimens with *w/c* = 0.35 to exhibit periods of sustained corrosion (greater than two weeks) in the top mat are the ECR(DCI)-10h-35 specimens, beginning at week 55 and continuing until week 65. Figure 3.32(b) shows that, with the exception of the ECR(RH)-10h-35 specimens at week 63, the bottom mats in all ECR specimens with *w/c* = 0.35 show a low probability of corrosion during the entire test.

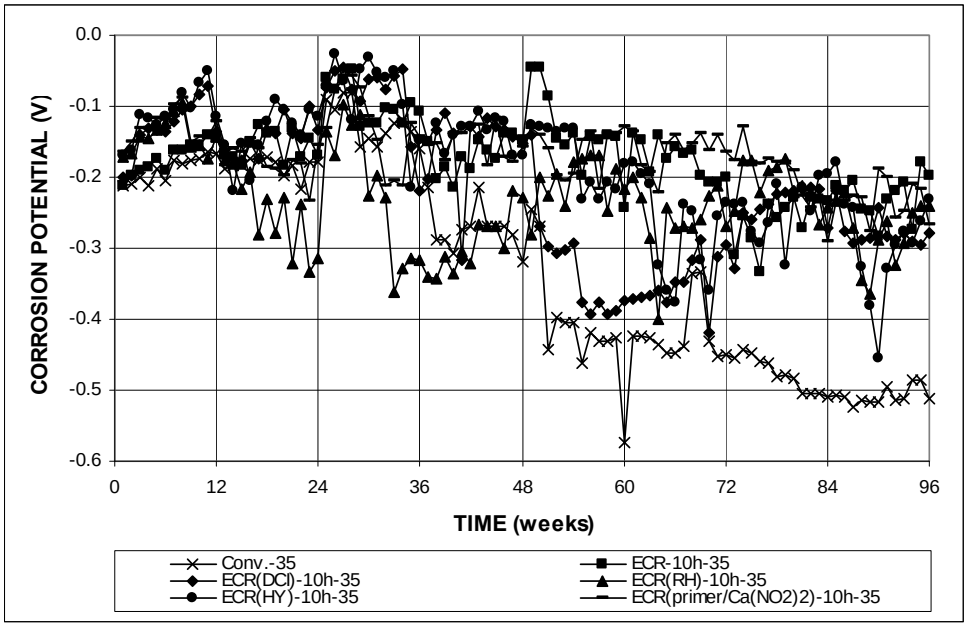

Figure 3.32 (a) – Average top mat corrosion potential, Southern Exposure test for specimens containing conventional steel, ECR, ECR in concrete with corrosion inhibitors, and ECR with a calcium nitrite primer, *w/c* = 0.35. Bars with ten holes in epoxy coating.

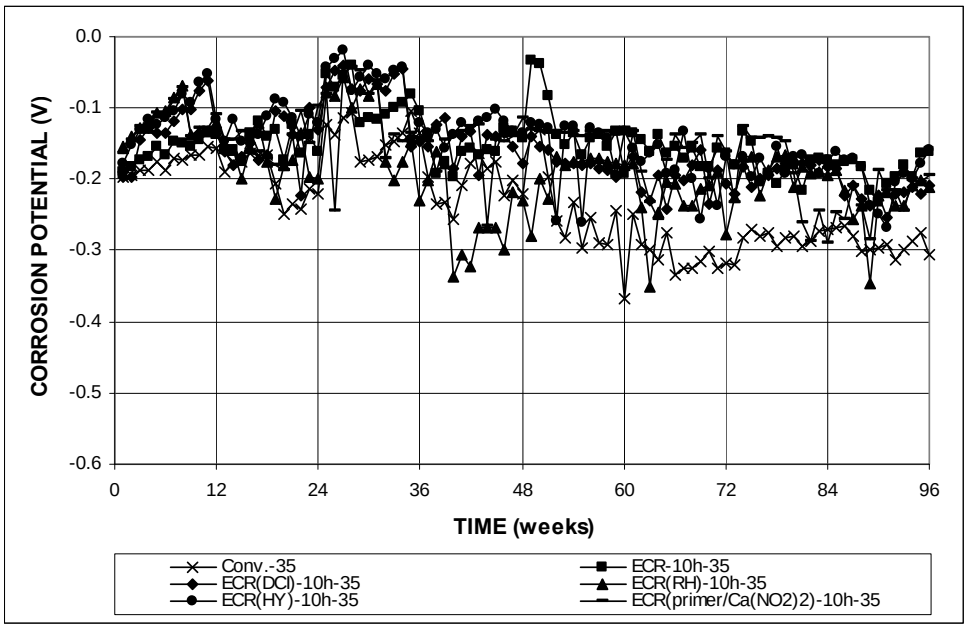

Figure 3.32 (b) – Average bottom mat corrosion potential, Southern Exposure test for specimens containing conventional steel, ECR, ECR in concrete with corrosion inhibitors, and ECR with a calcium nitrite primer, *w/c* = 0.35. Bars with ten holes in epoxy coating.

3.2.2 Cracked Beam Tests

Figures 3.33 and 3.34 show the average corrosion rates for the cracked beam tests with ECR containing four holes through the epoxy in concrete with *w/c* = 0.45. Figure 3.33(a) compares the high corrosion rate based on total area for conventional steel reinforcement with the low corrosion rates of the specimens containing epoxy-coated reinforcement. As shown in Figure 3.33(b) and 3.34, there is little discernable difference among ECR specimens, with the exception of the ECR(RH)-4h-45 specimens, which generally exhibit higher corrosion rates than the other ECR specimens beginning at week 35. As shown in Figure A.35(a), this increased corrosion rate is observed in one out of three specimens.

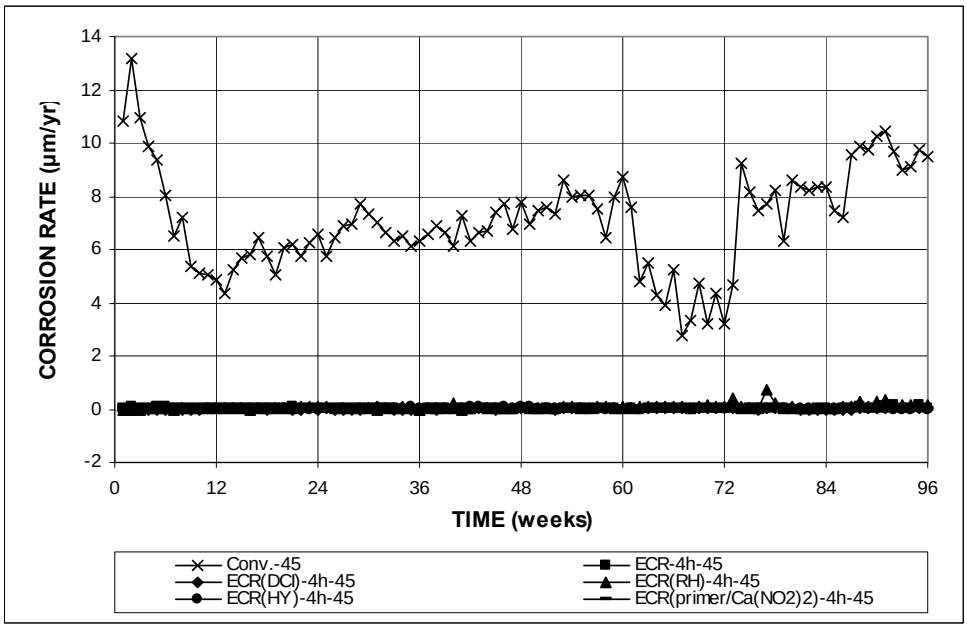

Figure 3.33 (a) – Average corrosion rate, cracked beam test for specimens containing conventional steel, ECR, ECR in concrete with corrosion inhibitors, and ECR with a calcium nitrite primer, *w/c* = 0.45. Bars with coating containing four holes through the epoxy.

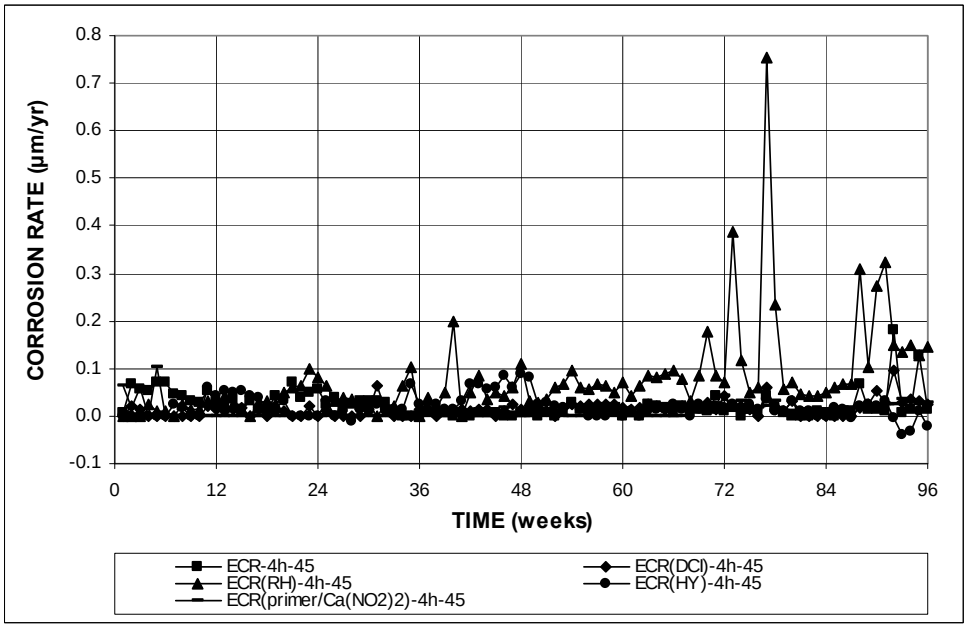

Figure 3.33 (b) – Average corrosion rate, cracked beam test for specimens containing ECR, ECR in concrete with corrosion inhibitors, and ECR with a calcium nitrite primer, *w/c* = 0.45. Bars with coating containing four holes through the epoxy. (Different scale)

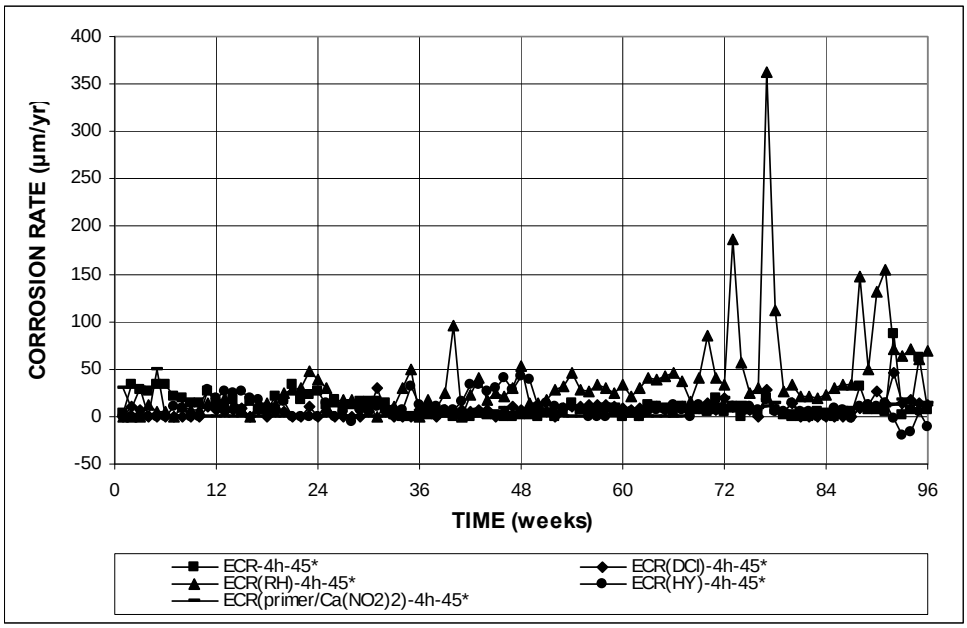

Figure 3.34 – Average corrosion rate based on exposed area, cracked beam test for specimens containing ECR, ECR in concrete with corrosion inhibitors, and ECR with a calcium nitrite primer, *w/c* = 0.45. Bars with coating containing four holes through the epoxy.

Figures 3.35 and 3.36 show the average corrosion rates for the CB specimens with ECR containing ten holes through the epoxy based on total and exposed area, respectively. Figure 3.35(a) shows that conventional steel exhibits significantly greater corrosion than any of the ECR specimens with ten holes through the epoxy. Figures 3.35(b) and 3.36 show that there is little discernable difference between the average corrosion rates of the ECR specimens with corrosion inhibitors, with the exception of the ECR(RH)-10h-45 specimens, which (like the ECR(RH)-4h-45 specimens) begin exhibiting slightly higher corrosion rates than other ECR specimens at week 17, and in general continues to exhibit the highest corrosion rate among ECR specimens shown in the figure for the remainder of the test.

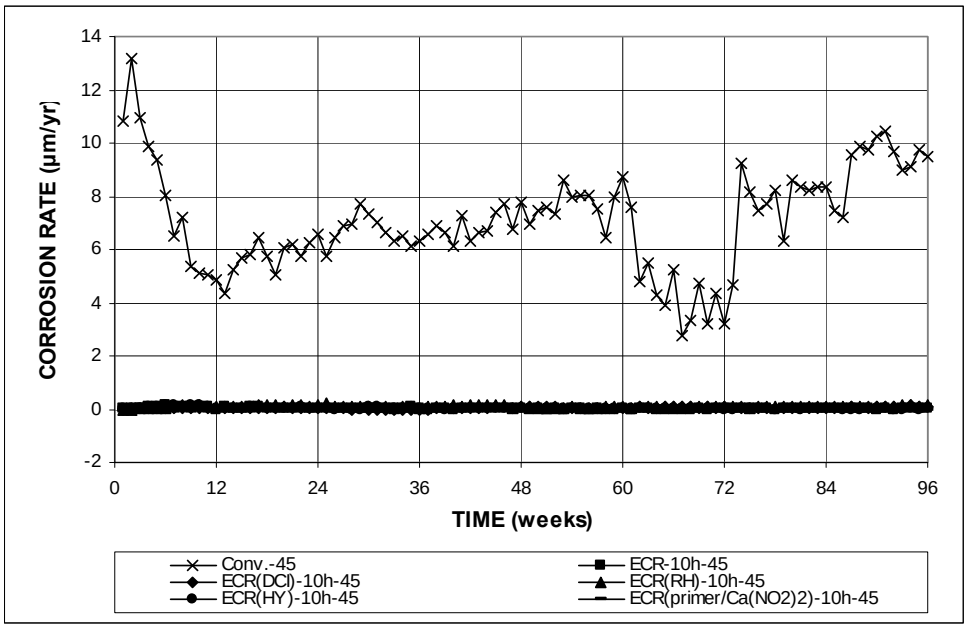

Figure 3.35 (a) – Average corrosion rate, cracked beam test for specimens containing conventional steel, ECR, ECR in concrete with corrosion inhibitors, and ECR with a calcium nitrite primer, *w/c* = 0.45. Bars with coating containing ten holes through the epoxy.

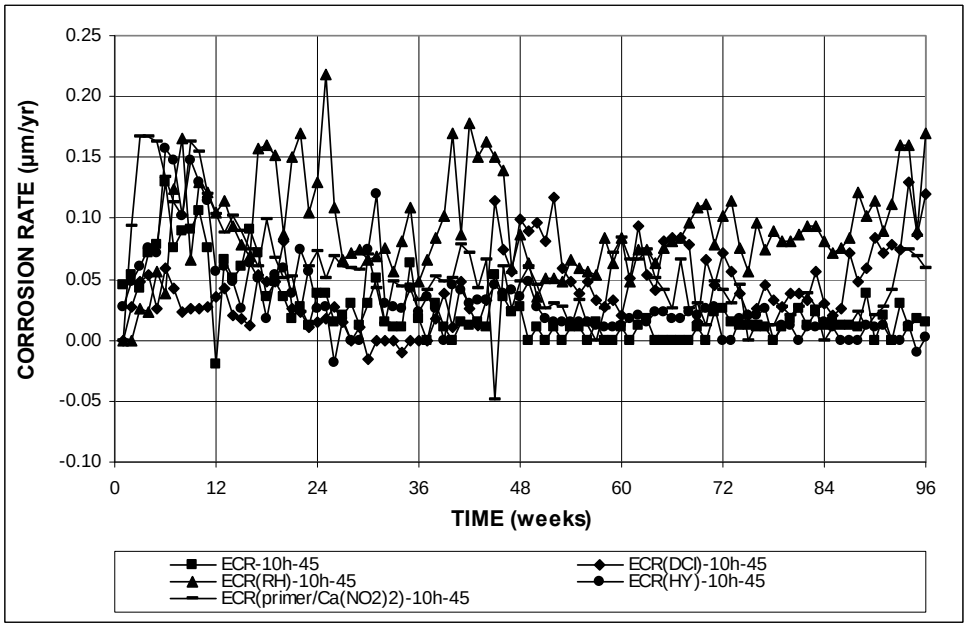

Figure 3.35 (b) – Average corrosion rate, cracked beam test for specimens containing ECR, ECR in concrete with corrosion inhibitors, and ECR with a calcium nitrite primer, *w/c* = 0.45. Bars with coating containing ten holes through the epoxy. (Different scale)

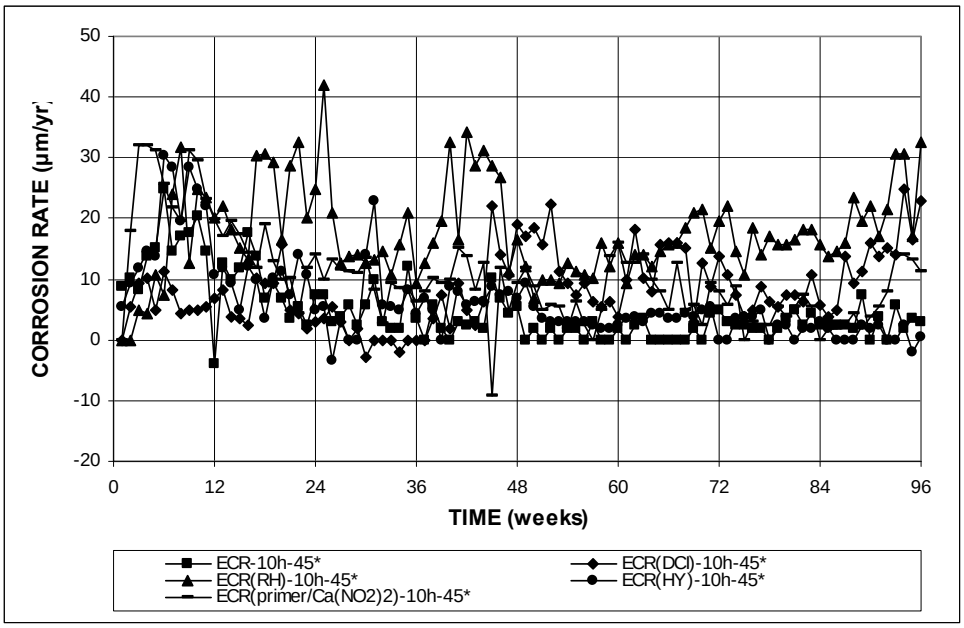

Figure 3.36 – Average corrosion rate based on exposed area, cracked beam test for specimens containing ECR, ECR in concrete with corrosion inhibitors, and ECR with a calcium nitrite primer, *w/c* = 0.45. Bars with coating containing ten holes through the epoxy.

Figures 3.37 and 3.38 show the average corrosion rates based on total and exposed area, respectively, for the CB specimens with ECR containing ten holes through the epoxy cast in concrete with *w/c* = 0.35. As shown in Figure 3.37(a), the conventional steel specimens again show higher corrosion rates than any of the ECR specimens. As shown in Figure 3.37(b) and 3.38, beginning at week 40, the ECR(primer/Ca(NO2)2)-10h-35 specimens begin exhibiting corrosion rates that are significantly higher than the other ECR specimens shown. Between weeks 40 and 96, the average corrosion rate of the ECR(primer/Ca(NO2)2)-10h-35 specimens remains elevated, ranging between 0.163 and 1.13 µm/yr based on total area and 31.2 and 218 µm/yr based on exposed area. As shown in Figure A.67(a), this increase in corrosion

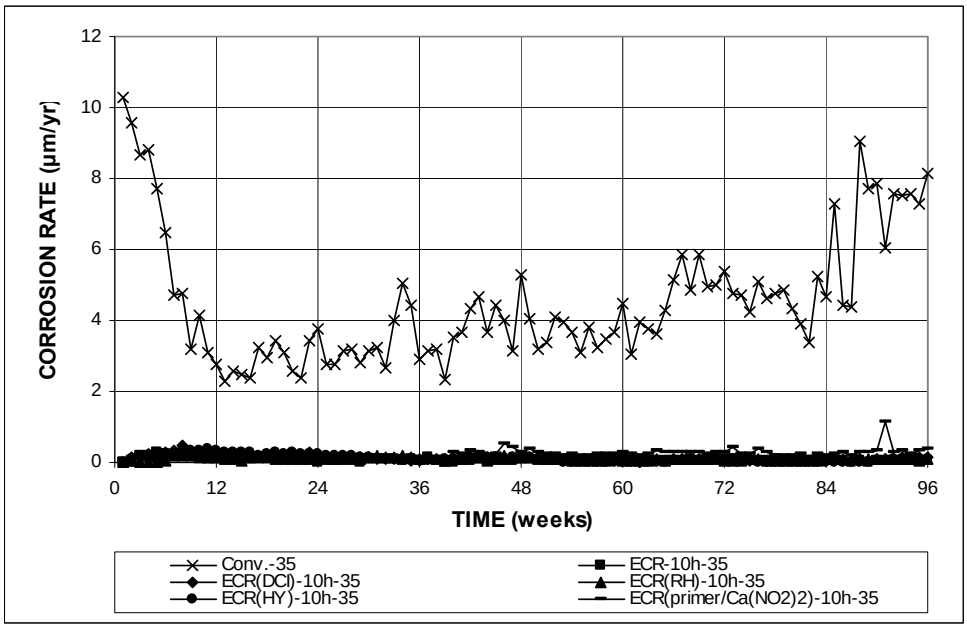

Figure 3.37 (a) – Average corrosion rate, cracked beam test for specimens containing conventional steel, ECR, ECR in concrete with corrosion inhibitors, and ECR with a calcium nitrite primer, *w/c* = 0.35. Bars with coating containing ten holes through the epoxy.

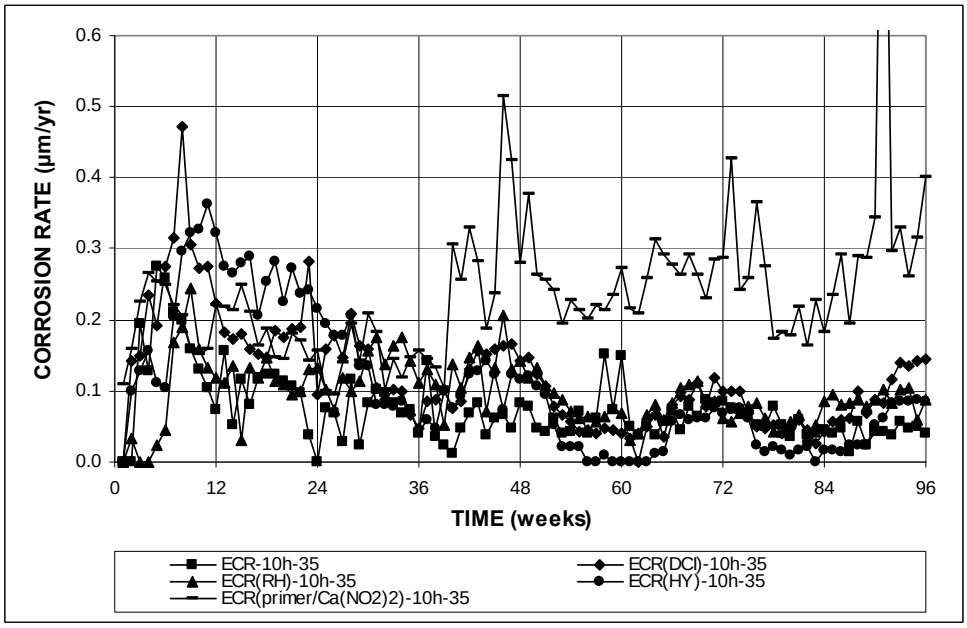

Figure 3.37 (b) – Average corrosion rate, cracked beam test for specimens containing ECR, ECR in concrete with corrosion inhibitors, and ECR with a calcium nitrite primer, *w/c* = 0.35. Bars with coating containing ten holes through the epoxy.

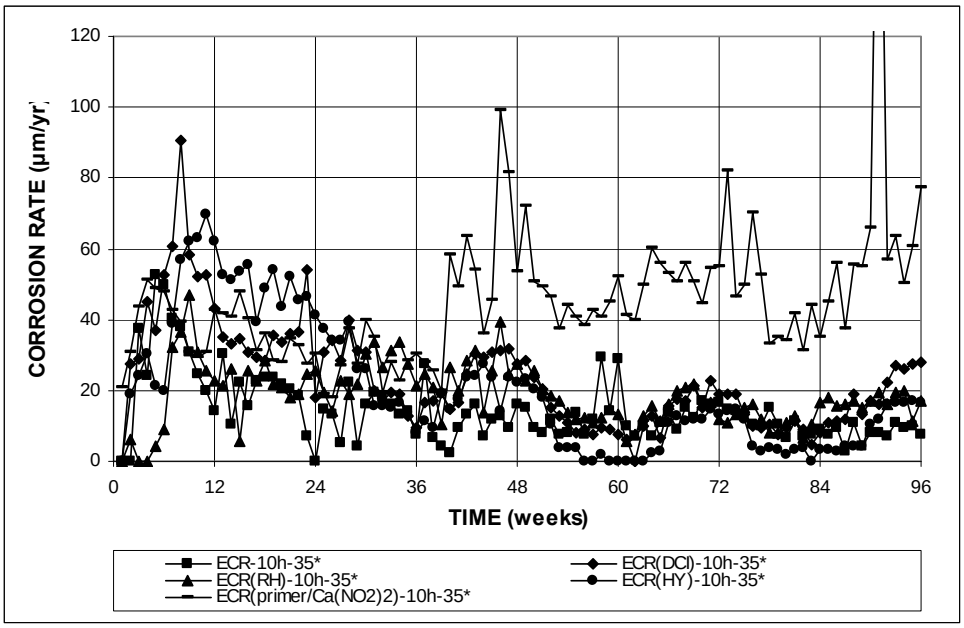

Figure 3.38 – Average corrosion rate based on exposed area, cracked beam test for specimens containing ECR, ECR in concrete with corrosion inhibitors, and ECR with a calcium nitrite primer, *w/c* = 0.35. Bars with coating containing ten holes through the epoxy.

rate is observed in two out of three specimens, although measurable corrosion is observed in all three specimens.

Figures 3.39 and 3.40 show the average corrosion losses based on total and exposed area, respectively, for the CB specimens with ECR containing four holes through the epoxy cast in concrete with *w/c* = 0.45. As shown in Figure 3.39, conventional steel exhibits higher corrosion losses than any of the ECR specimens in the figure. As shown in Figure 3.40, the ECR control specimens exhibit the highest losses among ECR specimens for the first 38 weeks of the test. Beginning at week 39, however, the average corrosion losses exhibited by the ECR(RH)-4h-45 specimens surpasses that of the ECR control specimens. This increased corrosion loss is observed in one out of the three specimens. The ECR(RH)-4h-45 specimens continue

to exhibit the highest corrosion loss among the ECR specimens for the remainder of the test. At week 49, the ECR(HY)-4h-45 specimens begin exhibiting higher average corrosion losses than the ECR controls specimen. As shown in Figure A.47(b), this increase in average corrosion loss is due to increased corrosion in one out of three specimens. The average corrosion loss of the Hycrete specimens remains higher than the ECR control specimens between weeks 49 and 92, after which the Hycrete specimens exhibit lower average corrosion losses than the ECR control specimens for the remainder of the test. The average corrosion losses of the ECR(DCI)-4h-45 and ECR(primer/Ca(NO2)2)-4h-45 specimens remain below that of the ECR control specimens for the entire test.

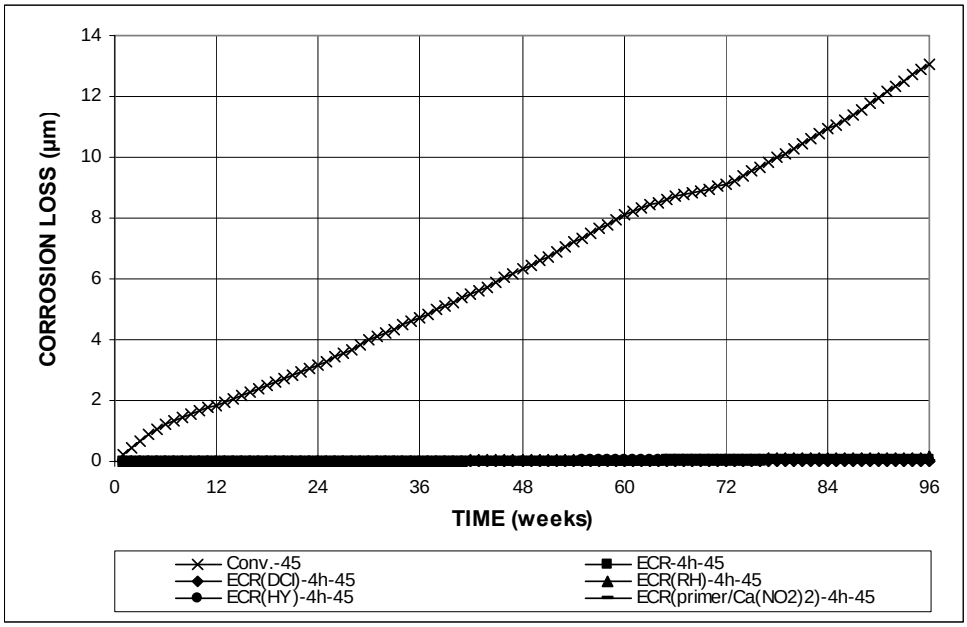

Figure 3.39 – Average corrosion loss, cracked beam test for specimens containing conventional steel, ECR, ECR in concrete with corrosion inhibitors, and ECR with a calcium nitrite primer, *w/c* = 0.45. Bars with four holes in epoxy coating.

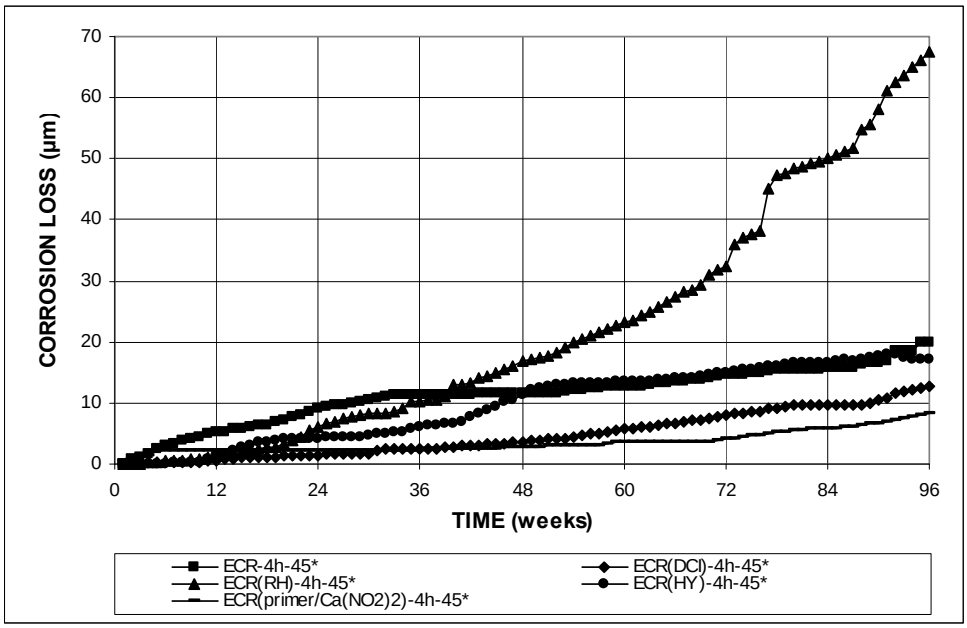

Figure 3.40 - Average corrosion loss based on exposed area, cracked beam test for specimens containing conventional steel, ECR, ECR in concrete with corrosion inhibitors, and ECR with a calcium nitrite primer, *w/c* = 0.45. Bars with four holes in epoxy coating.

Figure 3.41 and 3.42 show the average corrosion losses based on total and exposed area, respectively, for the CB specimens with ECR containing ten holes through the epoxy cast in concrete with *w/c* = 0.45. Figure 3.41 compares the high corrosion rates based on total area for specimens containing conventional steel reinforcement with the low corrosion rates of specimens containing epoxy-coated reinforcement. Figure 3.42 shows that for the first three weeks, the ECR control specimens exhibit the highest average corrosion loss among ECR specimens. At week four, the average corrosion loss measured in the ECR(primer/Ca(NO2)2)-10h-45 specimens surpasses that of the ECR controls specimens, and remains higher than any other ECR specimen until week 25. Beginning at week 25 and continuing for the remainder of the test, the ECR(RH)-10h-45 specimens exhibit the highest corrosion

losses among the ECR specimens. By week 5, the ECR(HY)-10h-45 specimens also exhibit higher average corrosion losses than those measured in the ECR control specimens. As shown in Figure A.51(b), measurable corrosion losses are observed in two out of three Hycrete specimens. The average corrosion losses of the ECR(DCI)-10h-45 specimens remain lower than the ECR control specimens for the first 57 weeks of the test, but the corrosion losses exhibited by these specimens ultimately surpass those of the ECR control specimens (at week 58) and of the ECR(HY)-10h-45 specimens (at week 78). The increase in average corrosion loss in the ECR(DCI)-10h-45 specimens is observed in one out of three specimens, as shown in Figure A.27(b).

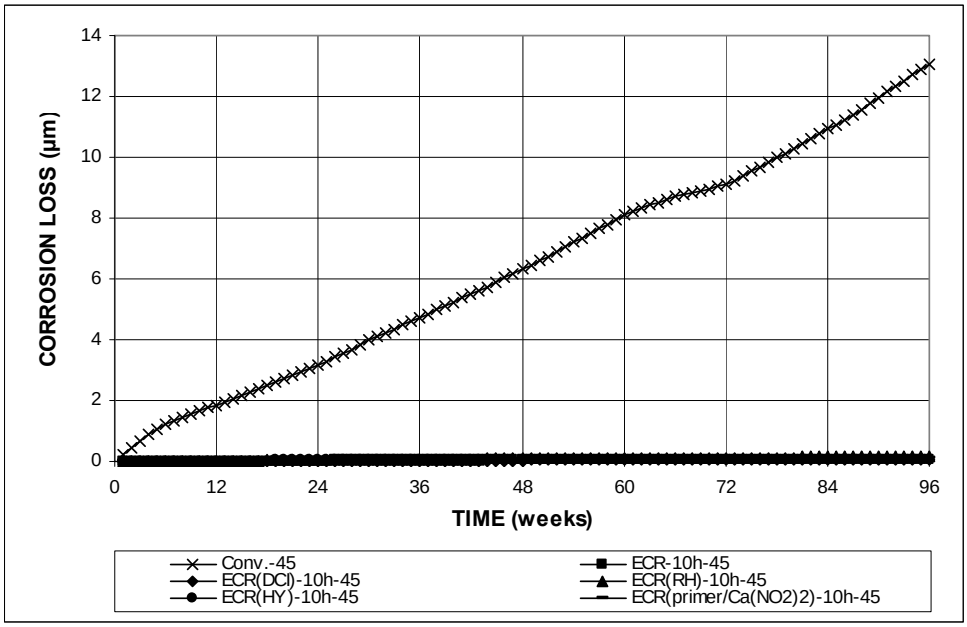

Figure 3.41 – Average corrosion loss, cracked beam test for specimens containing conventional steel, ECR, ECR in concrete with corrosion inhibitors, and ECR with a calcium nitrite primer, *w/c* = 0.45. Bars with ten holes in epoxy coating.

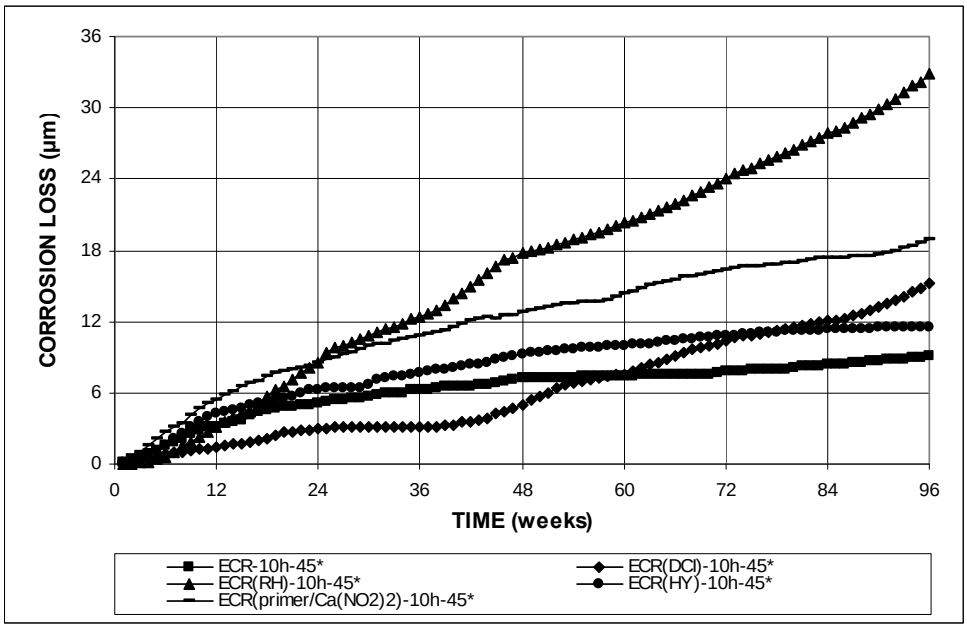

Figure 3.42 – Average corrosion loss based on exposed area, cracked beam test for specimens containing conventional steel, ECR, ECR in concrete with corrosion inhibitors, and ECR with a calcium nitrite primer, *w/c* = 0.45. Bars with ten holes in epoxy coating.

Figures 3.43 and 3.44 show the average corrosion losses based on total and exposed area, respectively, for the CB specimens with ECR containing ten holes through the epoxy cast in concrete with *w/c* = 0.35. Figure 3.43 compares the high corrosion rates based on total area for specimens containing conventional steel reinforcement with the low corrosion rates of specimens containing epoxy-coated reinforcement. As shown in Figure 3.44, after week 10, all ECR specimens with corrosion inhibitors exhibit higher corrosion losses than the ECR control specimens for the remainder of the test, with the exception of the ECR(RH)-10h-35 specimens, which do not surpass the ECR control specimens until week 33.

Table 3.5 summarizes the total average corrosion losses at 96 weeks for cracked beam ECR specimens cast with corrosion inhibitors. Based on total area, the

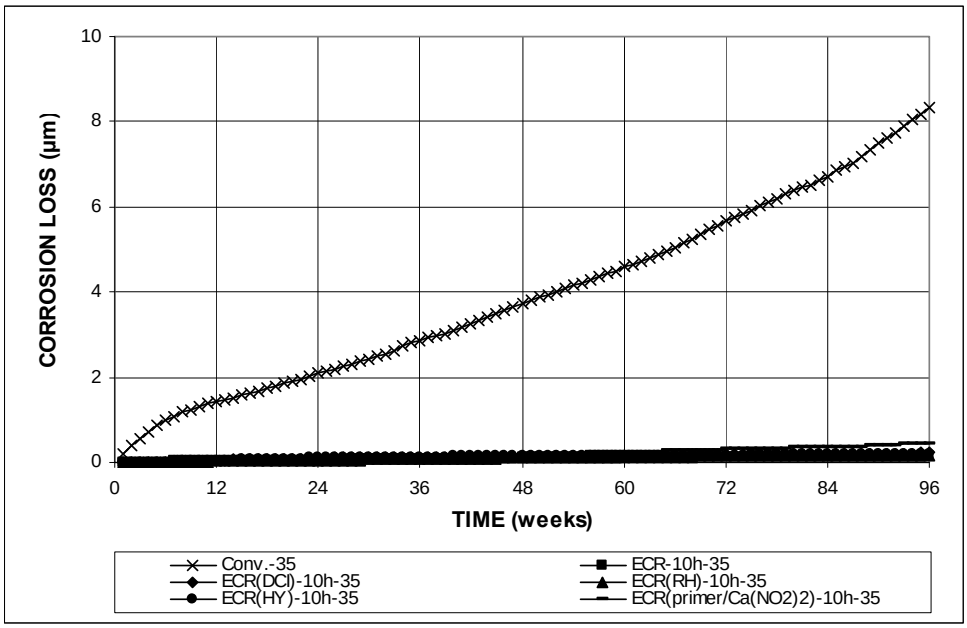

Figure 3.43 – Average corrosion loss, cracked beam test for specimens containing conventional steel, ECR, ECR in concrete with corrosion inhibitors, and ECR with a calcium nitrite primer, *w/c* = 0.35. Bars with ten holes in epoxy coating.

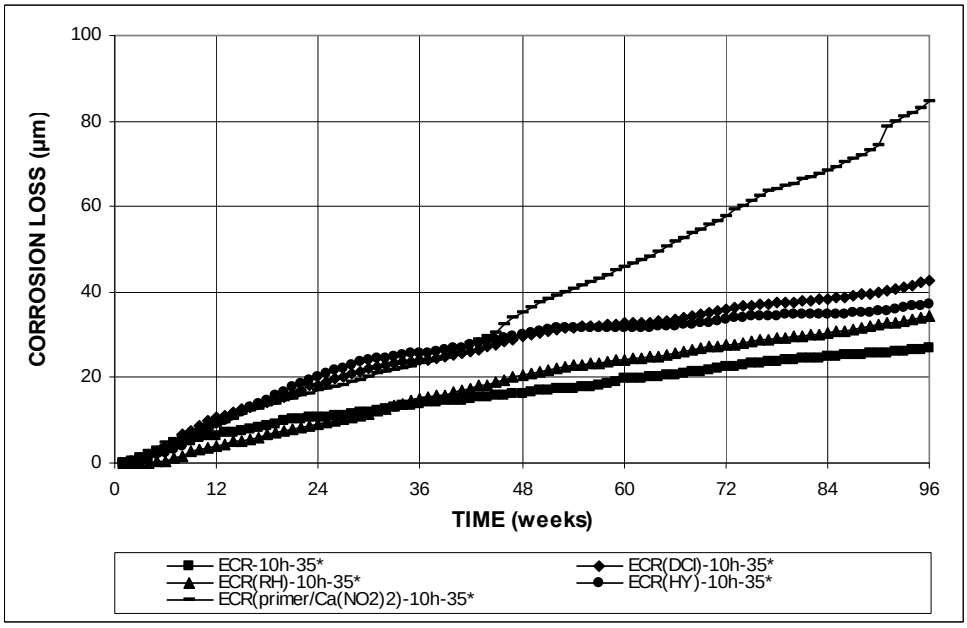

Figure 3.44 – Average corrosion loss based on exposed area, cracked beam test for specimens containing conventional steel, ECR, ECR in concrete with corrosion inhibitors, and ECR with a calcium nitrite primer, *w/c* = 0.35. Bars with ten holes in epoxy coating.

Table 3.5 – Average corrosion loss (μm) at week 96 as measured in the cracked beam test for specimens containing ECR in concrete with corrosion inhibitors and ECR with a calcium nitrite primer

Steel Designation[a]	Specimen			Average	Standard Deviation
	1	2	3		
Total Area					
ECR(DCI)-4h-45	0.025	0.048	0.007	0.026	0.021
ECR(DCI)-10h-45	0.044	0.155	0.039	0.079	0.065
ECR(DCI)-10h-35	0.124	0.095	0.449	0.223	0.197
ECR(RH)-4h-45	0.062	0.314	0.047	0.141	0.150
ECR(RH)-10h-45	0.240	0.134	0.138	0.171	0.060
ECR(RH)-10h-35	0.096	0.302	0.136	0.178	0.109
ECR(HY)-4h-45	0.010	0.005	0.092	0.036	0.049
ECR(HY)-10h-45	0.002	0.116	0.062	0.060	0.057
ECR(HY)-10h-35	0.144	0.159	0.278	0.194	0.073
ECR(primer/$Ca(NO_2)_2$)-4h-45	0.016	0.008	0.028	0.017	0.010
ECR(primer/$Ca(NO_2)_2$)-10h-45	0.152	0.059	0.084	0.098	0.048
ECR(primer/$Ca(NO_2)_2$)-10h-35	0.506	0.315	0.589	0.470	0.140
Exposed Area					
ECR(DCI)-4h-45*	12.1	22.9	3.17	12.72	9.87
ECR(DCI)-10h-45*	8.45	29.8	7.57	15.3	12.6
ECR(DCI)-10h-35*	23.8	18.2	86.3	42.8	37.8
ECR(RH)-4h-45*	29.6	151	22.5	67.6	72.0
ECR(RH)-10h-45*	46.1	25.7	26.6	32.8	11.6
ECR(RH)-10h-35*	18.5	58.0	26.2	34.3	20.9
ECR(HY)-4h-45*	4.79	2.39	44.0	17.1	23.4
ECR(HY)-10h-45*	0.31	22.4	12.0	11.6	11.0
ECR(HY)-10h-35*	27.7	30.6	53.4	37.2	14.1
ECR(primer/$Ca(NO_2)_2$)-4h-45*	7.81	3.80	13.2	8.28	4.73
ECR(primer/$Ca(NO_2)_2$)-10h-45*	29.2	11.4	16.1	18.9	9.23
ECR(primer/$Ca(NO_2)_2$)-10h-35*	97.3	60.5	113	90.3	27.0

[a] ECR(DCI) = ECR in concrete with DCI inhibitor.
ECR(Rheocrete) = ECR in concrete with Rheocrete inhibitor.
ECR (Hycrete) = normal ECR with Hycrete inhibitor.
4h = bar with four holes through epoxy, 10h = bar with 10 holes through epoxy.
45 = concrete with *w/c* =0.45; 35 = concrete with *w/c* =0.35.

* Corrosion loss calculation based on the exposed area of four or ten 3-mm (1/8-in.) diamter holes.

ECR(primer/Ca(NO2)2)-10h-35 and ECR(DCI)-10h-35 specimens exhibit the highest corrosion loss, with values of 0.470 and 0.223 μm, respectively. These are followed by the ECR(HY)-10h-35, ECR(RH)-10h-35, ECR(RH)-10h-45, and ECR(RH)-4h-45 specimens with losses of 0.194, 0.178, 0.171, and 0.141 μm, respectively. All other

ECR specimens exhibit losses of less than 0.1 μm based on total area. Based on exposed area, the ECR(primer/Ca(NO2)2)-10h-35 and ECR(RH)-4h-45 specimens exhibit the highest corrosion loss, with values of 90.3 and 67.6 μm, respectively. This is followed by the ECR(DCI)-10h-35, ECR(HY)-10h-35, and ECR(RH)-10h-35 specimens with losses of 42.8, 37.2, and 34.3 μm, respectively. All ten-hole specimens with a *w/c* ratio of 0.35 exhibit higher corrosion losses based on exposed area than their counterpart specimens with *w/c* = 0.45. The cause of the increased corrosion loss in these specimens is unknown. When comparing four and ten-hole specimens in concrete with a *w/c* of 0.45, the Hycrete and Rheocrete four-hole specimens exhibit higher corrosion losses than their ten-hole counterparts, while the DCI and primer/Ca(NO2)2 specimens exhibit lower corrosion losses than their ten hole counterparts. The lowest corrosion loss based on exposed area among the ECR specimens with corrosion inhibitors is observed in the ECR(primer/Ca(NO2)2)-4h-45 specimens, with a total corrosion loss of 8.28 μm.

Figures 3.45, 3.46 and 3.47 show the average mat-to-mat resistance for the ECR specimens with four holes through the epoxy with a *w/c* ratio of 0.45, ECR specimens with ten holes through the epoxy with a *w/c* ratio of 0.45, and ECR specimens with ten holes through the epoxy with a *w/c* ratio of 0.35, respectively. As shown in all three figures, the average mat-to-mat resistances for all specimens increases with time during the first 48 weeks of the test. After week 48, the scatter observed in the resistance readings increases, possibly due to additional cracking occurring in the specimen as previously discussed, and little information can be

drawn from this data. Figure 3.45 shows that ECR specimens containing four holes through the epoxy with corrosion inhibitors generally exhibit lower average mat-to-mat resistances than the ECR control specimens. Figure 3.46 shows that all ECR specimens with ten holes through the epoxy exhibit similar mat-to-mat resistances during the first 48 weeks of the test. Figure 3.47 shows that ECR control specimens generally exhibit higher average mat-to-mat resistances than the other ECR specimens. Specimens cast in concrete with a *w/c* ratio of 0.35 show lower mat-to-mat resistances than specimens cast in concrete with a *w/c* ratio of 0.45. This is contrary to what would be expected, since the decreased permeability of the concrete with the lower *w/c* ratio should decrease the efficiency of the pore solution electrolyte.

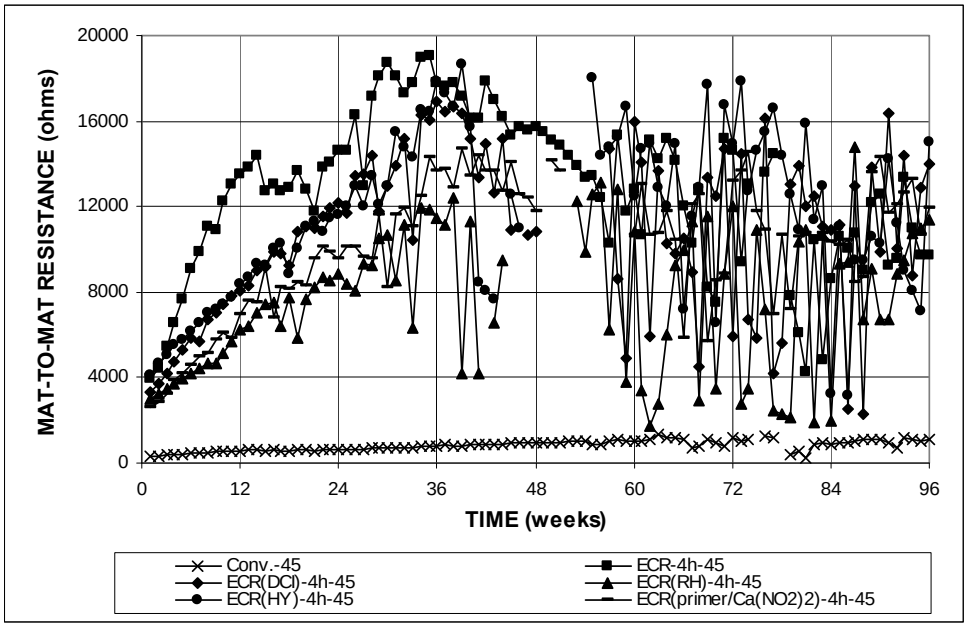

Figure 3.45 – Average mat-to-mat resistance, cracked beam test for specimens containing conventional steel, ECR, ECR in concrete with corrosion inhibitors, and ECR with a calcium nitrite primer, *w/c* = 0.45. Bars with four holes in epoxy coating.

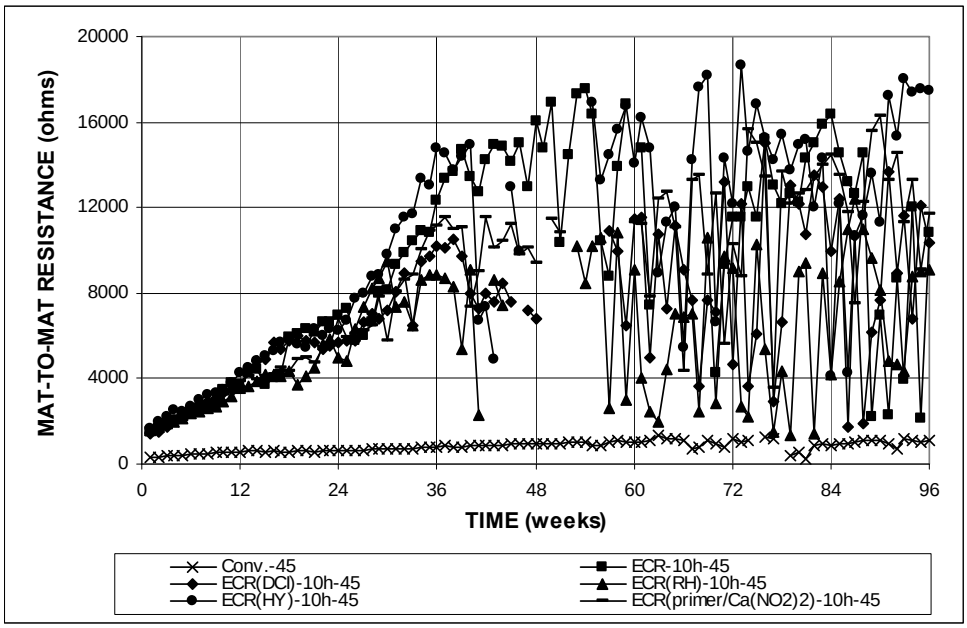

Figure 3.46 – Average mat-to-mat resistance, cracked beam test for specimens containing conventional steel, ECR, ECR in concrete with corrosion inhibitors, and ECR with a calcium nitrite primer, *w/c* = 0.45. Bars with ten holes in epoxy coating.

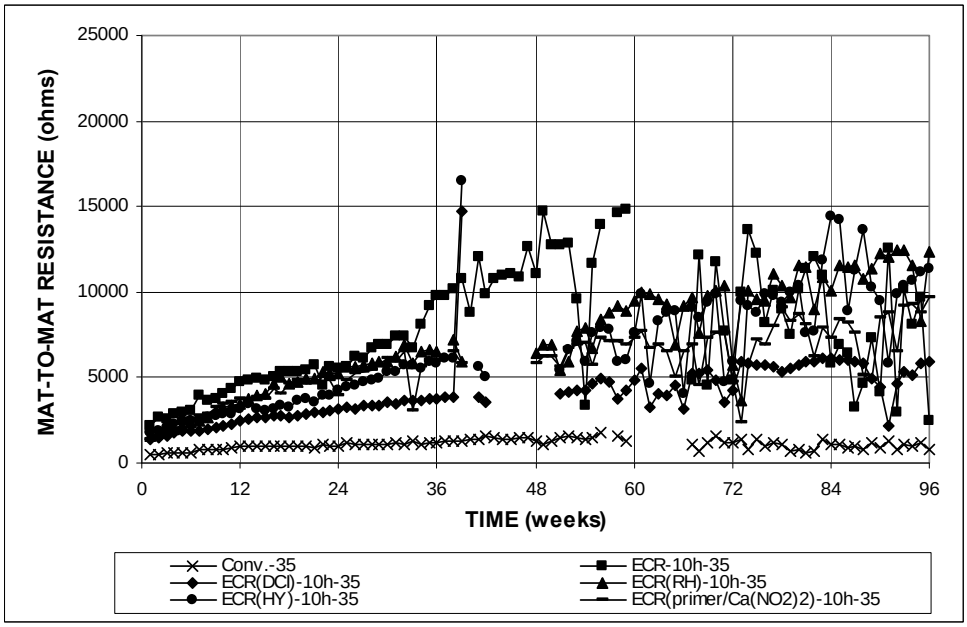

Figure 3.47 – Average mat-to-mat resistance, cracked beam test for specimens containing conventional steel, ECR, ECR in concrete with corrosion inhibitors, and ECR with a calcium nitrite primer, *w/c* = 0.35. Bars with ten holes in epoxy coating.

Figure 3.48 shows the average corrosion potentials versus a copper-copper sulfate electrode for the top and bottom mats of the CB specimens with ECR containing four holes through the epoxy cast in concrete with *w/c* = 0.45. As shown in Figure 3.48(a), a high probability of active corrosion, indicated by a corrosion potential more negative than –0.350 V, is first observed among ECR specimens in the top mats of the ECR-4h-45 and ECR(primer/Ca(NO2)2)-4h-45 specimens at week 2. These specimens continue to exhibit active corrosion for the remainder of the test. The ECR(DCI)-4h-45 specimens begin exhibiting corrosion activity in the top mat at week 3, and continues to show active corrosion for the remainder of the test with the exception of weeks 5, 6, and 33. The ECR(RH)-4h-45 specimens exhibit active corrosion in the top mat at weeks 4 and 5, appear to passivate during weeks 6 through 10, and then actively corrode from week 11 until the end of test. The latest initiation of corrosion is observed in the ECR(HY)-4h-45 specimens at week 11. These specimens continue to exhibit active corrosion for the remainder of the test. As shown in Figure 3.48(b), active corrosion observed in the bottom mats of the ECR specimens are generally isolated to periods of three weeks or less. The first specimens to exhibit active corrosion in the bottom bars for a period of more than three weeks are the ECR(RH)-45h-45 specimens, beginning at week 89 and continuing for the remainder of the test. The ECR(DCI)-4h-45 and ECR(HY)-4h-45 specimens also exhibit a sustained period of active corrosion in the bottom mat between weeks 92 through 95.

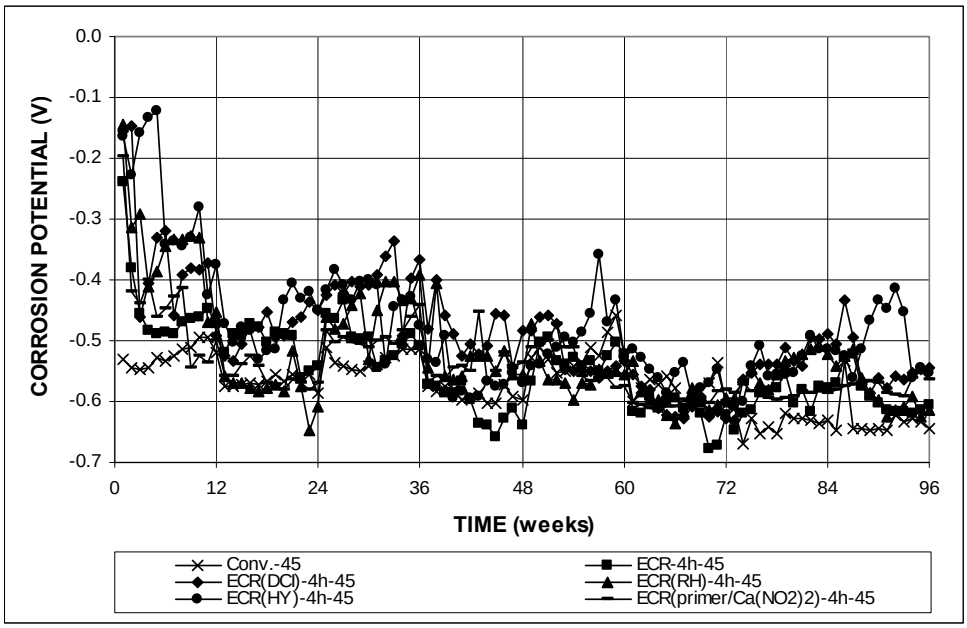

Figure 3.48 (a) – Average top mat corrosion potential, cracked beam test for specimens containing conventional steel, ECR, ECR in concrete with corrosion inhibitors, and ECR with a calcium nitrite primer, *w/c* = 0.45. Bars with four holes in epoxy coating.

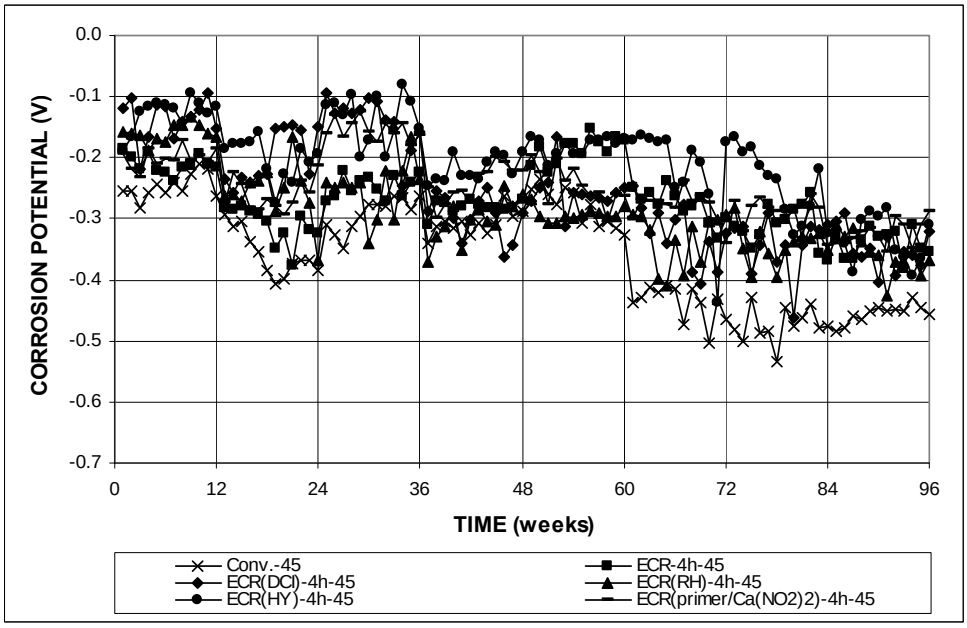

Figure 3.48 (b) – Average bottom mat corrosion potential, cracked beam test for specimens containing conventional steel, ECR, ECR in concrete with corrosion inhibitors, and ECR with a calcium nitrite primer, *w/c* = 0.45. Bars with four holes in epoxy coating.

Figure 3.49 shows the average corrosion potentials versus a copper-copper sulfate electrode for the top and bottom mats of the CB specimens with ECR containing ten holes through the epoxy cast in concrete with *w/c* = 0.45. As shown in Figure 3.49(a), all ECR specimens show active signs of corrosion in the top mat by week 4, and continue exhibiting active corrosion for the remainder of the test, with the exception of ECR(DCI)-10h-45 at week 33. As shown in Figure 3.49(b), the ECR control specimens are the only ECR specimens to show a high probability of active corrosion in the bottom mat for more than three consecutive weeks, beginning at week 91. All other ECR specimens exhibit active corrosion in the bottom mat during

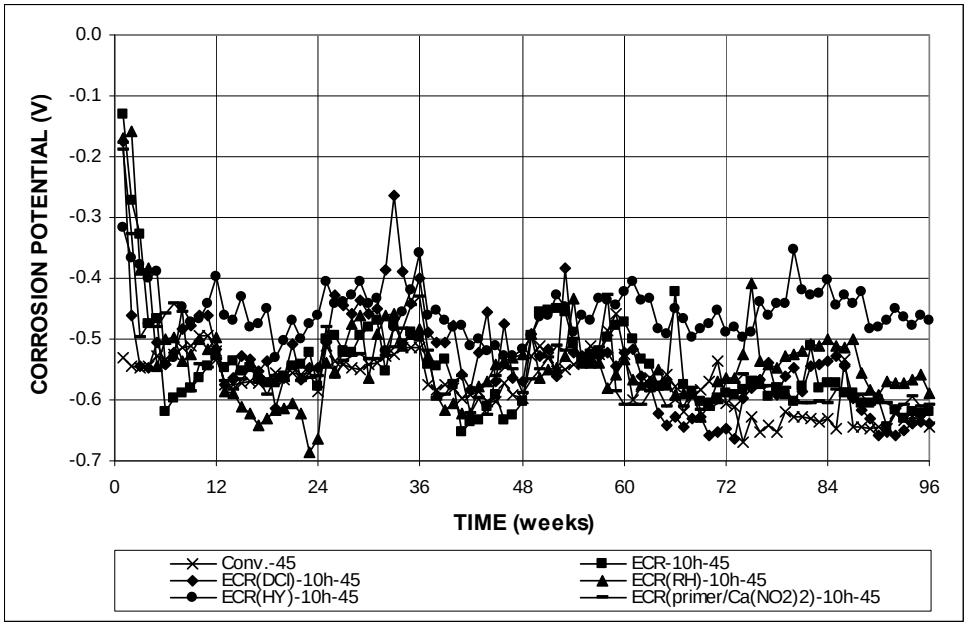

Figure 3.49 (a) – Average top mat corrosion potential, cracked beam test for specimens containing conventional steel, ECR, ECR in concrete with corrosion inhibitors, and ECR with a calcium nitrite primer, *w/c* = 0.45. Bars with ten holes in epoxy coating.

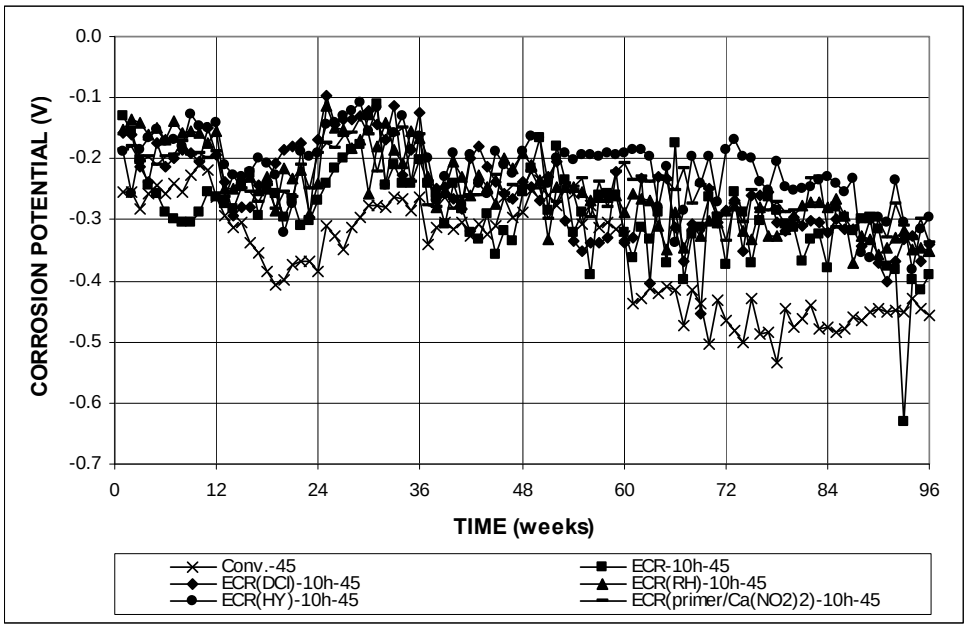

Figure 3.49 (b) – Average bottom mat corrosion potential, cracked beam test for specimens containing conventional steel, ECR, ECR in concrete with corrosion inhibitors, and ECR with a calcium nitrite primer, *w/c* = 0.45. Bars with ten holes in epoxy coating.

isolated periods of less than three weeks, with the exception of the ECR(primer/Ca(NO2)2-10h-45 specimens, which exhibit no active corrosion in the bottom mat during the entire test period.

Figure 3.50 shows the average corrosion potentials versus a copper-copper sulfate electrode for the top and bottom mats of the CB specimens with ECR containing ten holes through the epoxy cast in concrete with *w/c* = 0.35. Figure 3.50(a) shows that all ECR specimens exhibit active corrosion in the top mat by week 7, and continue to exhibit active corrosion for the remainder of the test with the exception of the ECR(HY)-10h-35 specimens at weeks 34, 56, 58, 62 and 63. As shown in Figure 3.50(b), the ECR(DCI)-10h-35 specimens are the only ECR specimen to exhibit active corrosion in the bottom mat for a period of time longer

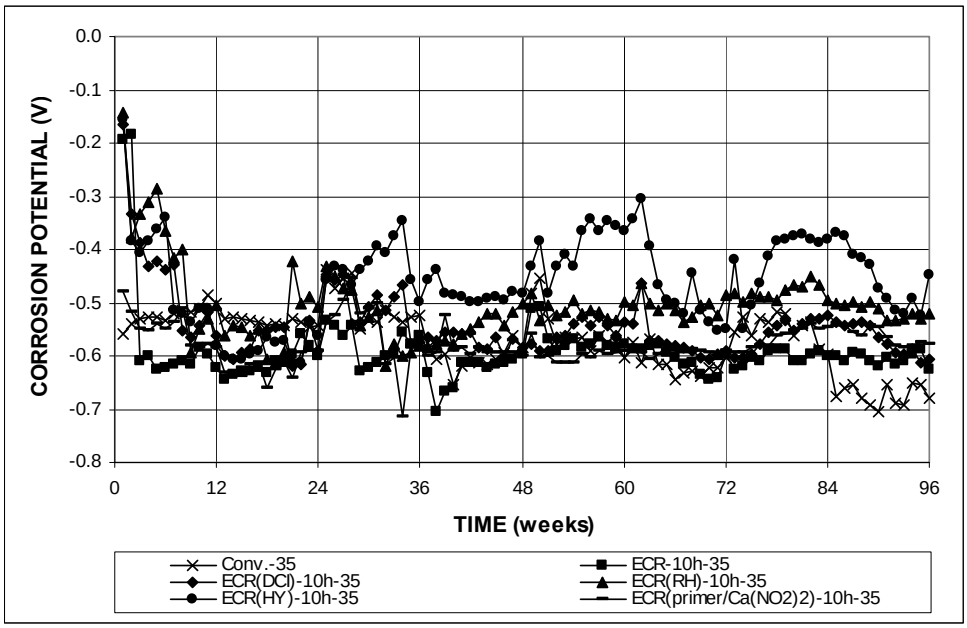

Figure 3.50 (a) – Average top mat corrosion potential, cracked beam test for specimens containing conventional steel, ECR, ECR in concrete with corrosion inhibitors, and ECR with a calcium nitrite primer, *w/c* = 0.35. Bars with ten holes in epoxy coating.

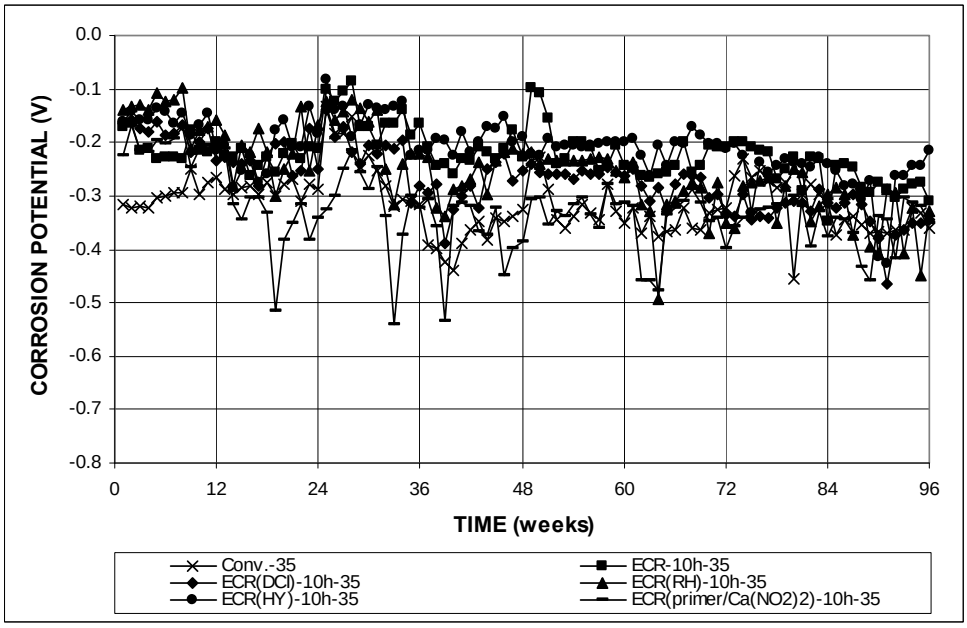

Figure 3.50 (b) – Average bottom mat corrosion potential, cracked beam test for specimens containing conventional steel, ECR, ECR in concrete with corrosion inhibitors, and ECR with a calcium nitrite primer, *w/c* = 0.35. Bars with ten holes in epoxy coating.

than three weeks, beginning at week 90. All other ECR specimens exhibit brief periods (less than three consecutive weeks) of active corrosion in the bottom mat, with the exception of the ECR-10h-35 control specimens, which never attain a corrosion potential less than –0.350 V in the bottom mat for the entire duration of the test.

3.3 Increased Adhesion ECR

This section presents the results of the Southern Exposure and cracked beam test specimens containing ECR with an increased adhesion between the epoxy coating and steel. Two types of ECR with improved adhesion epoxy coatings manufactured by DuPont and Valspar, along with ECR that was pretreated with zinc chromate prior to coating with a conventional epoxy, are evaluated. The high adhesion epoxy-coated bars are evaluated with the coatings penetrated with four or ten holes through the epoxy cast in concrete with w/c = 0.45. Each system is evaluated using three Southern Exposure and three cracked beam specimens.

3.3.1 Southern Exposure Test

Figures 3.51 and 3.52 show the average corrosion rates based on total and exposed area, respectively, for ECR specimens with increased adhesion cast in concrete with w/c = 0.45 and with four holes through the epoxy layer. Figure 3.51(a) compares the high corrosion rate based on total area for the control specimens containing conventional steel with the low corrosion rates of the specimens containing epoxy-coated reinforcement, including conventional ECR. As shown in

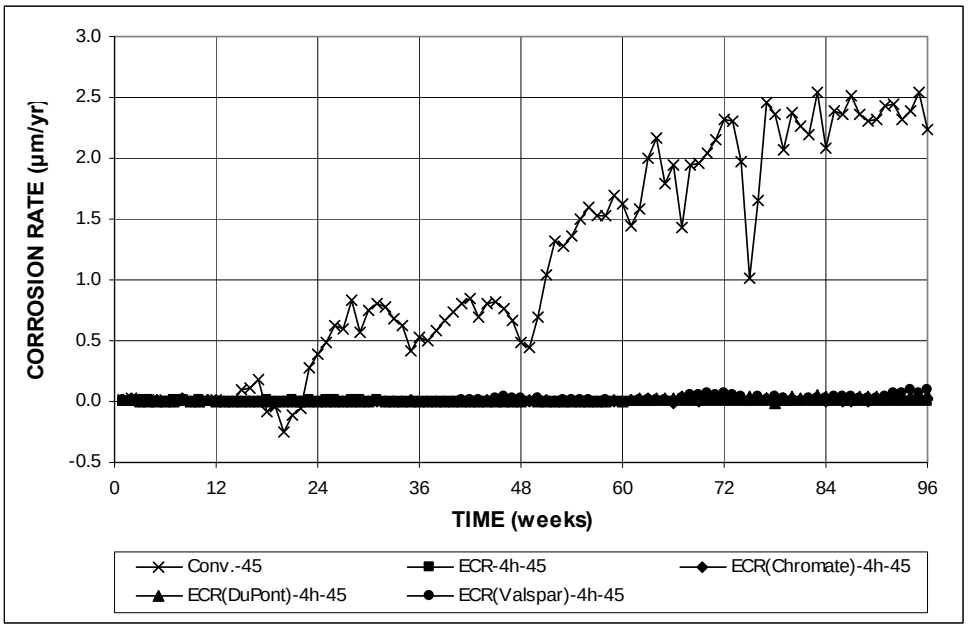

Figure 3.51 (a) – Average corrosion rate, Southern Exposure test for specimens containing conventional steel, ECR, and ECR with increased adhesion, *w/c* = 0.45. Bars with coating containing four holes through the epoxy.

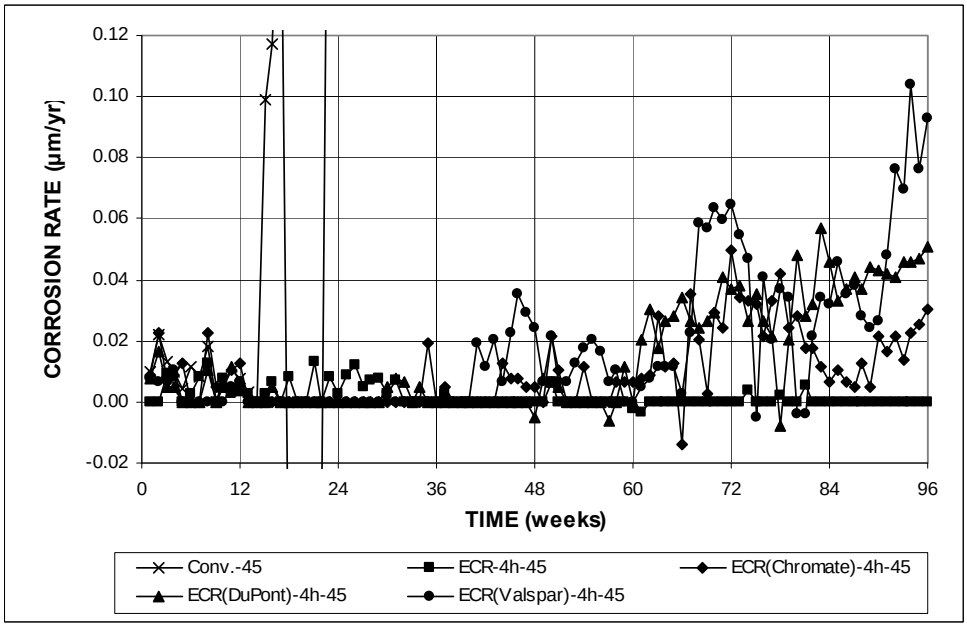

Figure 3.51 (b) – Average corrosion rate, Southern Exposure test for specimens containing conventional steel, ECR, and ECR with increased adhesion, *w/c* = 0.45. Bars with coating containing four holes through the epoxy. (Different scale)

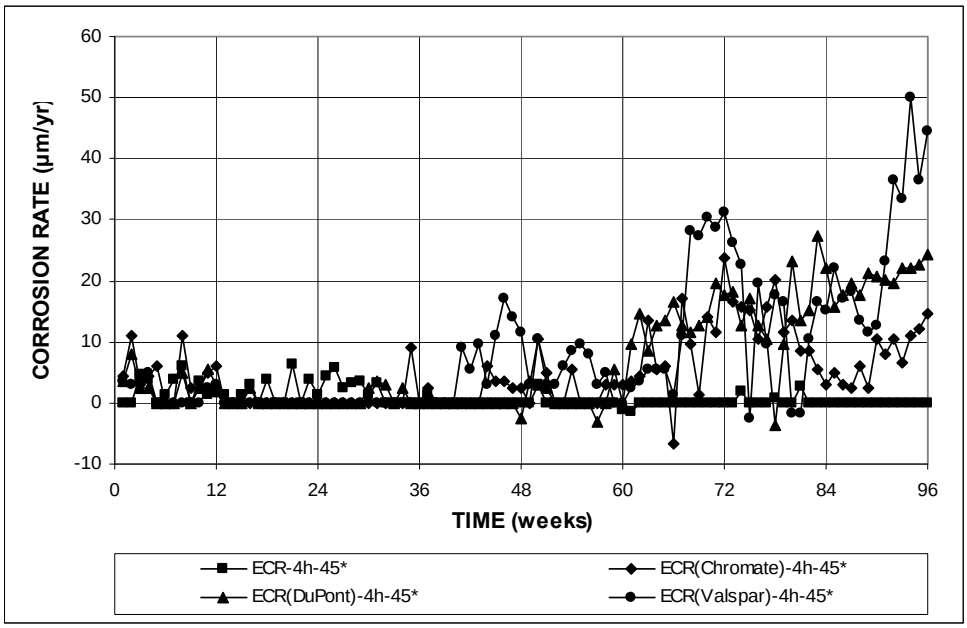

Figure 3.52 – Average corrosion rate based on exposed area, Southern Exposure test for specimens containing conventional ECR and ECR with increased adhesion, *w/c* = 0.45. Bars with coating containing four holes through the epoxy.

Figures 3.51(b) and 3.52, the ECR(Valspar)-4h-45 specimens begin exhibiting elevated corrosion rates at week 41 and continue to exhibit measurable corrosion for the remainder of the test. The ECR(DuPont)-4h-45 and ECR(Chromate)-4h-45 specimens exhibit sustained periods of measurable corrosion beginning at weeks 60 and 63, respectively.

Figures 3.53 and 3.54 show the average corrosion rates based on total and exposed area, respectively, for ECR specimens with increased adhesion cast in concrete with *w/c* = 0.45 and with ten holes through the epoxy layer. Figure 3.53(a), compares the high corrosion rate based on total area for the specimens containing conventional steel with the low corrosion rates of the specimens containing epoxy-coated reinforcement. As shown in Figures 3.53(b) and 3.54, the ECR(Chromate)-10h-

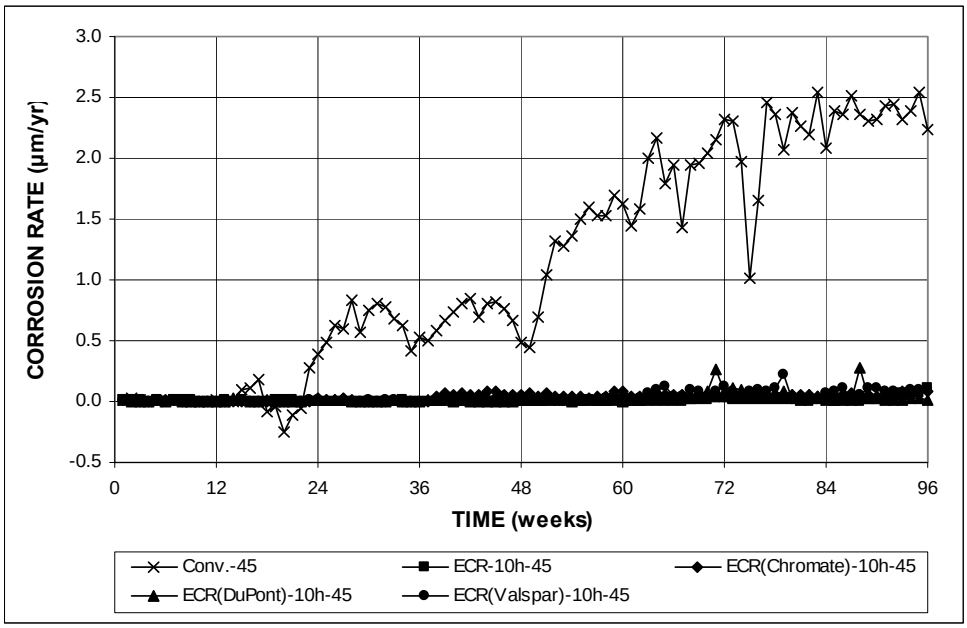

Figure 3.53 (a) – Average corrosion rate, Southern Exposure test for specimens containing conventional steel, ECR, and ECR with increased adhesion, *w/c* = 0.45. Bars with coating containing ten holes through the epoxy.

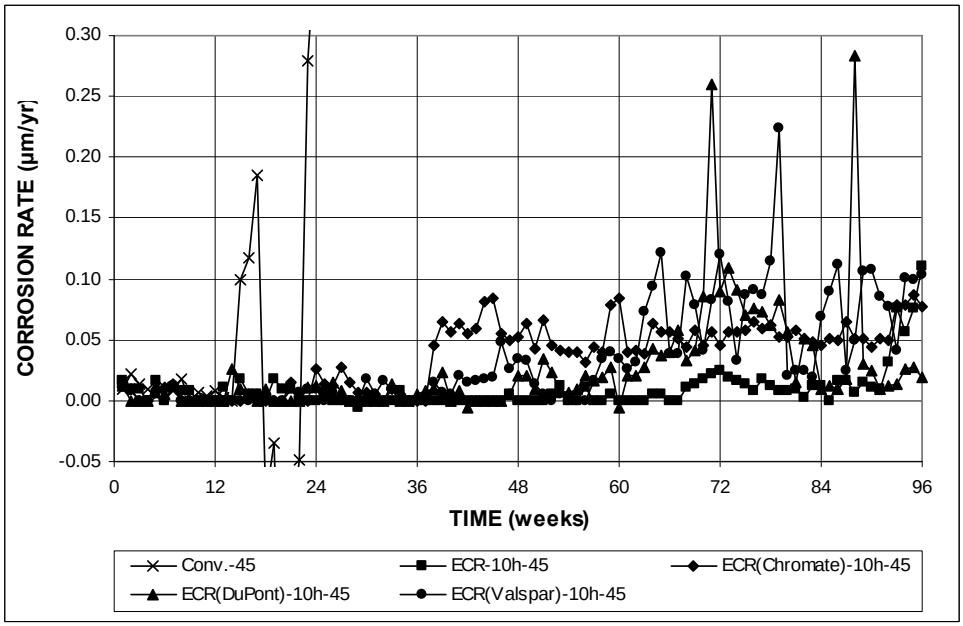

Figure 3.53 (b) – Average corrosion rate, Southern Exposure test for specimens containing conventional steel, ECR, and ECR with increased adhesion, *w/c* = 0.45. Bars with coating containing ten holes through the epoxy. (Different scale)

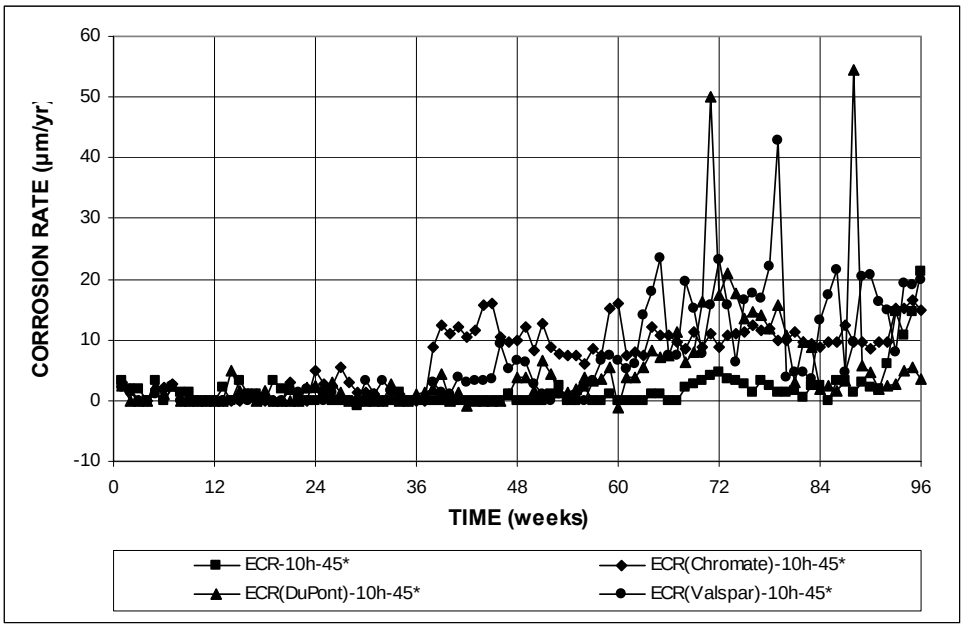

Figure 3.54 – Average corrosion rate based on exposed area, Southern Exposure test for specimens containing conventional ECR and ECR with increased adhesion, *w/c* = 0.45. Bars with coating containing ten holes through the epoxy.

45 specimens begin exhibiting corrosion rates that are higher than the other ECR specimens beginning at week 38, and continue until week 63, when all three increased adhesion ECR specimens begin exhibiting similar corrosion rates.

Figures 3.55 and 3.56 show the average corrosion losses, based on total and exposed area, respectively, for increased adhesion ECR specimens cast in concrete with a *w/c* ratio of 0.45 containing four holes through the epoxy layer. Figure 3.55 compares the high corrosion rate based on total area for the specimens containing conventional steel with the low corrosion rates of the specimens containing epoxy-coated reinforcement. As shown in Figure 3.56, the increased adhesion ECR holds no advantage over conventional ECR. The ECR(Chromate)-4h-45 and ECR(Valspar)-4h-45 specimens exhibit higher average corrosion losses than the ECR control specimens

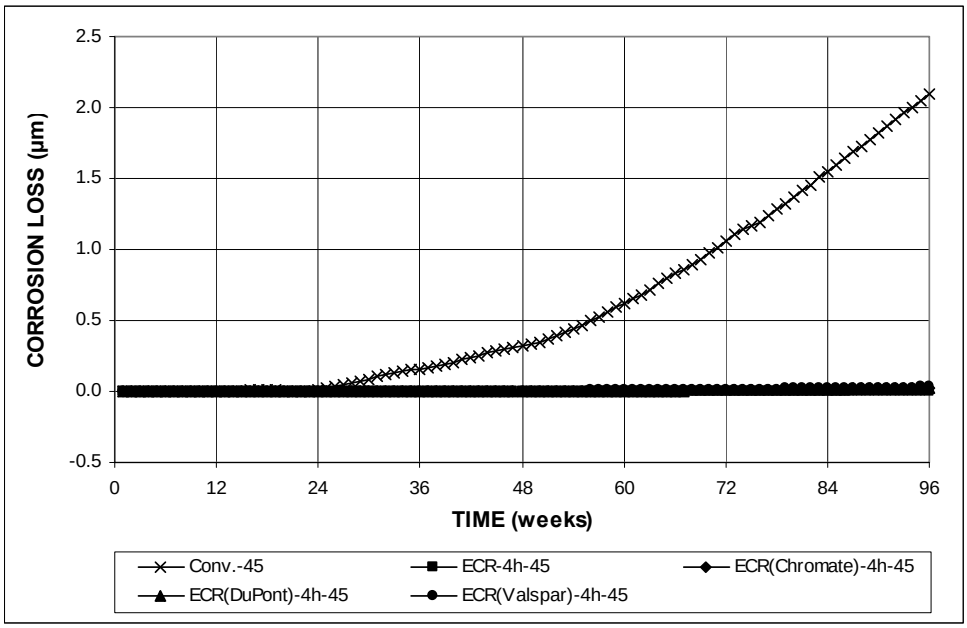

Figure 3.55 – Average corrosion loss, cracked beam test for specimens containing conventional steel, ECR, and ECR with increased adhesion, *w/c* = 0.45. Bars with coating containing four holes through the epoxy.

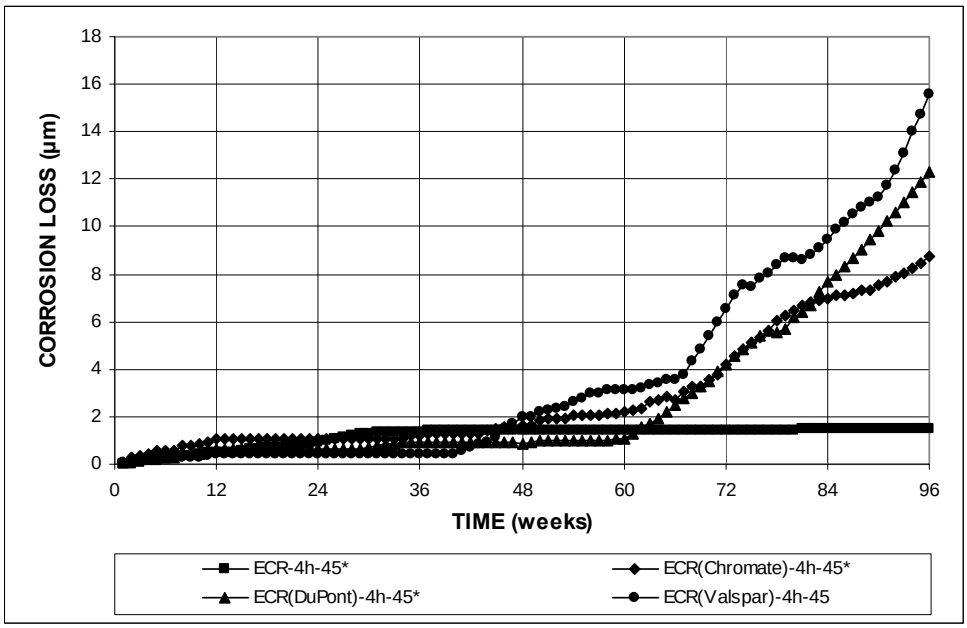

Figure 3.56 – Average corrosion loss based on exposed area, cracked beam test for specimens containing conventional ECR and ECR with increased adhesion, *w/c* = 0.45. Bars with coating containing four holes through the epoxy.

beginning at weeks 44 and 46, respectively. The average corrosion loss exhibited by the ECR(DuPont)-4h-45 specimens surpass that exhibited by the control specimens at week 62. Corrosion initiation, characterized by a discontinuity in the slope of the corrosion loss graph, is first observed in the ECR(Valspar)-4h-45 specimens at week 41. As shown in Figure A.89(b), this is due to corrosion that occurs in specimen ECR(Valspar)-4h-45-1 and to a lesser extent in specimen ECR(Valspar)-4h-45-2. At week 68, the corrosion rate of the ECR(Valspar)-4h-45 specimens appears to increase; this is due to corrosion initiation occurring in specimen 3, as shown in Figure A.89(b). At week 44, the ECR(Chromate) specimens begin to show indications of corrosion initiation, with a corrosion rate that initially remains low and then gradually increases with time. The last specimens to exhibit corrosion initiation are the ECR(DuPont)-4h-45 specimens at 61 weeks, with corrosion observed in all three specimens, as shown in Figure A.79(b).

Figures 3.57 and 3.58 show the average corrosion losses, based on total and exposed area, respectively, for increased adhesion ECR specimens cast in concrete with a *w/c* ratio of 0.45 containing bars with ten holes through the epoxy layer. Figure 3.57 compares the high corrosion losses based on total area for the specimens containing conventional steel with the low corrosion losses of the specimens containing epoxy-coated reinforcement. Figure 3.58 shows that for specimens with ten holes through the epoxy, the increased adhesion ECR holds no advantage over the ECR control specimens. Corrosion initiation is first observed in the ECR(Chromate)-10h-45 specimens at week 38. As shown in Figure A.73(b), this is due to corrosion

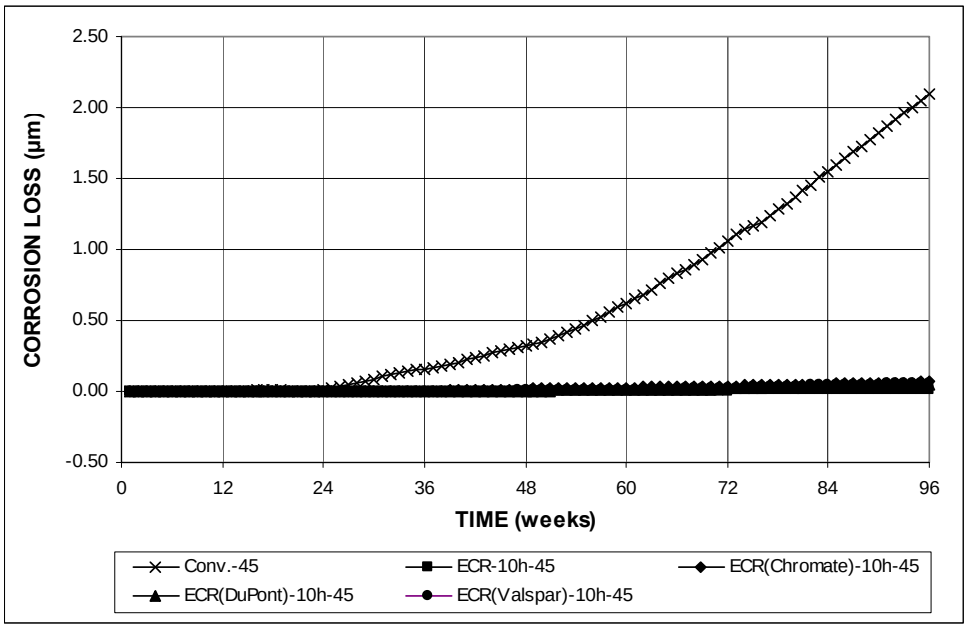

Figure 3.57 – Average corrosion loss, cracked beam test for specimens containing conventional steel, ECR, and ECR with increased adhesion, *w/c* = 0.45. Bars with coating containing ten holes through the epoxy.

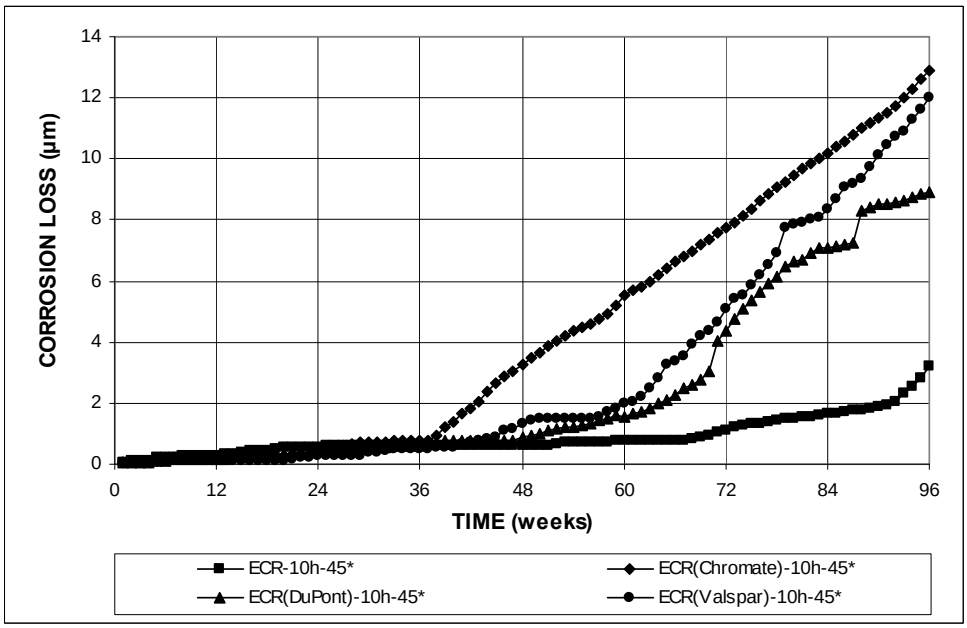

Figure 3.58 – Average corrosion loss based on exposed area, cracked beam test for specimens containing conventional ECR and ECR with increased adhesion, *w/c* = 0.45. Bars with coating containing ten holes through the epoxy.

initiation occurring in one out of three specimens. At week 38, corrosion also appears to initiate in the ECR(Valspar)-10h-45 specimens, although this initiation is less pronounced than the initiation observed in the ECR(Chromate)-10h-45 specimens. At week 50, the ECR(Valspar)-10h-45 specimens appear to passivate, and further corrosion activity is not observed in these specimens until week 57. At week 48, corrosion initiation is observed in the ECR(DuPont)-10h-45 specimens. By week 41, all of the increased adhesion ECR specimens exhibit higher average corrosion losses than the ECR control specimens.

Table 3.6 summarizes the total corrosion losses as measured in the Southern Exposure specimens with increased adhesion ECR. Based on total area, all ten-hole specimens exhibit higher corrosion loss than their four-hole counterparts. The ECR(Chromate)-10h-45 specimens exhibit the highest corrosion loss, 0.067 μm, followed closely by the ECR(Valspar)-10h-45 specimens with a corrosion loss of 0.063 μm. The ECR(DuPont)-10h-45 specimens exhibit the least amount of corrosion loss based on total area, 0.046 μm, among specimens with ten holes through the epoxy. For specimens with four holes through the epoxy, the ECR(Valspar)-4h-45 specimens exhibit the highest corrosion loss, 0.032 μm, followed by the ECR(DuPont)-4h-45 and ECR(Chromate)-4h-45 specimens, with corrosion losses of 0.026 and 0.018 μm, respectively. Based on exposed area, the ECR(Valspar)-4h-45 and ECR(Chromate)-10h-45 specimens exhibit the highest corrosion losses among the increased adhesion ECR specimens, with losses of 15.6 and 12.9 μm, respectively. The ECR(Chromate)-4h-45 and ECR(DuPont)-10h-45 specimens exhibit the lowest

corrosion loss based on exposed area among all of the increased adhesion ECR specimens, with losses of 8.76 and 8.90 μm, respectively. As previously mentioned, all increased adhesion specimens exhibit higher corrosion loss, based both on total and exposed area, than the ECR control specimens. In fact, based on exposed area, the total corrosion losses measured in the increased adhesion ECR specimens range from 5.8 to 10.3 times the amount of corrosion loss measured in the specimens containing conventional ECR. When analyzing the data from individual specimens, only two increased adhesion ECR specimens, ECR(Chromate)-4h-45-1 and ECR(Chromate)-10h-45-1, exhibit corrosion losses lower than the highest corrosion loss observed in a corresponding individual control specimen. From this data, it

Table 3.6 – Average corrosion loss (μm) at week 96 as measured in the Southern Exposure test for specimens increased adhesion ECR

Steel Designation[a]	Specimen			Average	Standard Deviation
	1	2	3		
Total Area					
ECR(Chromate)-4h-45	0.004	0.015	0.035	0.018	0.016
ECR(Chromate)-10h-45	0.011	0.068	0.123	0.067	0.056
ECR(DuPont)-4h-45	0.031	0.017	0.030	0.026	0.008
ECR(DuPont)-10h-45	0.029	0.060	0.050	0.046	0.016
ECR(Valspar)-4h-45	0.039	0.015	0.044	0.032	0.016
ECR(Valspar)-10h-45	0.054	0.044	0.090	0.063	0.024
Exposed Area					
ECR(Chromate)-4h-45*	2.11	7.28	16.9	8.76	7.50
ECR(Chromate)-10h-45*	2.04	13.0	23.7	12.9	10.8
ECR(DuPont)-4h-45*	14.7	7.99	14.3	12.3	3.77
ECR(DuPont)-10h-45*	5.52	11.5	9.68	8.90	3.07
ECR(Valspar)-4h-45*	18.8	7.00	21.0	15.6	7.51
ECR(Valspar)-10h-45*	10.3	8.53	17.2	12.0	4.58

[a] ECR(Chromate) = ECR with the chromate pretreatment.
ECR(DuPont) = ECR with high adhesion DuPont coating.
ECR(Valspar) = ECR with high adhesion Valspar coating.
4h = bar with four holes through epoxy, 10h = bar with 10 holes through epoxy.
45 = concrete with *w/c* =0.45; 35 = concrete with *w/c* =0.35.

* Corrosion loss calculation based on the exposed area of four or ten 3-mm (1/8-in.) diamter holes.

appears that the increased adhesion epoxies do not improve the corrosion performance of the reinforcement.

Figures 3.59 and 3.60 show the average mat-to-mat resistances for the increased adhesion ECR specimens cast with four and ten holes through the epoxy, respectively. For both four-hole and ten-hole specimens, the average mat-to-mat resistance of all specimens gradually increases with time. As shown in Figure 3.59, increased adhesion ECR specimens with four holes through the epoxy generally exhibit lower average mat-to-mat resistances than the control ECR specimens. After week 63, the scatter in the average mat-to-mat resistances for all specimens increases significantly, possibly due to additional cracking within the specimens, as previously discussed. No conclusions can be made from this data. However, the lower mat-to-

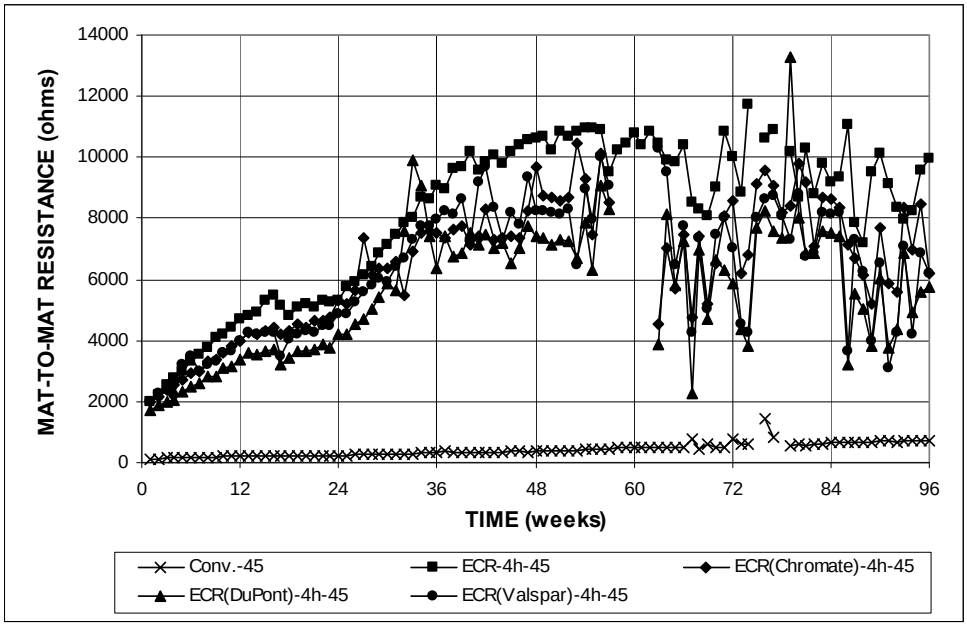

Figure 3.59 – Average mat-to-mat resistance, Southern Exposure test for specimens containing conventional steel, ECR, and ECR with increased adhesion, *w/c* = 0.45. Bars with four holes in epoxy coating.

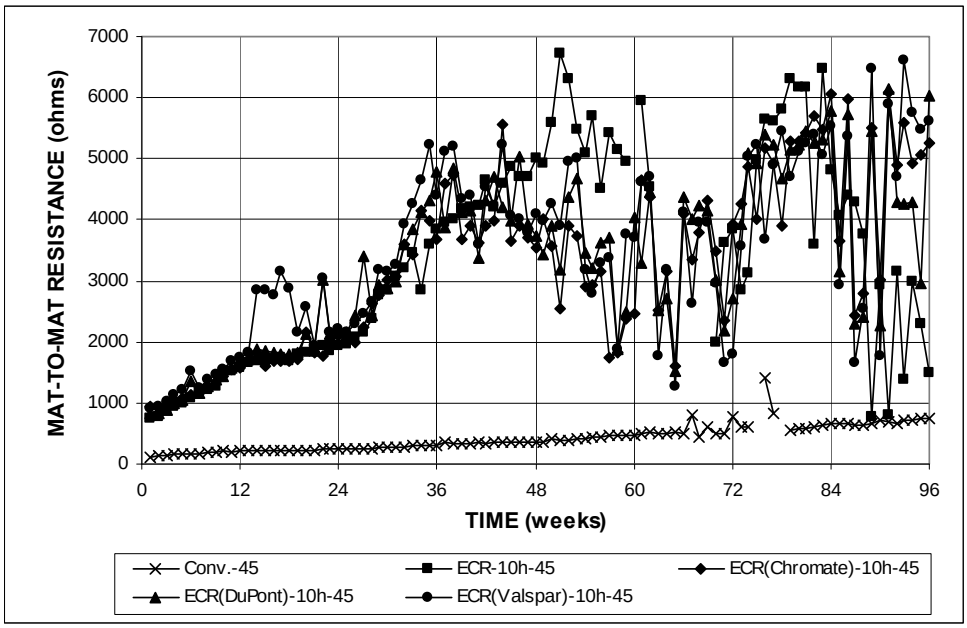

Figure 3.60 – Average mat-to-mat resistance, Southern Exposure test for specimens containing conventional steel, ECR, and ECR with increased adhesion, *w/c* = 0.45. Bars with four holes in epoxy coating.

mat resistances observed in the increased adhesion ECR specimens during the first 60 weeks suggests that the epoxy in these systems may not isolate the underlying steel as efficiently as the in the ECR control specimens. Figure 3.60 shows that for the first 48 weeks, ECR control specimens and increased adhesion ECR specimens exhibit similar mat-to-mat resistances, except for the ECR(Valspar)-10h-45 specimens between weeks 14 through 23 and weeks 32 through 38, which exhibit slightly higher mat-to-mat resistances than the other ECR specimens during these periods. No conclusions can be drawn from the data after week 48 due to the large amount of scatter present in the data.

Figure 3.61 shows the average top mat and bottom mat corrosion potentials versus a copper-copper sulfate electrode for increased adhesion ECR specimens with

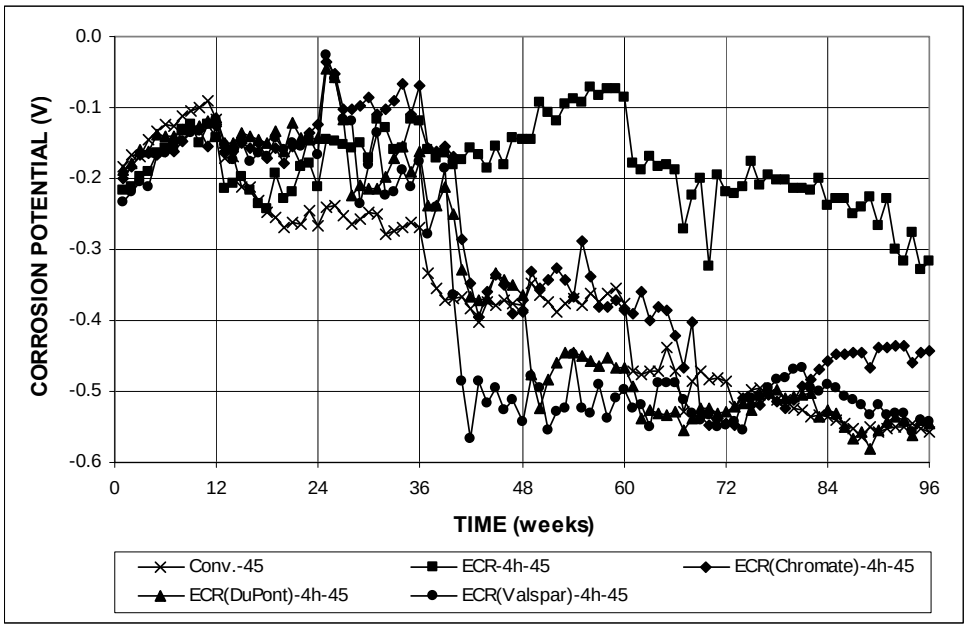

Figure 3.61 (a) – Average top mat corrosion potential, Southern Exposure test for specimens containing conventional steel, ECR, and ECR with increased adhesion, *w/c* = 0.45. Bars with four holes in epoxy coating.

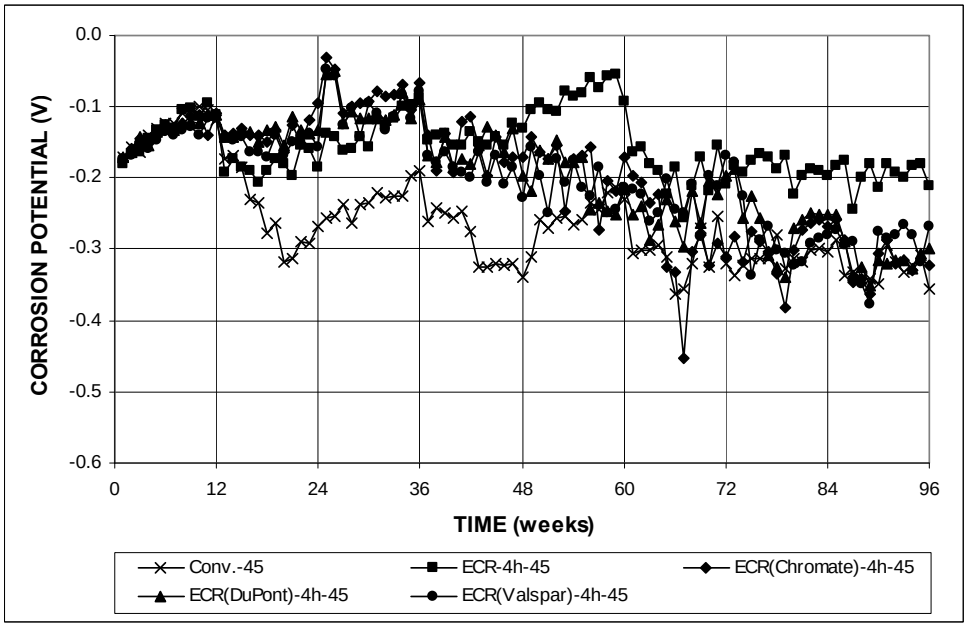

Figure 3.61 (b) – Average bottom mat corrosion potential, Southern Exposure test for specimens containing conventional steel, ECR, and ECR with increased adhesion, *w/c* = 0.45. Bars with four holes in epoxy coating.

four holes through the epoxy layer. As shown in Figure 3.61(a), active corrosion, characterized by a corrosion potential more negative than –0.350 V, is observed first in conventional steel before being observed in ECR specimens. Active corrosion is observed in the top mats of all three increased adhesion ECR systems as opposed to the ECR control specimens, which never exhibit active corrosion based on corrosion potential in the top mat during the study. The ECR(Valspar)-4h-45 specimens are the first group to exhibit active corrosion in the top mat at week 40, only two weeks after the conventional steel specimens begin to exhibit active corrosion in the top mat. The ECR(DuPont)-4h-45 and ECR(Chromate)-4h-45 specimens begin exhibiting active corrosion in the top mat at weeks 42 and 43, respectively. Once active corrosion is observed in the top mat of the increased adhesion ECR specimens, it is observed for the remainder of the test, with the exception of the ECR(DuPont)-4h-45 specimens at weeks 45 and 46 and the ECR(Chromate)-4h-45 specimens at weeks 45, 49, 51-53, and 55-56. As shown in Figure 3.61(b), average corrosion potentials in the bottom mats of the increased adhesion ECR specimens remain more positive than -0.350 V, indicating a low probability of corrosion, with the exception of the ECR(Chromate)-4h-45 specimens at weeks 67, 79, and 89, and the ECR(DuPont)-4h-45 and ECR(Valspar)-4h-45 specimens at week 89. The control specimens exhibit no active corrosion in the bottom mat during the study.

Figure 3.62 shows the average top mat and bottom mat corrosion potentials versus a copper-copper sulfate electrode for increased adhesion ECR specimens with ten holes through the epoxy layer. As with the increased adhesion ECR specimens

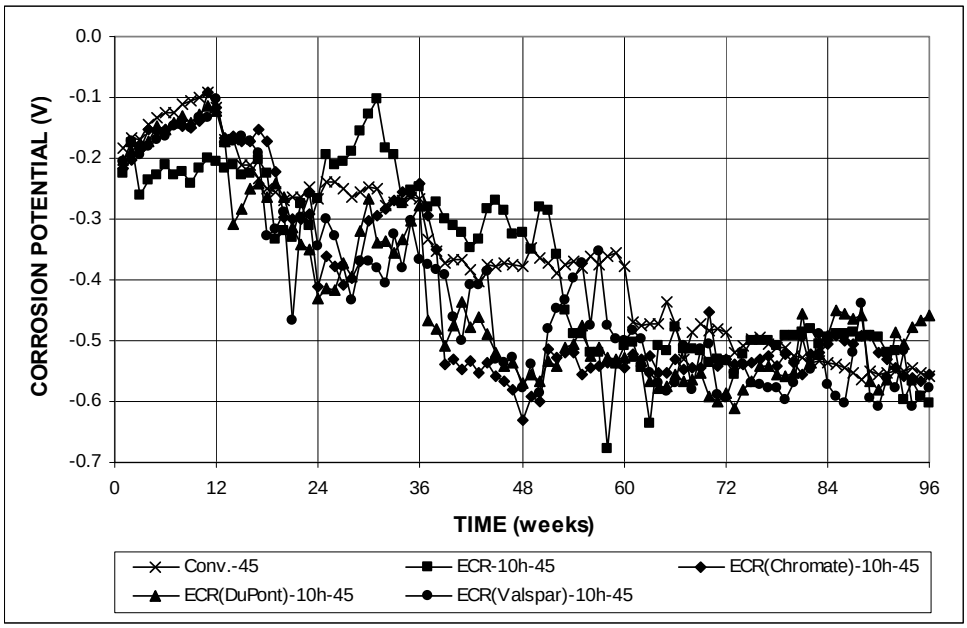

Figure 3.62 (a) – Average top mat corrosion potential, Southern Exposure test for specimens containing conventional steel, ECR, and ECR with increased adhesion, *w/c* = 0.45. Bars with ten holes in epoxy coating.

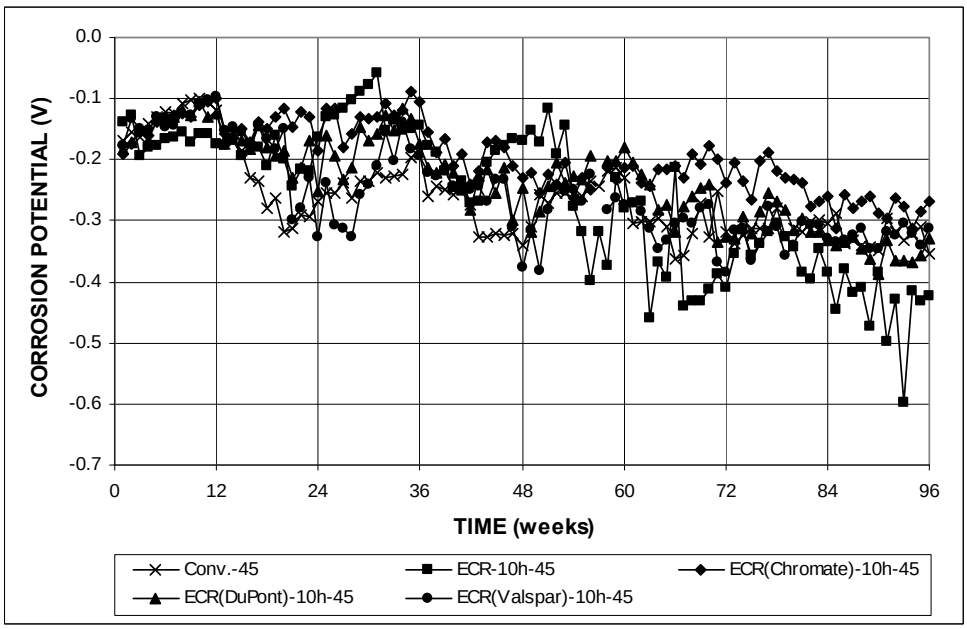

Figure 3.62 (b) – Average bottom mat corrosion potential, Southern Exposure test for specimens containing conventional steel, ECR, and ECR with increased adhesion, *w/c* = 0.45. Bars with ten holes in epoxy coating.

with four holes through the epoxy, the increased adhesion ECR specimens with ten holes through the epoxy begin exhibiting active corrosion in the top mat before the control ECR specimens. As shown in Figure 3.62(a), the first increased adhesion ECR specimens to exhibit active corrosion in the top mat are the ECR(Valspar)-10h-45 specimens at week 21, followed by the ECR(DuPont)-10h-45 and ECR(Chromate)-10h-45 specimens at weeks 23 and 24, respectively. As would be expected, the ten-hole specimens exhibit corrosion sooner than the four-hole specimens. This is due to a greater area of steel being exposed to the pore solution, which increases the probability of exposure to chloride ions. After an initial period of active corrosion that lasts for six weeks, the ECR(Chromate)-10h-45 and ECR(DuPont)-10h-45 specimens appear to enter a period of passivity lasting approximately eight weeks, after which active corrosion is exhibited for the remainder of the test. After week 21, the ECR(Valspar)-10h-45 specimens exhibit a five week passive period, but then exhibit active corrosion beginning at week 27 and continuing for the remainder of the test, with the exception of weeks 33 and 35.

Figure 3.62(b) shows that active corrosion in the bottom mat is first observed in the ECR(Valspar)-10h-45 specimens at week 71, and is again observed at weeks 72, 75, and 80. The ECR(DuPont)-10h-45 specimens exhibit corrosion in the bottom mat between weeks 89 and 95, excluding week 91. The ECR(Chromate)-10h-45 specimens are the only ECR specimens to not exhibit active corrosion in the bottom mat based on corrosion potential during the 96-week test.

3.3.2 Cracked Beam Tests

Figures 3.63 and 3.64 show the average corrosion rates based on total and exposed area, respectively, for ECR specimens with increased adhesion cast in concrete with *w/c* = 0.45 and with four holes through the epoxy layer. Figure 3.63(a) compares the high corrosion rates based on total area for the specimens containing conventional steel with the low corrosion rates of the specimens containing epoxy-coated reinforcement. As shown in Figures 3.63(b) and 3.64, all ECR specimens exhibit similar corrosion rates, with the exception of the ECR(Valspar)-4h-45 specimens at week 51 and the ECR(DuPont)-4h-45 specimens from week 62 to 96. The high corrosion rate exhibited by the ECR(Valspar)-4h-45 specimens at week 51

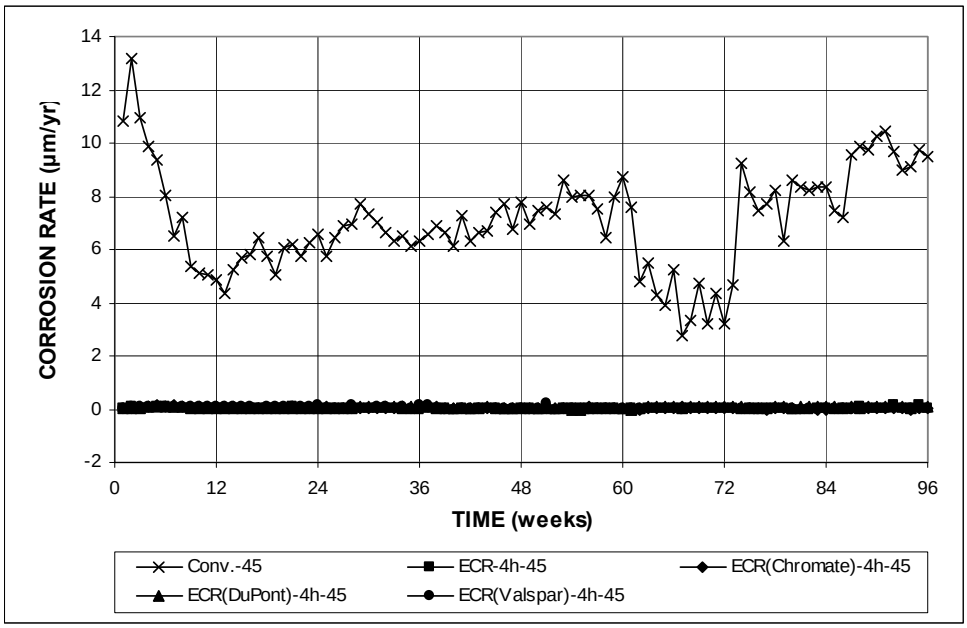

Figure 3.63 (a) – Average corrosion rate, cracked beam test for specimens containing conventional steel, ECR, and ECR with increased adhesion, *w/c* = 0.45. Bars with coating containing four holes through the epoxy.

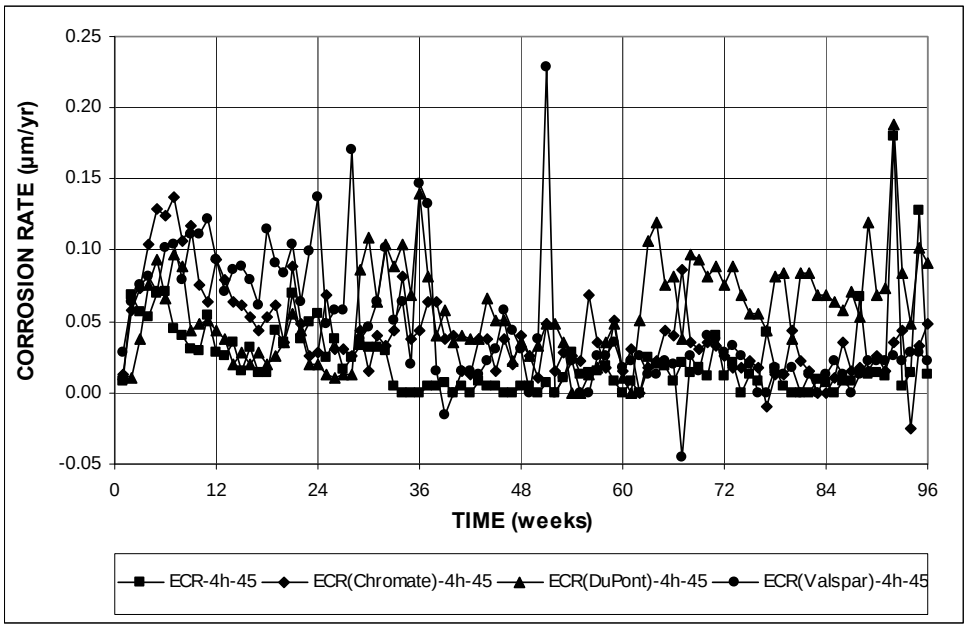

Figure 3.63 (b) – Average corrosion rate, cracked beam test for specimens containing conventional steel, ECR, and ECR with increased adhesion, *w/c* = 0.45. Bars with coating containing four holes through the epoxy. (Different scale)

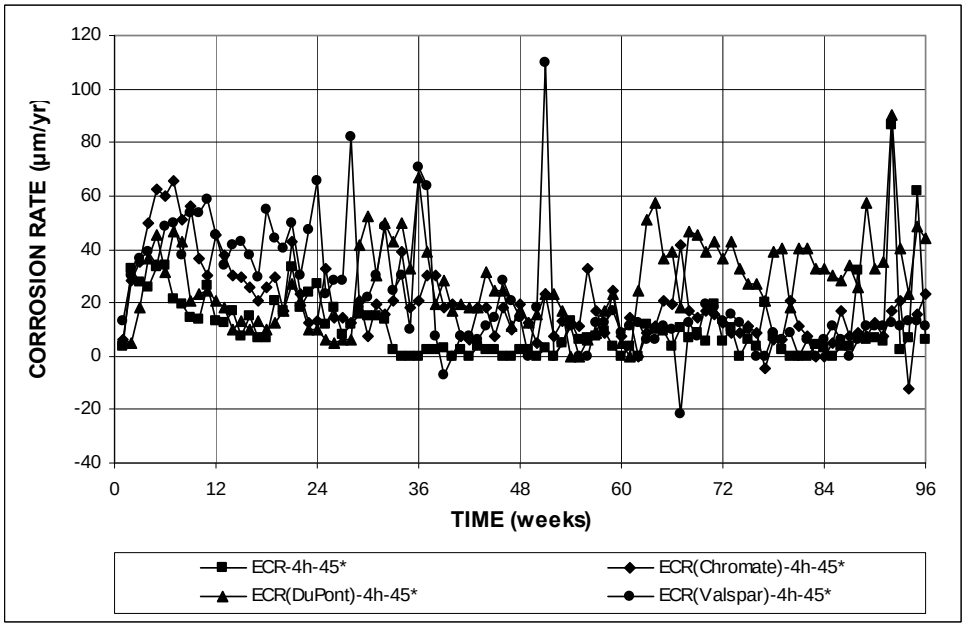

Figure 3.64 – Average corrosion rate based on exposed area, cracked beam test for specimens containing conventional steel, ECR, and ECR with increased adhesion, *w/c* = 0.45. Bars with coating containing four holes through the epoxy.

was observed in one specimen, and in all likelihood, is due to an aberrant reading. From weeks 62 through 96, the ECR(DuPont)-4h-45 specimens exhibit slightly higher corrosion rates than the other ECR specimens.

Figures 3.65 and 3.66 show the average corrosion rates based on total and exposed area, respectively, for ECR specimens with increased adhesion cast in concrete with *w/c* = 0.45 and with ten holes through the epoxy layer. Figure 3.65(a) compares the high corrosion rates based on total area for the specimens containing conventional steel with the low corrosion rates of the specimens containing epoxy-coated reinforcement. As shown in Figures 3.65(b) and 3.66, all high adhesion ECR specimens exhibit similar to or slightly higher than the ECR control specimens.

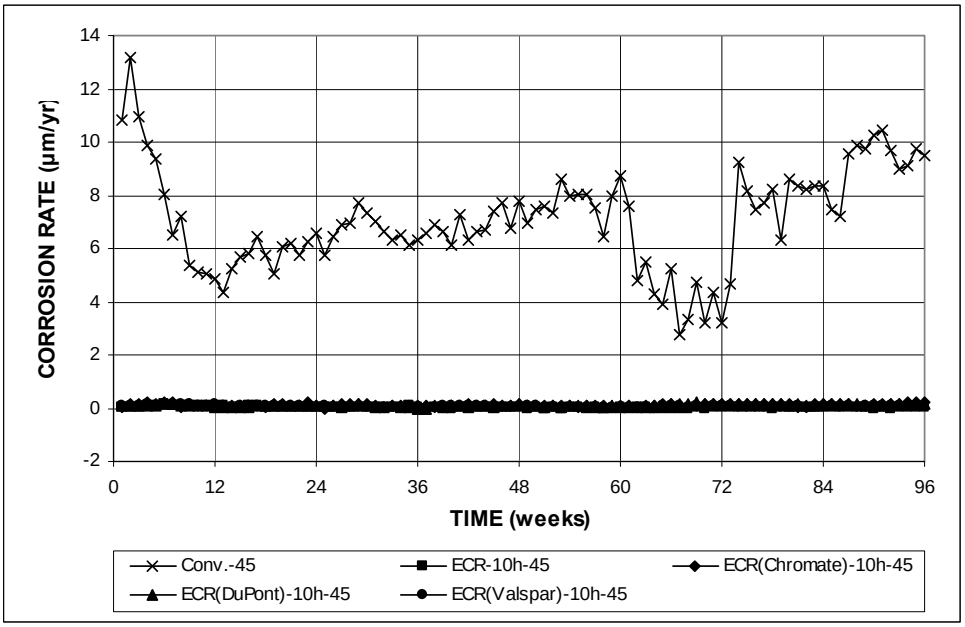

Figure 3.65 (a) – Average corrosion rate, cracked beam test for specimens containing conventional steel, ECR, and ECR with increased adhesion, *w/c* = 0.45. Bars with coating containing ten holes through the epoxy.

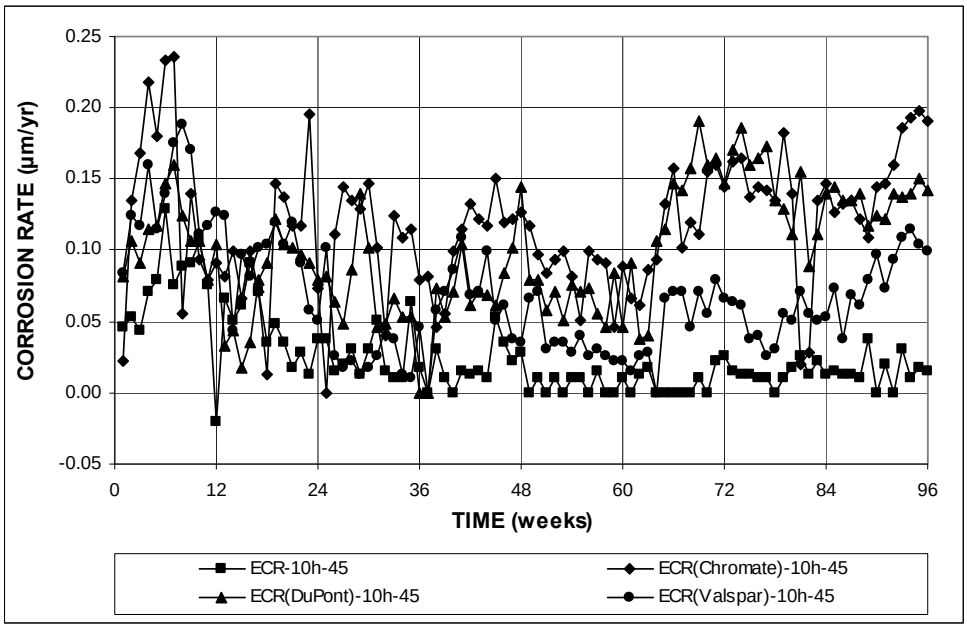

Figure 3.65 (b) – Average corrosion rate, cracked beam test for specimens containing conventional ECR and ECR with increased adhesion, *w/c* = 0.45. Bars with coating containing ten holes through the epoxy. (Different scale)

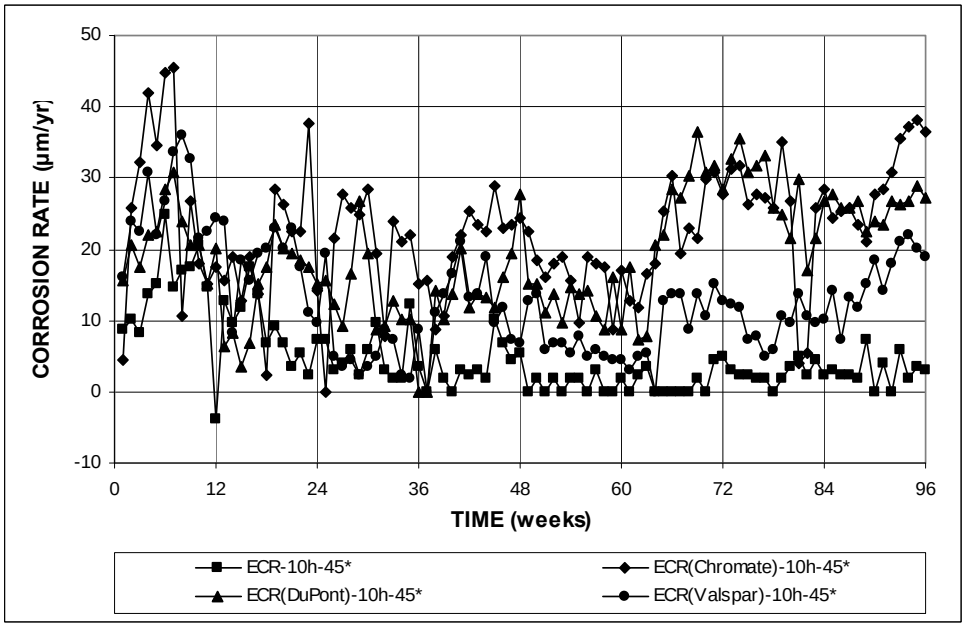

Figure 3.66 – Average corrosion rate based on exposed area, cracked beam test for specimens containing conventional ECR and ECR with increased adhesion, *w/c* = 0.45. Bars with coating containing ten holes through the epoxy.

Figures 3.67 and 3.68 show the average corrosion loss based on total and exposed area, respectively, for ECR specimens with increased adhesion cast in concrete with *w/c* = 0.45 and with four holes through the epoxy layer. Figure 3.67 compares the high corrosion rates based on total area for the specimens containing conventional steel with the low corrosion rates of the specimens containing epoxy-coated reinforcement. As shown in Figure 3.68, the ECR(Valspar)-4h-45 and ECR(Chromate)-4h-45 specimens exhibit similar corrosion losses for the first 18 weeks of the test and exhibit higher corrosion rates, characterized by the slope of the corrosion loss graph, than the ECR(DuPont)-4h-45 and ECR control specimens. After week 18, the ECR(Valspar)-4h-45 specimens exhibit higher corrosion losses than the other ECR specimens until week 79. The ECR(DuPont)-4h-45 specimens,

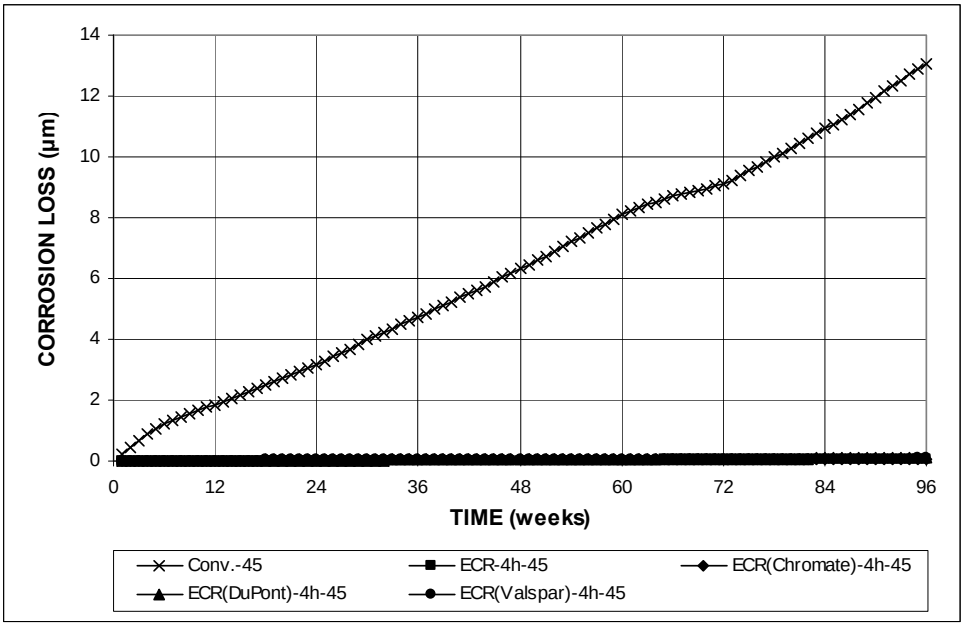

Figure 3.67 – Average corrosion loss, cracked beam test for specimens containing conventional steel, ECR, and ECR with increased adhesion, *w/c* = 0.45. Bars with coating containing four holes through the epoxy.

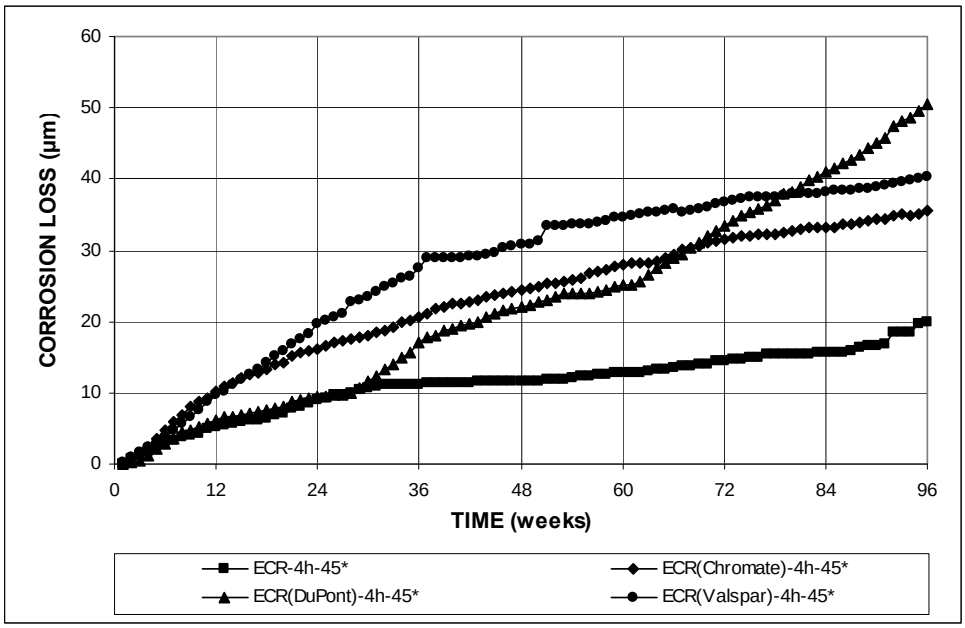

Figure 3.68 – Average corrosion loss based on exposed area, cracked beam test for specimens containing conventional ECR and ECR with increased adhesion, *w/c* = 0.45. Bars with coating containing four holes through the epoxy.

which initially exhibit corrosion losses similar to ECR control specimens, begin to show an increased corrosion rate at week 30, and by week 79, exhibit the highest corrosion loss of all the ECR specimens. At no point during the study did the increased adhesion ECR specimens show any advantage, in terms of corrosion loss, over the ECR control specimens.

Figures 3.69 and 3.70 show the average corrosion loss based on total and exposed area, respectively, for ECR specimens with increased adhesion cast in concrete with *w/c* = 0.45 and with ten holes through the epoxy layer. Figure 3.69 compares the high corrosion rates based on total area for the specimens containing conventional steel with the low corrosion rates of the specimens containing epoxy-coated reinforcement. As shown in Figure 3.70, the ECR(Chromate)-10h-45 and

ECR(Valspar)-10h-45 specimens show similar corrosion losses during the first 25 weeks of the test. At week 26, the ECR(Valspar)-10h-45 specimens appear to briefly passivate, while the ECR(Chromate)-10h-45 specimens continue to corrode at a nearly steady rate. After week 26, the ECR(Chromate)-10h-45 specimens continue to exhibit the highest corrosion losses of all the ECR specimens for the remainder of the test. Between weeks 26 and 55, the ECR(Valspar)-10h-45 and ECR(DuPont)-10h-45 specimens exhibit similar corrosion losses. Beginning at week 48, and continuing for the remainder of the test, the ECR(DuPont)-10h-45 specimens exhibit higher corrosion losses than the ECR(Valspar)-10h-45 specimens. During the entire test, the corrosion losses observed in the increased adhesion ECR specimens are higher than those observed in the ECR control specimens.

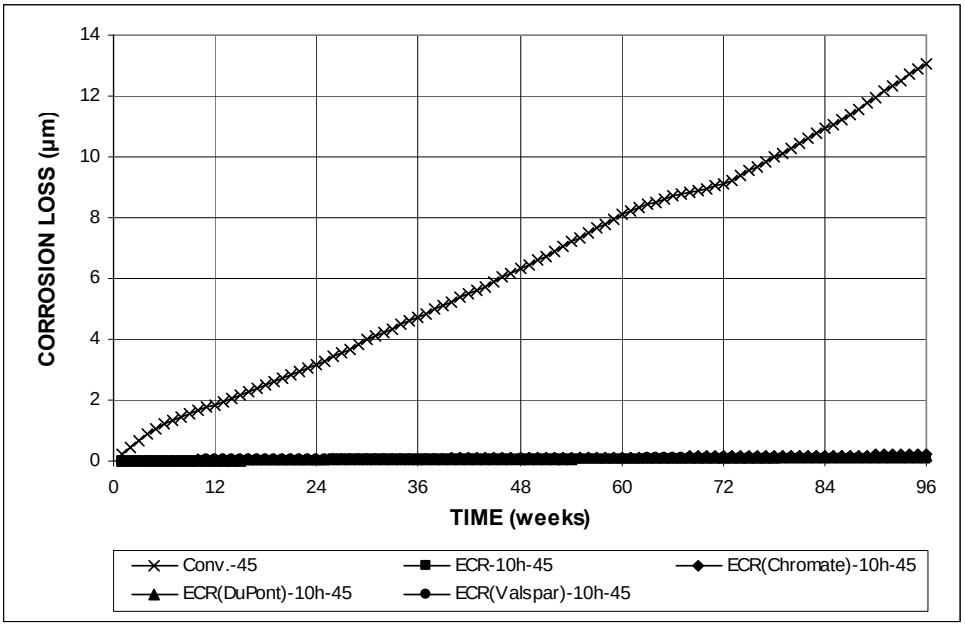

Figure 3.69 – Average corrosion loss, cracked beam test for specimens containing conventional steel, ECR, and ECR with increased adhesion, *w/c* = 0.45. Bars with coating containing ten holes through the epoxy.

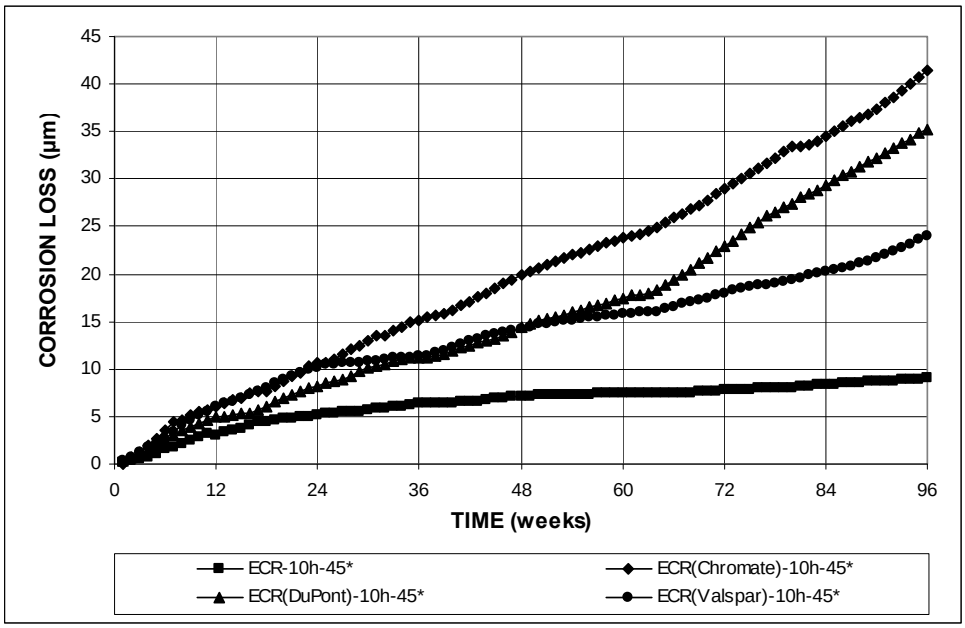

Figure 3.70 – Average corrosion loss based on exposed area, cracked beam test for specimens containing conventional ECR and ECR with increased adhesion, *w/c* = 0.45. Bars with coating containing ten holes through the epoxy.

Table 3.7 summarizes the total corrosion losses as measured in the cracked beam specimens containing increased adhesion ECR. Based on total area, all ten-hole specimens exhibit higher corrosion losses than their four-hole counterparts. Among the specimens with ten holes through the epoxy, the ECR(Chromate)-10h-45 and ECR(DuPont)-10h-45 specimens exhibit the highest corrosion losses, with values of 0.216 and 0.184 µm, respectively, based on total area. Among the specimens with four holes through the epoxy, the ECR(DuPont)-4h-45 and ECR(Valspar)-4h-45 specimens exhibit the highest corrosion loss based on exposed area, with values of 0.105 and 0.084 µm, respectively. Based on exposed area, the ECR(DuPont)-4h-45, ECR(Chromate)-10h-45, and ECR(Valspar)-4h-45 specimens exhibit the highest

corrosion loss among the increased adhesion ECR specimens, with losses of 50.4, 41.4, and 40.4 μm, respectively.

Table 3.7 – Average corrosion loss (μm) at week 96 as measured in the cracked beam test for specimens containing increased adhesion ECR

Steel Designation[a]	Specimen			Average	Standard Deviation
	1	2	3		
Total Area					
ECR(Chromate)-4h-45	0.066	0.058	0.099	0.074	0.022
ECR(Chromate)-10h-45	0.026	0.140	0.480	0.216	0.236
ECR(DuPont)-4h-45	0.124	0.137	0.054	0.105	0.045
ECR(DuPont)-10h-45	0.128	0.127	0.297	0.184	0.098
ECR(Valspar)-4h-45	0.172	0.071	0.009	0.084	0.082
ECR(Valspar)-10h-45	0.081	0.039	0.254	0.125	0.114
Exposed Area					
ECR(Chromate)-4h-45*	31.5	28.0	47.5	35.7	10.4
ECR(Chromate)-10h-45*	4.98	26.9	92.3	41.4	45.4
ECR(DuPont)-4h-45*	59.4	66.0	26.0	50.4	21.4
ECR(DuPont)-10h-45*	24.6	24.4	57.0	35.3	18.8
ECR(Valspar)-4h-45*	82.6	34.2	4.29	40.4	39.5
ECR(Valspar)-10h-45*	15.6	7.55	48.8	24.0	21.9

[a] ECR(Chromate) = ECR with the chromate pretreatment.
ECR(DuPont) = ECR with high adhesion DuPont coating.
ECR(Valspar) = ECR with high adhesion Valspar coating.
4h = bar with four holes through epoxy, 10h = bar with 10 holes through epoxy.
45 = concrete with *w/c* =0.45; 35 = concrete with *w/c* =0.35.

* Corrosion loss calculation based on the exposed area of four or ten 3-mm (1/8-in.) diamter holes.

Figures 3.71 and 3.72 show the average mat-to-mat resistances for the increased adhesion ECR specimens cast with four and ten holes through the epoxy, respectively. As in both Figures 3.71 and 3.72, the average mat-to-mat resistances of all specimens generally increase with time for the first 36 weeks. During this period, lower mat-to-mat resistances were measured in the increase adhesion ECR specimens with four holes through the epoxy than in the ECR control specimens with four holes through the epoxy. As previously mentioned, this may indicate that the increased

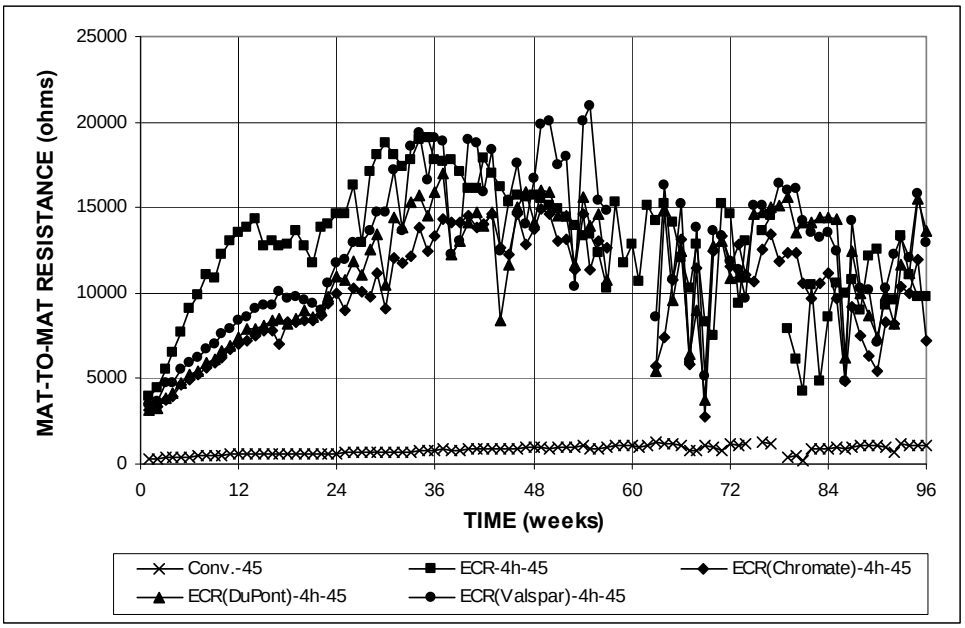

Figure 3.71 – Average mat-to-mat resistance, cracked beam test for specimens containing conventional steel, ECR, and ECR with increased adhesion, *w/c* = 0.45. Bars with four holes in epoxy coating.

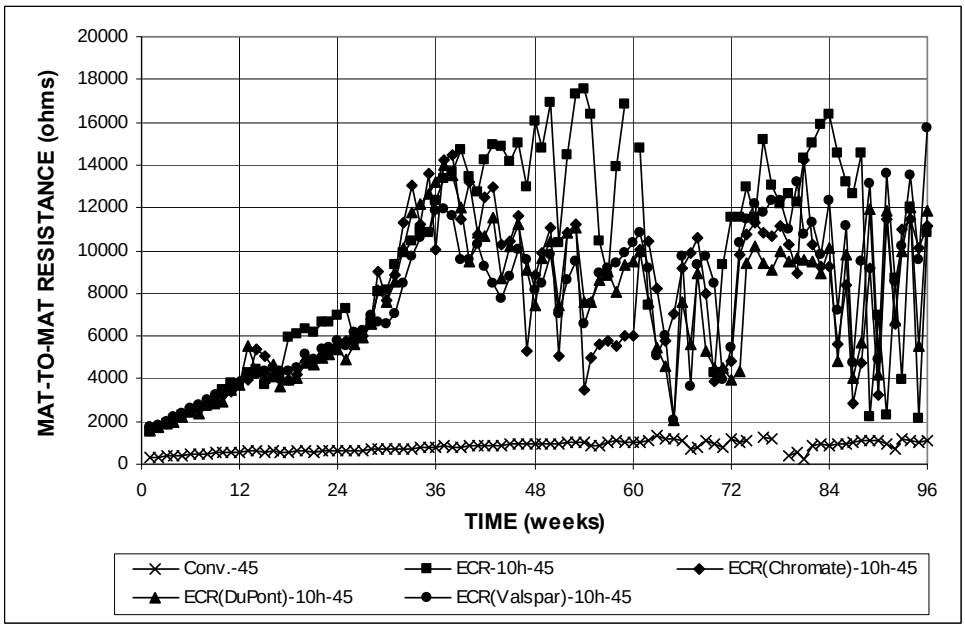

Figure 3.72 – Average mat-to-mat resistance, cracked beam test for specimens containing conventional steel, ECR, and ECR with increased adhesion, *w/c* = 0.45. Bars with ten holes in epoxy coating.

adhesion epoxy in these specimens may be less effective at isolating the underlying steel from the electrolyte than the conventional epoxy. For specimens with ten holes through the epoxy, increased adhesion ECR specimens and ECR control specimens exhibit similar mat-to-mat resistances during the first 36 weeks of the test. For all specimens, the mat-to-mat resistance readings taken after week 36 contain a large amount of scatter. As previously mentioned, additional cracking in the specimen may be periodically alter the increase in the mat-to-mat resistance measurements. Otherwise, few conclusions can be made from this data. It does appear that beyond week 36, the mat-to-mat resistances measured in the ECR control specimens remain somewhat higher than those measured in the increased adhesion ECR specimens.

Figure 3.73 shows the average top and bottom mat corrosion potentials versus a copper-copper sulfate electrode as measure in the increased adhesion ECR specimens with four holes through the epoxy layer. As shown in Figure 3.73(a), corrosion activity, characterized by a corrosion potential more negative than –0.350 V, is observed in the top mat of all specimens by week 3. As previously noted, this rapid onset of corrosion is attributable to the crack allowing moisture, oxygen, and chloride ions direct access to the top reinforcement. Except for the ECR(DuPont)-4h-45 specimens at weeks 25, 26 and 28, all increased adhesion ECR specimens exhibit active corrosion in the top mat from week 3 to the end of the test. As shown in Figure 3.73(b), little active corrosion is observed in the bottom mats of the increased adhesion ECR specimens during the test with the exception of the ECR(Valspar)-4h-

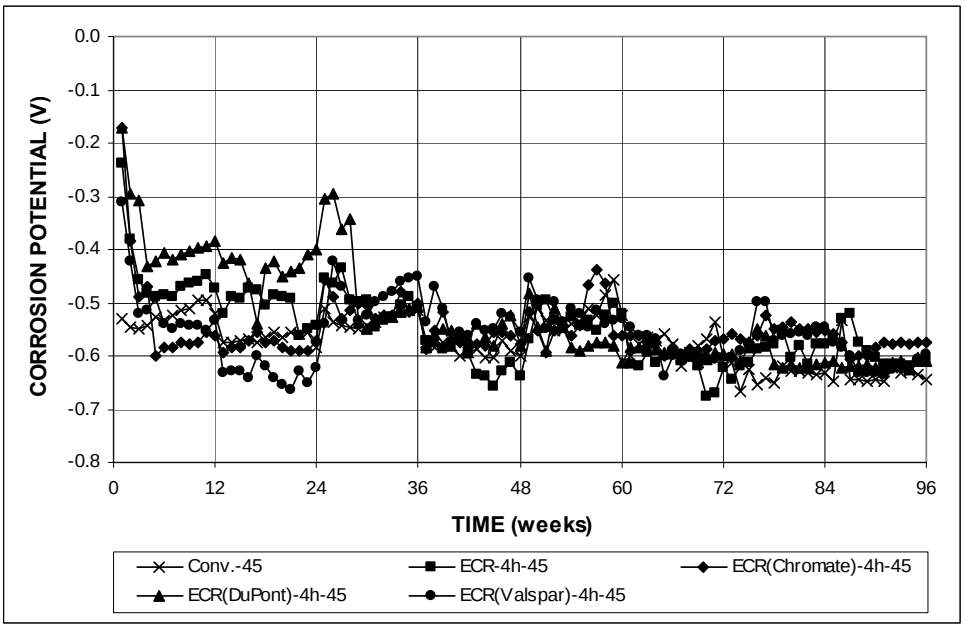

Figure 3.73 (a) – Average top mat corrosion potential, cracked beam test for specimens containing conventional steel, ECR, and ECR with increased adhesion, *w/c* = 0.45. Bars with four holes in epoxy coating.

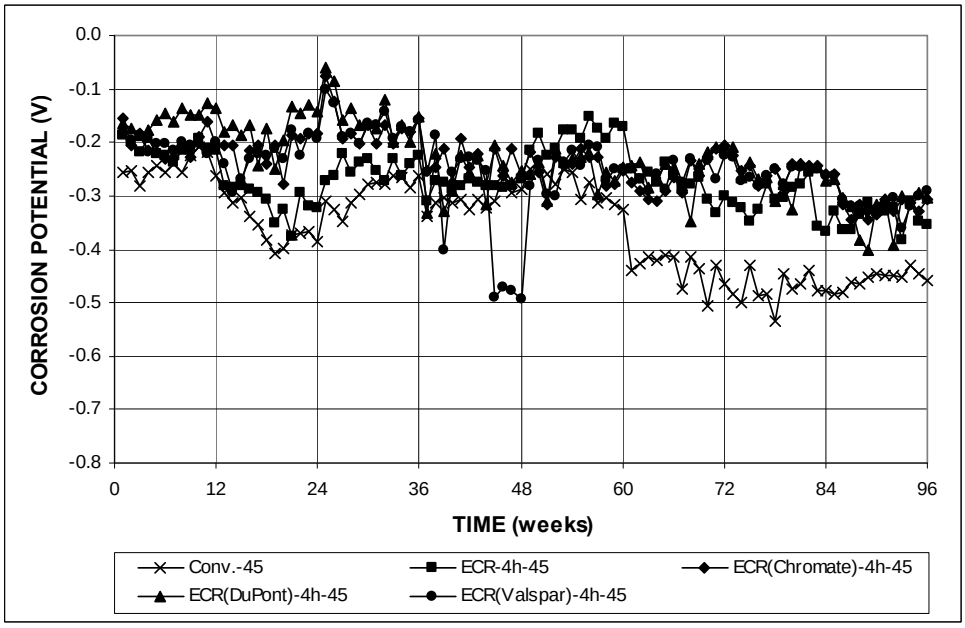

Figure 3.73 (b) – Average bottom mat corrosion potential, cracked beam test for specimens containing conventional steel, ECR, and ECR with increased adhesion, *w/c* = 0.45. Bars with four holes in epoxy coating.

45 specimens between weeks 45 through 48. Because active corrosion is observed by week 61 in the bottom bars of the conventional steel specimens, it is likely that the absence of corrosion activity in the bottom mats of the ECR specimens is due to the protection afforded by the epoxy layer.

Figure 3.74 shows the average top and bottom mat corrosion potentials measured in the increased adhesion ECR specimens with ten holes through the epoxy. As shown in Figure 3.74(a), active corrosion is observed in the top mat of all ECR specimens by week four. With the exception of the ECR(Valspar)-10h-45 specimens at week 7, the top mat corrosion potential for all ECR specimens remains more negative than –0.350 V for the remainder of the test. As shown in Figure 3.74(b), the corrosion potentials measured in the bottom mats of the increased adhesion ECR

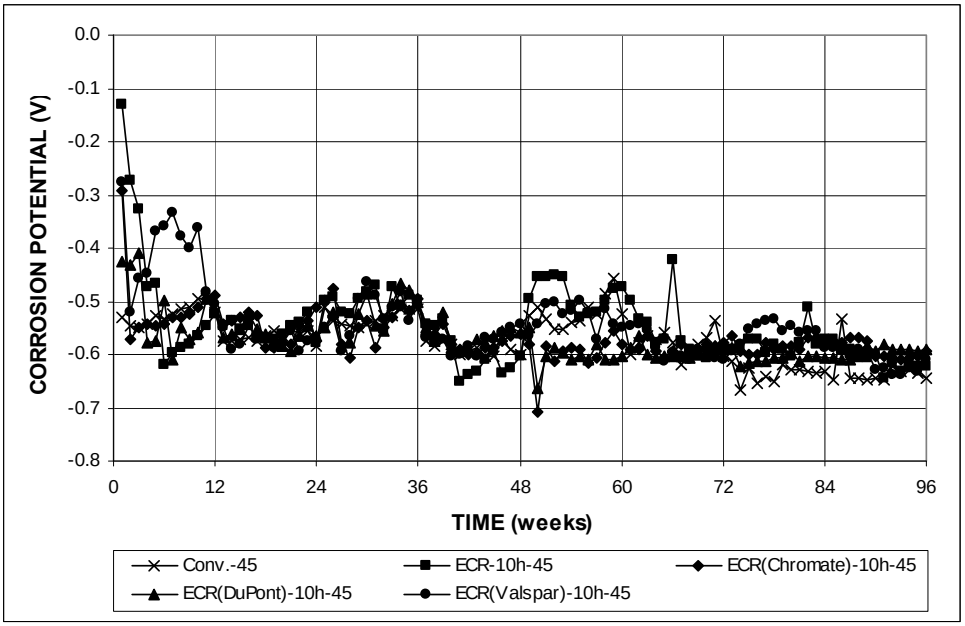

Figure 3.74 (a) – Average top mat corrosion potential, cracked beam test for specimens containing conventional steel, ECR, and ECR with increased adhesion, *w/c* = 0.45. Bars with ten holes in epoxy coating.

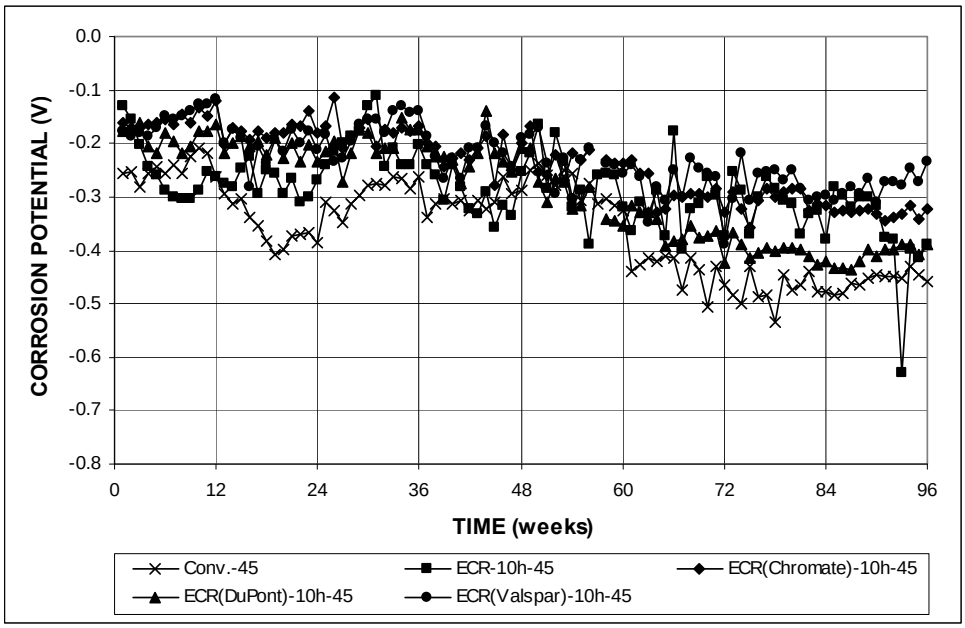

Figure 3.74 (b) – Average bottom mat corrosion potential, cracked beam test for specimens containing conventional steel, ECR, and ECR with increased adhesion, *w/c* = 0.45. Bars with ten holes in epoxy coating.

specimens generally indicate little corrosion activity, with the exception of the ECR(DuPont)-10h-45 specimens, which exhibit active corrosion between weeks 65 through 96.

3.4 Increased Adhesion ECR with DCI

This section presents the results of the Southern Exposure test specimens containing ECR with an increased adhesion cast in concrete containing DCI corrosion inhibitor designed to evaluate the combined effectiveness of the increased adhesion ECR with a corrosion inhibitor. Three Southern Exposure specimens were cast for each type of increased adhesion ECR evaluated. Each specimen had a *w/c* ratio of 0.45, and the epoxy-coating contained four holes.

Figures 3.75 and 3.76 show the average corrosion rates of the increased adhesion specimens cast with DCI based on total and exposed area, respectively, along with the results for the control specimens. Figure 3.75(a) compares the high corrosion rates based on total area for specimens containing conventional steel reinforcement with the low corrosion rates of specimens containing epoxy-coated reinforcement. Figures 3.75(b) and 3.76 show that between weeks 14 and 26, the ECR(Chromate)-DCI-4h-45 specimens exhibit a negative corrosion rate. During this period, corrosion potentials observed in the bottom mat are generally more negative than the potentials of top mat, indicating that electrons being produced at the bottom bar were flowing to the top bar. Between weeks 53 and 69, the ECR(Valspar)-DCI-4h-45 specimens exhibit slightly higher corrosion rates than the other ECR specimens.

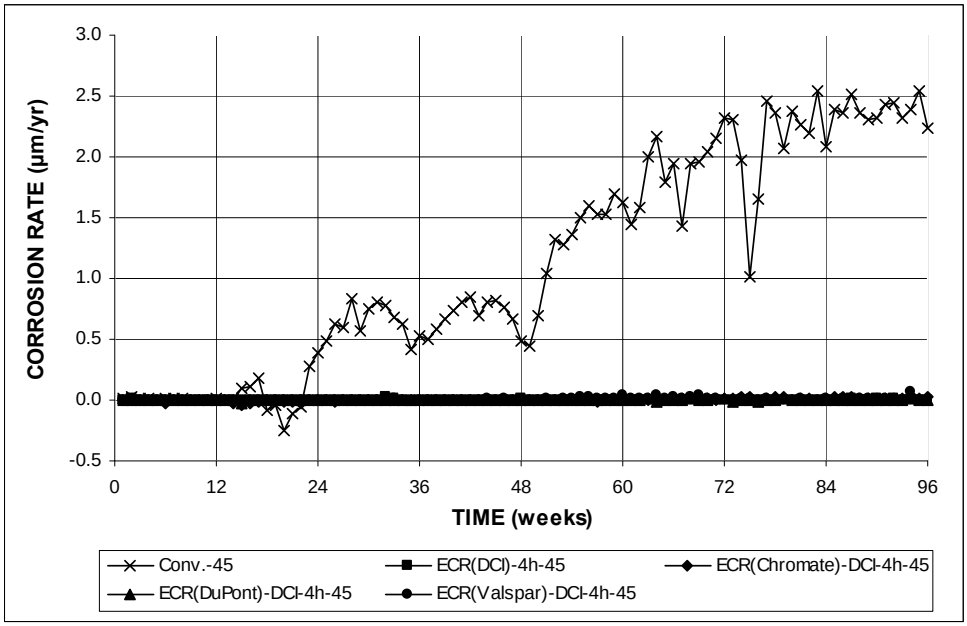

Figure 3.75 (a) – Average corrosion rate, Southern Exposure test for specimens containing conventional steel, ECR in concrete with DCI, and increased adhesion ECR in concrete with DCI, *w/c* = 0.45. Bars with coating containing four holes through the epoxy.

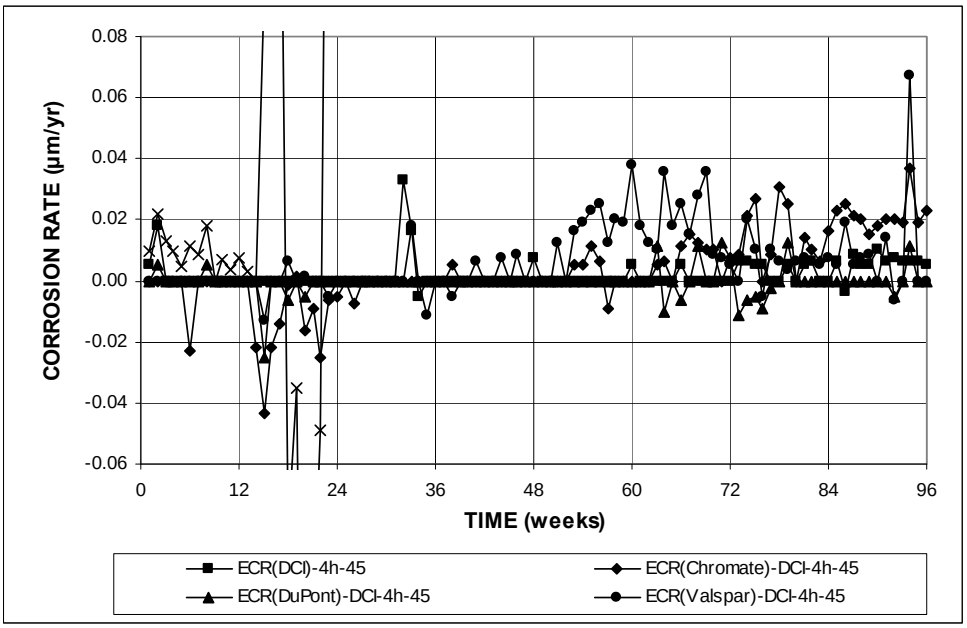

Figure 3.75 (b) – Average corrosion rate, Southern Exposure test for specimens containing conventional ECR in concrete with DCI and increased adhesion ECR in concrete with DCI, *w/c* = 0.45. Bars with coating containing four holes through the epoxy. (Different scale)

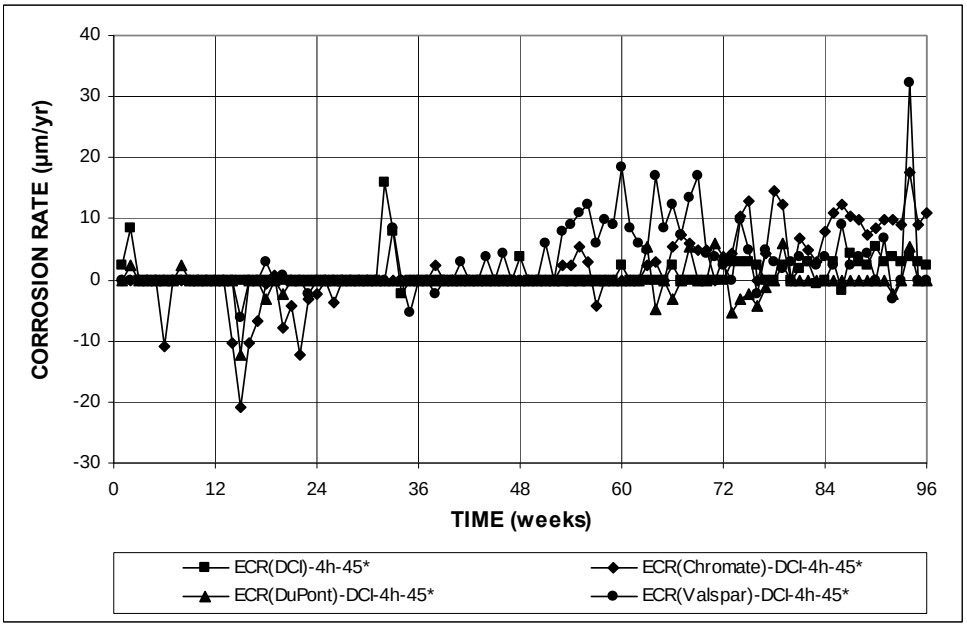

Figure 3.76 – Average corrosion rate based on exposed area, Southern Exposure test for specimens containing conventional ECR in concrete with DCI and increased adhesion ECR in concrete with DCI, *w/c* = 0.45. Bars with coating containing four holes through the epoxy.

This increase in corrosion rate was observed in one of three specimens, as shown Figure A.97(a). All other ECR specimens exhibit similar corrosion rates.

Figures 3.77 and 3.78 show the average corrosion losses of the increased adhesion ECR specimens with DCI, based on total and exposed area, respectively. Figure 3.77 compares the high corrosion rates based on total area for specimens containing conventional steel reinforcement with the low corrosion rates of specimens containing epoxy-coated reinforcement. As shown in Figure 3.78, all three increased adhesion ECR specimens with DCI initially exhibit lower corrosion losses than the ECR(DCI) control specimens. At week 53, there is a notable increase in the corrosion rate observed in the ECR(Valspar)-DCI-4h-45 specimens, as characterized by the increase in the slope of the corrosion loss plot. At week 55, the corrosion loss observed in the ECR(Valspar)-DCI-4h-45 specimens surpasses the corrosion loss of the ECR(DCI) control specimens, and remains higher than any other ECR specimen for the remainder of the test. Beginning at week 14, the ECR(Chromate)-DCI-4h-45 specimens begin exhibiting a negative corrosion loss due to the previously discussed negative macrocell currents observed between weeks 14 and 26. Between weeks 27 and 65, little corrosion activity is observed in the ECR(Chromate)-DCI-4h-45 specimens. At week 66, corrosion in the ECR(Chromate)-DCI-4h-45 specimens appears to initiate, and by week 86, the corrosion loss in these specimens has surpassed that of the ECR control specimens. No significant corrosion activity is observed in the ECR(DuPont)-DCI-4h-45 specimens during the study.

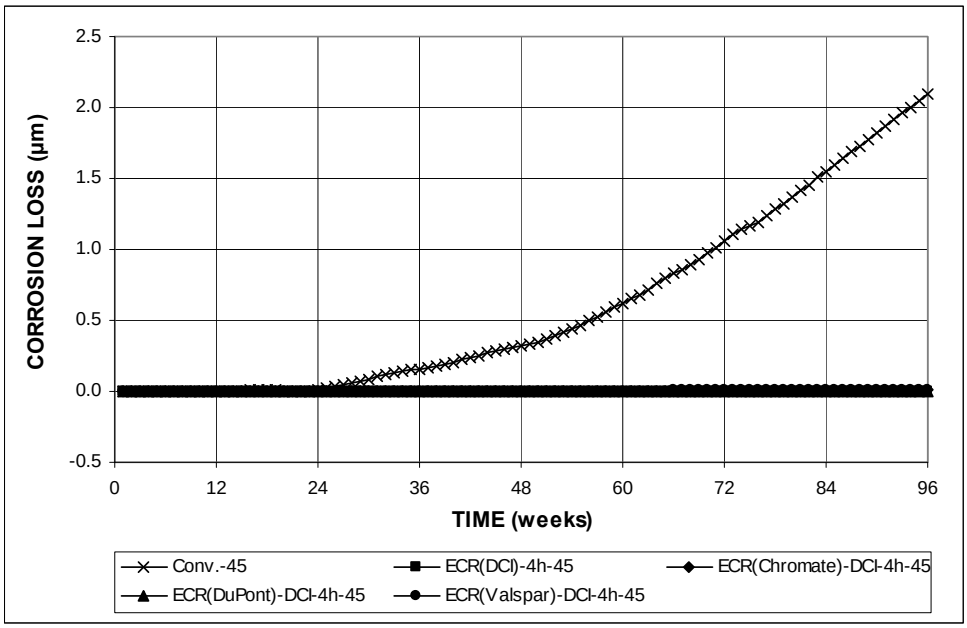

Figure 3.77 – Average corrosion loss, Southern Exposure test for specimens containing conventional steel, ECR in concrete with DCI, and increased adhesion ECR in concrete with DCI, *w/c* = 0.45. Bars with coating containing four holes through the epoxy.

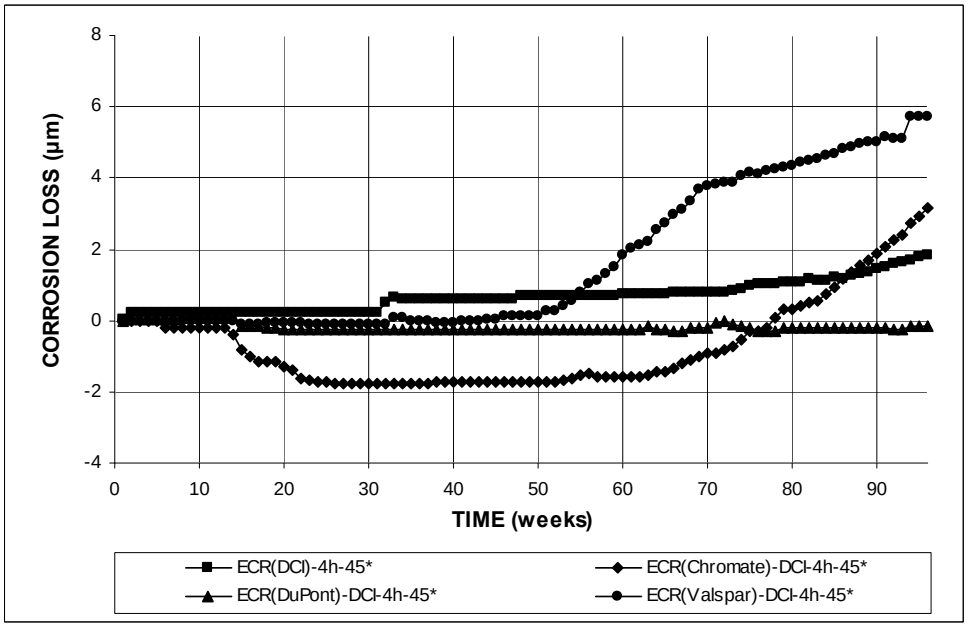

Figure 3.78 – Average corrosion loss based on exposed area, Southern Exposure test for specimens containing conventional ECR in concrete with DCI and increased adhesion ECR in concrete with DCI, *w/c* = 0.45. Bars with coating containing four holes through the epoxy.

Table 3.8 summarizes the corrosion losses as measured in the Southern Exposure specimens containing increased adhesion ECR in concrete with DCI. The ECR(Valspar)-DCI-4h-45 specimens exhibit the highest corrosion loss, 0.012 and 5.72 μm based on total and exposed area, respectively. The second highest corrosion loss is observed in the ECR(Chromate)-DCI-4h-45 specimens, with values of 0.007 and 3.14 μm, based on total and exposed area, respectively. The ECR(DuPont)-DCI-4h-45 specimens exhibit the least amount of corrosion loss upon termination of the test.

Table 3.8 – Average corrosion loss (μm) at week 96 as measured in the Southern Exposure test for specimens containing increased adhesion ECR in concrete with DCI

Steel Designation[a]	Specimen			Average	Standard Deviation
	1	2	3		
Total Area					
ECR(Chromate)-DCI-4h-45	0.002	0.000	0.018	0.007	0.010
ECR(DuPont)-DCI-4h-45	0.000	-0.001	0.001	0.000	0.001
ECR(Valspar)-DCI-4h-45	0.000	0.002	0.033	0.012	0.019
Exposed Area					
ECR(Chromate)-DCI-4h-45*	1.06	-0.211	8.59	3.14	4.76
ECR(DuPont)-DCI-4h-45*	-0.21	-0.493	0.282	-0.141	0.392
ECR(Valspar)-DC)-4h-45*	-0.070	1.161	16.1	5.72	8.99

[a] ECR(Chromate) = ECR with the chromate pretreatment.
ECR(DuPont) = ECR with high adhesion DuPont coating.
ECR(Valspar) = ECR with high adhesion Valspar coating.
4h = bar with four holes through epoxy
45 = concrete with *w/c* =0.45

* Corrosion loss calculation based on the exposed area of four or ten 3-mm (1/8-in.) diamter holes.

Figure 3.79 shows the average mat-to-mat resistance as measured in the increased adhesion ECR specimens with DCI. The average mat-to-mat resistance observed in the ECR specimens generally increases with time, with a noticeable increase in scatter past week 38. During the study, all increased adhesion ECR

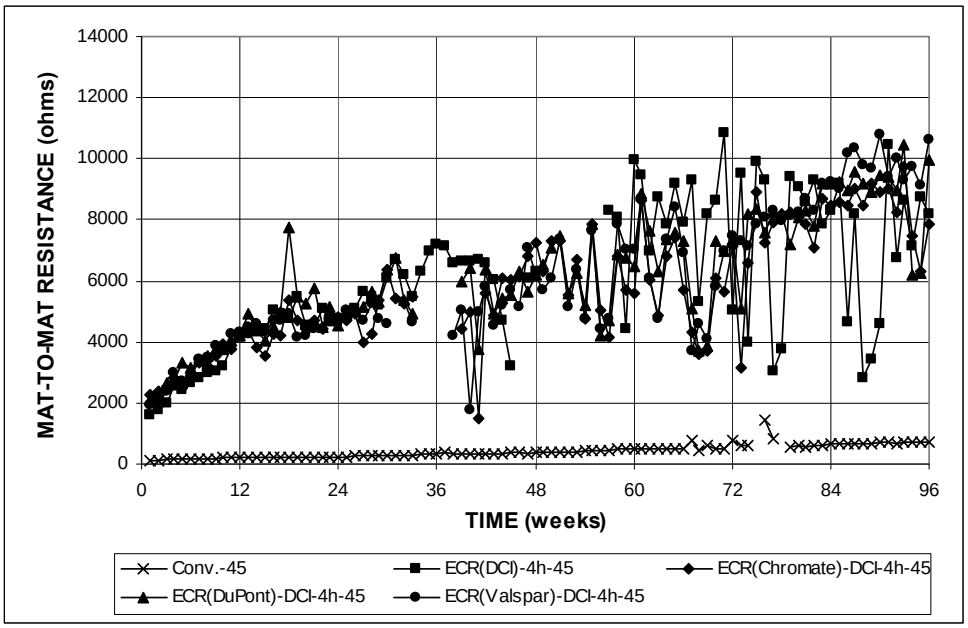

Figure 3.79 – Average mat-to-mat resistance, Southern Exposure test for specimens containing conventional steel, ECR in concrete with DCI, and increased adhesion ECR in concrete with DCI, *w/c* = 0.45. Bars with coating containing four holes through the epoxy.

specimens exhibit mat-to-mat resistances that are similar to specimens with conventional ECR specimens cast in concrete containing DCI corrosion inhibitor.

Figure 3.80 shows the average top and bottom mat corrosion potentials, respectively, versus a copper-copper sulfate electrode as measured in the increased adhesion ECR specimens with DCI. As shown in Figure 3.80(a), active corrosion, characterized by corrosion potentials more negative than –0.350 V, is observed in the top mat of the ECR(DuPont)-DCI-4h-45 specimens between weeks 63 and 65 and at week 68. Active corrosion is also observed in the top mat of the ECR(Chromate)-DCI-4h-45 specimens at week 68. No other corrosion was observed in the top mats of the increased adhesion ECR specimens with DCI during the course of the test. As shown in Figure 3.80(b), the bottom-mat corrosion potentials in the increased adhesion

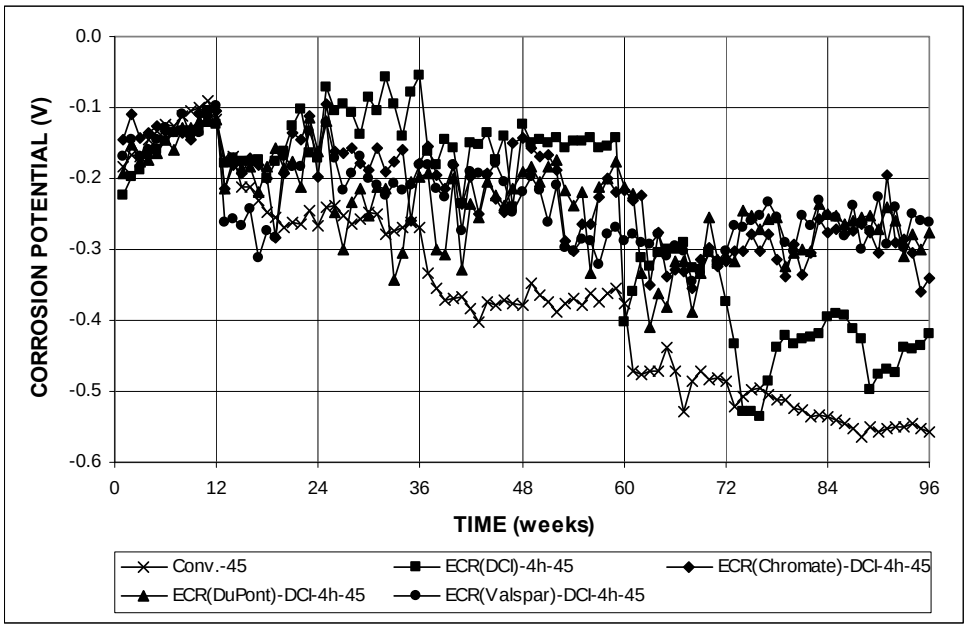

Figure 3.80 (a) – Average top mat corrosion potential, Southern Exposure test for specimens containing conventional steel, ECR in concrete with DCI, and increased adhesion ECR in concrete with DCI, *w/c* = 0.45. Bars with coating containing four holes through the epoxy.

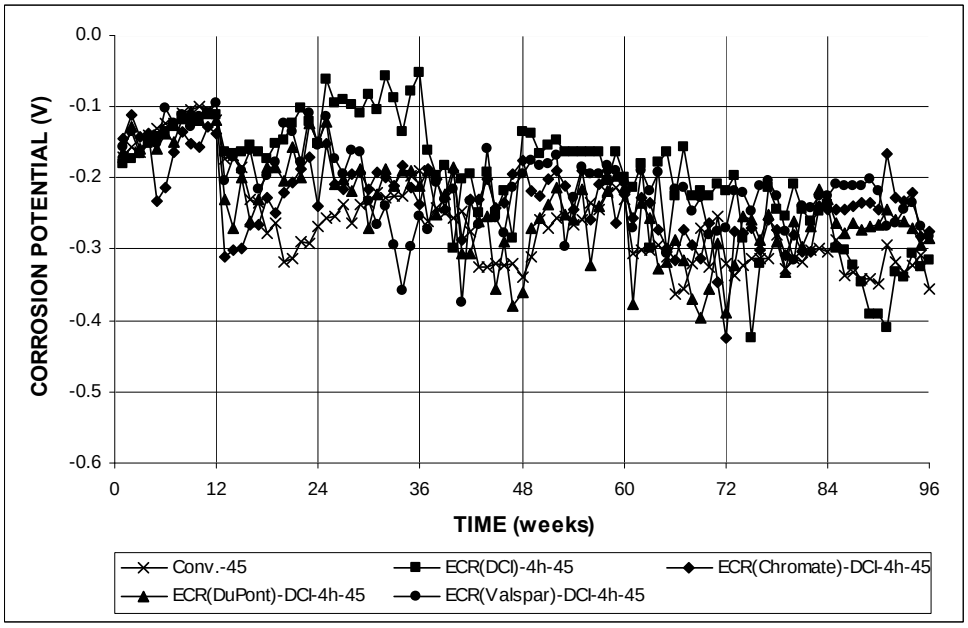

Figure 3.80 (b) – Average bottom mat corrosion potential, Southern Exposure test for specimens containing conventional steel, ECR in concrete with DCI, and increased adhesion ECR in concrete with DCI, *w/c* = 0.45. Bars with coating containing four holes through the epoxy.

ECR specimens with DCI generally indicate low corrosion activity, with the exception of the ECR(DuPont)-DCI-4h-45 specimens between weeks 68 through 72.

3.5 Multiple-coated Reinforcement

This section presents the results for the Southern Exposure and cracked beam test specimens containing multiple-coated ECR. These specimens have a layer comprised of 98% zinc and 2% aluminum between the steel and epoxy coating. The current study evaluates the multiple-coated reinforcement under two conditions: with both the epoxy and zinc layers penetrated, which exposes the underlying steel to the pore solution, and with only the epoxy layer penetrated. The reinforcement is evaluated with four and ten holes in the outer layer(s). Three Southern Exposure and three cracked beam specimens were fabricated for each test group.

3.5.1 Southern Exposure

Figures 3.81 and 3.82 show the average corrosion rates based on total and exposed area, respectively, for the Southern Exposure specimens containing multiple-coated reinforcement with four holes through the epoxy and with four holes through the epoxy and zinc layers. Figure 3.81(a) compares the high corrosion rates based on total area for the specimens containing conventional steel reinforcement with the low corrosion rates of the specimens containing multiple-coated reinforcement. The specimens containing multiple-coated reinforcement are the only ECR specimens which exhibit a discernable corrosion rate when compared to the conventional steel specimens using the scale shown in Figure 3.81(a). As shown in Figures 3.81(b) and

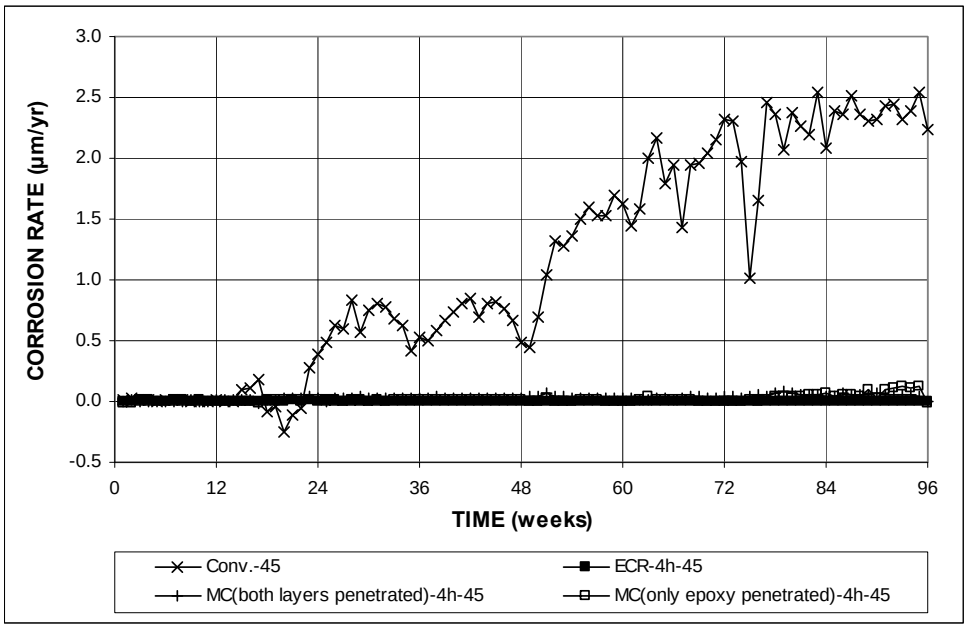

Figure 3.81 (a) – Average corrosion rate, Southern Exposure test for specimens containing conventional steel, ECR, and multiple-coated reinforcement in concrete with *w/c* = 0.45. Bars with coating containing four holes through the epoxy.

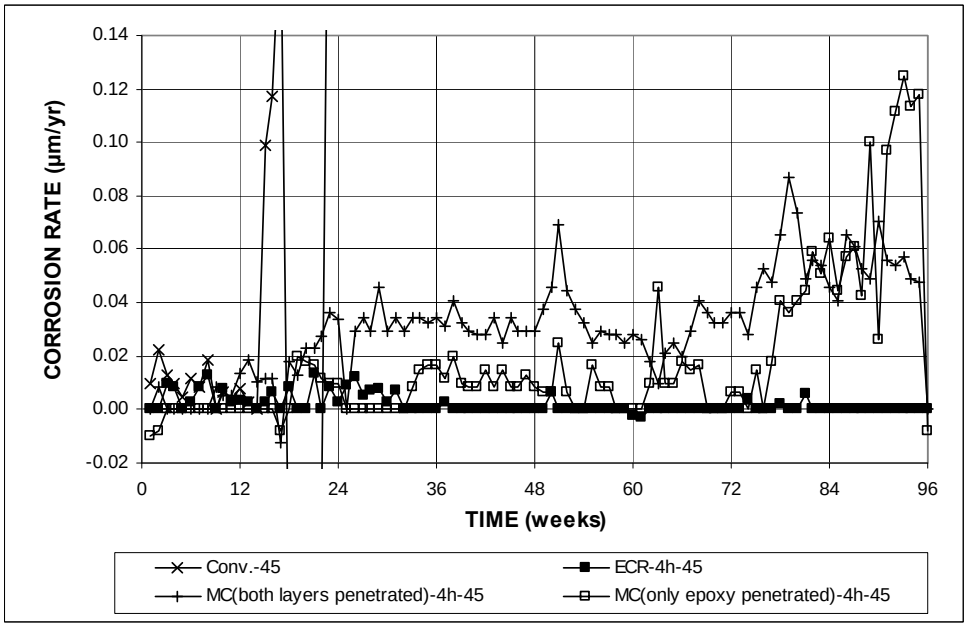

Figure 3.81 (b) – Average corrosion rate, Southern Exposure test for specimens containing conventional steel, ECR, and multiple-coated reinforcement in concrete with *w/c* = 0.45. Bars with coating containing four holes through the epoxy. (Different scale)

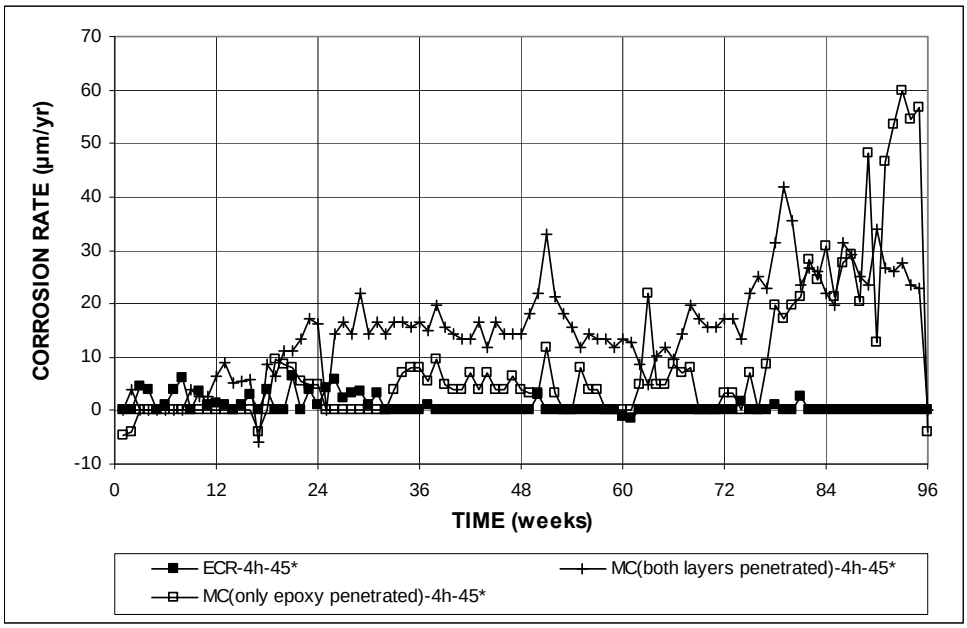

Figure 3.82 – Average corrosion rate based on exposed area, Southern Exposure test for specimens containing ECR and multiple-coated reinforcement in concrete with *w/c* = 0.45. Bars with coating containing four holes through the epoxy.

3.82, the multiple-coated bars with both layers penetrated generally exhibit higher corrosion rates than the multiple-coated bars with only the epoxy penetrated during the first 78 weeks of the test. The reason for this behavior is discussed later in this section. Between weeks 78 and 96, the multiple-coated bars with only the epoxy penetrated exhibit corrosion rates that are slightly higher or similar to the multiple-coated bars with both layers penetrated. This represents the only case in which the corrosion rate of the bars with only the epoxy penetrated exceeds the corrosion rate for bars with both layers penetrated.

Figures 3.83 and 3.84 show the average corrosion rates based on total and exposed area, respectively, for the Southern Exposure specimens containing multiple-coated reinforcement with ten holes through the epoxy and through the epoxy and

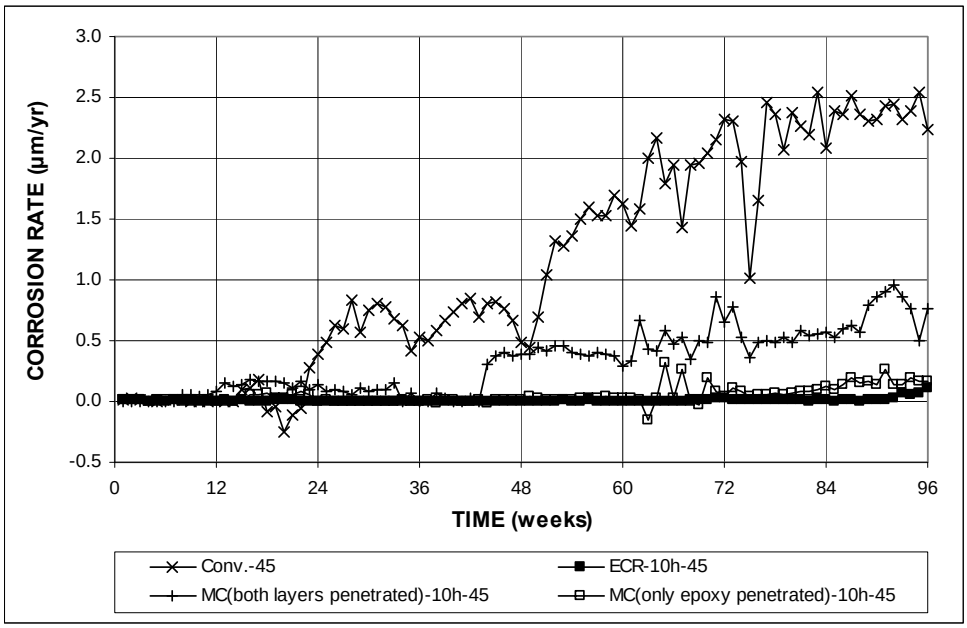

Figure 3.83 (a) – Average corrosion rate, Southern Exposure test for specimens containing conventional steel, ECR, and multiple-coated reinforcement in concrete with *w/c* = 0.45. Bars with coating containing ten holes through the epoxy.

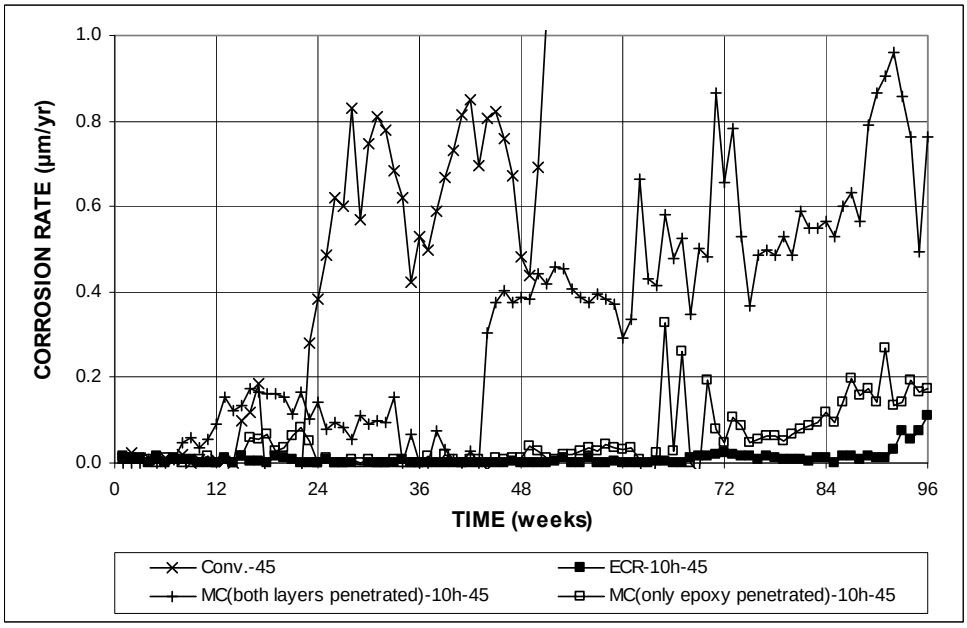

Figure 3.83 (b) – Average corrosion rate, Southern Exposure test for specimens containing conventional steel, ECR, and multiple-coated reinforcement in concrete with *w/c* = 0.45. Bars with coating containing ten holes through the epoxy. (Different scale)

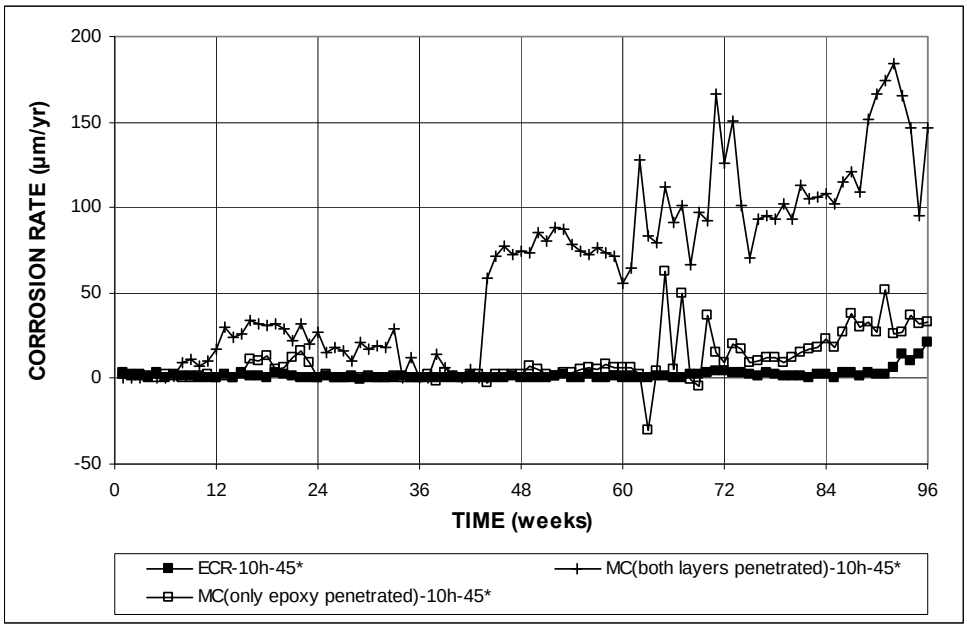

Figure 3.84 – Average corrosion rate based on exposed area, Southern Exposure test for specimens containing ECR and multiple-coated reinforcement in concrete with *w/c* = 0.45. Bars with coating containing ten holes through the epoxy.

zinc layers. As shown in Figure 3.83(a) conventional steel generally exhibits higher corrosion rates than the multiple-coated reinforcement, except at week 49, when both exhibit corrosion rates approximately equal to 0.45 µm/yr, based on total area. As shown in Figures 3.83(b) and 3.84, higher corrosion rates are typically observed in the multiple-coated bars with both layers penetrated than in the bars with only the epoxy layer penetrated.

Figures 3.85 and 3.86 present the average corrosion losses based on total and exposed area, respectively, for the test specimens containing multiple-coated reinforcement with four holes through only the epoxy, as well as specimens with four holes through the epoxy and zinc layers. As shown in Figure 3.85, conventional steel specimens exhibit higher corrosion losses than any specimen with multiple-coated

reinforcement. As shown in Figure 3.86, the multiple-coated bars with both layers penetrated exhibit higher corrosion losses than the bars with only the epoxy penetrated, with corrosion initiation occurring approximately at week 20 and steady-state corrosion continuing for the remainder of the test. From week 33 to week 77, the multiple-coated bars with only the epoxy penetrated exhibit a nearly steady-state corrosion rate, as indicated by the slope of the corrosion loss plot. At week 78, a marked increase is observed in the corrosion rate of these bars. As previously mentioned, between weeks 78 and 96, both types of multiple-coated bars exhibit similar corrosion rates. The higher corrosion rates observed in the multiple-coated bars can be attributed to the zinc of the top bar corroding to protect the exposed steel in the bottom bars. The zinc preferentially corrodes before steel because it is

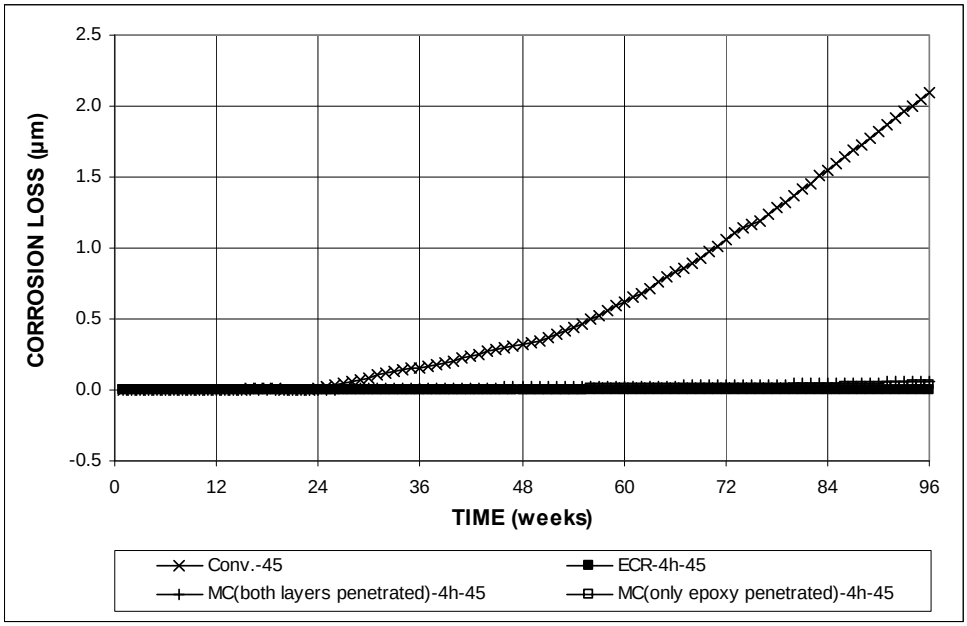

Figure 3.85 – Average corrosion loss, Southern Exposure test for specimens containing conventional steel, ECR, and multiple-coated reinforcement in concrete with *w/c* = 0.45. Bars with coating containing four holes through the epoxy.

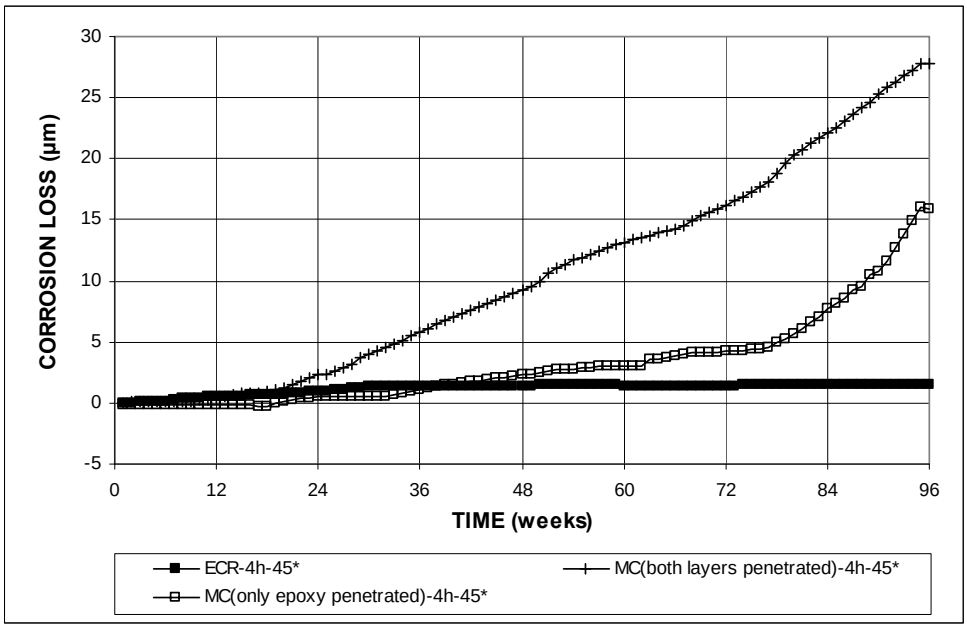

Figure 3.86 – Average corrosion loss based on exposed area, Southern Exposure test for specimens containing ECR and multiple-coated reinforcement in concrete with *w/c* = 0.45. Bars with coating containing four holes through the epoxy.

galvanically more active than iron, and therefore protects the steel from corrosion. As will be discussed in Section 3.8, a study by Darwin et al. (2007) shows that the critical chloride threshold for galvanized reinforcement (2.57 lb/yd^3) is higher than the chloride threshold for conventional steel reinforcement (1.63 lb/yd^3). The corrosion rate measured in the corrosion loss plots is due to macrocell corrosion only, and is therefore only indicative of the protection afforded to the steel in the bottom bars by the zinc in the top bars. The corrosion interaction between the zinc and steel in the top bar is not captured by the voltage drop readings from which the corrosion loss figures are derived.

Figures 3.87 and 3.88 show the average corrosion losses for the Southern Exposure specimens containing multiple-coated reinforcement with ten holes in the

epoxy only, as well as specimens with holes penetrating both the epoxy and zinc layers. As shown in Figure 3.87, the conventional steel specimens exhibit higher corrosion loses than the multiple-coated bars. As shown in Figures 3.87 and 3.88, multiple-coated bars with both layers penetrated exhibit higher corrosion losses than the bars with only the epoxy penetrated. Between weeks 12 and 43, the multiple-coated bars with both layers penetrated exhibit an average corrosion rate of 17.5 μm/yr based on exposed area. At week 44, the corrosion rate of the bars with both layers penetrated dramatically increases to an average of 100 μm/yr based on exposed area. The average corrosion rates observed in the bars with only the epoxy layer penetrated remain low until week 65, when corrosion initiation occurs as indicated the discontinuity in the slope of the corrosion loss graph. From week 65 to 96, the

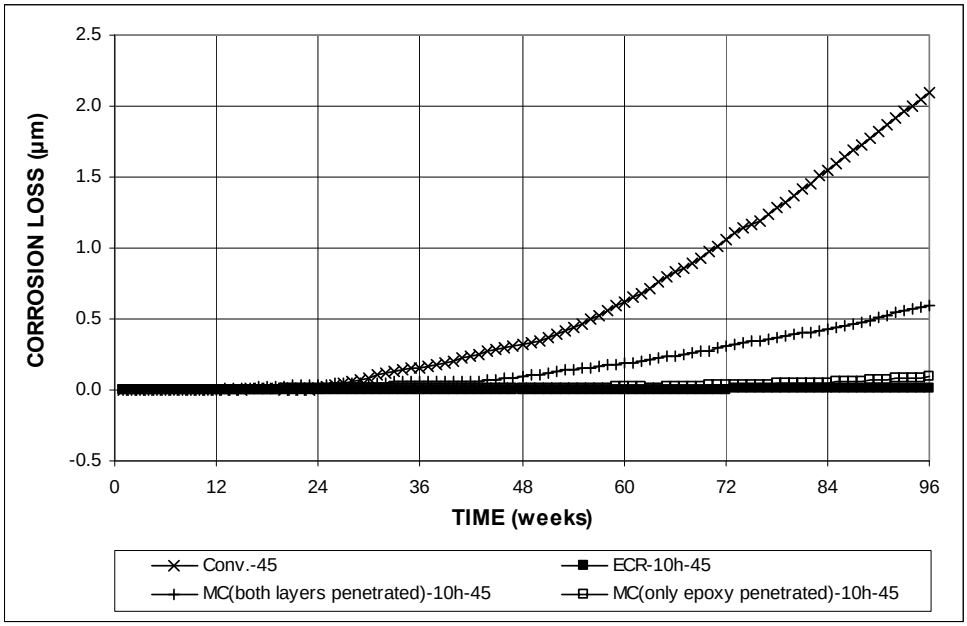

Figure 3.87 – Average corrosion loss, Southern Exposure test for specimens containing conventional steel, ECR, and multiple-coated reinforcement in concrete with *w/c* = 0.45. Bars with coating containing ten holes through the epoxy.

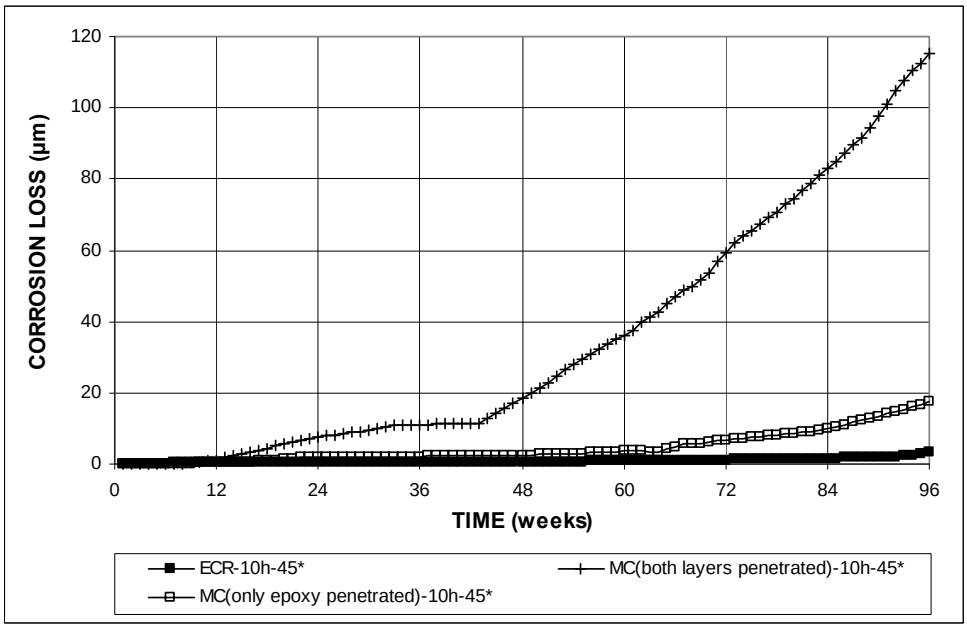

Figure 3.88 – Average corrosion loss based on exposed area, Southern Exposure test for specimens containing ECR and multiple-coated reinforcement in concrete with *w/c* = 0.45. Bars with coating containing ten holes through the epoxy.

multiple-coated bars with only the epoxy penetrated exhibit an average corrosion rate of 25.8 µm/yr, based on exposed area. As previously mentioned, the higher corrosion rates and losses observed in the bars with both layers penetrated is in all likelihood due to the zinc in the top bar preferentially corroding to protect the exposed steel in the bottom bars.

Table 3.9 summarizes the corrosion losses as measured in the Southern Exposure specimens containing multiple-coated reinforcement. Based on total area, the multiple-coated bars with 10 holes penetrating both epoxy and zinc layers exhibit the highest corrosion loss, 0.599 µm, followed by the bars with 10 holes penetrating only the epoxy, four holes penetrating both epoxy and zinc layers, and four holes penetrating only the epoxy layer with losses of 0.090, 0.058, and 0.033 µm,

respectively. Based on exposed area, it is clear that the reinforcement with both layers penetrated suffered more total corrosion loss than the bars with only the epoxy coating penetrated. The effect that the amount of damage present on the reinforcement surface has on corrosion loss is more pronounced for reinforcement with both epoxy and zinc layers penetrated (115 μm versus 27.7 μm for ten and four holes, respectively) than for reinforcement with only the epoxy layer penetrated (17.4 μm versus 15.9 μm, respectively). This also illustrates that corrosion loss measured in the specimens with both layers penetrated is due to the corrosion loss of the zinc layer in the top mat as it protects the exposed steel in the bottom mat. It is clear that as greater steel area is exposed in bottom bar, the greater the corrosion loss that is observed in the top mat.

Table 3.9 – Average corrosion loss (μm) at week 96 as measured in the Southern Exposure test for specimens containing multiple-coated reinforcement

Steel Designation[a]	Specimen			Average	Standard Deviation
	1	2	3		
Total Area					
MC(both layers penetrated)-4h-45	0.063	0.064	0.046	0.058	0.010
MC(both layers penetrated)-10h-45	0.521	0.708	0.569	0.599	0.097
MC(only epoxy penetrated)-4h-45	0.019	0.052	0.028	0.033	0.017
MC(only epoxy penetrated)-10h-45	0.026	0.179	0.066	0.090	0.079
Exposed Area					
MC(both layers penetrated)-4h-45*	30.5	30.7	22.0	27.7	5.00
MC(both layers penetrated)-10h-45*	100	136	109	115	18.7
MC(only epoxy penetrated)-4h-45*	8.96	25.2	13.5	15.9	8.38
MC(only epoxy penetrated)-10h-45*	5.06	34.4	12.7	17.4	15.2

[a] MC(both layers penetrated) = multiple coated bars with both zinc and epoxy layers penetrated.
MC(only epoxy penetrated) = mutiple coated bars with only epoxy layer penetrated.
4h = bar with four holes through epoxy, 10h = bar with 10 holes through epoxy.
45 = concrete with w/c =0.45

* Corrosion loss calculation based on the exposed area of four or ten 3-mm (1/8-in.) diamter holes.

Figures 3.89 and 3.90 show the average mat-to-mat resistance for Southern Exposure specimens containing multiple-coated reinforcement with four and ten

holes through the outer layer(s), respectively. As shown in Figure 3.89, multiple-coated reinforcement with four holes through the epoxy exhibit similar or slightly higher mat-to-mat resistance than the ECR control specimens for the first 35 weeks of the test. From week 44 until week 64, the multiple-coated reinforcement with both layers penetrated and with only the epoxy penetrated exhibit similar mat-to-mat resistances, which are lower than the ECR control specimens. From week 65 to 96, the multiple-coated bars with both layers penetrated exhibit mat-to-mat resistances similar to the ECR control specimens, while the multiple-coated bars with only the

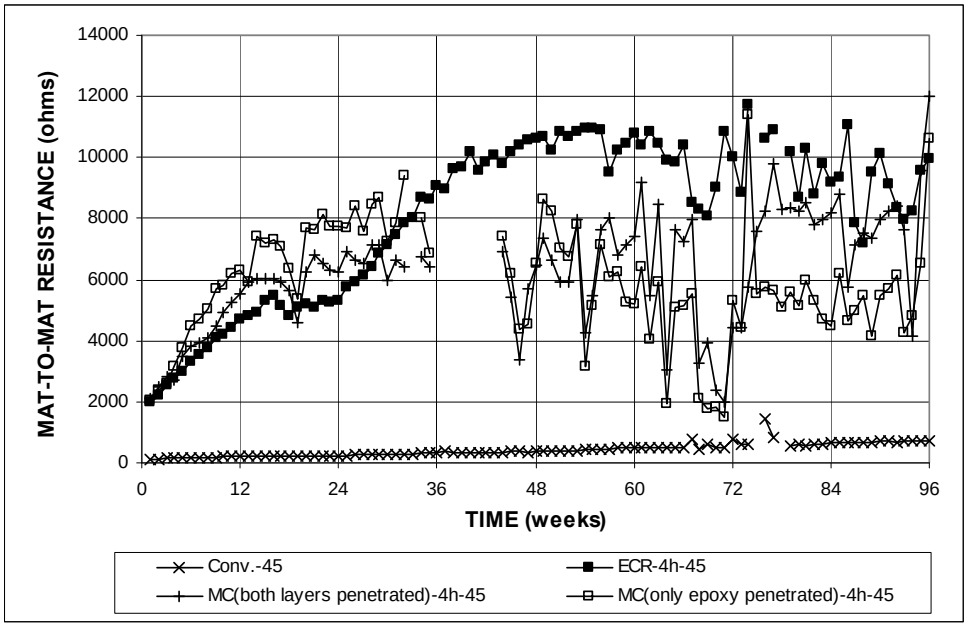

Figure 3.89 – Average mat-to-mat resistance, Southern Exposure test for specimens containing conventional steel, ECR, and multiple-coated reinforcement in concrete with *w/c* = 0.45. Bars with coating containing four holes through the epoxy.

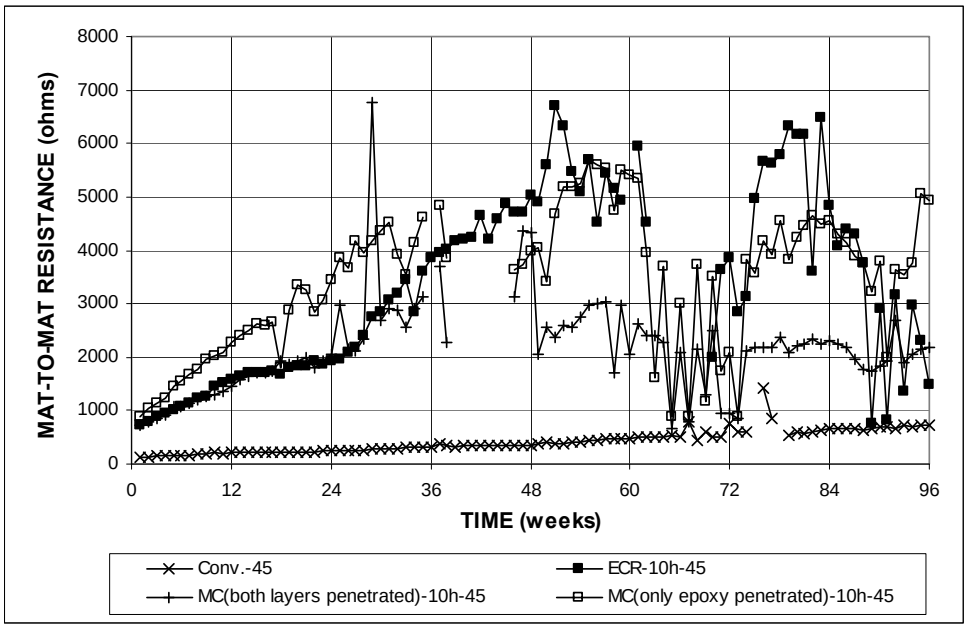

Figure 3.90 – Average mat-to-mat resistance, Southern Exposure test for specimens containing conventional steel, ECR, and multiple-coated reinforcement in concrete with *w/c* = 0.45. Bars with coating containing ten holes through the epoxy.

epoxy penetrated continue to exhibit mat-to-mat resistances that are lower than the control ECR specimens.

As shown in Figure 3.90, multiple-coated bars with ten holes penetrating only the epoxy layer exhibit higher mat-to-mat resistances than the multiple-coated bars with holes penetrating both epoxy and zinc layers and the ECR control bars, which exhibit similar mat-to-mat resistances during the first 37 weeks. Between weeks 46 and 96, a significant amount of scatter is present in the data, and no conclusions can be drawn from this data, except that the multiple-coated bars with both layers penetrated appear to generally exhibit lower mat-to-mat resistances than the ECR control specimens.

Figures 3.91 and 3.92 present the average corrosion potentials versus a copper-copper sulfate electrode in the top and bottom mats, respectively, for the Southern Exposure test specimens containing multiple-coated reinforcement with four and ten holes in the outer layer(s). As shown in Figure 3.91(a), both the MC(both layers penetrated)-4h-45 and MC(only epoxy penetrated)-4h-45 specimens exhibit more negative corrosion potentials in the top mats than the conventional steel and ECR reinforcement. These strongly negative corrosion potentials are an indicator of the high corrosion activity of the zinc coating. The corrosion potentials in the top mats for the multiple-coated bars range between – 0.360 V to –0.601 V for bars with both layers penetrated and between –0.183 V to – 0.590 V for bars with only the epoxy layer penetrated. For the first 18 weeks, the MC(only epoxy penetrated)-4h-45

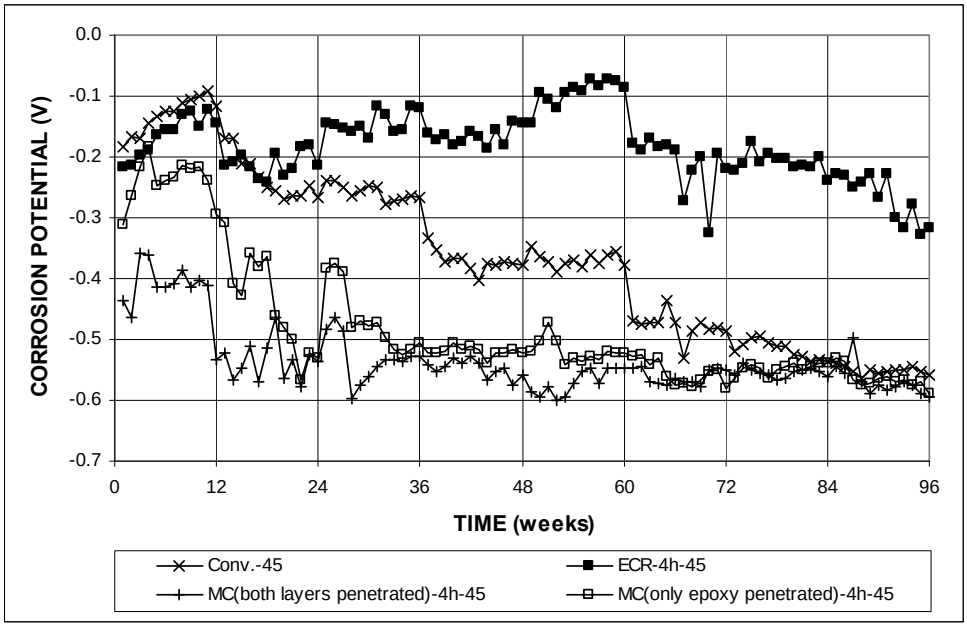

Figure 3.91 (a) – Average top mat corrosion potential, Southern Exposure test for specimens containing conventional steel, ECR, and multiple-coated reinforcement in concrete with *w/c* = 0.45. Bars with coating containing four holes through the epoxy.

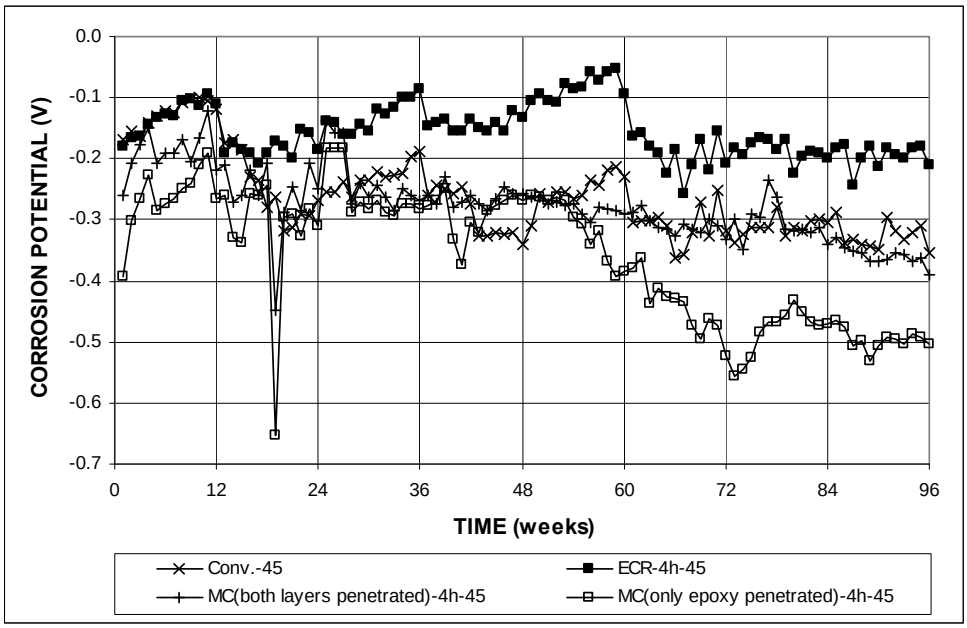

Figure 3.91 (b) – Average bottom mat corrosion potential, Southern Exposure test for specimens containing conventional steel, ECR, and multiple-coated reinforcement in concrete with *w/c* = 0.45. Bars with coating containing four holes through the epoxy.

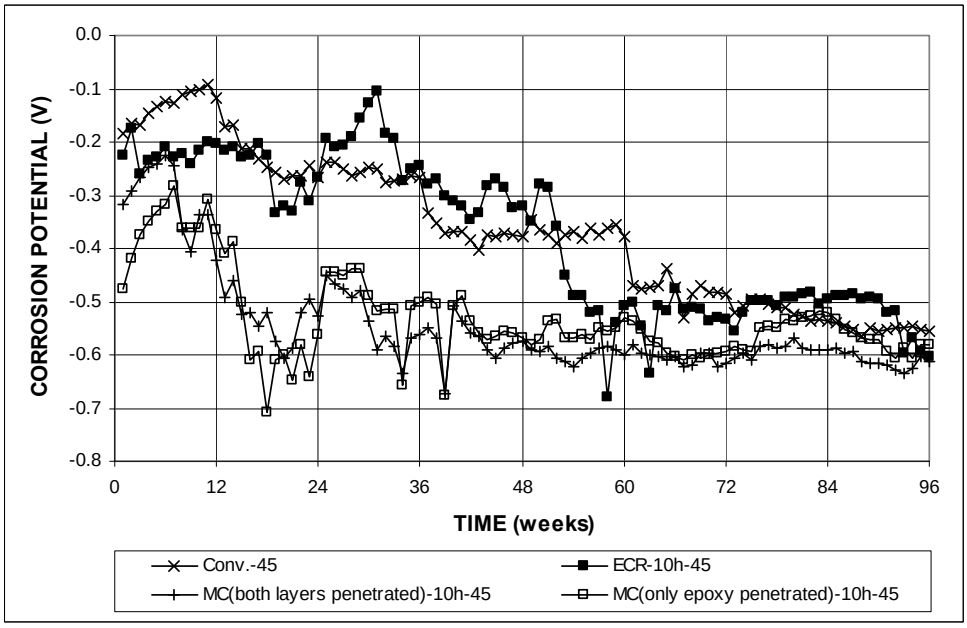

Figure 3.92 (a) – Average top mat corrosion potential, Southern Exposure test for specimens containing conventional steel, ECR, and multiple-coated reinforcement in concrete with *w/c* = 0.45. Bars with coating containing ten holes through the epoxy.

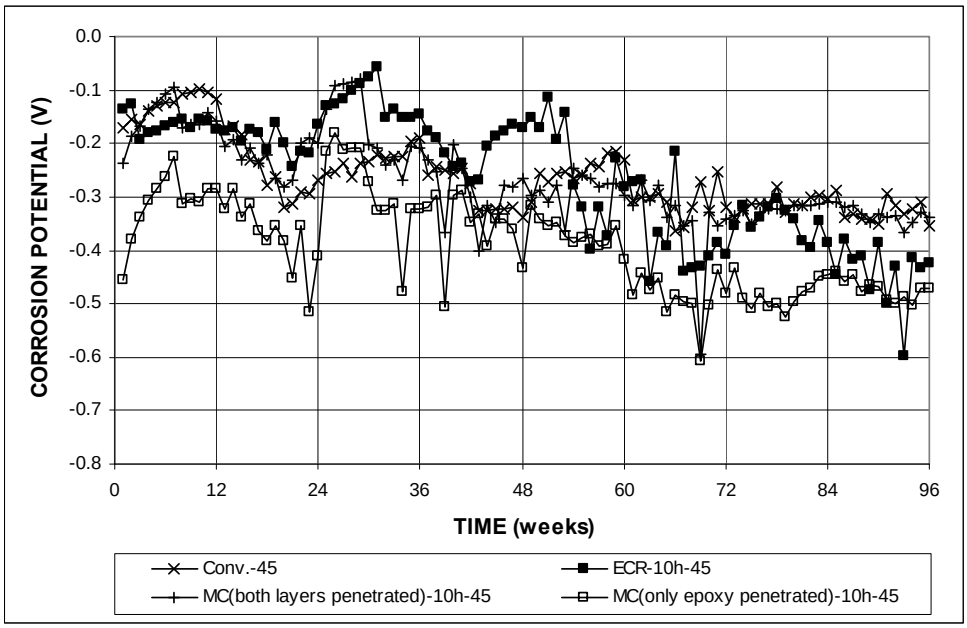

Figure 3.92 (b) – Average bottom mat corrosion potential, Southern Exposure test for specimens containing conventional steel, ECR, and multiple-coated reinforcement in concrete with *w/c* = 0.45. Bars with coating containing ten holes through the epoxy.

specimens exhibit corrosion potentials that are more positive than the MC(both layers penetrated)-4h-45 specimens, suggesting that the intact zinc layer was able to remain passive during this time period. However, from week 19 to week 96, both MC(only epoxy penetrated)-4h-45 and MC(both layers penetrated)-4h-45 exhibit similar corrosion potentials in the top mat.

As shown in Figure 3.91(b), both the MC(only epoxy penetrated)-4h-45 and MC(both layers penetrated)-4h-45 specimens generally exhibit corrosion potentials similar to those observed in the convention steel reinforcement for the first 56 weeks of the test. Between weeks 57 and 96, the MC(only epoxy penetrated)-4h-45 specimens exhibit the most negative corrosion potentials among the group while the

MC(both layers penetrated)-4h-45 specimens continue to show corrosion potentials that are similar to those observed in the conventional steel reinforcement.

As shown in Figure 3.92(a), the MC(only epoxy penetrated)-10h-45 specimens exhibit top mat corrosion potentials that are more negative than those observed in the conventional and ECR controls specimens during the entire test. The MC(both layers penetrated)-10h-45 specimens exhibit top mat corrosion potentials that are similar to those observed in the ECR control specimens during the first seven weeks of the test. After week 7, the top mat corrosion potential in the MC(both layers penetrated)-10h-45 specimens begins to drop. From week 43 to week 96, the top mat corrosion potentials in both MC specimens appear relatively stable, with potentials ranging from –0.570 to –0.636 V for the MC(both layers penetrated)-10h-45 specimens and from –0.518 to –0.609 V for the MC(both layers penetrated)-10-h-45 specimens. These strongly negative corrosion potentials are attributable to the high activity of the zinc coating. As shown Figure 3.92(b), the MC(only epoxy penetrated)-10h-45 specimens exhibit bottom mat corrosion potentials that are generally somewhat more negative than the ECR control specimens, yet are not as negative as the corrosion potentials that are observed in the top mat of these specimens. The bottom mat potentials in these specimens range from –0.180 to –0.606 V. The bottom mat corrosion potentials observed in the MC(both layers penetrated)-10h-45 specimens are very similar to those observed in the bottom mat of the conventional steel control specimens, and range between – 0.080 and –0.593 V.

3.5.2 Cracked Beam Tests

Figures 3.93 and 3.94 show the average corrosion rates based on total and exposed area, respectively, as measured in the cracked beam specimens fabricated with multiple-coated reinforcement containing either four holes in only the epoxy layer or four holes in both epoxy and zinc layers. Figure 3.93(a) compares the high corrosion rates based on total area for specimens containing conventional steel reinforcement with the low corrosion rates of the specimens containing multiple-coated reinforcement. As shown in Figures 3.93(b) and 3.94, both the MC(both layers penetrated)-4h-45 and MC(only epoxy penetrated)-4h-45 specimens exhibit higher corrosion rates than the ECR control specimens. During the first 52 weeks, the MC(both layers penetrated)-4h-45 specimens generally exhibit higher corrosion rates

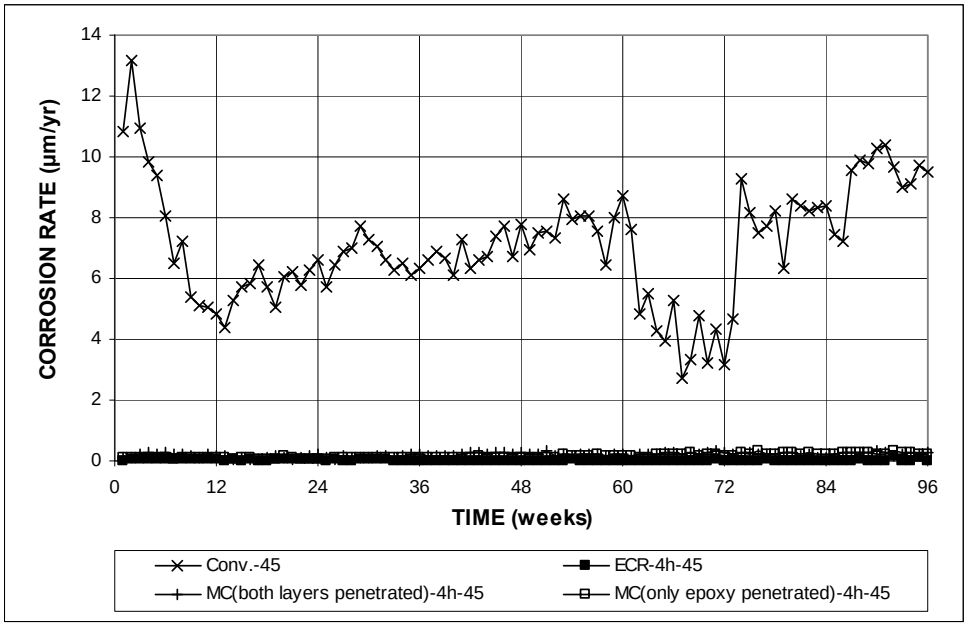

Figure 3.93 (a) – Average corrosion rate, cracked beam test for specimens containing conventional steel, ECR, and multiple-coated reinforcement in concrete with *w/c* = 0.45. Bars with coating containing four holes through the epoxy.

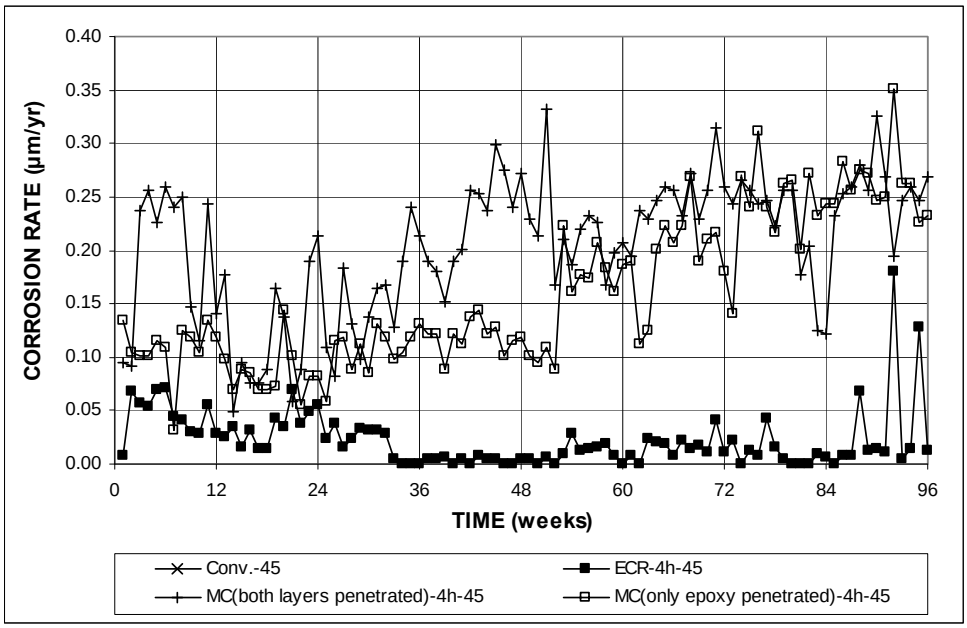

Figure 3.93 (b) – Average corrosion rate, cracked beam test for specimens containing conventional steel, ECR, and multiple-coated reinforcement in concrete with *w/c* = 0.45. Bars with coating containing four holes through the epoxy. (Different scale)

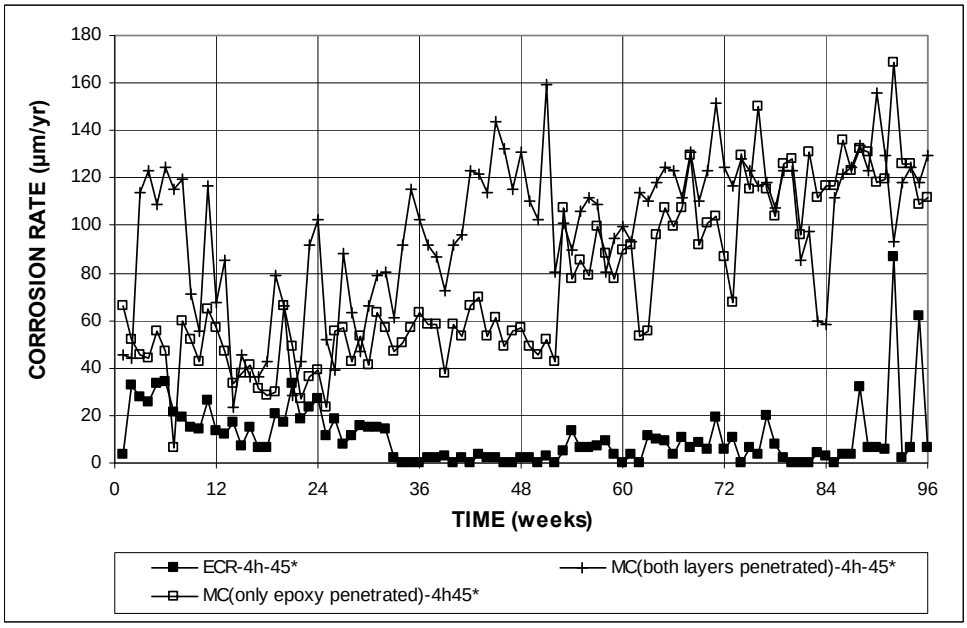

Figure 3.94 – Average corrosion rate based on exposed area, cracked beam test for specimens containing conventional ECR and multiple-coated reinforcement in concrete with *w/c* = 0.45. Bars with coating containing four holes through the epoxy.

than the MC(only epoxy penetrated)-4h-45 specimens, but from week 53 to the end of the test, similar corrosion rates are observed in both specimen groups.

Figures 3.95 and 3.96 show the average corrosion rates based on total and exposed area, respectively, for the cracked beam specimens fabricated with multiple-coated reinforcement containing ten holes in the outer layer(s). Figure 3.95(a) compares the high corrosion rates based on total area for specimens containing conventional steel reinforcement with the low corrosion rates of the specimens containing multiple-coated reinforcement. As shown in Figures 3.95(b) and 3.96, the MC(both layers penetrated)-10h-45 specimens exhibit higher corrosion rates than the MC(only epoxy penetrated)-10h-45 specimens for the entire 96 weeks of the test, except at week 84, when both specimens exhibit similar corrosion rates. Both the

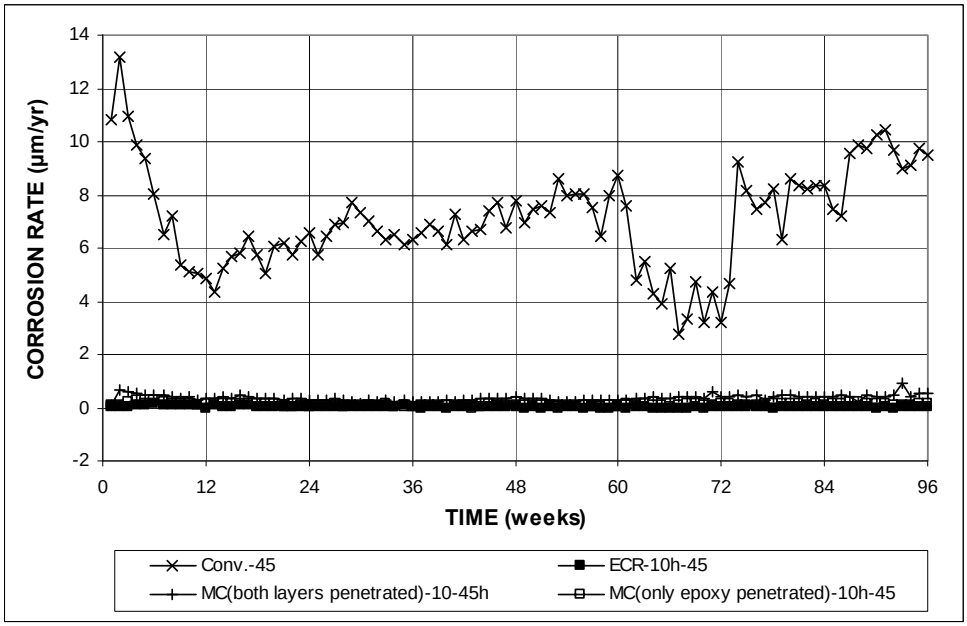

Figure 3.95 (a) – Average corrosion rate, cracked beam test for specimens containing conventional steel, ECR, and multiple-coated reinforcement in concrete with *w/c* = 0.45. Bars with coating containing ten holes through the epoxy.

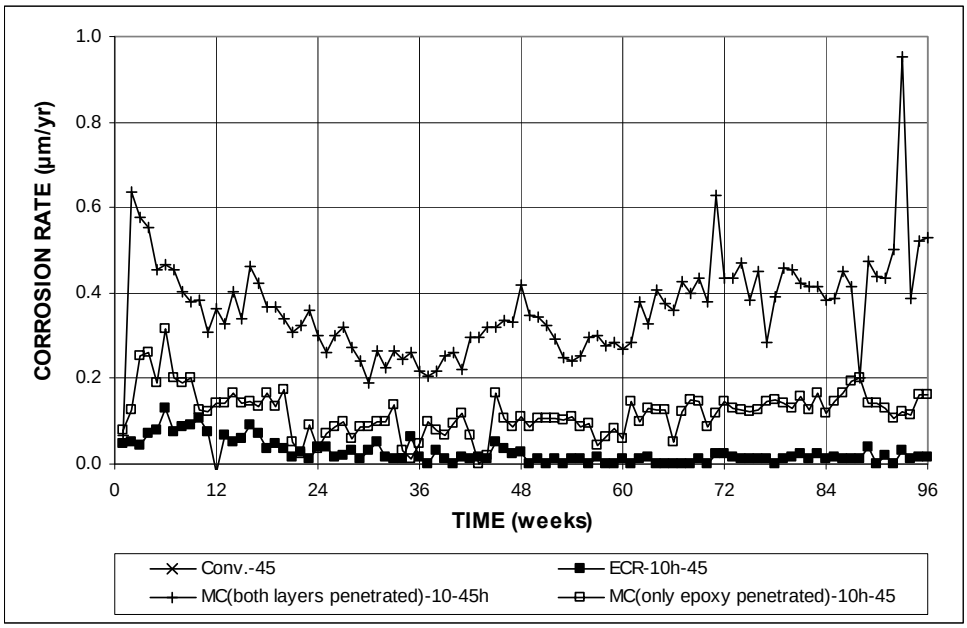

Figure 3.95 (b) – Average corrosion rate, cracked beam test for specimens containing conventional steel, ECR, and multiple-coated reinforcement in concrete with *w/c* = 0.45. Bars with coating containing ten holes through the epoxy. (Different scale)

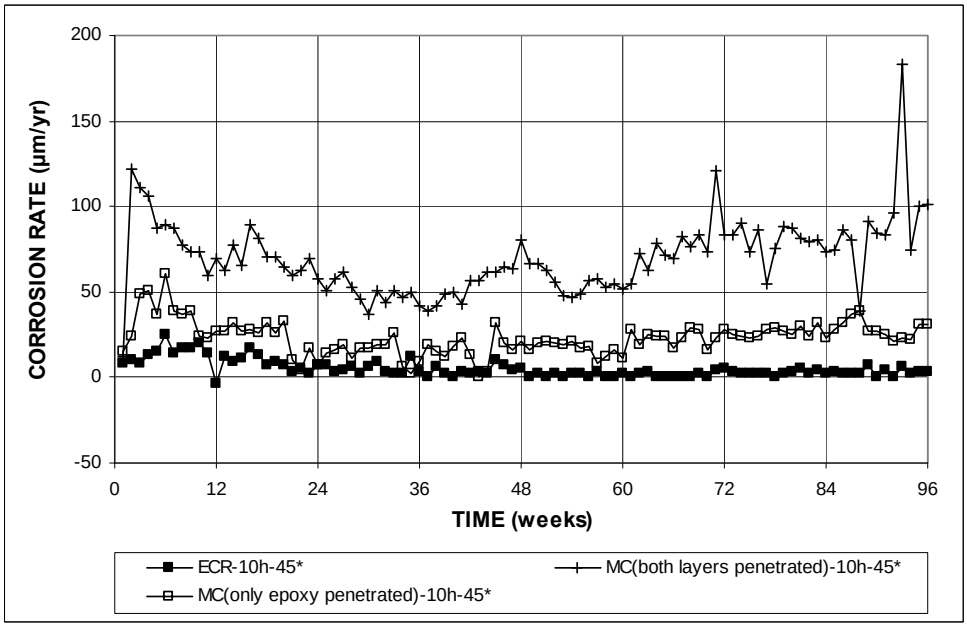

Figure 3.96 – Average corrosion rate based on exposed area, cracked beam test for specimens containing conventional ECR and multiple-coated reinforcement in concrete with *w/c* = 0.45. Bars with coating containing ten holes through the epoxy.

four-hole and the ten-hole multiple-coated reinforcement specimens exhibit higher corrosion rates than the ECR control specimens. During the study, the corrosion rate observed in the MC(both layers penetrated)-10h-45 specimens ranged from 0.066 to 0.952 μm/yr based on total area (12.6 to 183 μm/yr based on exposed area), while the corrosion rate in the MC(only epoxy penetrated)-10h-45 specimens ranged from 0 to 0.315 μm/yr based on total area (0 to 60.54 μm/yr based on exposed area).

Figures 3.97 and 3.98 show the corrosion losses based on total and exposed area, respectively, as measured in the cracked beam specimens fabricated with multiple-coated reinforcement containing four holes through the outer layer(s). Figure 3.97 compares the high corrosion rates based on total area for specimens containing conventional steel reinforcement with the low corrosion rates for the specimens

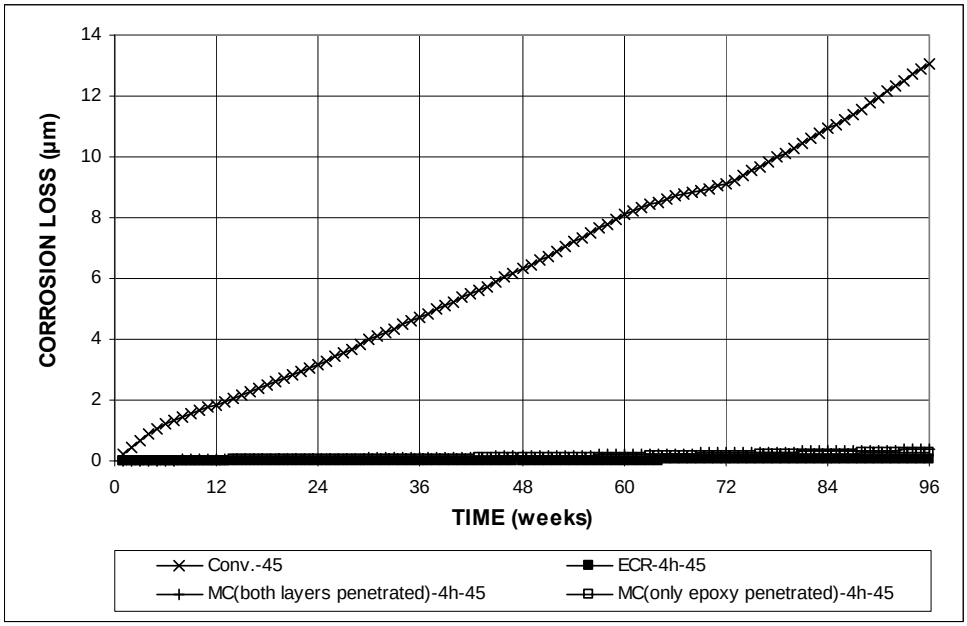

Figure 3.97 – Average corrosion loss, cracked beam test for specimens containing conventional steel, ECR, and multiple-coated reinforcement in concrete with *w/c* = 0.45. Bars with coating containing four holes through the epoxy.

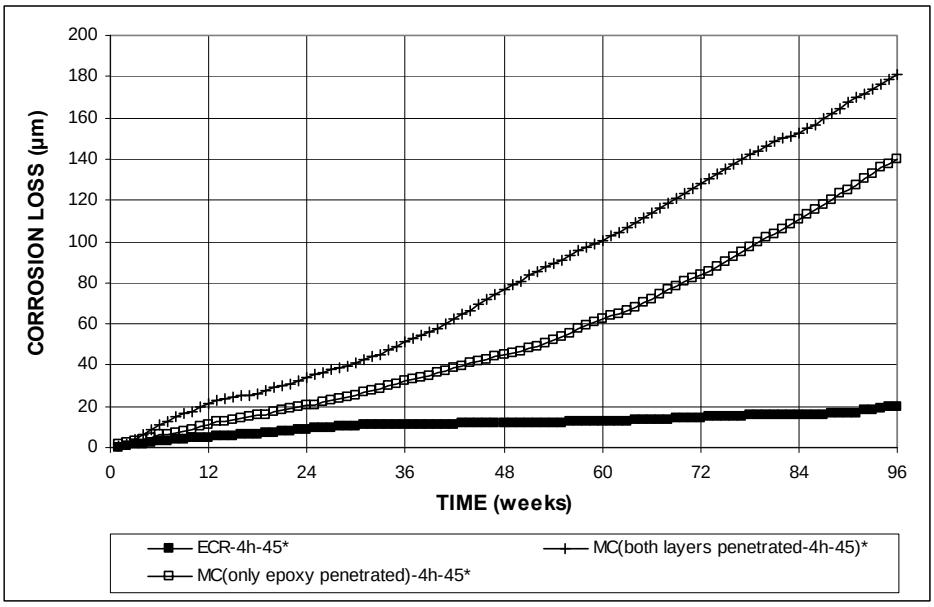

Figure 3.98 – Average corrosion loss based on exposed area, cracked beam test for specimens containing conventional ECR and multiple-coated reinforcement in concrete with *w/c* = 0.45. Bars with coating containing four holes through the epoxy.

containing multiple-coated reinforcement. As shown in Figure 3.98, both MC specimens exhibit higher corrosion rates (as characterized by the slope of the corrosion loss plot) and corrosion losses than the ECR control specimen. The MC(both layers penetrated)-4h-45 specimens exhibit higher corrosion losses than the MC(only epoxy penetrated)-4h-45 specimens. The higher corrosion loss observed in the specimens with both layers penetrated is due to the increased activity of zinc over iron. The higher corrosion loss is representative of the zinc in the top mat preferentially corroding to protect the steel in the bottom mat.

Figures 3.99 and 3.100 show the corrosion losses based on total and exposed area, respectively, for the MC specimens with ten holes through the outer layer(s). Figure 3.99 compares the high corrosion rates based on total area for specimens

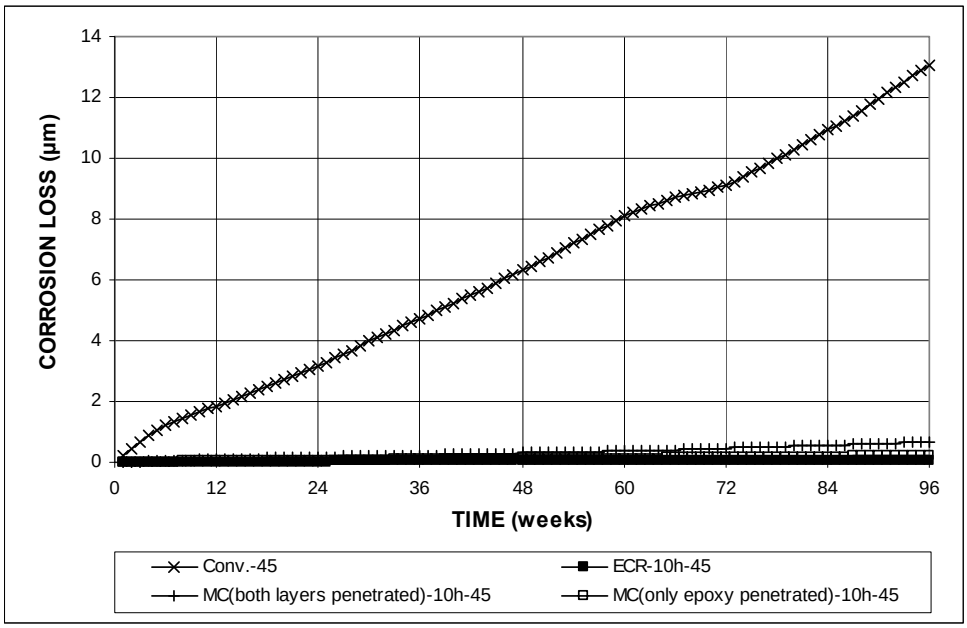

Figure 3.99 – Average corrosion loss, cracked beam test for specimens containing conventional steel, ECR, and multiple-coated reinforcement in concrete with *w/c* = 0.45. Bars with coating containing ten holes through the epoxy.

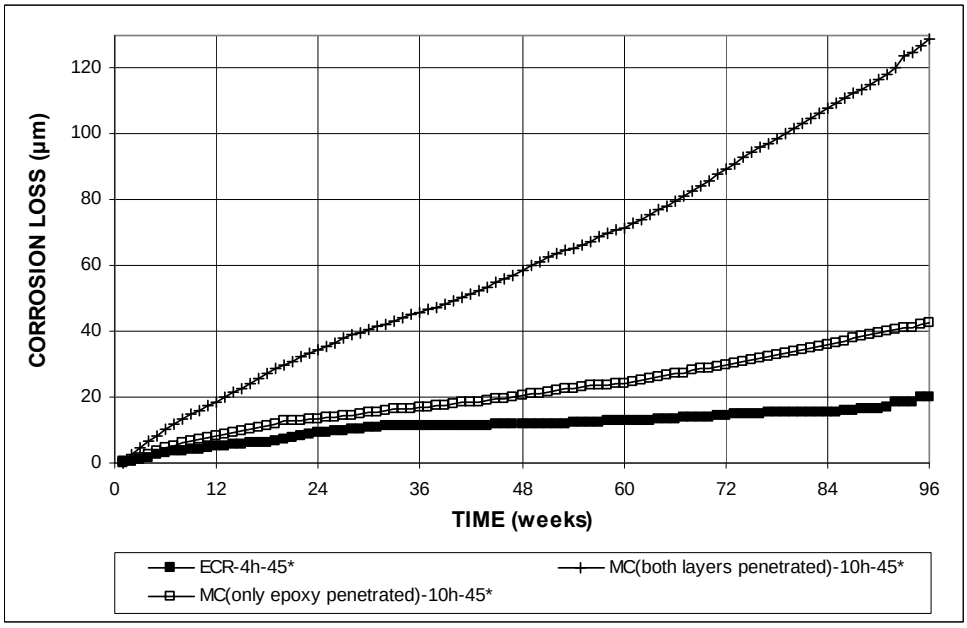

Figure 3.100 – Average corrosion loss based on exposed area, cracked beam test for specimens containing conventional ECR and multiple-coated reinforcement in concrete with *w/c* = 0.45. Bars with coating containing ten holes through the epoxy.

containing conventional steel reinforcement with the low corrosion rates of the specimens containing multiple-coated reinforcement. As shown in Figure 3.100, both MC specimens exhibit higher corrosion rates and corrosion losses than the ECR control specimens. The MC(both layers penetrated)-10h-45 specimens exhibit much higher corrosion losses than the MC(only epoxy penetrated)-10h-45 specimens, which exhibit corrosion losses about twice those of the ECR control specimens.

Table 3.10 summarizes the corrosion loss results at 96 weeks for the cracked beam specimens containing multiple-coated reinforcement with four and ten holes through the outer layer(s). Based on total area, the MC(both layers penetrated)-10h-45 specimens exhibit the highest corrosion loss, 0.672 μm, followed by the MC(both layers penetrated)-4h-45, MC(only epoxy penetrated)-4h-45, and MC(only epoxy penetrated)-10h-45 specimens, with losses of 0.377, 0.294, and 0.221 μm, respectively. The MC(only epoxy penetrated)-10h-45 specimens would be expected to exhibit more corrosion than the MC(only epoxy penetrated)-4h-45 specimens due to the increased exposure area afforded by the ten holes through the epoxy; however, they exhibit lower corrosion rates and lower corrosion losses than their four-hole counterparts. The reason for this behavior is unclear. It is also noteworthy that the MC(both layers penetrated)-4h-45 specimens exhibit higher corrosion loss than the MC(only epoxy penetrated)-10h-45 specimens, despite their advantage over the ten-hole specimens due to their smaller exposed area. This further illustrates that in specimens with both layers penetrated, the zinc layer in the top mats preferentially corrodes to protect the exposed steel in the bottom mat. Based on exposed area, the

MC(both layers penetrated)-4h-45 specimens exhibit the highest corrosion loss, 181 μm, followed by the MC(only epoxy penetrated)-4h-45, MC(both layers penetrated)-10h-45, and MC(only epoxy penetrated)-10h-45 specimens, with losses of 140, 129, and 42.5 μm, respectively. Thus, after adjusting the data for the differences in exposed area between the four and ten hole specimens, the multiple-coated specimens with four holes through the outer layer(s) exhibit higher corrosion losses than the specimens with ten holes through the outer layer(s), regardless of whether both layers are penetrated or whether only the epoxy layer is penetrated. This behavior is unique to the cracked beam specimens and is not observed in the Southern Exposure specimens.

Table 3.10 – Average corrosion loss (μm) at week 96 as measured in the cracked beam test for specimens containing multiple-coated reinforcement

Steel Designation[a]	Specimen			Average	Standard Deviation
	1	2	3		
Total Area					
MC(both layers penetrated)-4h-45	0.489	0.262	0.379	0.377	0.114
MC(both layers penetrated)-10h-45	0.214	1.27	0.532	0.672	0.541
MC(only epoxy penetrated)-4h-45	0.141	0.161	0.581	0.294	0.248
MC(only epoxy penetrated)-10h-45	0.159	0.106	0.398	0.221	0.156
Exposed Area					
MC(both layers penetrated)-4h-45*	235	126	182	181	54.6
MC(both layers penetrated)-10h-45*	41.1	244	102	129	104
MC(only epoxy penetrated)-4h-45*	64.9	76.0	279	140	120
MC(only epoxy penetrated)-10h-45*	30.5	20.7	76.4	42.5	29.7

[a] MC(both layers penetrated) = multiple coated bars with both zinc and epoxy layers penetrated.
MC(only epoxy penetrated) = mutiple coated bars with only epoxy layer penetrated.
4h = bar with four holes through epoxy, 10h = bar with 10 holes through epoxy.
45 = concrete with *w/c* =0.45

* Corrosion loss calculation based on the exposed area of four or ten 3-mm (1/8-in.) diamter holes.

Figures 3.101 and 3.102 show the average mat-to-mat resistance for cracked beam specimens containing multiple-coated reinforcement with four and ten holes through the outer layer(s), respectively. As shown in Figure 3.101, both the MC(both

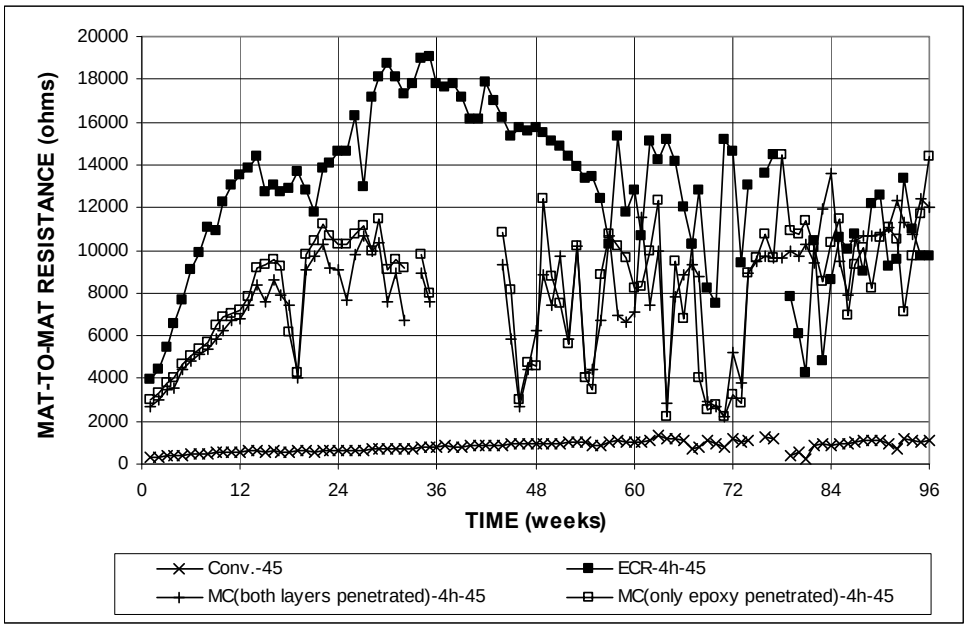

Figure 3.101 – Average mat-to-mat resistance, cracked beam test for specimens containing conventional steel, ECR, and multiple-coated reinforcement in concrete with *w/c* = 0.45. Bars with coating containing four holes through the epoxy.

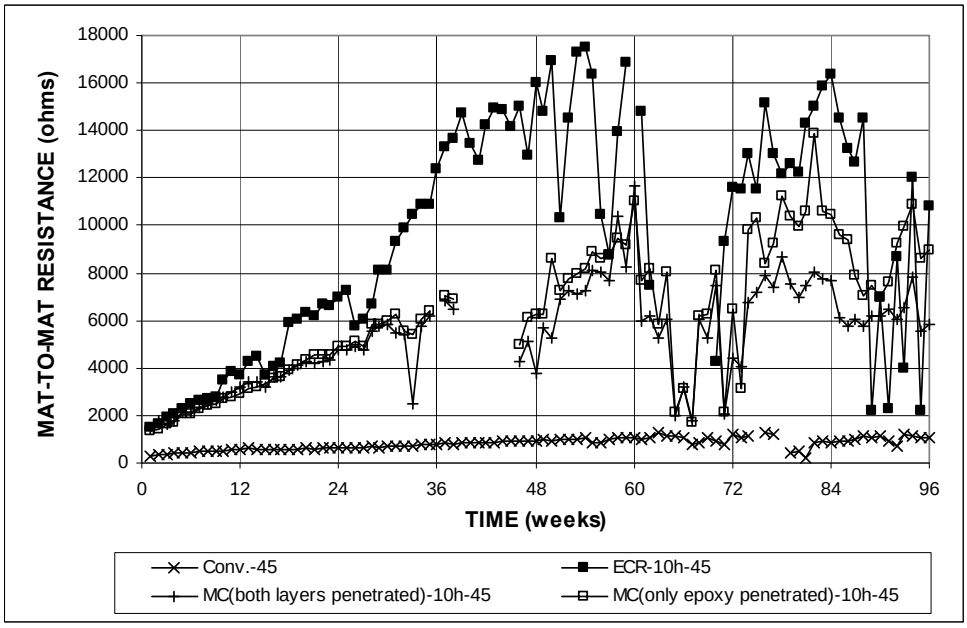

Figure 3.102 – Average mat-to-mat resistance, cracked beam test for specimens containing conventional steel, ECR, and multiple-coated reinforcement in concrete with *w/c* = 0.45. Bars with coating containing ten holes through the epoxy.

layers penetrated)-4h-45 and MC(only epoxy penetrated)-4h-45 specimens exhibit similar mat-to-mat resistances during the first 35 weeks of the test, which are lower than the resistance observed for the ECR control specimens. From week 43 through week 96, a high amount of scatter is present in the data; consequently, no conclusions can be made from this data. As previously mentioned, additional cracking occurring within the specimen may be periodically altering the resistance caused by the formation of corrosion and hydration products. As shown in Figure 3.102, both MC specimen types with ten holes exhibit lower average mat-to-mat resistances than the ECR control specimens during the first 36 weeks of the test, although the degree of difference is less than that observed between the ECR control specimens and the MC specimens with four holes through the outer layer(s). From week 48 to week 96, the average mat-to-mat resistance of both MC specimen types generally remains lower than the ECR control specimens, with the MC(only epoxy penetrated)-10h-45 specimens exhibiting average resistances equal to or greater than those observed in MC(both layers penetrated)-10h-45.

Figures 3.103 and 3.104 show the average top and bottom mat corrosion potentials versus a copper-copper sulfate electrode as measured in the cracked beams specimens containing multiple-coated reinforcement with four and ten holes through the outer layer(s), respectively. As shown in Figure 3.103(a), the MC(only epoxy penetrated)-4h-45 specimens exhibit the lowest top mat corrosion potentials during the first 13 weeks, followed by the MC(both layers penetrated)-4h-45, Conv.-45, and ECR-4h-45 specimens. From week 19 to the end of the test, both MC specimen types

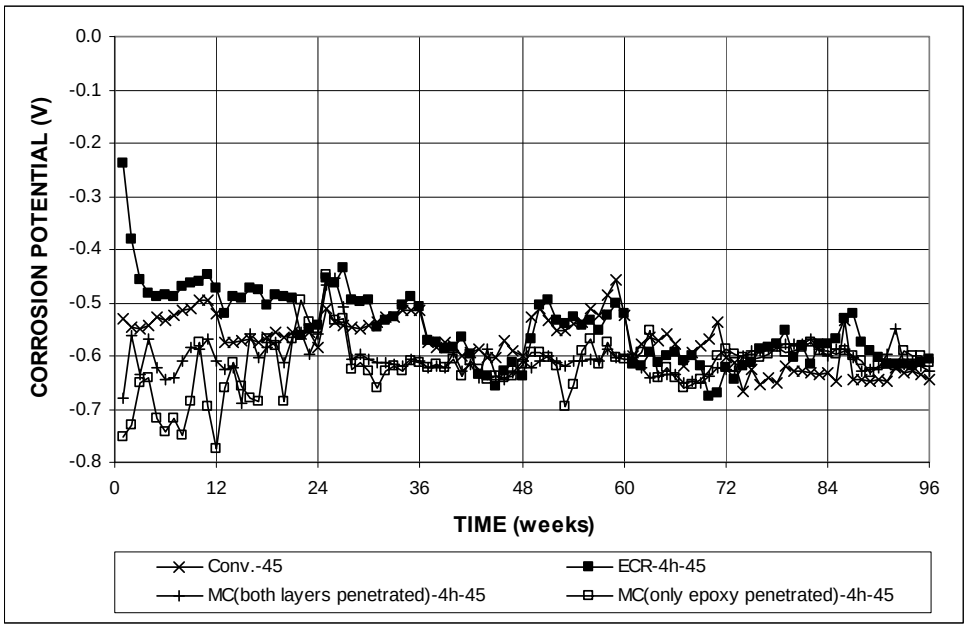

Figure 3.103 (a) – Average top mat corrosion potential, cracked beam test for specimens containing conventional steel, ECR, and multiple-coated reinforcement in concrete with *w/c* = 0.45. Bars with coating containing four holes through the epoxy.

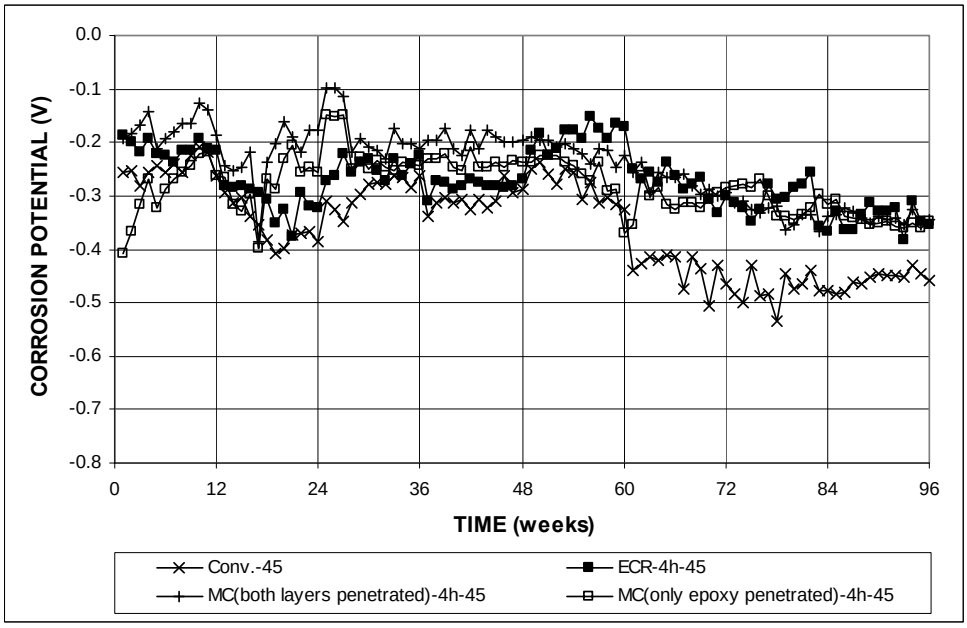

Figure 3.103 (b) – Average bottom mat corrosion potential, cracked beam test for specimens containing conventional steel, ECR, and multiple-coated reinforcement in concrete with *w/c* = 0.45. Bars with coating containing four holes through the epoxy.

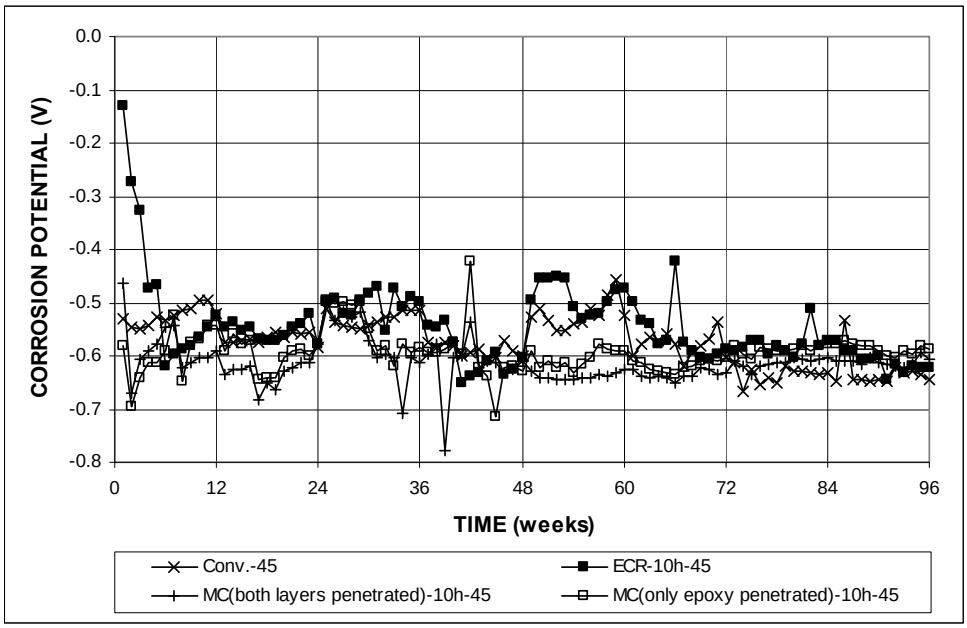

Figure 3.104 (a) – Average top mat corrosion potential, cracked beam test for specimens containing conventional steel, ECR, and multiple-coated reinforcement in concrete with *w/c* = 0.45. Bars with coating containing ten holes through the epoxy.

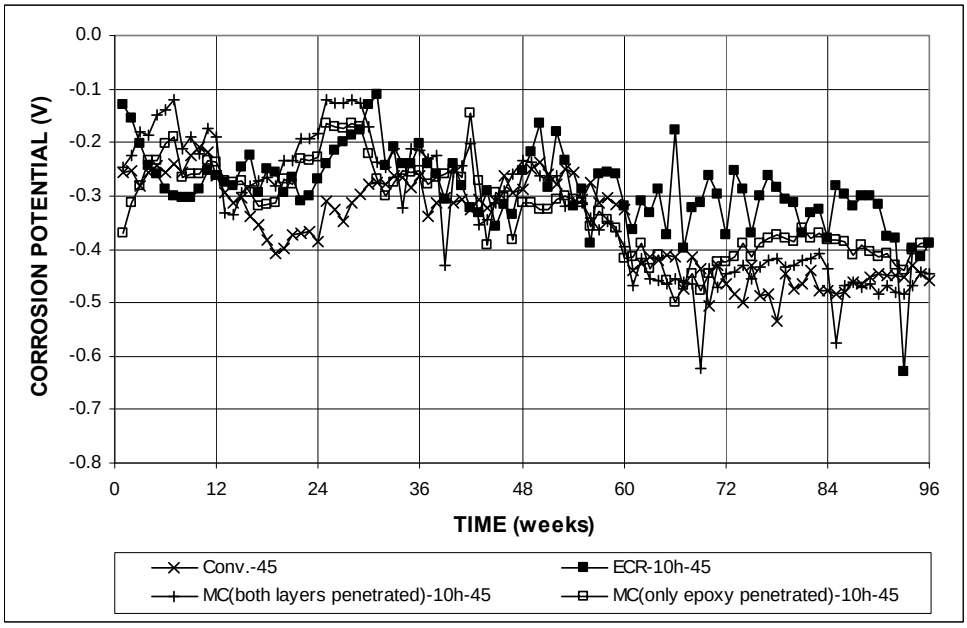

Figure 3.104 (b) – Average bottom mat corrosion potential, cracked beam test for specimens containing conventional steel, ECR, and multiple-coated reinforcement in concrete with *w/c* = 0.45. Bars with coating containing ten holes through the epoxy.

exhibit top mat corrosion potentials similar to those observed in the conventional steel and ECR control specimens, except between weeks 48 and 60, during which both control specimens exhibit top mat corrosion potentials that are slightly more positive than the MC specimens. During the testing period, the top mat corrosion potentials observed in the four-hole MC specimens range from –0.450 V to –0.688 V for the MC(both layers penetrated)-4h-45 specimens and from –0.477 V to –0.755 V for the MC(only epoxy penetrated)-4h-45 specimens. As shown in Figure 3.103(b), the bottom mat corrosion potentials observed in both MC specimens are similar to those observed in the ECR control specimens, and range from –0.097 V to –0.387 V and from –0.149 V to –0.408 V for the MC(both layers penetrated)-4h-45 and MC(only epoxy penetrated)-4h-45 specimens, respectively.

As shown in Figure 3.104(a), both MC specimens with ten holes through the outer layer(s) exhibit top mat corrosion potentials that are similar to those observed in the conventional steel and ECR control specimens, except between weeks 48 and 68, during which both MC specimens exhibit more negative corrosion potentials than those observed in the control specimens. During the study, the top mat corrosion potentials ranged from – 0.465 V to –0.799 V for the MC(both layers penetrated)-10h-45 specimens and from – 0.423 V to –0.715 V for the MC(only epoxy penetrated)-10h-45 specimens. As shown in Figure 3.104(b), the bottom mat corrosion potentials observed in the MC specimens are similar to those observed in the ECR control specimens during the first 56 weeks of the test. From week 57 through week 96, the bottom mat corrosion potentials exhibited in the MC specimens

are more typical of the bottom mat corrosion potentials measured in the conventional steel control specimens. The bottom mat corrosion potentials for the MC specimens range from –0.119 V to –0.622 V for the MC(both layers penetrated)-10h-45 specimens and between –0.144 V to –0.499 V for the MC(only epoxy penetrated)-10h-45 specimens.

3.6 Linear Polarization Resistance Tests

This section presents the results of the linear polarization resistance (LPR) tests conducted in this study. Linear polarization is used to measure the combined microcell and macrocell corrosion rates of the top and bottom mats of one Southern Exposure and one cracked beam specimen from each group of corrosion protection systems. For simplicity of notation and to distinguish the LPR results from the macrocell results based on the voltage drop across the 10-ohm resistor, the LPR results will be referred to as "microcell" rates and losses.

As described in Chapter 1, the polarization resistance test provides a measure of the corrosion rate of a metal in terms of a corrosion current density. Various criteria have been suggested for interpreting the corrosion current densities measured using the LPR test (Berke 1987, Clear 1989). For the test configuration used in the current study, Guo et al. (2006) used the guidelines presented by Broomfield (1997), presented in Table 3.11, to interpret the LPR test results. These guidelines were developed for LPR tests conducted on conventional steel specimens and are not applicable to epoxy-coated reinforcement. In addition to microcell corrosion rates,

Table 3.11 – LPR interpretation guidelines presented by Broomfield (1997)

Corrosion Current Density*	**Corrosion Rate**	**Corrosion Level**
$\mu A/cm^3$	μm/yr	
< 0.1	<1.16	Passive condition
0.1 to 0.5	1.16 to 5.8	Low to moderate corrosion
0.5 to 1.0	5.8 to 11.6	Moderate to high corrosion
> 1.0	> 11.6	High corrosion

* Stern-Geary constant, B = 26 mV

microcell corrosion losses will also be reported. As explained in Chapter 1, corrosion losses are calculated by numerically integrating the corrosion rates.

In the current study, separate LPR measurements are made every four weeks on the top and bottom mats. The first LPR measurements are made on the fourth week of testing for most specimens; however, the first LPR measurements were made as late as week 16 for some specimens. Since microcell corrosion losses are calculated by integrating the microcell corrosion rates, the corrosion losses in these specimens during this initial time step are calculated assuming a constant microcell corrosion rate over the time step, equal to the first microcell corrosion rate measured. In some instances, LPR measurements result in microcell corrosion rates that are uncharacteristically high when compared to microcell corrosion rates from the previous or following measurements. If these spikes in microcell corrosion rate are not accompanied by a corresponding increase in macrocell corrosion rate, it is concluded that these readings are aberrant and are not included in the microcell loss calculations. Instead, the uncharacteristically high corrosion rate is replaced by the microcell corrosion rate of the previous period.

Unless otherwise noted, the figures in this section show the microcell corrosion rates and microcell corrosion losses based on total area for the corrosion protection systems evaluated during the 96 week testing period. The total losses at 96 weeks are summarized in Table 3.12. Results for only the top mat are given in this section because the microcell corrosion rates measured in the bottom mats are usually at least one order of magnitude lower than the microcell corrosion rates measured in the top mat. Appendix D contains the microcell corrosion rates and losses based on the LPR test for the bottom mats for the specimens evaluated in this study. The microcell corrosion loss results reported in this section will be compared in Chapter 4 with the macrocell corrosion loss results reported in earlier in this chapter.

3.6.1 Conventional Steel and Epoxy-Coated Reinforcement

Figure 3.105 shows the microcell corrosion rates for the Southern Exposure specimens containing conventional steel and epoxy-coated reinforcement. The conventional steel reinforcement exhibits higher microcell corrosion rates than the ECR reinforcement throughout the test, with the Conv.-45 specimen showing higher microcell corrosion than the Conv.-35 specimen. This indicates that the lower *w/c* ratio provides some level of corrosion protection in uncracked concrete. The Conv.-45 specimen begins showing moderate to high corrosion (per Table 3.11) at week 52 and high corrosion at week 60. Between weeks 48 to 96, the Conv.-35 specimen showed low to moderate corrosion. The ECR-10h-45 specimen showed the greatest microcell corrosion rates among the ECR specimens, followed by the ECR-10h-35 and ECR-4h-45 specimen. The microcell corrosion rate measured in the ECR-10h-35

Table 3.12 – Total microcell corrosion losses (μm) at week 96 for Southern Exposure and cracked beam specimens, as measured using the linear polarization test.

Steel Designation[a]	Based on Total Area		Based on Exposed Area	
	Southern Exposure Test	Cracked Beam Test	Southern Exposure Test	Cracked Beam Test
Control				
Conv.-45	17.7	167	-	-
Conv.-35	2.50	131	-	-
ECR-4h-45	0.002	0.466	1.08	224
ECR-10h-45	0.143	0.471	27.4	90.4
ECR-10h-35	0.020	0.826	3.84	159
Corrosion inhibitors				
ECR(DCI)-4h-45	0.032	0.763	15.2	366
ECR(DCI)-10h-45	0.185	1.29	35.5	247
ECR(DCI)-10h-35	0.020	2.58	3.83	495
ECR(RH)-4h-45	0.002	2.22	0.961	1070
ECR(RH)-10h-45	0.024	1.16	4.55	223
ECR(RH)-10h-35	0.018	0.854	3.40	164
ECR(HY)-4h-45	0.005	0.357	2.25	171
ECR(HY)-10h-45	0.013	0.880	2.52	169
ECR(HY)-10h-35	0.008	0.811	1.6	156
ECR(primer/$Ca(NO_2)_2$)-4h-45	0.033	0.902	15.8	433
ECR(primer/$Ca(NO_2)_2$)-10h-45	0.029	1.03	5.55	198
ECR(primer/$Ca(NO_2)_2$)-10h-35	0.008	2.33	1.54	447
Multiple Coated Bars				
MC(both layers penetrated)-4h-45	0.931	1.44	447	690
MC(both layers penetrated)-10h-45	1.86	3.65	357	700
MC(only epoxy penetrated)-4h-45	0.803	3.77	386	1810
MC(only epoxy penetrated)-10h-45	0.681	1.66	131	318
Increased Adhesion ECR				
ECR(Chromate)-4h-45	0.029	1.73	14.1	829
ECR(Chromate)-10h-45	0.090	0.550	17.3	106
ECR(DuPont)-4h-45	0.106	0.525	50.9	252
ECR(DuPont)-10h-45	0.287	1.88	55.2	362
ECR(Valspar)-4h-45	0.142	1.91	68	918
ECR(Valspar)-10h-45	0.193	1.71	37.1	329
Increased Adhesion ECR with Corrosion Inhibitor DCI				
ECR(Chromate)-DCI-4h-45	0.080	-	38.4	-
ECR(DuPont)-DCI-4h-45	0.010	-	4.88	-
ECR(Valspar)-DCI-4h-45	0.004	-	1.76	-

[a] Conv. = conventional steel. ECR = conventional epoxy-coated reinforcement.
ECR(Chromate) = ECR with the chromate pretreatment.
ECR(DuPont) = ECR with high adhesion DuPont coating.
ECR(Valspar) = ECR with high adhesion Valspar coating.
ECR(DCI) = ECR in concrete with DCI inhibitor.
ECR(Rheocrete) = ECR in concrete with Rheocrete inhibitor.
ECR (Hycrete) = normal ECR with Hycrete inhibitor.
MC(both layers penetrated) = multiple coated bars with both zinc and epoxy layers penetrated.
MC(only epoxy penetrated) = mutiple coated bars with only epoxy layer penetrated.
4h = bar with four holes through epoxy, 10h = bar with 10 holes through epoxy.
45 = concrete with *w/c* =0.45; 35 = concrete with *w/c* =0.45.

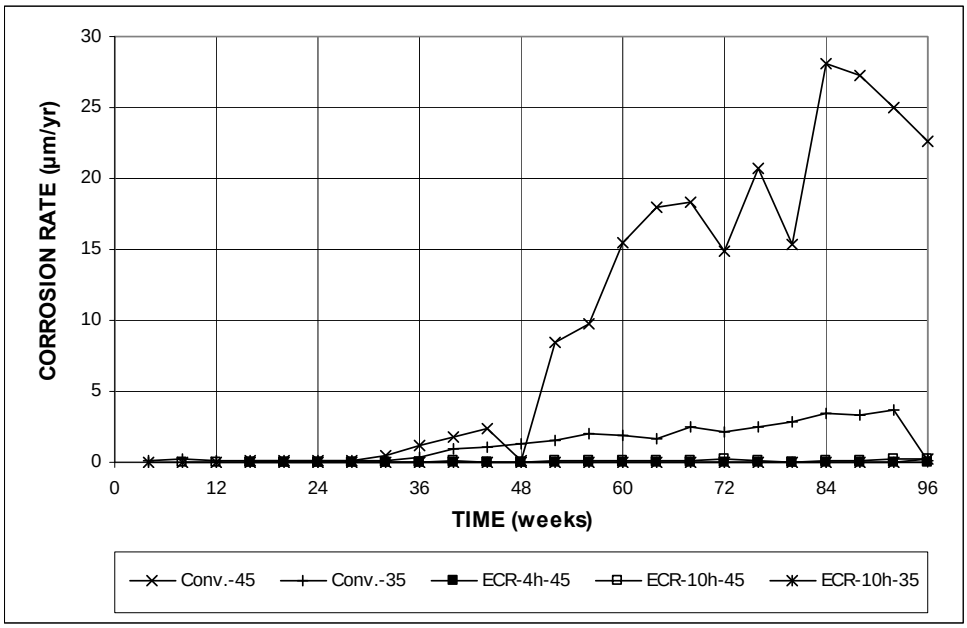

Figure 3.105 (a) – Microcell corrosion rate, LPR test for Southern Exposure specimens containing conventional and ECR with four and ten holes through the epoxy, *w/c* = 0.45 and 0.35.

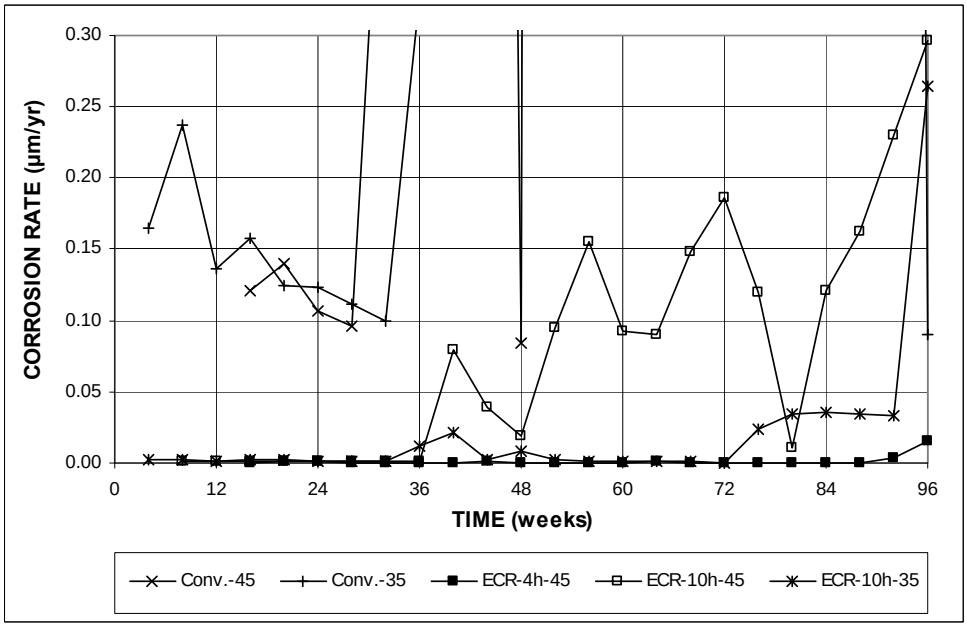

Figure 3.105 (b) – Microcell corrosion rate, LPR test for Southern Exposure specimens containing conventional and ECR with four and ten holes through the epoxy, *w/c* = 0.45 and 0.35. (Different scale)

specimen at week 96 is uncharacteristically high and is, in all likelihood, due to an aberrant reading. Consequently, this reading is not used when calculating the passive condition (<1.16 μm/yr). Again, the lower microcell corrosion rates observed in the ECR-10h-35 specimen, when compared with the ECR-10h-45 specimen, suggests that the lower permeability of the lower *w/c* ratio concrete helps delay corrosion initiation.

Figure 3.106 and Table 3.12 show the microcell corrosion losses for the Southern Exposure specimens containing conventional steel and epoxy-coated reinforcement. The Conv.-45 and Conv.-35 specimens exhibited the highest microcell corrosion losses among the control specimens, with losses at 96 weeks equal to 17.7 μm and 2.50 μm, respectively. Among the ECR control specimens, the

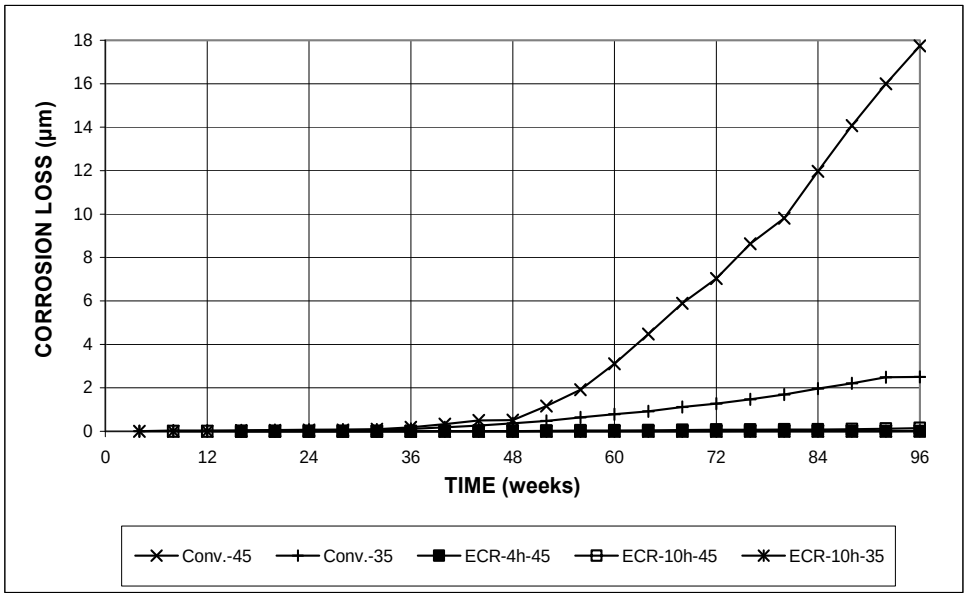

Figure 3.106 (a) – Microcell corrosion loss, LPR test for Southern Exposure specimens containing conventional and ECR with four and ten holes through the epoxy, *w/c* = 0.45 and 0.35.

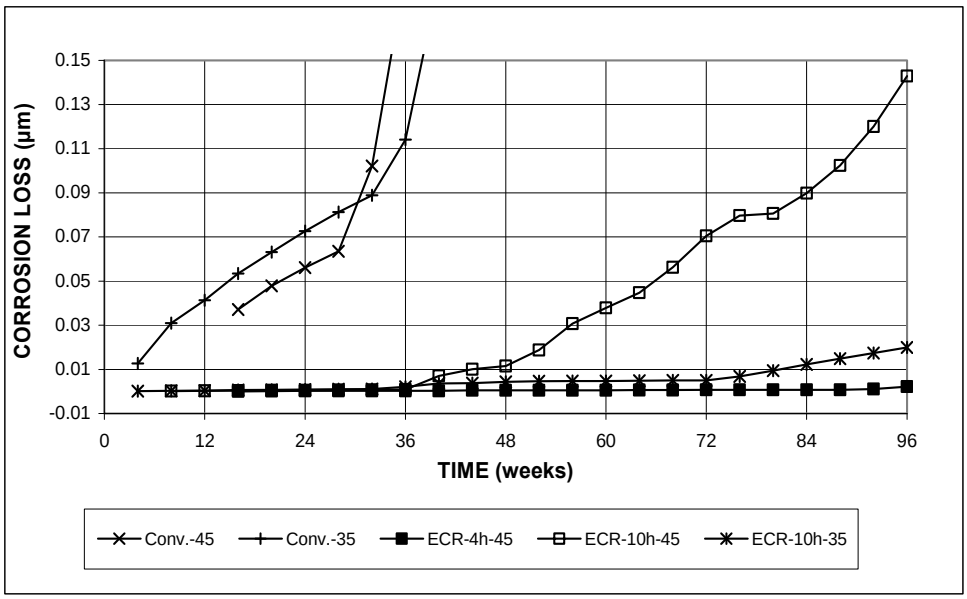

Figure 3.106 (b) – Microcell corrosion loss, LPR test for Southern Exposure specimens containing conventional and ECR with four and ten holes through the epoxy, *w/c* = 0.45 and 0.35. (Different scale)

ECR-10h-45 specimen exhibited the highest microcell corrosion loss, 0.143 µm at 96 weeks, followed by the ECR-10h-35 and ECR-4h-45 specimens with losses of 0.020 and 0.002 µm, respectively. Based on exposed area, the respective values are 27.4, 3.84, and 1.08 µm. The lower *w/c* ratio appears to have benefited the ECR-10h-35 specimen when compared with the ECR-10h-45 specimen.

Figure 3.107 shows the microcell corrosion rates for the cracked beam specimens containing conventional steel and epoxy-coated reinforcement. The Conv.-45 and Conv.-35 specimens generally exhibit similar microcell corrosion rates during the course of the test. This indicates that the *w/c* ratio has little effect on the microcell corrosion of reinforcement placed in cracked concrete, which is likely due to the direct access to the bar afforded to the chloride ions by the crack. It is also

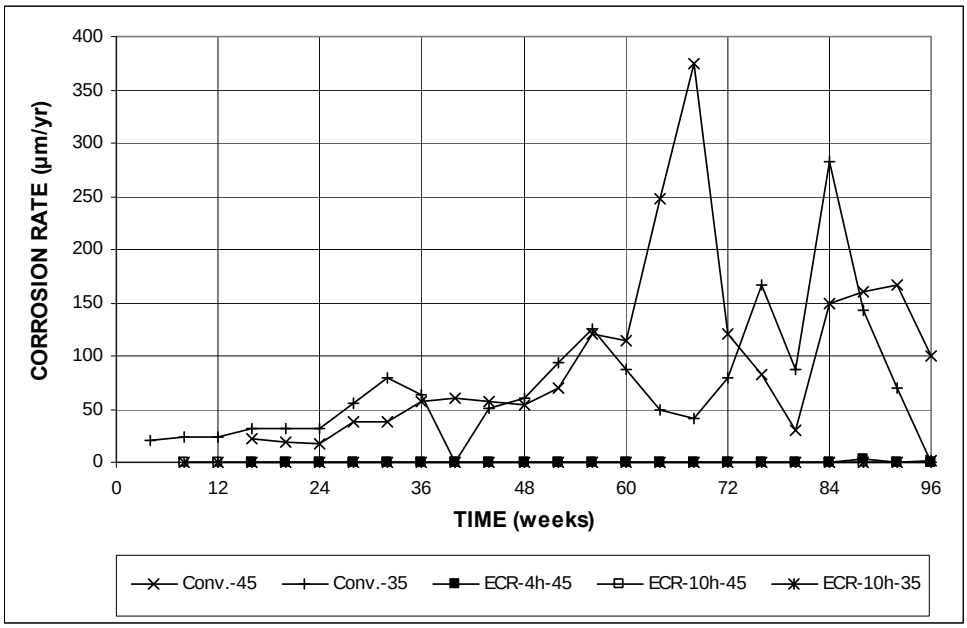

Figure 3.107 (a) – Microcell corrosion rate, LPR test for cracked beam specimens containing conventional and ECR with four and ten holes through the epoxy, *w/c* = 0.45 and 0.35.

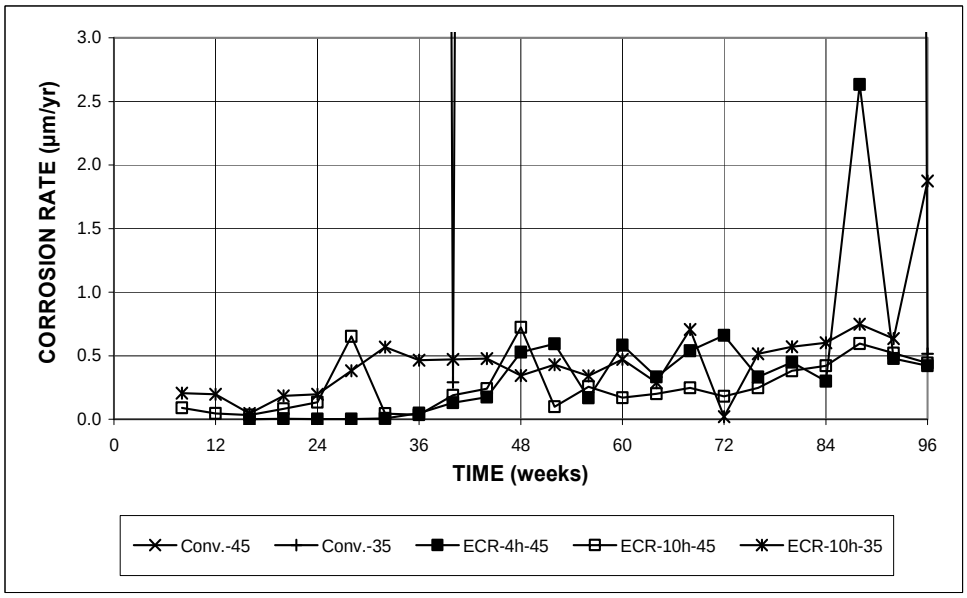

Figure 3.107 (b) – Microcell corrosion rate, LPR test for cracked beam specimens containing conventional and ECR with four and ten holes through the epoxy, *w/c* = 0.45 and 0.35. (Different scale)

observed that measurable microcell corrosion is observed in both the Conv.-45 and Conv.-35 specimens as early as the first LPR measurement. No significant amount of microcell corrosion is observed in the ECR specimens during the test, except for the ECR-4h-45 specimen at week 88 which exhibit a microcell corrosion rate of 2.63 μm/yr, and is in all likelihood due to an aberrant reading. Consequently, this LPR reading is not used when calculating the microcell corrosion loss for the ECR-4h-45 specimen. It is noted that the microcell corrosion rates are much higher than the macrocell corrosion rates presented earlier for these specimens.

The microcell corrosion losses for the cracked beam specimens containing conventional and epoxy reinforcement are presented in Figure 3.108 and Table 3.12. The Conv.-45 and Conv.-35 specimens show the highest 96-week microcell corrosion losses, 167 and 131 μm based on total area, respectively, among the control specimens.

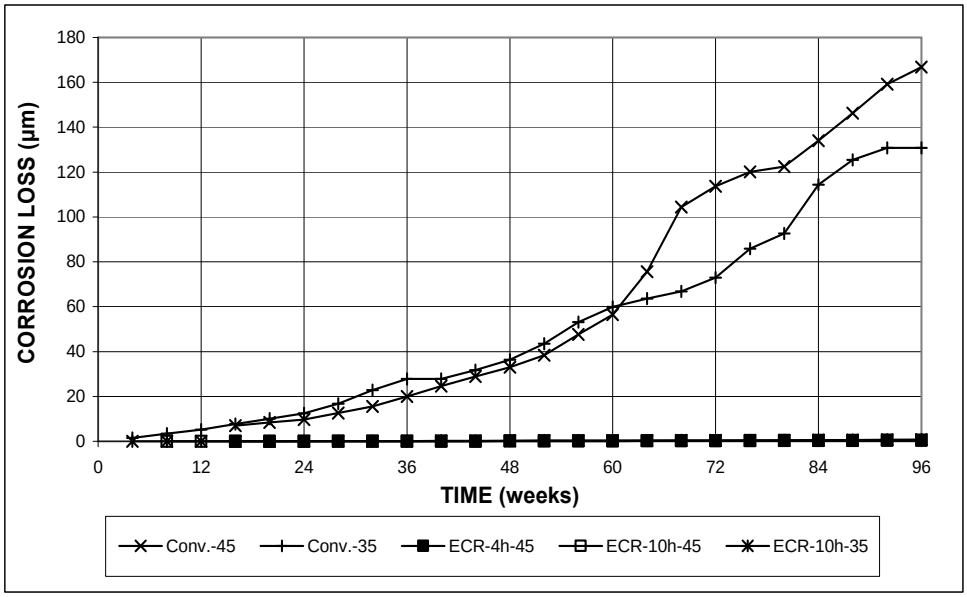

Figure 3.108 (a) – Microcell corrosion loss, LPR test for cracked beam specimens containing conventional and ECR with four and ten holes through the epoxy, *w/c* = 0.45 and 0.35.

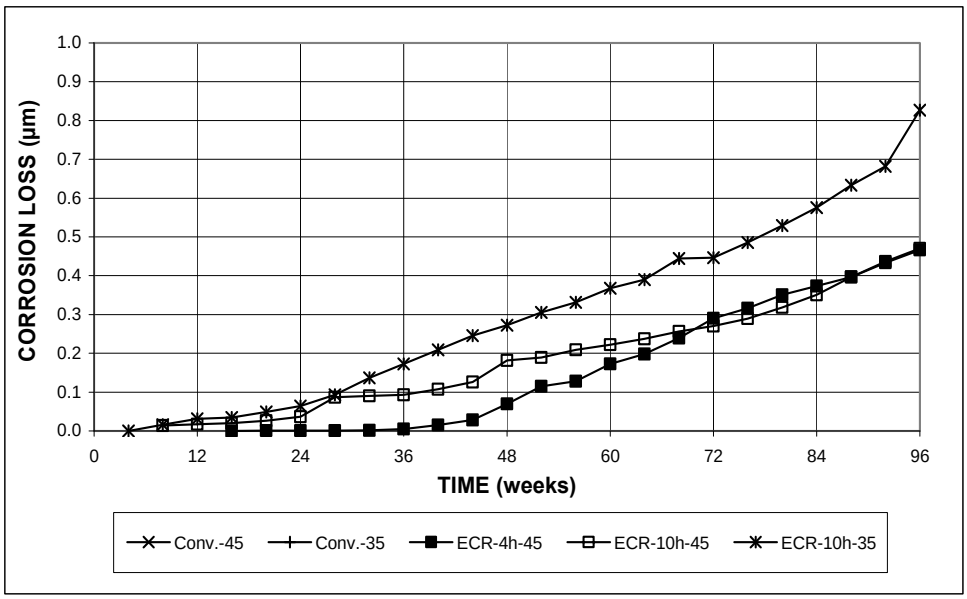

Figure 3.108 (b) – Microcell corrosion loss, LPR test for cracked beam specimens containing conventional and ECR with four and ten holes through the epoxy, *w/c* = 0.45 and 0.35.

Among the specimens containing ECR, the ECR-10h-35 specimen exhibits the highest corrosion loss, 0.826 µm, followed by the ECR-10h-45 and ECR-4h-45 specimens with losses of 0.471 and 0.466 µm based on total area, respectively. During the study, the Conv.-45 and Conv.-35 specimens exhibit similar corrosion rates and losses, indicating that the decreased *w/c* ratio affords no additional corrosion protection to the reinforcement. Similarly, the cumulative microcell corrosion losses observed in ECR specimens are all very similar during the course of the test, further indicating that a low w/c ratio affords no additional protection to the reinforcement against microcell corrosion in the presence of a crack.

3.6.2 Corrosion Inhibitors

This section presents the LPR test results for the Southern Exposure and cracked beam test specimens containing ECR cast in concrete containing corrosion

inhibitors. DCI, Rheocrete 222+, and Hycrete, as well as ECR containing a calcium nitrite primer between the epoxy and steel, are evaluated. Figures 3.109 through 3.111 show the microcell corrosion rates for the Southern Exposure specimens. For specimens with ECR containing four holes through the epoxy (Figure 3.109), the ECR(primer/Ca(NO2)2)-4h-45 and ECR(DCI)-4h-45 specimens exhibit significantly higher microcell corrosion rates than the control specimens, with corrosion rates surpassing 0.01 μm/yr at 76 weeks and 72 weeks, respectively. The corrosion rate observed for the ECR(DCI)-4h-45 specimen at week 80 is uncharacteristically high, and is, in all likelihood, due to an aberrant reading. Consequently, it is not used in calculating the microcell corrosion loss for this specimen. All other ECR specimens

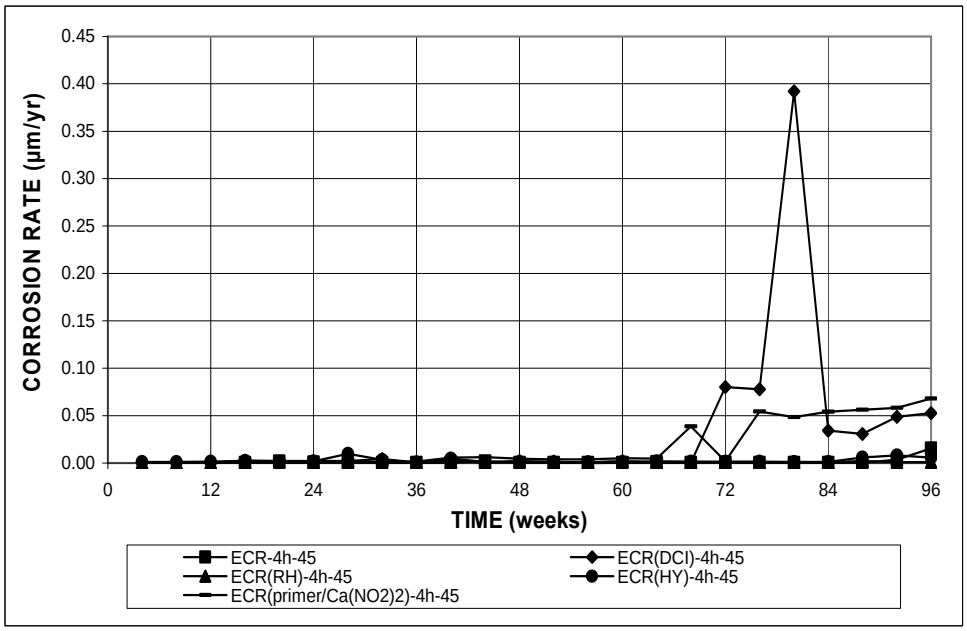

Figure 3.109 (a) – Microcell corrosion rate, LPR test for Southern Exposure specimens containing ECR, ECR in concrete with corrosion inhibitors, and ECR with a calcium nitrite primer, *w/c* = 0.45. Bars with coating containing four holes through the epoxy.

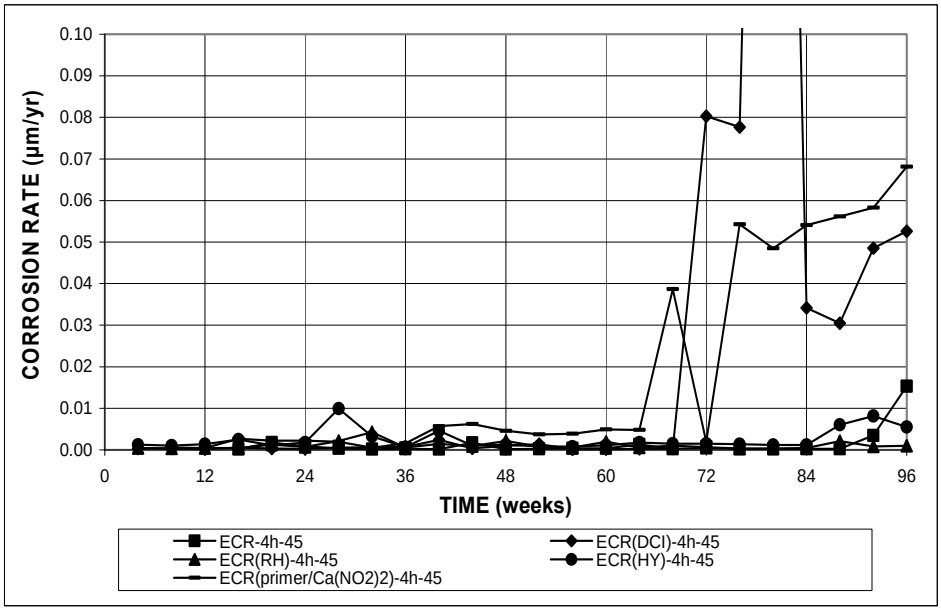

Figure 3.109 (b) – Microcell corrosion rate, LPR test for Southern Exposure specimens containing ECR, ECR in concrete with corrosion inhibitors, and ECR with a calcium nitrite primer, *w/c* = 0.45. Bars with coating containing four holes through the epoxy. (Different scale)

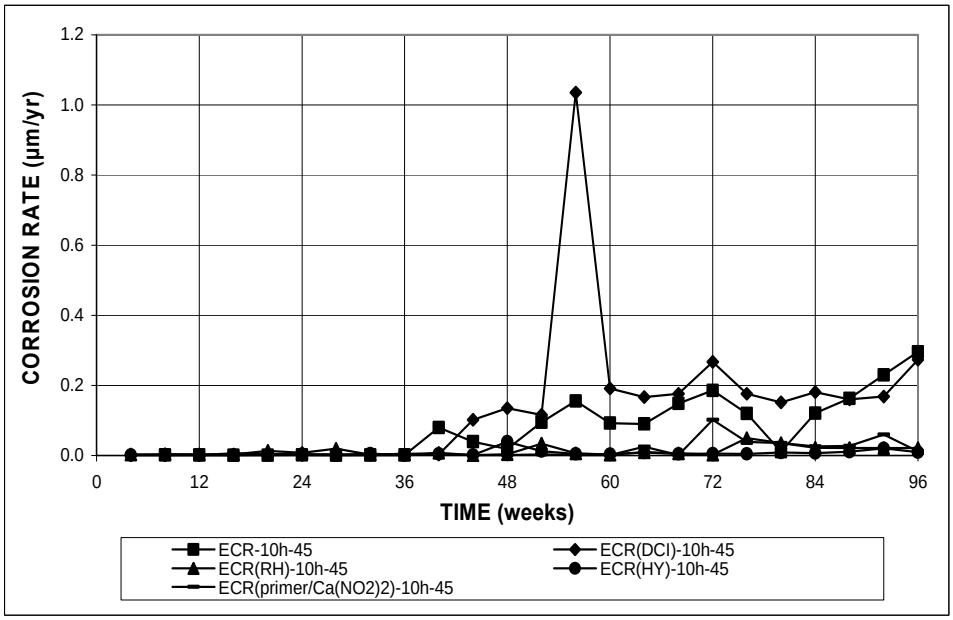

Figure 3.110 (a) – Microcell corrosion rate, LPR test for Southern Exposure specimens containing ECR, ECR in concrete with corrosion inhibitors, and ECR with a calcium nitrite primer, *w/c* = 0.45. Bars with coating containing ten holes through the epoxy.

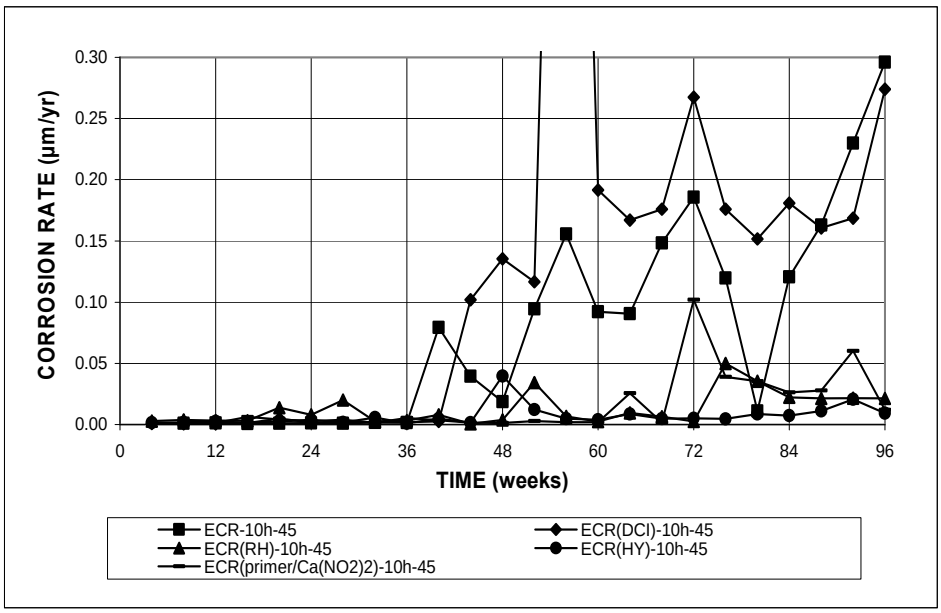

Figure 3.110 (b) – Microcell corrosion rate, LPR test for Southern Exposure specimens containing ECR, ECR in concrete with corrosion inhibitors, and ECR with a calcium nitrite primer, *w/c* = 0.45. Bars with coating containing ten holes through the epoxy. (Different scale)

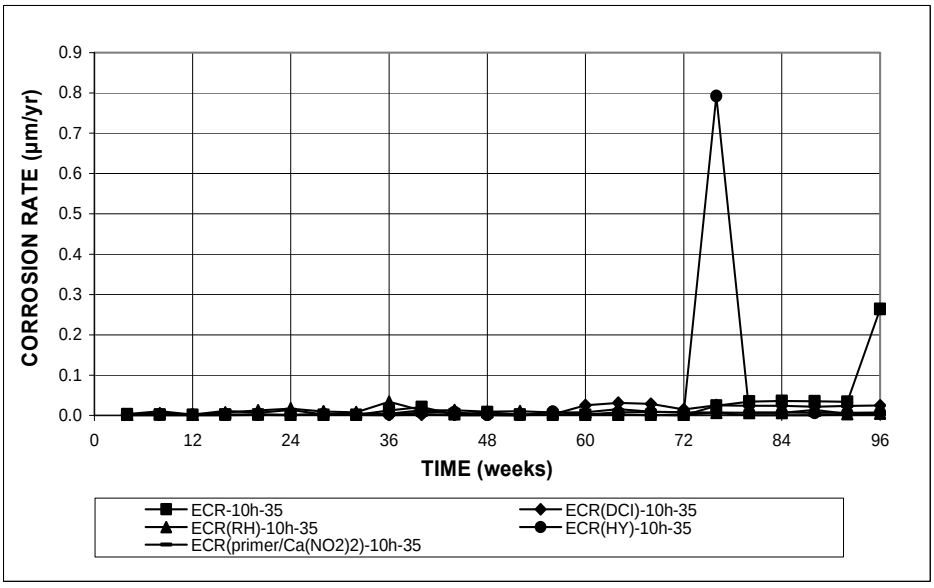

Figure 3.111 (a) – Microcell corrosion rate, LPR test for Southern Exposure specimens containing ECR, ECR in concrete with corrosion inhibitors, and ECR with a calcium nitrite primer, *w/c* = 0.35. Bars with coating containing ten holes through the epoxy.

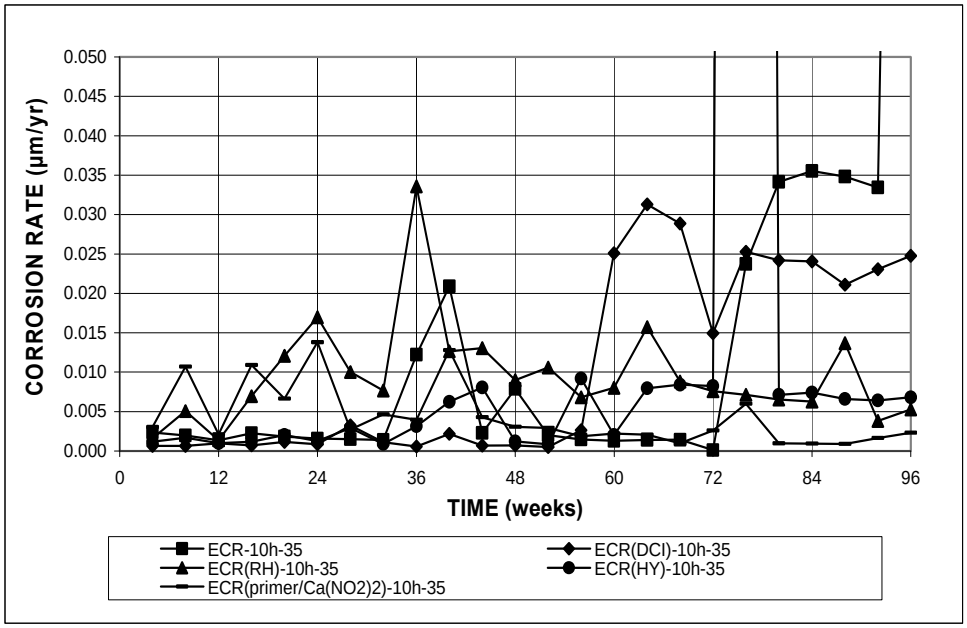

Figure 3.111 (b) – Microcell corrosion rate, LPR test for Southern Exposure specimens containing ECR, ECR in concrete with corrosion inhibitors, and ECR with a calcium nitrite primer, *w/c* = 0.35. Bars with coating containing ten holes through the epoxy. (Different scale)

exhibit corrosion rates similar to the control specimen, with corrosion rates remaining below 0.01 µm/yr during the 96 week study. As shown in Figure 3.110, the ECR(DCI)-10h-45 specimen exhibits higher microcell corrosion rates than the control specimen between weeks 44 to 84. All other ten-hole specimens with w/c = 0.45 have corrosion rates that generally remain below the corrosion rates observed for the control specimens. The high corrosion rate measured in the ECR(DCI)-10h-45 specimen at week 56 is due to an aberrant reading and is not used in the calculation of the microcell corrosion loss for this specimen. As shown in Figure 3.111, specimens containing ECR cast in concrete containing corrosion inhibitors with a *w/c* ratio of 0.35 exhibit microcell corrosion rates that are similar to or higher than the corrosion

rates observed in the ECR-10h-35 control specimen for the first 80 weeks of the test. The uncharacteristically high corrosion rate measured in the ECR(HY)-10h-35 specimen at week 76 is due to an aberrant reading and is not used in the calculation of the microcell corrosion loss for this specimen. Between week 84 and week 96, all ECR specimens with corrosion inhibitors exhibit lower microcell corrosion rates than the ECR controls specimen.

The microcell corrosion losses for the Southern Exposure specimens containing corrosion inhibitors are shown in Figures 3.112 to 3.114 and summarized in Table 3.12. For specimens containing ECR with four holes through the epoxy (Figure 3.112), all specimens with corrosion inhibitors exhibit corrosion losses that are equal to or greater than the ECR control specimens. Among these specimens, the

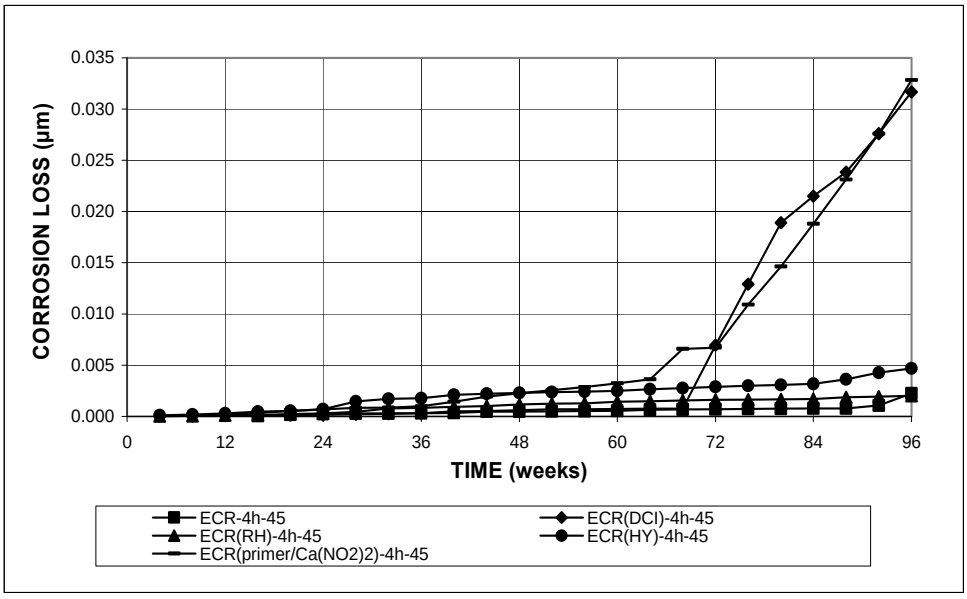

Figure 3.112 – Microcell corrosion loss, LPR test for Southern Exposure specimens containing ECR, ECR in concrete with corrosion inhibitors, and ECR with a calcium nitrite primer, *w/c* = 0.45. Bars with coating containing four holes through the epoxy.

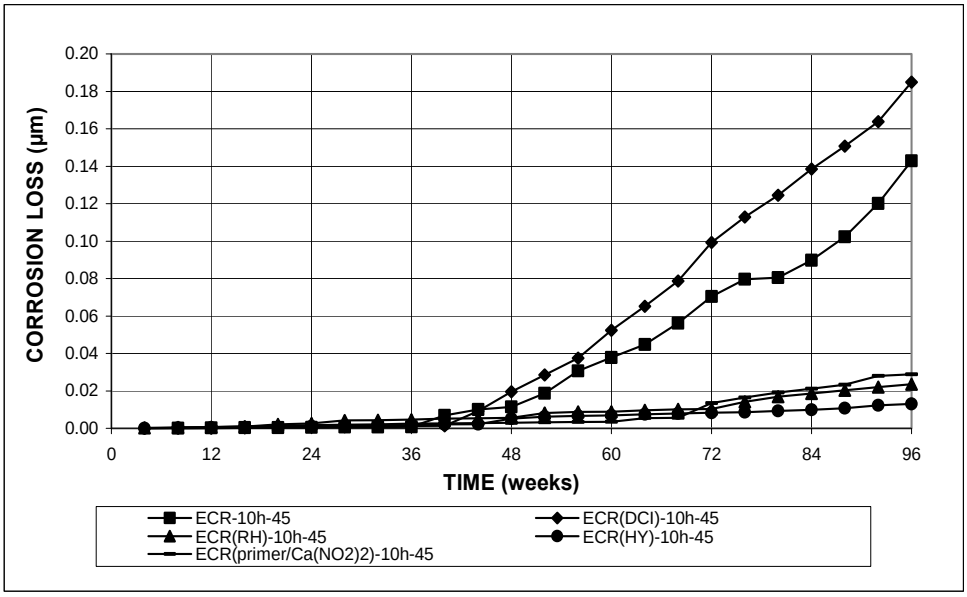

Figure 3.113 – Microcell corrosion loss, LPR test for Southern Exposure specimens containing ECR, ECR in concrete with corrosion inhibitors, and ECR with a calcium nitrite primer, *w/c* = 0.45. Bars with coating containing ten holes through the epoxy.

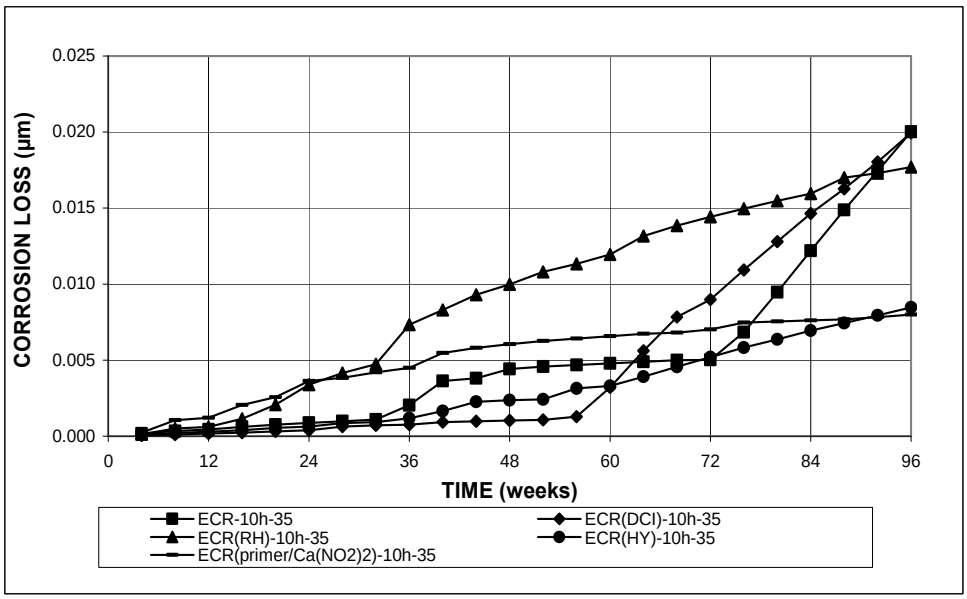

Figure 3.114 – Microcell corrosion loss, LPR test for Southern Exposure specimens containing ECR, ECR in concrete with corrosion inhibitors, and ECR with a calcium nitrite primer, *w/c* = 0.35. Bars with coating containing ten holes through the epoxy.

ECR(primer/Ca(NO_2)$_2$)-4h-45 specimen exhibits the highest microcell corrosion loss, 0.033 μm at week 96. As shown in Figure 3.113, specimens with a *w/c* ratio of 0.45 and ten holes through the epoxy exhibit corrosion losses less than the control specimen, except for the ECR(DCI)-10h-45 specimen, which begins exhibiting corrosion losses higher than the control specimen at week 48. The ECR(DCI)-10h-45 specimen had a total corrosion loss of 0.185 μm at week 96 (Table 3.12). Figure 3.114 shows that for specimens with 10 holes through the epoxy and concrete with a *w/c* ratio of 0.35, all specimens containing corrosion inhibitors exhibit corrosion losses higher than the control specimen for at least a portion of the study. However, by week 96, all specimens containing corrosion inhibitors exhibit corrosion losses that are equal to or lower than the control specimen (Table 3.12).

Figures 3.115 through 3.117 show the microcell corrosion rates for the cracked beam specimens. As shown in Figure 3.115, specimens with four holes through the epoxy exhibit corrosion rates of less than 1.0 μm/yr, with the exception of the ECR(RH)-4h-45 specimen during weeks 36 through 40 and 56 through 96, the ECR(primer/Ca(NO2)2)-4h-45 specimen at week 40 and the ECR-4h-45 specimen at week 88. Figure 3.116 shows that all 10-hole specimens in concrete with a *w/c* ratio of 0.45 exhibit similar or higher microcell corrosion rates than the control specimens, all with corrosion rates below 2.0 μm/yr. Specimens with 10 holes through the epoxy and concrete with a *w/c* ratio of 0.35 (Figure 3.117) exhibit corrosion rates less than 1.5 μm/yr except for the ECR(DCI)-10h-35 specimen at weeks 48 and 68 through 96 and the ECR(primer/Ca(NO2)2)-10h-35 specimen from weeks 56 to 96.

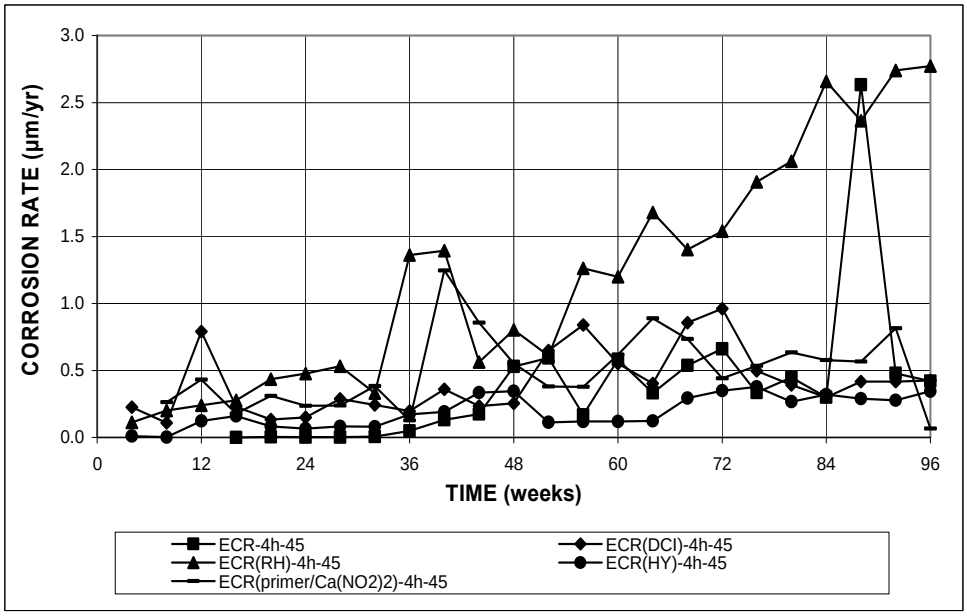

Figure 3.115 – Microcell corrosion rate, LPR test for cracked beam specimens containing ECR, ECR in concrete with corrosion inhibitors, and ECR with a calcium nitrite primer, *w/c* = 0.45. Bars with coating containing four holes through the epoxy.

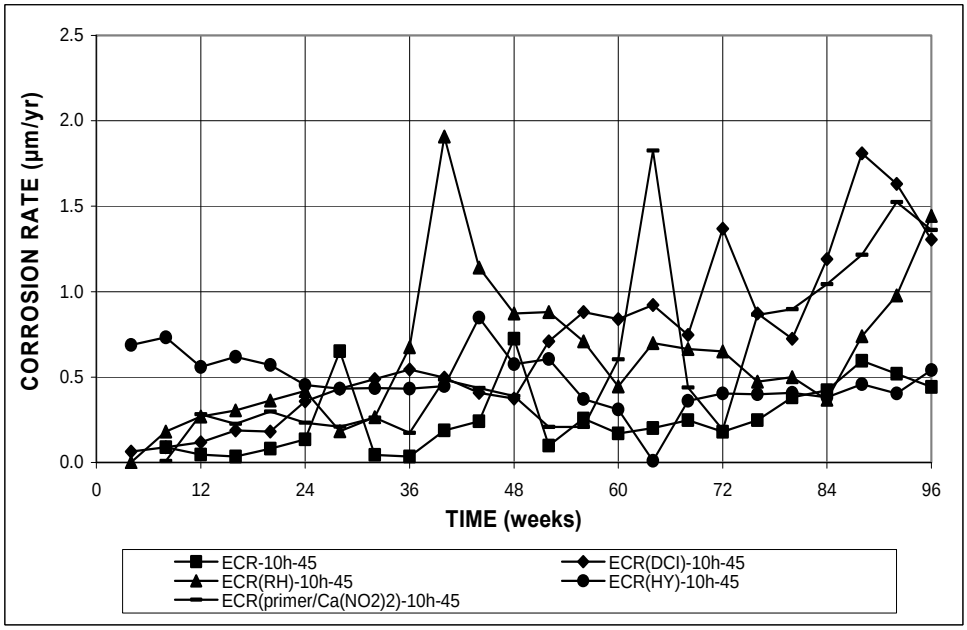

Figure 3.116 – Microcell corrosion rate, LPR test for cracked beam specimens containing ECR, ECR in concrete with corrosion inhibitors, and ECR with a calcium nitrite primer, *w/c* = 0.45. Bars with coating containing ten holes through the epoxy.

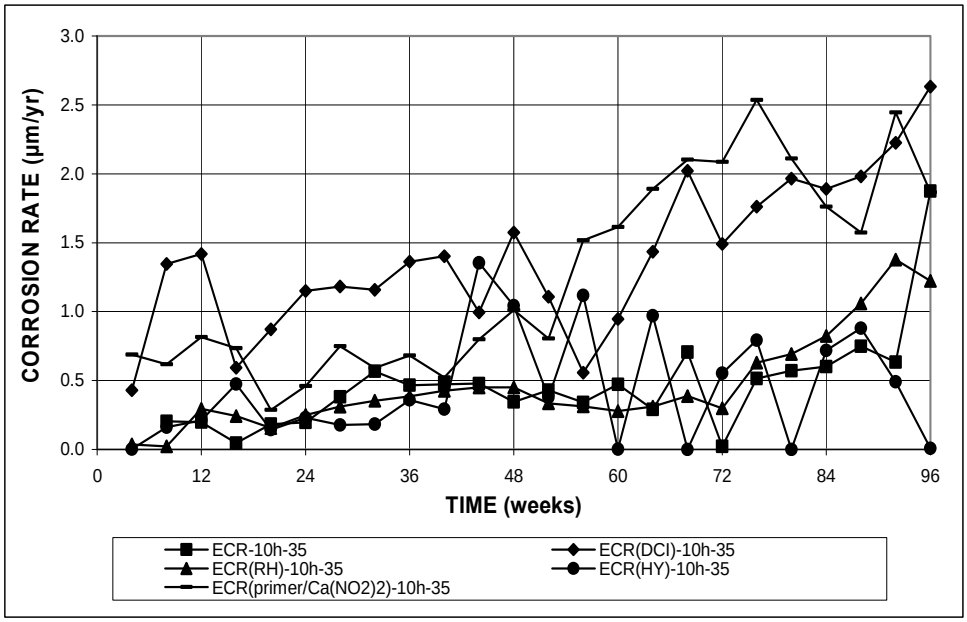

Figure 3.117 – Microcell corrosion rate, LPR test for cracked beam specimens containing ECR, ECR in concrete with corrosion inhibitors, and ECR with a calcium nitrite primer, *w/c* = 0.35. Bars with coating containing ten holes through the epoxy.

Figures 3.118 through 3.120 show the corrosion losses for the cracked beam specimens. Figure 3.118 shows that, among specimens with four holes through the epoxy and concrete with a *w/c* ratio of 0.45, all specimens, except the ECR(HY)-4h-45 specimen, exhibit higher corrosion losses than the control specimen throughout the duration of the test. The highest corrosion loss observed at week 96 among the four-hole specimens is 2.22 µm for the ECR(RH)-4h-45 specimen (Table 3.12). All other corrosion losses are below 1.0 µm. As shown in Figure 3.119, all specimens exhibit higher corrosion losses than the control specimen throughout the test. The total corrosion losses at week 96 range from 0.88 to 1.29 µm, with the highest corrosion loss observed in the ECR(DCI)-10h-45 specimen (Table 3.12). Figure 3.120 shows that specimens with 10 holes through the epoxy and concrete with a *w/c* ratio of 0.35

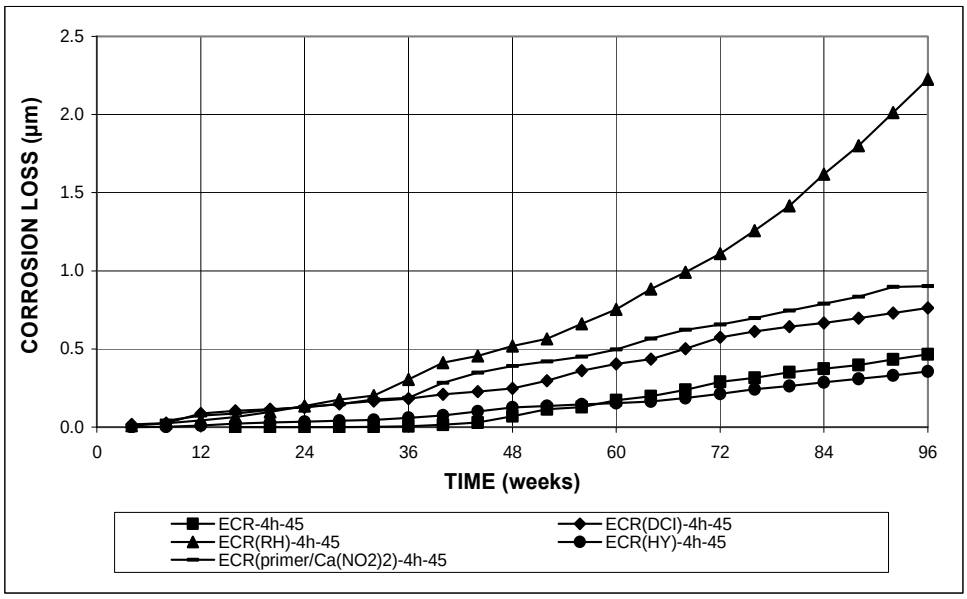

Figure 3.118 – Microcell corrosion loss, LPR test for cracked beam specimens containing ECR, ECR in concrete with corrosion inhibitors, and ECR with a calcium nitrite primer, *w/c* = 0.45. Bars with coating containing four holes through the epoxy.

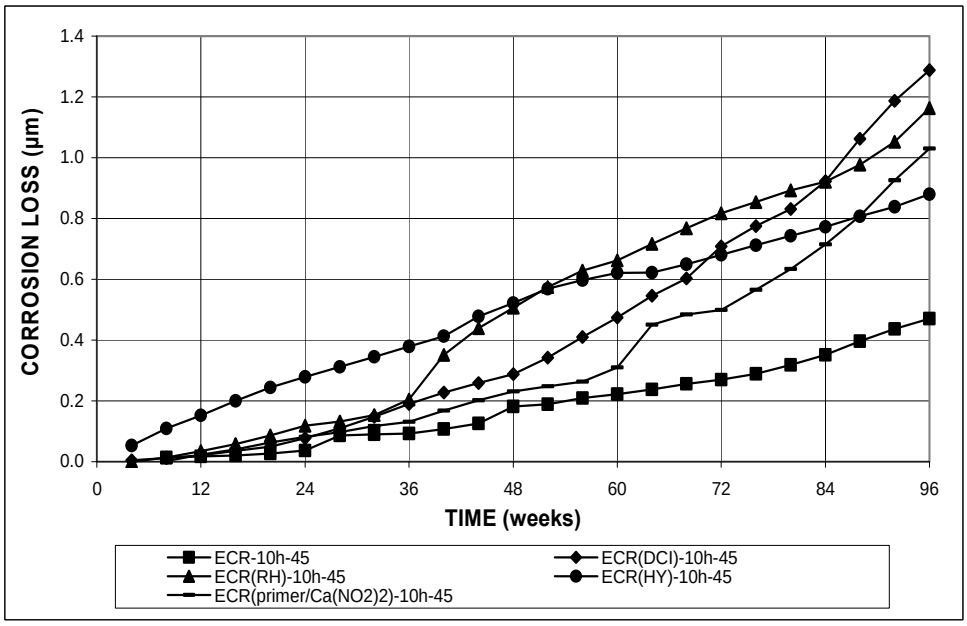

Figure 3.119 – Microcell corrosion loss, LPR test for cracked beam specimens containing ECR, ECR in concrete with corrosion inhibitors, and ECR with a calcium nitrite primer, *w/c* = 0.45. Bars with coating containing ten holes through the epoxy.

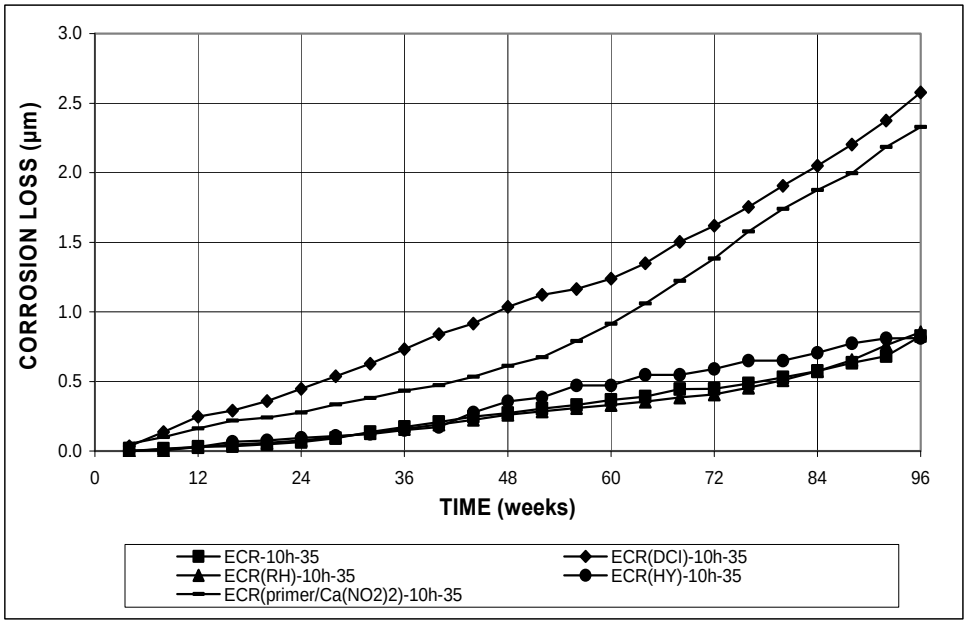

Figure 3.120 – Microcell corrosion loss, LPR test for cracked beam specimens containing ECR, ECR in concrete with corrosion inhibitors, and ECR with a calcium nitrite primer, *w/c* = 0.35. Bars with coating containing ten holes through the epoxy.

exhibit corrosion losses similar to the control specimen, with the exception of the ECR(DCI)-10h-35 and ECR(primer/Ca(NO2)2)-10h-35 specimens, which both show higher corrosion losses than the control specimens. The ECR(DCI)-10h-35 and ECR(primer/Ca(NO2)2)-10h-35 specimens exhibit a total corrosion loss at 96 week of 2.58 and 2.33 µm, respectively.

As shown in Table 3.12, in uncracked concrete (SE specimens), specimens containing corrosion inhibitors exhibit total corrosion losses that range from 9% to 1600% of the losses exhibited by conventional ECR, with five out of nine specimens containing corrosion inhibitors showing corrosion losses that are less than or equal to corrosion losses exhibited by the control specimens. Only one corrosion inhibitor, Rheocrete, consistently maintains or improves the corrosion performance of the

reinforcement when compared to the control specimen, with total 96-week corrosion losses ranging from 17% to 100% of the corrosion loss observed in the control specimens (100% meaning equal amount of corrosion loss). In the cracked beam tests, only two out of nine systems exhibit any advantage in corrosion protection over the conventional ECR. Both of these cases are specimens containing Hycrete corrosion inhibitor, the ECR(HY)-4h-45 and ECR(HY)-10h-35 specimens, which exhibit 77% and 98%, respectively, of the corrosion loss observed in the control specimens.

ECR with a calcium nitrite primer shows improved corrosion performance in two out of three cases in uncracked concrete. The ECR(primer/Ca(NO2)2)-10h-45 and ECR(primer/Ca(NO2)2)-10h-35 specimens exhibit total corrosion losses equal to 20% and 40%, respectively, of the corrosion losses observed for the conventional ECR. In cracked concrete, none of the specimens with ECR containing a calcium nitrite primer show an improvement over conventional ECR. Corrosion losses exhibited by these specimens ranged from 1.9 to 2.8 times the corrosion loss observed for the control specimens.

In uncracked concrete, a lower water-cement ratio (0.35 versus 0.45) provided additional corrosion protection in all specimens with corrosion inhibitors. The reduced *w/c* ratio, however, appears to provide little or no advantage in cracked concrete.

3.6.3 Increased Adhesion ECR

Figures 3.121 through 3.124 show the microcell corrosion rates and losses for Southern Exposure specimens. As shown in Figure 3.121, all high adhesion ECR specimens exhibit higher microcell corrosion rates than the ECR control specimens by week 40, and continue to exhibit higher corrosion rates for the remainder of the study. All microcell corrosion rates exhibited by the high adhesion ECR specimens remain below 0.3 μm/yr, except for the ECR(Valspar)-4h-45 specimen, which exhibits a microcell corrosion rate of 1.21 μm/yr at week 80. This uncharacteristically high microcell corrosion measurement is, in all likelihood, due to an aberrant reading. As a result, this reading is not used when calculating the corrosion loss for this specimen. Figure 3.122 shows the microcell corrosion rates for ECR specimens with high adhesion epoxy containing ten holes through the epoxy. High adhesion ECR specimens exhibit microcell corrosion rates similar to the ECR control specimen until week 62. After week 62, all high adhesion ECR specimens continue to exhibit corrosion rates higher than the ECR control specimen, except for the ECR(Chromate) specimen, which exhibit lower corrosion rates from weeks 84 to 96. Significant jumps in corrosion rate are observed for the ECR(Chromate) and ECR(Valspar) specimens at week 74. In all likelihood, these jumps are due to aberrant readings, and these readings are not used in the corrosion loss calculations for these specimens.

Figures 3.123 and 3.124 show the microcell corrosion losses for high adhesion ECR specimens with four and ten holes through the epoxy, respectively. Specimens

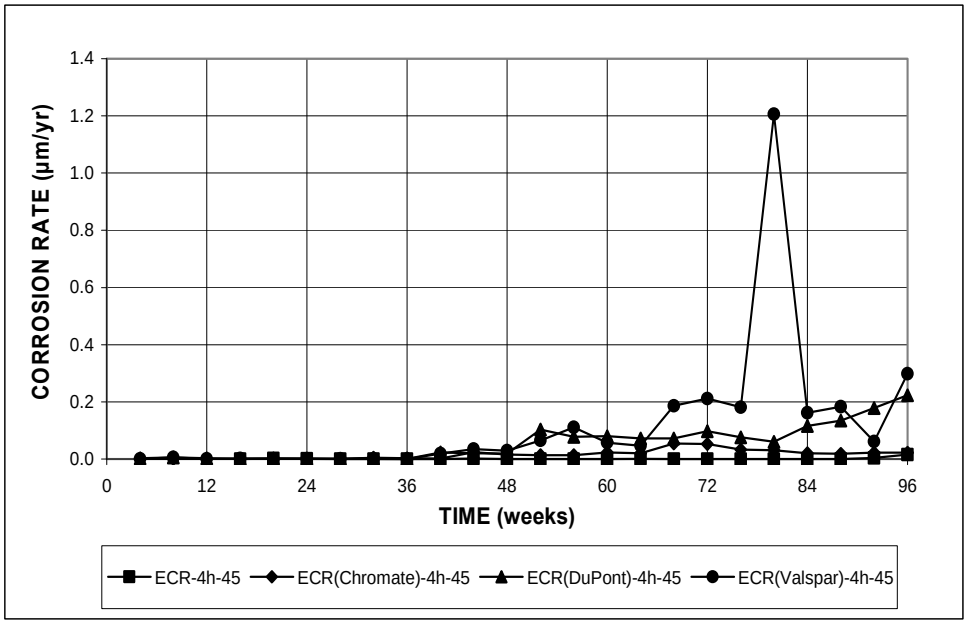

Figure 3.121 – Microcell corrosion rate, LPR test for Southern Exposure specimens containing ECR and ECR with increased adhesion, *w/c* = 0.45 Bars with coating containing four holes through the epoxy.

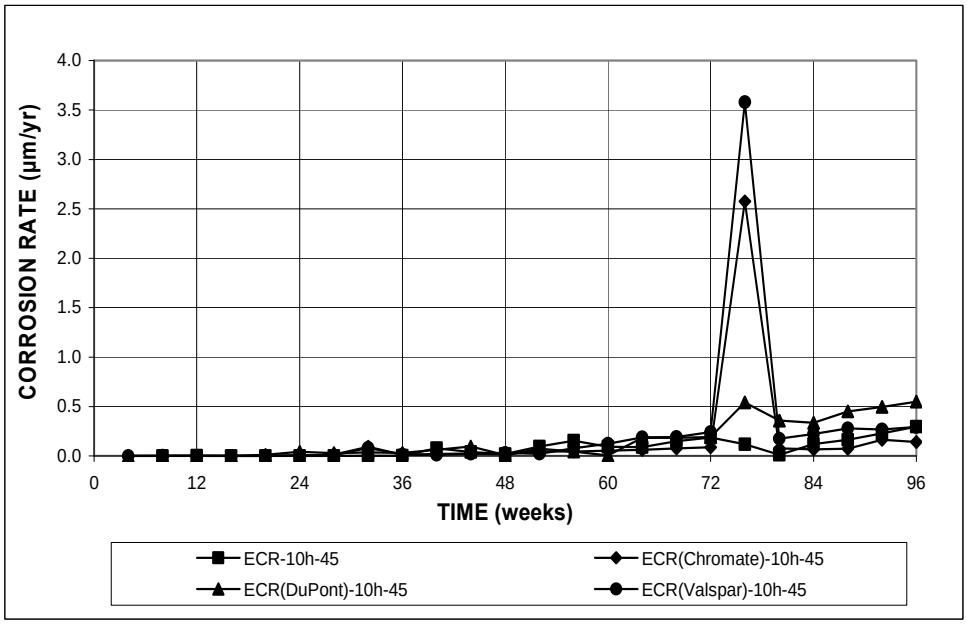

Figure 3.122 – Microcell corrosion rate, LPR test for Southern Exposure specimens containing ECR and ECR with increased adhesion, *w/c* = 0.45 Bars with coating containing ten holes through the epoxy.

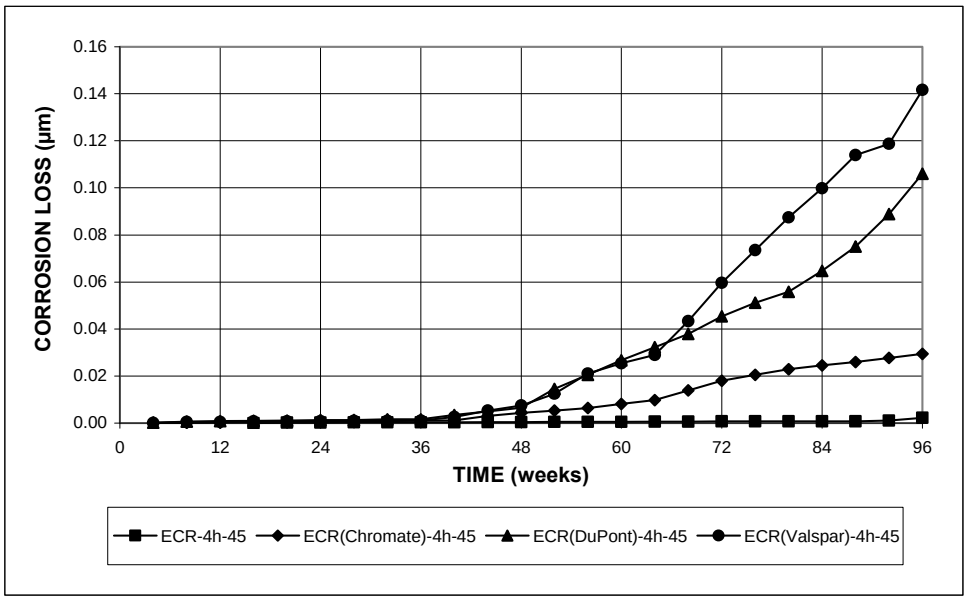

Figure 3.123 – Microcell corrosion loss, LPR test for Southern Exposure specimens containing ECR and ECR with increased adhesion, *w/c* = 0.45 Bars with coating containing four holes through the epoxy.

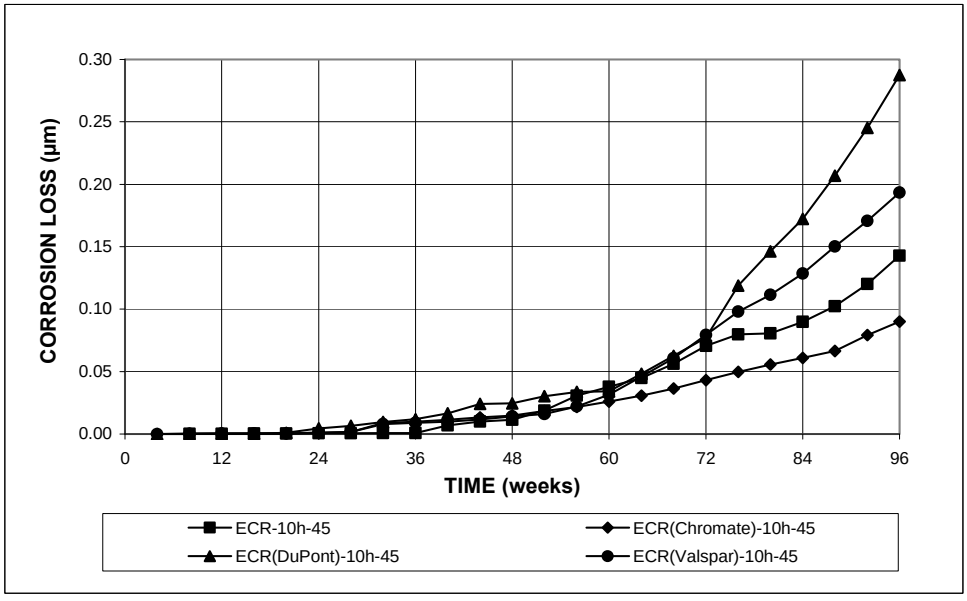

Figure 3.124 – Microcell corrosion loss, LPR test for Southern Exposure specimens containing ECR and ECR with increased adhesion, *w/c* = 0.45 Bars with coating containing ten holes through the epoxy.

with four holes through the epoxy exhibit corrosion losses similar to or higher than ECR control specimens. By week 72, all 10-hole specimens exhibit higher corrosion losses than the control specimen, with the exception of the ECR(Valspar)-10h-45 specimen, which continues to exhibit lower corrosion losses than the control specimens for the remainder of the test.

Microcell corrosion rates and losses measured in cracked beam specimens are shown in Figures 3.125 through 3.128. As shown in Figure 3.125, the ECR(Chromate)-4h-45 and ECR(Valspar)-4h-45 specimens consistently exhibit higher microcell corrosion rates than the ECR control specimen throughout the duration of the test. The ECR(DuPont)-4h-45 specimen exhibits microcell corrosion rates similar to ECR control specimens. The microcell corrosion rates of all high

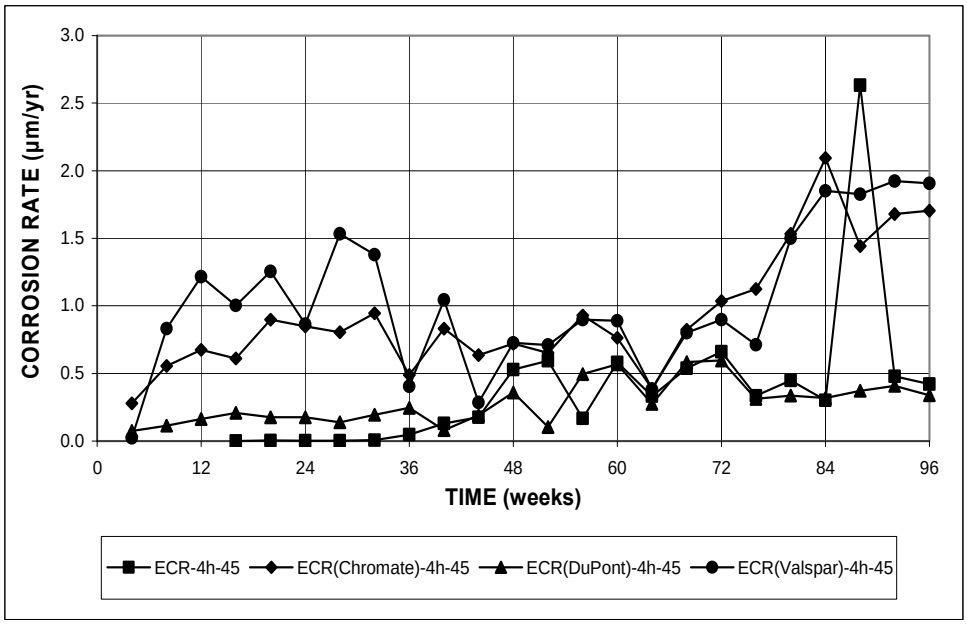

Figure 3.125 – Microcell corrosion rate, LPR test for cracked beam specimens containing ECR and ECR with increased adhesion, *w/c* = 0.45 Bars with coating containing four holes through the epoxy.

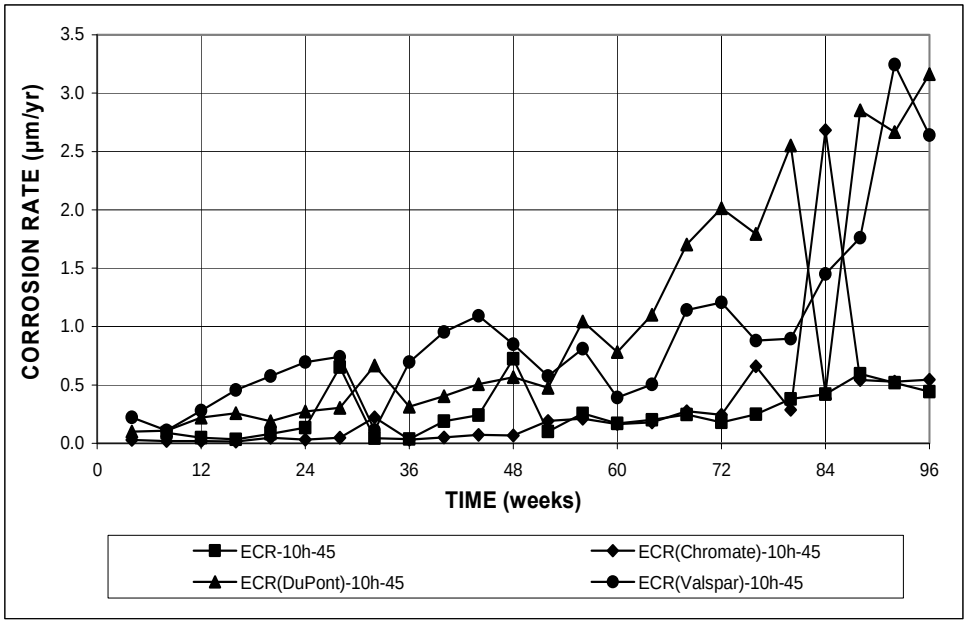

Figure 3.126 – Microcell corrosion rate, LPR test for cracked beam specimens containing ECR and ECR with increased adhesion, *w/c* = 0.45 Bars with coating containing ten holes through the epoxy.

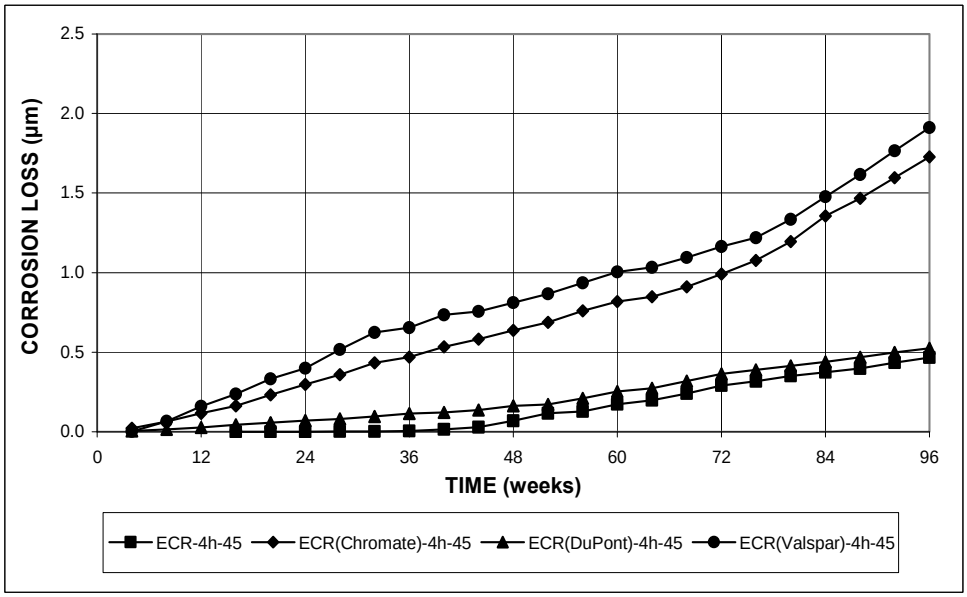

Figure 3.127 – Microcell corrosion loss, LPR test for cracked beam specimens containing ECR and ECR with increased adhesion, *w/c* = 0.45 Bars with coating containing four holes through the epoxy.

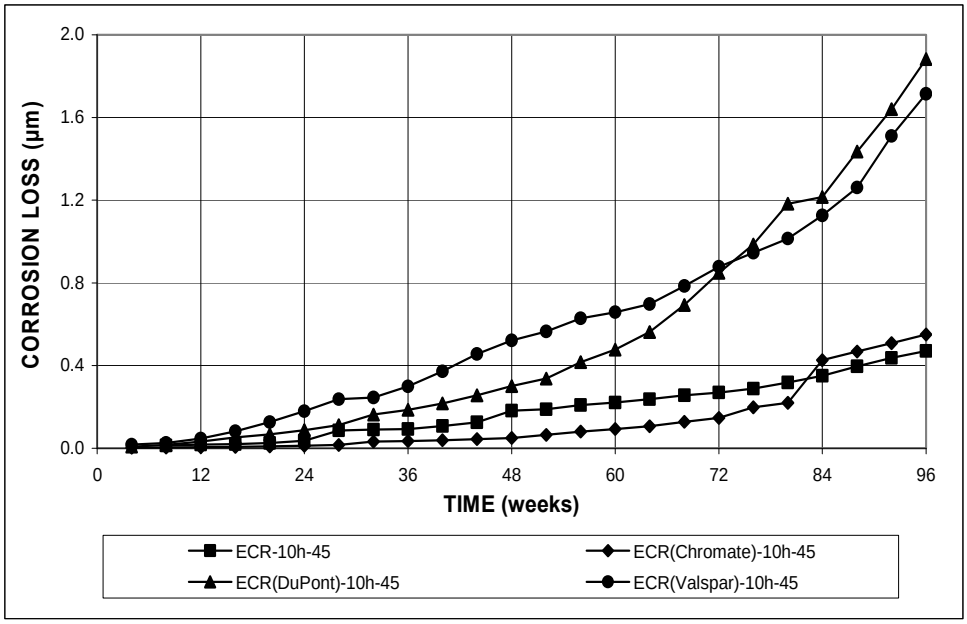

Figure 3.128 – Microcell corrosion loss, LPR test for cracked beam specimens containing ECR and ECR with increased adhesion, *w/c* = 0.45 Bars with coating containing ten holes through the epoxy.

adhesion ECR specimens remain below 2.5 µm/yr. Figure 3.126 shows that the ECR(Valspar)-10h-45 specimen exhibits higher microcell corrosion rates than the ECR control specimens throughout the test. The ECR(DuPont)-10h-45 specimen exhibits higher microcell corrosion rates than the ECR control specimens except for weeks 28 and 48, with corrosion rates of 0.302 and 0.567 µm/yr, respectively. The corrosion rates observed in the ECR(Chromate)-10h-45 specimen are generally comparable to those observed in the control specimen, with the exception of week 84, which is probably the result of an aberrant reading. For total corrosion losses (Figures 3.127 and 3.128), the ECR(Valspar)-4h-45, ECR(Chromate)-4h-45, ECR(Chromate)-10h-45, and ECR(DuPont)-10h-45 specimens all exhibit higher corrosion losses than the ECR control specimens throughout the test. The

ECR(DuPont)-4h-45 and ECR(Chromate)-10h-45 specimens exhibit corrosion losses similar to those observed in ECR control specimens.

Table 3.12 shows that the high adhesion ECR bars hold no advantage in corrosion protection over the conventional ECR bars, with the exception of the ECR(Chromate)-10h-45 Southern Exposure specimen, which exhibits 63% of the loss observed in the ECR control specimens with ten holes. The remaining specimens exhibit corrosion losses that range from 1.1 to 71 times the losses observed in SE and CB specimens containing conventional ECR.

3.6.4 Increased Adhesion with DCI

This section presents the LPR results for the Southern Exposure specimens containing high adhesion ECR cast in concrete containing calcium nitrite corrosion inhibitor (DCI). The results are presented in Figures 3.129 and 3.130. The combination of high adhesion ECR with DCI was not evaluated in the cracked beam test. Only specimens with ECR containing four holes through the epoxy coating are evaluated.

Figure 3.129 shows that between weeks 56 and 96, the ECR(Chromate)-4h-45 specimen exhibits higher microcell corrosion rates than the ECR(DCI)-4h-45 control specimen, except for week 80. As previously mentioned, the uncharacteristically high corrosion rate observed in the ECR(DCI)-4h-45 specimen at week 80 is most likely due to an aberrant reading, and is therefore not included when calculating the corrosion loss for this specimen. All other high adhesion ECR specimens cast in concrete containing DCI corrosion inhibitor exhibit corrosion rates similar to those

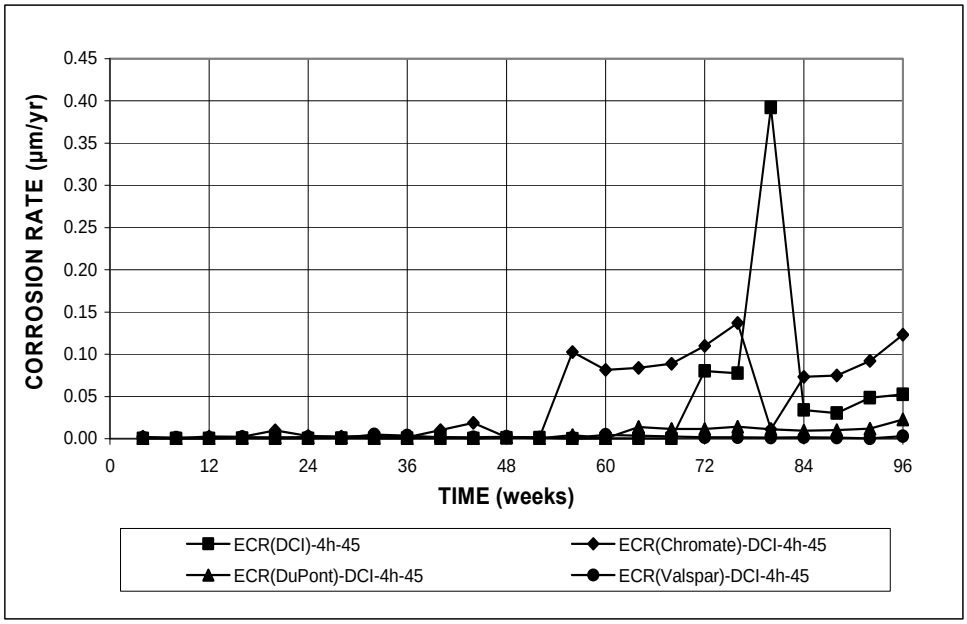

Figure 3.129 – Microcell corrosion rate, LPR test for Southern Exposure specimens containing ECR and ECR with increased adhesion cast in concrete containing DCI, *w/c* = 0.45 Bars with coating containing four holes through the epoxy.

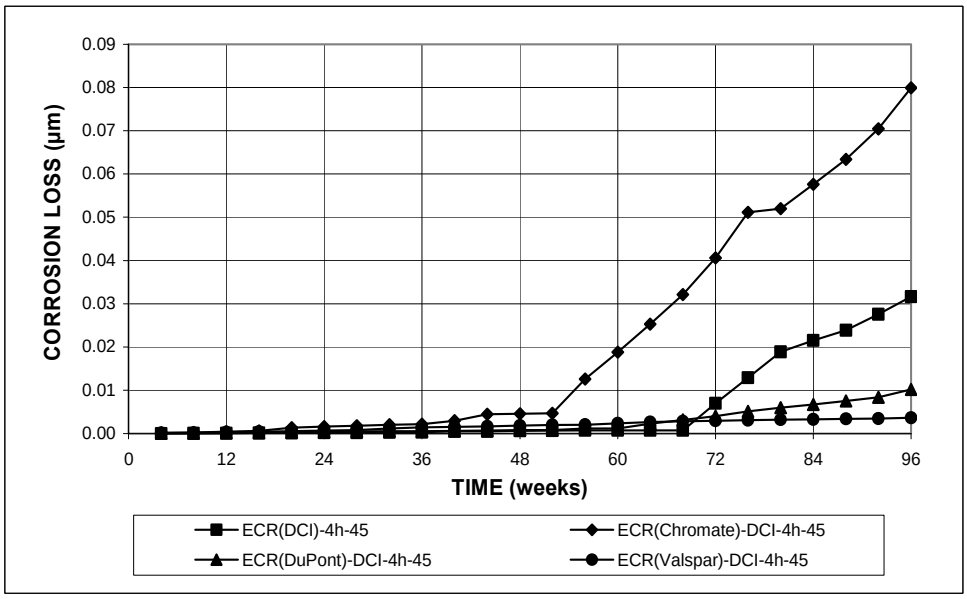

Figure 3.130 – Microcell corrosion loss, LPR test for Southern Exposure specimens containing ECR and ECR with increased adhesion cast in concrete containing DCI, *w/c* = 0.45 Bars with coating containing four holes through the epoxy.

observed in the ECR(DCI)4h-45 control specimen during the first 68 weeks of the test. These specimens exhibit lower corrosion rates than the control specimen from week 72 through 96. All microcell corrosion rates observed in ECR bars with increased adhesion remain below 0.15 μm/yr. Figure 3.130 shows that between weeks 52 and 96, the ECR(Chromate)-DCI-4h-45 specimen exhibits higher corrosion losses than the ECR(DCI)-4h-45 specimen. All other specimens exhibit corrosion losses comparable to or below that of the control specimen. As shown in Table 3.12, two specimens with high adhesion ECR systems with DCI, the ECR(DuPont) and ECR(Valspar) specimens, show improved resistance to corrosion when in the presence of DCI when compared with conventional ECR, with corrosion losses equal to 31.3% and 12.5%, respectively, of the corrosion loss observed in the specimen containing conventional ECR in concrete containing DCI. The ECR(Chromate) specimen, with a corrosion loss 2.50 times that of the control specimen, suggests that the ECR bars with a chromate pretreatment, when in the presence of DCI, offer no advantage over conventional epoxy-coated reinforcement in the presence of DCI.

3.6.5 Multiple-coated Reinforcement

This section presents the LPR results for the Southern Exposure and cracked beam specimens containing multiple-coated reinforcement. Figures 3.131 and 3.132 show the microcell corrosion rates and losses, respectively, for Southern Exposure specimens. As shown in Figure 3.131, specimens with multiple-coated reinforcement exhibit much higher microcell corrosion rates than ECR control specimens, beginning at week 32 and continuing for the remainder of the test. As previously discussed, this

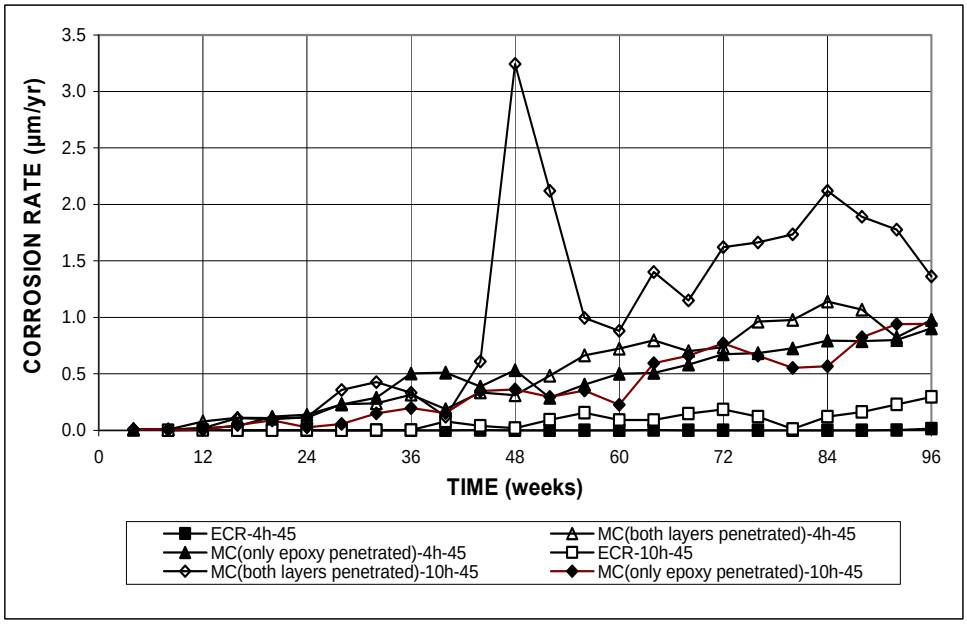

Figure 3.131 – Microcell corrosion rate, LPR test for Southern Exposure specimens containing ECR and multiple-coated bars, *w/c* = 0.45. 4h = four holes through the epoxy and 10h = 10 holes through the epoxy.

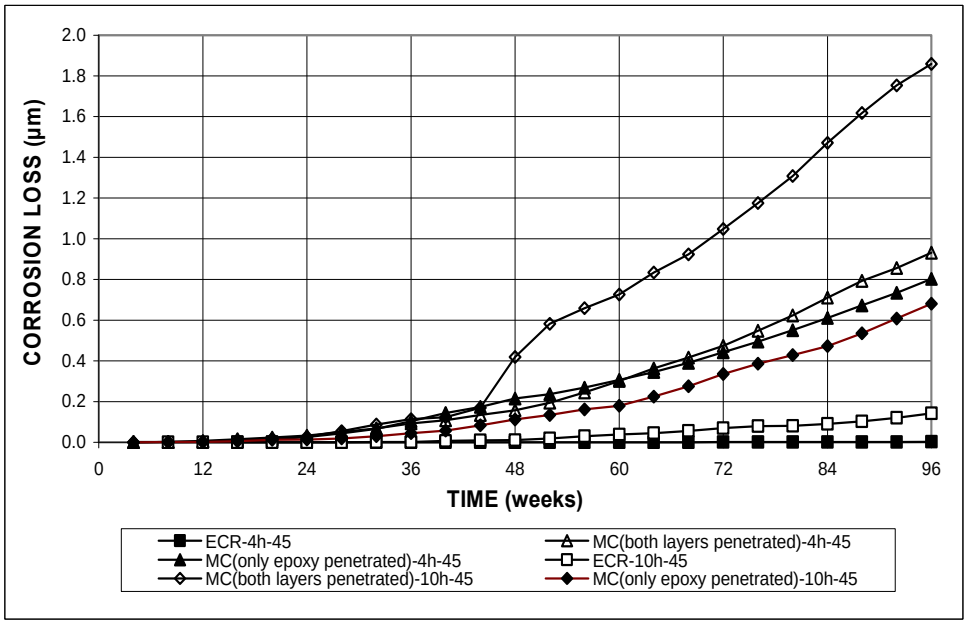

Figure 3.132 – Microcell corrosion loss, LPR test for Southern Exposure specimens containing ECR and multiple-coated bars, *w/c* = 0.45. 4h = four holes through the epoxy and 10h = 10 holes through the epoxy.

higher corrosion rate is in all likelihood attributable to the zinc layer, which is more galvanically active than iron. Between weeks 32 and 96, corrosion rates range from 0.187 to 1.14 µm/yr for the specimen with four holes through the epoxy and 0.121 to 3.24 µm/yr for the specimen with ten holes through the epoxy. Figure 3.132 shows that specimens containing multiple-coated reinforcement consistently exhibit higher corrosion losses than the ECR control specimens throughout the test. The specimen with both the epoxy and zinc layers penetrated exhibits higher corrosion losses than specimen with only the epoxy layer penetrated.

Figures 3.133 and 3.134 show the microcell corrosion rates and losses, respectively, for cracked beam specimens. As shown in Figure 3.133, specimens with multiple-coated reinforcement exhibit higher microcell corrosion rates than ECR

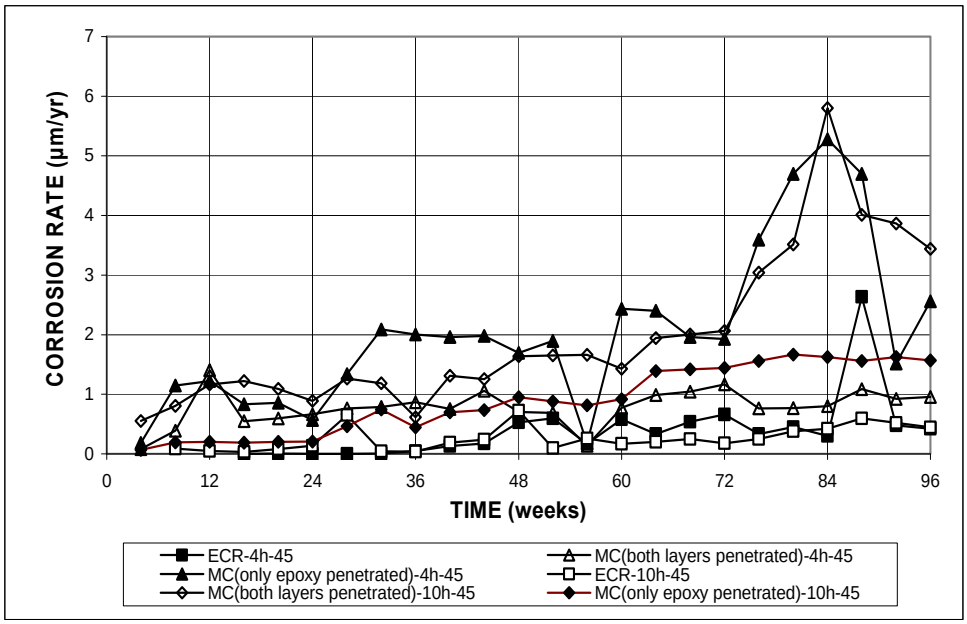

Figure 3.133 – Microcell corrosion rate, LPR test for cracked beam specimens containing ECR and multiple-coated bars, *w/c* = 0.45. 4h = four holes through the epoxy and 10h = 10 holes through the epoxy.

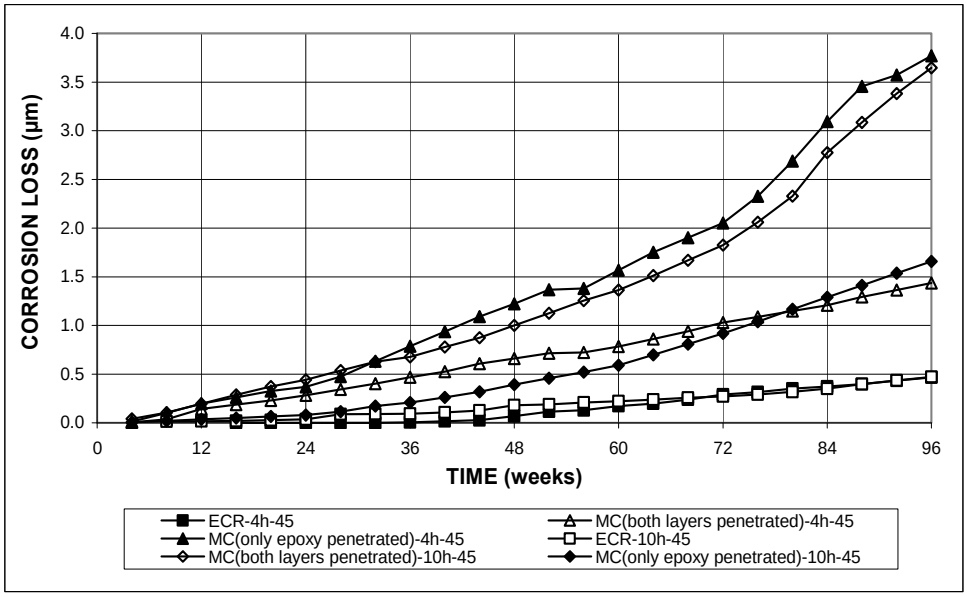

Figure 3.134 – Microcell corrosion loss, LPR test for cracked beam specimens containing ECR and multiple-coated bars, *w/c* = 0.45. 4h = four holes through the epoxy and 10h = 10 holes through the epoxy.

control specimens throughout the entire test. Microcell corrosion rates range from 0.078 to 5.28 µm/yr for the specimen with four holes through the epoxy and from 0.065 to 5.80 µm/yr for the specimen with ten holes through the epoxy. Figure 3.134 shows that specimens containing multiple-coated reinforcement exhibit higher corrosion losses than the ECR control specimens throughout the test. For the specimen containing four holes through the epoxy, the specimen with only the epoxy layer penetrated exhibits higher corrosion losses than the specimen with both layers penetrated. For specimens containing 10 holes through the epoxy, the specimen with only the epoxy layer penetrated exhibits lower corrosion losses than the specimen with both layers penetrated.

As shown in Table 3.12, multiple corrosion reinforcement shows no advantage over conventional ECR reinforcement based on the LPR results. Corrosion losses for specimens containing multiple-coated reinforcement ranged from 4.8 to 466 times the corrosion losses exhibited by ECR control specimens. Specimens with both the zinc and epoxy layers penetrated exhibit higher corrosion losses than specimens with only the epoxy layer penetrated, except for cracked beam specimens with four holes through the epoxy.

3.7 Post-Mortem Disbondment Analysis

As stated in Chapter 2, most Southern Exposure and cracked beam tests were conducted for a 96 week period, with some tests being extended to periods as long as 120 weeks. Upon completion of a test, the reinforcement within each specimen was extracted, inspected, and photographed. During inspection, it was noted that some ECR specimens exhibited disbondment between the epoxy layer and the underlying steel. This section presents the results of the disbondment measurements taken from the epoxy-coated reinforcement at the conclusion of the test. The procedure for measuring the disbondment of the epoxy coating is adapted from ASTM G8 and ASTM A775, and is described in Chapter 2. Two disbondment measurements are reported: the average radius of disbondment (r_d) and the total disbonded area (A_d). The average radius is obtained by averaging four different disbondment radii, which are measured at 0°, 90°, 180°, and 270°, as described in ASTM A775. The total disbonded area is measured as described in ASTM G8, and the value is corrected by subtracting the area of the original intentional defect in the epoxy. Values are

reported for two holes through the epoxy on the top face of the bar ("Side 1-A" and "Side 1-B") and for one hole on the bottom face of the bar ("Side 2-A"). For a given bar, the measurement for Side 2-A is directly opposite to the measurement for Side 1-A. If one or more individual disbondment radii are measured to be greater than 12 mm, they are counted as 12 mm when calculating the average disbondment radius and the average disbondment radius is preceded by a greater-than sign (>). The corresponding disbondment area is recorded as "TD" (total disbondment). The corrosion disbondment measurements report in this chapter will be compared to cathodic disbondment test results (Gong et al. 2006) in Chapter 4.

In addition to measuring disbondment of the epoxy-coating, the surface of the bar was visually inspected, and the appearance of any corrosion products was noted. Initially, the bars from each specimen were inspected twice. First, the bars were inspected immediately after being extracted from the concrete specimen, and the color of any corrosion product on the bar was noted. The bars were then allowed to sit for an hour, at which point they were inspected a second time, noting any change in coloration of the corrosion product. After inspecting several specimens in this manner, it became apparent that there was a tendency for the corrosion product to change color. Corrosion products that were originally black or dark brown would change to orange or light brown. This indicates that the corrosion products on the surface of the reinforcement originally formed in the absence of oxygen; the subsequent color change, which occurred after the reinforcement was extracted from the concrete, is due to exposure to oxygen.

As shown in Figures 3.135 through 3.139, a wide range surface conditions were observed after extracting the bars from the test specimens. Figure 3.135 shows the top and bottom bars of the Conv.-45-5 Southern Exposure specimen, which is representative of the surface conditions exhibited by conventional reinforcing upon extraction of the bars at the end of the test. Generally, top bars exhibit larger areas of corrosion product than bottom bars, while some portions of each bar remain free of corrosion product. This illustrates the variability in the distribution of chloride ions at

Figure 3.135 – Top and bottom bars of the Conv.-45-3 specimen at autopsy. Top bars are shown at the top of the figure and bottom bars are show at the bottom of the figure.

Figure 3.136 – Top and bottom bars of the ECR-4h-45-5 specimen at autopsy (before disbondment test). Top bars are shown at the top of the figure and bottom bars are show at the bottom of the figure.

Figure 3.137 – Top and bottom bars of the ECR(Chromate)-10h-45-2 specimen at autopsy (before disbondment test). Top bars are shown at the top of the figure and bottom bars are show at the bottom of the figure.

Figure 3.138 – Top bars of the ECR(Chromate)-10h-45-2 specimen at autopsy (after disbondment test).

Figure 3.139 – Top bars of the MC(both layers penetrated)-4h-45-3 specimen at autopsy (after disbondment test).

a given depth within the concrete; some portions of the bar are exposed to higher chloride concentrations than other portions, resulting in corrosion. The areas free of corrosion product remained passive due to either lower chloride concentrations within the concrete or because they became cathodic due to microcell corrosion. The color of the corrosion products varied between dark orange and dark brown.

Figure 3.136 shows the top and bottom bars of the ECR-4h-45-5 Southern Exposure specimen and is representative of the surface condition of ECR bars upon removal from the concrete. Bars with little to no disbondment also often come out clean. For example, see bottom bars in Figures 3.137 and 3.138. The epoxy coating is intact along the entire length of the top and bottom bars, with the exception of the holes that were intentionally drilled through the epoxy. The steel surface at each hole is shiny and free of any visible corrosion products.

Figures 3.137 and 3.138 shows the top and bottom bars of the ECR(Chromate)-10h-45-2 specimen before and after performing the disbondment evaluation, respectively. The surface condition of these bars is representative of a specimen that has undergone total disbondment. The steel surface at each hole intentionally drilled through the epoxy is entirely covered with corrosion products. Additionally, blistering of the epoxy coating due to formation of corrosion products beneath the epoxy is visible, and orange staining due to corrosion products can be seen on the surface of the epoxy. The epoxy is, in many instances, easily removed without the aid of a knife, and, as shown in Figure 1.138, the disbonded area is not confined solely to regions immediately surrounding the hole through the epoxy.

Figure 3.139 shows the top bars of the MC(both layers penetrated)-4h-45-3 specimen after performing the disbondment test. The epoxy coating exhibits significant disbondment, and the disbondment often extends beyond the immediate region surrounding the hole. The corrosion products observed have two distinct colors. At the site of the hole drilled through the zinc layer, a small area of dark brown and black corrosion product exists, which is due to the corrosion of the steel. The area of this corrosion product is small and confined to the immediate region of the hole. The second corrosion product is dark grey in color and is due to the corrosion of the zinc layer between the steel and the outer epoxy coating. Like the disbonded region, this corrosion product is not confined to the immediate region surrounding the hole through the epoxy, but extends more than 12 mm (0.5 in.) beyond the hole.

As shown in Table 3.13 for the ECR control specimens, the magnitude of disbondment observed in the top bars is greater than that observed in bottom bars. Specimens with 10 holes through the epoxy in concrete with *w/c* = 0.45 suffered the greatest amount of disbondment, with all three specimens exhibiting total disbondment, followed by specimens with 10 holes through the epoxy cast in concrete with *w/c* = 0.35 (one out of three specimens exhibiting total disbondment). None of the ECR-4h control specimens exhibited total disbondment. In general, all specimens containing ECR with 10 holes through the epoxy exhibit higher disbondment values than specimens containing four holes through the epoxy, with the exception of the

Table 3.13a – Disbondment measurements on top bars of Southern Exposure control specimens.

Specimen	Side 1-A						Side 1-B						Side 2-A						Comments
	A_d	Disbondment Radius (mm)				Avg. r_d	A_d	Disbondment Radius (mm)				Avg. r_d	A_d	Disbondment Radius (mm)				Avg. r_d	
	(cm^2)	0°	90°	180°	270°	(mm)	(cm^2)	0°	90°	180°	270°	(mm)	(cm^2)	0°	90°	180°	270°	(mm)	
ECR-4h-45-1	0.000	0	0	0	0	0.00	0.000	0	0	0	0	0.00	0.000	0	0	0	0	0.00	no rust
ECR-4h-45-2	0.000	0	0	0	0	0.00	0.000	0	0	0	0	0.00	0.000	0	0	0	0	0.00	no rust
ECR-4h-45-3	0.0903	0	1	0	0	0.25	0.0903	0	1	0	0	0.25	0.316	1	2	1	2	1.5	black discoloration
ECR-4h-45-4	1.32	5	6	5	4.5	5.1	1.41	5	5	5	5	5.0	1.22	4	4	5	5	4.5	black discoloration
ECR-4h-45-5	0.0903	0	0	0	1	0.25	0.000	0	0	0	0	0.00	0.000	0	0	0	0	0.00	no rust
ECR-4h-45-6	5.03	7	10	7	10	8.5	0.000	0	0	0	0	0.00	1.06	4	4	3	4	3.8	orange rust
ECR-10h-45-1	TD	>12	10	>12	9	>11	TD	>12	>12	>12	>12	>12	TD	>12	>12	>12	>12	>12	dark brown and black rust
ECR-10h-45-2	5.67	11	10	12	12	11	TD	>12	12	>12	12	>12	2.90	8	8	8	12	9.0	black rust
ECR-10h-45-3	TD	>12	>12	>12	10	>12	0.155	1	0	0	1	0.50	3.15	8	8	9	9	8.5	dark brown and black rust, light blistering
ECR-10h-35-1	0.445	2	2	2	2	2.0	0.606	3	2	3	2	2.5	0.381	1	3	2	2	2.0	no rust
ECR-10h-35-2	0.252	1	2	1	1	1.3	0.316	1	2	2	1	1.5	0.252	0	1	0	1	0.50	dark brown and black rust
ECR-10h-35-3	2.38	5	6	9	5	6.3	TD	12	8	>12	6	>9.5	1.09	4	5	3	4	4.0	dark brown and black rust

TD = Total Disbondment

Table 3.13b – Disbondment measurements on bottom bars of Southern Exposure control specimens.

Specimen	Side 1-A						Side 1-B						Side 2-A						Comments
	A_d	Disb. Radius (mm)				Avg. r_d	A_d	Disb. Radius (mm)				Avg. r_d	A_d	Disb. Radius (mm)				Avg. r_d	
	(cm^2)	0°	90°	180°	270°	(mm)	(cm^2)	0°	90°	180°	270°	(mm)	(cm^2)	0°	90°	180°	270°	(mm)	
ECR-4h-45-1	0.000	0	0	0	0	0.00	0.000	0	0	0	0	0.00	0.000	0	0	0	0	0.00	no rust
ECR-4h-45-2	0.000	0	0	0	0	0.00	0.000	0	0	0	0	0.00	0.000	0	0	0	0	0.00	no rust
ECR-4h-45-3	0.0903	0	0	0	1	0.25	0.000	0	0	0	0	0.00	0.000	0	0	0	0	0.00	no rust
ECR-4h-45-4	0.000	0	0	0	0	0.00	0.000	0	0	0	0	0.00	0.000	0	0	0	0	0.00	no rust
ECR-4h-45-5	0.0903	0	0	0	1	0.25	0.000	0	0	0	0	0.00	0.000	0	0	0	0	0.00	no rust
ECR-4h-45-6	0.000	0	0	0	0	0.00	0.000	0	0	0	0	0.00	0.000	0	0	0	0	0.00	no rust
ECR-10h-45-1	3.09	8	8	8	9	8.3	0.445	1	2	3	2	2.0	0.703	4	3	4	3	3.5	black rust
ECR-10h-45-2	1.48	5	5	5	5	5.0	1.28	5	5	5	4	4.8	2.32	10	8	6	8	8.0	dark brown and black rust
ECR-10h-45-3	0.703	3	3	3	4	3.3	0.0903	0	0	0	1	0.25	0.316	1.5	2	2	1.5	1.8	dark brown and black rust
ECR-10h-35-1	0.187	0	1	0	0	0.25	1.000	1	0	1	1	0.75	0.252	1	1	1	1	1.0	dark brown and black rust
ECR-10h-35-2	0.000	0	0	0	0	0.00	0.123	0	1	0	0	0.25	0.510	4	5	0	2	2.8	dark brown and black rust
ECR-10h-35-3	0.155	0	0	0	1	0.25	0.155	0	0	1	1	0.50	0.187	0	1	1	1	0.75	no rust

TD = Total Disbondment

MC(only epoxy penetrated), ECR(DuPont), and ECR(Valspar) specimens. Additionally, all 10-hole specimens cast in concrete with a *w/c* ratio of 0.35 exhibit less disbondment than 10-hole specimens cast in concrete with a *w/c* ratio of 0.45. Among all SE specimens, all exhibit disbondment in the top bars that is greater than or equal to the disbondment in the bottom bars, with the exception of the ECR(RH)-10h-35, ECR(primer/ $Ca(NO_2)_2$)-10h-35-3, MC(both layers penetrated)-4h-45-2, ECR(Valspar)-10h-45-3, and ECR(DuPont/DCI)-4h-45-3 specimens.

Table 3.14 shows that, among the specimens cast with corrosion inhibitors, the ECR(primer/$Ca(NO_2)_2$) specimens experienced the greatest number of total disbondment (TD) measurements, five overall. All three ECR(primer/$Ca(NO_2)_2$)-10h specimens exhibited total disbondment and two ECR(primer/$Ca(NO_2)_2$)-4h specimens exhibited total disbondment. ECR(DCI) exhibited the next greatest amount of total disbondment measurements (four total), followed by ECR(RH). The ECR(HY) specimens generally exhibit low disbondment measurements with the exception of ECR(HY)-10h-45 specimens.

Table 3.14a – Disbondment measurements on top bars of Southern Exposure specimens cast with corrosion inhibitors

	Side 1-A						Side 1-B						Side 2-A						
	A_d	Disbondment Radius (mm)				Avg. r_d	A_d	Disbondment Radius (mm)				Avg. r_d	A_d	Disbondment Radius (mm)				Avg. r_d	
Specimen	(cm^2)	0°	90°	180°	270°	(mm)	(cm^2)	0°	90°	180°	270°	(mm)	(cm^2)	0°	90°	180°	270°	(mm)	Comments
ECR(DCI)-4h-45-1	1.09	3	4	5	4	4.0	4.83	9	11	12	11	11	0.542	1	2	2	2	1.8	dark brown and black rust
ECR(DCI)-4h-45-2	2.19	6	6	6	6	6.0	3.74	8	9	8	9	8.5	2.70	8	8	7	8	7.8	dark brown and black rust
ECR(DCI)-4h-45-3	0.000	0	0	0	0	0.00	TD	>12	11	>12	10	>11	0.639	2	2	2	2	2.0	dark brown and black rust, light blistering
ECR(DCI)-10h-45-1	1.15	4	4	4	5	4.3	TD	10	9	>12	11	>11	0.639	2	3	2	3	2.5	dark brown and black rust
ECR(DCI)-10h-45-2	TD	>12	>12	>12	>12	>12	TD	>12	>12	>12	>12	>12	0.768	3	2	2	3	2.5	dark brown and black rust
ECR(DCI)-10h-45-3	N/A[1]	N/A[1]	N/A[1]	N/A[1]	N/A[1]	N/A[1]	N/A[1]	N/A[1]	N/A[1]	N/A[1]	N/A[1]	N/A[1]	N/A[1]	N/A[1]	N/A[1]	N/A[1]	N/A[1]	N/A[1]	dark brown and black rust, light blistering
ECR(DCI)-10h-35-1	TD	>12	12	>12	7	>11	TD	>12	12	>12	12	>12	5.03	10	10	10	12	11	dark brown and black rust
ECR(DCI)-10h-35-2	0.000	0	0	0	0	0.00	0.000	0	0	0	0	0.00	0.000	0	0	0	0	0.00	dark brown and black rust
ECR(DCI)-10h-35-3	0.832	3	3	4	3	3.3	3.80	4	4	10	12	7.5	0.316	2	2	2	2	2.0	dark brown and black rust
ECR(RH)-4h-45-1	0.252	1	1	1	1	1.0	0.284	1	2	1	2	1.5	0.219	1	1	1	1	1.0	no rust
ECR(RH)-4h-45-2	2.41	8	7	7	6	7.0	TD	>12	>12	>12	>12	>12	TD	>12	>12	>12	>12	>12	dark orange, brown and black rust
ECR(RH)-4h-45-3	0.187	1	1	1	1	1.0	0.284	2	1	1	1	1.3	0.000	0	0	0	0	0.00	no rust
ECR(RH)-10h-45-1	3.09	5	10	7	10	8.0	TD	>12	10	9	9	>10	1.03	4	4	4	4	4.0	dark brown and black rust
ECR(RH)-10h-45-2	0.000	0	0	0	0	0.00	0.000	0	0	0	0	0.00	0.000	0	0	0	0	0.00	no rust
ECR(RH)-10h-45-3	TD	>12	>12	>12	>12	>12	TD	>12	>12	>12	>12	>12	0.961	3	4	4	3	3.5	dark brown and black rust
ECR(RH)-10h-35-1	0.000	0	0	0	0	0.00	0.316	1	0	1	0	0.50	0.000	0	0	0	0	0.00	no rust
ECR(RH)-10h-35-2	0.000	0	0	0	0	0.00	0.316	1	1	0	0	0.50	0.000	0	0	0	0	0.00	no rust
ECR(RH)-10h-35-3	0.510	2	2	2	2	2.0	0.832	3	3	2	2	2.5	0.316	1	0	1	1	0.75	no rust
ECR(HY)-4h-45-1	0.187	0	1	0	0	0.25	0.187	0	1	0	0	0.25	0.000	0	0	0	0	0.00	no rust
ECR(HY)-4h-45-2	0.252	0	0	1	0	0.25	0.510	2	3	2	2	2.3	0.000	0	0	0	0	0.00	no rust
ECR(HY)-4h-45-3	0.187	0	0	1	0	0.25	2.19	3	10	5	5	5.8	0.000	0	0	0	0	0.00	dark brown and black rust
ECR(HY)-10h-45-1	0.348	1	2	2	1	1.5	4.03	8	11	4	7	7.5	0.000	0	0	0	0	0.00	dark brown and black rust
ECR(HY)-10h-45-2	0.000	0	0	0	0	0.00	0.316	0	4	0	1	1.3	0.000	0	0	0	0	0.00	dark brown and black rust
ECR(HY)-10h-45-3	0.000	0	0	0	0	0.00	5.93	6	12	9	12	9.8	0.187	1	1	0	0	0.50	dark brown and black rust
ECR(HY)-10h-35-1	0.252	1	2	2	1	1.5	0.316	1	2	2	2	1.8	0.155	0	1	0	0	0.25	dark brown and black rust
ECR(HY)-10h-35-2	0.000	0	0	0	0	0.00	0.000	0	0	0	0	0.00	0.000	0	0	0	0	0.00	no rust
ECR(HY)-10h-35-3	0.000	0	0	0	0	0.00	0.768	2	2	3	5	3.0	0.000	0	0	0	0	0.00	dark brown and black rust
ECR(primer/$Ca(NO_2)_2$)-4h-45-1	0.316	1	1	1	2	1.3	0.381	1	2	2	1	1.5	0.000	0	0	0	0	0.00	no rust
ECR(primer/$Ca(NO_2)_2$)-4h-45-2	2.45	5	9	6	11	7.8	TD	7	12	>12	12	>11	1.03	5	3	5	4	4.3	dark brown and black rust
ECR(primer/$Ca(NO_2)_2$)-4h-45-3	1.09	5	4	5	3	4.3	TD	10	12	>12	7	>10	1.28	5	5	4	4	4.5	dark brown and black rust
ECR(primer/$Ca(NO_2)_2$)-10h-45-1	3.03	7	7	7	6	6.8	TD	11	10	>12	8	>10	2.96	9	6	9	7	7.8	dark orange, brown and black rust
ECR(primer/$Ca(NO_2)_2$)-10h-45-2	TD	>12	>12	>12	>12	>12	TD	>12	>12	>12	>12	>12	1.99	6	6	4	6	5.5	dark brown and black rust, light blistering
ECR(primer/$Ca(NO_2)_2$)-10h-45-3	1.22	4	4	4	4	4.0	TD	>12	8	>12	10	>11	1.28	4	4	4	4	4.0	dark brown and black rust
ECR(primer/$Ca(NO_2)_2$)-10h-35-1	0.510	2	4	4	2	3.0	1.61	6	4	4	5	4.8	0.574	2	3	5	2	3.0	no rust
ECR(primer/$Ca(NO_2)_2$)-10h-35-2	1.41	5	4	5	5	4.8	2.19	7	4	6	5	5.5	0.961	4	3	3	3	3.3	black rust
ECR(primer/$Ca(NO_2)_2$)-10h-35-3	0.252	1	1	1	0	0.75	0.510	0	2	2	3	1.8	0.316	1	1	1	1	1.0	no rust

TD = Total Disbondment

Table 3.14b – Disbondment measurements on bottom bars of Southern Exposure specimens cast with corrosion inhibitors

Specimen	Side 1-A						Side 1-B						Side 2-A						Comments
		Disb. Radius (mm)				Avg.		Disb. Radius (mm)				Avg.		Disb. Radius (mm)				Avg.	
	A_d (cm^2)	0°	90°	180°	270°	r_d (mm)	A_d (cm^2)	0°	90°	180°	270°	r_d (mm)	A_d (cm^2)	0°	90°	180°	270°	r_d (mm)	
ECR(DCI)-4h-45-1	0.000	0	0	0	0	0.00	0.000	0	0	0	0	0.00	0.000	0	0	0	0	0.00	no rust
ECR(DCI)-4h-45-2	0.000	0	0	0	0	0.00	0.187	1	1	0	0	0.50	0.000	0	0	0	0	0.00	no rust
ECR(DCI)-4h-45-3	0.000	0	0	0	0	0.00	0.000	0	0	0	0	0.00	0.000	0	0	0	0	0.00	no rust
ECR(DCI)-10h-45-1	0.000	0	0	0	0	0.00	0.000	0	0	0	0	0.00	0.000	0	0	0	0	0.00	no rust
ECR(DCI)-10h-45-2	0.000	0	0	0	0	0.00	0.000	0	0	0	0	0.00	0.000	0	0	0	0	0.00	no rust
ECR(DCI)-10h-45-3	N/A[1]	N/A[1]	N/A[1]	N/A[1]	N/A[1]	N/A[1]	N/A[1]	N/A[1]	N/A[1]	N/A[1]	N/A[1]	N/A[1]	N/A[1]	N/A[1]	N/A[1]	N/A[1]	N/A[1]	N/A[1]	no rust
ECR(DCI)-10h-35-1	0.000	0	0	0	0	0.00	0.219	0	1	1	1	0.75	0.832	3	3	4	3	3.3	no rust
ECR(DCI)-10h-35-2	0.000	0	0	0	0	0.00	0.000	0	0	0	0	0.00	0.000	0	0	0	0	0.00	no rust
ECR(DCI)-10h-35-3	0.000	0	0	0	0	0.00	0.000	0	0	0	0	0.00	0.000	0	0	0	0	0.00	no rust
ECR(RH)-4h-45-1	0.000	0	0	0	0	0.00	0.000	0	0	0	0	0.00	0.000	0	0	0	0	0.00	no rust
ECR(RH)-4h-45-2	0.735	3	3	3	3	3.0	0.961	4	4	3	4	3.8	0.768	4	4	3	3	3.5	no rust
ECR(RH)-4h-45-3	0.000	0	0	0	0	0.00	0.000	0	0	0	0	0.00	0.000	0	0	0	0	0.00	black rust
ECR(RH)-10h-45-1	0.219	1	1	1	1	1.0	0.252	1	2	1	1	1.3	0.123	0	1	0	1	0.50	no rust
ECR(RH)-10h-45-2	0.000	0	0	0	0	0.00	0.000	0	0	0	0	0.00	0.000	0	0	0	0	0.00	no rust
ECR(RH)-10h-45-3	0.0903	1	0	0	0	0.25	0.413	2	2	2	2	2.0	0.252	1	1	1	1	1.0	no rust
ECR(RH)-10h-35-1	0.000	0	0	0	0	0.00	0.000	0	0	0	0	0.00	0.000	0	0	0	0	0.00	no rust
ECR(RH)-10h-35-2	0.606	1	2	2	2	1.8	0.671	3	2	2	3	2.5	0.768	3	2	2	3	2.5	no rust
ECR(RH)-10h-35-3	0.000	0	0	0	0	0.00	0.252	0	1	1	1	0.75	0.187	0	1	0	0	0.25	no rust
ECR(HY)-4h-45-1	0.000	0	0	0	0	0.00	0.574	0	1	0	1	0.50	0.000	0	0	0	0	0.00	no rust
ECR(HY)-4h-45-2	0.000	0	0	0	0	0.00	0.000	0	0	0	0	0.00	0.252	0	1	0	2	0.75	no rust
ECR(HY)-4h-45-3	0.187	0	1	0	0	0.25	0.252	0	0	2	0	0.50	0.000	0	0	0	0	0.00	no rust
ECR(HY)-10h-45-1	0.000	0	0	0	0	0.00	0.000	0	0	0	0	0.00	0.000	0	0	0	0	0.00	no rust
ECR(HY)-10h-45-2	0.000	0	0	0	0	0.00	0.000	0	0	0	0	0.00	0.000	0	0	0	0	0.00	no rust
ECR(HY)-10h-45-3	0.000	0	0	0	0	0.00	0.000	0	0	0	0	0.00	0.000	0	0	0	0	0.00	no rust
ECR(HY)-10h-35-1	0.000	0	0	0	0	0.00	0.252	1	1	1	1	1.0	0.000	0	0	0	0	0.00	small amount of orange rust
ECR(HY)-10h-35-2	0.000	0	0	0	0	0.00	0.000	0	0	0	0	0.00	0.000	0	0	0	0	0.00	no rust
ECR(HY)-10h-35-3	0.000	0	0	0	0	0.00	0.000	0	0	0	0	0.00	0.000	0	0	0	0	0.00	no rust
ECR(primer/$Ca(NO_2)_2$)-4h-45-1	0.000	0	0	0	0	0.00	0.000	0	0	0	0	0.00	0.000	0	0	0	0	0.00	no rust
ECR(primer/$Ca(NO_2)_2$)-4h-45-2	0.000	0	0	0	0	0.00	0.187	0	0	0	1	0.25	0.284	1	2	1	1	1.3	no rust
ECR(primer/$Ca(NO_2)_2$)-4h-45-3	0.000	0	0	0	0	0.00	0.000	0	0	0	0	0.00	0.000	0	0	0	0	0.00	no rust
ECR(primer/$Ca(NO_2)_2$)-10h-45-1	0.252	2	2	2	2	2.0	0.445	2	1	4	3	2.5	0.381	3	2	3	3	2.8	small amount of black rust
ECR(primer/$Ca(NO_2)_2$)-10h-45-2	0.510	5	5	4	3	4.3	1.03	6	5	6	4	5.3	2.25	11	9	7	11	9.5	dark brown and black rust
ECR(primer/$Ca(NO_2)_2$)-10h-45-3	0.000	0	0	0	0	0.00	0.000	0	0	0	0	0.00	0.155	0	1	0	0	0.25	no rust
ECR(primer/$Ca(NO_2)_2$)-10h-35-1	0.316	0	1	1	1	0.75	0.316	1	1	1	1	1.0	0.000	0	0	0	0	0.00	no rust
ECR(primer/$Ca(NO_2)_2$)-10h-35-2	0.639	2	2	2	2	2.0	1.09	4	3	2	4	3.3	1.15	3	5	3	3	3.5	small amount of orange rust
ECR(primer/$Ca(NO_2)_2$)-10h-35-3	0.252	1	0	0	1	0.50	0.510	2	2	2	2	2.0	0.510	3	2	1	2	2.0	small amount of orange rust

TD = Total Disbondment

As shown in Table 3.15, multiple-coated bars exhibited a greater amount of disbondment than the control ECR specimens. All but one MC bar with only the epoxy penetrated exhibited total disbondment. Three out of six MC specimens with both layers penetrated exhibited total disbondment; two with 10 holes through the epoxy and one with four holes through the epoxy. One MC specimen, MC(both layers penetrated)-4h-45-2, exhibited total disbondment on a bottom bar.

As shown in Table 3.16, all high adhesion ECR specimens exhibited total disbondment, with the exception of ECR(Valspar)-4h-45-4. The magnitude of disbondment observed in the high adhesion bars is greater than that observed in any other specimen group.

Table 3.15a – Disbondment measurements on top bars of Southern Exposure specimens containing multiple-coated reinforcement

	Side 1-A						Side 1-B						Side 2-A						
	A_d	Disbondment Radius (mm)				Avg. r_d	A_d	Disbondment Radius (mm)				Avg. r_d	A_d	Disbondment Radius (mm)				Avg. r_d	
Specimen	(cm^2)	0°	90°	180°	270°	(mm)	(cm^2)	0°	90°	180°	270°	(mm)	(cm^2)	0°	90°	180°	270°	(mm)	Comments
MC(both layers penetrated)-4h-45-1	2.38	5	5	4	9	5.8	0.000	0	0	0	0	0.00	0.155	3	0	1	1	1.3	dark grey
MC(both layers penetrated)-4h-45-2	2.15	5	11	4	5	6.3	0.000	0	0	0	0	0.00	0.000	0	0	0	0	0.00	orange and dark brown rust
MC(both layers penetrated)-4h-45-3	TD	10	11	>12	6	>9.8	0.000	0	0	0	0	0.00	0.000	0	0	0	0	0.00	dark brown and grey rust
MC(both layers penetrated)-10h-45-1	2.15	6	6	6	7	6.3	TD	>12	8	>12	6	>9.5	0.381	0	1	4	2	1.8	dark brown and grey rust
MC(both layers penetrated)-10h-45-2	2.06	6	7	6	7	6.5	2.25	3	7	10	7	6.8	0.252	1	1	1	2	1.3	orange, dark brown and dark grey rust, light blistering
MC(both layers penetrated)-10h-45-3	0.187	7	6	8	7	7.0	TD	>12	6	>12	12	>11	0.000	0	0	0	0	0.00	dark brown and dakr grey rust, light blistering
MC(only epoxy penetrated)-4h-45-1	1.86	9	6	5	4	6.0	TD	>12	9	8	12	>10	0.000	0	0	0	0	0.00	orange, dark brown and dark grey rust
MC(only epoxy penetrated)-4h-45-2	TD	>12	12	11	8	>11	TD	>12	12	>12	12	>12	0.187	2	2	2	2	2.0	dark brown and dark grey rust
MC(only epoxy penetrated)-4h-45-3	TD	8	12	>12	9	>10	TD	>12	12	>12	12	>12	0.000	0	0	0	0	0.00	dark brown and dark grey rust, white discoloration
MC(only epoxy penetrated)-10h-45-1	TD	>12	>12	>12	6	>11	TD	>12	>12	8	>12	>11	0.219	1	1	0	2	1.0	dark brown and grey rust
MC(only epoxy penetrated)-10h-45-2	2.45	6	9	4	7	6.5	TD	>12	10	>12	12	>12	0.735	2	4	4	3	3.3	orange, dark brown and dark grey rust
MC(only epoxy penetrated)-10h-45-3	1.90	5	4	5	5	4.8	5.15	11	6	12	12	10	0.413	2	2	2	1	1.8	dark brown and grey rust

TD = Total Disbondment

Table 3.15b – Disbondment measurements on bottom bars of Southern Exposure specimens containing multiple-coated reinforcement

	Side 1-A						Side 1-B						Side 2-A						
	A_d	Disb. Radius (mm)				Avg. r_d	A_d	Disb. Radius (mm)				Avg. r_d	A_d	Disb. Radius (mm)				Avg. r_d	
Specimen	(cm^2)	0°	90°	180°	270°	(mm)	(cm^2)	0°	90°	180°	270°	(mm)	(cm^2)	0°	90°	180°	270°	(mm)	Comments
MC(both layers penetrated)-4h-45-1	0.123	1	0	0	1	0.50	0.155	1	0	1	1	0.75	0.000	0	0	0	0	0.00	no rust
MC(both layers penetrated)-4h-45-2	0.000	0	0	0	0	0.00	TD	>12	12	>12	12	>12	0.000	0	0	0	0	0.00	no rust
MC(both layers penetrated)-4h-45-3	0.000	0	0	0	0	0.00	0.000	0	0	0	0	0.00	0.000	0	0	0	0	0.00	no rust
MC(both layers penetrated)-10h-45-1	0.000	0	0	0	0	0.00	0.000	0	0	0	0	0.00	0.316	3	3	1	1	2.0	grey rust
MC(both layers penetrated)-10h-45-2	0.000	0	0	0	0	0.00	0.000	0	0	0	0	0.00	0.000	0	0	0	0	0.00	no rust
MC(both layers penetrated)-10h-45-3	0.000	0	0	0	0	0.00	0.000	0	0	0	0	0.00	0.000	0	0	0	0	0.00	no rust
MC(only epoxy penetrated)-4h-45-1	0.000	0	0	0	0	0.00	0.000	0	0	0	0	0.00	0.000	0	0	0	0	0.00	no rust
MC(only epoxy penetrated)-4h-45-2	0.000	0	0	0	0	0.00	0.000	0	0	0	0	0.00	0.187	1	1	1	1	1.0	small amount of grey rust
MC(only epoxy penetrated)-4h-45-3	0.000	0	0	0	0	0.00	0.000	0	0	0	0	0.00	0.000	0	0	0	0	0.00	no rust
MC(only epoxy penetrated)-10h-45-1	0.000	0	0	0	0	0.00	0.000	0	0	0	0	0.00	0.000	0	0	0	0	0.00	no rust
MC(only epoxy penetrated)-10h-45-2	0.000	0	0	0	0	0.00	0.000	0	0	0	0	0.00	0.510	3	2	2	3	2.5	dark brown and grey rust
MC(only epoxy penetrated)-10h-45-3	0.000	0	0	0	0	0.00	0.000	0	0	0	0	0.00	0.000	0	0	0	0	0.00	no rust

TD = Total Disbondment

Table 3.16a – Disbondment measurements on top bars of Southern Exposure specimens containing ECR with increased adhesion epoxy

	Side 1-A						Side 1-B						Side 2-A						
	A_d	Disbondment Radius (mm)				Avg. r_d	A_d	Disbondment Radius (mm)				Avg. r_d	A_d	Disbondment Radius (mm)				Avg. r_d	
Specimen	(cm^2)	0°	90°	180°	270°	(mm)	(cm^2)	0°	90°	180°	270°	(mm)	(cm^2)	0°	90°	180°	270°	(mm)	Comments
ECR(Chromate)-4h-45-1	3.35	7	6	7	8	7.0	TD	9	7	>12	10	>9.5	1.35	5	4	4	3	4.0	dark brown and black rust
ECR(Chromate)-4h-45-2	TD	>12	>12	>12	>12	>12	TD	>12	>12	>12	>12	>12	3.22	6	6	6	12	7.5	dark brown and black rust, light blistering
ECR(Chromate)-4h-45-3	TD	>12	>12	>12	>12	>12	TD	>12	>12	>12	>12	>12	5.41	10	12	10	12	11	dark brown rust, light blistering
ECR(Chromate)-4h-45-4	4.83	8	8	12	12	10	TD	>12	12	>12	12	>12	1.48	4	3	4	4	3.8	dark brown rust, light blistering
ECR(Chromate)-10h-45-1	TD	>12	>12	>12	>12	>12	TD	>12	>12	>12	>12	>12	TD	>12	>12	>12	>12	>12	dark brown rust
ECR(Chromate)-10h-45-2	TD	>12	>12	>12	12	>12	TD	>12	12	>12	12	>12	TD	>12	12	>12	12	>12	dark brown and black rust, heavy blistering
ECR(Chromate)-10h-45-3	2.70	7	5	5	10	6.8	TD	7	12	>12	10	>10	2.25	5	5	8	6	6.0	dark brown and black rust, moderate blistering
ECR(DuPont)-4h-45-1	TD	>12	>12	>12	>12	>12	TD	>12	>12	>12	>12	>12	TD	>12	>12	>12	>12	>12	gold, orange and black rust
ECR(DuPont)-4h-45-2	TD	>12	>12	>12	>12	>12	TD	>12	>12	>12	>12	>12	TD	>12	>12	>12	>12	>12	gold and black rust, light blistering
ECR(DuPont)-4h-45-3	TD	>12	>12	>12	>12	>12	TD	>12	>12	>12	>12	>12	TD	>12	>12	>12	>12	>12	gold and black rust
ECR(DuPont)-4h-45-4	TD	>12	>12	>12	>12	>12	TD	>12	>12	>12	>12	>12	4.70	10	8	11	9	9.5	gold and black rust
ECR(DuPont)-10h-45-1	TD	>12	>12	>12	>12	>12	TD	>12	>12	>12	>12	>12	TD	>12	>12	>12	>12	>12	gold and black rust
ECR(DuPont)-10h-45-2	TD	>12	>12	>12	>12	>12	TD	>12	>12	>12	>12	>12	TD	>12	>12	>12	>12	>12	gold and black rust
ECR(DuPont)-10h-45-3	TD	>12	>12	>12	>12	>12	TD	>12	>12	>12	>12	>12	TD	>12	>12	>12	>12	>12	gold and black rust, light blistering
ECR(Valspar)-4h-45-1	TD	>12	>12	>12	>12	>12	TD	>12	>12	>12	>12	>12	5.74	10	12	10	12	11	dark brown and black rust, light blistering
ECR(Valspar)-4h-45-2	TD	>12	>12	>12	>12	>12	TD	>12	>12	>12	>12	>12	TD	>12	>12	>12	>12	>12	dark brown and black rust, light blistering
ECR(Valspar)-4h-45-3	TD	>12	>12	>12	>12	>12	TD	>12	>12	>12	>12	>12	TD	>12	>12	>12	>12	>12	dark brown and black rust, light blistering
ECR(Valspar)-4h-45-4	1.09	4	4	4	5	4.3	1.28	5	5	4	4	4.5	0.000	0	0	0	0	0.00	dark orange rust
ECR(Valspar)-10h-45-1	TD	>12	>12	>12	>12	>12	TD	>12	>12	>12	>12	>12	TD	>12	>12	>12	>12	>12	dark brown and black rust, light blistering
ECR(Valspar)-10h-45-2	TD	>12	12	>12	>12	>12	TD	>12	12	>12	>12	>12	TD	>12	12	>12	>12	>12	dark brown and black rust, moderate blistering
ECR(Valspar)-10h-45-3	0.000	0	0	0	0	0.00	TD	11	11	>12	12	>12	4.45	10	8	11	12	10	dark brown and black rust

TD = Total Disbondment

Table 3.16b – Disbondment measurements on bottom bars of Southern Exposure specimens containing ECR with increased adhesion epoxy

	Side 1-A						Side 1-B						Side 2-A						
		Disb. Radius (mm)				Avg.		Disb. Radius (mm)				Avg.		Disb. Radius (mm)				Avg.	
Specimen	A_d (cm^2)	0°	90°	180°	270°	r_d (mm)	A_d (cm^2)	0°	90°	180°	270°	r_d (mm)	A_d (cm^2)	0°	90°	180°	270°	r_d (mm)	Comments
ECR(Chromate)-4h-45-1	0.000	0	0	0	0	0.00	0.000	0	0	0	0	0.00	0.000	0	0	0	0	0.00	no rust
ECR(Chromate)-4h-45-2	0.316	1	2	1	2	1.5	0.574	2	3	4	4	3.3	0.252	0	1	0	1	0.50	dark brown and black rust
ECR(Chromate)-4h-45-3	0.000	0	0	0	0	0.00	0.000	0	0	0	0	0.00	3.48	10	9	5	9	8.3	black rust
ECR(Chromate)-4h-45-4	0.187	0	0	1	1	0.50	0.252	1	1	1	1	1.0	0.123	0	1	0	1	0.50	no rust
ECR(Chromate)-10h-45-1	0.284	1	0	1	2	1.0	0.316	0	1	1	2	1.0	0.413	2	1	1	2	1.5	no rust
ECR(Chromate)-10h-45-2	0.252	1	2	1	2	1.5	0.703	4	3	3	3	3.3	0.000	0	0	0	0	0.00	no rust
ECR(Chromate)-10h-45-3	0.671	1	2	2	4	2.3	0.606	2	3	2	2	2.3	0.219	0	0	1	1	0.50	small amount of brown rust
ECR(DuPont)-4h-45-1	0.187	0	2	0	1	0.75	0.639	2	2	2	2	2.0	4.57	9	10	10	10	9.8	orange and gold rust
ECR(DuPont)-4h-45-2	0.000	0	0	0	0	0.00	0.252	1	1	0	1	0.75	0.316	0	2	1	1	1.0	orange rust
ECR(DuPont)-4h-45-3	0.000	0	0	0	0	0.00	3.54	9	9	9	9	9.0	1.80	5	7	6	8	6.5	gold rust
ECR(DuPont)-4h-45-4	0.000	0	0	0	0	0.00	1.54	5	4	4	5	4.5	1.22	4	4	4	4	4.0	gold rust
ECR(DuPont)-10h-45-1	1.15	4	5	3	5	4.3	1.67	5	7	5	6	5.8	0.381	2	2	2	2	2.0	gold rust
ECR(DuPont)-10h-45-2	0.123	1	1	1	1	1.0	0.897	5	4	2	3	3.5	0.897	4	3	3	5	3.8	gold rust
ECR(DuPont)-10h-45-3	1.09	4	4	4	4	4.0	1.86	5	6	6	6	5.8	0.897	3	4	3	3	3.3	gold and black rust
ECR(Valspar)-4h-45-1	0.000	0	0	0	0	0.00	0.381	3	0	1	2	1.5	0.252	0	1	1	0	0.50	no rust
ECR(Valspar)-4h-45-2	0.445	2	2	1	1	1.5	1.41	2	4	6	9	5.3	TD	>12	>12	>12	>12	>12	black rust
ECR(Valspar)-4h-45-3	0.000	0	0	0	0	0.00	3.41	8	7	4	10	7.3	2.12	5	7	5	6	5.8	black rust
ECR(Valspar)-4h-45-4	0.000	0	0	0	0	0.00	0.000	0	0	0	0	0.00	0.000	0	0	0	0	0.00	no rust
ECR(Valspar)-10h-45-1	1.15	4	6	4	5	4.8	3.86	10	10	8	10	9.5	2.32	9	8	5	8	7.5	orange and black rust
ECR(Valspar)-10h-45-2	0.000	0	0	0	0	0.00	0.316	2	2	2	2	2.0	0.000	0	0	0	0	0.00	no rust
ECR(Valspar)-10h-45-3	2.77	4	7	7	9	6.8	3.03	9	8	6	6	7.3	3.67	8	9	10	9	9.0	black rust

TD = Total Disbondment

Table 3.17 shows that the magnitude of disbondment observed for the high adhesion ECR cast in specimens with DCI corrosion inhibitor is less than that observed in high adhesion ECR cast in plain concrete. Only one specimen, ECR(Valspar/DCI)-4h-45-3, exhibited total disbondment. It should be noted that only high adhesion ECR with four holes through the epoxy was evaluated in conjunction with DCI corrosion inhibitor. Generally, bars with four holes through the epoxy exhibit less disbondment than bars with ten holes through the epoxy.

Disbondment measurements taken on cracked beam specimens are summarized in Tables 3.18 through 3.21. As shown in Table 3.18, ECR control specimens experienced severe disbondment, with all but one specimen, ECR-4h-4h-6, exhibiting total disbondment in the top bars. None of the bottom bars in the ECR control specimens exhibited total disbondment. Table 3.19 shows that the cracked beam specimens cast with corrosion inhibitors also exhibited severe disbondment,

Table 3.17a – Disbondment measurements on top bars of Southern Exposure specimens containing ECR with increased adhesion epoxy cast with concrete containing DCI corrosion inhibitor

	Side 1-A						Side 1-B						Side 2-A						
	A_d	Disbondment Radius (mm)				Avg. r_d	A_d	Disbondment Radius (mm)				Avg. r_d	A_d	Disbondment Radius (mm)				Avg. r_d	
Specimen	(cm^2)	0°	90°	180°	270°	(mm)	(cm^2)	0°	90°	180°	270°	(mm)	(cm^2)	0°	90°	180°	270°	(mm)	Comments
ECR(Chromate/DCI)-4h-45-1	0.187	1	1	1	2	1.3	5.15	>12	12	10	10	>11	0.219	1	1	0	0	0.50	dark brown and black rust, light blistering
ECR(Chromate/DCI)-4h-45-2	0.000	0	0	0	0	0.00	0.000	0	0	0	0	0.00	0.000	0	0	0	0	0.00	no rust
ECR(Chromate/DCI)-4h-45-3	0.000	0	0	0	0	0.00	1.54	5	3	6	7	5.3	0.961	4	3	5	4	4.0	dark brown and black rust
ECR(DuPont/DCI)-4h-45-1	0.000	0	0	0	0	0.00	5.41	8	12	5	12	9.3	0.800	2	2	3	2	2.3	orange, dark brown and black rust
ECR(DuPont/DCI)-4h-45-2	0.000	0	0	0	0	0.00	0.000	0	0	0	0	0.00	0.000	0	0	0	0	0.00	no rust
ECR(DuPont/DCI)-4h-45-3	0.000	0	0	0	0	0.00	0.000	0	0	0	0	0.00	0.187	1	2	1	1	1.3	no rust
ECR(Valspar/DCI)-4h-45-1	0.542	2	2	2	2	2.0	0.574	3	2	2	2	2.3	0.284	2	2	1	1	1.5	black rust
ECR(Valspar/DCI)-4h-45-2	0.768	6	2	1	0	2.3	1.67	5	5	6	5	5.3	0.000	0	0	0	0	0.00	dark orange, brown and black rust
ECR(Valspar/DCI)-4h-45-3	TD	1	4	>12	1	>4.5	2.25	6	7	7	6	6.5	2.77	7	6	8	7	7.0	dark orange, brown and black rust

TD = Total Disbondment

Table 3.17b – Disbondment measurements on bottom bars of Southern Exposure specimens containing ECR with increased adhesion epoxy cast with concrete containing DCI corrosion inhibitor

	Side 1-A						Side 1-B						Side 2-A						
	A_d	Disb. Radius (mm)				Avg. r_d	A_d	Disb. Radius (mm)				Avg. r_d	A_d	Disb. Radius (mm)				Avg. r_d	
Specimen	(cm^2)	0°	90°	180°	270°	(mm)	(cm^2)	0°	90°	180°	270°	(mm)	(cm^2)	0°	90°	180°	270°	(mm)	Comments
ECR(Chromate/DCI)-4h-45-1	0.000	0	0	0	0	0.00	0.000	0	0	0	0	0.00	0.000	0	0	0	0	0.00	no rust
ECR(Chromate/DCI)-4h-45-2	0.000	0	0	0	0	0.00	0.000	0	0	0	0	0.00	0.000	0	0	0	0	0.00	no rust
ECR(Chromate/DCI)-4h-45-3	0.252	1	1	0	0	0.50	0.252	2	1	0	0	0.75	0.510	2	2	2	2	2.0	no rust
ECR(DuPont/DCI)-4h-45-1	0.000	0	0	0	0	0.00	0.000	0	0	0	0	0.00	0.000	0	0	0	0	0.00	no rust
ECR(DuPont/DCI)-4h-45-2	0.000	0	0	0	0	0.00	0.000	0	0	0	0	0.00	0.000	0	0	0	0	0.00	gold rust
ECR(DuPont/DCI)-4h-45-3	0.187	0	1	1	1	0.75	0.445	1	2	2	2	1.8	0.961	4	4	4	4	4.0	gold rust
ECR(Valspar/DCI)-4h-45-1	0.000	0	0	0	0	0.00	0.000	0	0	0	0	0.00	0.000	0	0	0	0	0.00	no rust
ECR(Valspar/DCI)-4h-45-2	0.000	0	0	0	0	0.00	0.000	0	0	0	0	0.00	0.000	0	0	0	0	0.00	no rust
ECR(Valspar/DCI)-4h-45-3	0.187	1	1	1	1	1.0	0.252	1	1	1	1	1.0	0.510	2	1	1	2	1.5	black rust

TD = Total Disbondment

Table 3.18a – Disbondment measurements on top bars of cracked beam control specimens.

	Side 1-A						Side 1-B						Side 2-A						
	A_d	Disbondment Radius (mm)				Avg. r_d	A_d	Disbondment Radius (mm)				Avg. r_d	A_d	Disbondment Radius (mm)				Avg. r_d	
Specimen	(cm^2)	0°	90°	180°	270°	(mm)	(cm^2)	0°	90°	180°	270°	(mm)	(cm^2)	0°	90°	180°	270°	(mm)	Comments
ECR-4h-45-1	TD	>12	>12	>12	>12	>12	1.41	5	4	4	4	4.3	TD	11	>12	>12	8	>11	dark brown and black rust, light blistering
ECR-4h-45-2	TD	>12	>12	>12	>12	>12	TD	>12	>12	>12	>12	>12	TD	>12	>12	>12	>12	>12	dark brown and black rust
ECR-4h-45-3	TD	>12	11	>12	>12	>12	TD	>12	>12	>12	>12	>12	TD	10	>12	>12	>12	>12	dark brown and black rust
ECR-4h-45-4	1.54	4	4	3	5	4.0	TD	>12	>12	>12	>12	>12	TD	>12	>12	>12	>12	>12	dark brown and black rust, light blistering
ECR-4h-45-5	TD	>12	>12	>12	>12	>12	TD	>12	>12	>12	>12	>12	TD	>12	>12	>12	>12	>12	dark brown and black rust, light blistering
ECR-4h-45-6	3.15	7	10	6	10	8.3	4.64	10	12	10	10	11	5.67	12	12	12	12	12	dark brown and black rust
ECR-10h-45-1	TD	>12	>12	>12	>12	>12	TD	>12	>12	>12	>12	>12	TD	>12	>12	>12	>12	>12	dark brown and black rust, light blistering
ECR-10h-45-2	TD	>12	>12	>12	>12	>12	TD	>12	>12	>12	>12	>12	TD	>12	>12	>12	>12	>12	dark brown and black rust, light blistering
ECR-10h-45-3	TD	>12	>12	>12	>12	>12	TD	>12	>12	>12	>12	>12	TD	>12	>12	>12	>12	>12	dark brown and black rust
ECR-10h-35-1	5.99	10	11	12	11	11	TD	>12	>12	>12	>12	>12	TD	>12	>12	12	>12	>12	dark brown and black rust
ECR-10h-35-2	TD	>12	>12	>12	>12	>12	TD	>12	>12	>12	>12	>12	TD	>12	>12	>12	>12	>12	dark brown and black rust, light blistering
ECR-10h-35-3	TD	9	>12	>12	>12	>11	TD	>12	>12	>12	>12	>12	TD	10	>12	10	>12	>11	dark brown and black rust, light blistering

TD = Total Disbondment

Table 3.18b – Disbondment measurements on bottom bars of cracked beam control specimens.

Specimen	Side 1-A						Side 1-B						Side 2-A						Comments
	A_d	Disb. Radius (mm)				Avg. r_d	A_d	Disb. Radius (mm)				Avg. r_d	A_d	Disb. Radius (mm)				Avg. r_d	
	(cm^2)	0°	90°	180°	270°	(mm)	(cm^2)	0°	90°	180°	270°	(mm)	(cm^2)	0°	90°	180°	270°	(mm)	
ECR-4h-45-1	0.000	0	0	0	0	0.00	1.09	4	4	5	4	4.3	1.48	4	4	4	5	4.3	no rust
ECR-4h-45-2	0.000	0	0	0	0	0.00	1.28	5	4	5	4	4.5	1.28	4	6	5	4	4.8	no rust
ECR-4h-45-3	0.000	0	0	0	0	0.00	0.768	3	3	4	4	3.5	0.252	2	2	2	2	2.0	black rust
ECR-4h-45-4	1.15	4	4	4	4	4.0	1.28	6	5	5	5	5.3	4.54	10	10	10	10	10	dark brown and black rust
ECR-4h-45-5	0.000	0	0	0	0	0.00	0.000	0	0	0	0	0.00	2.51	7	7	7	7	7.0	black rust
ECR-4h-45-6	0.000	0	0	0	0	0.00	0.316	2	2	1	2	1.8	0.000	0	0	0	0	0.00	black rust
ECR-10h-45-1	0.381	2	2	2	1	1.8	0.445	2	2	2	2	2.0	0.316	2	2	2	1	1.8	no rust
ECR-10h-45-2	0.000	0	0	0	0	0.00	0.000	0	0	0	0	0.00	1.41	4	6	5	5	5.0	black rust
ECR-10h-45-3	0.000	0	0	0	0	0.00	0.000	0	0	0	0	0.00	1.93	6	6	7	6	6.3	black rust
ECR-10h-35-1	1.35	4	4	5	5	4.5	1.15	4	4	5	5	4.5	1.35	5	4	5	4	4.5	black rust
ECR-10h-35-2	1.80	5	6	6	6	5.8	2.12	7	6	6	7	6.5	1.22	4	4	4	4	4.0	black rust
ECR-10h-35-3	1.54	6	5	5	5	5.3	1.74	6	6	6	5	5.8	1.28	4	5	4	5	4.5	black rust

TD = Total Disbondment

Table 3.19a – Disbondment measurements on top bars of cracked beam specimens cast with corrosion inhibitors

Specimen	Side 1-A						Side 1-B						Side 2-A						Comments
	A_d	Disbondment Radius (mm)				Avg. r_d	A_d	Disbondment Radius (mm)				Avg. r_d	A_d	Disbondment Radius (mm)				Avg. r_d	
	(cm^2)	0°	90°	180°	270°	(mm)	(cm^2)	0°	90°	180°	270°	(mm)	(cm^2)	0°	90°	180°	270°	(mm)	
ECR(DCI)-4h-45-1	TD	>12	12	>12	12	>12	TD	>12	12	>12	12	>12	3.74	7	11	7	12	9.3	dark brown and black rust
ECR(DCI)-4h-45-2	3.48	8	12	4	8	8.0	TD	10	>12	>12	12	>12	3.93	8	12	5	12	9.3	dark brown and black rust
ECR(DCI)-4h-45-3	TD	>12	>12	>12	>12	>12	TD	>12	>12	>12	>12	>12	TD	8	>12	8	>12	>10	dark brown and black rust
ECR(DCI)-10h-45-1	TD	>12	>12	>12	>12	>12	TD	>12	>12	>12	>12	>12	TD	10	>12	8	>12	>11	dark brown and black rust, light blistering
ECR(DCI)-10h-45-2	TD	>12	12	>12	12	>12	TD	>12	12	>12	12	>12	5.54	12	8	12	10	11	dark brown and black rust, light blistering
ECR(DCI)-10h-45-3	TD	>12	>12	>12	>12	>12	TD	>12	>12	>12	>12	>12	TD	8	>12	8	>12	>10	dark brown and black rust, light blistering
ECR(DCI)-10h-35-1	5.41	10	8	12	11	10	TD	>12	>12	>12	>12	>12	3.74	9	10	10	9	9.5	orange, dark brown and black rust
ECR(DCI)-10h-35-2	4.83	12	7	13	6	9.5	TD	>12	>12	>12	>12	>12	5.99	12	>12	8	5	>9.3	dark brown and black rust, light blistering
ECR(DCI)-10h-35-3	TD	>12	>12	>12	>12	>12	TD	>12	>12	>12	>12	>12	6.64	11	12	9	8	10	dark brown and black rust, heavy blistering
ECR(RH)-4h-45-1	TD	>12	>12	>12	>12	>12	TD	>12	>12	>12	>12	>12	6.19	>12	12	9	>12	>11	orange, dark brown and black rust, moderate blistering
ECR(RH)-4h-45-2	3.86	8	10	7	7	8.0	TD	>12	>12	>12	>12	>12	TD	>12	>12	>12	>12	>12	dark brown and black rust, light blistering
ECR(RH)-4h-45-3	TD	>12	>12	>12	>12	>12	TD	>12	>12	>12	>12	>12	TD	>12	>12	>12	>12	>12	dark brown and black rust, heavy blistering
ECR(RH)-10h-45-1	TD	>12	>12	>12	>12	>12	TD	>12	>12	>12	>12	>12	TD	>12	>12	>12	>12	>12	orange, dark brown and black rust, heavy blistering
ECR(RH)-10h-45-2	TD	>12	>12	>12	>12	>12	TD	>12	>12	>12	>12	>12	TD	>12	>12	>12	>12	>12	orange, dark brown and black rust, heavy blistering
ECR(RH)-10h-45-3	TD	>12	>12	>12	>12	>12	TD	>12	>12	>12	>12	>12	4.70	7	10	9	10	9.0	dark brown and black rust, moderate blistering
ECR(RH)-10h-35-1	TD	>12	>12	>12	>12	>12	TD	>12	>12	>12	>12	>12	1.86	5	7	6	2	5.0	dark brown and black rust, light blistering
ECR(RH)-10h-35-2	TD	>12	>12	>12	>12	>12	TD	>12	>12	>12	>12	>12	5.80	>12	12	7	10	>10	dark brown and black rust, heavy blistering
ECR(RH)-10h-35-3	TD	>12	>12	>12	>12	>12	TD	>12	>12	>12	>12	>12	TD	>12	>12	10	>12	>12	orange, dark brown and black rust, light blistering
ECR(HY)-4h-45-1	3.80	7	10	6	11	8.5	5.74	10	12	11	12	11	3.80	6	10	6	11	8.3	orange, dark brown and black rust, light blistering
ECR(HY)-4h-45-2	TD	>12	>12	>12	>12	>12	TD	>12	>12	>12	>12	>12	TD	6	>12	7	>12	>9.3	orange, dark brown and black rust, light blistering
ECR(HY)-4h-45-3	TD	>12	10	11	11	>11	TD	>12	9	>12	11	>11	2.77	5	11	7	7	7.5	orange, dark brown and black rust, moderate blistering
ECR(HY)-10h-45-1	TD	>12	>12	>12	>12	>12	TD	>12	>12	>12	>12	>12	1.74	5	6	6	6	5.8	orange, dark brown and black rust, light blistering
ECR(HY)-10h-45-2	TD	>12	>12	>12	>12	>12	TD	>12	>12	>12	>12	>12	3.80	7	7	5	12	7.8	dark brown and black rust, light blistering
ECR(HY)-10h-45-3	TD	>12	>12	>12	>12	>12	TD	>12	>12	>12	>12	>12	4.51	8	12	6	12	9.5	dark brown and black rust
ECR(HY)-10h-35-1	TD	>12	>12	>12	>12	>12	TD	>12	>12	>12	>12	>12	TD	12	>12	10	>12	>12	dark brown and black rust
ECR(HY)-10h-35-2	TD	>12	>12	>12	>12	>12	TD	>12	>12	>12	>12	>12	5.35	10	10	11	11	11	orange, dark brown and black rust, moderate blistering
ECR(HY)-10h-35-3	TD	>12	>12	>12	>12	>12	TD	>12	>12	>12	>12	>12	5.15	10	12	8	12	11	dark brown and black rust
ECR(primer/$Ca(NO_2)_2$)-4h-45-1	TD	>12	12	>12	12	>12	TD	>12	12	>12	12	>12	2.83	7	7	7	8	7.3	dark brown and black rust
ECR(primer/$Ca(NO_2)_2$)-4h-45-2	TD	>12	>12	>12	12	>12	TD	>12	12	>12	12	>12	TD	>12	12	>12	12	>12	dark brown and black rust, light blistering
ECR(primer/$Ca(NO_2)_2$)-4h-45-3	0.832	3	4	3	5	3.8	TD	>12	12	>12	12	>12	TD	>12	>12	>12	>12	>12	orange, dark brown and black rust, light blistering
ECR(primer/$Ca(NO_2)_2$)-10h-45-1	TD	>12	12	>12	12	>12	TD	>12	12	>12	12	>12	3.15	8	12	5	12	9.3	orange, dark brown and black rust
ECR(primer/$Ca(NO_2)_2$)-10h-45-2	TD	>12	12	>12	12	>12	TD	>12	12	>12	12	>12	2.25	7	7	7	8	7.3	orange, dark brown and black rust, light blistering
ECR(primer/$Ca(NO_2)_2$)-10h-45-3	TD	>12	12	>12	12	>12	TD	>12	12	>12	12	>12	3.03	8	12	6	12	9.5	dark brown and black rust, light blistering
ECR(primer/$Ca(NO_2)_2$)-10h-35-1	TD	>12	>12	>12	>12	>12	TD	>12	>12	>12	>12	>12	0.381	1	2	1	2	1.5	dark brown and black rust, light blistering
ECR(primer/$Ca(NO_2)_2$)-10h-35-2	TD	>12	10	>12	10	>11	TD	>12	8	>12	10	>11	1.61	6	6	3	6	5.3	dark brown and black rust, light blistering
ECR(primer/$Ca(NO_2)_2$)-10h-35-3	TD	>12	11	>12	12	>12	TD	>12	5	>12	>12	>10	5.28	10	>12	7	7	>9.0	dark brown and black rust, light blistering

TD = Total Disbondment

Table 3.19b – Disbondment measurements on bottom bars of cracked beam specimens cast with corrosion inhibitors

Specimen	Side 1-A						Side 1-B						Side 2-A						Comments
	A_d	Disb. Radius (mm)				Avg. r_d	A_d	Disb. Radius (mm)				Avg. r_d	A_d	Disb. Radius (mm)				Avg. r_d	
	(cm^2)	0°	90°	180°	270°	(mm)	(cm^2)	0°	90°	180°	270°	(mm)	(cm^2)	0°	90°	180°	270°	(mm)	
ECR(DCI)-4h-45-1	0.639	4	3	2	2	2.8	0.703	3	3	3	2	2.8	0.639	2	3	2	4	2.8	black rust
ECR(DCI)-4h-45-2	0.510	2	2	1	2	1.8	0.639	2	3	3	2	2.5	0.000	0	0	0	0	0.00	black rust
ECR(DCI)-4h-45-3	0.510	3	2	2	2	2.3	0.639	3	2	2	3	2.5	0.000	0	0	0	0	0.00	black rust
ECR(DCI)-10h-45-1	0.000	0	0	0	0	0.00	0.000	0	0	0	0	0.00	0.381	2	1	2	1	1.5	black rust
ECR(DCI)-10h-45-2	0.316	1	2	1	1	1.3	0.510	3	3	1	2	2.3	0.000	0	0	0	0	0.00	black rust
ECR(DCI)-10h-45-3	0.445	2	2	2	2	2.0	0.703	3	4	4	3	3.5	0.574	3	2	2	4	2.8	black rust
ECR(DCI)-10h-35-1	0.316	2	2	0	1	1.3	3.41	8	8	8	9	8.3	2.32	6	5	5	5	5.3	black rust
ECR(DCI)-10h-35-2	2.45	7	7	6	6	6.5	2.83	7	9	8	6	7.5	3.67	8	9	8	9	8.5	black rust
ECR(DCI)-10h-35-3	1.99	6	8	6	4	6.0	1.99	6	7	6	5	6.0	1.74	4	6	6	4	5.0	black rust
ECR(RH)-4h-45-1	0.961	3	3	4	3	3.3	1.80	5	5	6	5	5.3	1.67	5	6	5	5	5.3	black rust
ECR(RH)-4h-45-2	1.61	4	4	5	4	4.3	2.38	5	5	5	5	5.0	5.54	10	10	12	10	11	black rust
ECR(RH)-4h-45-3	1.41	5	4	5	5	4.8	2.45	5	7	6	8	6.5	4.51	8	10	9	8	8.8	black rust
ECR(RH)-10h-45-1	2.70	6	11	6	6	7.3	2.70	5	12	6	6	7.3	TD	>12	12	>12	>12	>12	black rust
ECR(RH)-10h-45-2	0.639	4	3	4	3	3.5	1.99	8	6	7	4	6.3	5.99	11	12	11	12	12	black rust
ECR(RH)-10h-45-3	1.15	4	4	4	4	4.0	1.28	4		5	5	3.5	0.252	7	1	1	1	2.5	black rust
ECR(RH)-10h-35-1	1.22	3	4	4	3	3.5	1.22	4	4	4	6	4.5	1.28	3	5	4	4	4.0	black rust
ECR(RH)-10h-35-2	1.80	6	6	5	4	5.3	2.32	5	7	5	6	5.8	1.48	5	4	5	3	4.3	black rust
ECR(RH)-10h-35-3	0.510	2	3	2	2	2.3	1.28	4	4	5	3	4.0	1.28	4	5	4	3	4.0	black rust
ECR(HY)-4h-45-1	0.000	0	0	0	0	0.00	0.187	0	1	1	1	0.75	0.000	0	0	0	0	0.00	no rust
ECR(HY)-4h-45-2	0.219	1	1	1	0	0.75	0.735	2	2	3	2	2.3	0.000	0	0	0	0	0.00	black rust
ECR(HY)-4h-45-3	0.000	0	0	0	0	0.00	0.000	0	0	0	0	0.00	0.000	0	0	0	0	0.00	no rust
ECR(HY)-10h-45-1	0.000	0	0	0	0	0.00	0.252	1	1	1	1	1.0	0.000	0	0	0	0	0.00	small amount of orange rust
ECR(HY)-10h-45-2	0.000	0	0	0	0	0.00	0.574	3	3	4	2	3.0	0.219	1	0	1	2	1.0	black rust
ECR(HY)-10h-45-3	0.000	0	0	0	0	0.00	0.000	0	0	0	0	0.00	0.542	2	2	3	2	2.3	black rust
ECR(HY)-10h-35-1	0.606	2	2	3	3	2.5	1.35	5	4	4	4	4.3	1.12	4	3	3	4	3.5	black rust
ECR(HY)-10h-35-2	0.574	1	0	0	1	0.50	1.93	6	6	5	5	5.5	1.99	5	5	5	5	5.0	black rust
ECR(HY)-10h-35-3	0.000	0	0	0	0	0.00	1.80	6	4	5	4	4.8	1.48	5	4	5	4	4.5	black rust
ECR(primer/$Ca(NO_2)_2$)-4h-45-1	1.09	4	4	4	4	4.0	1.54	5	6	5	5	5.3	1.22	4	3	3	5	3.8	black rust
ECR(primer/$Ca(NO_2)_2$)-4h-45-2	0.000	0	0	0	0	0.00	0.252	1	2	2	1	1.5	0.123	1	0	1	2	1.0	small amount of black rust
ECR(primer/$Ca(NO_2)_2$)-4h-45-3	1.35	6	4	5	4	4.8	1.67	5	5	5	5	5.0	0.897	6	6	5	7	6.0	black rust
ECR(primer/$Ca(NO_2)_2$)-10h-45-1	0.897	4	3	4	2	3.3	1.03	5	4	4	4	4.3	1.48	6	4	5	6	5.3	black rust
ECR(primer/$Ca(NO_2)_2$)-10h-45-2	0.000	0	0	0	0	0.00	0.832	5	3	3	3	3.5	0.897	2	1	1	1	1.3	black rust
ECR(primer/$Ca(NO_2)_2$)-10h-45-3	0.510	3	2	2	1	2.0	0.832	5	3	4	2	3.5	2.25	7	8	5	6	6.5	black rust
ECR(primer/$Ca(NO_2)_2$)-10h-35-1	0.316	1	0	0	1	0.50	3.28	10	7	8	6	7.8	3.74	8	5	6	6	6.3	small amount of brown rust
ECR(primer/$Ca(NO_2)_2$)-10h-35-2	3.41	10	6	8	8	8.0	4.90	>12	8	12	9	>10	3.74	9	12	10	6	9.3	black rust
ECR(primer/$Ca(NO_2)_2$)-10h-35-3	0.510	0	3	1	4	2.0	1.86	0	3	10	6	4.8	1.28	4	3	4	4	3.8	black rust

TD = Total Disbondment

with all but one specimen, ECR(HY)-4h-45-1 exhibiting total disbondment in the top bars. None of the bottom bars exhibited total disbondment, with ECR(HY)-4h-45-3 exhibiting no disbondment at all.

As shown in Table 3.20, two out of six MC specimens with both layers penetrated exhibited total disbondment in the top bar while three out of six MC specimens with only the outer epoxy layer penetrated exhibited total disbondment in the top bar. None of the bottom MC bars exhibited total disbondment. In fact, only four out of twelve MC bottom bars exhibited any amount of disbondment at all. All four of these specimens had both epoxy and zinc layers penetrated.

Table 3.20a – Disbondment measurements on top bars of cracked beam specimens containing multiple-coated reinforcement

	Side 1-A						Side 1-B						Side 2-A						
	A_d	Disbondment Radius (mm)				Avg. r_d	A_d	Disbondment Radius (mm)				Avg. r_d	A_d	Disbondment Radius (mm)				Avg. r_d	
Specimen	(cm^2)	0°	90°	180°	270°	(mm)	(cm^2)	0°	90°	180°	270°	(mm)	(cm^2)	0°	90°	180°	270°	(mm)	Comments
MC(both layers penetrated)-4h-45-1	2.09	4	5	8	5	5.5	3.25	8	7	8	7	7.5	0.123	1	0	0	0	0.25	orange, dark brown and grey rust
MC(both layers penetrated)-4h-45-2	4.41	5	9	11	7	8.0	3.51	10	5	11	9	8.8	0.000	0	0	0	0	0.00	dark brown and grey rust
MC(both layers penetrated)-4h-45-3	2.35	5	7	6	7	6.3	3.77	10	9	8	9	9.0	0.000	0	0	0	0	0.00	orange, dark brown and grey rust
MC(both layers penetrated)-10h-45-1	1.74	4	6	9	6	6.3	TD	>12	12	>12	6	>11	0.000	0	0	0	0	0.00	orange, dark brown and grey rust
MC(both layers penetrated)-10h-45-2	1.41	5	5	5	5	5.0	1.74	8	5	7	7	6.8	0.000	0	0	0	0	0.00	brown and grey rust
MC(both layers penetrated)-10h-45-3	TD	9	6	>12	12	>9.8	TD	8	8	>12	9	>9.3	0.000	0	0	0	0	0.00	orange, dark brown and grey rust
MC(only epoxy penetrated)-4h-45-1	1.61	4	6	8	5	5.8	2.25	5	5	8	6	6.0	0.000	0	0	0	0	0.00	orange, dark brown and grey rust
MC(only epoxy penetrated)-4h-45-2	1.74	7	8	6	6	6.8	TD	>12	10	12	>12	>12	0.316	0	1	1	2	1.0	dark brown and grey rust
MC(only epoxy penetrated)-4h-45-3	TD	>12	12	>12	12	>12	TD	>12	12	>12	>12	>12	2.12	10	9	7	8	8.5	bright orange, dark brown and grey rust, light blistering
MC(only epoxy penetrated)-10h-45-1	2.80	7	7		5	4.8	2.64	9	5	12	7	8.3	0.413	1	2	1	2	1.5	orange, dark brown and grey rust
MC(only epoxy penetrated)-10h-45-2	0.735	3	4	4	4	3.8	TD	11	8	>12	6	>9.3	0.000	0	0	0	0	0.00	grey rust, light blistering
MC(only epoxy penetrated)-10h-45-3	1.28	5	5	4	4	4.5	1.28	4	5	4	4	4.3	0.000	0	0	0	0	0.00	dark brown and grey rust, light blistering

TD = Total Disbondment

Table 3.20b – Disbondment measurements on bottom bars of cracked beam specimens containing multiple-coated reinforcement

	Side 1-A						Side 1-B						Side 2-A						
	A_d	Disb. Radius (mm)				Avg. r_d	A_d	Disb. Radius (mm)				Avg. r_d	A_d	Disb. Radius (mm)				Avg. r_d	
Specimen	(cm^2)	0°	90°	180°	270°	(mm)	(cm^2)	0°	90°	180°	270°	(mm)	(cm^2)	0°	90°	180°	270°	(mm)	Comments
MC(both layers penetrated)-4h-45-1	0.000	0	0	0	0	0.00	0.574	3	2	3	3	2.8	0.000	0	0	0	0	0.00	dark brown and grey rust
MC(both layers penetrated)-4h-45-2	0.000	0	0	0	0	0.00	0.000	0	0	0	0	0.00	0.348	2	2	2	2	2.0	small amount of brown rust; grey rust
MC(both layers penetrated)-4h-45-3	0.000	0	0	0	0	0.00	0.000	0	0	0	0	0.00	0.000	0	0	0	0	0.00	no rust
MC(both layers penetrated)-10h-45-1	0.000	0	0	0	0	0.00	0.413	2	2	2	0.6	1.6	0.000	0	0	0	0	0.00	dark brown and grey rust
MC(both layers penetrated)-10h-45-2	0.000	0	0	0	0	0.00	0.000	0	0	0	0	0.00	0.284	1	2	0	1	1.0	small amount of orange rust with grey rust
MC(both layers penetrated)-10h-45-3	0.000	0	0	0	0	0.00	0.000	0	0	0	0	0.00	0.000	0	0	0	0	0.00	no rust
MC(only epoxy penetrated)-4h-45-1	0.000	0	0	0	0	0.00	0.000	0	0	0	0	0.00	0.000	0	0	0	0	0.00	no rust
MC(only epoxy penetrated)-4h-45-2	0.000	0	0	0	0	0.00	0.000	0	0	0	0	0.00	0.000	0	0	0	0	0.00	small amount of orange rust with grey rust
MC(only epoxy penetrated)-4h-45-3	0.000	0	0	0	0	0.00	0.000	0	0	0	0	0.00	0.000	0	0	0	0	0.00	no rust
MC(only epoxy penetrated)-10h-45-1	0.000	0	0	0	0	0.00	0.000	0	0	0	0	0.00	0.000	0	0	0	0	0.00	no rust
MC(only epoxy penetrated)-10h-45-2	0.000	0	0	0	0	0.00	0.000	0	0	0	0	0.00	0.000	0	0	0	0	0.00	no rust
MC(only epoxy penetrated)-10h-45-3	0.000	0	0	0	0	0.00	0.000	0	0	0	0	0.00	0.000	0	0	0	0	0.00	no rust

TD = Total Disbondment

Table 3.21 shows that all increased adhesion ECR specimens exhibited disbondment in the top bars. Three specimens, ECR(DuPont)-4h-45-2, ECR(DuPont)-4h-45-3, and ECR(Valspar)-4h-45-1 exhibited total disbondment on a bottom bar.

The results of the disbondment measurements show that for both Southern Exposure and cracked beam specimens, the severity of disbondment is generally greater in top bars than in bottom bars. Since corrosion products were found beneath the disbonded epoxy, it would appear that corrosion initiates at the exposed metal specimens versus Southern Exposure specimens. These observations suggest that the

Table 3.21a – Disbondment measurements on top bars of cracked beam specimens containing ECR with increased adhesion epoxy

	Side 1-A						Side 1-B						Side 2-A						
	A_d	Disbondment Radius (mm)				Avg. r_d	A_d	Disbondment Radius (mm)				Avg. r_d	A_d	Disbondment Radius (mm)				Avg. r_d	
Specimen	(cm^2)	0°	90°	180°	270°	(mm)	(cm^2)	0°	90°	180°	270°	(mm)	(cm^2)	0°	90°	180°	270°	(mm)	Comments
ECR(Chromate)-4h-45-1	TD	>12	>12	>12	>12	>12	TD	>12	>12	>12	>12	>12	TD	>12	>12	>12	>12	>12	orange, dark brown and black rust, light blistering
ECR(Chromate)-4h-45-2	TD	>12	12	>12	12	>12	TD	>12	12	>12	12	>12	2.51	5	5	5	12	6.8	dark brown and black rust, light blistering
ECR(Chromate)-4h-45-3	TD	6	>12	5	>12	>8.8	TD	>12	>12	>12	>12	>12	3.86	6	7	9	12	8.5	dark brown and black rust
ECR(Chromate)-4h-45-4	6.12	10	6	12	10	9.5	TD	>12	>12	>12	>12	>12	TD	>12	>12	>12	>12	>12	dark brown and black rust, light blistering
ECR(Chromate)-10h-45-1	TD	11	12	>12	12	>12	TD	>12	>12	>12	>12	>12	TD	>12	>12	10	>12	>12	dark brown and black rust, light blistering
ECR(Chromate)-10h-45-2	TD	5	>12	>12	>12	>10	TD	>12	>12	>12	>12	>12	TD	>12	>12	12	>12	>12	dark brown and black rust, light blistering
ECR(Chromate)-10h-45-3	TD	>12	>12	>12	>12	>12	TD	>12	>12	>12	>12	>12	TD	>12	>12	>12	>12	>12	dark brown and black rust, moderate blistering
ECR(DuPont)-4h-45-1	3.28	5	12	4	12	8.3	TD	>12	12	>12	12	>12	TD	>12	>12	11	>12	>12	gold and black rust
ECR(DuPont)-4h-45-2	TD	>12	>12	>12	>12	>12	TD	>12	>12	>12	>12	>12	TD	>12	>12	>12	>12	>12	orange, dark brown and black rust, light blistering
ECR(DuPont)-4h-45-3	3.54	7	10	8	9	8.5	TD	>12	>12	>12	>12	>12	TD	>12	>12	>12	>12	>12	gold and black rust
ECR(DuPont)-4h-45-4	3.93	7	12	7	11	9.3	TD	10	>12	8	>12	>11	TD	9	>12	11	>12	>11	gold and black rust
ECR(DuPont)-10h-45-1	TD	>12	>12	>12	>12	>12	TD	>12	>12	>12	>12	>12	TD	>12	>12	>12	>12	>12	gold, dark brown and black rust, heavy blistering
ECR(DuPont)-10h-45-2	TD	>12	>12	>12	>12	>12	TD	>12	>12	>12	>12	>12	TD	>12	>12	>12	>12	>12	gold, orange, brown and black rust, light blistering
ECR(DuPont)-10h-45-3	TD	>12	>12	>12	>12	>12	TD	>12	>12	>12	>12	>12	TD	>12	>12	>12	>12	>12	gold, dark brown and black rust, light blistering
ECR(Valspar)-4h-45-1	TD	>12	12	>12	12	>12	TD	>12	12	>12	12	>12	TD	>12	12	>12	12	>12	dark brown and black rust, light blistering
ECR(Valspar)-4h-45-2	TD	>12	>12	>12	>12	>12	TD	>12	>12	>12	>12	>12	TD	>12	>12	>12	>12	>12	dark brown and black rust
ECR(Valspar)-4h-45-3	TD	>12	>12	>12	>12	>12	TD	>12	>12	>12	>12	>12	TD	>12	>12	>12	>12	>12	dark brown and black rust
ECR(Valspar)-4h-45-4	4.83	12	12	8	12	11	TD	>12	>12	>12	>12	>12	TD	>12	>12	>12	>12	>12	dark brown and black rust
ECR(Valspar)-10h-45-1	TD	>12	>12	>12	>12	>12	TD	>12	>12	>12	>12	>12	TD	>12	>12	>12	>12	>12	dark brown and black rust, heavy blistering
ECR(Valspar)-10h-45-2	TD	>12	>12	>12	>12	>12	TD	>12	>12	>12	>12	>12	TD	>12	>12	>12	>12	>12	orange, dark brown and black rust, light blistering
ECR(Valspar)-10h-45-3	TD	>12	>12	>12	>12	>12	TD	>12	>12	>12	>12	>12	TD	>12	>12	>12	>12	>12	orange, dark brown and black rust, light blistering

TD = Total Disbondment

Table 3.21b – Disbondment measurements on bottom bars of cracked beam specimens containing ECR with increased adhesion epoxy

	Side 1-A						Side 1-B						Side 2-A						
	A_d	Disb. Radius (mm)				Avg. r_d	A_d	Disb. Radius (mm)				Avg. r_d	A_d	Disb. Radius (mm)				Avg. r_d	
Specimen	(cm^2)	0°	90°	180°	270°	(mm)	(cm^2)	0°	90°	180°	270°	(mm)	(cm^2)	0°	90°	180°	270°	(mm)	Comments
ECR(Chromate)-4h-45-1	1.61	5	9	4	3	5.3	1.61	4	5	5	4	4.5	0.961	3	4	4	4	3.8	orange and black rust
ECR(Chromate)-4h-45-2	0.187	1	1	1	1	1.0	1.41	5	4	4	5	4.5	0.252	1	1	1	1	1.0	black rust
ECR(Chromate)-4h-45-3	0.187	0	0	1	2	0.75	0.574	2	3	3	2	2.5	0.123	0	0	1	0	0.25	no rust
ECR(Chromate)-4h-45-4	0.510	2	2	2	1	1.8	0.639	4	3	2	3	3.0	0.381	1	2	2	2	1.8	black rust
ECR(Chromate)-10h-45-1	0.187	1	1	2	1	1.3	0.252	1	1	2	1	1.3	0.123	1	0	1	0	0.50	black rust
ECR(Chromate)-10h-45-2	0.316	1	1	0	1	0.75	0.832	3	1	3	3	2.5	0.510	2	2	2	1	1.8	black rust
ECR(Chromate)-10h-45-3	0.000	0	0	0	0	0.00	1.35	2	4	10	1	4.3	0.961	5	5	3	4	4.3	black rust
ECR(DuPont)-4h-45-1	0.897	2	3	4	4	3.3	1.22	4	4	4	5	4.3	3.09	7	9	8	8	8.0	orang and gold rust
ECR(DuPont)-4h-45-2	TD	>12	>12	>12	>12	>12	0.832	4	3	3	3	3.3	3.86	9	8	8	1	6.5	gold rust
ECR(DuPont)-4h-45-3	0.000	0	0	0	0	0.00	1.67	5	6	5	6	5.5	TD	>12	>12	>12	>12	>12	gold rust
ECR(DuPont)-4h-45-4	1.22	4	3	4	3	3.5	1.54	5	5	4	5	4.8	0.574	3	2	2	3	2.5	gold and black rust
ECR(DuPont)-10h-45-1	1.03	4	4	3	2	3.3	1.28	5	4	6	4	4.8	0.510	3	2	2	2	2.3	gold and black rust
ECR(DuPont)-10h-45-2	0.510	6	5	3	5	4.8	0.961	6	5	4	5	5.0	0.316	3	3	3	4	3.3	gold and black rust
ECR(DuPont)-10h-45-3	2.77	6	9	7	8	7.5	3.03	9	9	8	8	8.5	3.03	6	10	6	8	7.5	gold and black rust
ECR(Valspar)-4h-45-1	TD	11	>12	11	>12	>12	TD	11	>12	11	>12	>12	TD	11	>12	8	>12	>11	black rust
ECR(Valspar)-4h-45-2	0.000	0	0	0	0	0.00	2.48	7	6	8	6	6.8	1.93	6	6	5	5	5.5	black rust
ECR(Valspar)-4h-45-3	2.45	9	8	4	6	6.8	3.03	9	9	7	8	8.3	3.41	7	8	7	9	7.8	black rust
ECR(Valspar)-4h-45-4	1.15	4	4	4	4	4.0	1.45	4	7	5	2	4.5	0.542	2	2	2	2	2.0	black rust
ECR(Valspar)-10h-45-1	1.48	3	5	4	5	4.3	1.80	6	5	6	4	5.3	0.961	5	3	3	4	3.8	black rust
ECR(Valspar)-10h-45-2	2.12	7	5	4	5	5.3	2.45	6	6	7	5	6.0	2.45	5	6	5	5	5.3	black rust
ECR(Valspar)-10h-45-3	2.77	10	7	4	8	7.3	3.48	8	9	7	9	8.3	3.61	6	10	9	9	8.5	black rust

TD = Total Disbondment

disbondment is a result of the corrosion occurring in bars as a result of exposure to moisture or chlorides, or both.

For the purposes of evaluating the performance of each corrosion protection system, it is useful to compare systems based on the average radius and area of

disbondment. However, as previously mentioned, any disbondment radius that is measured to be greater than 12 mm (0.5 in.) is not explicitly measured; rather the radius is recorded as ">12mm" and the disbondment is recorded as "TD" (total disbondment). Consequently, the method for considering these values in the averaged results is not straightforward. For the average results reported in this report, all disbondment radii readings that are greater than 12 mm (0.5 in.) are treated as if they were equal to 12 mm (0.5 in.). All disbondment areas that are recorded as "TD" are treated as if they were equal to 4.52 cm^2 (0.701 in^2.), which corresponds to the area of a circle with a radius equal to 12 mm (0.5 in.).

The balance of this section will present the average disbonded areas and radii observed in the corrosion protection systems evaluated in this study. While both average disbondment radius and area are presented for each specimen, these two measurements are closely correlated. As a result, for the purposes of clarity, comparisons between systems will be discussed in terms of disbonded area only. Furthermore, since the magnitude of disbondment that is observed in the top bars is much greater than that observed in the bottom bars (with only one exception, which will be discussed subsequently), only the top bar disbondment results will be discussed.

The average disbonded areas and radii observed on the reinforcement in Southern Exposure specimens are summarized in Table 3.22. Among the specimens containing conventional epoxy-coated reinforcement, the ECR-10h-45 specimens exhibit the greatest amount of disbondment, with an average disbonded

Table 3.22 – Average disbondment measurements on top and bottom bars of Southern Exposure specimens.

Steel Designation[a]	Top Bar Averages		Bottom Bar Averages	
	A_d (cm^2)	r_d (mm)	A_d (cm^2)	r_d (mm)
ECR-4h-45	0.590	1.63	0.0100	0.0277
ECR-10h-45	3.83	10.0	1.16	4.10
ECR-10h-35	1.14	3.30	0.285	0.723
ECR(DCI)-4h-45	2.25	5.77	0.0208	0.0567
ECR(DCI)-10h-45	2.69	7.35	0.000	0.000
ECR(DCI)-10h-35	2.11	5.10	0.117	0.467
ECR(RH)-4h-45	1.41	3.99	0.274	1.13
ECR(RH)-10h-45	2.07	5.50	0.150	0.677
ECR(RH)-10h-35	0.254	0.713	0.276	0.877
ECR(HY)-4h-45	0.390	1.01	0.141	0.223
ECR(HY)-10h-45	1.20	2.28	0.000	0.000
ECR(HY)-10h-35	0.166	0.733	0.0280	0.110
ECR(primer/Ca(NO2)2)-4h-45	1.73	4.98	0.0523	0.173
ECR(primer/Ca(NO2)2)-10h-45	3.17	8.10	0.558	2.96
ECR(primer/Ca(NO2)2)-10h-35	0.926	3.10	0.531	1.66
MC(both layers penetrated)-4h-45	1.02	2.60	0.533	1.47
MC(both layers penetrated)-10h-45	1.81	5.60	0.0351	0.223
MC(only epoxy penetrated)-4h-45	2.74	6.97	0.0208	0.110
MC(only epoxy penetrated)-10h-45	2.71	6.83	0.0567	0.277
ECR(Chromate)-4h-45	3.90	9.60	0.432	1.32
ECR(Chromate)-10h-45	4.07	10.5	0.385	1.50
ECR(DuPont)-4h-45	4.54	11.8	1.17	3.20
ECR(DuPont)-10h-45	4.52	12.0	0.996	3.73
ECR(Valspar)-4h-45	3.69	9.73	1.04	2.84
ECR(Valspar)-10h-45	4.01	10.4	1.90	5.22
ECR(Chromate/DCI)-4h-45	0.895	2.47	0.113	0.367
ECR(DuPont/DCI)-4h-45	0.711	1.44	0.177	0.733
ECR(Valspar/DCI)-4h-45	1.49	3.47	0.105	0.400

[a] ECR(Chromate) = ECR with the chromate pretreatment.
ECR(DuPont) = ECR with high adhesion DuPont coating.
ECR(Valspar) = ECR with high adhesion Valspar coating.
ECR(DCI) = ECR in concrete with DCI inhibitor.
ECR(Rheocrete) = ECR in concrete with Rheocrete inhibitor.
ECR (Hycrete) = normal ECR with Hycrete inhibitor.
MC(both layers penetrated) = multiple coated bars with both zinc and epoxy layers penetrated.
MC(only epoxy penetrated) = mutiple coated bars with only epoxy layer penetrated.
4h = bar with four holes through epoxy, 10h = bar with 10 holes through epoxy.
45 = concrete with *w/c* =0.45; 35 = concrete with *w/c* =0.45.

area of 3.83 cm^2 (0.594 in^2.), followed by the ECR-10h-35 and ECR-4h-45 specimens, with average disbonded areas of 1.14 cm^2 (0.177 in^2) and 0.590 cm^2 (0.0915 in^2), respectively. The greater amount of disbondment observed in bars containing ten holes through the epoxy layer is expected, since the greater exposed area in ten-hole specimens provides less protection against corrosion.

Among Southern Exposure specimens containing ECR with four holes through the epoxy cast in the presence of corrosion inhibitors, the specimens containing Hycrete show an advantage over conventional ECR reinforcement cast in concrete without corrosion inhibitors, with an average disbonded area of disbondment of 0.390 cm^2 (0.0605 in^2.). All specimens containing ECR with ten holes through the epoxy cast in concrete containing corrosion inhibitors, regardless of *w/c* ratio, exhibit less disbondment than the conventional ECR control specimens, with the exception of the ECR(DCI)-10h-35 specimens, which exhibit an average disbonded area of 2.11 cm^2 (0.327 in.). Of the four systems that exhibit greater disbondment than the control specimens, three contain some form of calcium nitrite (the ECR(DCI)-4h-45, ECR(DCI)-10h-35 and ECR(primer/$Ca(NO_2)_2$)-4h-45 specimens).

Among the SE specimens containing ECR with improved adhesion epoxy, all specimens exhibit greater disbondment than the control specimens. Among the specimens with four holes through the epoxy, the ECR(DuPont)-4h-45 specimens exhibit the highest average disbonded area, 4.54 cm^2 (0.704 in^2.), followed by the ECR(Chromate)-4h-45 and ECR(Valspar)-4h-45 specimens, with average disbonded areas of 3.90 cm^2 (0.605 in^2.) and 3.69 cm^2 (0.572 in^2.), respectively. Among the 10-

hole specimens, the ECR(DuPont)-10h-45 specimens exhibit the greatest average disbonded area, 4.52 cm^2 (0.701 in^2.), followed by the ECR(Chromate)-10h-45 and ECR(Valspar)-10h-45 specimens, with disbonded areas of 4.07 cm^2 (0.631 in^2.) and 4.01 cm^2 (0.622 in^2.), respectively.

For SE specimens containing increased adhesion ECR cast in the presence of DCI corrosion inhibitor, all systems exhibit less disbondment than the control specimens. This behavior is unexpected, since specimens containing calcium nitrite and conventional ECR generally exhibited greater disbondment than the control specimens. Furthermore, all of the specimens containing increased adhesion ECR in concrete without corrosion inhibitors exhibited greater disbondment than control specimens.

For SE specimens containing multiple-coated reinforcement, both of the groups containing four holes through the epoxy exhibit greater disbondment than the control specimens, with average disbonded areas of 2.74 cm^2 (0.425 in^2.) and 1.02 cm^2 (0.158 in.) for the MC(only epoxy penetrated)-4h-45 and MC(both layers penetrated)-4h-45 specimens, respectively. For the 10-hole specimens, both the MC(only epoxy penetrated)-10h-45 and MC(both layers penetrated)-10h-45 specimens exhibited less disbondment than the control specimens, with average disbonded areas of 2.71 cm^2 (0.420 $in.^2$) and 1.81 cm^2 (0.281 $in.^2$), respectively. Specimens with only the epoxy layer penetrated exhibit greater disbondment than specimens with both the epoxy and zinc layers penetrated. One possible explanation for this behavior is that when the underlying steel is exposed, it forces the anodic

region of the zinc to be more concentrated within the immediate area surround the exposed steel, whereas in bars with no exposed steel, the anodic area of the zinc may be distributed over a greater area of the bar.

The average disbondment areas and radii observed on the reinforcement in cracked beam specimens are summarized in Table 3.23. All specimens containing corrosion inhibitors and containing four holes through the epoxy exhibit higher disbonded areas than the conventional ECR control specimens, with the exception of the ECR(primer/$Ca(NO_2)_2$) specimens, which exhibit an average disbonded area of 3.92 cm^2 (0.608 $in.^2$) Among specimens with ten holes through the epoxy and a *w/c* ratio of 0.45, only the ECR(HY) and ECR(primer/$Ca(NO_2)_2$) specimens exhibit smaller disbonded areas than control specimens, with respective areas of 4.13 cm^2 (0.640 $in.^2$) and 3.95 cm^2 (0.612 $in.^2$). Among specimens with ten holes through the epoxy and a *w/c* ratio of 0.35, only the ECR(RH) specimens exhibit a lower average disbonded area than control specimens, with an area of 4.37 cm^2 (0.678 $in.^2$).

All specimens containing improved adhesion ECR exhibit average disbonded areas that are greater than or equal to the average disbonded areas measured in control specimens. For specimens with four holes through the epoxy, average disbonded areas range from 4.29 cm^2 (0.665 $in.^2$) in the ECR(DuPont) specimens to 4.55 cm^2 (0.705 $in.^2$) in the ECR(Valspar) specimens. All ten-hole specimens exhibit average disbonded areas equal to 4.52 cm^2 (0.701 $in.^2$), which is characteristic of total disbondment, as defined previously.

Table 3.23 – Average disbondment measurements on top and bottom bars of cracked beam specimens.

Steel Designation[a]	Top Bar Averages		Bottom Bar Averages	
	A_d (cm^2)	r_d (mm)	A_d (cm^2)	r_d (mm)
ECR-4h-45	4.18	10.7	0.886	2.85
ECR-10h-45	4.52	12.0	0.498	1.90
ECR-10h-35	4.68	11.7	1.51	5.03
ECR(DCI)-4h-45	4.25	10.6	0.475	1.93
ECR(DCI)-10h-45	4.63	11.7	0.325	1.50
ECR(DCI)-10h-35	4.97	10.7	2.30	6.07
ECR(RH)-4h-45	4.63	11.7	2.48	6.03
ECR(RH)-10h-45	4.54	11.7	2.36	6.50
ECR(RH)-10h-35	4.37	10.9	1.38	4.17
ECR(HY)-4h-45	4.30	10.0	0.127	0.417
ECR(HY)-10h-45	4.13	10.6	0.176	0.800
ECR(HY)-10h-35	4.68	12.0	1.21	3.40
ECR(primer/Ca(NO2)2)-4h-45	3.92	10.4	0.905	3.51
ECR(primer/Ca(NO2)2)-10h-45	3.95	10.7	0.970	3.30
ECR(primer/Ca(NO2)2)-10h-35	3.82	9.20	2.56	5.83
MC(both layers penetrated)-4h-45	2.17	5.03	0.102	0.533
MC(both layers penetrated)-10h-45	2.05	5.37	0.0774	0.443
MC(only epoxy penetrated)-4h-45	2.40	7.17	0.000	0.000
MC(only epoxy penetrated)-10h-45	1.52	4.07	0.000	0.000
ECR(Chromate)-4h-45	4.43	10.7	0.704	2.53
ECR(Chromate)-10h-45	4.52	11.7	0.503	1.87
ECR(DuPont)-4h-45	4.29	11.0	2.00	5.48
ECR(DuPont)-10h-45	4.52	12.0	1.49	5.23
ECR(Valspar)-4h-45	4.55	12.0	2.50	6.80
ECR(Valspar)-10h-45	4.52	12.0	2.35	6.00

[a] ECR(Chromate) = ECR with the chromate pretreatment.
ECR(DuPont) = ECR with high adhesion DuPont coating.
ECR(Valspar) = ECR with high adhesion Valspar coating.
ECR(DCI) = ECR in concrete with DCI inhibitor.
ECR(Rheocrete) = ECR in concrete with Rheocrete inhibitor.
ECR (Hycrete) = normal ECR with Hycrete inhibitor.
MC(both layers penetrated) = multiple coated bars with both zinc and epoxy layers penetrated.
MC(only epoxy penetrated) = mutiple coated bars with only epoxy layer penetrated.
4h = bar with four holes through epoxy, 10h = bar with 10 holes through epoxy.
45 = concrete with *w/c* =0.45; 35 = concrete with *w/c* =0.45.

All specimens containing multiple-coated reinforcement exhibit less disbondment than the control specimens. Average disbonded areas range from 1.52

cm^2 (0.236 $in.^2$) for the MC(only epoxy penetrated)-10h-45 specimens to 2.40 cm^2 (0.372 $in.^2$) for the MC(only epoxy penetrated)-4h-45 specimens.

3.8 Critical Chloride Corrosion Threshold

As discussed previously in Chapter 2, samples were taken from SE specimens upon corrosion initiation, at 48 weeks, and at 96 weeks. Corrosion initiation is defined to have occurred when either a macrocell corrosion rate of 0.3 μm/yr or a top mat corrosion potential less than -0.350 V (vs. CSE) is observed. The chloride concentration required to initiate corrosion is called the critical chloride corrosion threshold. This section presents the critical chloride corrosion threshold data for the SE specimens evaluated in this study. Chloride concentrations for samples taken from SE specimens at 48 and 96 weeks are included in Appendix C.

Initially, two concrete powder samples were taken from each specimen for chloride analysis upon corrosion initiation. As the study progressed, it was decided to increase this number to six samples per specimen. Consequently, some specimens have only two chloride measurements while others have up to six. Additionally, the sampling procedure described in Chapter 2 at times did not produce the 3 grams of sample required to complete the chloride analysis. Consequently, throughout this section, a lack of data due to an inadequate sample is indicated in tables by the symbol (†).

When interpreting the chloride concentrations presented within this section, it is important to note that, due to the variable nature of chloride diffusion through

concrete, a the average chloride concentration of the sample group may or may not be representative of the true average chloride content within the specimen. Ji et al. (2005) studied the critical chloride threshold of conventional steel, duplex stainless steel, and MMFX microcomposite steel reinforcement in modified Southern Exposure (MSE) specimens. The MSE specimens were identical to the Southern Exposure specimens used in the current study, except that each top bar had a separate electrical connection to two bottom bars. Therefore, the top bars were not electrically connected and were individually monitored for corrosion initiation. A statistical analysis was performed to determine, for a level of confidence of 95%, the sample size required to estimate the true chloride content of the specimen within specific limits. The results showed that sample sizes of 8, 12, 19, 34, and 76 are required to estimate the true average chloride content of the specimen for specified errors of, respectively, 30, 25, 20, 15, and 10%.

As stated previously, a maximum of six samples is collected to determine the critical chloride threshold for each specimen, and in many instances, the limited quantity of sample produced by the sampling procedure resulted in less than six samples per specimen. As a result, the chloride thresholds reported within this study, while somewhat useful for comparisons between corrosion protection systems, may not be representative of the true chloride thresholds for each system.

Table 3.24 summarizes the critical chloride thresholds for SE specimens containing conventional steel and epoxy-coated reinforcement. Higher chloride threshold values represent corrosion protection systems that are more resilient against

Table 3.24 – Critical chloride thresholds for conventional steel and epoxy-coated reinforcement

Specimen	Age (weeks)	Rate (µm/yr)	Top Mat Potential (V)	Water Soluble Cl^- (kg/m^3) 1	2	3	4	5	6	Average (kg/m^3)	SD[a]	COV[b]
Conv.-45-1	84	0.107	-0.351	2.32	3.89	2.17	1.80	3.33	0.56	2.35	1.17	0.50
Conv.-45-2	15	0.480	-0.387	†	†	†	†	†	†	†	†	†
Conv.-45-3	43	0.335	-0.383	0.80	0.56	†	†	†	†	0.68	0.17	0.25
Conv.-45-4	25	0.499	-0.328	0.62	0.58	†	†	†	†	0.60	0.03	0.04
Conv.-45-5	50	0.358	-0.316	3.07	1.24	†	†	†	†	2.15	1.30	0.60
Conv.-45-6	35	0.351	-0.309	2.39	2.03	†	†	†	†	2.21	0.25	0.11
										1.81	1.12	0.62
Conv.-35-1	52	0.381	-0.292	1.46	0.86	3.03	2.73	1.95	1.50	1.92	0.83	0.43
Conv.-35-2	49	0.297	-0.262	0.86	0.63	†	†	†	†	0.75	0.16	0.21
Conv.-35-3	38	0.000	-0.388	1.80	1.98	†	†	†	†	1.89	0.13	0.07
										1.68	0.79	0.47
ECR-4h-45-1	70	0.000	-0.390	4.57	5.35	4.19	3.84	†	†	4.49	0.65	0.14
ECR-4h-45-2	70	0.000	-0.537	†	†	†	†	†	†	†	†	†
ECR-4h-45-3[c]	-	-	-	-	-	-	-	-	-	-	-	-
ECR-4h-45-4	84	0.000	-0.511	4.42	3.63	4.63	†	†	†	4.23	0.53	0.13
ECR-4h-45-5[c]	-	-	-	-	-	-	-	-	-	-	-	-
ECR-4h-45-6	92	0.000	-0.594	3.93	3.22	2.81	8.46	7.79	4.53	5.12	2.41	0.47
										4.72	1.65	0.35
ECR-10h-45-1	19	0.053	-0.530	2.65	4.18	†	†	†	†	3.42	1.08	0.32
ECR-10h-45-2	53	0.008	-0.560	10.26	7.75	9.06	9.84	†	†	9.23	1.10	0.12
ECR-10h-45-3	52	0.011	-0.486	7.86	8.80	†	†	†	†	8.33	0.66	0.08
										7.55	2.72	0.36
ECR-10h-35-1[c]	-	-	-	-	-	-	-	-	-	-	-	-
ECR-10h-35-2[c]	-	-	-	-	-	-	-	-	-	-	-	-
ECR-10h-35-3[c]	-	-	-	-	-	-	-	-	-	-	-	-
										-	-	-

[a]Standard Deviation

[b]Coefficient of Variation

[c]No corrosion initiation observed in specimen

† Sample quantity insufficent for testing

corrosion initiation. For each specimen, the chloride concentration of the individual samples is reported, along with the mean, standard deviation, and coefficient of variation for the specimen. Additionally, an overall mean, standard deviation, and coefficient of variation of all the samples for each corrosion protection system are reported. The conventional steel specimens cast in concrete with a *w/c* ratio of 0.45 exhibited an average chloride thresholds ranging from 0.60 to 2.35 kg/m^3 (1.01 to 3.96 lb/yd^3), with an average of 1.81 kg/m^3 (3.05 lb/yd^3) and a coefficient of variation of 0.62. Conventional steel in concrete with a *w/c* ratio of 0.35 exhibited corrosion

thresholds ranging from 0.75 to 1.92 kg/m^3 (1.26 to 3.24 lb/yd^3) with an average of 1.68 kg/m3 (2.83 lb/yd^3) and a coefficient of variation of 0.47. The lower chloride threshold observed in the specimens with a *w/c* ratio of 0.35 is not expected; however, as previously mentioned, the number of samples taken from each system (14 and 10 samples for specimens with a *w/c* ratio of 0.45 and 0.35, respectively) is not adequate to be able to accurately estimate the true chloride threshold in these specimens to better than about 25% accuracy.

The ECR-4h specimens exhibited an average chloride threshold of 4.72 kg/m^3 (7.96 lb/yd^3) and a coefficient of variation of 0.35, with values ranging from 4.23 to 5.12 kg/m^3 (7.13 to 8.63 lb/yd^3). Two of the six ECR-4h-45 specimens did not exhibit significant corrosion during the test and, therefore, provide no chloride threshold data. The ECR-10h-45 specimens exhibited an average threshold values of 7.55 kg/m^3 (12.7 lb/yd^3) and a coefficient of variation of 0.36, with values ranging from 3.42 to 9.23 kg/m^3 (5.77 to 15.6 lb/yd^3). The higher threshold value of epoxy-coated reinforcement compared with conventional steel reinforcement is due to the additional protection against moisture and chlorides afforded to the steel by the epoxy coating and the reduced probability of reaching the threshold chloride concentration at the exposed regions on the bars, as will be discussed later in this section. However, the higher average threshold value observed in the ECR-10h specimens, compared to the ECR-4h specimens, is unexpected, since the greater area of exposed steel in the ECR-10h specimens should theoretically cause these specimens to have a lower chloride threshold. This discrepancy is again, in all likelihood, attributable to the low

number of samples collected from each system. Corrosion initiation was not observed in the ECR-10h-35 specimens during the 96 week test.

Table 3.25 summarizes the critical chloride threshold values for SE specimens containing epoxy-coated reinforcement cast in concrete containing corrosion inhibitors. Among specimens with four holes through the epoxy, the ECR(HY) specimens exhibited the lowest average corrosion threshold, 1.19 kg/m^3 (2.01 lb/yd^3) and a coefficient of variation of 0.72; however, only six samples, all from one specimen, had sufficient quantities for chloride testing. Therefore, it is not clear if this low chloride threshold is representative of the true chloride threshold of epoxy-coated reinforcement in the presence of Hycrete. The ECR(DCI) specimens exhibited the highest chloride threshold, ranging from 4.51 to 5.72 kg/m^3 (7.60 to 9.64 lb/yd^3), with an average threshold of 5.42 kg/m^3 (9.14 lb/yd^3) and a coefficient of variation of 0.22.

For specimens with 10 holes through the epoxy and *w/c* = 0.45, the ECR(HY) specimens exhibited the lowest average corrosion threshold, 0.93 kg/m^3 (1.57 lb/yd^3), with values ranging from 0.79 to 1.02 kg/m^3 (1.33 to 1.72 lb/yd^3) and a coefficient of variation of 0.41. The ECR(primer/Ca$(NO_2)_2$) specimens exhibited the highest corrosion thresholds, with values ranging from 6.34 to 13.75 kg/m^3 (10.7 to 23.2 lb/yd^3), an average of 8.48 kg/m^3 (14.3 lb/yd^3), and a coefficient of variation of 0.38. This chloride threshold is uncharacteristically high, especially for specimen ECR(primer/Ca$(NO_2)_2$)10h-45-2 specimen, which was obtained by averaging only two samples. Based on the chloride threshold values reported for other specimens

Table 3.25 – Critical chloride thresholds for epoxy-coated reinforcement cast in concrete with corrosion inhibitors

Specimen	Age (weeks)	Rate (µm/yr)	Top Mat Potential (V)	Water Soluble Cl^- (kg/m^3) 1	2	3	4	5	6	Average (kg/m^3)	SD[a]	COV[b]
ECR(DCI)-4h-45-1	60	0.015	-0.520	5.97	3.04	†	†	†	†	4.51	2.07	0.46
ECR(DCI)-4h-45-2	60	0.011	-0.535	†	†	†	†	†	†	†	†	†
ECR(DCI)-4h-45-3	73	0.019	-0.582	4.57	5.35	6.92	5.35	5.95	6.18	5.72	0.81	0.14
										5.42	1.18	0.22
ECR(DCI)-10h-45-1	56	0.023	-0.526	†	†	†	†	†	†	†	†	†
ECR(DCI)-10h-45-2	69	0.000	-0.349	7.22	5.24	4.83	†	†	†	5.76	1.28	0.22
ECR(DCI)-10h-45-3	41	0.050	-0.598	7.34	7.45	7.00	†	†	†	7.26	0.23	0.03
										6.51	1.16	0.18
ECR(DCI)-10h-35-1	50	0.027	-0.509	†	†	†	†	†	†	†	†	†
ECR(DCI)-10h-35-2	87	0.000	-0.363	1.35	1.35	1.27	5.02	3.26	3.71	2.66	1.57	0.59
ECR(DCI)-10h-35-3	56	0.000	-0.387	1.05	1.66	1.50	†	†	†	1.40	0.32	0.23
										2.24	1.40	0.63
ECR(RH)-4h-45-1	84	0.000	-0.501	†	†	†	†	†	†	†	†	†
ECR(RH)-4h-45-2	57	0.133	-0.635	2.62	2.06	1.81	†	†	†	2.16	0.41	0.19
ECR(RH)-4h-45-3	62	0.000	-0.391	1.61	3.26	4.49	2.58	4.79	3.48	3.37	1.19	0.35
										2.97	1.13	0.38
ECR(RH)-10h-45-1	44	0.034	-0.488	†	†	†	†	†	†	†	†	†
ECR(RH)-10h-45-2[c]	-	-	-	-	-	-	-	-	-	-	-	-
ECR(RH)-10h-45-3	74	0.053	-0.563	5.13	3.74	3.12				4.00	1.03	0.26
										4.00	1.03	0.26
ECR(RH)-10h-35-1[c]	-	-	-	-	-	-	-	-	-	-	-	-
ECR(RH)-10h-35-2	30	0.027	-0.386	1.61	1.42	†	†	†	†	1.52	0.13	0.09
ECR(RH)-10h-35-3	21	0.000	-0.437	0.97	0.49	†	†	†	†	0.73	0.34	0.47
										1.12	0.50	0.45
ECR(HY)-4h-45-1	40	0.000	-0.395	†	†	†	†	†	†	†	†	†
ECR(HY)-4h-45-2	52	0.004	-0.370	0.10	0.67	0.56	1.57	2.06	2.17	1.19	0.86	0.72
ECR(HY)-4h-45-3	88	0.008	-0.490	†	†	†	†	†	†	†	†	†
										1.19	0.86	0.72
ECR(HY)-10h-45-1	29	0.000	-0.419	0.97	0.60	†	†	†	†	0.79	0.26	0.34
ECR(HY)-10h-45-2[c]	-	-	-	-	-	-	-	-	-	-	-	-
ECR(HY)-10h-45-3	46	0.030	-0.531	1.01	0.56	1.50	†	†	†	1.02	0.47	0.46
										0.93	0.38	0.41
ECR(HY)-10h-35-1	64	0.023	-0.557	0.90	0.30	†	†	†	†	0.60	0.42	0.71
ECR(HY)-10h-35-2	70	0.000	-0.401	0.65	0.19	0.46	†	†	†	0.43	0.23	0.54
ECR(HY)-10h-35-3	56	0.000	-0.393	0.34	0.34	0.37	†	†	†	0.35	0.02	0.05
										0.44	0.23	0.52
ECR(primer/$Ca(NO_2)_2$)-4h-45-1	51	0.008	-0.412	5.18	3.73	†	†	†	†	4.45	1.02	0.23
ECR(primer/$Ca(NO_2)_2$)-4h-45-2	45	0.027	-0.517	†	†	†	†	†	†	†	†	†
ECR(primer/$Ca(NO_2)_2$)-4h-45-3	38	0.000	-0.519	3.41	3.58	†	†	†	†	3.49	0.13	0.04
										3.97	0.81	0.20
ECR(primer/$Ca(NO_2)_2$)-10h-45-1	47	0.000	-0.540	5.17	6.82	7.04	†	†	†	6.34	1.02	0.16
ECR(primer/$Ca(NO_2)_2$)-10h-45-2	37	0.351	-0.438	14.82	12.69	†	†	†	†	13.75	1.51	0.11
ECR(primer/$Ca(NO_2)_2$)-10h-45-3	69	0.099	-0.605	8.72	6.92	6.29	7.86	†	†	7.45	1.07	0.14
										8.48	3.19	0.38
ECR(primer/$Ca(NO_2)_2$)-10h-35-1[c]	-	-	-	-	-	-	-	-	-	-	-	-
ECR(primer/$Ca(NO_2)_2$)-10h-35-2	57	0.008	-0.385	3.29	1.24	1.42	1.57	0.60	0.71	1.47	0.97	0.66
ECR(primer/$Ca(NO_2)_2$)-10h-35-3[c]	-	-	-	-	-	-	-	-	-	-	-	-
										1.47	0.97	0.66

[a]Standard Deviation

[b]Coefficient of Variation

[c]No corrosion initiation observed in specimen

† Sample quantity insufficent for testing

evaluated in this study that contain a calcium nitrite primer beneath the epoxy coating, it is expected that the true threshold for these specimens is lower.

For specimens with 10 holes through the epoxy and *w/c* = 0.35, the ECR(HY) specimens exhibited the lowest average corrosion threshold, 0.44 kg/m^3 (0.74 lb/yd^3), with values ranging from 0.35 to 0.6 kg/m^3 (0.59 to 1.01 lb/yd^3) and a coefficient of variation of 0.52. The ECR(DCI) specimens exhibited the highest average corrosion threshold, 2.24 kg/m^3 (3.78 lb/yd^3), with values ranging from 1.40 to 2.66 kg/m^3 (2.36 to 4.48 lb/yd^3) and a coefficient of variation of 0.63. Due to the limited quantity of material produced when sampling the specimens, chloride threshold data are not available for one of the three specimens.

The critical chloride corrosion thresholds for SE specimens containing epoxy-coated reinforcement with increased adhesion epoxy are presented in Table 3.26. For specimens with four holes through the epoxy, the ECR(DuPont) specimens exhibited the lowest average corrosion threshold, 6.89 kg/m^3 (11.6 lb/yd^3), with values ranging from 4.23 to 8.74 kg/m^3 (7.13 to 14.7 lb/yd^3) and a coefficient of variation of 0.36. The ECR(Chromate) specimens exhibited the highest corrosion threshold, with values ranging from 5.52 to 8.44 kg/m^3 (9.3 to 14.2 lb/yd^3), an average threshold of 7.53 kg/m^3 (12.7 lb/yd^3) and a coefficient of variation of 0.29.

For specimens with 10 holes through the epoxy, the ECR(DuPont) specimens exhibited the lowest average corrosion threshold, 3.37 kg/m^3 (5.68 lb/yd^3), with values ranging from 1.55 to 5.39 kg/m^3 (2.61 to 9.09 lb/yd^3) and a coefficient of variation of 0.67. The ECR(Valspar) specimens exhibited the highest average corrosion

Table 3.26 – Critical chloride thresholds for epoxy-coated reinforcement with increased adhesion epoxy

Specimen	Age (weeks)	Rate (µm/yr)	Top Mat Potential (V)	Water Soluble Cl^- (kg/m^3) 1	2	3	4	5	6	Average (kg/m^3)	SD[a]	COV[b]
ECR(Chromate)-4h-45-1	43	0.000	-0.466	7.67	3.37	†	†	†	†	5.52	3.04	0.55
ECR(Chromate)-4h-45-2	69	0.000	-0.55	8.76	8.41	7.65	†	†	†	8.27	0.57	0.07
ECR(Chromate)-4h-45-3	41	0.008	-0.543	10.37	6.51	†	†	†	†	8.44	2.73	0.32
										7.53	2.19	0.29
ECR(Chromate)-10h-45-1	25	0.000	-0.388	1.68	3.18	†	†	†	†	2.43	1.06	0.44
ECR(Chromate)-10h-45-2	20	0.000	-0.583	4.03	3.40	†	†	†	†	3.72	0.45	0.12
ECR(Chromate)-10h-45-3	39	0.160	-0.57	3.63	4.87	†	†	†	†	4.25	†	†
										3.47	1.06	0.30
ECR(DuPont)-4h-45-1	49	0.000	-0.401	9.58	7.90	†	†	†	†	8.74	1.19	0.14
ECR(DuPont)-4h-45-2	41	0.000	-0.521	7.99	7.41	†	†	†	†	7.70	0.41	0.05
ECR(DuPont)-4h-45-3	28	0.000	-0.462	6.03	2.43	†	†	†	†	4.23	2.54	0.60
										6.89	2.46	0.36
ECR(DuPont)-10h-45-1	21	0.008	-0.406	0.86	2.24	†	†	†	†	1.55	0.98	0.63
ECR(DuPont)-10h-45-2	14	0.076	-0.581	1.29	3.03	†	†	†	†	2.16	1.23	0.57
ECR(DuPont)-10h-45-3	39	0.01	-0.395	7.22	5.28	3.67	†	†	†	5.39	1.78	0.33
										3.37	2.26	0.67
ECR(Valspar)-4h-45-1	40	0.000	-0.492	8.20	8.08	†	†	†	†	8.14	0.08	0.01
ECR(Valspar)-4h-45-2	41	0.000	-0.465	7.26	7.30	7.05	7.28	†	†	7.22	0.12	0.02
ECR(Valspar)-4h-45-3	29	0.000	-0.502	8.87	5.39	†	†	†	†	7.13	2.46	0.35
										7.43	1.03	0.14
ECR(Valspar)-10h-45-1	26	0.008	-0.442	6.63	3.56	†	†	†	†	5.09	2.17	0.43
ECR(Valspar)-10h-45-2	18	0.011	-0.626	3.96	1.57	†	†	†	†	2.76	1.69	0.61
ECR(Valspar)-10h-45-3	40	0.015	-0.45	†	†	†	†	†	†	†	†	†
										3.93	2.08	0.53

[a]Standard Deviation

[b]Coefficient of Variation

† Sample quantity insufficent for testing

threshold, with values ranging from 2.76 to 5.09 kg/m^3 (4.65 to 8.58 lb/yd^3), an average of 3.93 kg/m^3 (6.62 lb/yd^3), and a coefficient of variation of 0.53. Due to the limited quantity of sample produced when sampling the specimens, chloride threshold data is not available for one of the three specimens.

Table 3.27 summarizes the critical chloride thresholds for SE specimens containing increased adhesion ECR with four holes through the epoxy, cast in concrete containing DCI corrosion inhibitor. The ECR(Chromate/DCI) specimens exhibited the lowest average corrosion threshold, 2.17 kg/m^3 (3.66 lb/yd^3), with

Table 3.27 – Critical chloride thresholds for epoxy-coated reinforcement with increased adhesion epoxy cast in concrete containing DCI

Specimen	Age (weeks)	Rate (µm/yr)	Top Mat Potential (V)	Water Soluble Cl^- (kg/m^3) 1	2	3	4	5	6	Average (kg/m^3)	SD[a]	COV[b]
ECR(Chromate/DCI)-4h-45-1	45	0.000	-0.352	2.78	2.66	1.32	†	†	†	2.25	0.81	0.36
ECR(Chromate/DCI)-4h-45-2	35	0.008	-0.368	0.77	1.12	1.71	†	†	†	1.20	0.48	0.40
ECR(Chromate/DCI)-4h-45-3	64	0.000	-0.365	4.84	†	†	†	†	†	4.84	-	-
										2.17	1.40	0.64
ECR(DuPont/DCI)-4h-45-1	56	0.004	-0.483	1.87	4.87	4.94	†	†	†	3.89	1.75	0.45
ECR(DuPont/DCI)-4h-45-2	69	0.000	-0.36	3.61	3.37	†	†	†	†	3.49	0.17	0.05
ECR(DuPont/DCI)-4h-45-3	63	0.019	-0.505	13.19	9.43	†	†	†	†	11.31	2.66	0.23
										5.90	3.99	0.68
ECR(Valspar/DCI)-4h-45-1[c]	-	-	-	-	-	-	-	-	-	-	-	-
ECR(Valspar/DCI)-4h-45-2	14	0.000	-0.426	1.72	1.38	†	†	†	†	1.55	0.24	0.15
ECR(Valspar/DCI)-4h-45-3	51	0.038	-0.418	8.18	9.81	9.32	†	†	†	9.10	0.83	0.09
										6.08	4.18	0.69

[a]Standard Deviation

[b]Coefficient of Variation

[c]No corrosion initiation observed in specimen

† Sample quantity insufficent for testing

values ranging from 1.2 to 4.84 kg/m^3 (2.02 to 8.16 lb/yd^3) and a coefficient of variation of 0.64. The ECR(Valspar/DCI) specimens exhibited the highest average corrosion threshold, with values ranging from 1.55 to 9.10 kg/m^3 (2.61 to 15.3 lb/yd^3), an average of 6.08 kg/m^3 (10.2 lb/yd^3), and a coefficient of variation of 0.69. One of the three specimens did not exhibit corrosion initiation during the test, and consequently, no corrosion threshold data is available for this specimen.

Table 3.28 presents the critical chloride corrosion thresholds for the multiple-coated reinforcement with both the epoxy and zinc layers penetrated. Chloride analyses were also performed on samples taken from SE specimens containing multiple-coated reinforcement with only the epoxy layer penetrated. As previously discussed, due to the small number of available samples, these data are of limited value in determining the chloride threshold of the zinc. Additionally, these data may not be representative of the chloride threshold of zinc because the concrete is sampled from various locations along the length of the bar, and most of the bar is protected by

Table 3.28 – Critical chloride thresholds for multiple-coated reinforcement with both layers penetrated

Specimen	Age (weeks)	Rate (µm/yr)	Top Mat Potential (V)	Water Soluble Cl^- (kg/m^3) 1	2	3	4	5	6	Average (kg/m^3)	SD[a]	COV[b]
MC(both layers penetrated)-4h-45-1[c]	-	-	-	-	-	-	-	-	-	-	-	-
MC(both layers penetrated)-4h-45-2[c]	-	-	-	-	-	-	-	-	-	-	-	-
MC(both layers penetrated)-4h-45-3	11	0.167	-0.406	0.82	0.60	†	†	†	†	0.71	0.16	0.22
										0.71	0.16	0.22
MC(both layers penetrated)-10h-45-1[c]	-	-	-	-	-	-	-	-	-	-	-	-
MC(both layers penetrated)-10h-45-2	14	0.280	-0.575	1.87	1.09	†	†	†	†	1.48	0.56	0.38
MC(both layers penetrated)-10h-45-3	12	0.039	-0.392	1.01	0.90	†	†	†	†	0.95	0.08	0.08
										1.22	0.44	0.36

[a]Standard Deviation

[b]Coefficient of Variation

[c]Top mat potential always < -0.350 V

† Sample quantity insufficent for testing

the epoxy coating. However, similar data was collected by Darwin et al. (2007) for galvanized reinforcement using a testing procedure similar to that implemented in the current study. Data from that study provides a more representative chloride threshold for zinc, since the reinforcement in that study was not epoxy-coated and a larger number of samples were collected. A total of twelve beam specimens (identical to a cracked beam specimen but fabricated without the crack) containing galvanized reinforcement were evaluated, and the results of that study are presented in Table 3.29. The galvanized reinforcement is similar to the exposed regions of the multiple-coated reinforcement with only the epoxy penetrated in that both consist of conventional steel coated with a layer of zinc that is exposed to the concrete pore solution.

As shown in Table 3.28, three of the six MC specimens with both layers penetrated consistently exhibited top mat corrosion potentials more negative than – 0.350 V (vs. CSE) from the beginning of the study. Consequently, corrosion initiation in these specimens was never clearly identifiable and no samples were taken from them. Of the specimens with four holes, only specimen MC(both layers

Table 3.29 – Critical chloride thresholds for galvanized reinforcement from Darwin et al. (2007). Chloride concentrations have been converted to kg/m^3.

Specimens[a]	Side[b]	Age (weeks)	Rate (μm/yr)	Top Potential (V)	Water soluble Cl$^-$ (kg/m^3)				
					1	2	3	4	5
B-Zn-45N-1	1	12	1.77	-0.805	1.72	3.37	1.78	4.21	3.08
	2				3.03	4.56	2.54	5.76*	2.77
B-Zn-45N-2	1	24	2.30	-0.566	2.84	1.91	1.31	1.46	2.51
	2				2.92	2.66	3.48	2.58	2.88
B-Zn-45N-3	1	18	1.12	-0.664	4.38	5.13*	3.89	1.38	1.35
	2				0.60	4.08	3.65	4.42	3.18
B-Zn-45N-4	1	6	3.04	-0.642	0.19	0.56	0.22	0.62	0.52
	2				0.34	0.51	0.90	0.27	1.38
B-Zn-45N-5	1	7	3.69	-0.718	1.50	2.43	0.34	1.35	1.46
	2				4.27	2.90	0.75	0.67	1.12
B-Zn-45N-6	1	6	0.00	-0.624	0.64	0.71	0.82	0.37	0.60
	2				0.82	0.26	0.15	0.30	0.34
B-Zn-45N-7	1	21	0.44	-0.524	1.87	4.64	0.86	1.50	1.76
	2				0.64	0.86	1.61	2.28	1.83
B-Zn-45N-8	1	16	0.65	-0.613	0.64	2.28	0.49	0.60	0.71
	2				2.66	2.88	2.96	4.30	3.11
B-Zn-45N-9	1	36	0.37	-0.541	3.29	1.05	1.61	2.10	1.20
	2				4.04	4.42	6.44*	4.71*	4.98*
B-Zn-45N-10	1	9	1.02	-0.592	0.75	0.30	0.32	0.19	0.21
	2				0.30	0.15	0.30	0.52	1.42
B-Zn-45N-11	1	9	0.98	-0.563	0.90	0.94	0.22	0.30	0.30
	2				0.67	1.27	1.27	0.82	1.23
B-Zn-45N-12	1	16	1.06	-0.580	0.52	1.16	1.98	0.64	0.62
	2				3.27	0.28	1.01	0.22	2.66

Specimens[a]	Side[b]	Water soluble Cl- (kg/m^3)					Average (kg/m^3)	SD[c]	COV[c]
		6	7	8	9	10			
B-Zn-45N-1	1	2.32	3.07	3.55	1.80	1.50	2.79	0.96	0.35
	2	3.03	4.49	3.22	2.51	2.96			
B-Zn-45N-2	1	2.28	1.87	0.90	2.54	1.91	1.99	0.78	0.39
	2	0.75	2.21	1.05	1.95	0.86			
B-Zn-45N-3	1	1.01	1.09	1.38	1.60	0.85	2.28	1.31	0.58
	2	2.73	1.12	2.58	4.86*	3.26			
B-Zn-45N-4	1	0.82	1.05	1.01	0.41	0.82	0.71	0.44	0.61
	2	0.34	0.64	0.41	1.20	0.49			
B-Zn-45N-5	1	0.75	1.01	0.39	1.61	1.24	1.35	0.94	0.69
	2	0.82	1.46	0.22	1.83	0.60			
B-Zn-45N-6	1	0.22	0.13	0.24	1.38	0.22	0.69	0.54	0.78
	2	0.88	0.49	0.64	2.06	0.94			
B-Zn-45N-7	1	5.20*	2.81	1.65	1.05	1.01	1.87	1.12	0.60
	2	1.65	3.89	1.05	1.12	4.12			
B-Zn-45N-8	1	0.52	1.78	2.77	1.23	1.31	2.23	1.30	0.59
	2	4.45	2.96	4.38	3.67	2.32			
B-Zn-45N-9	1	0.94	1.42	1.68	0.94	0.97	2.06	1.28	0.62
	2	5.65*	5.76*	5.58*	6.70*	4.23			
B-Zn-45N-10	1	1.98	1.09	0.64	0.37	0.26	0.68	0.54	0.80
	2	0.82	0.71	0.45	0.22	0.86			
B-Zn-45N-11	1	0.26	1.20	0.52	0.30	0.49	0.77	0.45	0.58
	2	0.56	1.05	0.71	0.45	0.45			
B-Zn-45N-12	1	0.75	0.64	0.71	1.16	0.52	1.13	1.02	0.90
	2	0.26	3.74	5.16*	0.22	0.34			
					Average		1.52		

[a]Beam Specimens
[b]10 chloride samples taken from each side of the bar per specimen
[c]SD = Standard Deviation, COV = Coefficient of Variation
*Outlier sample

penetrated)-4h-45-3 exhibited corrosion initiation, with a critical chloride threshold of 0.71 kg/m^3 (1.20 lb/yd^3) and a coefficient of variation of 0.22. For MC bars with 10 holes penetrating both layers, two out of three specimens exhibited corrosion initiation, with chloride threshold values of 0.95 and 1.48 kg/m^3 (1.6 and 2.5 lb/yd^3), giving an average of 1.22 kg/m^3 (2.06 lb/yd^3) and a coefficient of variation of 0.36. As shown in Table 3.29, galvanized reinforcement exhibited an average corrosion threshold of 1.52 kg/m^3 (2.57 lb/yd^3).

Several important observations can be made based on the results of the critical chloride corrosion threshold analysis. The chloride threshold observed for the conventional steel reinforcement in this study [1.68 to 1.81 kg/m^3 (2.83 to 3.05 lb/yd^3)] is higher than that reported in the literature reviewed in Chapter 1 [0.59 to 0.89 kg/m^3 (1.0 to 1.5 lb/yd^3)]. When evaluating conventional steel using modified Southern Exposure and beam specimens, Darwin et al. (2007) reported a critical chloride threshold of 0.967 kg/m^3 (1.63 lb/yd^3). The discrepancy between the chloride threshold observed for the conventional steel specimens in this study and the lower corrosion thresholds reported in literature is, in all likelihood, attributable to the limited number of samples evaluated in this study, combined with the variable nature of concrete.

The critical chloride threshold for epoxy-coated reinforcement is several times higher than that of conventional reinforcement. This is a result of the protection that the epoxy coating provides for the steel against chlorides, moisture, and oxygen. The transport of chloride ions through uncracked concrete is primarily governed by

diffusion, which follows Fick's second law. The major variables affecting chloride diffusion through a reinforced concrete are the concentration of chloride ions at the surface of the concrete and the diffusion coefficient, which depends on the material properties of the concrete. Since concrete is a heterogeneous material, the diffusion of chlorides through concrete is not entirely uniform. Therefore, a reinforcing bar at a given depth of concrete will not likely experience uniform chloride concentrations along its length. Consequently, corrosion initiation may occur when only a portion of the rebar is exposed to chloride concentrations that reach the critical chloride threshold concentration. For concrete containing damaged epoxy-coated reinforcement, corrosion initiation will not occur until the chloride concentration at the site of the damage reaches the critical chloride threshold. Chloride concentrations at other locations on the surface of the bar, where the epoxy is intact, may be higher or lower than the critical chloride threshold. This results in raising the effective critical chloride threshold of the reinforcement.

Among the corrosion inhibitors evaluated, specimens with Hycrete consistently exhibited the lowest chloride thresholds followed by specimens containing Rheocrete. In fact, specimens with corrosion inhibitors held no advantage over control specimens with the exception of ECR(DCI)-4h-45 and ECR(primer/$Ca(NO_2)_2$)-10h-45, both of which exhibited higher average corrosion thresholds than corresponding control specimens. However, it is bears reiterating that these results are based on a statistically small number of samples, and therefore, these results are subject to a large range of error.

ECR with increased adhesion exhibited threshold values that were higher than conventional ECR for bars containing four holes through the epoxy, but exhibited thresholds that were smaller than conventional ECR for bars containing ten holes through the epoxy. However, the small number of samples tested, from which the average threshold values are calculated, makes it difficult to establish whether the increased adhesion epoxy affects the chloride threshold of the reinforcement. Since, for epoxy-coated reinforcement, corrosion initiates at a damage site in the epoxy where the underlying steel is exposed, the increased adhesion epoxy would not be expected to affect the chloride threshold of the reinforcement. The use of DCI corrosion inhibitor in combination with increased adhesion ECR exhibited no beneficial effect on the critical chloride thresholds of the increased adhesion ECR.

Although the multiple-coated reinforcement exhibited corrosion thresholds that were lower than the corrosion threshold for conventional steel, the small quantity of data available for these specimens again makes it impossible to draw definitive conclusions. The critical chloride threshold for galvanized reinforcement reported by Darwin et al. (2007) is similar to the uncharacteristically high critical chloride threshold measured for the conventional steel reinforcement in this study, but is higher than the chloride threshold reported for conventional steel in the literature. This suggests that the zinc coating will provide additional protection against corrosion of the steel, and may extend the time to corrosion initiation of the reinforcement, although the effects of the zinc corrosion products on the serviceability of the concrete should be investigated.

CHAPTER 4

EVALUATION

This chapter presents an evaluation of the results reported in Chapter 3. Microcell and macrocell corrosion losses of each system are compared for the Southern Exposure and cracked beam specimens. Comparisons are also made between corrosion loss (both microcell and macrocell) and the disbonded area for specimens containing epoxy-coated reinforcement. A Student's t-test analysis is performed to identify statistically significant differences between corrosion protection systems. Finally, the performance of each corrosion protection system considered in this study is compared with the performance of conventional epoxy-coated reinforcement.

4.1 Microcell Versus Macrocell Corrosion

This section compares the microcell and macrocell corrosion losses observed in Southern Exposure and cracked beam specimens at week 96. For all specimens reported in this section, corrosion losses are calculated based on the total area of the bar. This is primarily done because the autopsies (Section 3.7) clearly show that the actual area of corrosion is not confined to the immediate region of the holes through the epoxy, but extends various distances away from the hole under the epoxy. The actual area of corrosion can vary substantially from one specimen to the other.

Therefore, corrosion losses reported in terms of the total area of the bar provide more unbiased values for comparison between systems than losses reported in terms of exposed area. Microcell corrosion losses measured for the top bars in the specimens are used for the comparison with the macrocell corrosion losses because they are representative of the corrosion that occurs within a bridge deck and are an order of magnitude higher than microcell corrosion losses observed in the bottom bars. Table 4.1 summarizes the 96-week macrocell and microcell corrosion losses for the specimens evaluated in this study. Corrosion losses reported for specimens with a *w/c* ratio of 0.45 are averaged for specimens containing four and ten holes through the epoxy layer. It is worth repeating that the microcell results represent a single specimen of each type for each corrosion protection system, while the macrocell results represent the average of three or six specimens. The microcell losses exceed the macrocell losses in all cases except for the ECR(primer/$Ca(NO_2)_2$) and ECR(Valspar)-DCI Southern Exposure specimens.

4.1.1 Southern Exposure Tests

The comparison between macrocell and microcell corrosion losses for the Southern Exposure specimens is shown in Figures 4.1 and 4.2. Results for specimens containing conventional steel reinforcement have not been included in these figures because the corrosion losses observed in these specimens are several orders of magnitude higher than those for any other specimen and thus skew the linear relationship between the specimens containing epoxy-coated reinforcement. As shown in Figure 4.1, macrocell corrosion loss generally increases with microcell

Table 4.1 – Total microcell and macrocell corrosion losses (μm) at week 96 for Southern Exposure and cracked beam specimens. Corrosion losses are expressed in terms of total area.

Steel Designation[a]	Southern Exposure		Cracked Beam	
	Microcell	Macrocell	Microcell	Macrocell
***w/c* ratio = 0.45[b]**				
Conv.	17.7	2.10	167	13.1
ECR	0.073	0.010	0.468	0.044
ECR(DCI)	0.108	0.008	1.03	0.053
ECR(RH)	0.013	0.004	1.69	0.156
ECR(HY)	0.009	0.000	0.619	0.048
ECR(primer/$Ca(NO_2)_2$)	0.031	0.039	0.966	0.058
MC(both layers penetrated)	1.39	0.343	2.54	0.524
MC(only epoxy penetrated)	0.742	0.062	2.71	0.256
ECR(Chromate)	0.060	0.043	1.14	0.145
ECR(DuPont)	0.197	0.036	1.20	0.144
ECR(Valspar)	0.167	0.048	1.81	0.104
ECR(Chromate)-DCI	0.080	0.007	-	-
ECR(DuPont)-DCI	0.010	0.000	-	-
ECR(Valspar)-DCI	0.004	0.012	-	-
***w/c* ratio = 0.35**				
Conv.	2.50	2.12	131	8.34
ECR	0.020	0.008	0.826	0.139
ECR(DCI)	0.020	0.007	2.58	0.223
ECR(RH)	0.018	0.003	0.854	0.178
ECR(HY)	0.008	0.001	0.811	0.194
ECR(primer/$Ca(NO_2)_2$)	0.008	0.002	2.33	0.470

[a] Conv. = conventional steel. ECR = conventional epoxy-coated reinforcement.
ECR(Chromate) = ECR with the chromate pretreatment.
ECR(DuPont) = ECR with high adhesion DuPont coating.
ECR(Valspar) = ECR with high adhesion Valspar coating.
ECR(DCI) = ECR in concrete with DCI inhibitor.
ECR(Rheocrete) = ECR in concrete with Rheocrete inhibitor.
ECR (Hycrete) = normal ECR with Hycrete inhibitor.
MC(both layers penetrated) = multiple coated bars with both zinc and epoxy layers penetrated.
MC(only epoxy penetrated) = mutiple coated bars with only epoxy layer penetrated.

[b] Corrosion losses reported for specimens with a *w/c* ratio of 0.45 area averaged value of corrosion losses in four and ten-hole specimens.

corrosion loss. The multiple-coated specimens with both layers penetrated exhibit the highest macrocell and microcell corrosion losses among the epoxy-coated specimens with a *w/c* ratio of 0.45, followed by the MC(only epoxy penetrated) specimens. The ECR(DuPont) and ECR(Valspar) specimens exhibit higher macrocell and microcell

corrosion losses than the control ECR specimens. Among the remaining corrosion protection systems, the ECR(primer/$Ca(NO_2)_2$), ECR(Chromate), and ECR(Valspar)-DCI specimens exhibit higher macrocell corrosion losses than the ECR specimens while the ECR(DCI) and ECR(Chromate)-DCI specimens exhibit higher microcell corrosion losses than the ECR control specimens. The remaining specimens, ECR(RH), ECR(HY) and ECR(DuPont)-DCI, exhibit both microcell and macrocell corrosion losses that are less than those exhibited by the ECR control specimens.

Guo et al. (2005) presented guidelines, originally presented by Kirkup (2002), for evaluating the strength of a linear relationship between a set of data based on the coefficient of determination R^2 and the correlation coefficient R. A value of R near to zero indicates that no linear relationship exists between the two variables. A coefficient R greater than or equal to 0.8 indicates a strong linear relationship between the two variables. For small sample sizes, it is possible to obtain a correlation coefficient R that is greater than 0.8 when there is no significant linear correlation between the two variables. The coefficient of determination R^2 is a measure of the percent of data that is closest to the line of best fit. For example, if $R^2 = 0.81$, then 81% of the variation between the x and y variables can be explained by the linear relationship between x and y.

The correlation coefficient for the data shown in Figure 4.1 is 0.93, with a coefficient of determination equal to 0.86, indicating a strong linear correlation between the macrocell and microcell corrosion losses. This means that 86% of the variation between the macrocell and microcell corrosion losses is linear. Therefore,

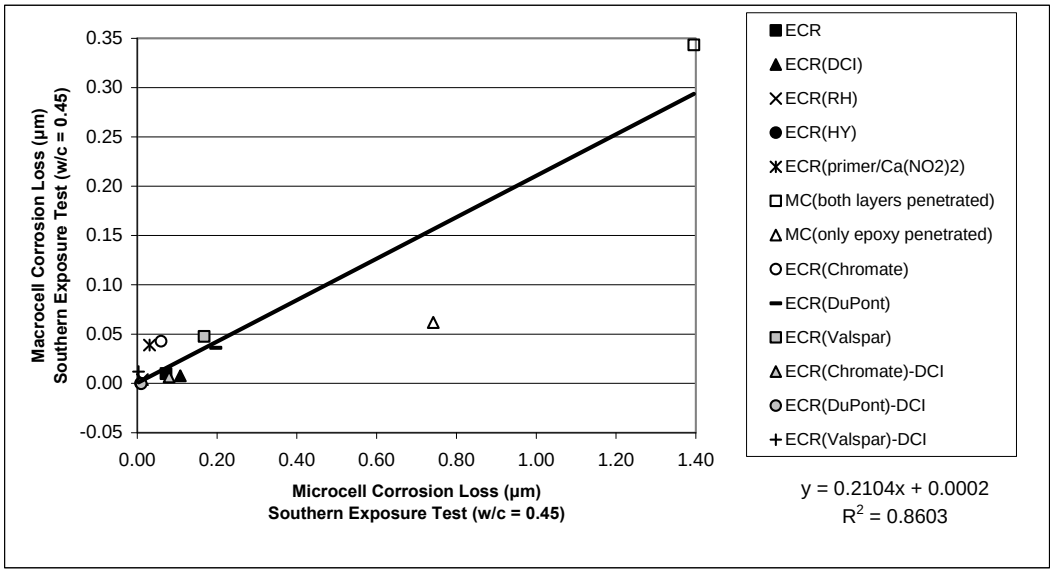

Figure 4.1 – Microcell versus macrocell total corrosion losses at week 96 for Southern Exposure test specimens containing ECR, w/c = 0.45. Total corrosion losses for ECR specimens are average values of specimens with four and 10 holes through the epoxy. Corrosion losses based on total area.

macrocell corrosion loss tends to increase with microcell corrosion loss, as initially observed. The best fit line through the data (Figure 4.1) indicates that the macrocell losses equal about one-fifth the microcell losses in these tests.

As shown in Figure 4.2 for specimens with a *w/c* ratio of 0.35, those with a corrosion inhibitor exhibit macrocell corrosion losses that are lower than the control ECR specimens. The figure also shows that the microcell corrosion losses are about an order of magnitude higher than the macrocell corrosion loss, and that with one exception the macrocell corrosion losses tend to increase as microcell corrosion losses increase. The one exception, ECR(HY), is enough to indicate an opposite trend, and only that specimen exhibits higher microcell corrosion loss than the ECR control specimen. Because of the scatter, the correlation coefficient is equal to only

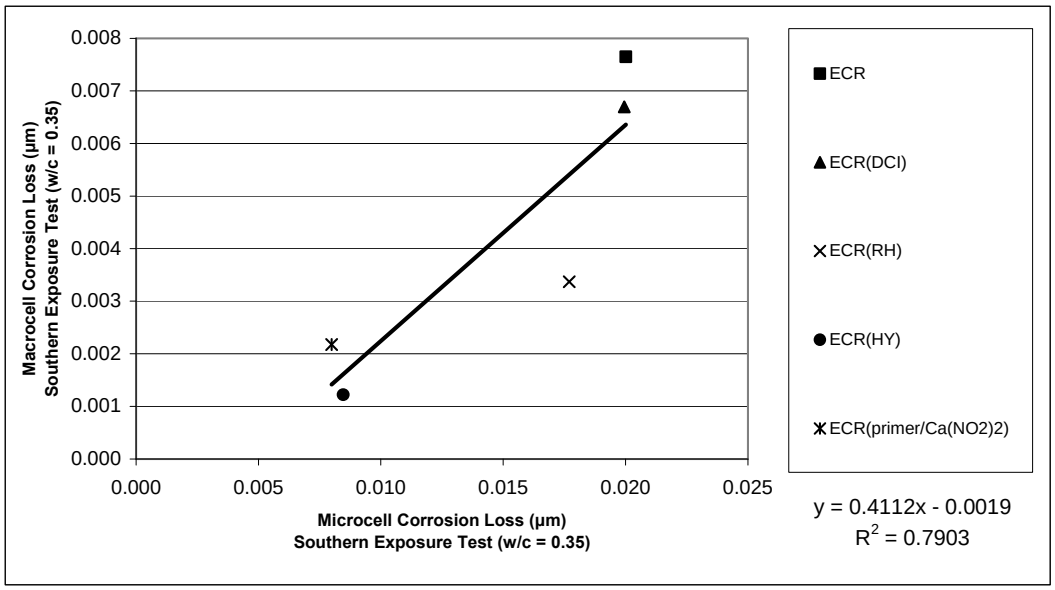

Figure 4.2 – Microcell versus macrocell total corrosion losses at week 96 for Southern Exposure test specimens containing ECR, *w/c* = 0.35. Corrosion losses based on total area.

0.219, and there appears to be no significant linear correlation between the macrocell and microcell corrosion rates in the specimens with a *w/c* ratio of 0.35. Without the ECR(HY) specimens, the correlation coefficient *R* is 0.87, indicating a strong linear trend.

4.1.2 Cracked Beam Tests

The comparisons between macrocell and microcell corrosion losses in the cracked beam specimens are shown in Figures 4.3 and 4.4. Figure 4.3 shows that for specimens with a *w/c* of 0.45, the microcell corrosion loss is about eight times larger than the macrocell corrosion loss and that the macrocell corrosion loss tends to increase with microcell corrosion loss. Specimens containing multiple-coated reinforcement exhibit the highest microcell and macrocell corrosion rates. Among the remainder of the specimens, the ECR(RH) specimens exhibit the highest macrocell

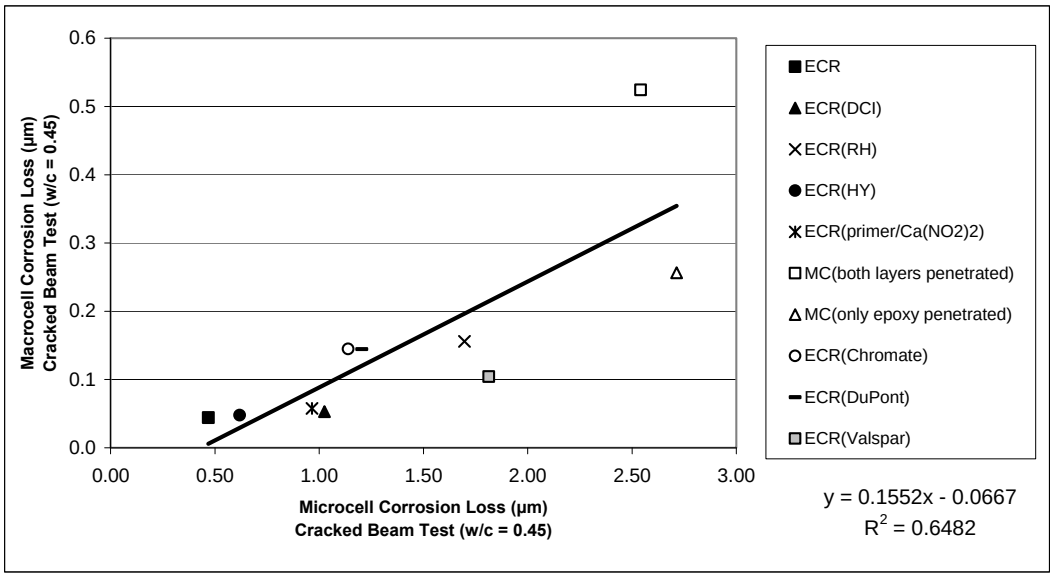

Figure 4.3 – Microcell versus macrocell total corrosion losses at week 96 for cracked beam test specimens containing ECR, *w/c* = 0.45. Total corrosion losses for ECR specimens are average values of specimens with four and 10 holes through the epoxy. Corrosion losses based on total area.

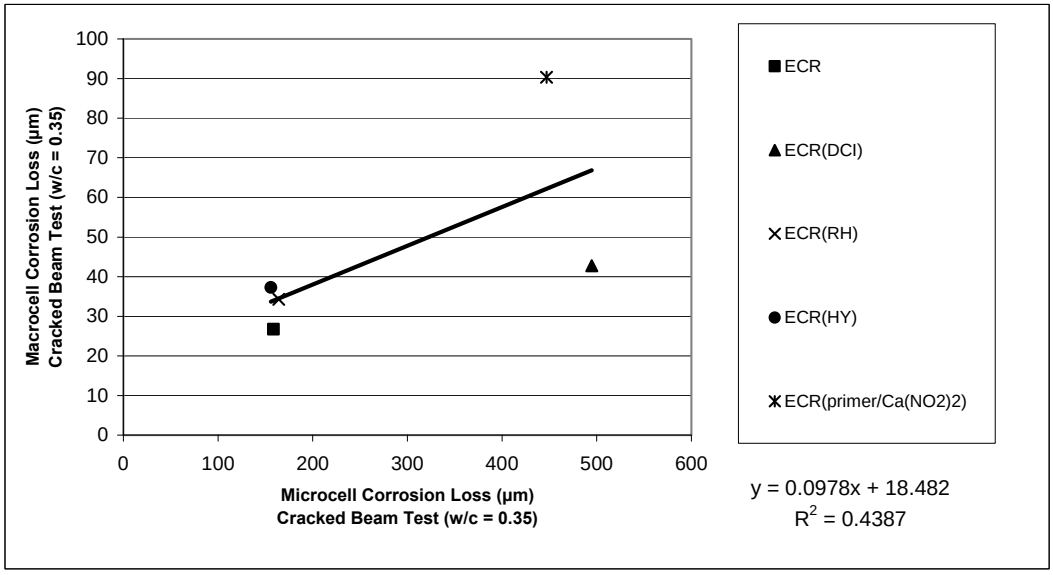

Figure 4.4 – Microcell versus macrocell total corrosion losses at week 96 for cracked beam test specimens containing ECR, *w/c* = 0.35. Corrosion losses based on total area.

corrosion loss, while the ECR(Valspar) specimens exhibit the highest microcell corrosion loss. All specimens exhibit both higher macrocell and microcell corrosion losses than the ECR control specimens. The correlation coefficient *R* is equal to 0.81, which suggests a moderately significant linear relationship between macrocell and microcell corrosion loss, albeit not as strong as the linear relationship observed among the Southern Exposure specimens.

Figure 4.4 shows that all cracked beam specimens with a *w/c* ratio of 0.35 exhibit a higher macrocell corrosion loss than the control ECR specimens. In this case, the microcell corrosion losses are an order of magnitude larger than macrocell corrosion losses, and the macrocell corrosion losses tend to increase with microcell corrosion loss, although there is a moderate amount of scatter in the data. In terms of microcell corrosion, the ECR(DCI) specimens exhibit the highest corrosion loss, followed by the ECR(primer/$Ca(NO_2)_2$) and ECR(RH) specimens. Only the ECR(HY) specimens exhibit a microcell corrosion loss lower than that of the ECR control specimens. The correlation coefficient *R* of 0.66 indicates that a significant linear relationship does not exist between the macrocell and microcell corrosion losses observed in the cracked beam specimens with a *w/c* ratio of 0.35.

4.2 Corrosion Loss Versus Disbonded Area

This section presents the comparison between the corrosion loss (both macrocell and microcell) and the average top bar disbonded area in the Southern

Table 4.2 – Average top bar disbonded area, macrocell and microcell corrosion losses in Southern Exposure and cracked beam specimens upon autopsy.

Steel Designation[a]	Age	Southern Exposure			Cracked Beam		
		Disbonded Area (cm^2)	Macrocell Loss (µm)	Microcell Loss (µm)	Disbonded Area (cm^2)	Macrocell Loss (µm)	Microcell Loss (µm)
ECR-4h-45	112	0.590	0.004	0.041	4.18	0.045	0.73
ECR-10h-45	120	3.83	0.052	0.247	4.52	0.059	0.76
ECR-10h-35	120	1.14	0.009	0.048	4.68	0.160	1.12
ECR(DCI)-4h-45	96	2.25	0.004	0.032	4.25	0.026	0.76
ECR(DCI)-10h-45	96	2.69	0.012	0.185	4.63	0.079	1.29
ECR(DCI)-10h-35	96	2.11	0.007	0.020	4.97	0.223	2.58
ECR(RH)-4h-45	96	1.41	0.010	0.002	4.63	0.141	2.22
ECR(RH)-10h-45	96	2.07	-0.002	0.024	4.54	0.171	1.16
ECR(RH)-10h-35	96	0.254	0.003	0.018	4.37	0.178	0.85
ECR(HY)-4h-45	96	0.390	-0.002	0.005	4.30	0.036	0.36
ECR(HY)-10h-45	96	1.20	0.002	0.013	4.13	0.060	0.88
ECR(HY)-10h-35	96	0.166	0.001	0.008	4.68	0.194	0.81
ECR(primer/$Ca(NO_2)_2$)-4h-45	96	1.73	0.014	0.033	3.92	0.017	0.90
ECR(primer/$Ca(NO_2)_2$)-10h-45	96	3.17	0.066	0.029	3.95	0.100	1.03
ECR(primer/$Ca(NO_2)_2$)-10h-35	96	0.926	0.002	0.008	3.82	0.440	2.33
MC(both layers penetrated)-4h-45	96	1.02	0.058	0.931	2.17	0.377	1.44
MC(both layers penetrated)-10h-45	96	1.81	0.599	1.859	2.05	0.672	3.65
MC(only epoxy penetrated)-4h-45	96	2.74	0.033	0.803	2.40	0.294	3.77
MC(only epoxy penetrated)-10h-45	96	2.71	0.090	0.681	1.52	0.221	1.66
ECR(Chromate)-4h-45	114[b]	3.90	0.027	0.036	4.43	0.085	2.27
ECR(Chromate)-10h-45	110[c]	4.07	0.079	0.116	4.52	0.221	0.66
ECR(DuPont)-4h-45	114[b]	4.54	0.043	0.166	4.29	0.131	0.65
ECR(DuPont)-10h-45	110[c]	4.52	0.053	0.396	4.52	0.202	2.53
ECR(Valspar)-4h-45	114[b]	3.69	0.049	0.204	4.55	0.092	2.53
ECR(Valspar)-10h-45	110[c]	4.01	0.072	0.247	4.52	0.133	2.25
ECR(Chromate)-DCI-4h-45	96	0.895	0.007	0.080	-	-	-
ECR(DuPont)-DCI-4h-45	96	0.711	0.000	0.010	-	-	-
ECR(Valspar)-DCI-4h-45	96	1.49	0.012	0.004	-	-	-

[a] Conv. = conventional steel. ECR = conventional epoxy-coated reinforcement.
ECR(Chromate) = ECR with the chromate pretreatment.
ECR(DuPont) = ECR with high adhesion DuPont coating.
ECR(Valspar) = ECR with high adhesion Valspar coating.
ECR(DCI) = ECR in concrete with DCI inhibitor.
ECR(Rheocrete) = ECR in concrete with Rheocrete inhibitor.
ECR (Hycrete) = normal ECR with Hycrete inhibitor.
MC(both layers penetrated) = multiple coated bars with both zinc and epoxy layers penetrated.
MC(only epoxy penetrated) = mutiple coated bars with only epoxy layer penetrated.
4h = bar with four holes through epoxy, 10h = bar with 10 holes through epoxy.
45 = concrete with *w/c* =0.45; 35 = concrete with *w/c* =0.45.

[b] Age of specimens 1 and 2 is 114 weeks. Age of specimen 3 is 112 weeks

[c] Age of specimens 1 and 2 is 110 weeks. Age of specimen 3 is 96 weeks

Exposure and cracked beam specimens containing epoxy-coated reinforcement. Corrosion loss and disbondment data are summarized in Table 4.2.

4.2.1 Southern Exposure Tests

A comparison between the average disbonded area A_d and the *macrocell* corrosion loss at specimen autopsy is shown in Figure 4.5. For each corrosion protection system, data for four and ten-hole specimens, as well as specimens with a *w/c* ratio of 0.35, is plotted individually on the same plot. For simplicity, the number of holes and the water-cement ratio are not identified in the figure. With a correlation coefficient R equal to 0.13, there appears to be no significant linear relationship between disbonded area and macrocell corrosion. The resulting trend line exhibits a slope of about 1.6 $cm^2/\mu m$, whereas most of the data exhibit a much steeper slope (about 29 times steeper). The MC specimens with the zinc protective layer, however, are clearly identifiable as statistical outliers, with the specimens with both layers penetrated being far more so than the specimens with only the epoxy penetrated. Although the MC specimens exhibit an average magnitude of disbonded area, they exhibit higher than typical macrocell corrosion losses. Therefore, it appears that corrosion losses in the zinc specimens are more confined to the immediate vicinity of the damaged area than they are in conventional epoxy-coated reinforcement. Once the MC specimens are removed (Figure 4.6), the remaining data exhibits a correlation coefficient R equal to 0.84, indicating that a good linear relationship exists between the macrocell corrosion loss and top bar disbonded area in the Southern Exposure specimens. The average disbonded area tends to increase as macrocell corrosion loss increases.

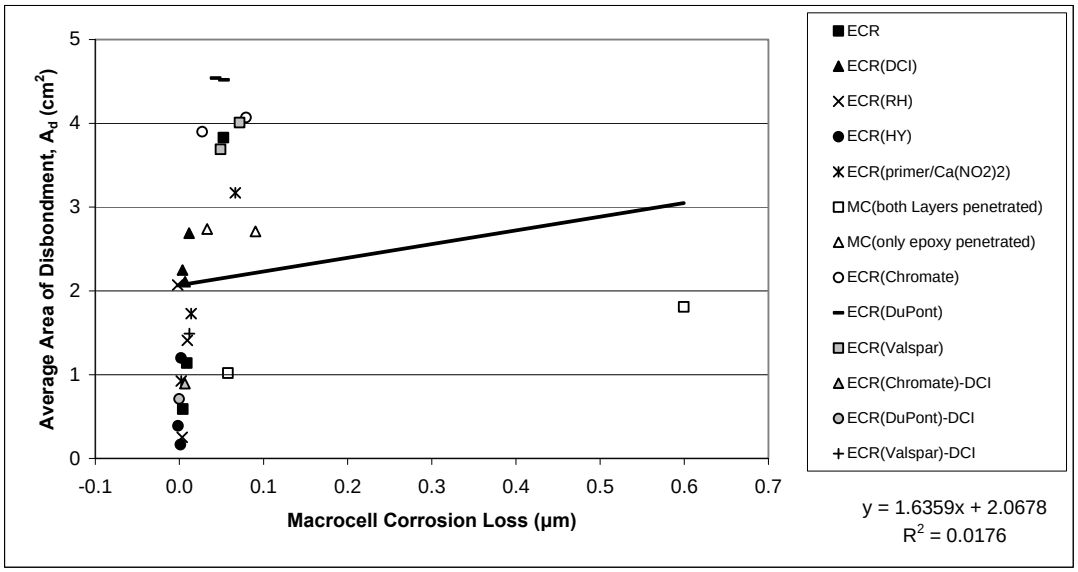

Figure 4.5 – Disbonded area versus macrocell corrosion loss for the Southern Exposure test specimens. Corrosion loss is based on total area.

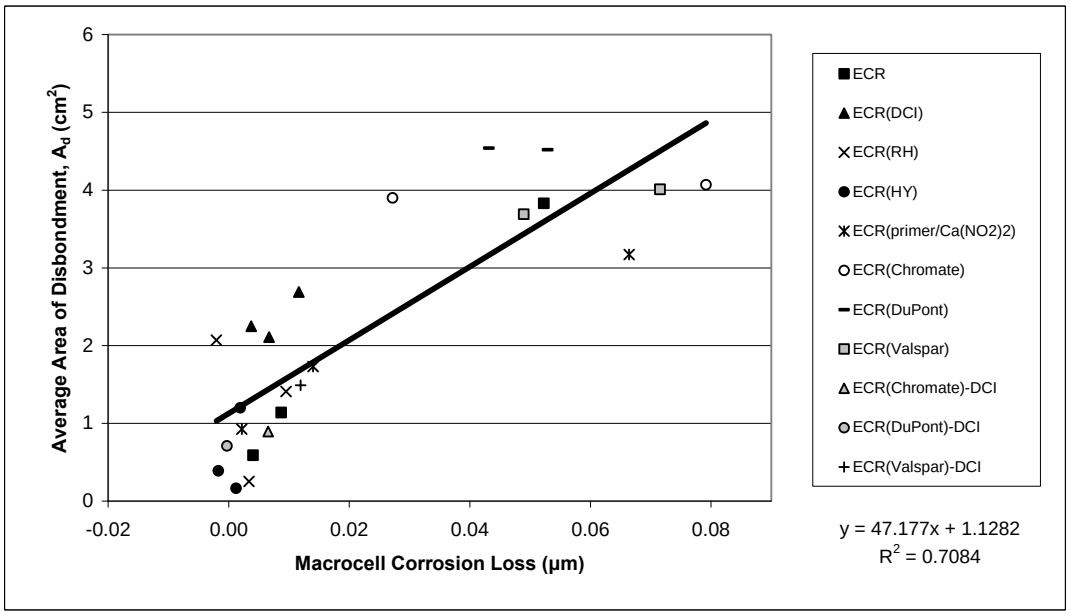

Figure 4.6 – Disbonded area versus macrocell corrosion loss for the Southern Exposure test specimens. Specimens containing zinc coatings have been excluded. Corrosion loss is based on total area.

Figure 4.7 shows the relationship between the average disbonded area and the *microcell* corrosion loss in the Southern Exposure test specimens. As observed for macrocell corrosion loss, specimens containing zinc coatings exhibit high corrosion losses compared with the remaining corrosion protection systems evaluated. The resulting correlation coefficient *R*, 0.12, indicates that a significant linear relationship does not exist between disbonded area and microcell corrosion loss when all specimens are considered. After removing the outlying MC specimens (Figure 4.8),

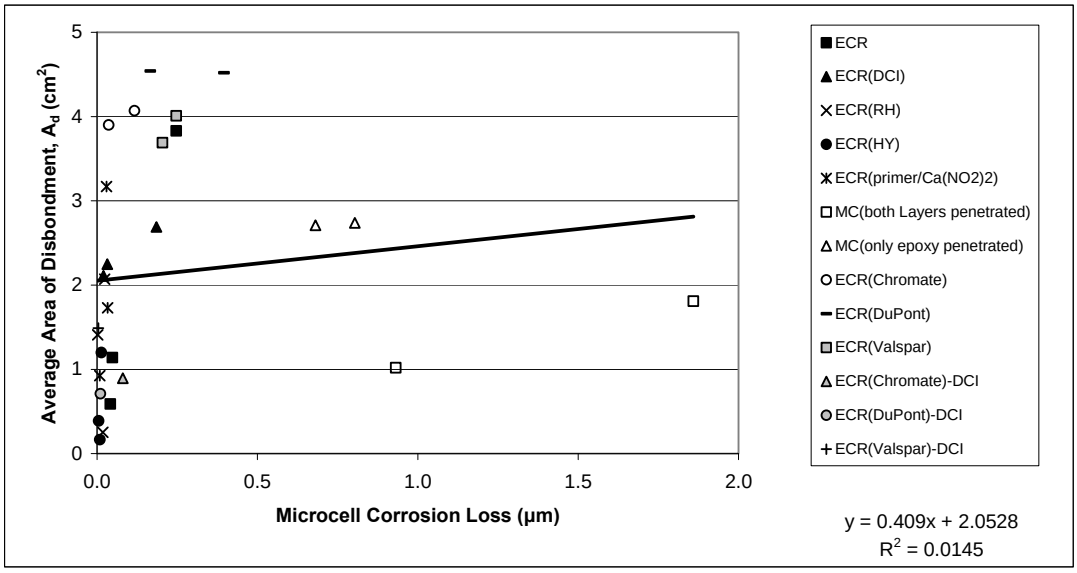

Figure 4.7 – Disbonded area versus microcell corrosion loss for the Southern Exposure test specimens. Corrosion loss is based on total area.

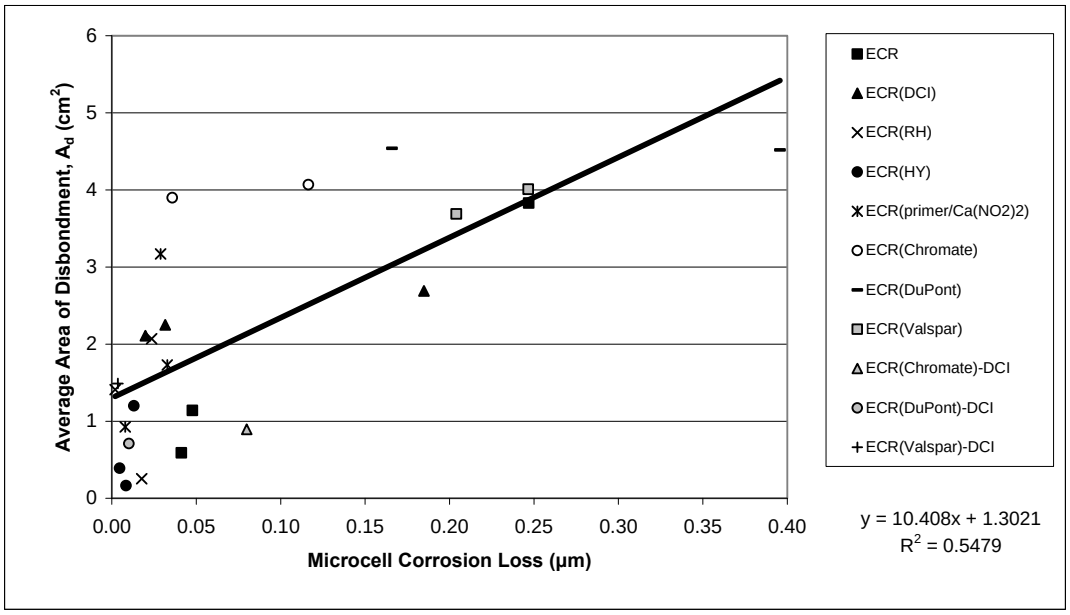

Figure 4.8 – Disbonded area versus microcell corrosion loss for the Southern Exposure test specimens. Specimens containing zinc coatings have been excluded. Corrosion loss is based on total area.

however, a weak linear relationship is observed between disbonded area and microcell corrosion loss, with a resulting correlation coefficient *R* equal to 0.74 and a coefficient of determination R^2 equal to 0.55. This means that 55% of the total variation in microcell corrosion loss can be explained by a linear relationship between average disbonded area and microcell corrosion loss. The figure also shows that disbonded area tends to increase as microcell corrosion loss increases.

4.2.2 Cracked Beam Tests

Figure 4.9 shows the relationship between average top bar disbonded area and *macrocell* corrosion loss in the cracked beam test specimens. The MC specimens and one group of ECR(primer/$Ca(NO_2)_2$) specimens appear as outliers. The MC

specimens exhibit smaller disbonded areas, between 1.52 to 2.54 cm^2 (0.24 to 0.39 $in.^2$), which are similar to the disbonded areas observed for Southern Exposure specimens. This may indicate that the multiple-coated reinforcement is less susceptible to corrosion disbondment than conventional ECR in environments of severe chloride exposure, such as occurs in CB specimens. The outlying ECR(primer/$Ca(NO_2)_2$) specimen exhibits a disbonded area similar to other specimens but exhibits about twice the macrocell corrosion loss. After removing the outliers (see Figure 4.10), the resulting linear regression yields a correlation coefficient *R* equal to 0.66, indicating that a weak linear relationship exists between disbonded area and macrocell corrosion loss. The average area of disbondment

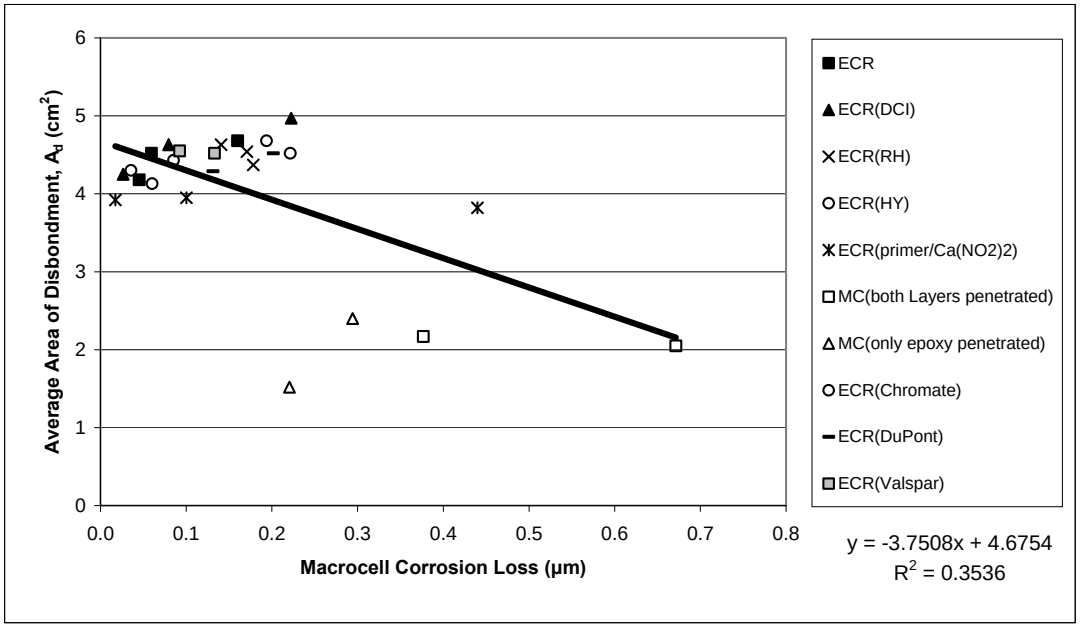

Figure 4.9 – Disbonded area versus macrocell corrosion loss for the cracked beam test specimens. Corrosion loss is based on total area.

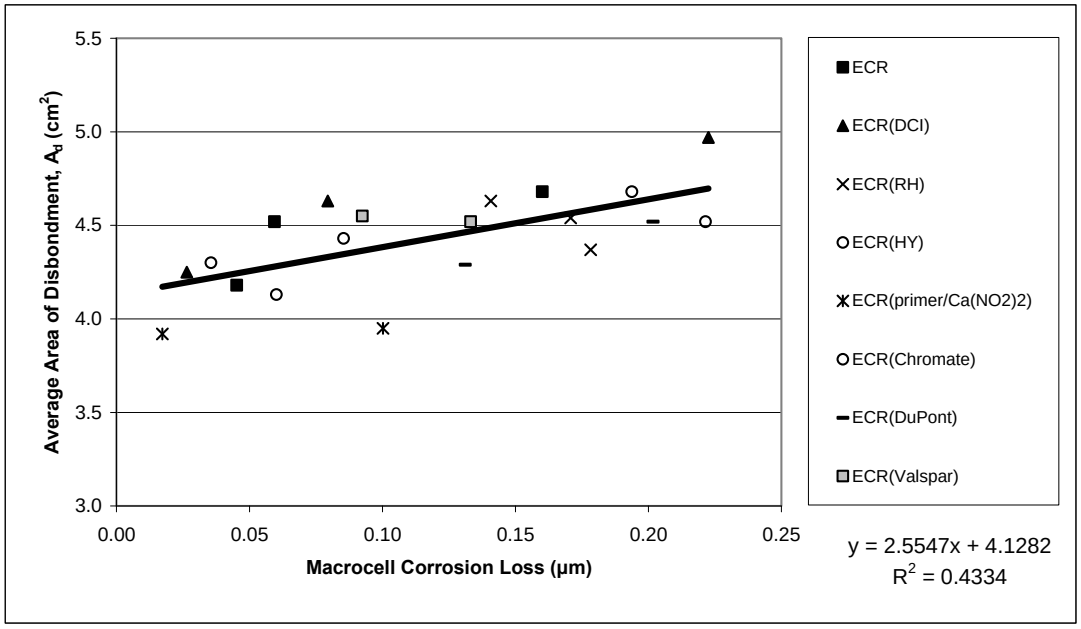

Figure 4.10 – Disbonded area versus macrocell corrosion loss for the cracked beam test specimens, with outlying data removed. Corrosion loss is based on total area.

increases about 0.29 cm^2 (0.05 in.^{2}) for each 0.05 µm increase in macrocell corrosion loss. Unlike the wide distribution of disbonded areas observed in the SE specimens, which exhibit disbonded areas ranging from 0.17 to 4.54 cm^2 (0.03 to 0.70 in.^{2}), the disbonded areas for all specimens fall between 4 to 5 cm^2 (0.62 to 0.78 in.^{2}). This, however, may be due to the manner in which totally disbonded bars ("TD") were averaged into the results. As described in Chapter 3, if any disbondment measurement included a disbonded radius greater than 12 mm (0.47 in.), the disbonded area was not explicitly measured; rather, the area was recorded as "TD". For the purposes of averaging these results, "TD" is treated as an area equal to 4.52 cm^2 (0.70 in.^{2}), which is equivalent to the area of a circle with a radius of 12 mm

(0.47 in.). Since many of the disbonded areas in CB specimens were recorded as "TD", the averaged values shown in Figure 4.10, in all likelihood, underestimate the true disbonded area for these specimens. Nevertheless, it is clear that bars in CB specimens exhibit higher disbonded areas than SE specimens.

Figure 4.11 shows a comparison between average top bar disbonded area and *microcell* corrosion loss. As in Figure 4.9, the multiple-coated specimens appear as outliers. The MC specimens exhibit smaller disbonded areas than the other CB specimens. Figure 4.12 shows the same data shown in Figure 4.11, except with the outlier data removed. The resulting correlation coefficient is equal to 0.50, indicating that no significant linear relationship exists between disbonded area and macrocell corrosion loss in the cracked beam specimens. However, it appears that the average area of disbondment tends to increase with microcell corrosion loss. As previously stated, the disbonded areas are between about 4 and 5 cm^2 (0.62 to 0.78 $in.^2$) due to the manner in which specimens which exhibited total disbondment are averaged into the results.

The comparisons between corrosion loss and disbonded area show that a clear relationship exists in Southern Exposure specimens in which the disbonded area tends to increase with both microcell and macrocell corrosion, and that the relationship can reasonably be approximated as linear. This relationship is not as strong for the cracked beam specimens. However, as previously stated, the many cracked beam specimens were recorded as being totally disbonded, and the true area of disbondment for these specimens were not recorded. The resulting underestimation of the true

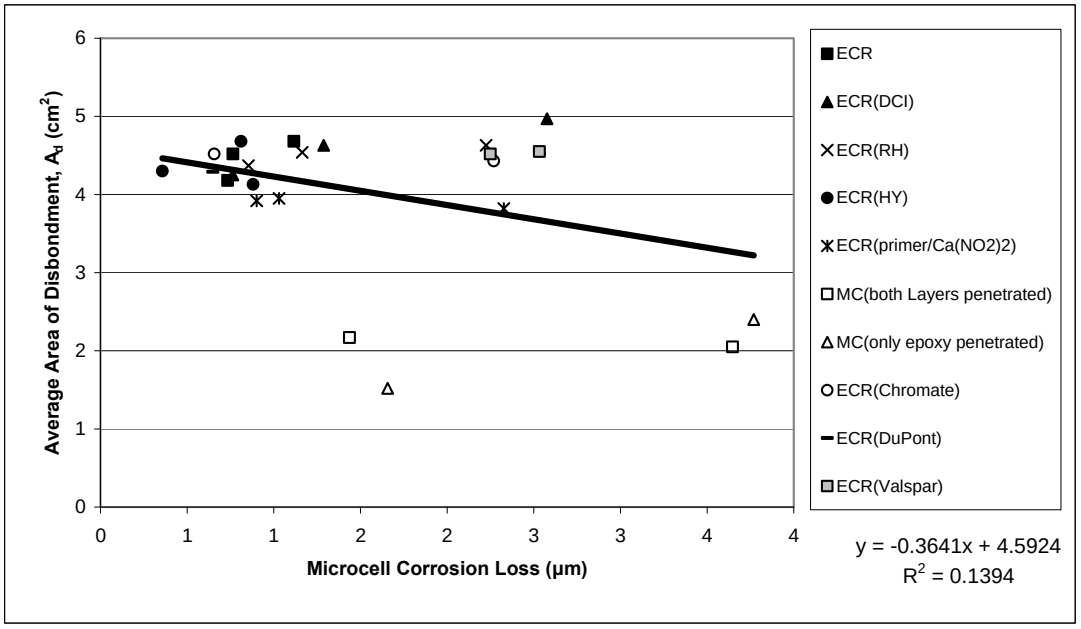

Figure 4.11 – Disbonded area versus microcell corrosion loss for the cracked beam test specimens. Corrosion loss is based on total area.

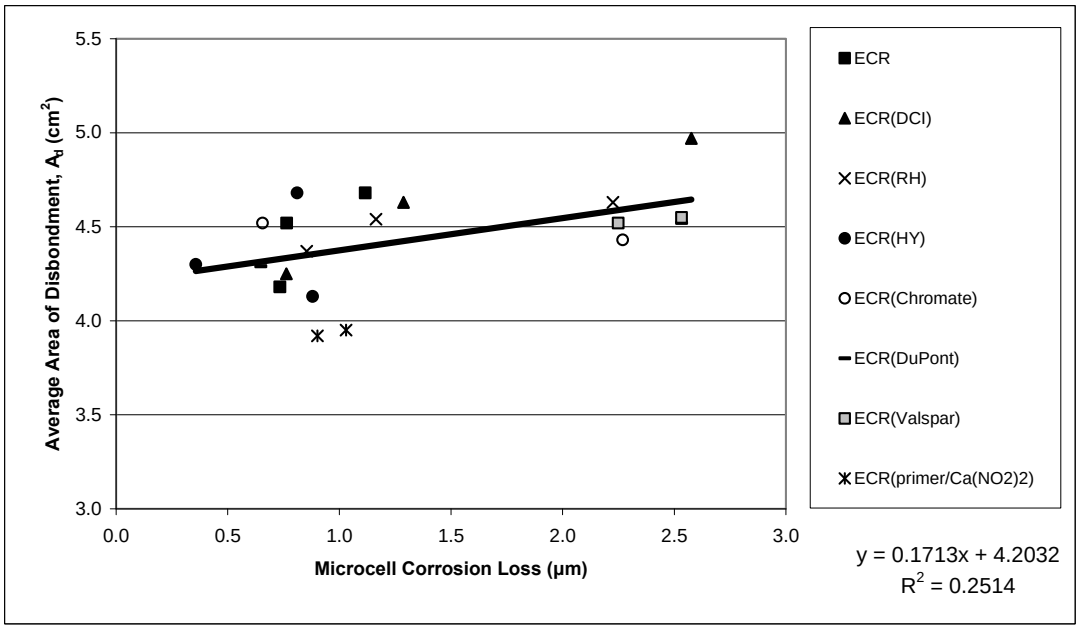

Figure 4.12 – Disbonded area versus microcell corrosion loss for the cracked beam test specimens, with outlying data removed. Corrosion loss is based on total area.

disbonded area for these specimens may be the main reason that the relationship between corrosion loss and disbonded area is weaker for the cracked beams specimens than for the Southern Exposure specimens. The relationship between corrosion loss and disbonded area suggests that the disbondment of the epoxy is caused by corrosion of the underlying steel to which the epoxy was bonded, and not due to any deficiency in the adhesion of the epoxy coating itself.

4.3 Statistical Difference Between Corrosion Protection Systems

This section presents a statistical comparison between the corrosion protection systems evaluated in this study. The Student's t-test provides a method to determine whether two populations of unknown variance are statistically different using a relatively small sample size from each population. In this study, the 96-week macrocell corrosion losses are used to statistically compare each corrosion protection system with its related control system. The t-test starts by forming the null hypothesis H_0:

$$H_0 : \mu_1 - \mu_2 = 0 \tag{4.1}$$

where

μ_1 = mean of population 1

μ_2 = mean of population 2

The null hypothesis states that there is no statistical difference between the means of the two independent populations. The alternative hypothesis H_1 states that the two means are not the same. The actual variance of each population is not

known; therefore, using the assumption that the two populations are normally distributed and their variances are not equal, the t-statistic is given by:

$$t_{stat} = \frac{\left(\overline{X}_1 - \overline{X}_2\right) - \left(\mu_1 - \mu_2\right)}{\sqrt{\left(\frac{s_2^{\,2}}{n_1} + \frac{s_2^{\,2}}{n_2}\right)}} \tag{4.2}$$

where

$\overline{X}_i$ = mean of the sample from population *i*

$s_i^{\,2}$ = variance of the sample from population *i*

n_i = size of the sample from population *i*

i = 1, 2

$\mu_1 - \mu_2$ = 0, the null hypothesis [Eq (4.1)]

The t-statistic is compared to the value obtained from the t-distribution t_{crit}. If the absolute value of t_{stat} is greater than the value for t_{crit}, the null hypothesis is rejected. The value of the t-statistic t_{crit} depends on the level of significance α and the number of degrees of freedom υ of the t-distribution. The significance level is defined as the probability that the test will reject the null hypothesis $\mu_1 = \mu_2$ when, in fact, it is true and should be accepted (also known as a Type I error). In this study, the significance level is the probability that the t-test will erroneously conclude that the corrosion losses between two corrosion protection systems are statistically different, when in fact they are statistically the same. The confidence level *X*%, which equals $1 - \alpha$, is the probability that the null hypothesis is accepted when it is true. The number of degrees of freedom υ of the t-distribution is given as

$$\upsilon = \frac{\left(\frac{{s_1}^2}{n_1} + \frac{{s_2}^2}{n_2}\right)^2}{\frac{{s_1}^4}{{n_1}^2(n_1 - 1)} + \frac{{s_2}^4}{{n_2}^2(n_2 - 1)}} \tag{4.3}$$

Tables containing values for t_{crit} corresponding to various levels of confidence are widely published in statistics textbooks. In the current study, a Microsoft Excel spreadsheet was used to calculate the values of t_{crit} for four different levels of significance, 0.20, 0.10, 0.05, and 0.02, assuming population variances are not equal. The results for the Student's t-test are shown in Table 4.4 for Southern Exposure specimens and in Table 4.5 for the cracked beam specimens. In these tables, the two corrosion protection systems being compared and the t_{stat} statistic are shown along with the t_{crit} statistic corresponding to each level of significance. If t_{crit} is less than t_{stat}, a "Y" is shown to indicate that, for the given level of significance, the difference between the corrosion losses of the systems is statistically significant. An "N" indicates that there is no significant statistical difference between the corrosion losses of the corrosion protection systems.

The results of the Student's t-test for comparing corrosion protection systems in Southern Exposure specimens are summarized in Table 4.3. For specimens containing conventional steel reinforcement, there is no statistically significant difference between the corrosion losses measured in specimens with *w/c* = 0.45 (1.75 μm) and *w/c* = 0.35 (2.12 μm). This does not mean that a lower water-cement ratio does not provide additional protection against corrosion; as was shown in Chapter 3, the lower *w/c* ratio provides a significant delay in corrosion initiation. However, by

Table 4.3 – Student's t-test for 96-week macrocell corrosion losses in Southern Exposure specimens based on total area

Control Specimen[a]		Test Specimen[a]			t_{crit}[c]			
	$\overline{X}$[d] (μm)		$\overline{X}$[d] (μm)	t_{stat}[b]	X%: 80% 90% 95% 98%			
					α: 0.2 0.1 0.05 0.02			
Conv.-45	1.75	Conv.-35	2.12	-0.322	1.886 N	2.920 N	4.303 N	6.965 N
Conv.-45	1.75	ECR-4h-45	0.003	3.986	1.476 Y	2.015 Y	2.571 Y	3.365 Y
Conv.-45	1.75	ECR-10h-45	0.017	3.955	1.476 Y	2.015 Y	2.571 Y	3.365 Y
Conv.-35	2.12	ECR-10h-35	0.008	2.015	1.886 Y	2.920 N	4.303 N	6.965 N
ECR-10h-45	0.047	ECR-10h-35	0.139	1.81	1.638 Y	2.353 N	3.182 N	4.541 N
ECR-4h-45	0.003	ECR(DCI)-4h-45	0.004	-0.299	1.886 N	2.920 N	4.303 N	6.965 N
ECR-10h-45	0.017	ECR(DCI)-10h-45	0.012	0.626	1.638 N	2.353 N	3.182 N	4.541 N
ECR-10h-35	0.008	ECR(DCI)-10h-35	0.007	0.235	1.638 N	2.353 N	3.182 N	4.541 N
ECR-4h-45	0.003	ECR(RH)-4h-45	0.010	-0.619	1.886 N	2.920 N	4.303 N	6.965 N
ECR-10h-45	0.017	ECR(RH)-10h-45	-0.003	3.637	1.638 Y	2.353 Y	3.182 Y	4.541 N
ECR-10h-35	0.008	ECR(RH)-10h-35	0.003	1.688	1.886 N	2.920 N	4.303 N	6.965 N
ECR-4h-45	0.003	ECR(HY)-4h-45	-0.002	6.379	1.440 Y	1.943 Y	2.447 Y	3.143 Y
ECR-10h-45	0.017	ECR(HY)-10h-45	0.002	3.184	1.886 Y	2.920 Y	4.303 N	6.965 N
ECR-10h-35	0.008	ECR(HY)-10h-35	0.001	1.873	1.638 Y	2.353 N	3.182 N	4.541 N
ECR-4h-45	0.003	ECR(primer/Ca(NO2)2)-4h-45	0.014	-1.738	1.886 N	2.920 N	4.303 N	6.965 N
ECR-10h-45	0.017	ECR(primer/Ca(NO2)2)-10h-45	0.064	-1.265	1.886 N	2.920 N	4.303 N	6.965 N
ECR-10h-35	0.008	ECR(primer/Ca(NO2)2)-10h-35	0.002	2.185	1.886 Y	2.920 N	4.303 N	6.965 N
ECR-4h-45	0.003	MC(both layers penetrated)-4h-45	0.058	-9.043	1.886 Y	2.920 Y	4.303 Y	6.965 Y
ECR-10h-45	0.017	MC(both layers penetrated)-10h-45	0.599	-10.357	1.886 Y	2.920 Y	4.303 Y	6.965 Y
ECR-4h-45	0.003	MC(only epoxy penetrated)-4h-45	0.033	-2.968	1.886 Y	2.920 Y	4.303 N	6.965 N
ECR-10h-45	0.017	MC(only epoxy penetrated)-10h-45	0.090	-1.605	1.886 N	2.920 N	4.303 N	6.965 N
ECR-4h-45	0.003	ECR(Chromate)-4h-45	0.018	-1.672	1.886 N	2.920 N	4.303 N	6.965 N
ECR-10h-45	0.017	ECR(Chromate)-10h-45	0.067	-1.538	1.886 N	2.920 N	4.303 N	6.965 N
ECR-4h-45	0.003	ECR(DuPont)-4h-45	0.026	-4.929	1.886 Y	2.920 Y	4.303 Y	6.965 N
ECR-10h-45	0.017	ECR(DuPont)-10h-45	0.046	-2.897	1.886 Y	2.920 N	4.303 N	6.965 N
ECR-4h-45	0.003	ECR(Valspar)-4h-45	0.032	-3.239	1.886 Y	2.920 Y	4.303 N	6.965 N
ECR-10h-45	0.017	ECR(Valspar)-10h-45	0.063	-3.171	1.886 Y	2.920 Y	4.303 N	6.965 N
ECR(DCI)-4h-45	0.004	ECR(Chromate)-DCI-4h-45	0.007	-0.466	1.886 N	2.920 N	4.303 N	6.965 N
ECR(DCI)-4h-45	0.004	ECR(DuPont)-DCI-4h-45	0.000	2.053	1.886 Y	2.920 N	4.303 N	6.965 N
ECR(DCI)-4h-45	0.004	ECR(Valspar)-DCI-4h-45	0.012	-0.745	1.886 N	2.920 N	4.303 N	6.965 N

[a] For explaination of of specimen nomenclature, see Table 2.3 in Chapter 2.

[b] t_{stat} = t-statistic calculated from the t-test;

[c] t_{crit} = t-value obtained from the Student's t-distribution for given α
α = level of significance; X% = level of confidence
Y = statistically significant difference exists between groups
N = no statistically significant difference exists between group

[d] $\overline{X}$ = mean macrocell corrosion loss

the end of the test, both groups exhibited similar corrosion losses; hence the Student's t-test concludes that the difference between the two groups is not statistically significant. The average corrosion losses exhibited by four-hole and ten-hole ECR specimens, 0.003 and 0.017 μm, respectively, are statistically different than conventional steel reinforcement is significant with α = 0.02, indicating that there is a strong statistical difference between conventional steel and epoxy-coated

reinforcement based on corrosion losses. The difference between conventional steel, with an average corrosion loss of 2.12 μm, and epoxy-coated reinforcement with ten holes in concrete with *w/c* of 0.35, with an average corrosion loss of 0.008 μm, is significant at $\alpha = 0.2$.

Among the Southern Exposure specimens cast with concrete containing corrosion inhibitors, only one specimen group, ECR(DCI), with an average corrosion loss of 0.004 μm, exhibits no statistically significant difference from the ECR-4h-45 specimens (0.003 μm). Among specimens cast with Rheocrete, the difference between the ECR-10h-45 specimens (average corrosion loss equal to 0.017 μm) and ECR(RH)-10h-45 specimens (average corrosion loss equal to –0.003 μm) is significant at $\alpha = 0.05$. The remaining specimens containing Rheocrete, ECR(RH)-4h-45 (average corrosion loss equal to 0.010 μm) and ECR(RH)-10h-35 specimens (average corrosion loss equal to 0.003 μm), exhibit no statistical difference from control specimens. All three Hycrete test groups exhibit differences from the ECR control specimens, with ECR(HY)-4h-45 (corrosion loss equal to -0.002 μm) significant at $\alpha = 0.02$, ECR(HY)-10h-45 (corrosion loss equal to 0.002 μm) significant at $\alpha = 0.1$, and ECR(HY)-10h-35 (corrosion loss equal to 0.001 μm) significant at $\alpha = 0.2$. The difference between the ECR-10h-35 specimens and the ECR(primer/$Ca(NO_2)_2$)-10h-35 specimens (corrosion loss equal to 0.002 μm) is significant at $\alpha = 0.2$. The remaining specimens containing ECR with an encapsulated calcium nitrite primer beneath the epoxy do not exhibit a significant difference from control specimens.

For specimens containing multiple-coated (MC) bars, both the four-hole specimens (average corrosion loss equal to 0.058 μm) and ten-hole specimens (average corrosion loss equal to 0.599 μm) with both layers penetrated exhibit a significant difference from the ECR control specimens, significant at $\alpha = 0.02$. The difference between the specimens containing four holes through only the epoxy (corrosion loss equal to 0.033 μm) and the conventional ECR specimens is significant at $\alpha = 0.1$. The difference between the MC specimens with ten holes through the epoxy (corrosion loss equal to 0.090 μm) and the conventional ECR is not significant.

Among specimens containing improved adhesion ECR, the ECR(Chromate) specimens (corrosion losses of 0.018 μm for four-hole specimens and 0.067 μm for ten-hole specimens) exhibit no significant difference from conventional ECR specimens. The difference between the ECR(DuPont)-4h-45 specimens (corrosion loss equal to 0.026 μm) and the ECR-4h-45 specimens is significant at $\alpha = 0.05$. The difference between the ECR(DuPont)-10h-45 specimens (corrosion loss equal to 0.046 μm) and the ECR-10h-45 specimens is significant at $\alpha = 0.2$. The difference between both ECR(Valspar) groups (corrosion losses of 0.032 and 0.063 μm for four and ten-hole specimens, respectively) and the conventional ECR specimens is significant at $\alpha = 0.1$. Among specimens containing improved adhesion ECR cast in concrete containing DCI, only the specimen contain DuPont ECR (zero corrosion loss) exhibits a statistical difference from ECR(DCI) specimens, significant at $\alpha = 0.2$.

The results of the Student's t-test for comparing corrosion protection systems in cracked beam specimens are summarized in Table 4.4. For specimens containing

Table 4.4 – Student's t-test for 96-week macrocell corrosion losses in cracked beam specimens based on total area

Control Specimen[a]		Test Specimen[a]			t_{crit}[c]			
	$\overline{X}$[d] (μm)		$\overline{X}$[d] (μm)	t_{stat}[b]	X%: 80% 90% 95% 98% α: 0.2 0.1 0.05 0.02			
Conv.-45	13.1	Conv.-35	8.34	2.011	1.476 Y	2.015 N	2.571 N	3.365 N
Conv.-45	13.1	ECR-4h-45	0.041	7.695	1.476 Y	2.015 Y	2.571 Y	3.365 Y
Conv.-45	13.1	ECR-10h-45	0.047	7.691	1.476 Y	2.015 Y	2.571 Y	3.365 Y
Conv.-35	8.34	ECR-10h-35	0.139	5.027	1.886 Y	2.920 Y	4.303 Y	6.965 N
ECR-10h-45	0.047	ECR-10h-35	0.139	-4.273	1.638 Y	2.353 Y	3.182 Y	4.541 N
ECR-4h-45	0.041	ECR(DCI)-4h-45	0.026	0.966	1.533 N	2.132 N	2.776 N	3.747 N
ECR-10h-45	0.047	ECR(DCI)-10h-45	0.079	-0.773	1.886 N	2.920 N	4.303 N	6.965 N
ECR-10h-35	0.139	ECR(DCI)-10h-35	0.223	-0.731	1.886 N	2.920 N	4.303 N	6.965 N
ECR-4h-45	0.041	ECR(RH)-4h-45	0.141	-1.140	1.886 N	2.920 N	4.303 N	6.965 N
ECR-10h-45	0.047	ECR(RH)-10h-45	0.171	-3.156	1.638 Y	2.353 Y	3.182 N	4.541 N
ECR-10h-35	0.139	ECR(RH)-10h-35	0.178	-0.614	1.886 N	2.920 N	4.303 N	6.965 N
ECR-4h-45	0.041	ECR(HY)-4h-45	0.036	0.200	1.886 N	2.920 N	4.303 N	6.965 N
ECR-10h-45	0.047	ECR(HY)-10h-45	0.060	-0.346	1.638 N	2.353 N	3.182 N	4.541 N
ECR-10h-35	0.139	ECR(HY)-10h-35	0.194	-1.248	1.886 N	2.920 N	4.303 N	6.965 N
ECR-4h-45	0.041	ECR(primer/Ca(NO2)2)-4h-45	0.017	2.107	1.440 Y	1.943 Y	2.447 N	3.143 N
ECR-10h-45	0.047	ECR(primer/Ca(NO2)2)-10h-45	0.098	-1.548	1.638 N	2.353 N	3.182 N	4.541 N
ECR-10h-35	0.139	ECR(primer/Ca(NO2)2)-10h-35	0.470	-4.041	1.886 Y	2.920 Y	4.303 N	6.965 N
ECR-4h-45	0.041	MC(both layers penetrated)-4h-45	0.377	-5.055	1.886 Y	2.920 Y	4.303 Y	6.965 N
ECR-10h-45	0.047	MC(both layers penetrated)-10h-45	0.672	-1.995	1.886 Y	2.920 N	4.303 N	6.965 N
ECR-4h-45	0.041	MC(only epoxy penetrated)-4h-45	0.294	-1.758	1.886 N	2.920 N	4.303 N	6.965 N
ECR-10h-45	0.047	MC(only epoxy penetrated)-10h-45	0.221	-1.893	1.886 Y	2.920 N	4.303 N	6.965 N
ECR-4h-45	0.041	ECR(Chromate)-4h-45	0.074	-2.048	1.533 Y	2.132 N	2.776 N	3.747 N
ECR-10h-45	0.047	ECR(Chromate)-10h-45	0.216	-1.223	1.886 N	2.920 N	4.303 N	6.965 N
ECR-4h-45	0.041	ECR(DuPont)-4h-45	0.105	-2.299	1.886 Y	2.920 N	4.303 N	6.965 N
ECR-10h-45	0.047	ECR(DuPont)-10h-45	0.184	-2.307	1.886 Y	2.920 N	4.303 N	6.965 N
ECR-4h-45	0.041	ECR(Valspar)-4h-45	0.084	-0.877	1.886 N	2.920 N	4.303 N	6.965 N
ECR-10h-45	0.047	ECR(Valspar)-10h-45	0.125	-1.140	1.886 N	2.920 N	4.303 N	6.965 N

[a] For explaination of of specimen nomenclature, see Table 2.3 in Chapter 2.

[b] t_{stat} = t-statistic calculated from the t-test;

[c] t_{crit} = t-value obtained from the Student's t-distribution for given α
α = level of significance; X% = level of confidence
Y = statistically significant difference exists between groups
N = no statistically significant difference exists between group

[d] $\overline{X}$ = mean macrocell corrosion loss

conventional steel reinforcement, the difference between specimens with *w/c* = 0.45 (corrosion loss equal to 13.1 μm) and *w/c* = 0.35 (corrosion loss equal to 8.34 μm) is statistically significant at α = 0.2. This further suggests that, while a low *w/c* ratio affords no additional protection to the top bar in cracked concrete, it may have a limited effect on corrosion rates by reducing the availability of oxygen to the bottom bars, thus limiting the cathodic reaction. The differences between specimens containing ECR (corrosion losses of 0.041 and 0.047 μm for four and ten-hole specimens, respectively) and specimens containing conventional steel reinforcement

in concrete with *w/c* = 0.45 are significant at α = 0.02. The difference between the Conv.-35 and ECR-10h-35 specimens (corrosion loss equal to 0.139 μm) is significant at α = 0.05.

Among specimens cast with concrete containing corrosion inhibitors, all but three specimen groups exhibit no statistically significant difference from the corresponding ECR control specimens. The difference between the ECR(RH)-10h-45 specimens (corrosion loss equal to 0.171 μm) and the ECR-10h-45 specimens is significant at α = 0.1. The difference between the ECR(primer/$Ca(NO_2)_2$)-4h-45 specimens (corrosion loss equal to 0.017 μm) and ECR-4h-45 specimens is significant at α = 0.1, and the difference between the ECR(primer/$Ca(NO_2)_2$)-10h-35 specimens (corrosion loss equal to 0.470 μm) and ECR-10h-35 specimens is significant at α = 0.1.

For specimens containing multiple-coated reinforcement, three out of four specimen groups exhibit statistically significant differences from the ECR control specimens. For specimens with both the epoxy and zinc layer penetrated, the difference between the four-hole specimens (corrosion loss equal to 0.377 μm) and the ECR-4h-45 specimens is significant at α = 0.05, while the difference between the ten-hole specimens (corrosion loss equal to 0.672 μm) and the ECR-10h-45 specimens is significant at α = 0.2. For specimens with only the epoxy coating penetrated, the difference between the ten-hole specimens (corrosion loss equal to 0.221 μm) and the ECR-10h-45 specimens is significant at α = 0.2, while the

difference between four-hole specimens (corrosion loss equal to 0.294 μm) and ECR-4h-45 specimens is not significant.

Among specimens containing ECR with improved adhesion epoxy, ECR(Chromate)-4h-45 (corrosion loss equals 0.074 μm) exhibits a statistically significant difference from the ECR-4h-45 control specimens (corrosion loss equal to 0.041 μm), significant at $\alpha = 0.2$. The differences between both the ECR(DuPont)-4h-45 and ECR(DuPont)-10h-45 (corrosion losses of 0.105 and 0.184 μm, respectively) and the corresponding control specimens (corrosion losses of 0.041 and 0.047 μm, respectively) is significant at $\alpha = 0.2$. All other specimens exhibit no statistically significant difference from control specimens.

4.4 Comparison Between Cathodic Disbondment and Corrosion Disbondment

This section presents a comparison between cathodic disbondment, as measured in accordance with ASTM A775, and the corrosion disbondment reported in Chapter 3. Gong et. al (2006) reported the cathodic disbondment test results for the ECR, ECR with improved adhesion epoxy, and MC bars evaluated in this study. These results are reproduced in Table 4.5, along with the average corrosion disbondment measurements reported in Chapter 3.

As shown in Table 4.5, the disbonded area observed at the conclusion of the Southern Exposure and cracked beam tests is higher than the disbonded area observed in the cathodic disbondment test. For the Southern Exposure specimens, corrosion disbonded areas range from 1.1 to 20 times the disbonded area measured in the cathodic disbondment test. For cracked beam specimens, corrosion disbonded areas

Table 4.5 – Corrosion disbondment and cathodic disbondment test results for conventional ECR, ECR with high adhesion between epoxy and steel, ECR containing an encapsulated calcium nitrite primer, and multiple-coated steel.

Steel Designation[a]	Southern Exposure Corrosion Disbonded Area (cm^2)	Cracked Beam Corrosion Disbonded Area (cm^2)	Cathodic Disbonded Area[1] (cm^2)
ECR	1.85	4.46	1.73
ECR(primer/$Ca(NO_2)_2$)	1.94	3.90	0.670
MC[2]	2.73	1.96	0.270
ECR(Chromate)	3.99	4.48	0.200
ECR(DuPont)	4.53	4.41	0.650
ECR(Valspar)	3.85	4.54	1.51

[1] Data from Gong et. al (2006)

[2] Specimens with only the epoxy layer penetrated

range from 2.6 to 22 times the disbonded area measured in the cathodic disbondment test. As previously mentioned, cracked beam specimens exhibit larger average corrosion disbonded areas than Southern Exposure specimens. There appears to be little correlation between cathodic disbonded area and corrosion disbonded area. Therefore, the results of the cathodic disbondment test, as specified in ASTM A775, do not appear to be a reliable indicator of corrosion disbondment performance of in-service epoxy-coated reinforcement.

4.5 Comparison Between Corrosion Protection Systems

This section presents a comparison between the corrosion protection systems evaluated in this study, based on the results of the Southern Exposure and cracked beam tests. Comparisons are made between conventional epoxy-coated reinforcement and conventional steel and between conventional epoxy-coated reinforcement and the other corrosion protection systems evaluated in this study.

Comparisons between corrosion protection systems are made based on both macrocell and microcell corrosion losses at 96 weeks, as well as disbonded area. Unless otherwise noted, corrosion losses are reported in terms of total area of the bar. Macrocell corrosion losses at 96 weeks are reported in Table 4.3 for Southern Exposure specimens and Table 4.4 for cracked beam specimens. Microcell corrosion losses are reported in Table 3.12 in Chapter 3.

4.5.1 Conventional Steel and Epoxy-Coated Reinforcement

In both the Southern Exposure and cracked beam specimens, epoxy-coated reinforcement exhibits superior corrosion resistance when compared to conventional bare steel reinforcement, both in terms of corrosion loss calculated based on the total area of the bar and the exposed area of the steel. The SE specimens with a *w/c* ratio of 0.45 containing ECR with four holes exhibit microcell and macrocell corrosion losses equal to 0.011% (Table 3.12) and 0.17% (Table 4.3), respectively, of that observed in specimens containing conventional steel reinforcement. ECR specimens with ten holes exhibit 0.81% of the microcell corrosion loss observed for conventional steel specimens. In terms of macrocell corrosion loss, the ECR-10h-45 specimens exhibit 0.97% of the corrosion loss observed for conventional steel specimens. The difference between both four and ten-hole specimens and the conventional steel specimens, based on macrocell losses, is statistically significant at $\alpha = 0.02$ (Section 4.3). As reported in Table 3.2 of Chapter 3, the macrocell corrosion losses based on exposed area exhibited by the ECR specimens are comparable to the losses observed in conventional steel specimens. Similar behavior is observed when

comparing microcell corrosion losses of ECR specimens with conventional steel specimens (Table 3.12, Chapter 3).

In the cracked beam specimens, specimens with a *w/c* ratio of 0.45 containing ECR with four holes through the epoxy exhibit microcell and macrocell corrosion losses equal to 0.28% (Table 3.12) and 0.31% (Table 4.4), respectively, of those in the CB specimens containing conventional steel reinforcement. The ECR-10h-45 specimens respectively exhibit 0.28% (Table 3.12) and 0.36% (Table 4.4) of the microcell and macrocell corrosion losses exhibited in conventional steel specimens. For both ECR-4h and ECR-10h specimens, the difference based on macrocell losses is statistically significant at $\alpha = 0.02$ (Section 4.3). In terms of exposed area, the ECR specimens exhibit similar or slightly higher macrocell corrosion losses (Chapter 3, Table 3.3) and microcell losses (Chapter 3, Table 3.12) than conventional steel specimens. The reason that ECR specimens exhibit higher corrosion losses based on exposed area is, in all likelihood, because the corrosion losses reported for the conventional steel specimens are based on the total area of the bar, all of which may not be corroding. This results in an underestimation of the local corrosion loss on the conventional steel specimens. Similarly, corrosion loss calculations based on exposed area assume an anodic area equal to the combined area exposed by the drilled holes in the epoxy. The autopsies, reported in Chapter 3, show that corrosion is not confined to the immediate site of the damaged epoxy, but progresses away from the damaged site beneath the epoxy layer due to crevice corrosion. Consequently, corrosion losses based on exposed area overestimate the thickness of the local

corrosion loss on epoxy-coated bars. Comparisons between corrosion losses based on total and exposed area must, therefore, be made judiciously.

For the conventional steel reinforcement cast in uncracked concrete, the SE specimens with a *w/c* ratio of 0.35 exhibit a microcell corrosion loss equal to 14% of the corrosion loss observed in the SE specimens with a *w/c* ratio equal to 0.45 (Table 3.12). In terms of macrocell corrosion, the specimens with a *w/c* ratio of 0.35 exhibit a 96-week corrosion loss that is nearly identical to that observed for the specimens with a *w/c* ratio of 0.45 (Table 4.3). However, based on Figure 3.3, it is clear that, even in terms of macrocell corrosion, a low *w/c* ratio affords additional protection to the reinforcement by delaying corrosion initiation. For conventional steel reinforcement in cracked concrete, the specimens with a *w/c* ratio equal to 0.35 exhibit 78% of the microcell corrosion loss (Table 3.12) and 64% the macrocell corrosion loss (Table 4.4) exhibited by the specimens with a 0.45 *w/c* ratio; the latter difference is statistically significant at $\alpha = 0.2$.

For conventional epoxy-coated reinforcement in uncracked concrete, specimens with a *w/c* ratio of 0.35 and ten holes through the epoxy exhibit 14% of the microcell corrosion loss (Table 3.12) and 47% of the macrocell corrosion loss (Table 4.3) of specimens with a *w/c* ratio of 0.45. Based on macrocell corrosion, the difference between the two systems is significant at $\alpha = 0.2$ (Table 4.3). For ECR in cracked concrete, the specimens with the lower *w/c* ratio exhibit *higher* corrosion losses than those with the higher *w/c* ratio. Specifically, the cracked beam specimens with a *w/c* ratio of 0.35 exhibit 1.8 times the microcell corrosion loss (Table 3.12) and

3.0 times the macrocell corrosion loss (Table 4.3) of the specimens with a *w/c* ratio of 0.45. The difference based on macrocell loss is significant at $\alpha = 0.05$ (Section 4.3). In terms of corrosion-induced disbondment (Table 4.2), the ECR in concrete with a *w/c* ratio of 0.35 exhibits 0.30 and 1.04 times the disbonded area of ECR in concrete with a *w/c* ratio of 0.45, for uncracked and cracked concrete, respectively.

From these results, it can be seen that a low *w/c* ratio provides additional corrosion protection for the conventional steel reinforcement and epoxy-coated reinforcement in uncracked concrete. Not only are 96-week corrosion losses lower for the specimens with the low *w/c* ratio than for the specimens with the higher *w/c* ratio, but corrosion initiation is delayed as well. In cracked concrete, however, the low *w/c* ratio provides much less corrosion protection.

As stated in Chapter 1, Gong et al. (2006) showed that for epoxy-coated reinforcement with 3.2-mm (1/8-inch) diameter holes through the epoxy, an average corrosion loss of about 2500 μm based on exposed area is required to cause concrete cracking. This is 100 times higher than the 25 μm of corrosion loss that will cause concrete cracking when conventional steel reinforcement is used. Based on exposed area, specimens containing ECR exhibit macrocell losses ranging from 1.47 to 3.21 μm for Southern Exposure specimens (Table 3.2) and from 9.04 to 26.7 μm in cracked beam specimens (Table 3.3). Microcell corrosion losses for ECR specimens range from 1.08 to 27.4 μm for Southern Exposure specimens and from 90.4 to 224 μm for cracked beam specimens (Table 3.12). In light of these values, all specimens containing ECR, whether in cracked or uncracked concrete, exhibit corrosion losses

that are well below that required to cause concrete cracking. In contrast, in most cases, the specimens containing conventional steel reinforcement approach or exceed a corrosion loss of 25 μm. Therefore, epoxy-coated reinforcement is expected to extend the service life of bridge decks well beyond the service life of bridge decks containing conventional steel reinforcement. Furthermore, these results suggest that in terms of *corrosion-induced surface deterioration*, the expected service life of a concrete bridge deck containing epoxy-coated reinforcement would extend beyond 75 years.

4.5.2 Corrosion Inhibitors

Based on the results presented in Table 4.3 for the Southern Exposure tests, all specimens with a *w/c* ratio of 0.45 containing ECR cast in concrete with a corrosion inhibitor exhibit lower macrocell corrosion losses than the ECR control specimens, with the exception of the four and ten-hole ECR(primer/$Ca(NO_2)_2$) specimens and the four-hole ECR(DCI) and ECR(RH) specimens. However, the differences between the conventional ECR and these specimens are not statistically significant. Two specimen groups, ECR(RH)-10h-45 and ECR(HY)-4h-45, exhibit negative macrocell corrosion loss, indicating, as discussed in Chapter 3, that the bottom bars are supplying electrons to the top bars. The difference between the conventional ECR specimens and the ECR(RH)-10h-45 and ECR(HY)-4h-45 specimens is significant at α = 0.05 and 0.02, respectively. Among the specimens that exhibit a positive macrocell corrosion loss, the ECR(HY)-10h-45 specimens exhibit the lowest macrocell corrosion losses at 12% of those exhibited by the ECR specimens

(difference is significant with α = 0.1), as shown in Table 4.2. The difference between the ECR(DCI)-10h-45 specimens and the conventional ECR specimens is not statistically significant. In terms of microcell corrosion losses (Table 3.12), all four-hole specimens containing corrosion inhibitors exhibit losses that are greater than or equal to corrosion losses for conventional ECR specimens, although the microcell corrosion losses in ECR specimens both with and without inhibitors are very low (maximum of 0.033 μm based on total area, exhibited by the ECR(primer/$(CaNO_2)_2$)-4h specimens). As shown in Table 3.12, the ECR(DCI)-10h-45 specimens are the only ten-hole specimens to exhibit higher microcell corrosion losses than the conventional ECR specimens, with a value equal to 129% that of the conventional ECR specimens. All other ten-hole specimens exhibit 9 to 20% the corrosion loss of the conventional ECR specimens. In terms of corrosion-induced disbondment (Table 4.2), ECR cast in concrete with a *w/c* ratio of 0.45 and containing corrosion inhibitors exhibits 31% [ECR(HY)-10h-45] to 381% [ECR(DCI)-4h-45] of the disbonded area exhibited by conventional ECR with the same number of holes through the epoxy.

As shown in Table 4.4, among ECR specimens cast with corrosion inhibitors in cracked concrete, only the ECR(primer/$Ca(NO_2)_2$)-4h-45 specimens exhibit a lower macrocell corrosion loss (41%) than the ECR control specimens, where the difference is statistically significant (α = 0.1). The ECR(RH)-10h-45 specimens, which perform well in uncracked concrete, exhibit 364% of the macrocell corrosion loss observed in the conventional ECR specimens, with the difference being

significant at α = 0.1. The differences between the remaining specimens and conventional ECR specimens are not statistically significant. In terms of microcell corrosion loss (Table 3.12), all cracked beam specimens cast with corrosion inhibitors and with a *w/c* ratio of 0.45 exhibit greater corrosion losses than the conventional ECR specimens, with the exception of the ECR(HY)-4h-45 specimens, which exhibit 77% the corrosion loss of the conventional ECR specimens. These results show that, while corrosion inhibitors may increase the corrosion protection afforded by ECR in uncracked concrete, they are not effective in cracked concrete. As shown in Table 4.2, corrosion disbonded areas of the epoxy range between 87% [ECR(primer/$Ca(NO_2)_2$-10h-45] to 111% [ECR(RH)-4h-45] of the disbonded area exhibited by the conventional ECR specimens with the same number of holes through the epoxy.

The effect of a lower *w/c* ratio (0.35) was also investigated in combination with the use of ECR and corrosion inhibitors. All SE specimens with a *w/*c ratio of 0.35 exhibit corrosion losses (both macrocell and microcell) that are lower than or similar to corrosion losses for the ECR control specimens (see Tables 4.3 and 3.12). This suggests that the lower *w/c* ratio enhances the effectiveness of the corrosion inhibitors. In terms of corrosion disbondment (Table 4.2), all Southern Exposure specimens cast with corrosion inhibitors in concrete with a *w/c* ratio of 0.35 exhibit smaller disbonded areas than the conventional ECR specimens at the same *w/c* ratio, with the exception of the ECR(DCI)-10h-35 specimens, which exhibit 185% of the disbonded area of the conventional ECR specimens. Among the remaining three

specimen groups, disbonded areas range from 15% [ECR(HY)-10h-35] to 81% [ECR(primer/$Ca(NO_2)_2$)-10h-35] of the disbonded area observed for the conventional ECR specimens cast without a corrosion inhibitor.

For the cracked beam specimens containing corrosion inhibitors, all specimens exhibit higher macrocell corrosion losses (Table 4.4) than the ECR specimens without corrosion inhibitors, but the difference is only statistically significant for the ECR(primer/$Ca(NO_2)_2$)-10h-35 specimens (at α = 0.1). When compared to analogous specimens with a *w/c* ratio of 0.45, all of the specimens with *w/c* = 0.35 exhibit higher macrocell corrosion losses. In terms of microcell corrosion loss (Table 3.12), all specimens with *w/c* = 0.35 exhibit similar or higher corrosion losses than the ECR specimens cast without corrosion inhibitors. When compared to similar specimens with *w/c* = 0.45, the specimens with *w/c* = 0.35 exhibit microcell corrosion losses that are similar to or greater than the losses for the 0.45 *w/c* specimens, except for the ECR(RH)-10h-35 specimen, which exhibits 74% the microcell corrosion loss of the ECR(RH)-10h-45 specimen. As shown in Table 4.2, the corrosion disbonded areas are 82% to 106% of those observed in control specimens. The corrosion losses observed for the SE and CB specimens indicate that a low *w/c* ratio may enhance the corrosion protection provided to the reinforcement by corrosion inhibitors in uncracked concrete but does not provide a measureable benefit in cracked concrete.

4.5.3 Increased Adhesion ECR

The Southern Exposure test results for specimens containing ECR with increased adhesion epoxy show that, in terms of macrocell corrosion loss, increased adhesion ECR holds no advantage over conventional epoxy-coated reinforcement. Macrocell corrosion losses (Table 4.3) range between 2.7 to 10.7 [ECR(DuPont)-10h-45 and ECR(Valspar)-4h-45 specimens, respectively] times the corrosion losses in the conventional ECR specimens. The difference is significant for all specimens except for the ECR(Chromate) specimens (both four and ten-hole specimens), which exhibit no statistical difference from conventional ECR specimens. In terms of microcell corrosion loss (Table 3.12), only the ECR(Chromate)-10h-45 specimens exhibit lower corrosion losses (63%) than the conventional ECR specimens. The remaining specimens exhibit a broad range of microcell corrosion losses that range from 1.3 [ECR(Valspar)-10h-45] to 71 [ECR(Valspar)-4h-45] times the corrosion losses for the conventional ECR specimens. The corrosion disbonded areas (Table 4.2) in the epoxy range from 1.1 to 77 times that exhibited by ECR control specimens.

For cracked beam specimens containing improved adhesion ECR, all specimen groups exhibit higher macrocell corrosion losses (Table 4.4) than the conventional ECR specimens. The difference is significant in three of the eight groups: the ECR(Chromate)-4h-45, ECR(DuPont)-4h-45, and ECR(DuPont)-10h-45 specimens, all with $\alpha = 0.2$. In terms of microcell corrosion loss (Table 3.12), all specimens containing improved adhesion ECR exhibit greater corrosion losses than conventional ECR specimens, with losses ranging between 1.1 [ECR(DuPont)-4h-45]

to 4.1 [ECR(Valspar)-4h-45] times the losses observed in the conventional ECR specimens. The corrosion disbonded areas (Table 4.2) for the increased adhesion epoxies are similar to those exhibited by the control ECR specimens. These results indicate that ECR with improved adhesion epoxy, while effective at protecting against corrosion, affords no additional protection compared to conventional ECR. Additionally, although bars with the improved adhesion epoxy have less cathodic disbondment than the conventional ECR bars, they exhibit no advantage in terms of corrosion disbonded area.

4.5.4 Increased Adhesion ECR in Concrete Containing Calcium Nitrite

For increased adhesion ECR cast in concrete containing calcium nitrite (DCI-S), only the ECR(DuPont)-DCI specimens exhibit lower macrocell corrosion losses than conventional ECR cast in concrete containing DCI (Table 4.3). The ECR(DuPont)-DCI specimens exhibit a negligible amount of macrocell corrosion loss. The Student's t-test indicates that the difference between the ECR(DuPont)-DCI and the ECR(DCI) specimens is significant at $\alpha = 0.2$ and that no statistically significant difference exists between the remaining specimens and the ECR(DCI) specimens. The ECR(Valspar) and ECR(DuPont) specimens exhibit 13% and 31%, respectively, of the microcell corrosion loss (Table 3.12) exhibited by the ECR(DCI) specimens, while the ECR(Chromate) specimens exhibit 2.5 times the microcell corrosion loss exhibited by ECR(DCI) specimens. The corrosion disbonded areas (Table 4.2) for the increased adhesion specimens containing DCI range from 32% to 66% of that exhibited by the conventional ECR cast in concrete containing DCI. These results

show that, in general, the combination of increased adhesion ECR and DCI affords a level of corrosion protection similar to that afforded by conventional ECR cast in concrete containing DCI.

4.5.5 Multiple-Coated Reinforcement

In Southern Exposure specimens containing multiple-coated reinforcement, all specimens exhibit much greater corrosion losses than the control specimens containing conventional epoxy-coated reinforcement. In terms of macrocell corrosion loss (Table 4.3), specimens with both the epoxy and zinc layers penetrated exhibit the greatest amount of corrosion loss, 19 and 35 times the macrocell corrosion losses observed in the conventional ECR specimens with four and ten-holes, respectively. The Student's t-test indicates that the difference between both systems and the conventional ECR specimens is significant at $\alpha = 0.02$. The four-hole specimens with only the epoxy layer damaged exhibit 11 times the macrocell corrosion losses observed for the conventional ECR specimen; the difference between the two systems is significant at $\alpha = 0.1$. The MC(only epoxy penetrated)-10h-45 specimens exhibit 5.3 times the macrocell corrosion loss observed for the ECR-10h-45 specimens, although the difference between the two systems is not significantly significant. In terms of microcell corrosion loss (Table 3.12), specimens with both layers penetrated exhibit 13 and 466 times the loss exhibited by the conventional ECR specimens for the ten and four-hole specimens, respectively. Specimens with only the epoxy layer penetrated exhibit 4.8 and 402 times the microcell corrosion rate of conventional ECR specimens (for ten and four-hole specimens, respectively). As shown in Table

4.2, the ten-hole specimens exhibit less disbonded area than the conventional ECR specimens (47% for specimens with both layers penetrated and 71% for specimens with only the epoxy penetrated). The four-hole specimens exhibit higher disbonded areas than conventional ECR specimens (1.7 times higher for specimens with both layers penetrated and 4.6 times higher for specimens with only the epoxy layer penetrated). The cracked beam specimens also exhibit much higher macrocell and microcell corrosion losses than the control specimens containing conventional ECR. The macrocell corrosion losses (Table 4.4) range from 4.7 to 14.3 times the corrosion losses observed in the conventional ECR specimens. Microcell corrosion losses (Table 3.12) range from 3.1 to 8.1 times the corrosion losses observed in conventional ECR specimens. With the exception of the microcell corrosion loss observed for the CB specimens containing four holes through the epoxy, specimens with both protective layers penetrated exhibit much higher corrosion losses than specimens with only the epoxy layer penetrated. This is, in all likelihood, the result of the zinc corroding preferentially to protect the exposed steel. While the corrosion losses observed in the MC specimens are much higher than any other ECR specimens in the study, it must be remembered that the high corrosion losses are due to zinc corrosion. The corrosion products formed as the result of the zinc corrosion are different than the products formed due to the corrosion of the steel. While it has been shown that a corrosion loss of 2500 μm (0.10 in.) would be required to cause concrete cracking due to the corrosion of conventional ECR bars, this value may or may not be valid for corrosion of zinc within concrete. Further evaluation is needed to determine the

amount of zinc corrosion that is required to cause concrete to crack. It is noted that concrete cracking is not observed in any of the specimens containing epoxy-coated or multiple-coated reinforcement in this study and that all MC specimens exhibit microcell and macrocell corrosion losses well below 2500 μm (0.10 in.). Furthermore, although the MC specimens exhibit much higher corrosion losses than the ECR specimens, a corresponding increase in the area of disbonded epoxy does not occur. As shown in Table 4.2, the MC bars in Southern Exposure specimens exhibit 47% to 464% of the corrosion disbonded area exhibited by conventional ECR, and the MC bars in cracked beam specimens exhibit 34% to 57% the corrosion disbonded area exhibited by conventional ECR, which are similar to the results found in the other corrosion protection systems evaluated in this study. Much of the corrosion in the MC specimens, as with the ECR specimens, occurs beneath the epoxy, where there is a limited availability of oxygen. The corrosion products that are formed in the absence of oxygen pose less of a threat to concrete serviceability because their low volume limits their ability to exert pressure to cause tensile stresses in the concrete. All of these considerations suggest that the increased corrosion losses observed in the MC specimens may not be detrimental in terms of bridge deck serviceability, and overall, when multiple-coated reinforcement is compared to conventional ECR purely on the basis of corrosion loss, the multiple-coated reinforcement appears to provide similar corrosion protection.

CHAPTER 5

CONCLUSIONS AND RECOMMENDATIONS

5.1 Summary

This report presents the results of the evaluation of multiple corrosion protection systems for reinforcing steel in concrete. The corrosion protection systems evaluated in this study include:

- Conventional steel reinforcement;
- Conventional epoxy-coated reinforcement (ECR);
- Conventional ECR cast in concrete with water-cement ratios of 0.45 and 0.35 containing one of three corrosion inhibitors, calcium nitrite (DCI-S), Rheocrete 222+, or Hycrete;
- ECR with a primer containing microencapsulated calcium nitrite between the steel and the epoxy;
- ECR with increased adhesion between the epoxy and the steel, including ECR with a chromate pretreatment of the steel prior to the application of the epoxy and ECR coated with improved adhesion epoxy by DuPont and Valspar;
- The three increased adhesion ECR systems cast in concrete containing DCI-S corrosion inhibitor; and
- Multiple-coated reinforcement, with a zinc layer (98% zinc, 2% aluminum), with a nominal thickness of 0.05 mm (2 mils), between the epoxy and the steel.

The corrosion protection systems specified above are evaluated using Southern Exposure (SE) and cracked beam (CB) tests. The corrosion performance of each system is evaluated using macrocell corrosion rates and losses, mat-to-mat resistance, and corrosion potential measurements. Linear polarization resistance measurements are also used to determine microcell corrosion rates and losses. Critical chloride thresholds are measured for each system, and chloride concentrations are measured at 48 and 96 weeks. Upon termination of each test, the reinforcement in each specimen is inspected, and if disbondment is observed, the area of disbonded epoxy is measured.

The relationship between macrocell and microcell corrosion losses in the Southern Exposure and cracked beam specimens is evaluated, along with the relationship between corrosion loss (both macrocell and microcell) and disbonded area in ECR specimens. Finally, the Student's t-test is used to determine the statistical significance of observed differences in performance among the corrosion protection systems.

5.2 Conclusions

The following conclusions are based on the results and observations presented in this report.

1. Of the systems evaluated in this study, conventional steel exhibits the greatest amount of corrosion.

2. ECR, whether in uncracked or cracked concrete, exhibits low corrosion losses. Corrosion losses in these specimens are well below the magnitude of corrosion loss required to cause corrosion-induced surface deterioration.
3. In general, concrete with a *w/c* ratio of 0.35 provides more protection against corrosion than concrete with a *w/c* ratio of 0.45 when cracks are not present in the concrete. However, the lower *w/c* ratio provides little or no additional corrosion protection in cracked concrete.
4. In uncracked concrete, corrosion inhibitors provide additional protection against corrosion. This protection is enhanced by a lower *w/c* ratio. In cracked concrete, however, corrosion inhibitors afford no additional protection against corrosion.
5. Though improved adhesion ECR is effective in preventing corrosion, it exhibits no better corrosion performance than conventional ECR.
6. Improved adhesion ECR, when used in conjunction with the corrosion inhibitor DCI-S, affords a level of corrosion protection similar to that afforded by conventional ECR cast in concrete containing DCI-S.
7. Multiple-coated reinforcement exhibits greater corrosion losses than conventional epoxy-coated reinforcement, but the corrosion products that form as a result of the zinc corrosion are different than the products formed due to the corrosion of steel. Therefore, the increased corrosion losses observed for the multiple-coated reinforcement do not necessarily suggest that it is less effective in protecting against corrosion-induced surface deterioration.

Corrosion losses in MC specimens are below the magnitude of corrosion loss required to cause such deterioration.

8. The relationship between microcell and macrocell corrosion loss is stronger for SE specimens than for CB specimens. Furthermore, the relationship is stronger in specimens with a *w/c* ratio of 0.45 than for specimens with a *w/c* ratio of 0.35.
9. The average area of disbonded epoxy tends to increase as both macrocell and microcell losses increase. With the multiple-coated specimens excluded, disbonded area increases with increases in both macrocell and microcell corrosion loss. This relationship is stronger in SE specimens than in CB specimens, and in both cases, disbonded area shows greater correlation with macrocell corrosion loss than with microcell corrosion loss.
10. For a given level of corrosion loss, multiple-coated bars exhibit less corrosion disbondment than conventional ECR bars.
11. The corrosion disbonded areas observed in Southern Exposure and cracked beam specimens are, respectively, 1.1 to 20 and 2.6 to 22 times the disbonded area measured in cathodic disbondment tests (ASTM A775) for the ECR used in this study. Therefore, the cathodic disbondment test does not appear to be a reliable indicator of corrosion disbondment performance of in-service epoxy-coated reinforcement.
12. The effective critical chloride threshold for epoxy-coated reinforcement is several times higher than that of conventional reinforcement. This is due to

the protection that the epoxy coating provides for the steel against chlorides, moisture, and oxygen. For concrete containing damaged epoxy-coated reinforcement, corrosion initiation will not occur until the chloride concentration at the site of the damage reaches the critical chloride threshold of steel. This results in raising the effective critical chloride threshold of the reinforcement.

5.3 Recommendations

1. Conventional epoxy-coated reinforcement is recommended for use in both top and bottom mats of reinforced concrete bridge decks.
2. A low *w/c* ratio and/or corrosion inhibitors should not be used as the primary means of corrosion protection in concrete bridge decks. This is because, although they provide additional protection in uncracked concrete, they afford little to no additional protection in cracked concrete.
3. Multiple-coated reinforcement may be used in reinforced concrete bridge decks that are subjected to corrosive environments.
4. The relationship between corrosion loss and corrosion disbonded area in ECR should be investigated further. If developed further, this relationship could be useful in predicting the service life of structures containing epoxy-coated reinforcement.
5. Since the cathodic disbondment test does not accurately predict the corrosion disbondment that occurs within a specimen, a new test method for predicting the corrosion disbondment of in-service ECR should be developed.

REFERENCES

AASHTO T 260-94 (1997). "Standard Method of Test for Sampling and Testing for Chloride Ion in Concrete and Concrete Raw Materials," *Standard Specifications for Transportation Materials and Methods of Sampling and Testing*, 19th Ed., Part II - Tests, American Association of State Highway and Transportation Officials, pp. 925-931.

ASTM A 775-04a (2004). "Standard Specification for Epoxy-Coated Steel Reinforcing Bars," ASTM International, West Conshohocken, PA.

ASTM C 192/C 192M-00 (2000). "Practice for Making and Curing Concrete Test Specimens in the Laboratory," ASTM International, West Conshohocken, PA, pp. 126-133.

ASTM C 876-91 "Standard Test Method for Half-Cell Potentials of Uncoated Reinforcing Steel in Concrete," *ASTM International*, West Conshohocken, PA, pp. 457-462.

ASTM G 8-96 (1996). "Standard Test Methods for Cathodic Disbonding of Pipeline Coatings," ASTM International, West Conshohocken, PA, pp. 864-872.

Andrade, C. and González, J. A. (1978). "Quantitative Measurements of Corrosion Rate of Reinforcing Steels Embedded in Concrete Using Polarization Resistance Measurements," *Werkstoffe und Korrosion*, Vol. 29, No. 8, pp. 515-519.

Ann, K. Y., Jung, H. S., Kim, H. S., Kim, S. S. and Moon, H. Y. (2006). "Effect of Calcium Nitrite-based Corrosion Inhibitor in Preventing Corrosion of Embedded Steel in Concrete," *Cement and Concrete Research*, Vol. 36, No. 3, pp. 530-535.

Berke, N.S. (1987). "The Effects of Calcium Nitrite and Mix Design on the Corrosion Resistance of Steel in Concrete (Part 2, Long-Term Results)," *Proc., Corrosion-87 Symposium on Corrosion of Metals in Concrete*, National Association of Corrosion Engineers, Houston, TX, pp. 124-144.

Berke, N. S. and Rosenberg, A. (1989). "Technical Review of Calcium Nitrite Corrosion Inhibitor in Concrete," *Transportation Research Record*, Vol. No. 1211, pp. 19-27.

Berke, N. S., Hicks, M. C., and Tourney, P. G. (1993). "Evaluation of Concrete Corrosion Inhibitors," *Proceedings, 12th International Corrosion Congress, Houston, Texas*, pp. 3271-3286.

Bernard, E. and Verbeck, G.J. (1975). "Corrosion of Metals in Concrete – Needed Research," *SP 49-4*, ACI International, pp. 39-46.

Bertolini, L., Elsener, B., Pedeferri, P. and Polder, R. (2004). *Corrosion of Steel in Concrete: Prevention, Diagnosis, Repair*, Wiley-VCH, Weinheim, 392 pp.

Bola, M. M. B. and Newtson, C. M. (2005). "Field Evaluation of Marine Structures Containing Calcium Nitrite," *Journal of Performance of Constructed Facilities*, Vol. 19, No. 1, pp. 28-35.

Broomfield, J. P. (1997). *Corrosion of Steel in Concrete: Understanding, Investigation, and Repair*, E & FN Spon, UK, 240 pp.

Brown, M.C., Weyers, R.E., and Sprinkel, M.M. (2006). "Service Life Extension of Virginia Bridge Decks Afforded by Epoxy-Coated Reinforcement," *Journal of ASTM International*, Vol. 3, No.2, 13 pp.

Civjan, S. A. (2005). "Effectiveness of Corrosion Inhibiting Admixture Combinations in Structural Concrete," *Cement and Concrete Composites*, Vol. 27, No. 6, pp. 688-703.

Civjan, S. A. (2005). "A New Corrosion Inhibitor for Concrete Construction," *Third International Conference on Construction Materials: Performance, Innovations and Structural Implications, ConMat '05*, Vancouver, British Columbia, Aug.

Civjan, S. A., LaFave, J. M., Lovett, D., Sund, D. J. and Trybulski, J. (2003), "Performance Evaluation and Economic Analysis of Combinations of Durability Enhancing Admixtures (Mineral and Chemical) in Structural Concrete for the Northeast U.S.A.," *NETCR36*, The New England Transportation Consortium, Storrs, CT, Feb., 166 pp.

Clear, K.C. (1989). "Measuring Rate of Corrosion of Steel in Field Concrete Structure," *Transportation Research Record*, No. 1211, pp. 28-38.

Darwin, D., Browning, J., O'Reilly, M., and Xing, L. (2007). "Critical Chloride Corrosion Threshold for Galvanized Reinforcing Bars," *SL Report* No. 07-2, The University of Kansas Center for Research, Inc., Lawrence, KS, 28 pp.

Diamond, S. (1986). "Chloride Concentrations in Concrete Pore Solutions Resulitng From Calcium and Sodium Chloride Admixtures," *Cement, Concrete, and Aggregates*, Vol. 8, No. 2, pp. 97-102.

Gaidis, J. M. (2004). "Chemistry of Corrosion Inhibitors," *Cement and Concrete Composites*, Vol. 26, No. 3, pp. 181-189.

Glass, G. K. and Buenfeld, N. R. (1997). "The Presentation of the Chloride Threshold Level for Corrosion of Steel in Concrete," *Corrosion Science*, Vol. 39, No. 5, pp. 1001-1013.

Gong, L., Darwin, D., Browning, J. P., and Locke, C. E. (2006). "Evaluation of Multiple Corrosion Protection Systems and Stainless Steel Clad Reinforcement for Reinforced Concrete," *SM Report* No. 82, University of Kansas Center for Research, Lawrence, KS, 504 pp.

Gouda, V. K. (1970). "Corrosion and Corrosion inhibition of Reinforcing Steel, I. Immersed in Alkaline Solutions," *British Corrosion Journal*, Vol. 5, No. 5, pp. 198-203.

Gu, P. and Beaudoin, J. J. (1998). "Obtaining Effective Half-Cell Potential Measurements in Reinforced Concrete Structures," *Construction Technology Updates*, Vol. 18, National Research Council of Canada, 4 pp.

Guo, G., Darwin, D., Browning, J. P. and Locke, C. E. (2006), "Laboratory and Field Tests of Multiple Corrosion Protection Systems for Reinforced Concrete Bridge Components and 2205 Pickled Stainless Steel," *SM Report* No. 85, University of Kansas Center for Research, Lawrence, Kansas, 776 pp.

Hansson, C. M., Mammoliti, L. and Hope, B. B. (1998). "Corrosion Inhibitors in Concrete - Part I: The Principles," *Cement and Concrete Research*, Vol. 28, No. 12, pp. 1775-1781.

Hausmann, D. A. (1967). "Steel Corrosion in Concrete," *Materials Protection*, Vol. 6, No. 11, pp. 19-23.

Hunkeler, F. (2005). "Corrosion in Reinforced Concrete: Processes and Mechanisms," *Corrosion in Reinforced Concrete Structures*, 1st Ed., Böhni, H., Woodhead Publishing Limited, Cambridge, pp. 1-45

Hussain, S. E., Al-Gahtani, A. S. and Rasheeduzzafar (1996). "Chloride Threshold for Corrosion of Reinforcement in Concrete," *ACI Materials Journal*, Vol. 93, No. 6, pp. 534-538.

Ji, J., Darwin, D., and Browning, J. P. (2005), "Corrosion Resistance of Duplex Stainless Steels and MMFX Microcomposite Steel for Reinforced Concrete Bridge Decks," *SM Report* No. 80, University of Kansas Center for Research, Inc., Lawrence, Kansas, 456 pp.

Jones, D. A. (1996). *Principles and Prevention of Corrosion*, Prentice Hall, Upper Saddle River, NJ, 572 pp.

Kepler, J. L., Darwin, D. and Locke, C. E. (2000). "Evaluation of Corrosion Protection Methods for Reinforced Concrete Highway Structures," *SM Report* No. 58, University of Kansas Center for Research, Lawrence, KS, 221 pp.

Kirkup, Les (2002). *Data Analysis with Excel: An Introduction for Physical Scientists*, Cambridge University Press, Cambridge, United Kingdom, 446 pp.

Lindquist, W. D., Darwin, D., Browning, J. P. (2005). "Cracking and Chloride Contents in Reinforced Concrete Bridge Decks," *SM Report* No. 78, Univeristy of Kansas Center for Research, Lawrence, KS, 453 pp.

Lindquist, W. D., Darwin, D., Browning, J. P., and Miller, G. (2006). "Effect of Cracking on Chloride Content in Concrete Bridge Decks," *ACI Materials Journal*, Vol. 103, No. 6, pp. 467-473.

Manning, D. G. (1996). "Corrosion Performance of Epoxy-Coated Reinforcing Steel: North American Experience," *Construction and Building Materials*, Vol. 10, No. 5, pp. 349-365.

McDonald, D. B., Pfeifer, D. W. and Sherman, M. R. (1998). "Corrosion Evaluation of Epoxy-Coated, Metallic-Clad and Solid Metallic Reinforcing Bars in Concrete," *FHWA-RD-98-153*, Federal Highway Administration, McLean, VA, 127 pp.

Mehta, P. K. and Monteiro, P. J. M. (2006). *Concrete: Microstructure, Properties, and Materials*, 3rd Ed., McGraw-Hill, New York, 659 pp.

Mindess, S., Young, J. F. and Darwin, D. (2003). *Concrete*, 2nd Ed., Pearson Education, Inc., Upper Saddle River, NJ, 644 pp.

Nmai, C. K., Farrington, S. A., and Bobrowski, G. (1992). "Organic-Based Corrosion-Inhibiting Admixture for Reinforced Concrete," *Concrete International*, Vol. 14, No. 4, pp. 45-51.

Ormellese, M., Berra, M., Bolzoni, F. and Pastore, T. (2006). "Corrosion Inhibitors for Chlorides Induced Corrosion in Reinforced Concrete Structures," *Cement and Concrete Research*, Vol. 36, No. pp. 536-547.

Pfeifer, D. W. (2000). "High Performance Concrete and Reinforcing Steel with a 100-Year Service Life," *PCI Journal*, Vol. 45, No. 3, pp. 46-54.

Pyc, W. A., Zemajtis, J., Weyers, R. E., and Sprinkel, M. M. (1999). "Evaluating Corrosion-Inhibiting Admixtures," *Concrete International*, Vol. 21, No. 4, pp. 39-44.

Pyc, W. A., Weyers, R. E., Weyers, R. M., Mokarem, D. W., and Zemajtis, J. (2000). "Field Performance of Epoxy-Coated Reinforcing Steel in Virginia Bridge Decks," *VTRC 00-R16*, Virginia Transportation Research Council, 38 pp.

Stern, M. and Geary, A. L. (1957). "Electrochemical Polarization. I. A Theoretical Analysis of the Shape Polarization Curves," *Journal of the Electrochemical Society*, Vol. 104, No. 1, pp. 56-63.

Torres-Acosta, A. and Sagüés, A. (2004). "Concrete Cracking by Localizad Steel Corrosion – Geometric Effects," *ACI Materials Journal*, Vol. 101, No. 6, pp. 501-507.

Virmani, Y. P. (1990). "Effectiveness of Calcium Nitrite Admixtures as a Corrosion Inhibitor," *Public Roads*, Vol. 54, No.1, pp. 171-182.

Yunovich, M., Thompson, N. G. Balvanyos, T., and Lave, L. (2002). "Highway Bridges," Appendix D, *Corrosion Cost and Preventive Strategies in the United States*, by G. H. Koch, M. PO., H. Broongers, N. G. Thompson, Y.P. Virmani, and J.H. Payer, Report No. FHWA-RD-01-156, Federal Highway Administration, McLean, VA, 773 pp.

APPENDIX A

CORROSION RATES, TOTAL CORROSION LOSSES, AND CORROSION POTENTIALS FOR INDIVIDUAL SPECIMENS

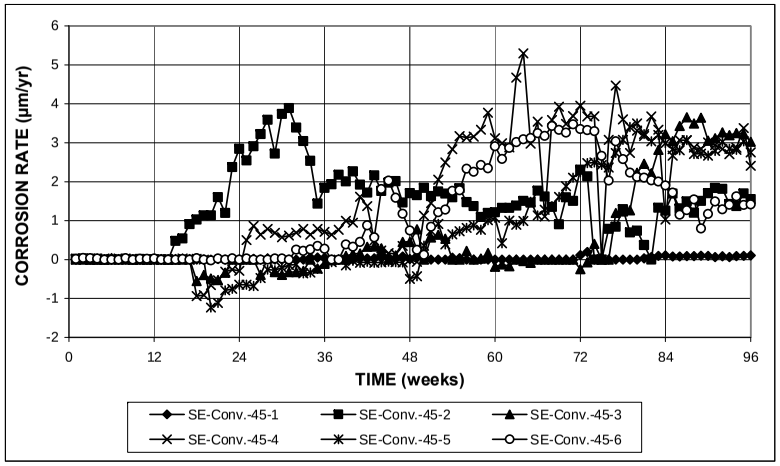

(a)

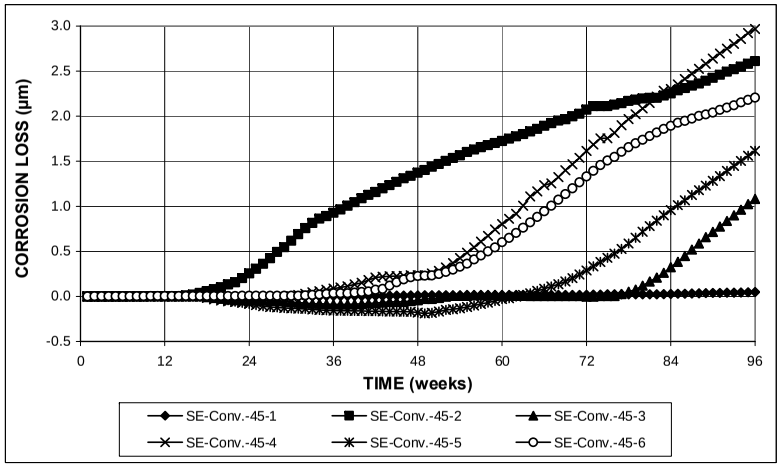

(b)

Figure A.1 – (a) Corrosion rates and (b) total corrosion loss in the Southern Exposure test for specimens with conventional steel, w/c = 0.45.

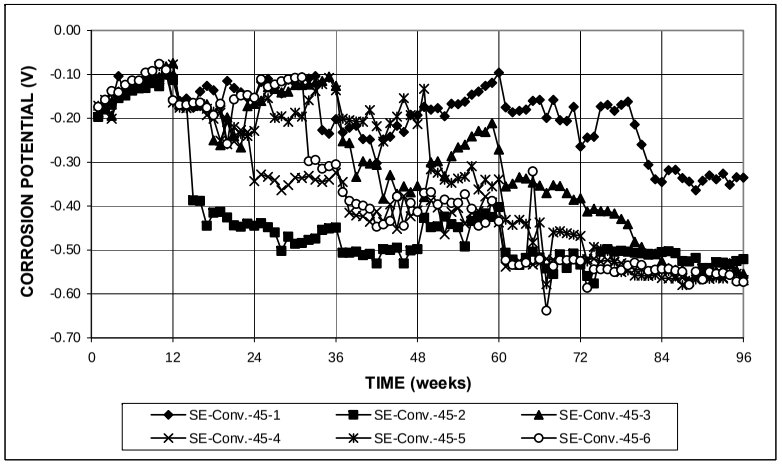

(a)

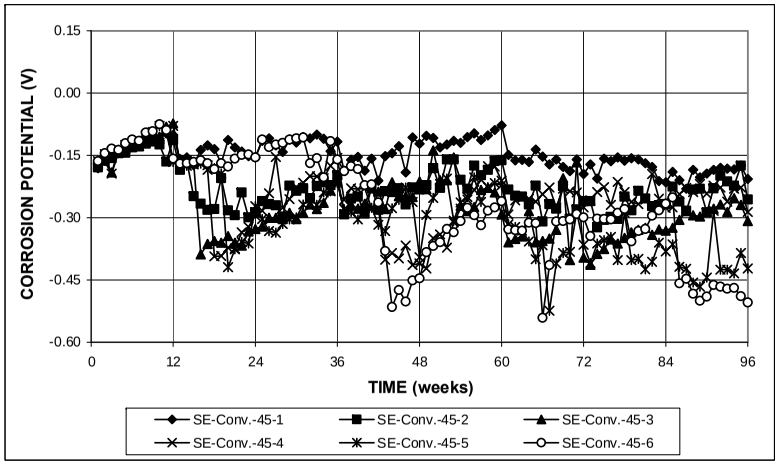

(b)

Figure A.2 – (a) Top mat corrosion potentials and (b) bottom mat corrosion potentials, with respect to the copper-copper sulfate electrode, in the Southern Exposure test for specimens with conventional steel, w/c = 0.45.

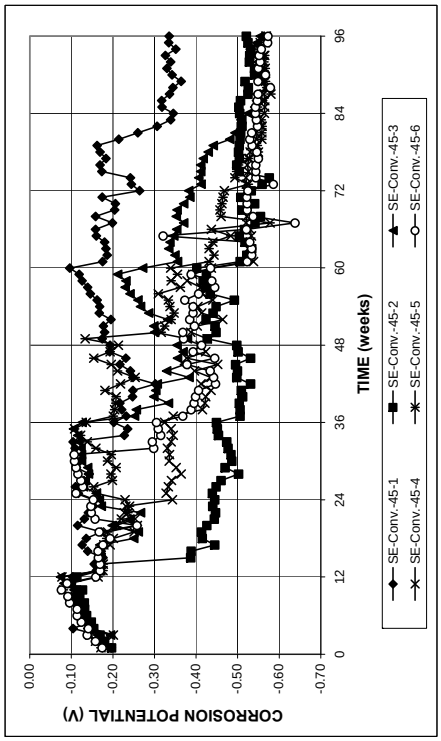

(a)

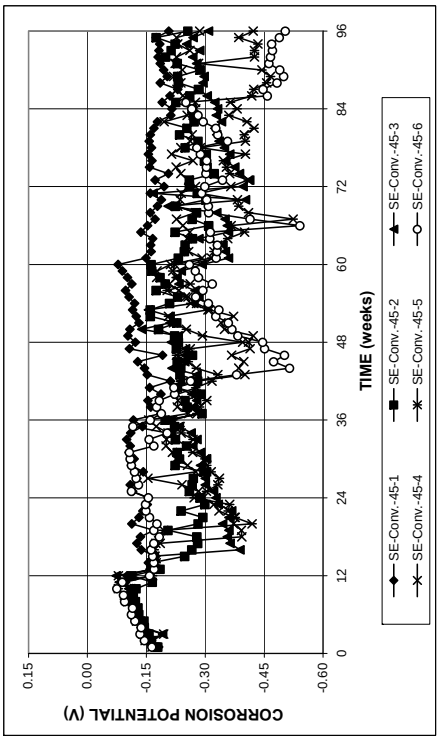

(b)

Figure A.4 – (a) Top mat corrosion potentials and (b) bottom mat corrosion potentials, with respect to the copper-copper sulfate electrode, in the Cracked Beam test for specimens with conventional steel, w/c = 0.45.

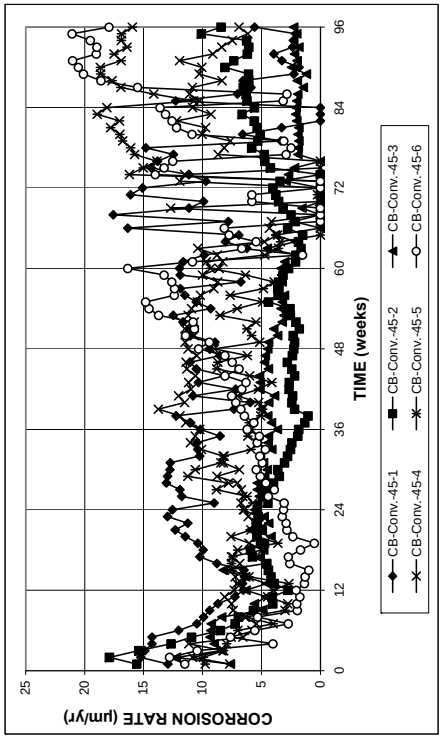

(a)

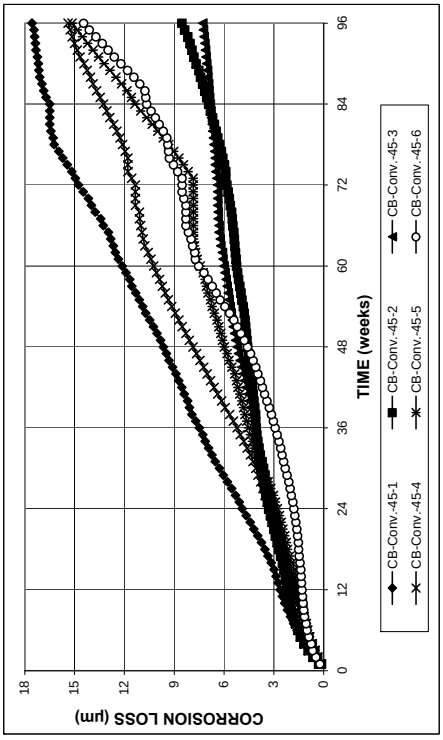

(b)

Figure A.3 – (a) Corrosion rates and (b) total corrosion loss in the Cracked Beam test for specimens with conventional steel, w/c = 0.45.

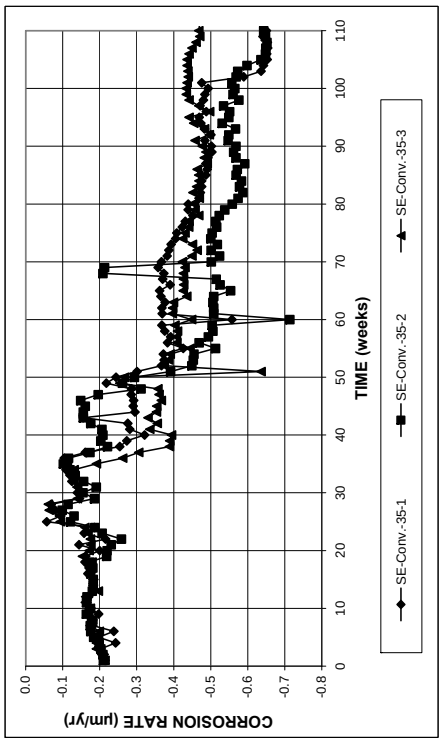

(a)

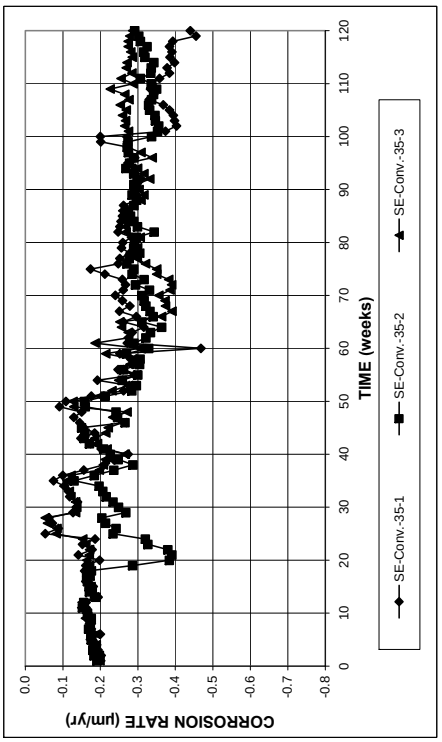

(b)

Figure A.6 – (a) Top mat corrosion potentials and (b) bottom mat corrosion potentials, with respect to the copper-copper sulfate electrode, in the Southern Exposure test for specimens with conventional steel, w/c = 0.35.

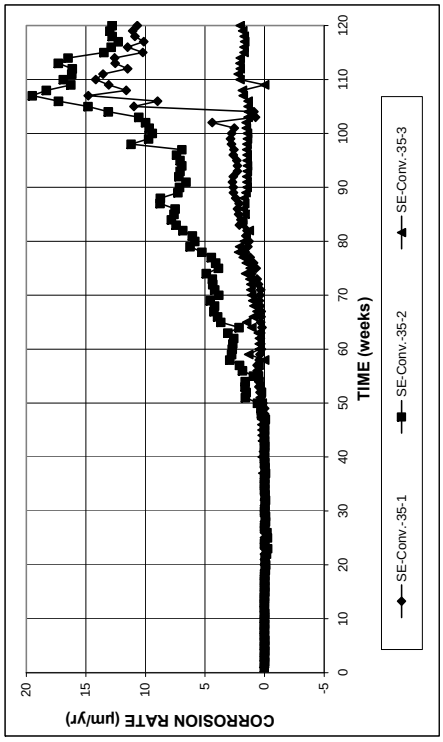

(a)

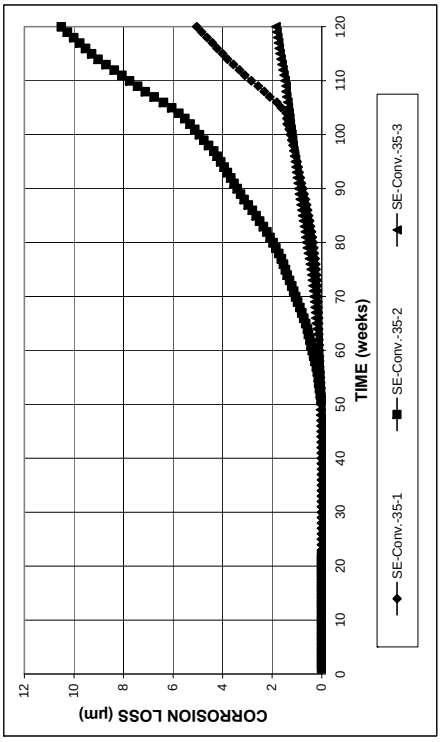

(b)

Figure A.5 – (a) Corrosion rates and (b) total corrosion loss in the Southern Exposure test for specimens with conventional steel, w/c = 0.35.

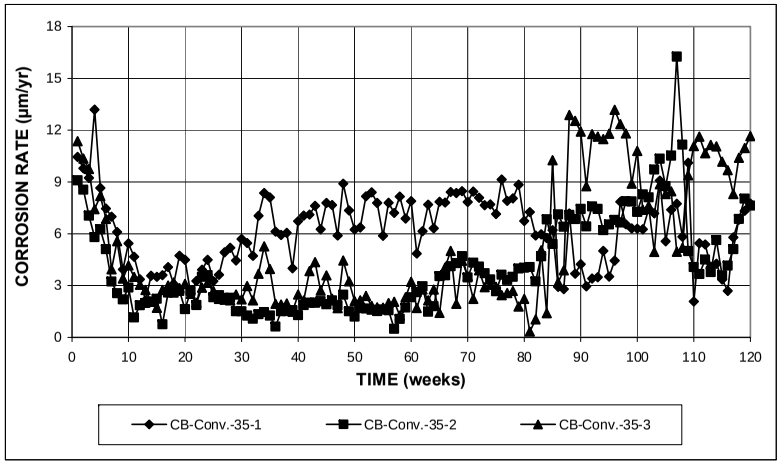

(a)

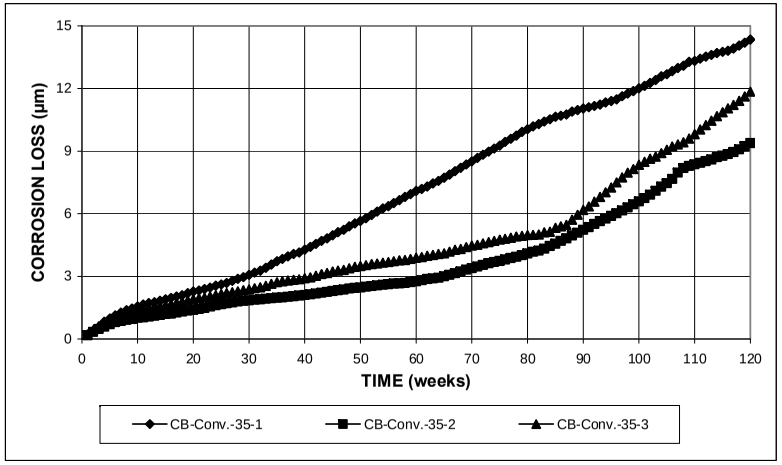

(b)

Figure A.7 – (a) Corrosion rates and (b) total corrosion loss in the Cracked Beam test for specimens with conventional steel, w/c = 0.35.

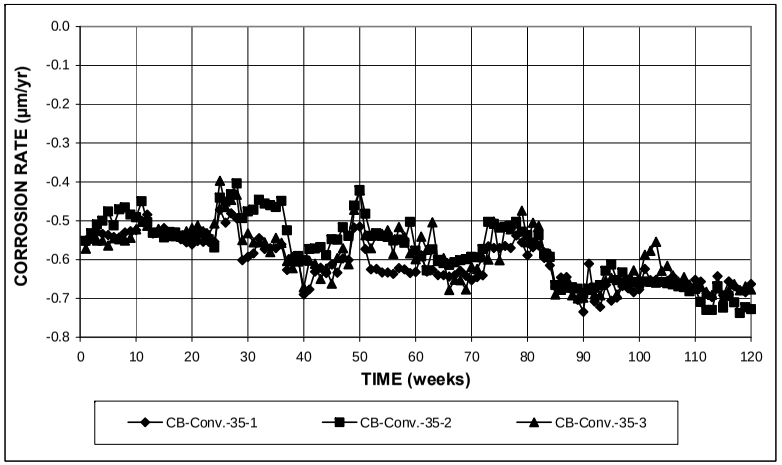

(a)

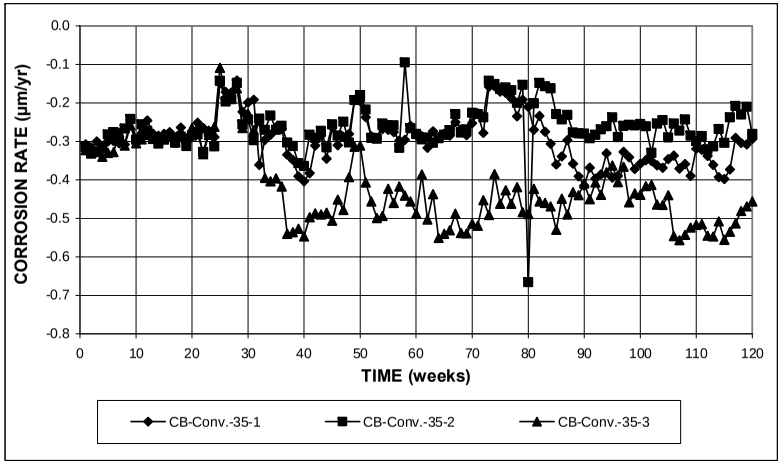

(b)

Figure A.8 – (a) Top mat corrosion potentials and (b) bottom mat corrosion potentials, with respect to the copper-copper sulfate electrode, in the Cracked Beam test for specimens with conventional steel, w/c = 0.35.

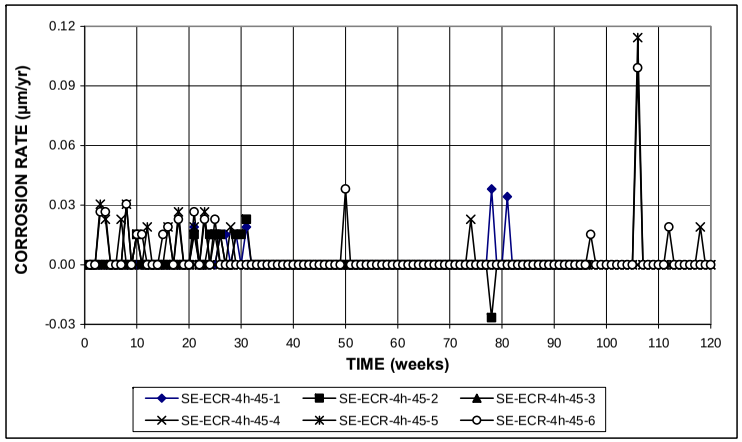

(a)

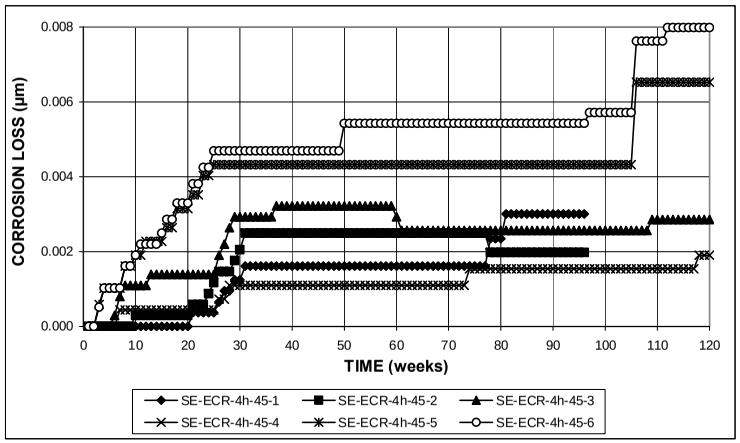

(b)

Figure A.9 – (a) Corrosion rates and (b) total corrosion loss based on total area of the bar in the Southern Exposure test for specimens with ECR (four 3-mm (1/8-in.) diameter holes), w/c = 0.45.

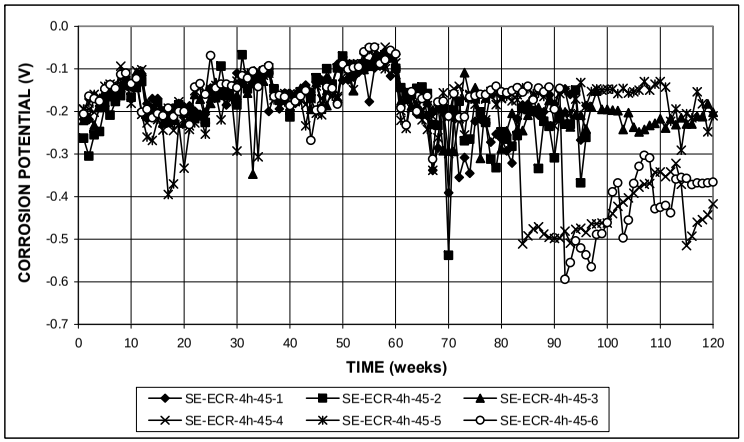

(a)

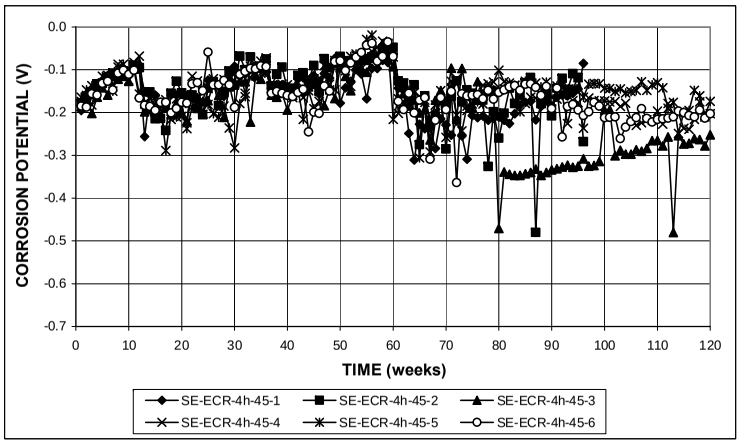

(b)

Figure A.10 – (a) Top mat corrosion potentials and (b) bottom mat corrosion potentials, with respect to the copper-copper sulfate electrode, in the Southern Exposure test for specimens with ECR (four 3-mm (1/8-in.) diameter holes), w/c = 0.45.

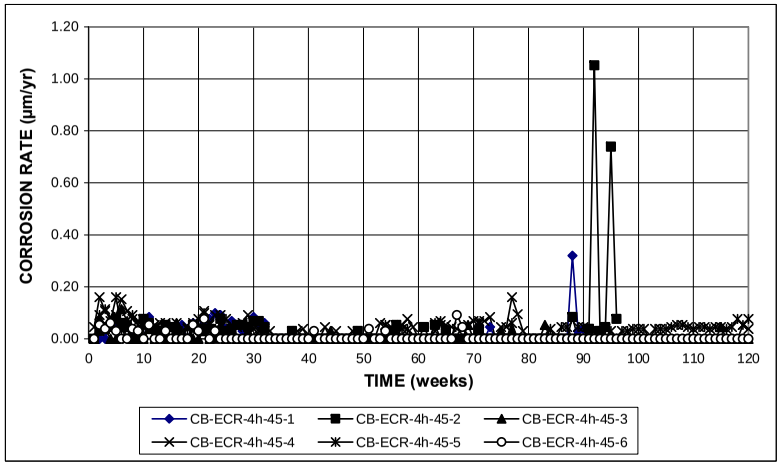

(a)

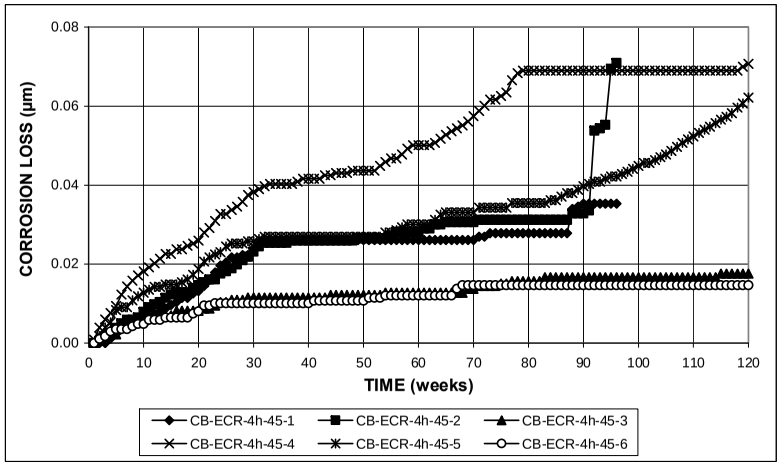

(b)

Figure A.11 – (a) Corrosion rates and (b) total corrosion loss based on total area of the bar in the Cracked Beam test for specimens with ECR (four 3-mm (1/8-in.) diameter holes), w/c = 0.45.

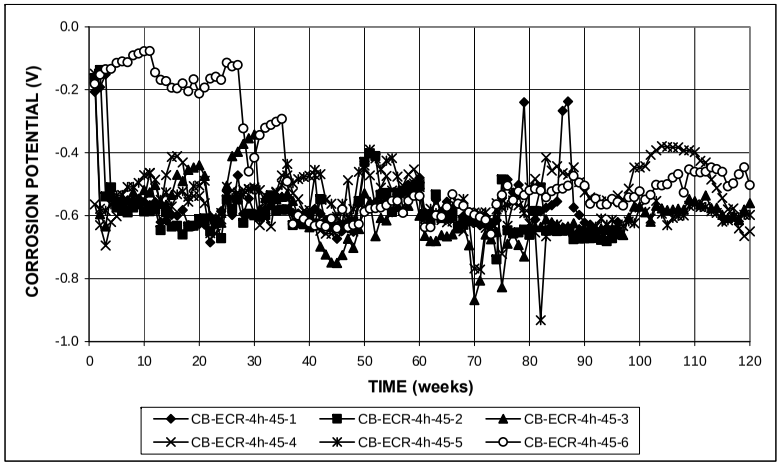

(a)

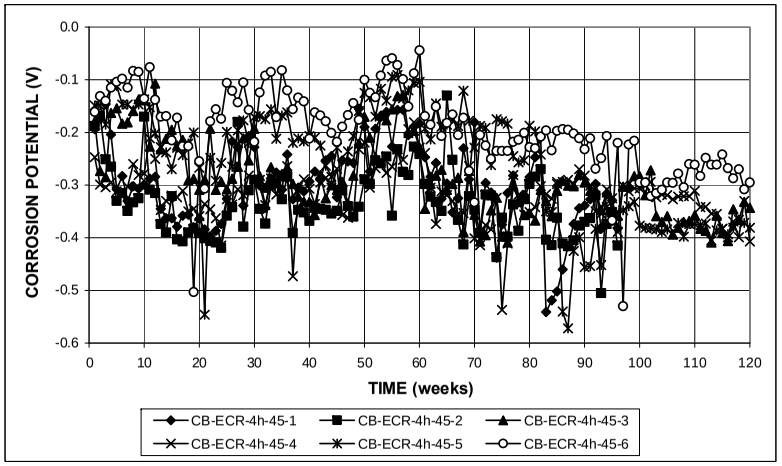

(b)

Figure A.12 – (a) Top mat corrosion potentials and (b) bottom mat corrosion potentials, with respect to the copper-copper sulfate electrode, in the Cracked Beam test for specimens with ECR (four 3-mm (1/8-in.) diameter holes), w/c = 0.45.

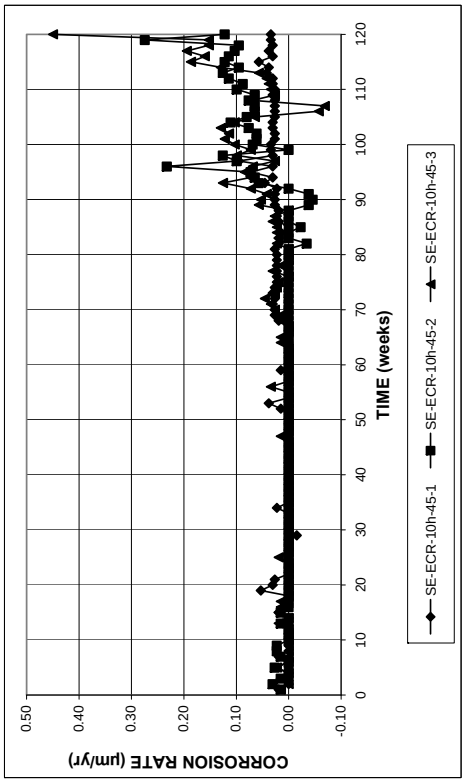

Figure A.13 – (a) Corrosion rates and (b) total corrosion loss based on total area of the bar in the Southern Exposure test for specimens with ECR (ten 3-mm (1/8-in.) diameter holes). w/c = 0.45.

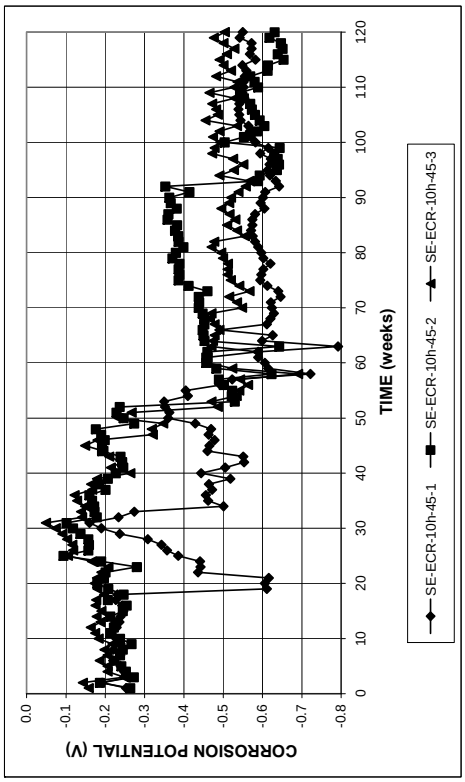

Figure A.14 – (a) Top mat corrosion potentials and (b) bottom mat corrosion potentials, with respect to the copper-copper sulfate electrode, in the Southern Exposure test for specimens with ECR (ten 3-mm (1/8-in.) diameter holes), w/c = 0.45.

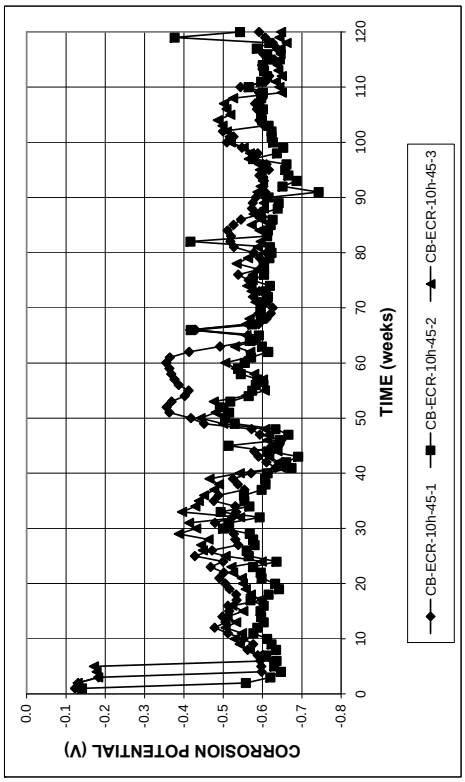

(a)

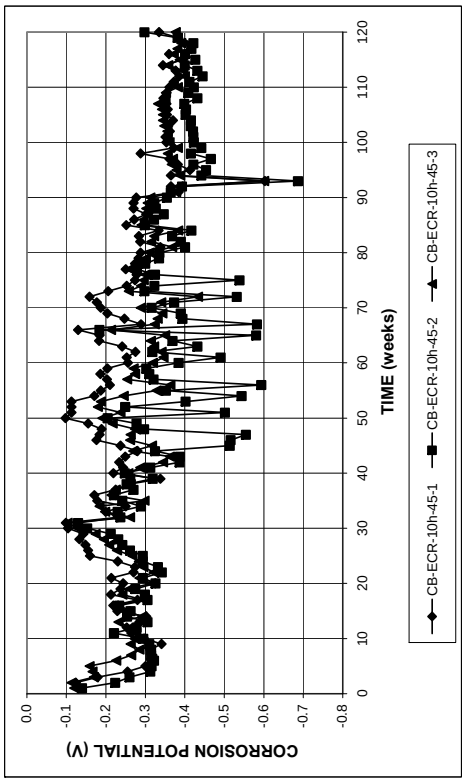

(b)

Figure A.16 – (a) Top mat corrosion potentials and (b) bottom mat corrosion potentials, with respect to the copper-copper sulfate electrode, in the Cracked Beam test for specimens with ECR (ten 3-mm (1/8-in.) diameter holes), w/c = 0.45.

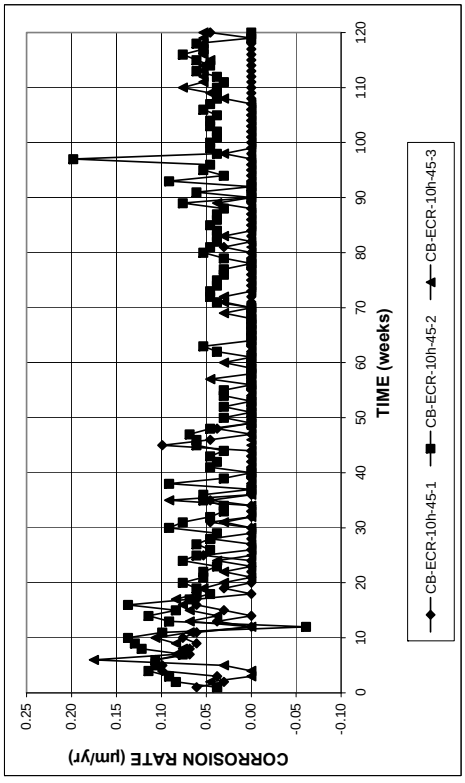

(a)

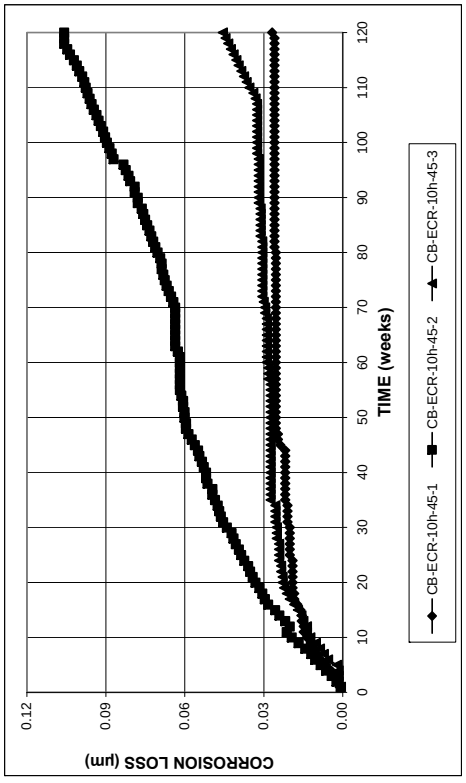

(b)

Figure A.15 – (a) Corrosion rates and (b) total corrosion loss based on total area of the bar in the Cracked Beam test for specimens with ECR (ten 3-mm (1/8-in.) diameter holes), w/c = 0.45.

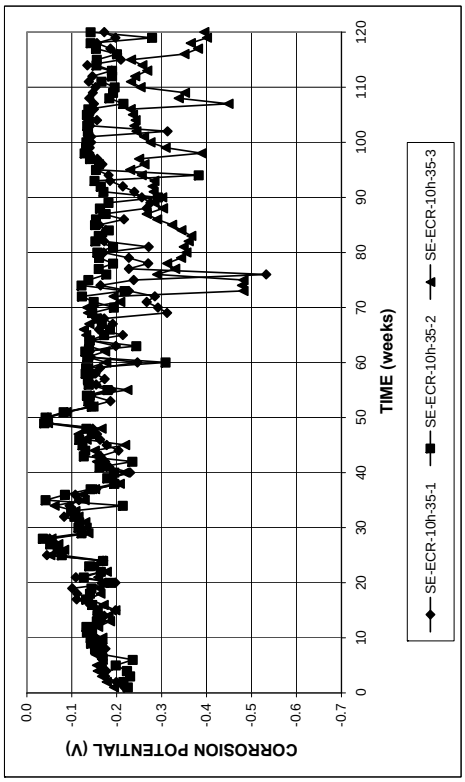

(a)

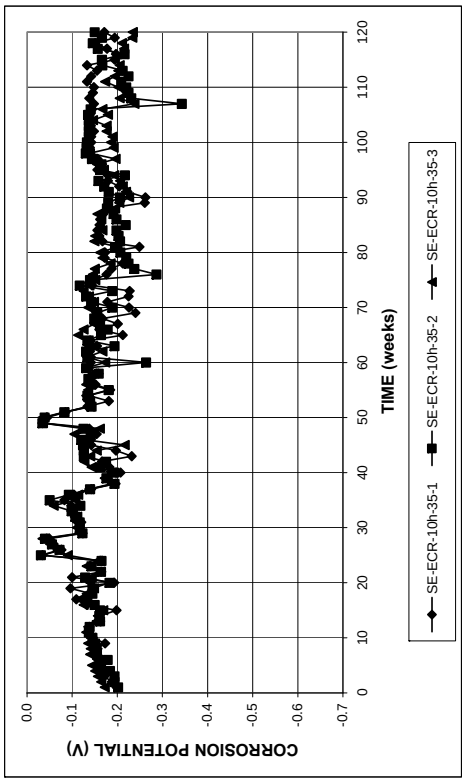

(b)

Figure A.18 – (a) Top mat corrosion potentials and (b) bottom mat corrosion potentials, with respect to the copper-copper sulfate electrode, in the Southern Exposure test for specimens with ECR (ten 3-mm (1/8-in.) diameter holes), w/c = 0.35.

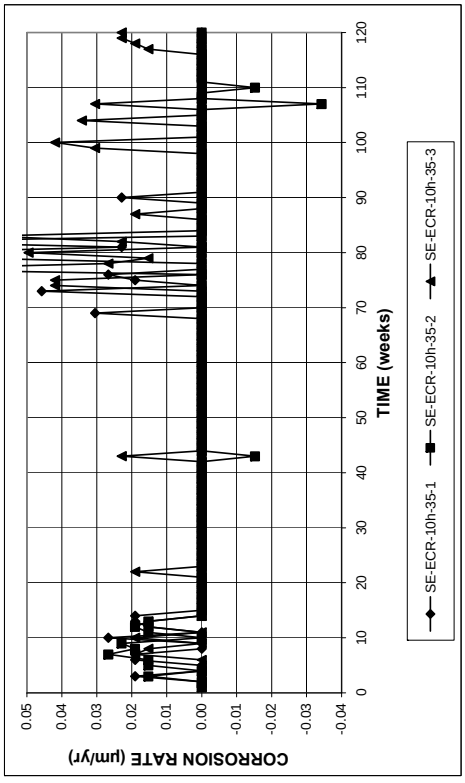

(a)

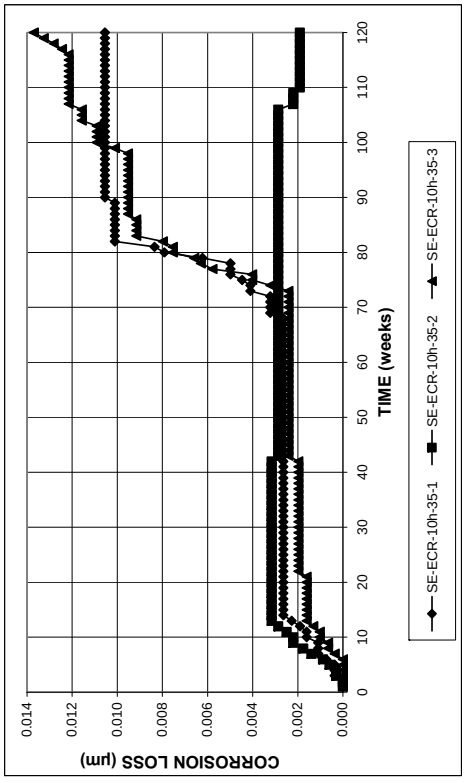

(b)

Figure A.17 – (a) Corrosion rates and (b) total corrosion loss based on total area of the bar in the Southern Exposure test for specimens with ECR (ten 3-mm (1/8-in.) diameter holes), w/c = 0.35.

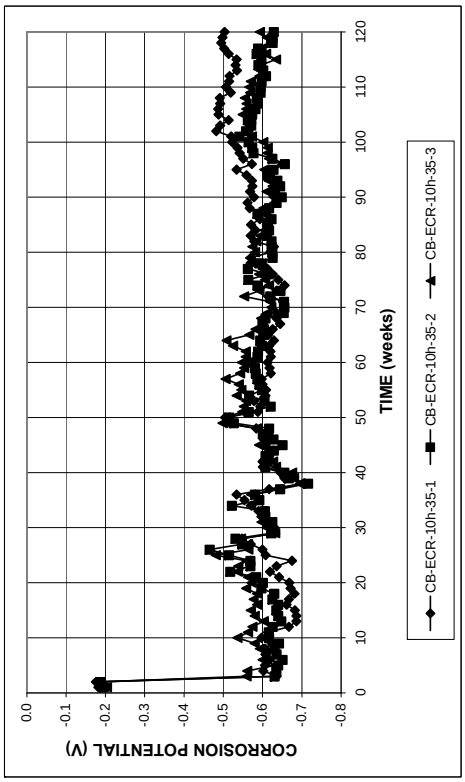

(a)

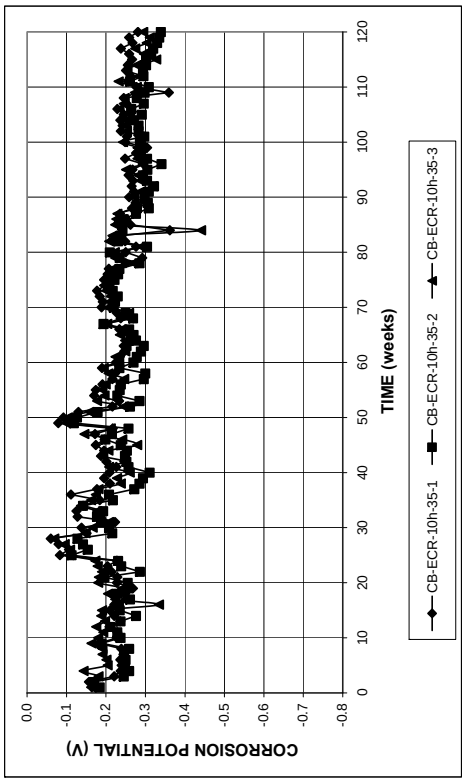

(b)

Figure A.20 – (a) Top mat corrosion potentials and (b) bottom mat corrosion potentials, with respect to the copper-copper sulfate electrode, in the Cracked Beam test for specimens with ECR (ten 3-mm (1/8-in.) diameter holes), w/c = 0.35.

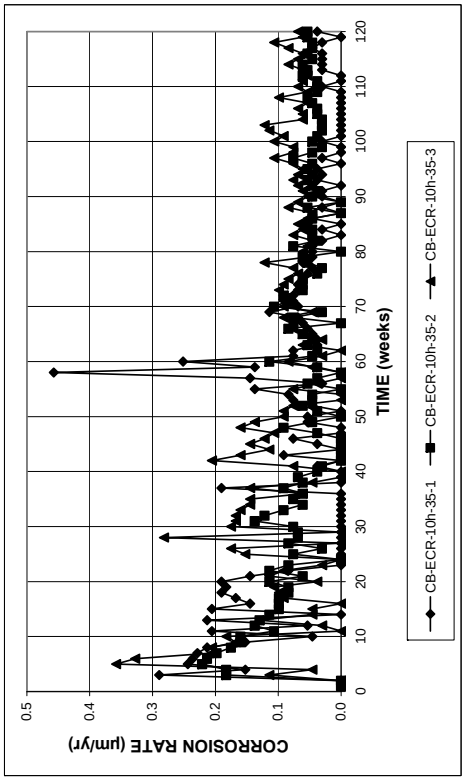

(a)

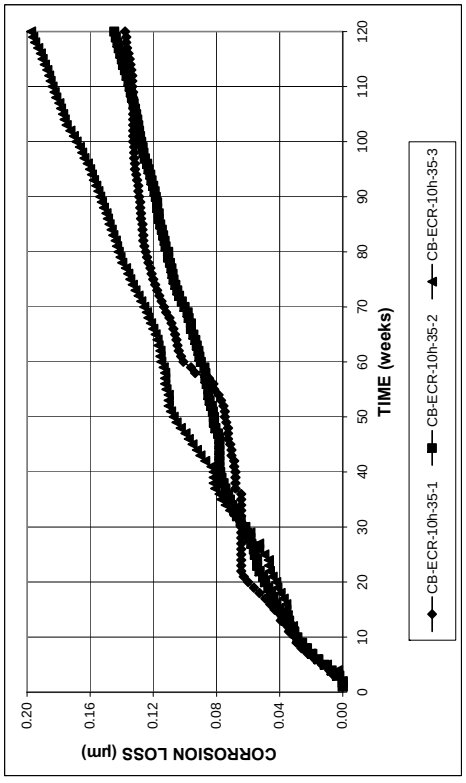

(b)

Figure A.19 – (a) Corrosion rates and (b) total corrosion loss based on total area of the bar in the Cracked Beam test for specimens with ECR (ten 3-mm (1/8-in.) diameter holes), w/c = 0.35.

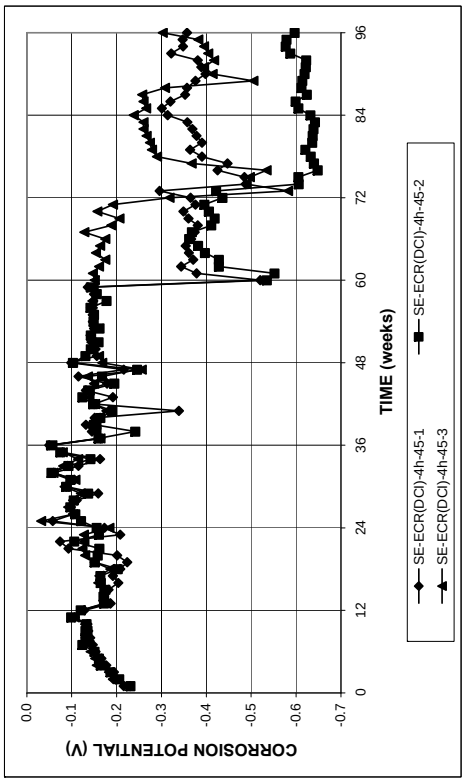

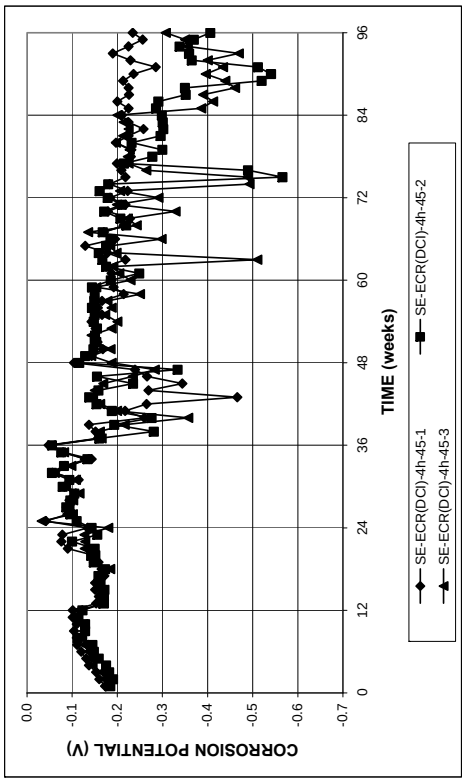

Figure A.22 – (a) Top mat corrosion potentials and (b) bottom mat corrosion potentials, with respect to the copper-copper sulfate electrode, in the Southern Exposure test for specimens with ECR in concrete with DCI (four 3-mm (1/8-in.) diameter holes), w/c = 0.45.

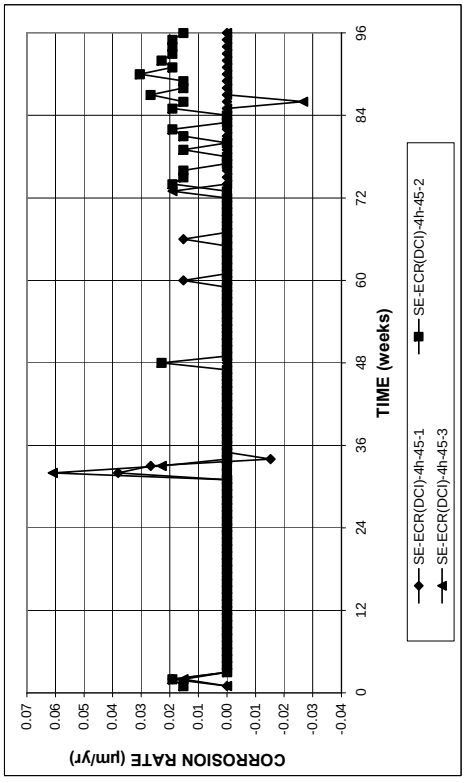

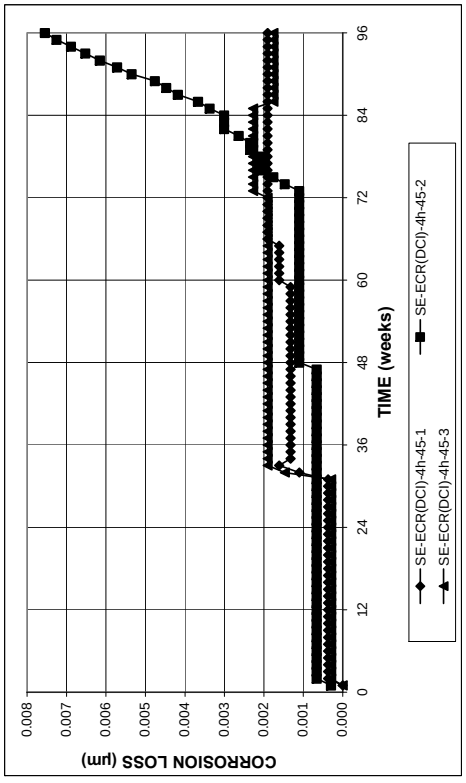

Figure A.21 – (a) Corrosion rates and (b) total corrosion loss based on total area of the bar in the Southern Exposure test for specimens with ECR in concrete with DCI (four 3-mm (1/8-in.) diameter holes), w/c = 0.45.

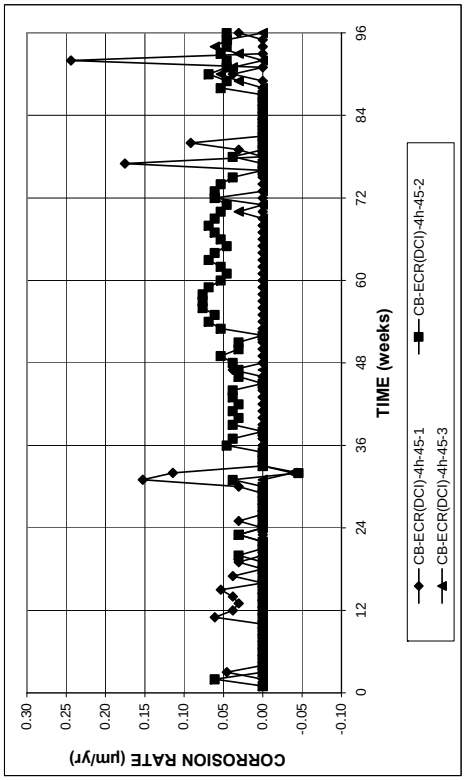

Figure A.23 – (a) Corrosion rates and (b) total corrosion loss based on total area of the bar in the Cracked Beam test for specimens with ECR in concrete with DCI (four 3-mm (1/8-in.) diameter holes), w/c = 0.45.

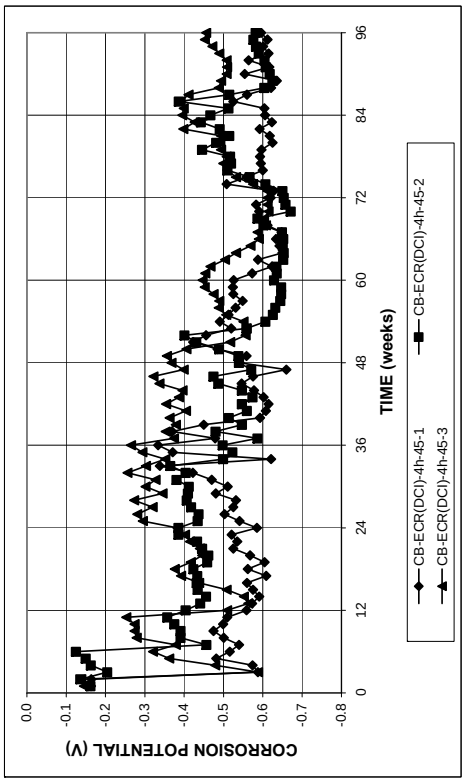

Figure A.24 – (a) Top mat corrosion potentials and (b) bottom mat corrosion potentials, with respect to the copper-copper sulfate electrode, in the Cracked Beam test for specimens with ECR in concrete with DCI (four 3-mm (1/8-in.) diameter holes), w/c = 0.45.

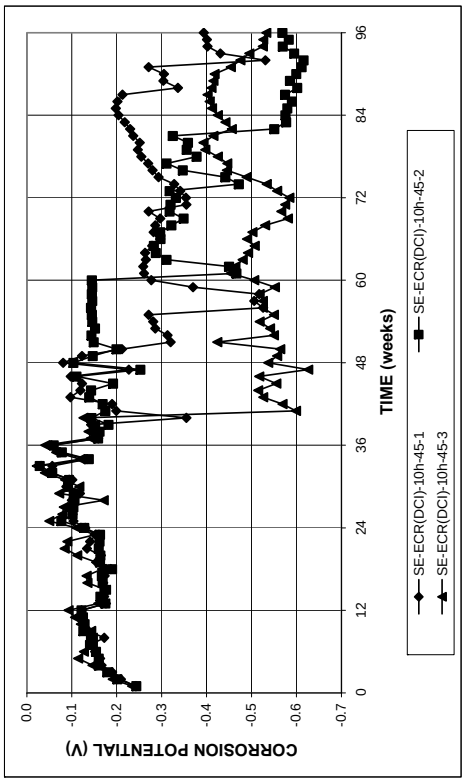

(a)

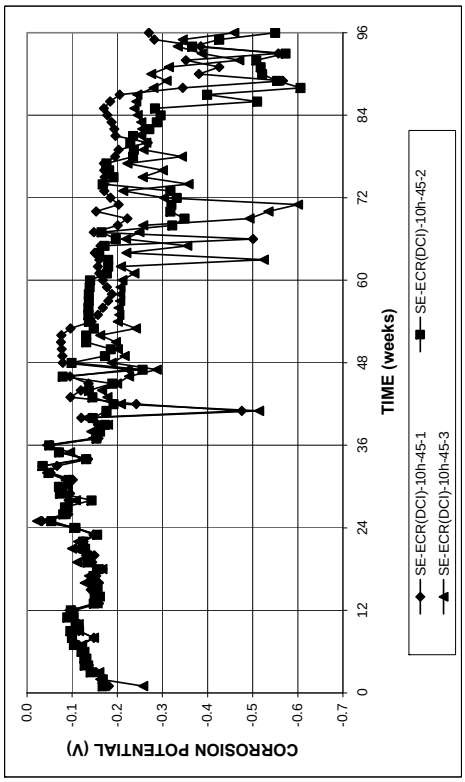

(b)

Figure A.26 – (a) Top mat corrosion potentials and (b) bottom mat corrosion potentials, with respect to the copper-copper sulfate electrode, in the Southern Exposure test for specimens with ECR in concrete with DCI (ten 3-mm (1/8-in.) diameter holes), w/c = 0.45.

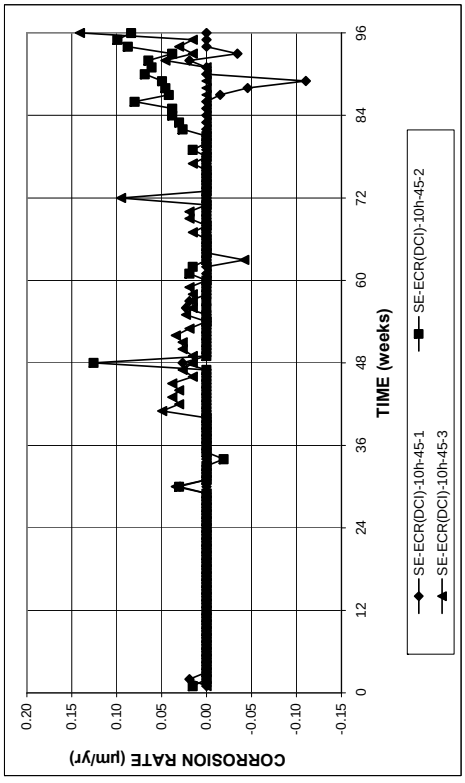

(a)

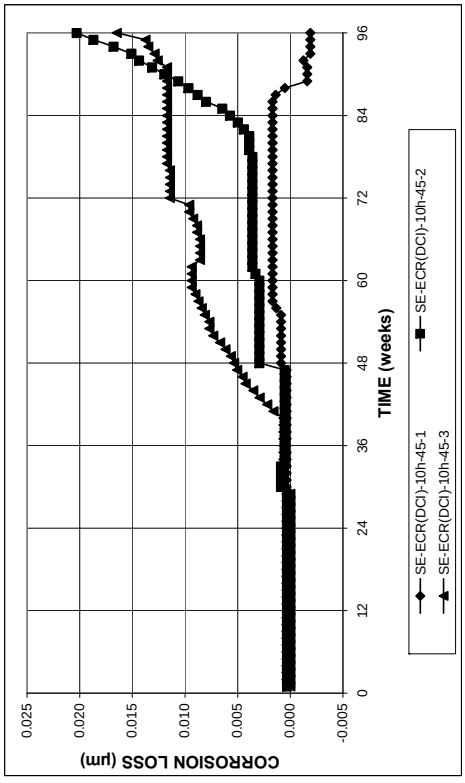

(b)

Figure A.25 – (a) Corrosion rates and (b) total corrosion loss based on total area of the bar in the Southern Exposure test for specimens with ECR in concrete with DCI (ten 3-mm (1/8-in.) diameter holes), w/c = 0.45.

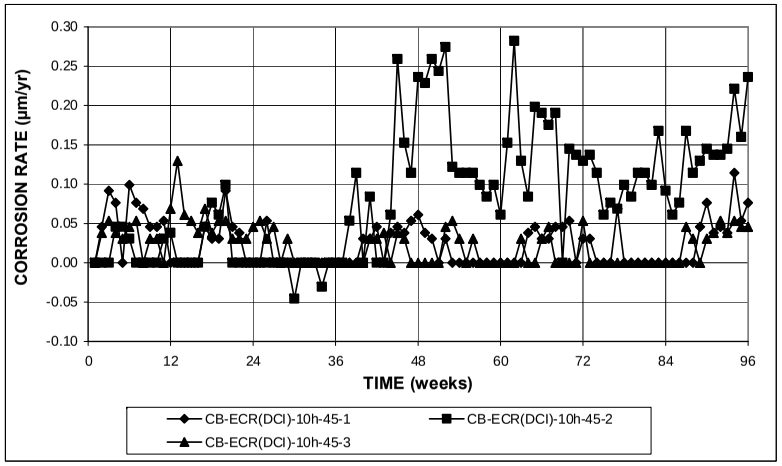

(a)

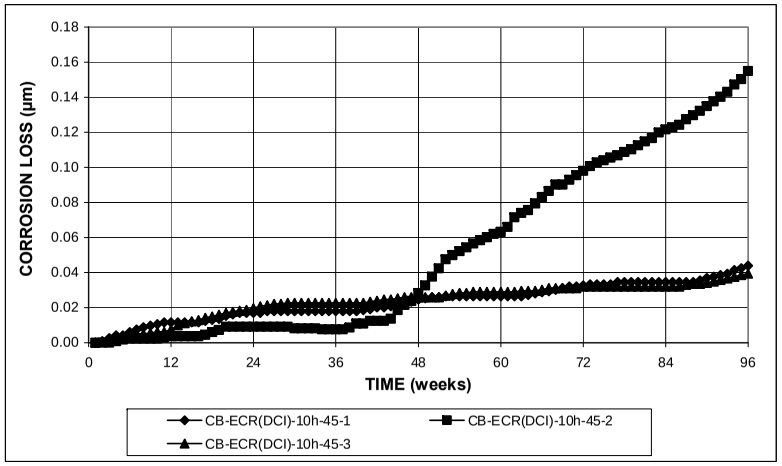

(b)

Figure A.27 – (a) Corrosion rates and (b) total corrosion loss based on total area of the bar in the Cracked Beam test for specimens with ECR in concrete with DCI (ten 3-mm (1/8-in.) diameter holes), w/c = 0.45.

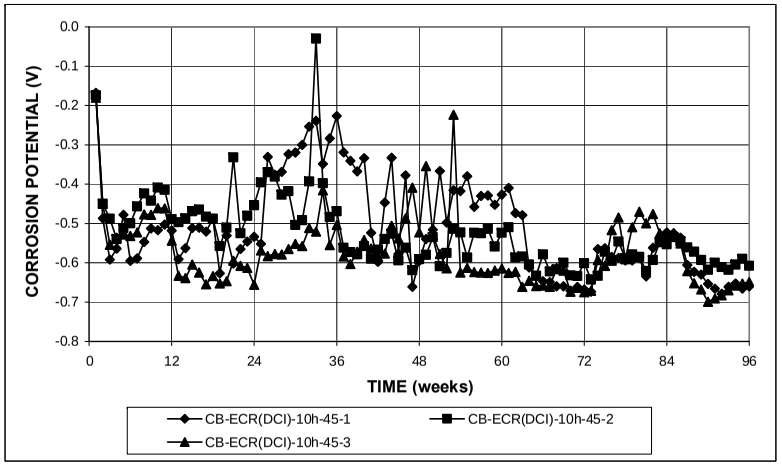

(a)

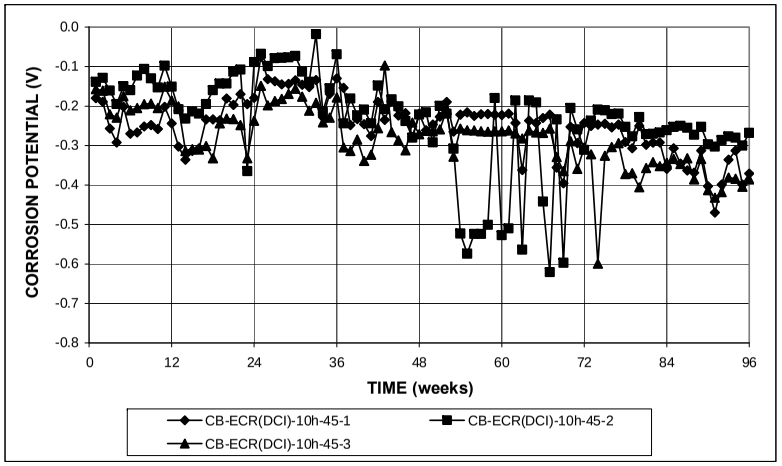

(b)

Figure A.28 – (a) Top mat corrosion potentials and (b) bottom mat corrosion potentials, with respect to the copper-copper sulfate electrode, in the Cracked Beam test for specimens with ECR in concrete with DCI (ten 3-mm (1/8-in.) diameter holes), w/c = 0.45.

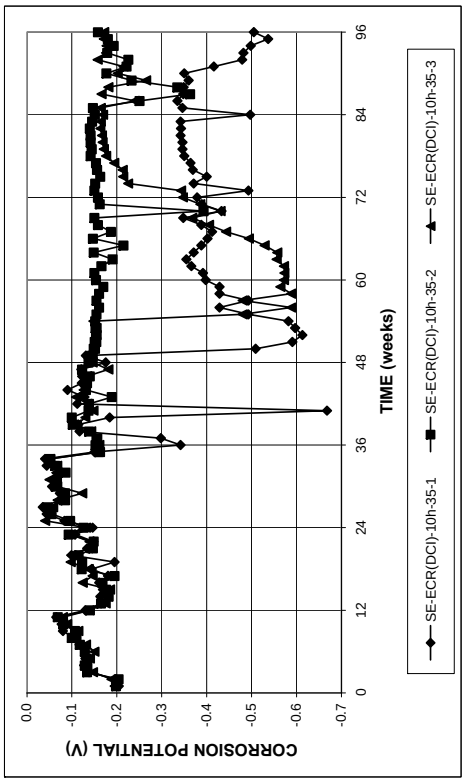

(a)

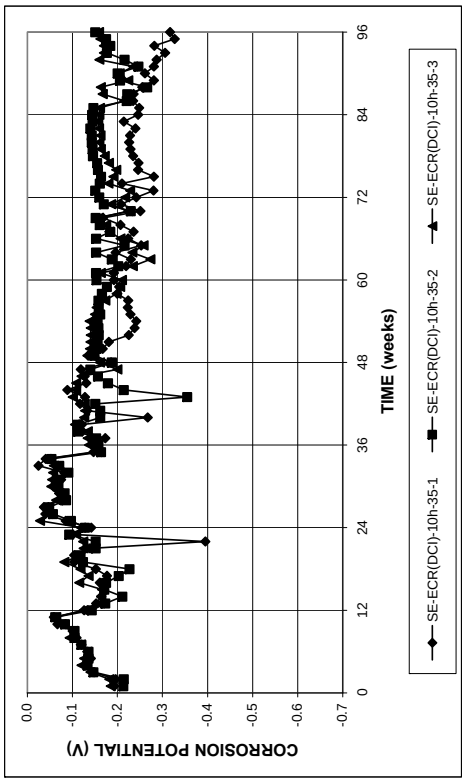

(b)

Figure A.30 – (a) Top mat corrosion potentials and (b) bottom mat corrosion potentials, with respect to the copper-copper sulfate electrode, in the Southern Exposure test for specimens with ECR in concrete with DCI (ten 3-mm (1/8-in.) diameter holes), w/c = 0.35.

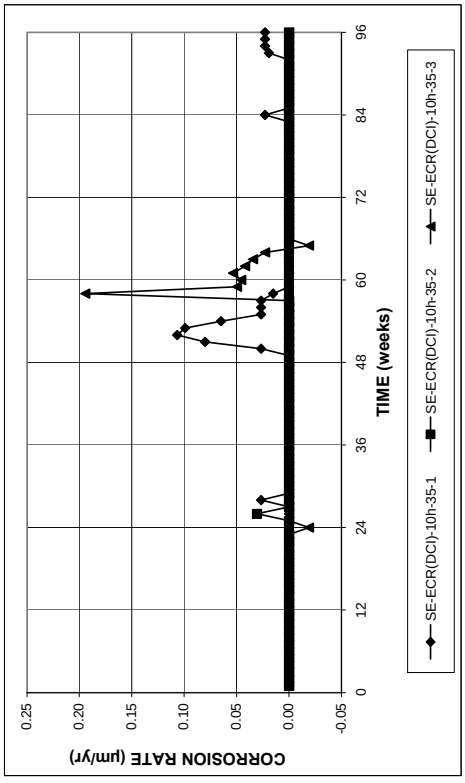

(a)

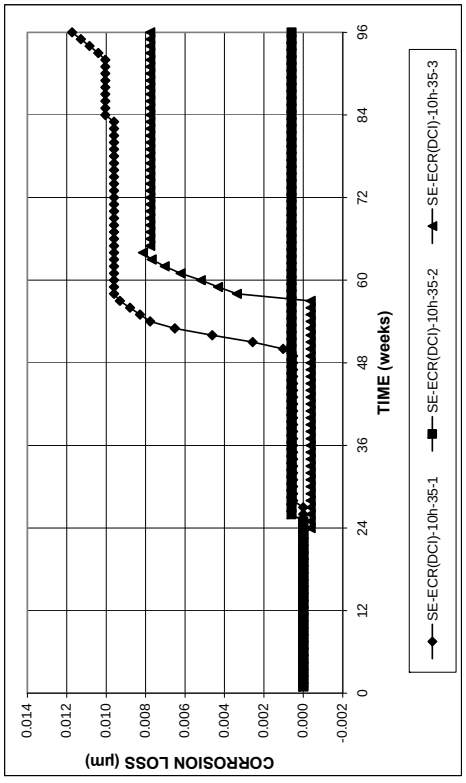

(b)

Figure A.29 – (a) Corrosion rates and (b) total corrosion loss based on total area of the bar in the Southern Exposure test for specimens with ECR in concrete with DCI (ten 3-mm (1/8-in.) diameter holes), w/c = 0.35.

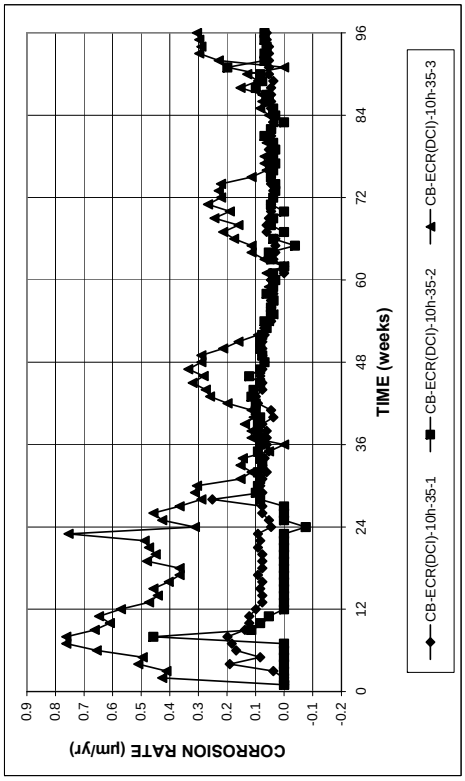

Figure A.31 – (a) Corrosion rates and (b) total corrosion loss based on total area of the bar in the Cracked Beam test for specimens with ECR in concrete with DCI (ten 3-mm (1/8-in.) diameter holes), w/c = 0.35.

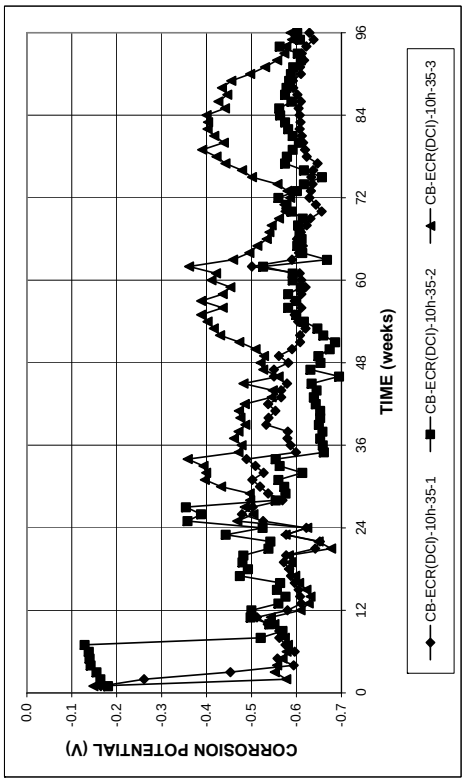

Figure A.32 – (a) Top mat corrosion potentials and (b) bottom mat corrosion potentials, with respect to the copper-copper sulfate electrode, in the Cracked Beam test for specimens with ECR in concrete with DCI (ten 3-mm (1/8-in.) diameter holes), w/c = 0.35.

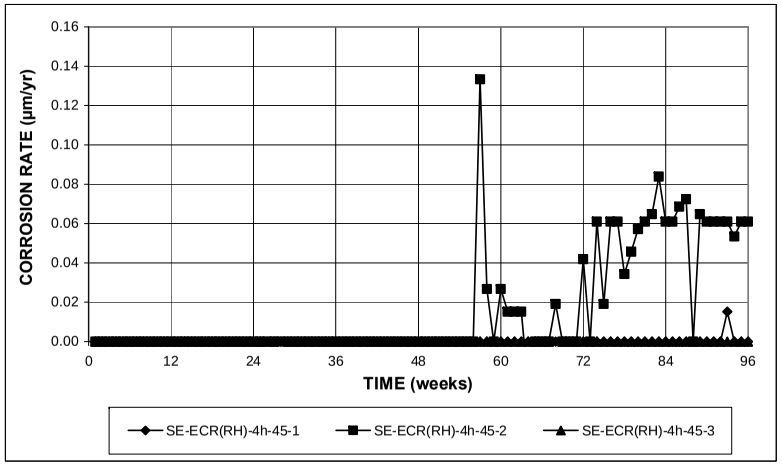

(a)

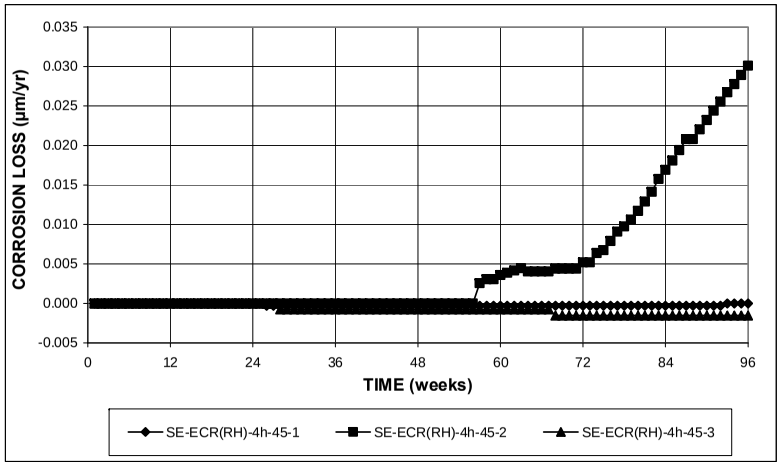

(b)

Figure A.33 – (a) Corrosion rates and (b) total corrosion loss based on total area of the bar in the Southern Exposure test for specimens with ECR in concrete with Rheocrete (four 3-mm (1/8-in.) diameter holes), w/c = 0.45.

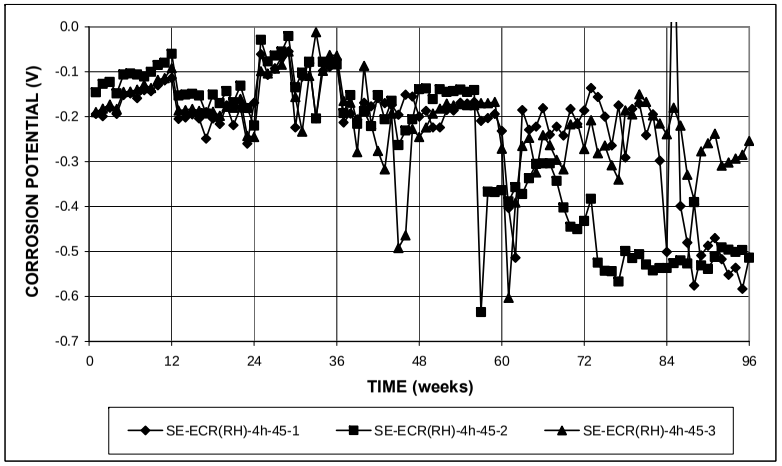

(a)

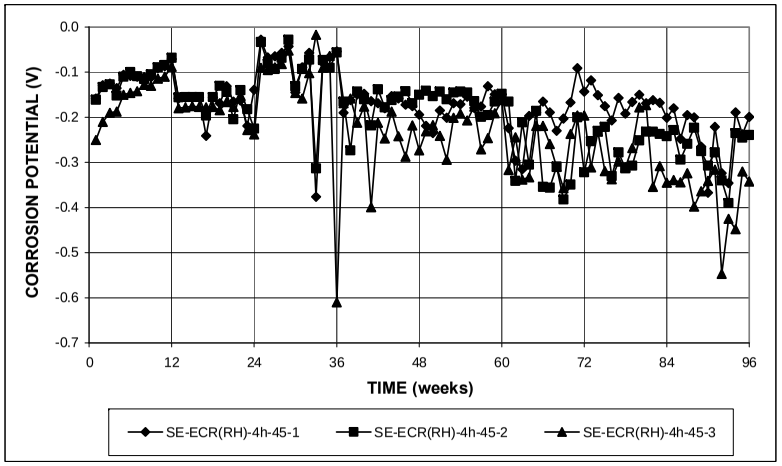

(b)

Figure A.34 – (a) Top mat corrosion potentials and (b) bottom mat corrosion potentials, with respect to the copper-copper sulfate electrode, in the Southern Exposure test for specimens with ECR in concrete with Rheocrete (four 3-mm (1/8-in.) diameter holes), w/c = 0.45.

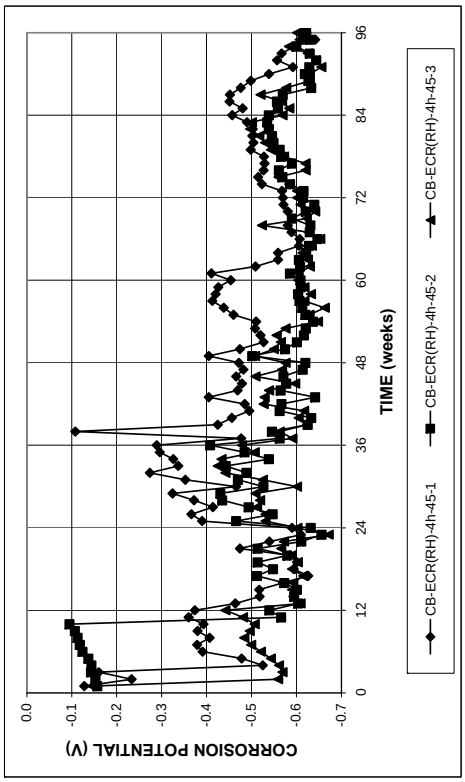

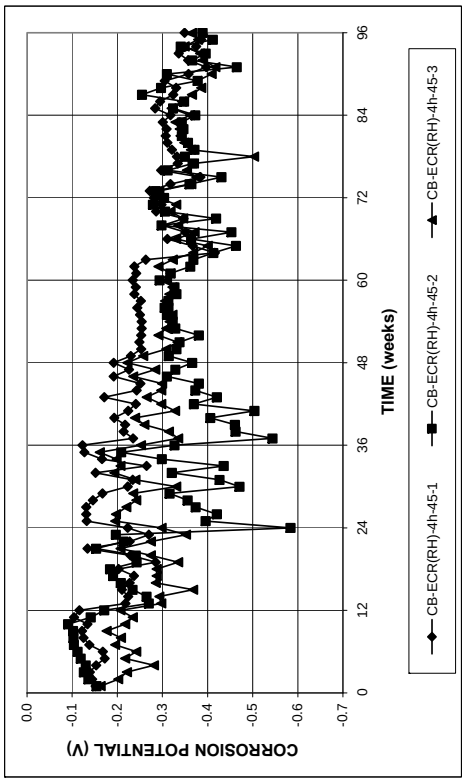

Figure A.36 – (a) Top mat corrosion potentials and (b) bottom mat corrosion potentials, with respect to the copper-copper sulfate electrode, in the Cracked Beam test for specimens with ECR in concrete with Rheocrete (four 3-mm (1/8-in.) diameter holes), w/c = 0.45.

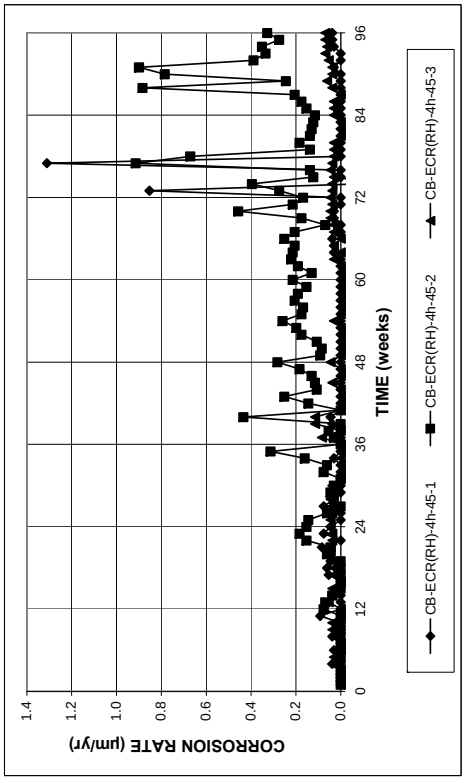

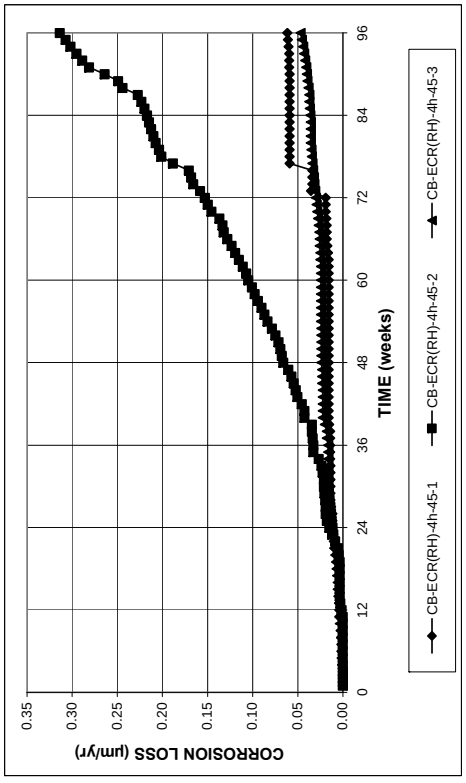

Figure A.35 – (a) Corrosion rates and (b) total corrosion loss based on total area of the bar in the Cracked Beam test for specimens with ECR in concrete with Rheocrete (four 3-mm (1/8-in.) diameter holes), w/c = 0.45.

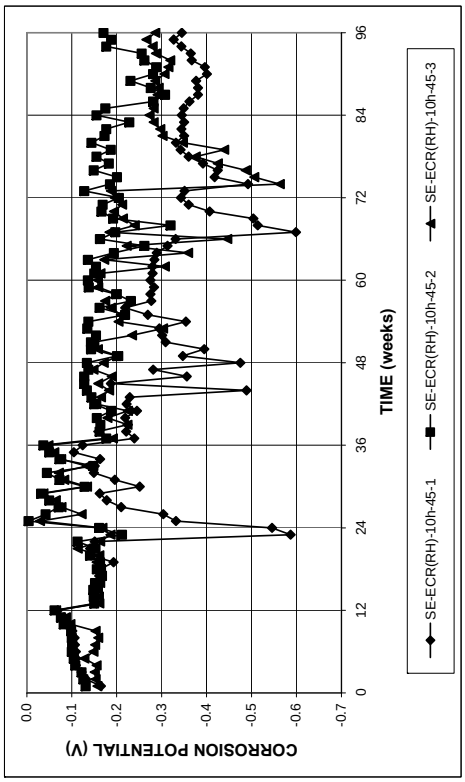

(a)

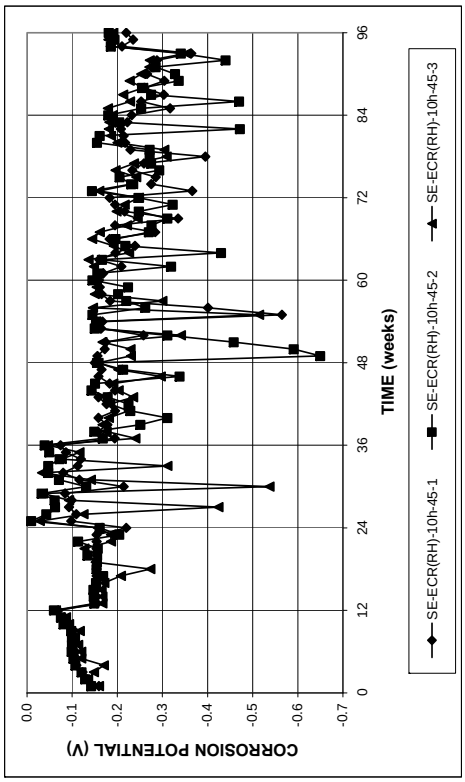

(b)

Figure A.38 – (a) Top mat corrosion potentials and (b) bottom mat corrosion potentials, with respect to the copper-copper sulfate electrode, in the Southern Exposure test for specimens with ECR in concrete with Rheocrete (ten 3-mm (1/8-in.) diameter holes), w/c = 0.45.

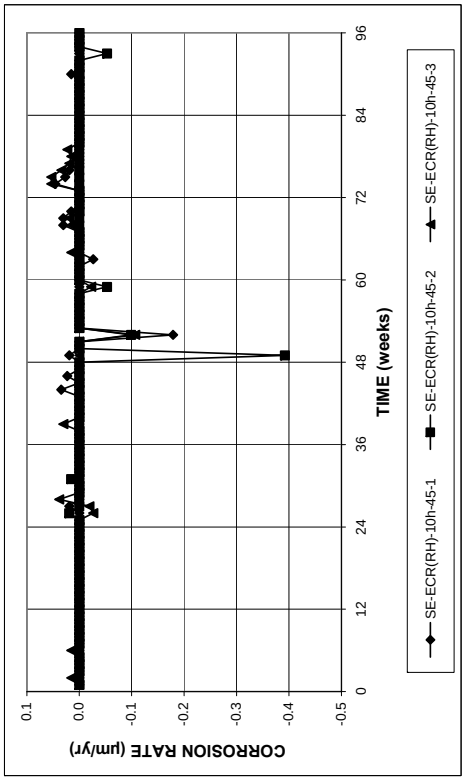

(a)

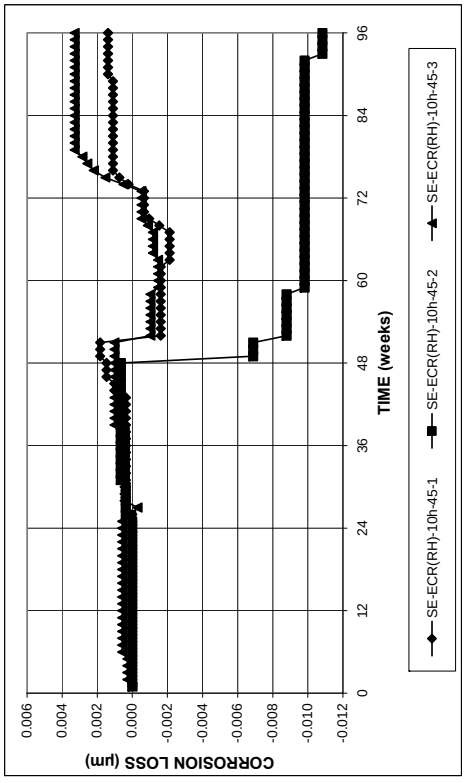

(b)

Figure A.37 – (a) Corrosion rates and (b) total corrosion loss based on total area of the bar in the Southern Exposure test for specimens with ECR in concrete with Rheocrete (ten 3-mm (1/8-in.) diameter holes), w/c = 0.45.

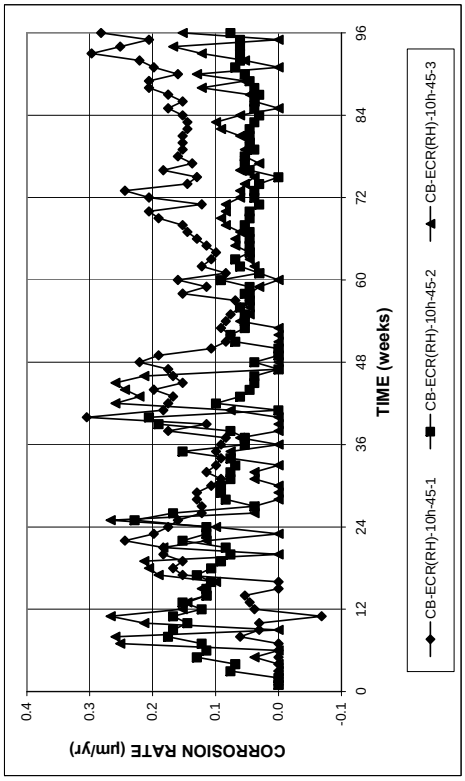

Figure A.39 – (a) Corrosion rates and (b) total corrosion loss based on total area of the bar in the Cracked Beam test for specimens with ECR in concrete with Rheocrete (ten 3-mm (1/8-in.) diameter holes), w/c = 0.45.

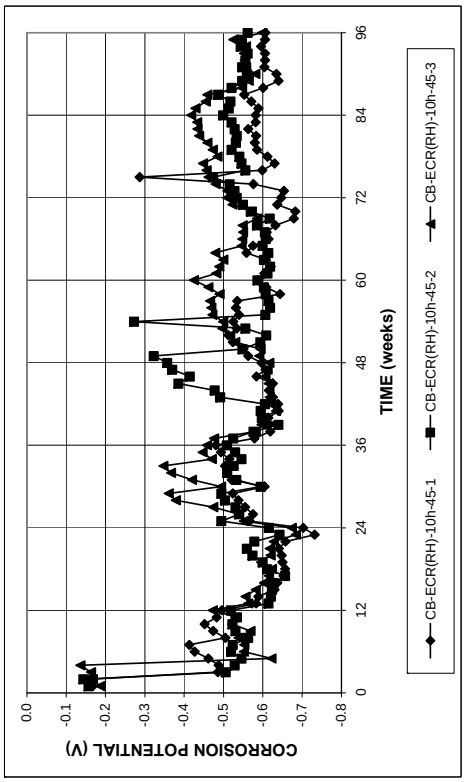

Figure A.40 – (a) Top mat corrosion potentials and (b) bottom mat corrosion potentials, with respect to the copper-copper sulfate electrode, in the Cracked Beam test for specimens with ECR in concrete with Rheocrete (ten 3-mm (1/8-in.) diameter holes), w/c = 0.45.

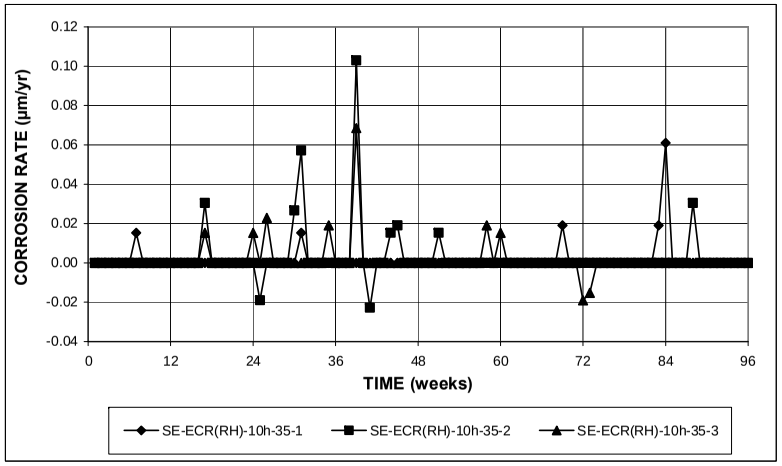

(a)

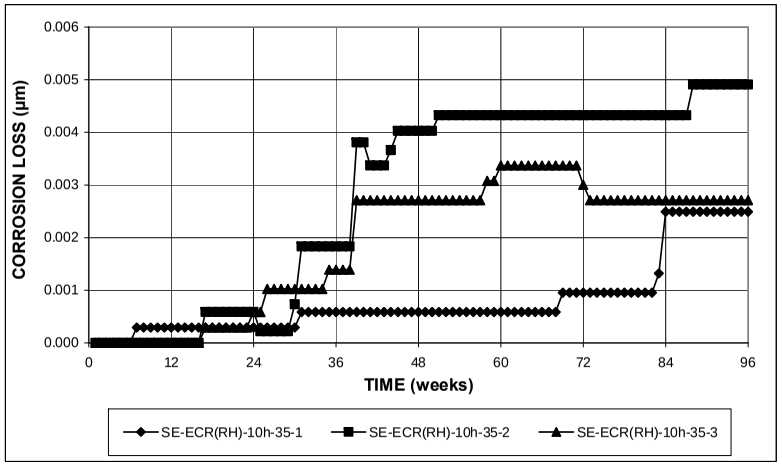

(b)

Figure A.41 – (a) Corrosion rates and (b) total corrosion loss based on total area of the bar in the Southern Exposure test for specimens with ECR in concrete with Rheocrete (ten 3-mm (1/8-in.) diameter holes), w/c = 0.35.

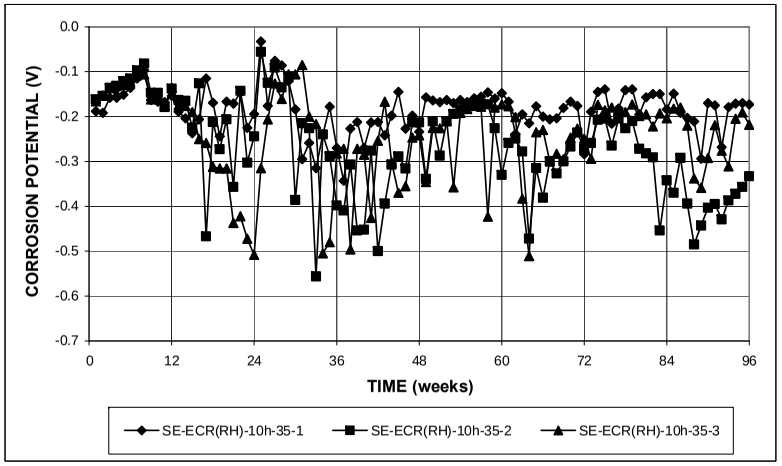

(a)

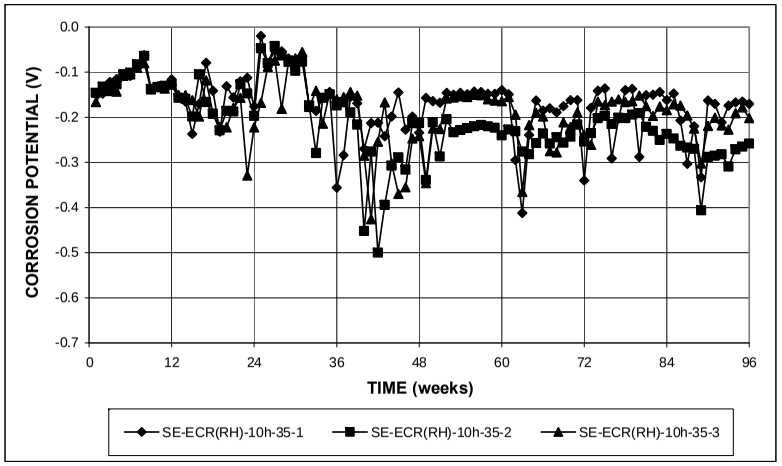

(b)

Figure A.42 – (a) Top mat corrosion potentials and (b) bottom mat corrosion potentials, with respect to the copper-copper sulfate electrode, in the Southern Exposure test for specimens with ECR in concrete with Rheocrete (ten 3-mm (1/8-in.) diameter holes), w/c = 0.35.

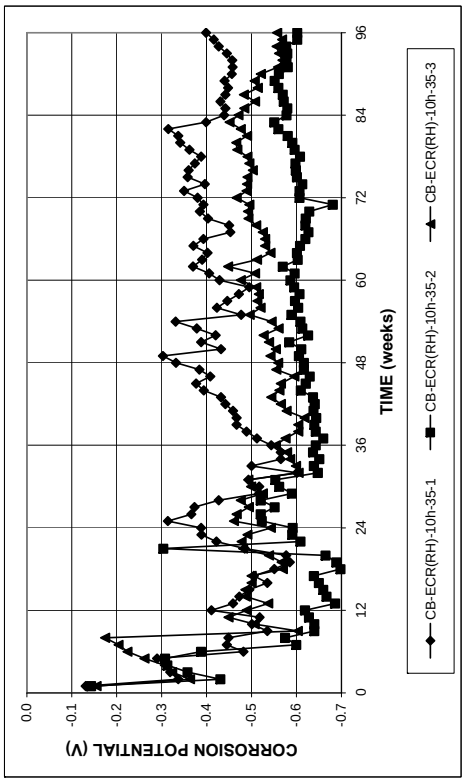

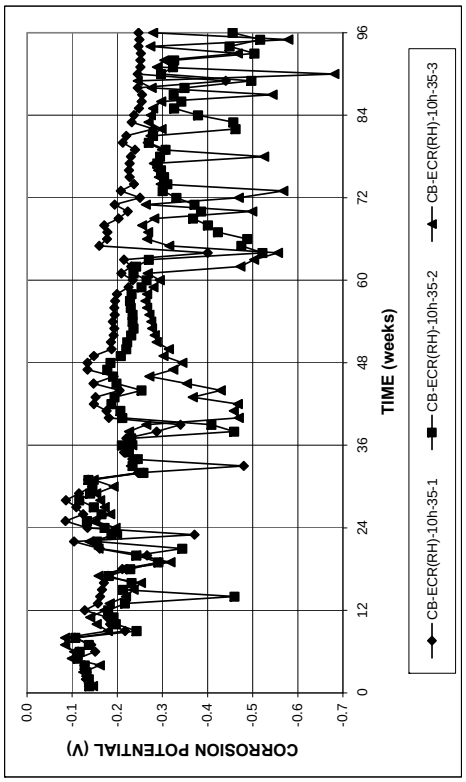

Figure A.44 – (a) Top mat corrosion potentials and (b) bottom mat corrosion potentials, with respect to the copper-copper sulfate electrode, in the Cracked Beam test for specimens with ECR in concrete with Rheocrete (ten 3-mm (1/8-in.) diameter holes), w/c = 0.35.

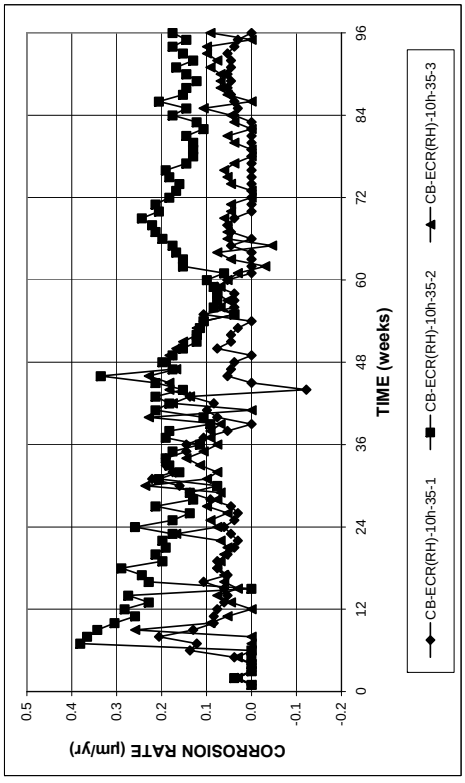

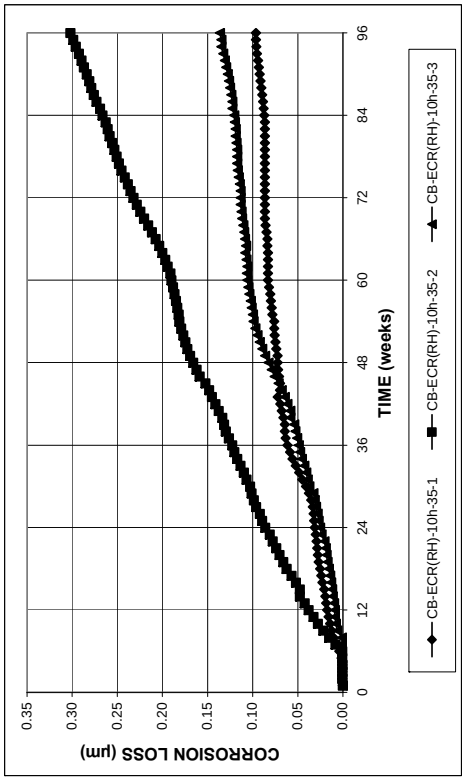

Figure A.43 – (a) Corrosion rates and (b) total corrosion loss based on total area of the bar in the Cracked Beam test for specimens with ECR in concrete with Rheocrete (ten 3-mm (1/8-in.) diameter holes), w/c = 0.35.

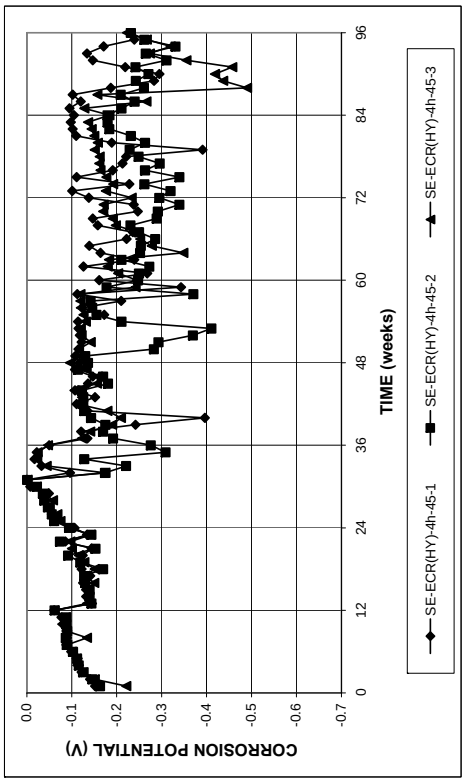

(a)

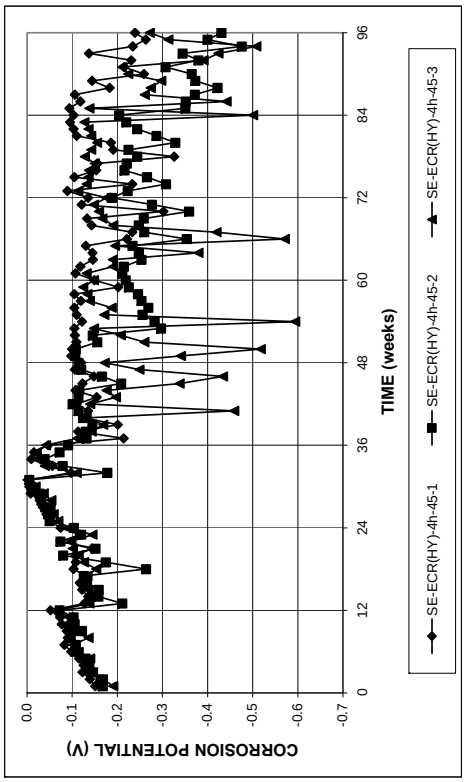

(b)

Figure A.46 – (a) Top mat corrosion potentials and (b) bottom mat corrosion potentials, with respect to the copper-copper sulfate electrode, in the Southern Exposure test for specimens with ECR in concrete with Hycrete (four 3-mm (1/8-in.) diameter holes), w/c = 0.45.

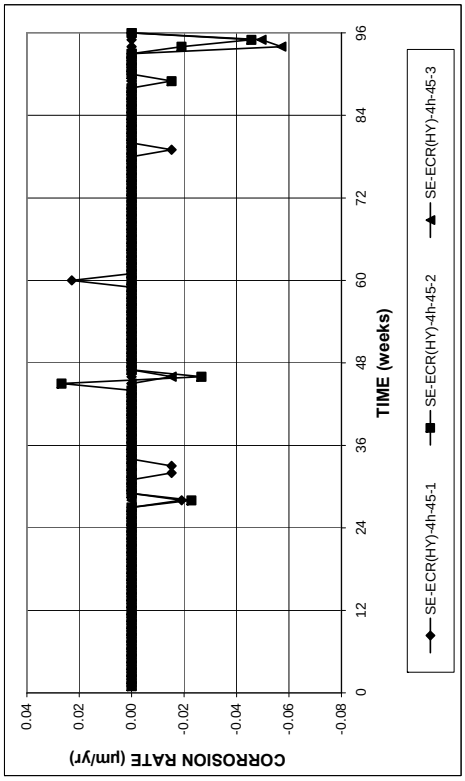

(a)

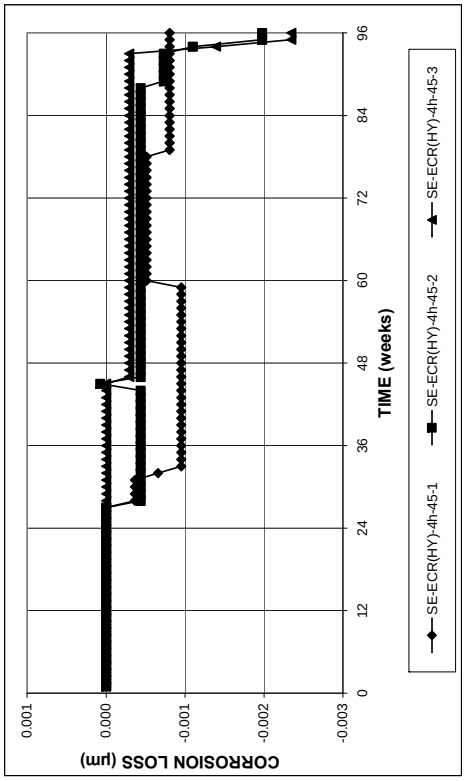

(b)

Figure A.45 – (a) Corrosion rates and (b) total corrosion loss based on total area of the bar in the Southern Exposure test for specimens with ECR in concrete with Hycrete (four 3-mm (1/8-in.) diameter holes), w/c = 0.45.

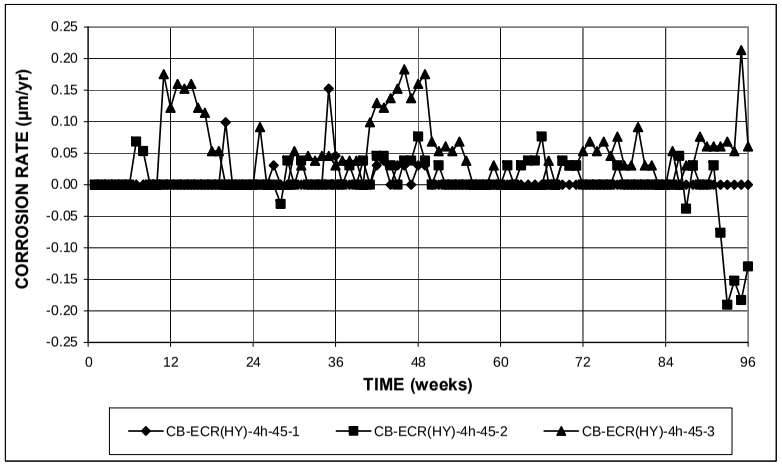

(a)

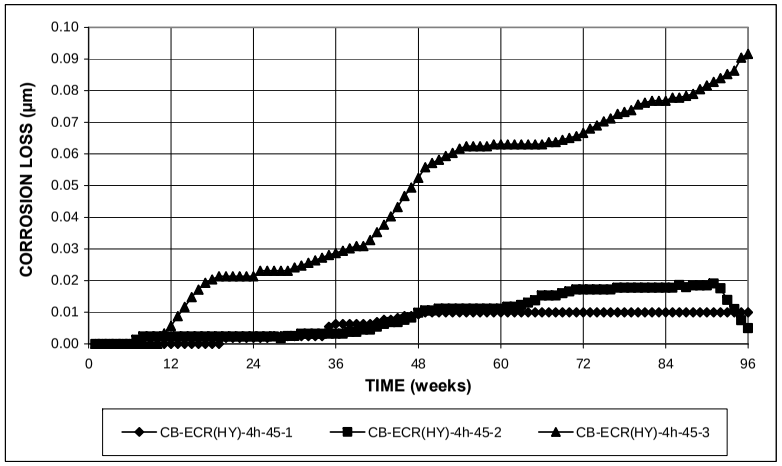

(b)

Figure A.47 – (a) Corrosion rates and (b) total corrosion loss based on total area of the bar in the Cracked Beam test for specimens with ECR in concrete with Hycrete (four 3-mm (1/8-in.) diameter holes), w/c = 0.45.

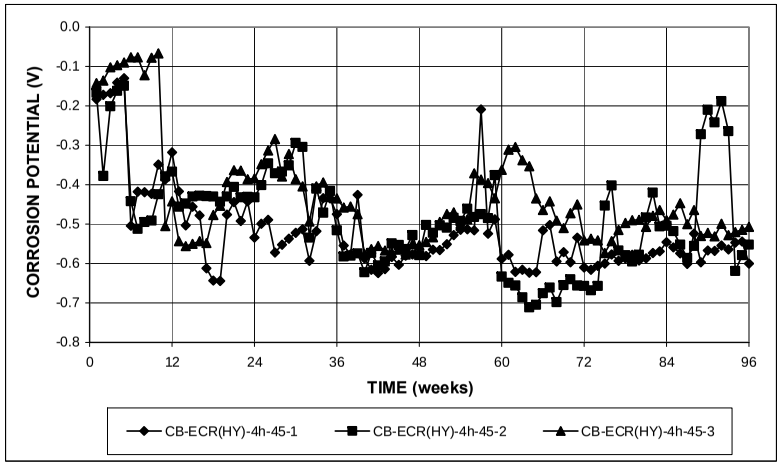

(a)

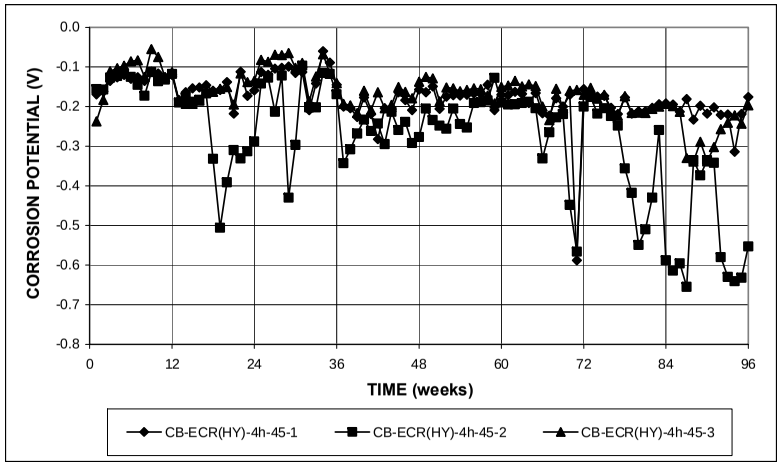

(b)

Figure A.48 – (a) Top mat corrosion potentials and (b) bottom mat corrosion potentials, with respect to the copper-copper sulfate electrode, in the Cracked Beam test for specimens with ECR in concrete with Hycrete (four 3-mm (1/8-in.) diameter holes), w/c = 0.45.

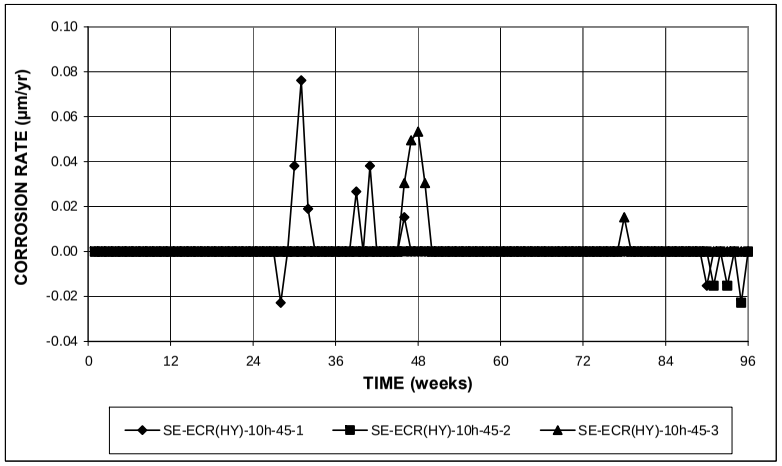

(a)

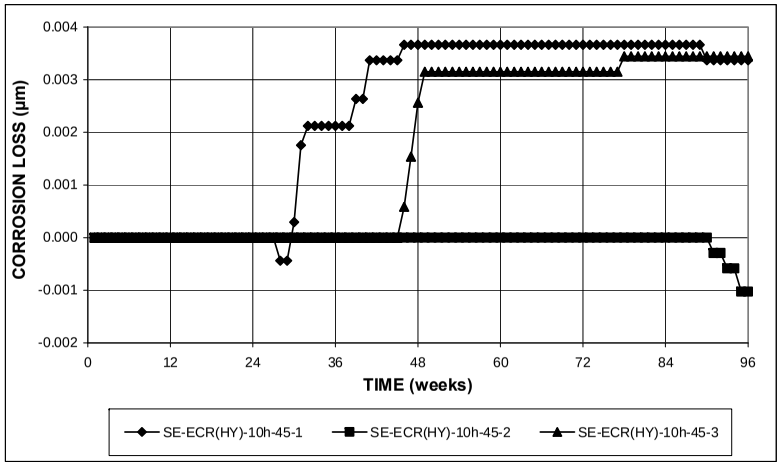

(b)

Figure A.49 – (a) Corrosion rates and (b) total corrosion loss based on total area of the bar in the Southern Exposure test for specimens with ECR in concrete with Hycrete (ten 3-mm (1/8-in.) diameter holes), w/c = 0.45.

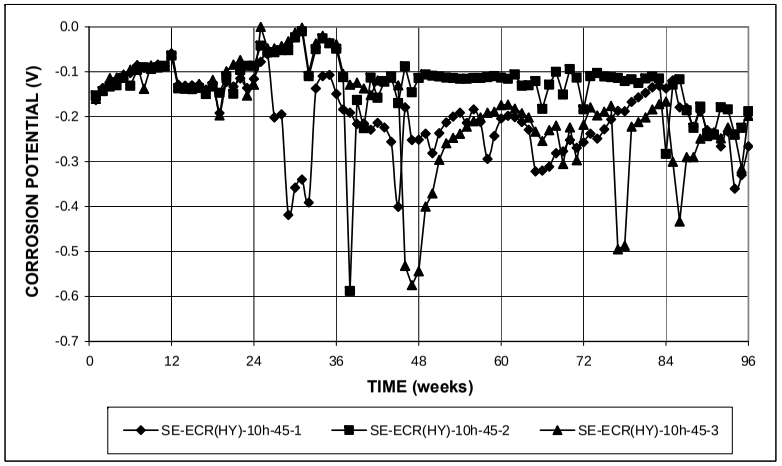

(a)

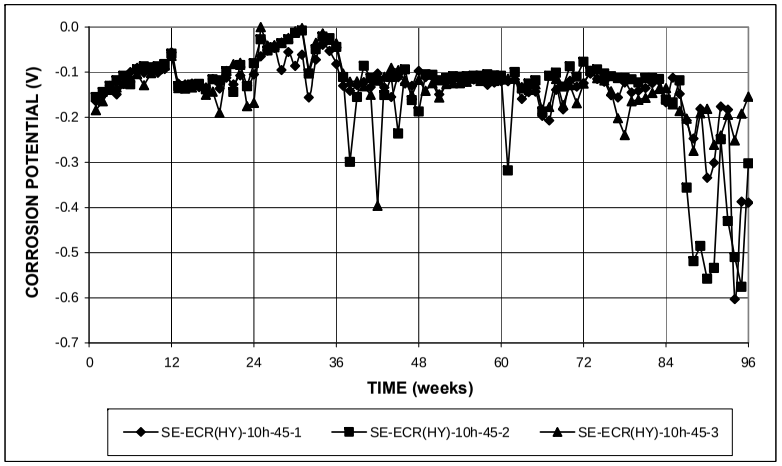

(b)

Figure A.50 – (a) Top mat corrosion potentials and (b) bottom mat corrosion potentials, with respect to the copper-copper sulfate electrode, in the Southern Exposure test for specimens with ECR in concrete with Hycrete (ten 3-mm (1/8-in.) diameter holes), w/c = 0.45.

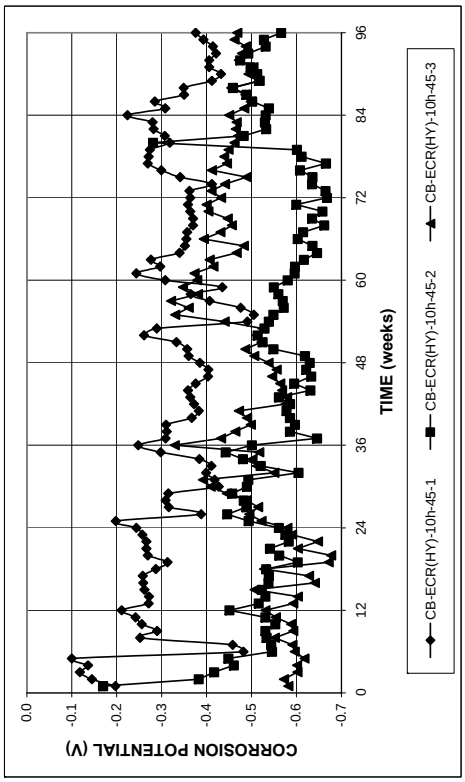

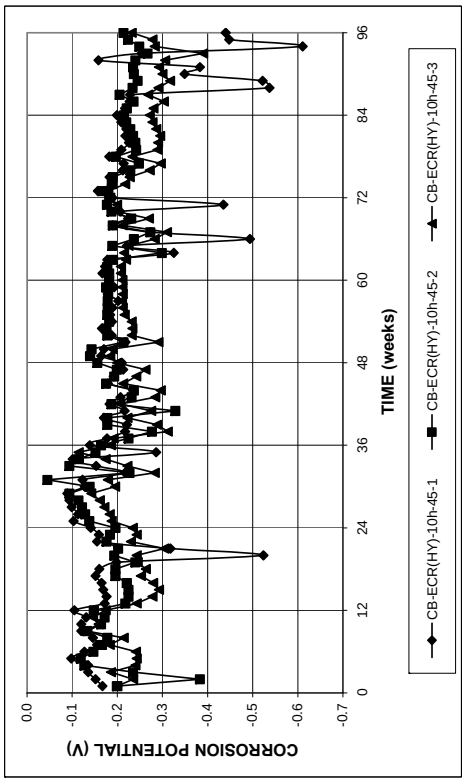

Figure A.52 – (a) Top mat corrosion potentials and (b) bottom mat corrosion potentials, with respect to the copper-copper sulfate electrode, in the Cracked Beam test for specimens with ECR in concrete with Hycrete (ten 3-mm (1/8-in.) diameter holes), w/c = 0.45.

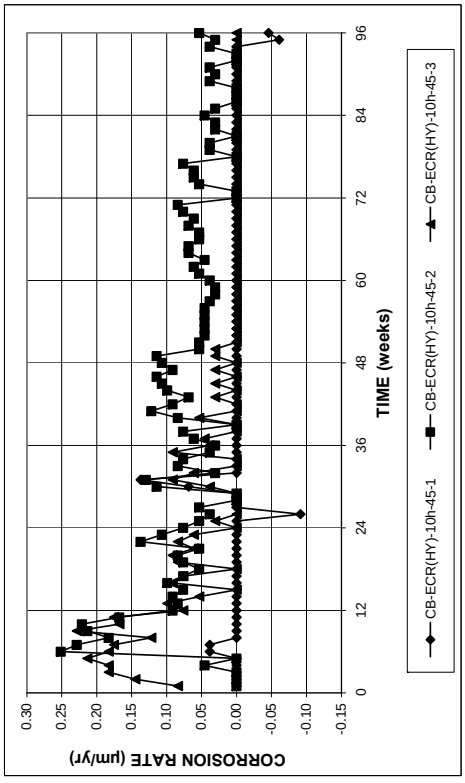

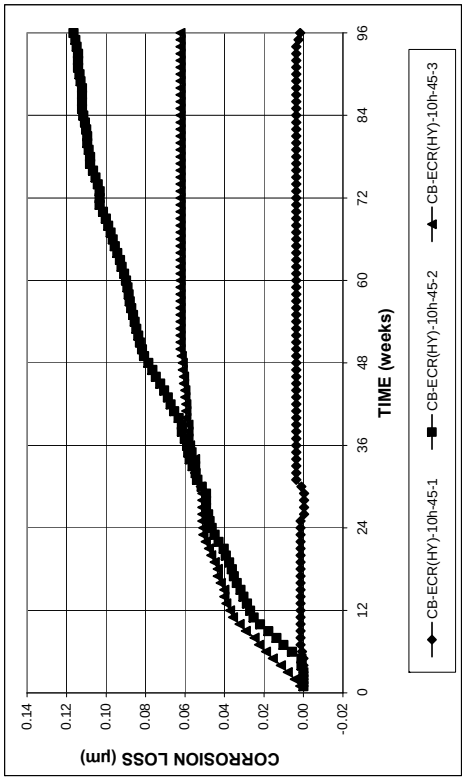

Figure A.51 – (a) Corrosion rates and (b) total corrosion loss based on total area of the bar in the Cracked Beam test for specimens with ECR in concrete with Hycrete (ten 3-mm (1/8-in.) diameter holes), w/c = 0.45.

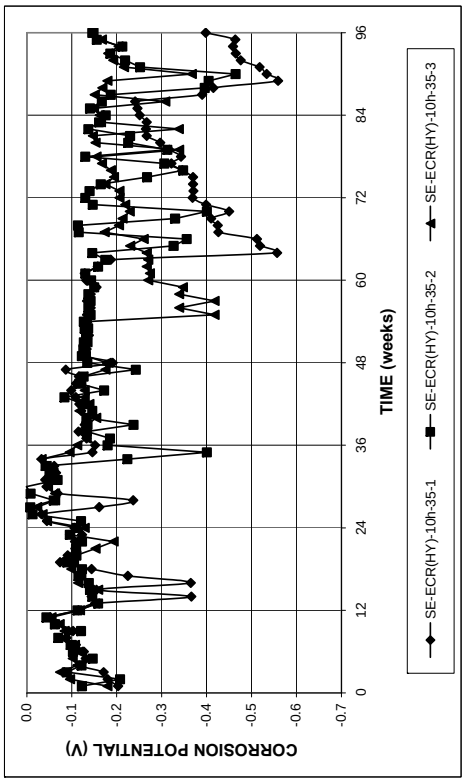

Figure A.54 – (a) Top mat corrosion potentials and (b) bottom mat corrosion potentials, with respect to the copper-copper sulfate electrode, in the Southern Exposure test for specimens with ECR in concrete with Hycrete (ten 3-mm (1/8-in.) diameter holes), w/c = 0.35.

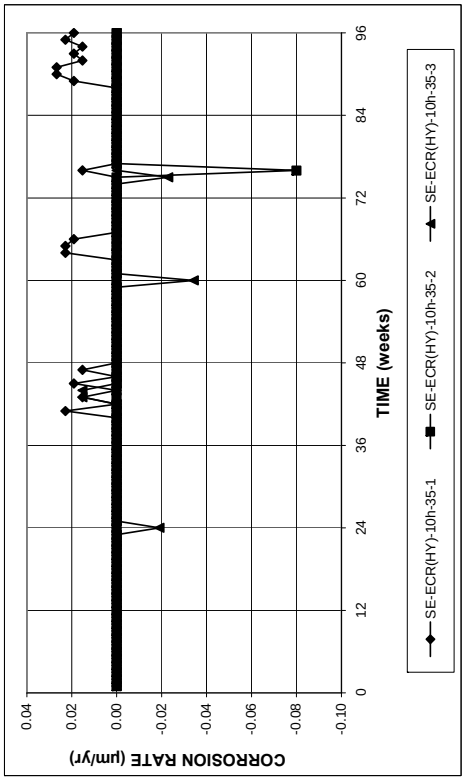

Figure A.53 – (a) Corrosion rates and (b) total corrosion loss based on total area of the bar in the Southern Exposure test for specimens with ECR in concrete with Hycrete (ten 3-mm (1/8-in.) diameter holes), w/c = 0.35.

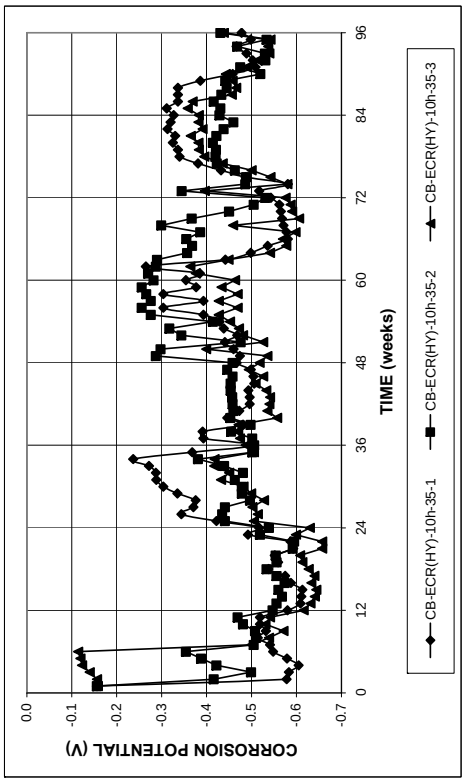

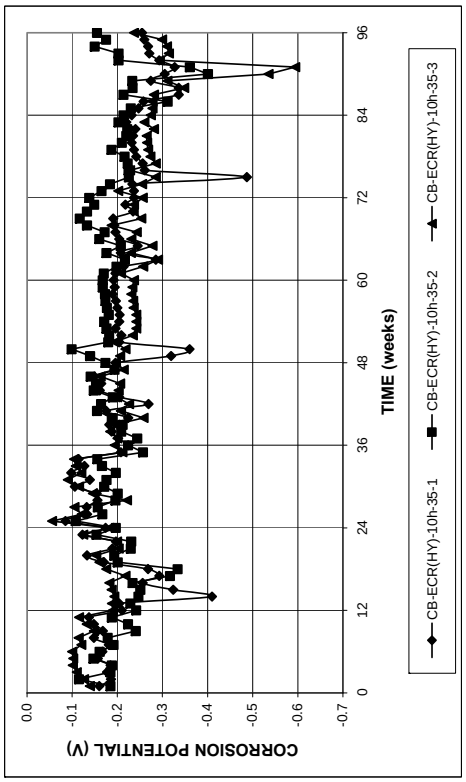

Figure A.56 – (a) Top mat corrosion potentials and (b) bottom mat corrosion potentials, with respect to the copper-copper sulfate electrode, in the Cracked Beam test for specimens with ECR in concrete with Hycrete (ten 3-mm (1/8-in.) diameter holes), w/c = 0.35.

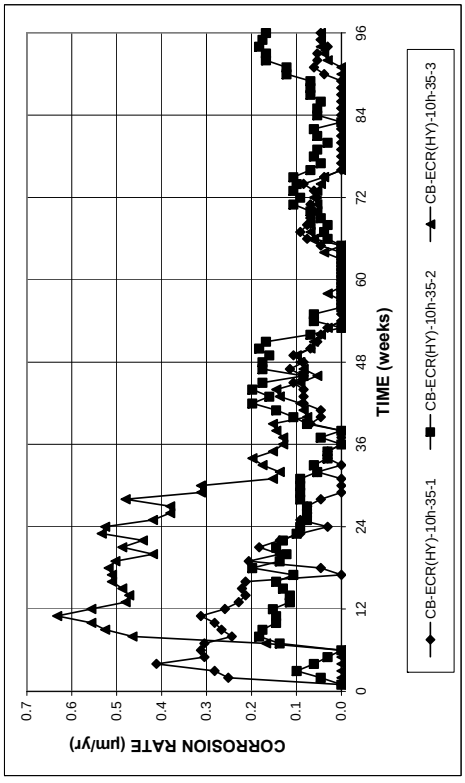

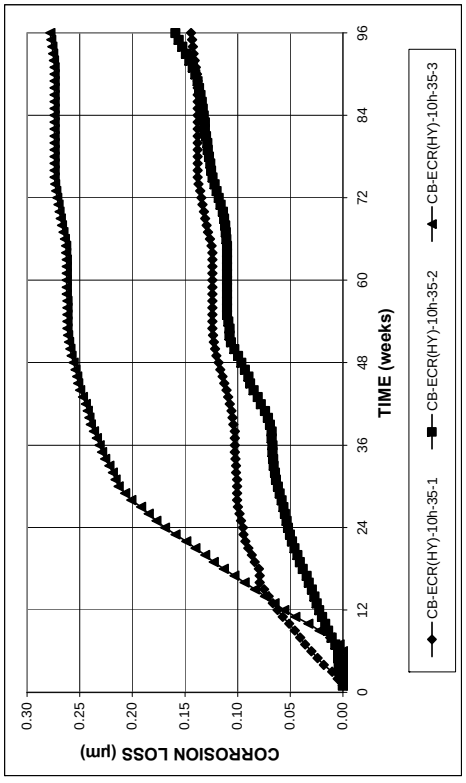

Figure A.55 – (a) Corrosion rates and (b) total corrosion loss based on total area of the bar in the Cracked Beam test for specimens with ECR in concrete with Hycrete (ten 3-mm (1/8-in.) diameter holes), w/c = 0.35.

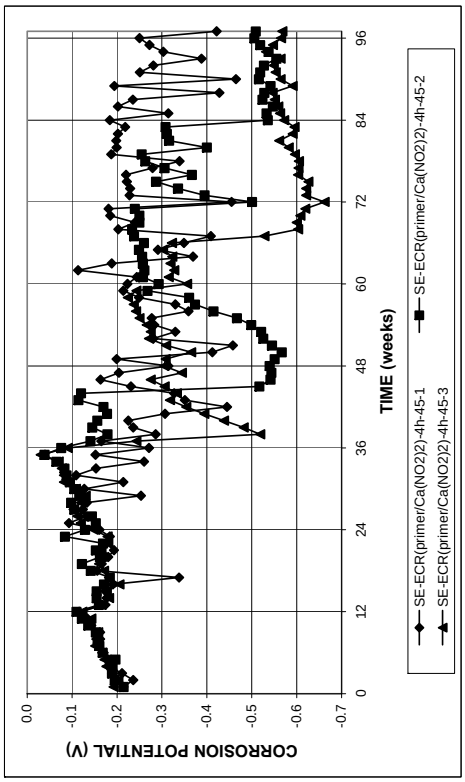

(a)

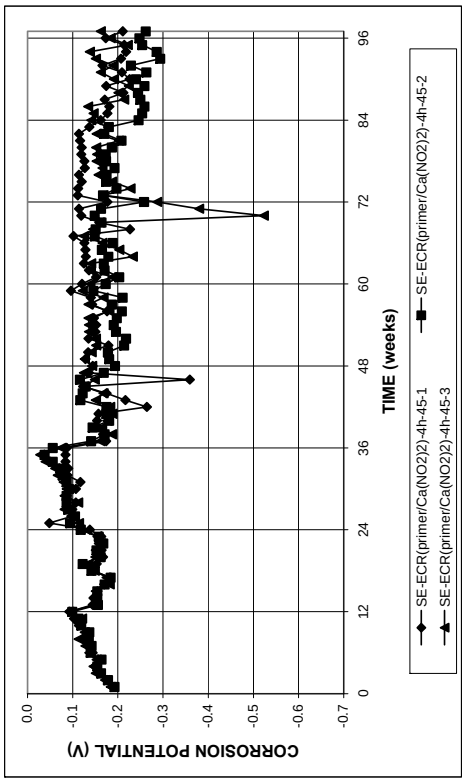

(b)

Figure A.58 – (a) Top mat corrosion potentials and (b) bottom mat corrosion potentials, with respect to the copper-copper sulfate electrode, in the Southern Exposure test for specimens with ECR with calcium nitrite primer (four 3-mm (1/8-in.) diameter holes), w/c = 0.45.

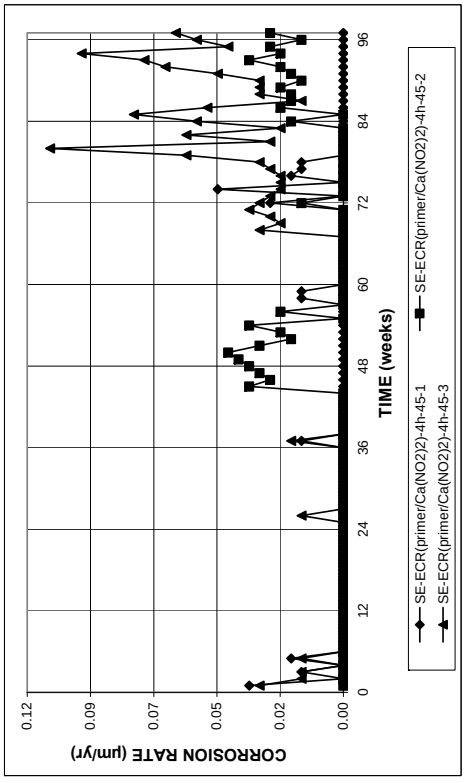

(a)

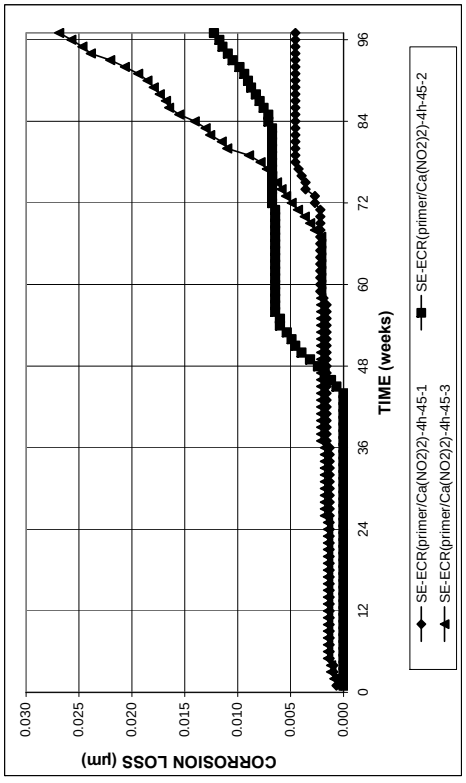

(b)

Figure A.57 – (a) Corrosion rates and (b) total corrosion loss based on total area of the bar in the Southern Exposure test for specimens with ECR with calcium nitrite primer (four 3-mm (1/8-in.) diameter holes), w/c = 0.45.

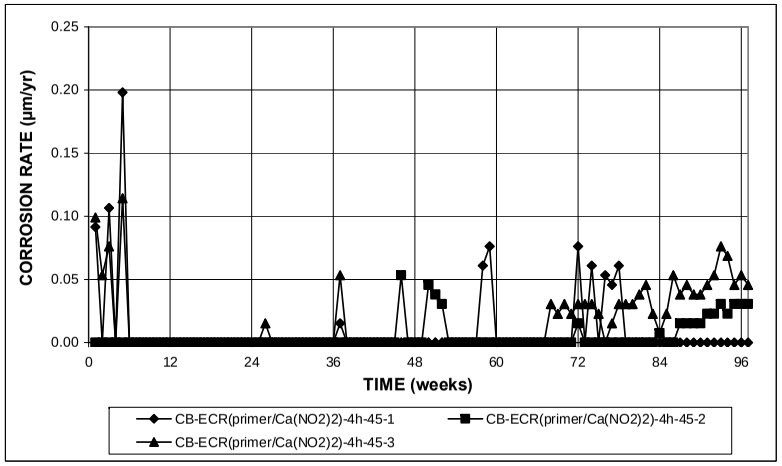

(a)

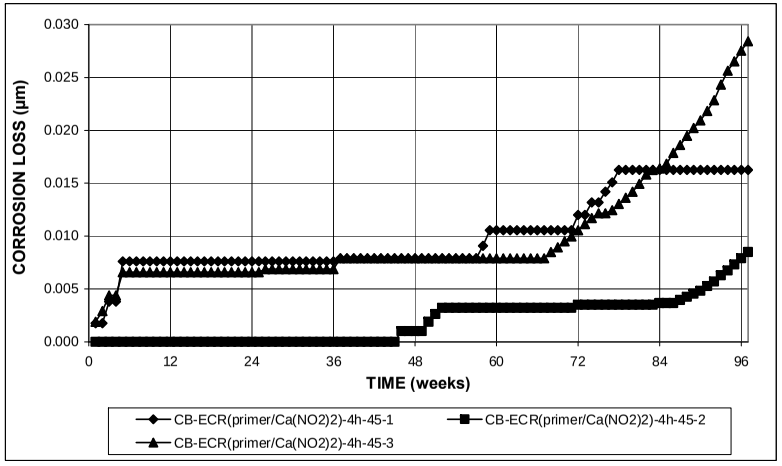

(b)

Figure A.59 – (a) Corrosion rates and (b) total corrosion loss based on total area of the bar in the Cracked Beam test for specimens with ECR with calcium nitrite primer (four 3-mm (1/8-in.) diameter holes), w/c = 0.45.

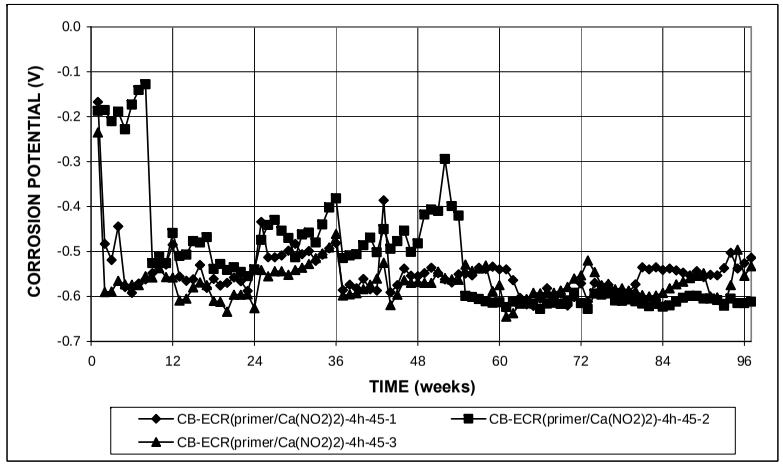

(a)

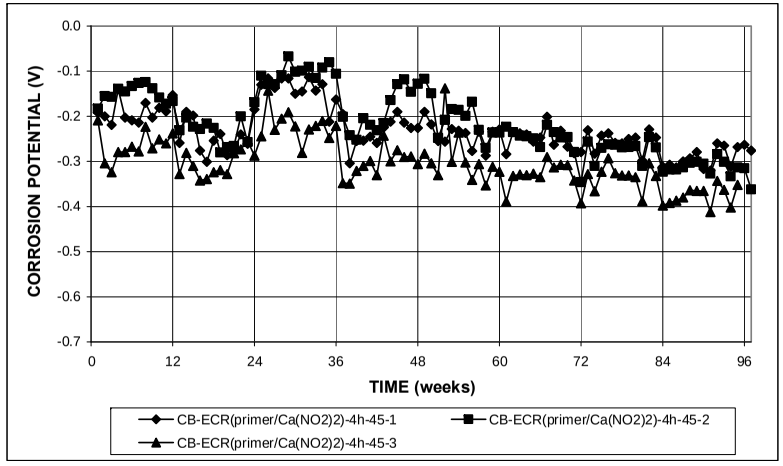

(b)

Figure A.60 – (a) Top mat corrosion potentials and (b) bottom mat corrosion potentials, with respect to the copper-copper sulfate electrode, in the Cracked Beam test for specimens with ECR with calcium nitrite primer (four 3-mm (1/8-in.) diameter holes), w/c = 0.45.

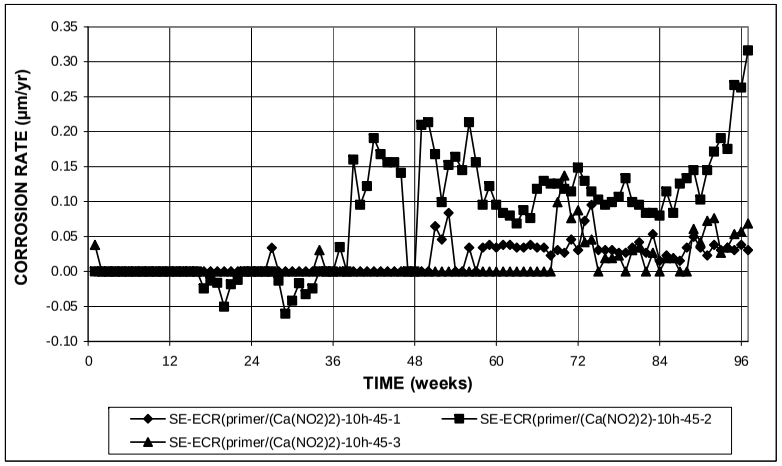

(a)

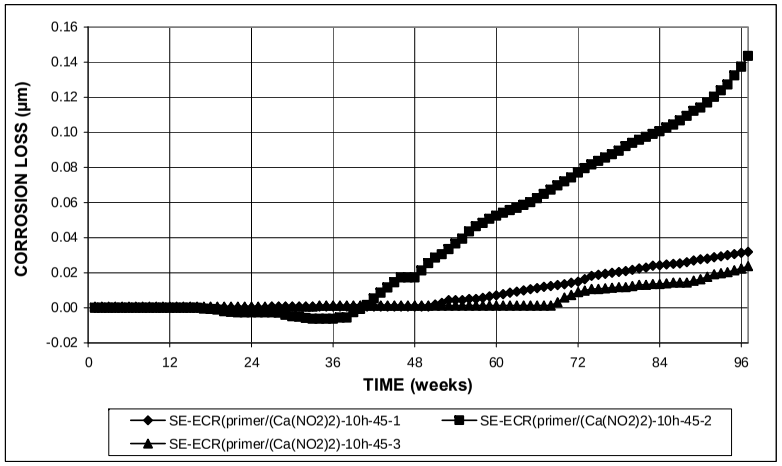

(b)

Figure A.61 – (a) Corrosion rates and (b) total corrosion loss based on total area of the bar in the Southern Exposure test for specimens with ECR with calcium nitrite primer (ten 3-mm (1/8-in.) diameter holes), w/c = 0.45.

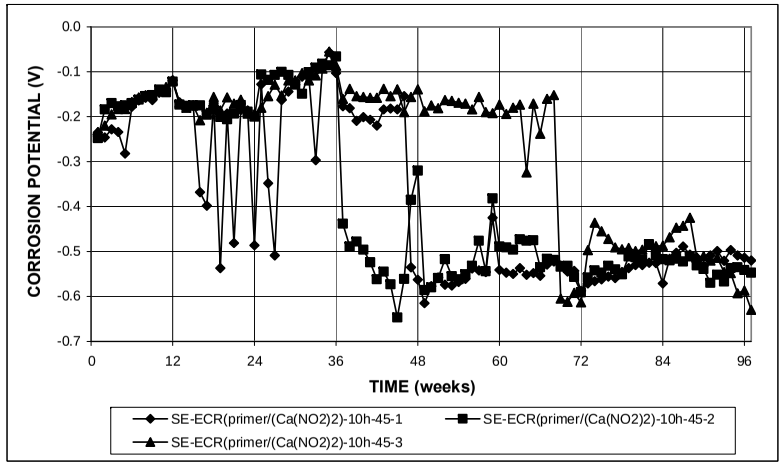

(a)

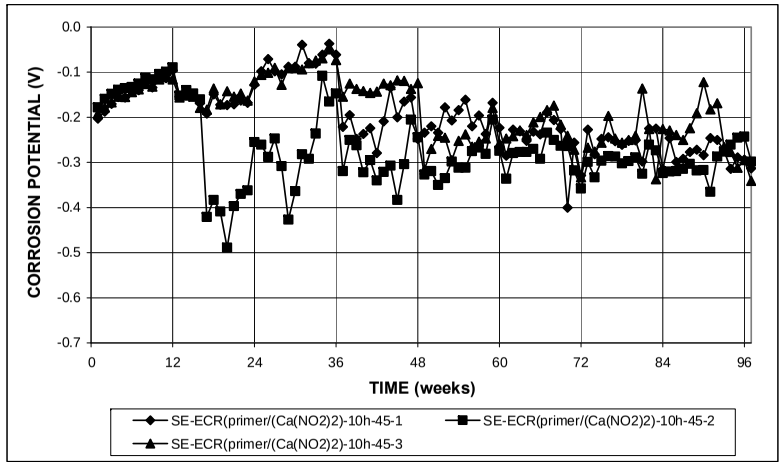

(b)

Figure A.62 – (a) Top mat corrosion potentials and (b) bottom mat corrosion potentials, with respect to the copper-copper sulfate electrode, in the Southern Exposure test for specimens with ECR with calcium nitrite primer (ten 3-mm (1/8-in.) diameter holes), w/c = 0.45.

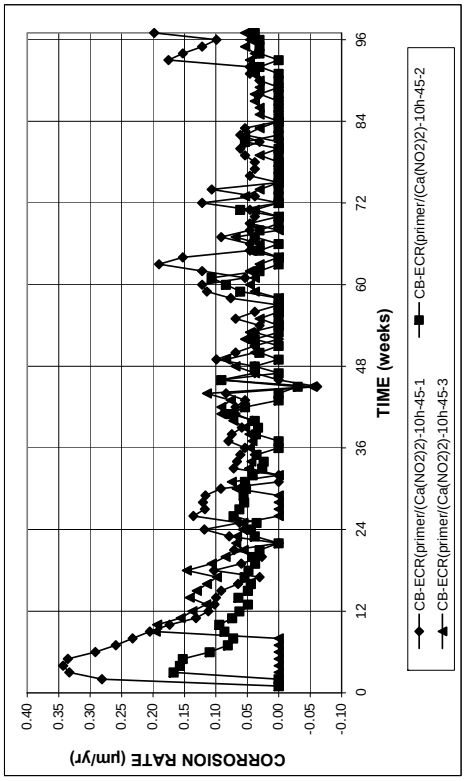

Figure A.63 – (a) Corrosion rates and (b) total corrosion loss based on total area of the bar in the Cracked Beam test for specimens with ECR with calcium nitrite primer (ten 3-mm (1/8-in.) diameter holes), w/c = 0.45.

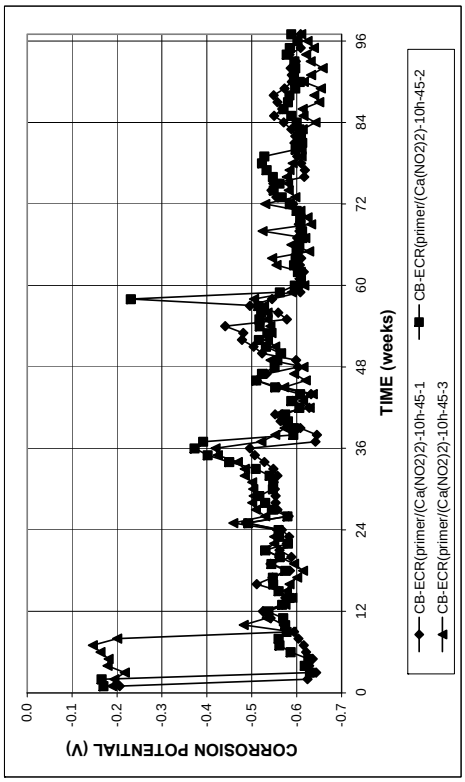

Figure A.64 – (a) Top mat corrosion potentials and (b) bottom mat corrosion potentials, with respect to the copper-copper sulfate electrode, in the Cracked Beam test for specimens with ECR with calcium nitrite primer (ten 3-mm (1/8-in.) diameter holes), w/c = 0.45.

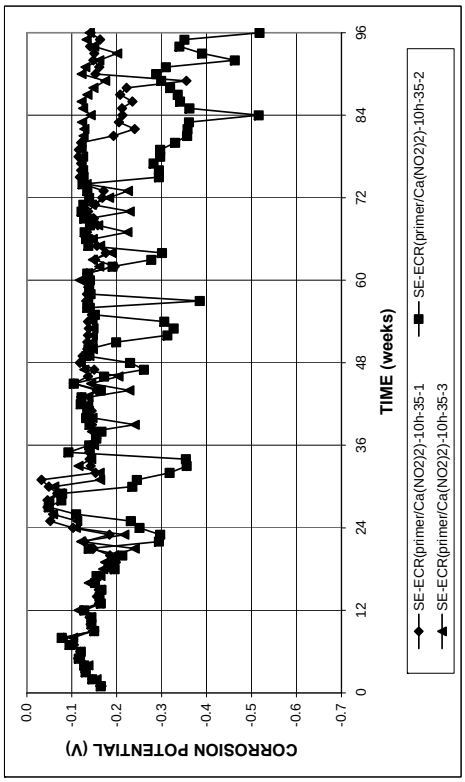

(a)

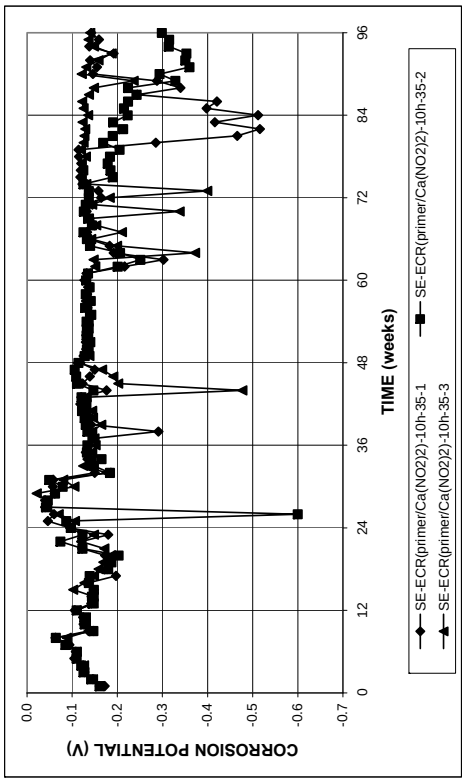

(b)

Figure A.66 – (a) Top mat corrosion potentials and (b) bottom mat corrosion potentials, with respect to the copper-copper sulfate electrode, in the Southern Exposure test for specimens with ECR with calcium nitrite primer (ten 3-mm (1/8-in.) diameter holes), w/c = 0.35.

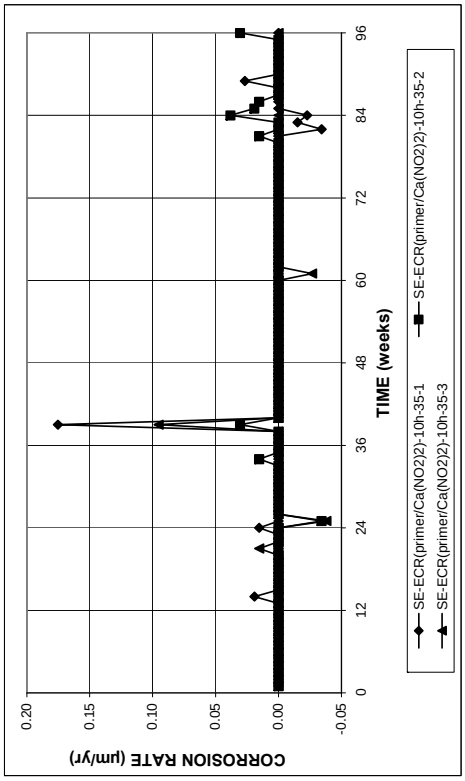

(a)

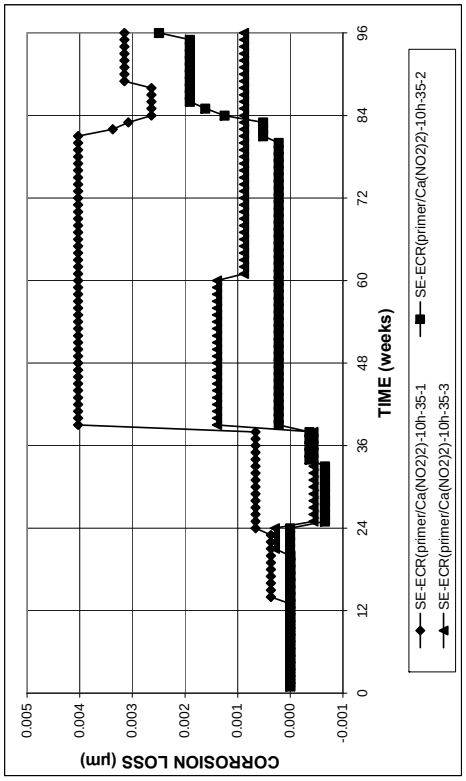

(b)

Figure A.65 – (a) Corrosion rates and (b) total corrosion loss based on total area of the bar in the Southern Exposure test for specimens with ECR with calcium nitrite primer (ten 3-mm (1/8-in.) diameter holes), w/c = 0.35.

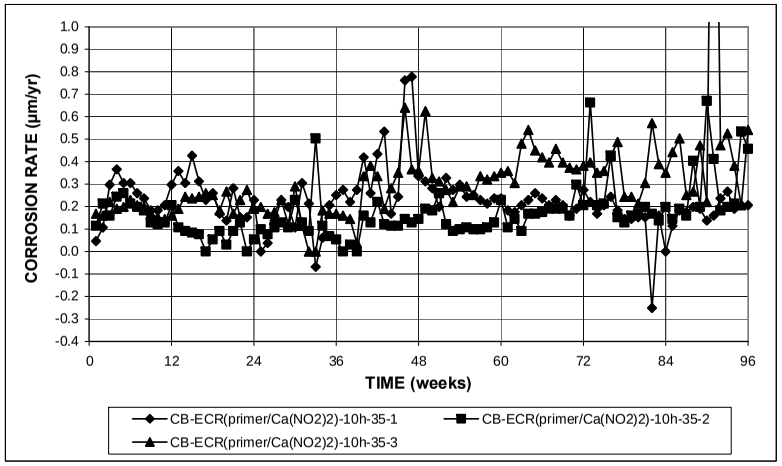

(a)

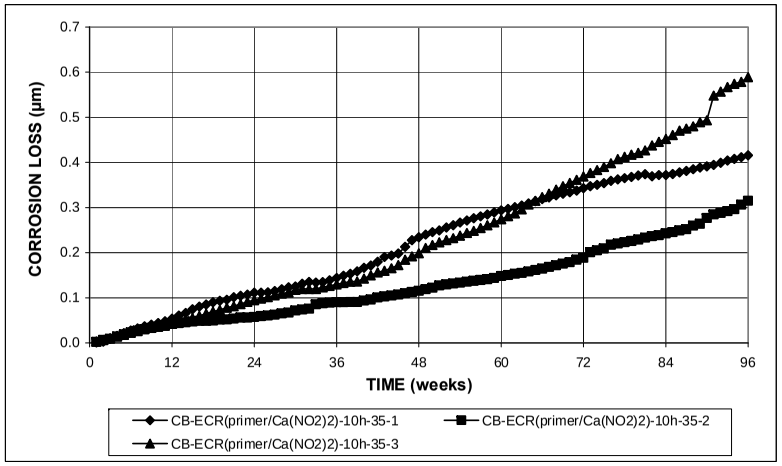

(b)

Figure A.67 – (a) Corrosion rates and (b) total corrosion loss based on total area of the bar in the Cracked Beam test for specimens with ECR with calcium nitrite primer (ten 3-mm (1/8-in.) diameter holes), w/c = 0.35.

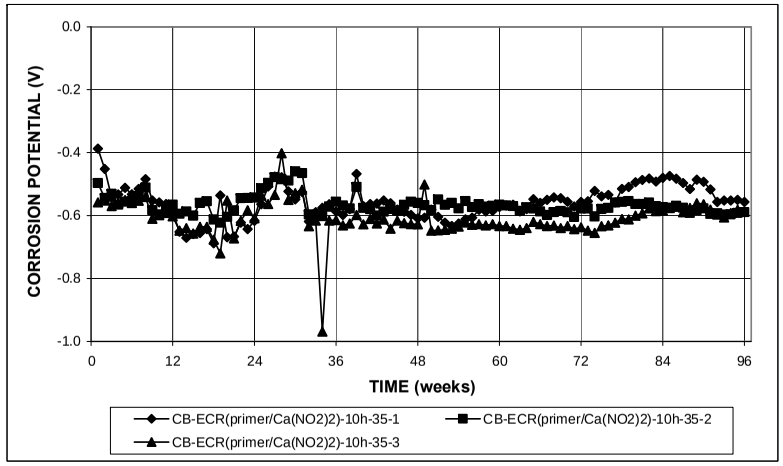

(a)

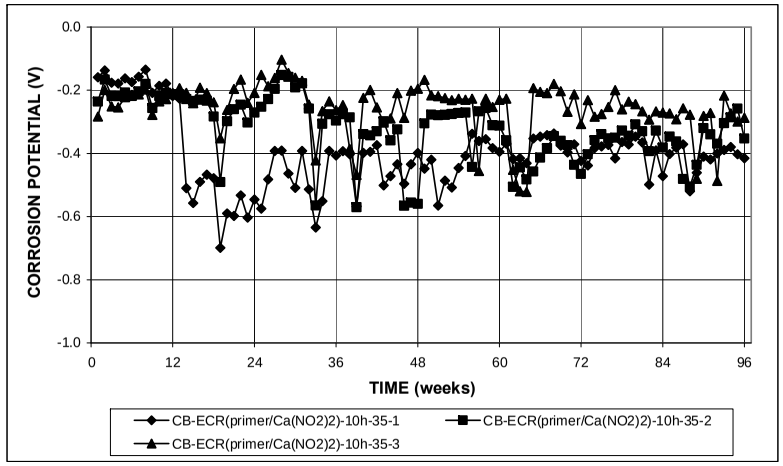

(b)

Figure A.68 – (a) Top mat corrosion potentials and (b) bottom mat corrosion potentials, with respect to the copper-copper sulfate electrode, in the Cracked Beam test for specimens with ECR with calcium nitrite primer (ten 3-mm (1/8-in.) diameter holes), w/c = 0.35.

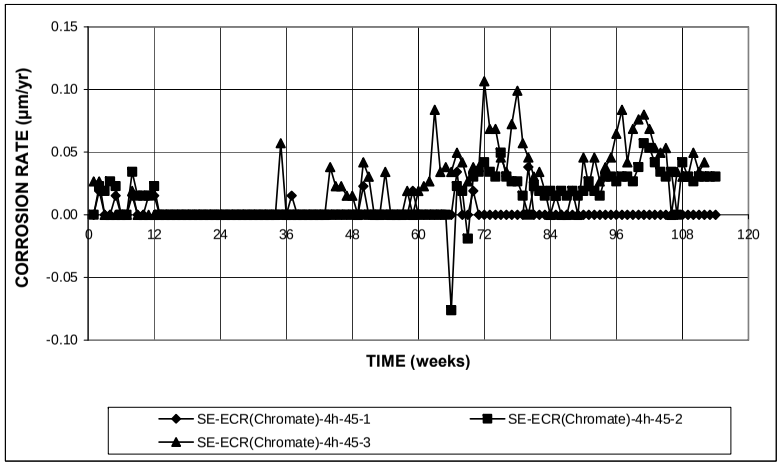

(a)

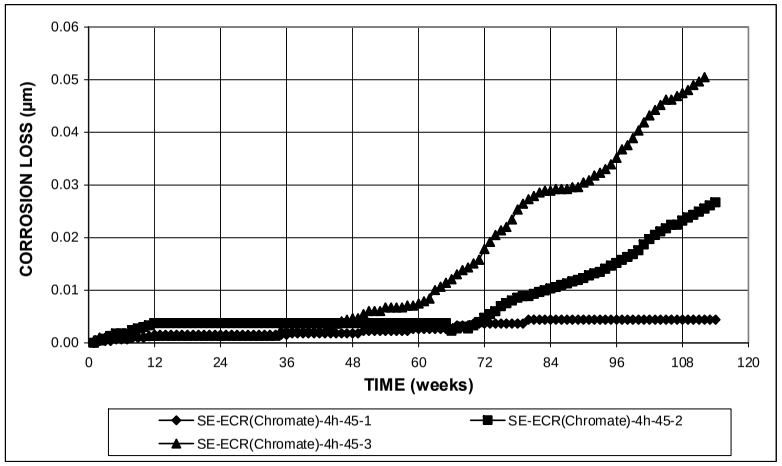

(b)

Figure A.69 – (a) Corrosion rates and (b) total corrosion loss based on total area of the bar in the Southern Exposure test for specimens with ECR with chromate pretreatment (four 3-mm (1/8-in.) diameter holes), w/c = 0.45.

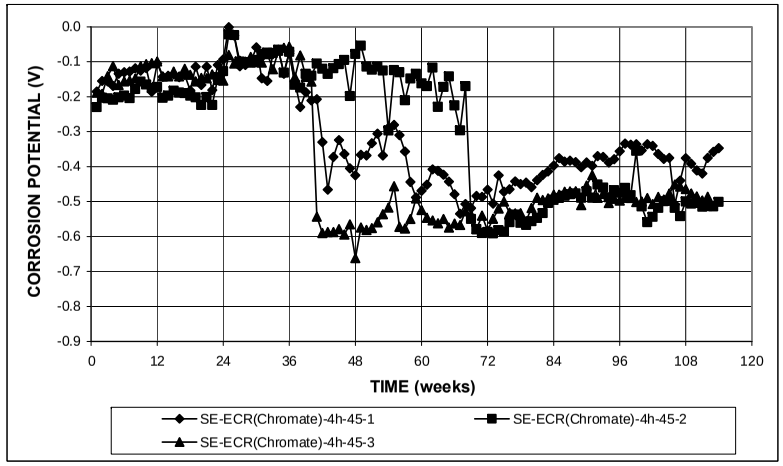

(a)

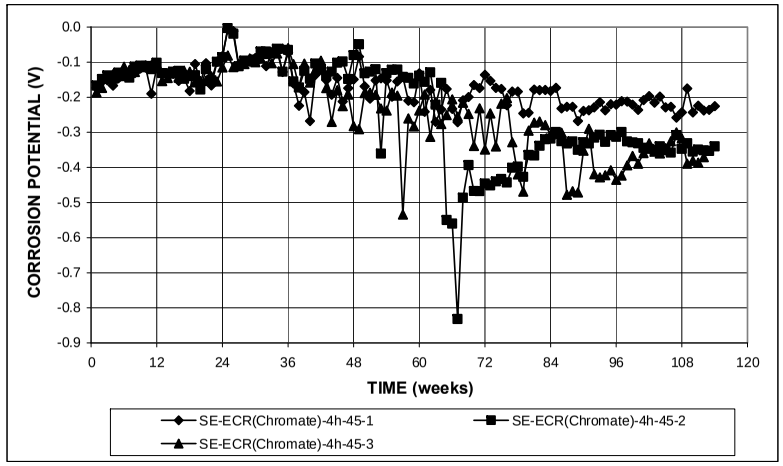

(b)

Figure A.70 – (a) Top mat corrosion potentials and (b) bottom mat corrosion potentials, with respect to the copper-copper sulfate electrode, in the Southern Exposure test for specimens with ECR with chromate pretreatment (four 3-mm (1/8-in.) diameter holes), w/c = 0.45.

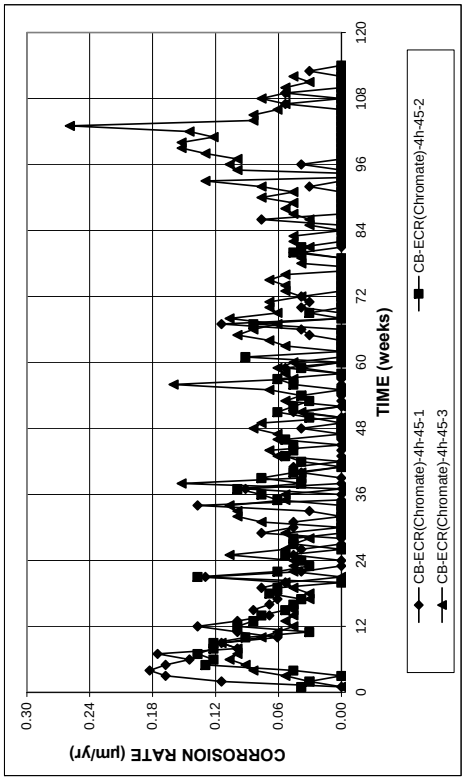

Figure A.71 – (a) Corrosion rates and (b) total corrosion loss based on total area of the bar in the Cracked Beam test for specimens with ECR with chromate pretreatment (four 3-mm (1/8-in.) diameter holes), w/c = 0.45.

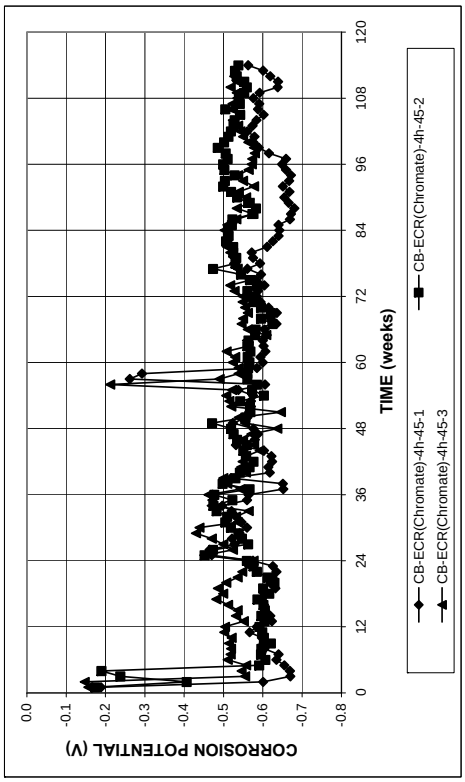

Figure A.72 – (a) Top mat corrosion potentials and (b) bottom mat corrosion potentials, with respect to the copper-copper sulfate electrode, in the Cracked Beam test for specimens with ECR with chromate pretreatment (four 3-mm (1/8-in.) diameter holes), w/c = 0.45.

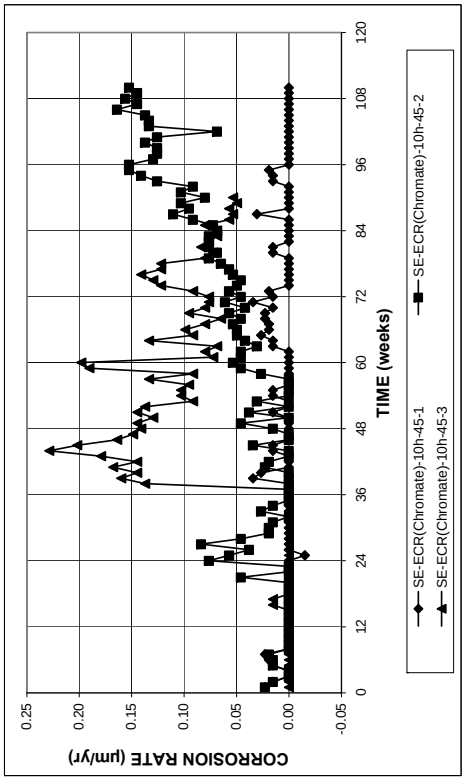

Figure A.73 – (a) Corrosion rates and (b) total corrosion loss based on total area of the bar in the Southern Exposure test for specimens with ECR with chromate pretreatment (ten 3-mm (1/8-in.) diameter holes), w/c = 0.45.

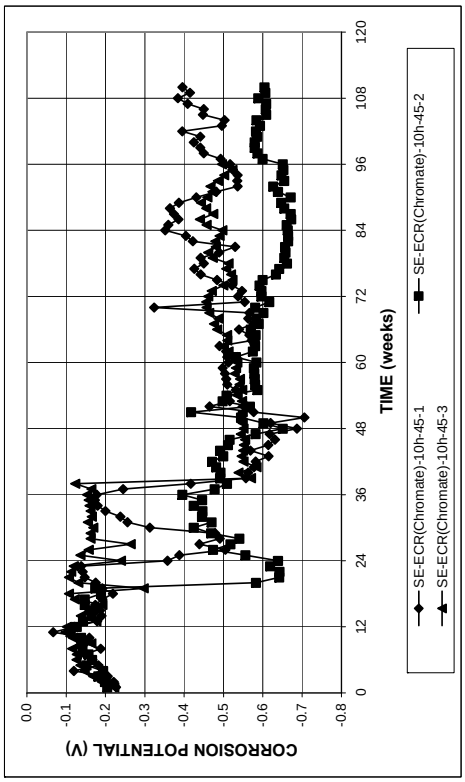

Figure A.74 – (a) Top mat corrosion potentials and (b) bottom mat corrosion potentials, with respect to the copper-copper sulfate electrode, in the Southern Exposure test for specimens with ECR with chromate pretreatment (ten 3-mm (1/8-in.) diameter holes), w/c = 0.45.

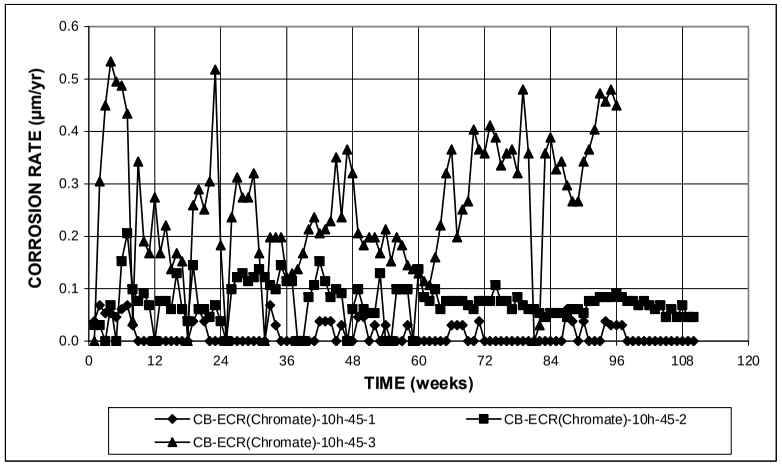

(a)

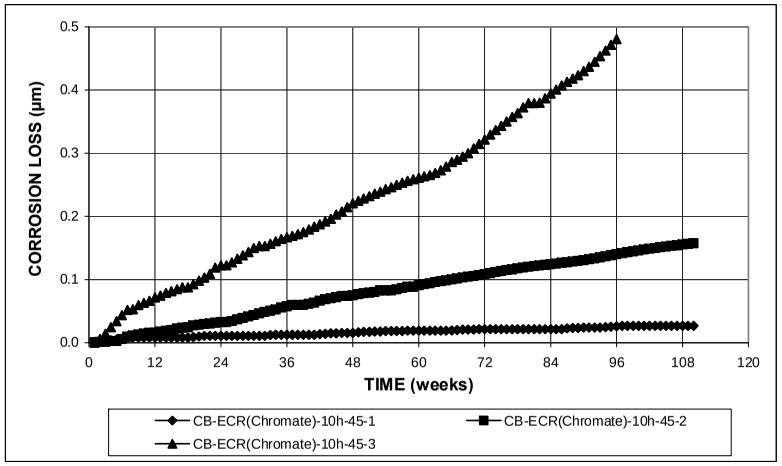

(b)

Figure A.75 – (a) Corrosion rates and (b) total corrosion loss based on total area of the bar in the Cracked Beam test for specimens with ECR with chromate pretreatment (ten 3-mm (1/8-in.) diameter holes), w/c = 0.45.

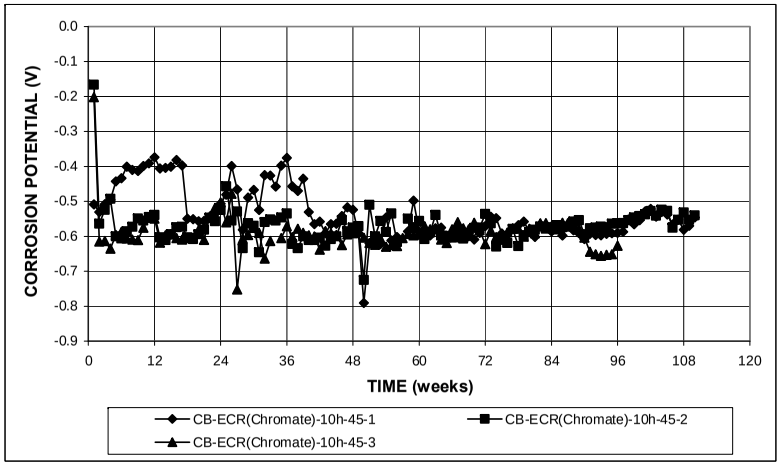

(a)

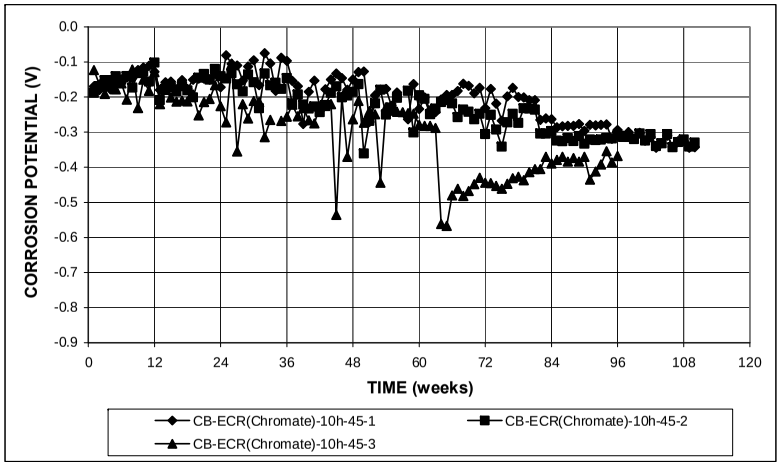

(b)

Figure A.76 – (a) Top mat corrosion potentials and (b) bottom mat corrosion potentials, with respect to the copper-copper sulfate electrode, in the Cracked Beam test for specimens with ECR with chromate pretreatment (ten 3-mm (1/8-in.) diameter holes), w/c = 0.45.

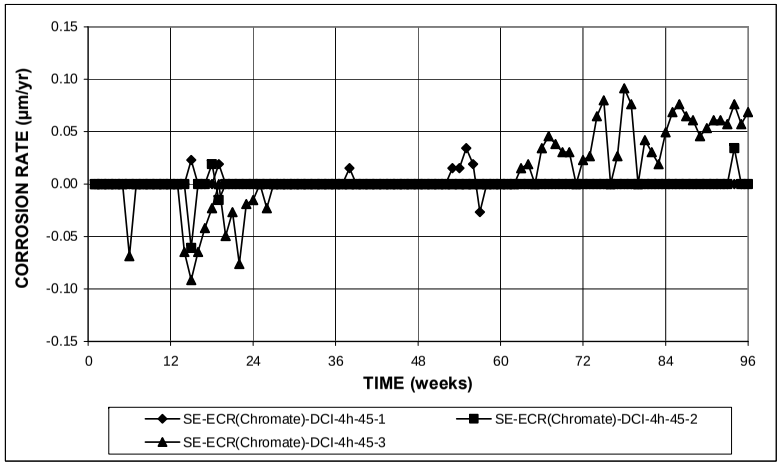

(a)

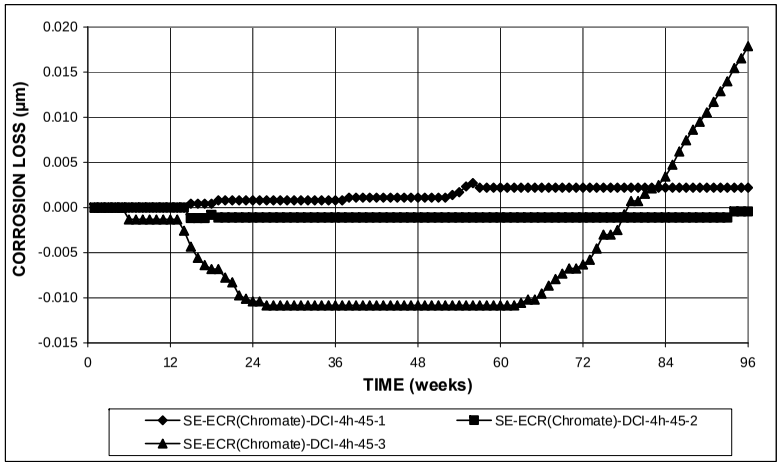

(b)

Figure A.77 – (a) Corrosion rates and (b) total corrosion loss based on total area of the bar in the Southern Exposure test for specimens with ECR with chromate pretreatment (four 3-mm (1/8-in.) diameter holes) in concrete with DCI, w/c = 0.45.

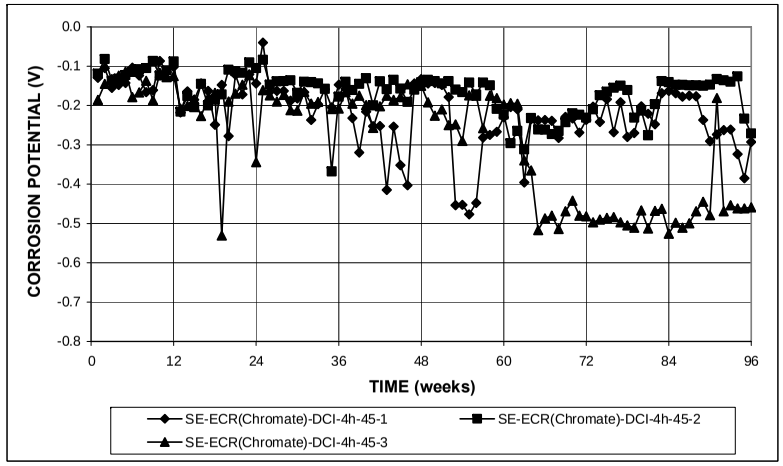

(a)

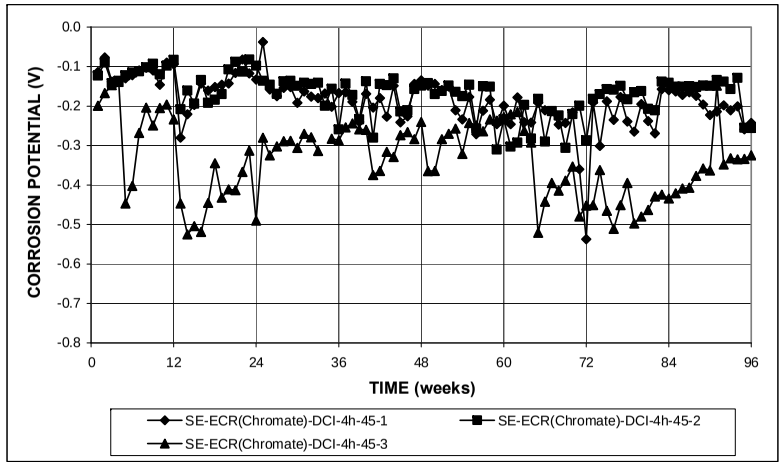

(b)

Figure A.78 – (a) Top mat corrosion potentials and (b) bottom mat corrosion potentials, with respect to the copper-copper sulfate electrode, in the Southern Exposure test for specimens with ECR with chromate pretreatment (four 3-mm (1/8-in.) diameter holes) in concrete with DCI, w/c = 0.45.

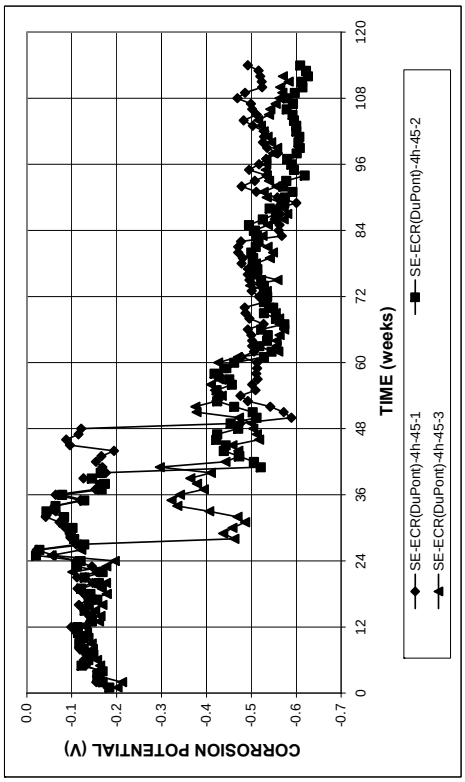

(a)

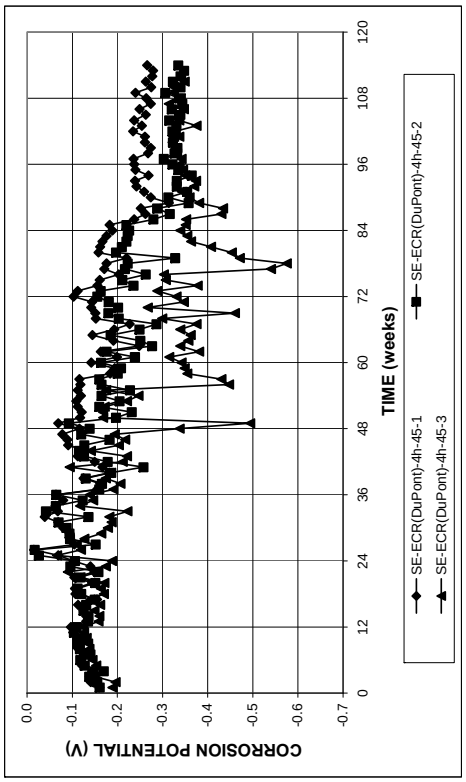

(b)

Figure A.80 – (a) Top mat corrosion potentials and (b) bottom mat corrosion potentials, with respect to the copper-copper sulfate electrode, in the Southern Exposure test for specimens with ECR with DuPont coating (four 3-mm (1/8-in.) diameter holes), w/c = 0.45.

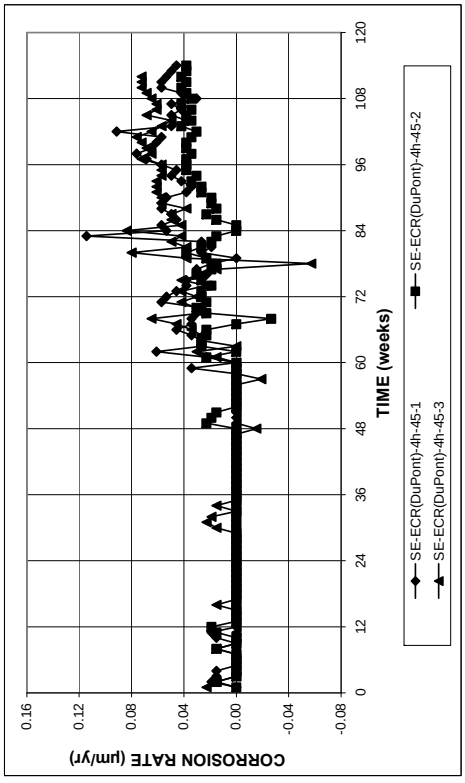

(a)

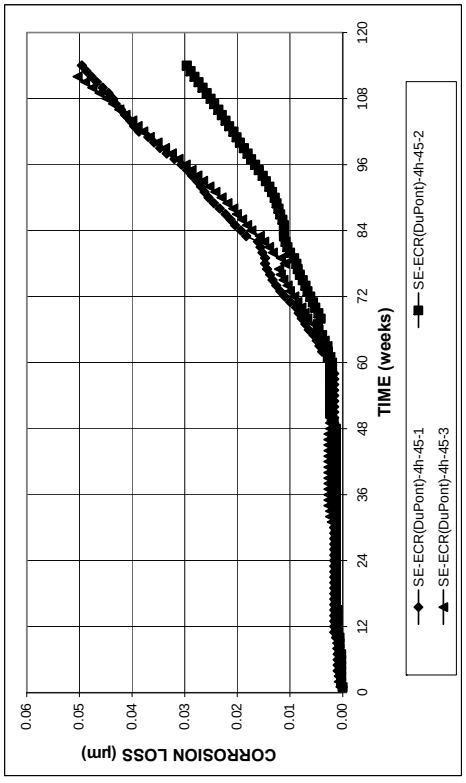

(b)

Figure A.79 – (a) Corrosion rates and (b) total corrosion loss based on total area of the bar in the Southern Exposure test for specimens with ECR with DuPont coating (four 3-mm (1/8-in.) diameter holes), w/c = 0.45.

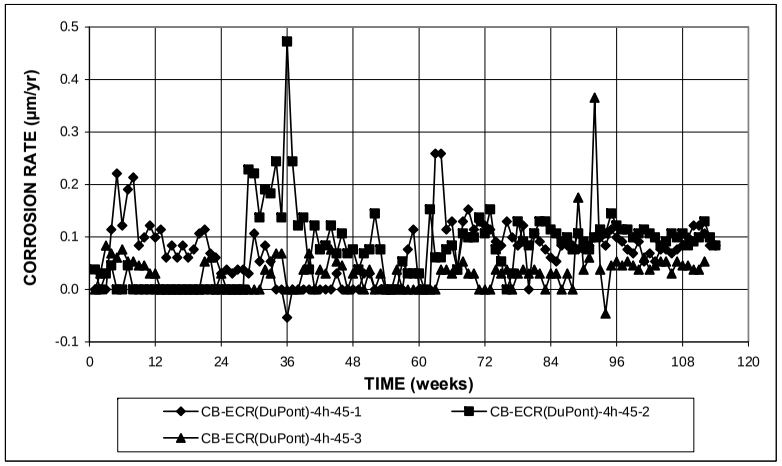

(a)

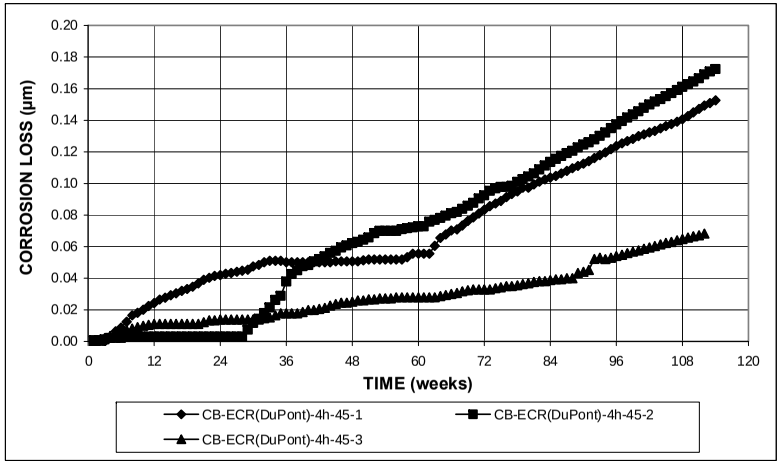

(b)

Figure A.81 – (a) Corrosion rates and (b) total corrosion loss based on total area of the bar in the Cracked Beam test for specimens with ECR with DuPont coating (four 3-mm (1/8-in.) diameter holes), w/c = 0.45.

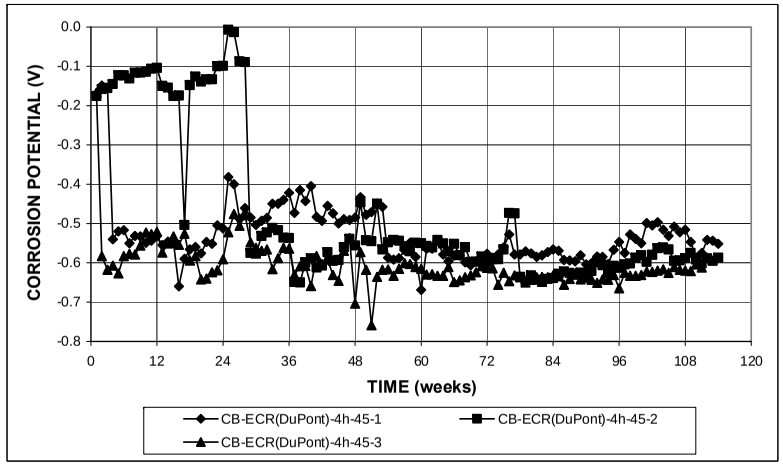

(a)

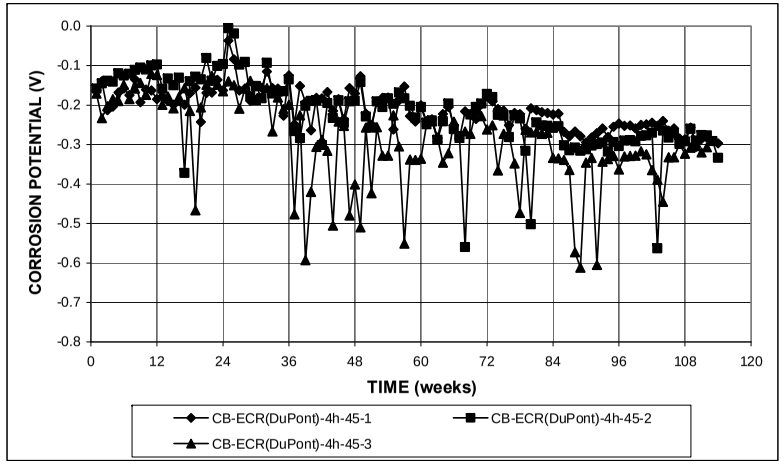

(b)

Figure A.82 – (a) Top mat corrosion potentials and (b) bottom mat corrosion potentials, with respect to the copper-copper sulfate electrode, in the Cracked Beam test for specimens with ECR with DuPont coating (four 3-mm (1/8-in.) diameter holes), w/c = 0.45.

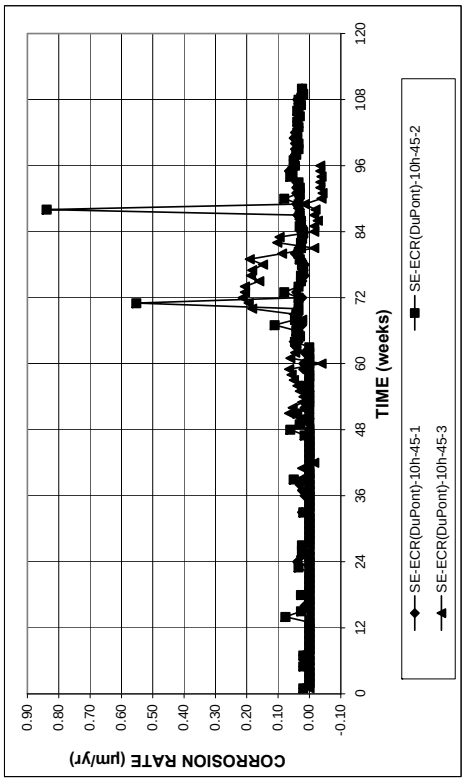

(a)

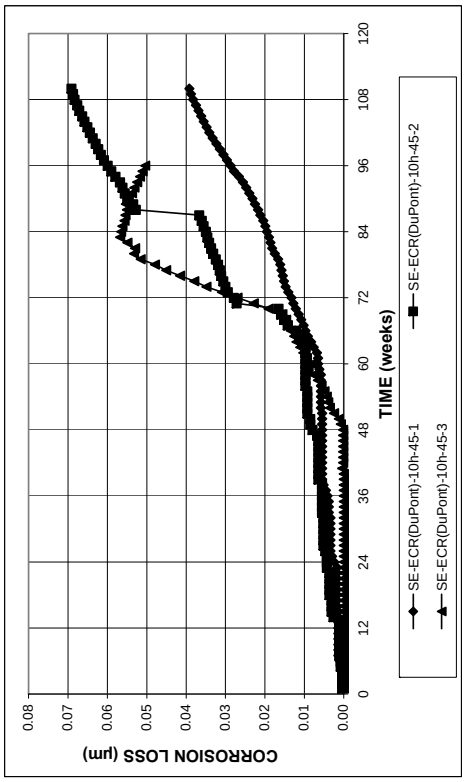

(b)

Figure A.83 – (a) Corrosion rates and (b) total corrosion loss based on total area of the bar in the Southern Exposure test for specimens with ECR with DuPont coating (ten 3-mm (1/8-in.) diameter holes), w/c = 0.45.

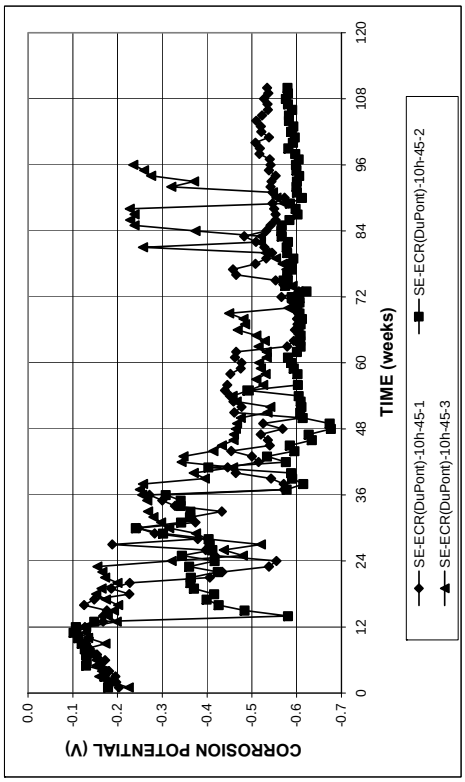

(a)

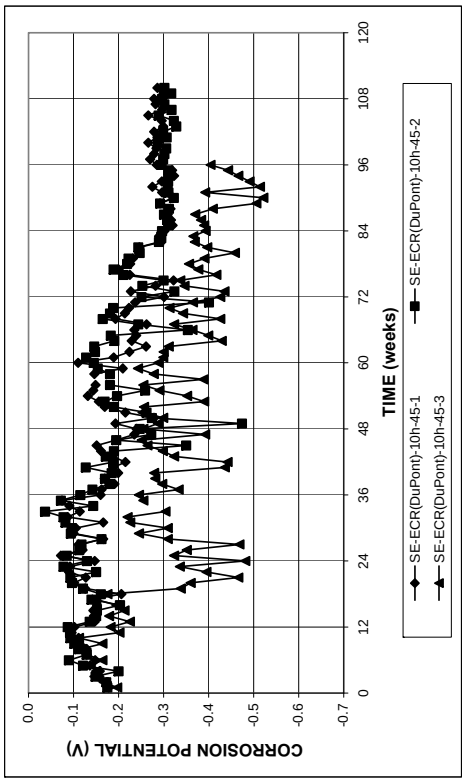

(b)

Figure A.84 – (a) Top mat corrosion potentials and (b) bottom mat corrosion potentials, with respect to the copper-copper sulfate electrode, in the Southern Exposure test for specimens with ECR with DuPont coating (ten 3-mm (1/8-in.) diameter holes), w/c = 0.45.

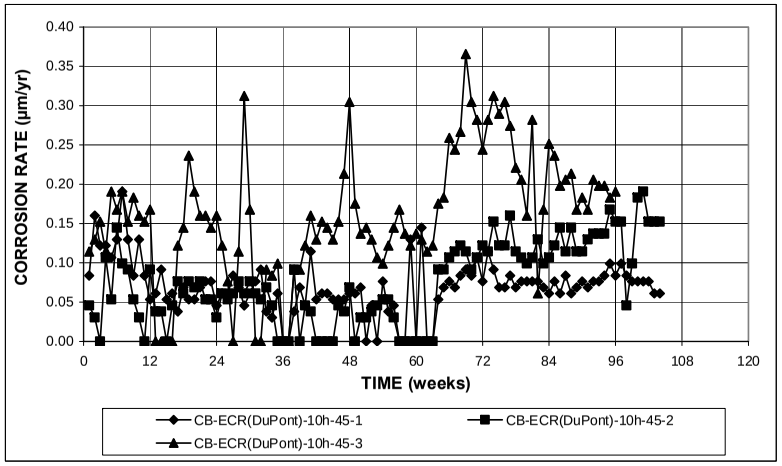

(a)

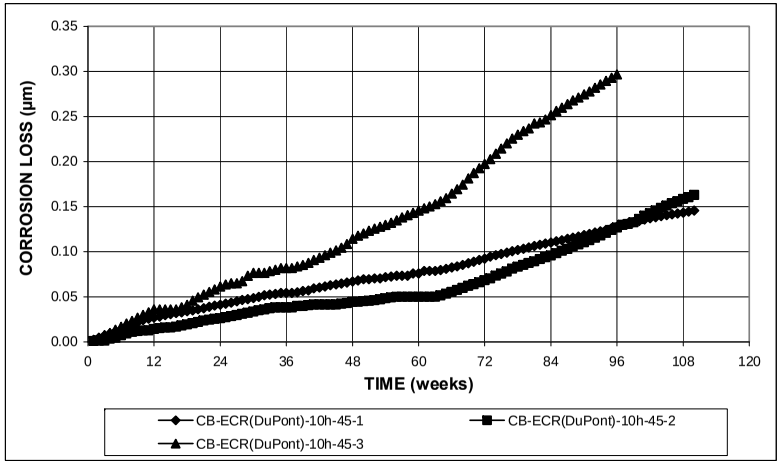

(b)

Figure A.85 – (a) Corrosion rates and (b) total corrosion loss based on total area of the bar in the Cracked Beam test for specimens with ECR with DuPont coating (ten 3-mm (1/8-in.) diameter holes), w/c = 0.45.

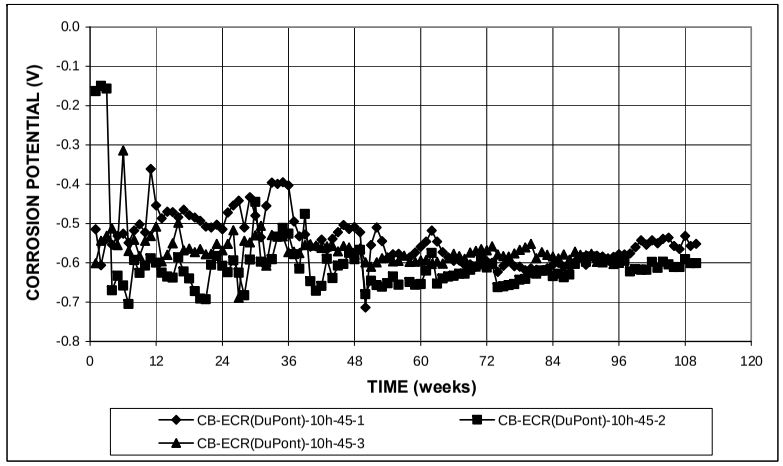

(a)

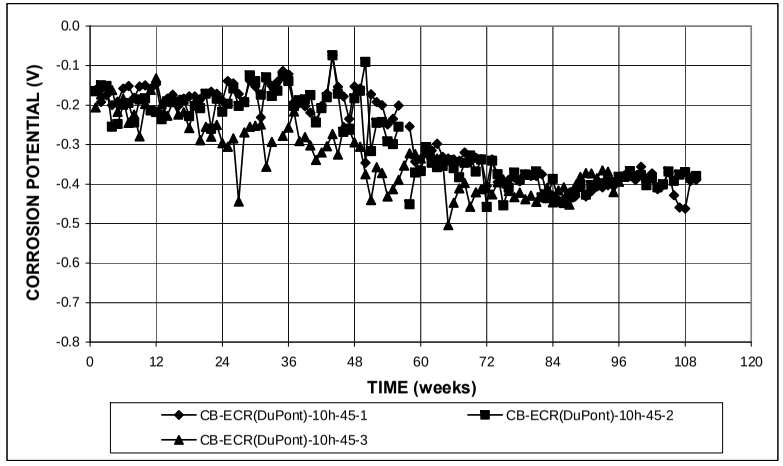

(b)

Figure A.86 – (a) Top mat corrosion potentials and (b) bottom mat corrosion potentials, with respect to the copper-copper sulfate electrode, in the Cracked Beam test for specimens with ECR with DuPont coating (ten 3-mm (1/8-in.) diameter holes), w/c = 0.45.

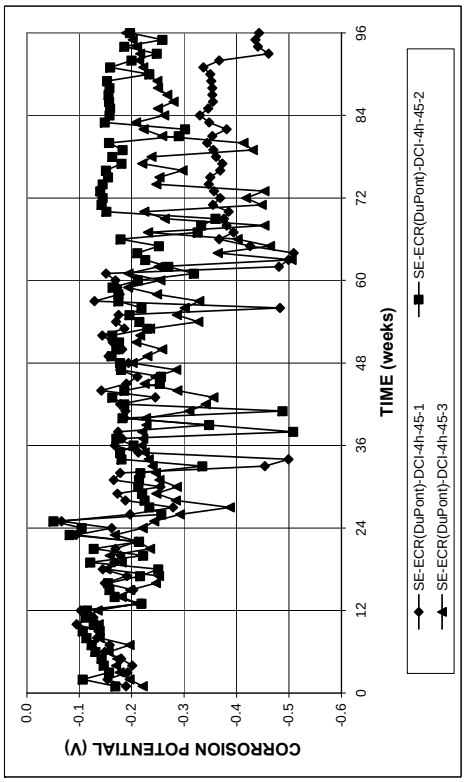

(a)

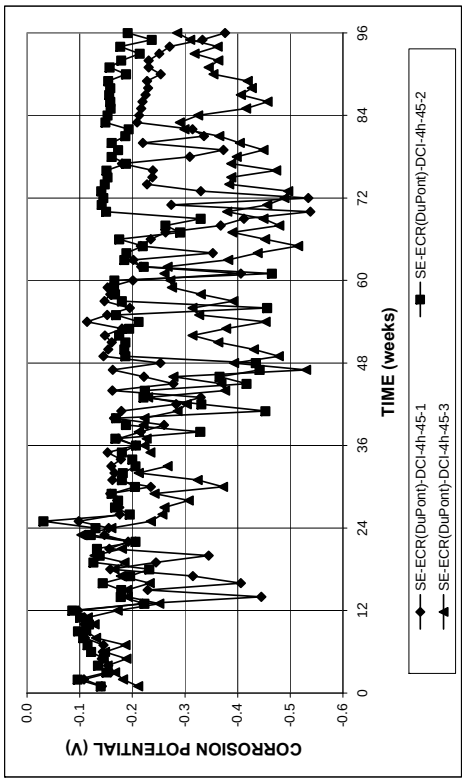

(b)

Figure A.88 – (a) Top mat corrosion potentials and (b) bottom mat corrosion potentials, with respect to the copper-copper sulfate electrode, in the Southern Exposure test for specimens with ECR with DuPont coating (four 3-mm (1/8-in.) diameter holes) in concrete with DCI, w/c = 0.45.

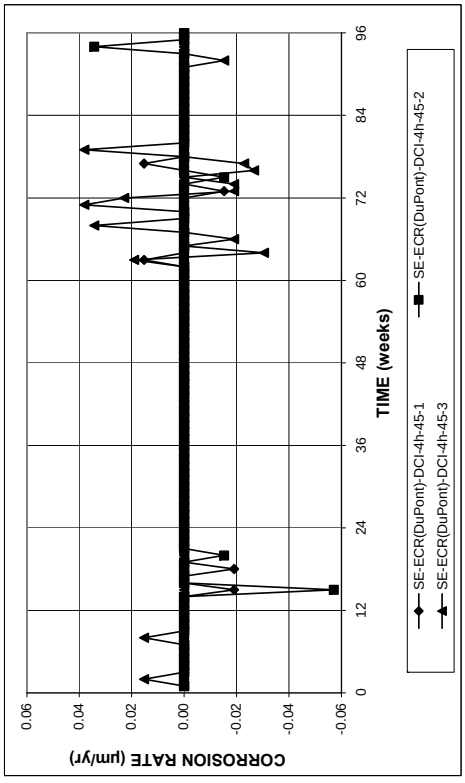

(a)

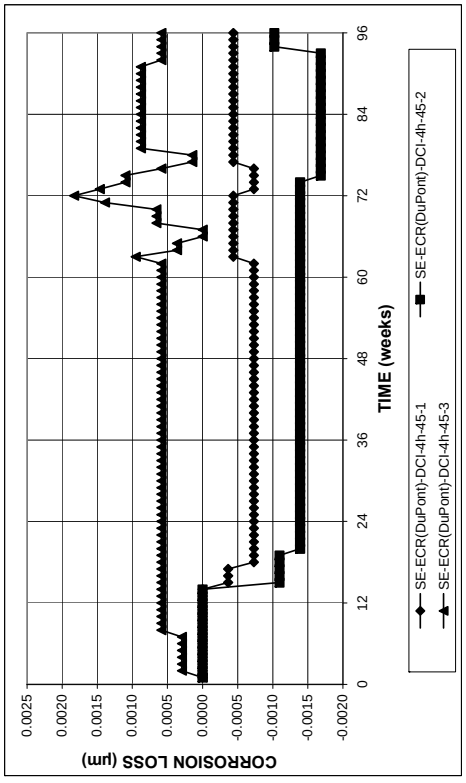

(b)

Figure A.87 – (a) Corrosion rates and (b) total corrosion loss based on total area of the bar in the Southern Exposure test for specimens with ECR with DuPont coating (four 3-mm (1/8-in.) diameter holes) in concrete with DCI, w/c = 0.45.

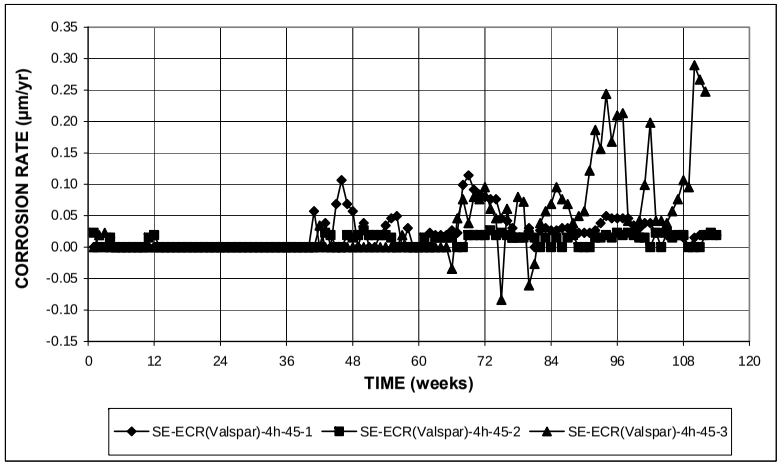

(a)

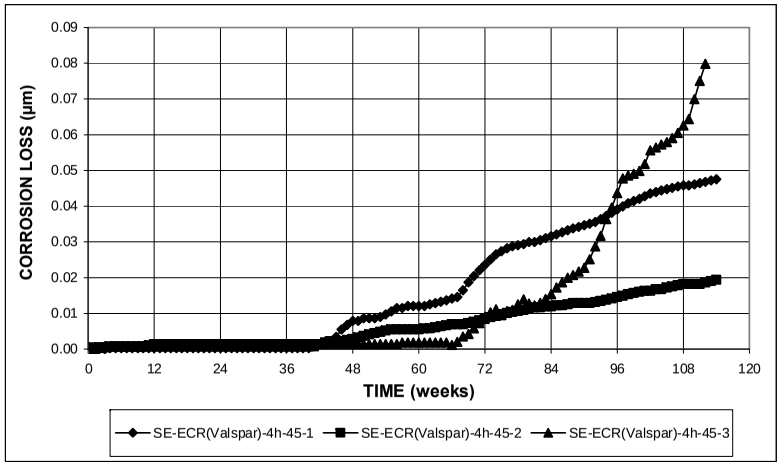

(b)

Figure A.89 – (a) Corrosion rates and (b) total corrosion loss based on total area of the bar in the Southern Exposure test for specimens with ECR with Valspar coating (four 3-mm (1/8-in.) diameter holes), w/c = 0.45.

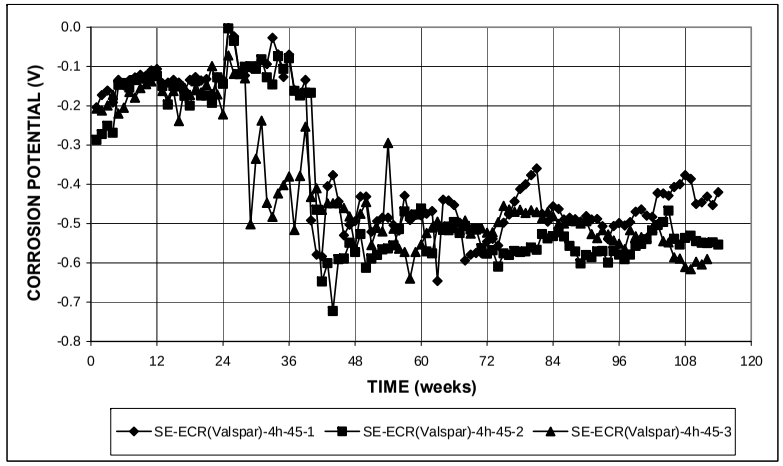

(a)

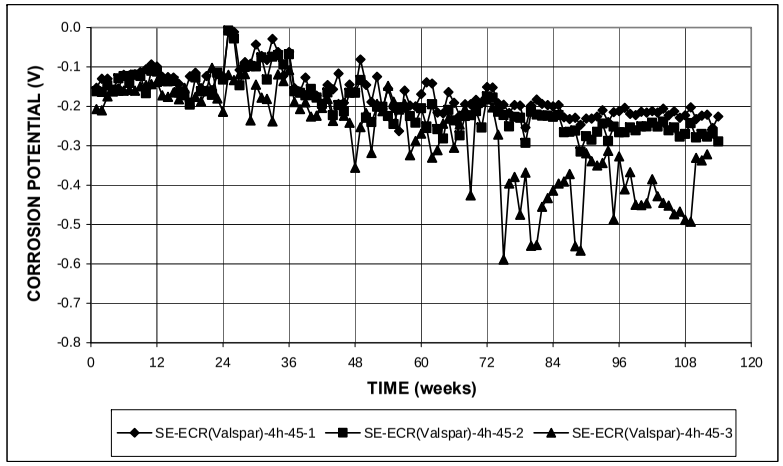

(b)

Figure A.90 – (a) Top mat corrosion potentials and (b) bottom mat corrosion potentials, with respect to the copper-copper sulfate electrode, in the Southern Exposure test for specimens with ECR with Valspar coating (four 3-mm (1/8-in.) diameter holes), w/c = 0.45.

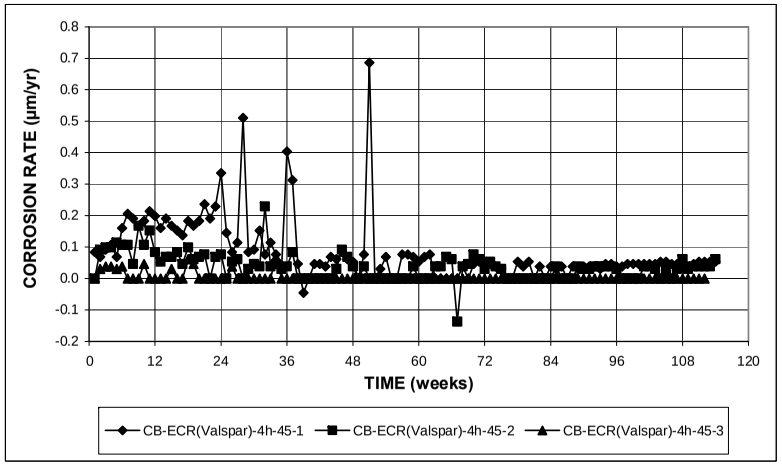

(a)

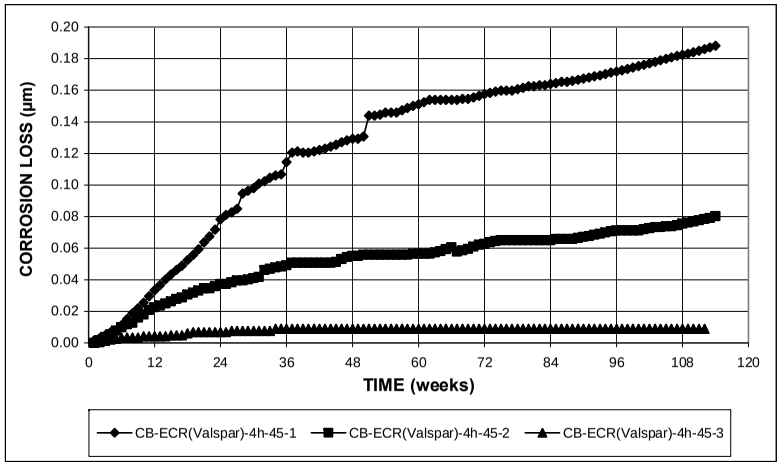

(b)

Figure A.91 – (a) Corrosion rates and (b) total corrosion loss based on total area of the bar in the Cracked Beam test for specimens with ECR with Valspar coating (four 3-mm (1/8-in.) diameter holes), w/c = 0.45.

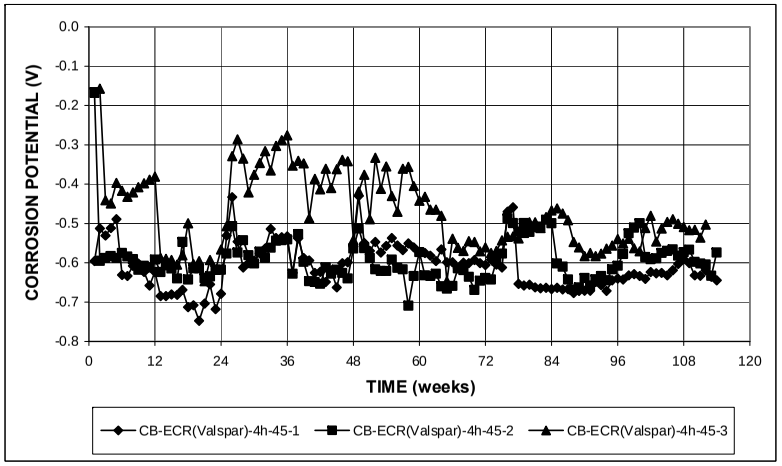

(a)

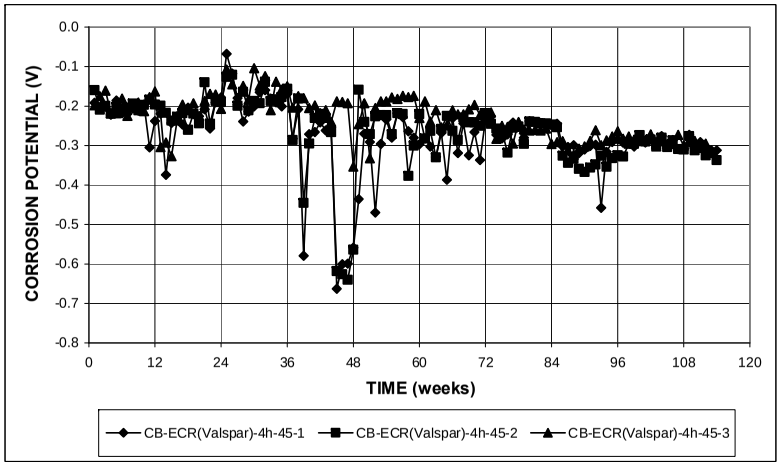

(b)

Figure A.92 – (a) Top mat corrosion potentials and (b) bottom mat corrosion potentials, with respect to the copper-copper sulfate electrode, in the Cracked Beam test for specimens with ECR with Valspar coating (four 3-mm (1/8-in.) diameter holes), w/c = 0.45.

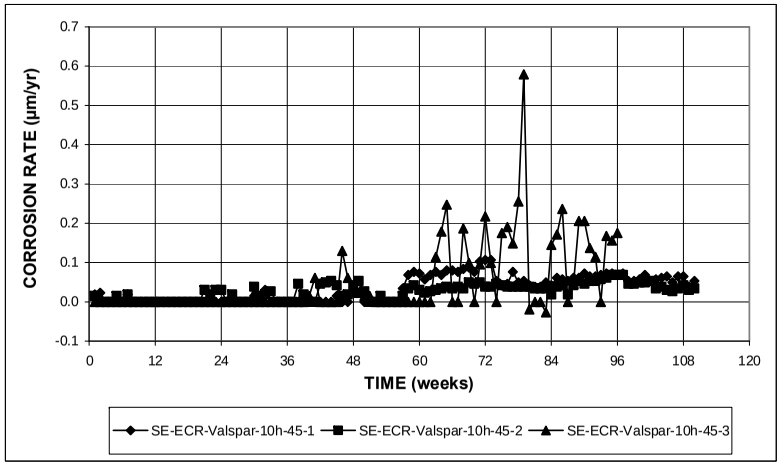

(a)

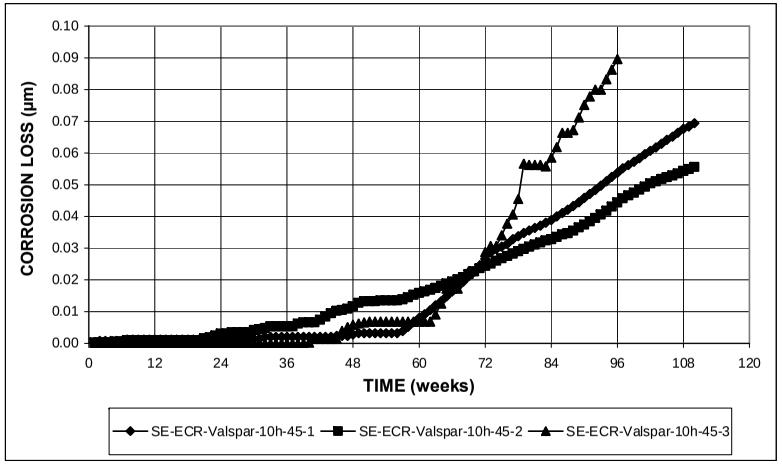

(b)

Figure A.93 – (a) Corrosion rates and (b) total corrosion loss based on total area of the bar in the Southern Exposure test for specimens with ECR with Valspar coating (ten 3-mm (1/8-in.) diameter holes), w/c = 0.45.

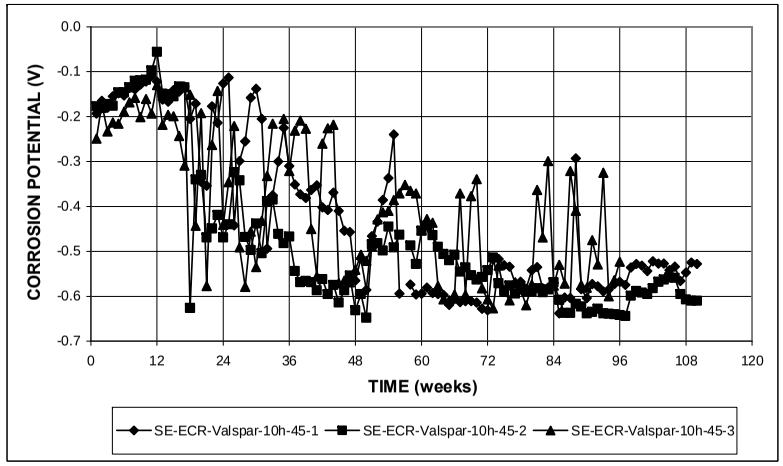

(a)

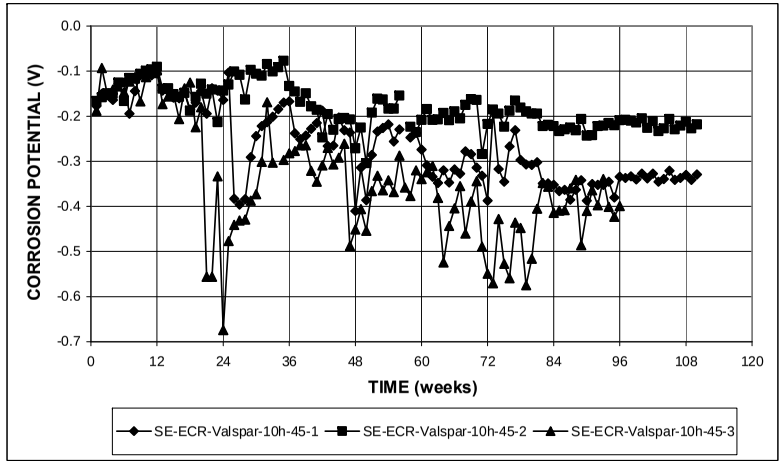

(b)

Figure A.94 – (a) Top mat corrosion potentials and (b) bottom mat corrosion potentials, with respect to the copper-copper sulfate electrode, in the Southern Exposure test for specimens with ECR with Valspar coating (ten 3-mm (1/8-in.) diameter holes), w/c = 0.45.

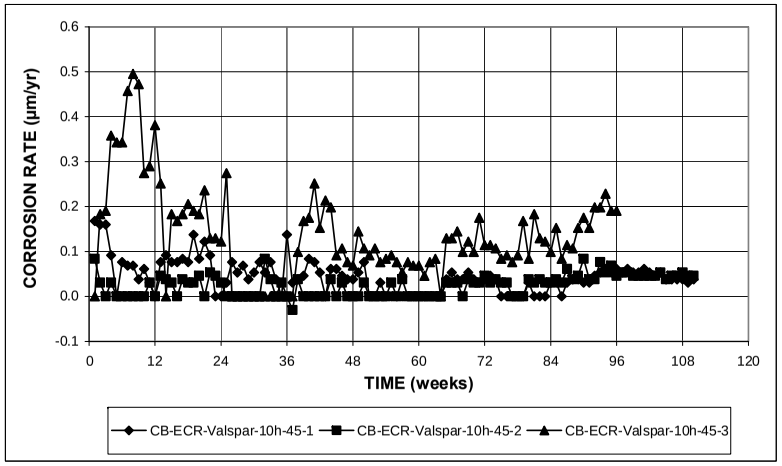

(a)

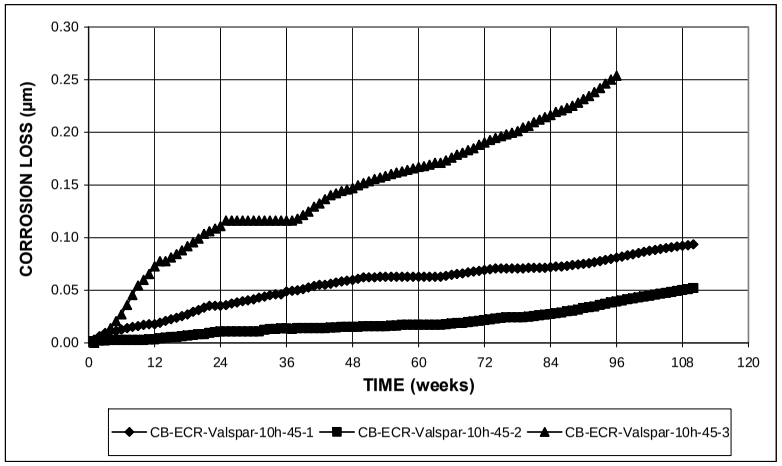

(b)

Figure A.95 – (a) Corrosion rates and (b) total corrosion loss based on total area of the bar in the Cracked Beam test for specimens with ECR with Valspar coating (ten 3-mm (1/8-in.) diameter holes), w/c = 0.45.

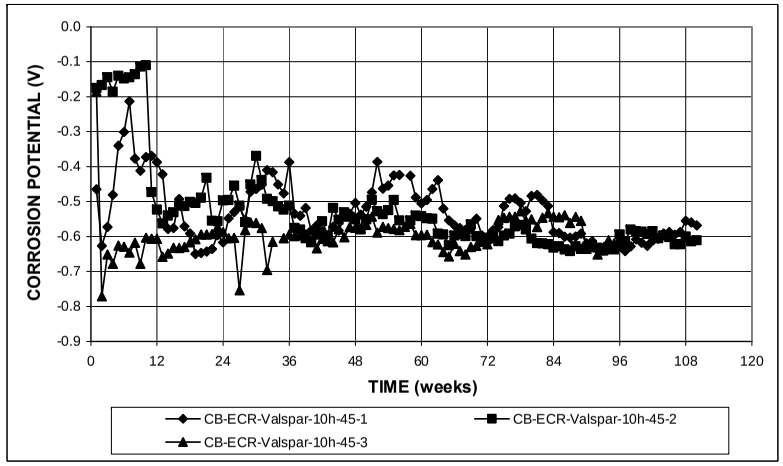

(a)

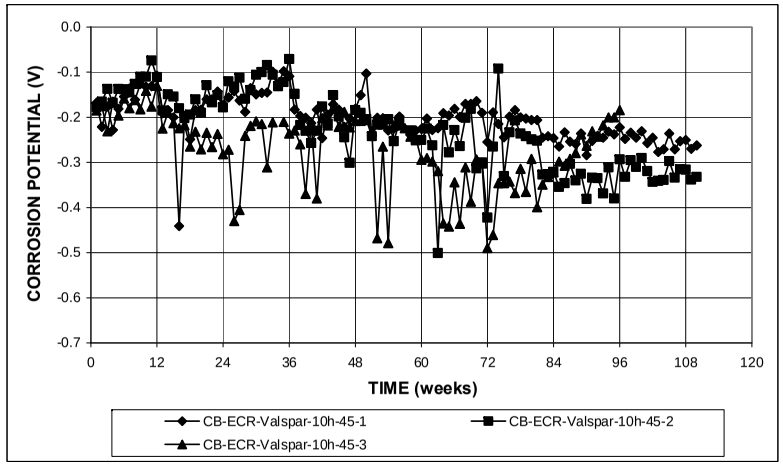

(b)

Figure A.96 – (a) Top mat corrosion potentials and (b) bottom mat corrosion potentials, with respect to the copper-copper sulfate electrode, in the Cracked Beam test for specimens with ECR with Valspar coating (ten 3-mm (1/8-in.) diameter holes), w/c = 0.45.

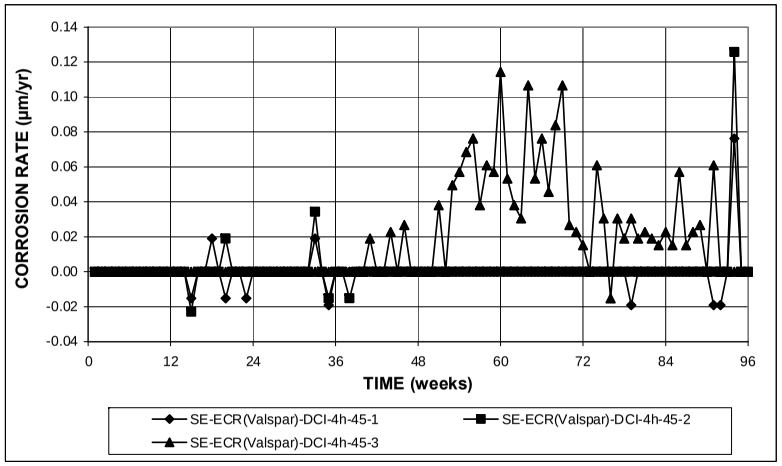

(a)

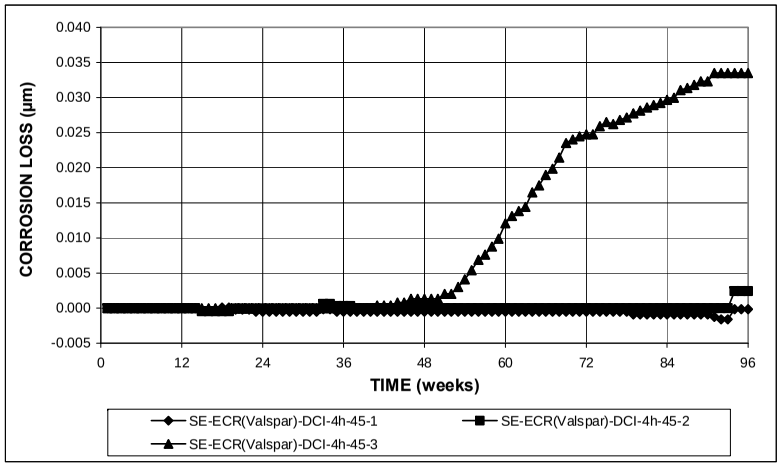

(b)

Figure A.97 – (a) Corrosion rates and (b) total corrosion loss based on total area of the bar in the Southern Exposure test for specimens with ECR with Valspar coating (four 3-mm (1/8-in.) diameter holes) in concrete with DCI, w/c = 0.45.

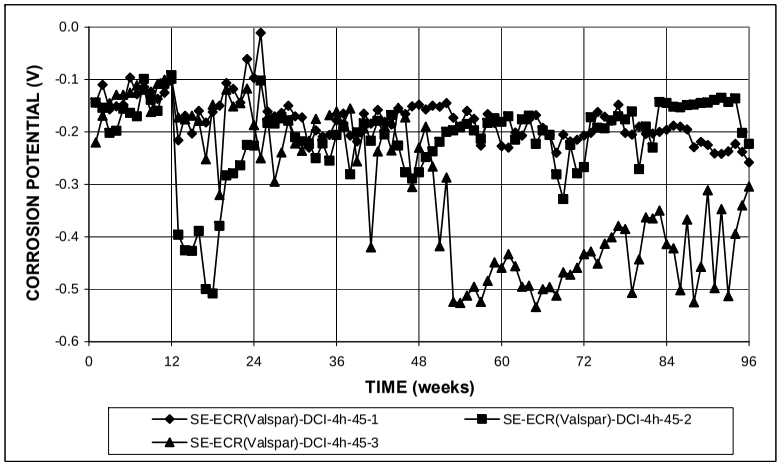

(a)

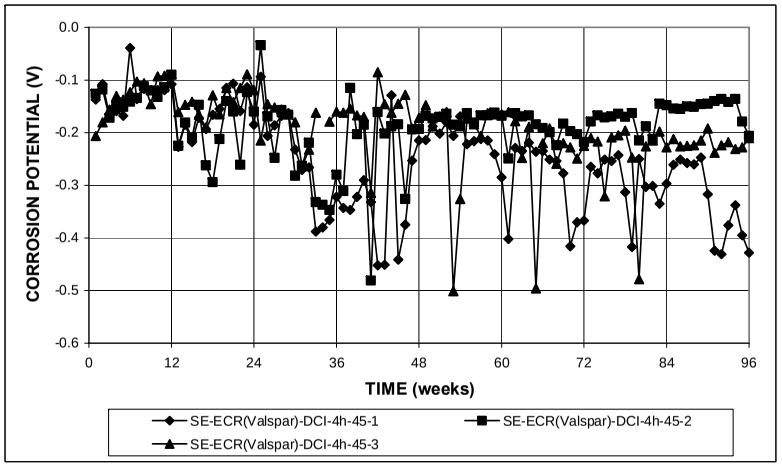

(b)

Figure A.98 – (a) Top mat corrosion potentials and (b) bottom mat corrosion potentials, with respect to the copper-copper sulfate electrode, in the Southern Exposure test for specimens with ECR with Valspar coating (four 3-mm (1/8-in.) diameter holes) in concrete with DCI, w/c = 0.45.

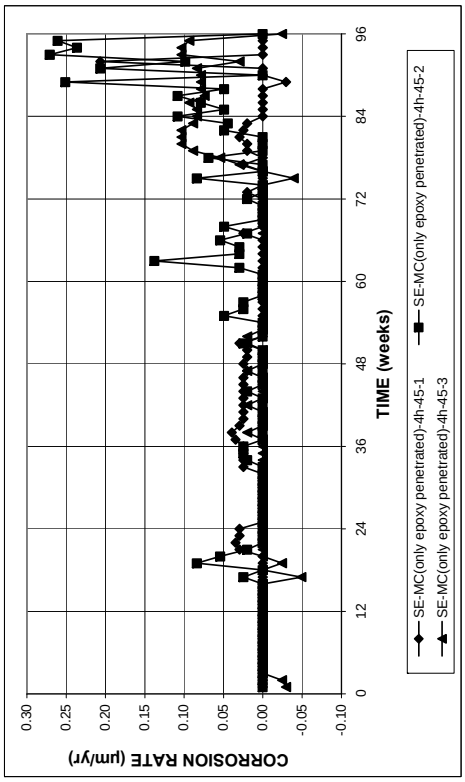

Figure A.99 – (a) Corrosion rates and (b) total corrosion loss based on total area of the bar in the Southern Exposure test for specimens with multiple coated bar (four 3-mm (1/8-in.) diameter holes, only epoxy penetrated), w/c = 0.45.

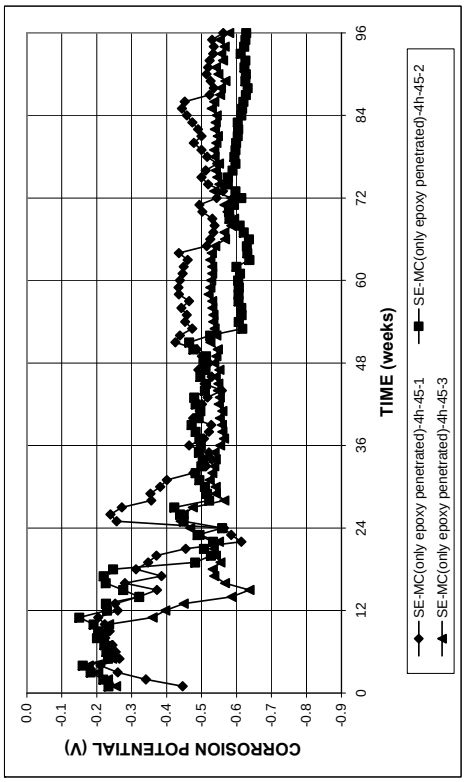

Figure A.100 – (a) Top mat corrosion potentials and (b) bottom mat corrosion potentials, with respect to the copper-copper sulfate electrode, in the Southern Exposure test for specimens with multiple coated bars (four 3-mm (1/8-in.) diameter holes, only epoxy penetrated), w/c = 0.45.

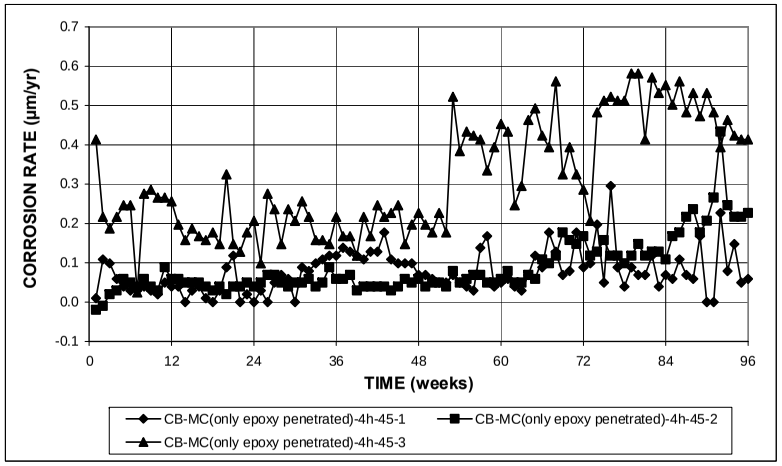

(a)

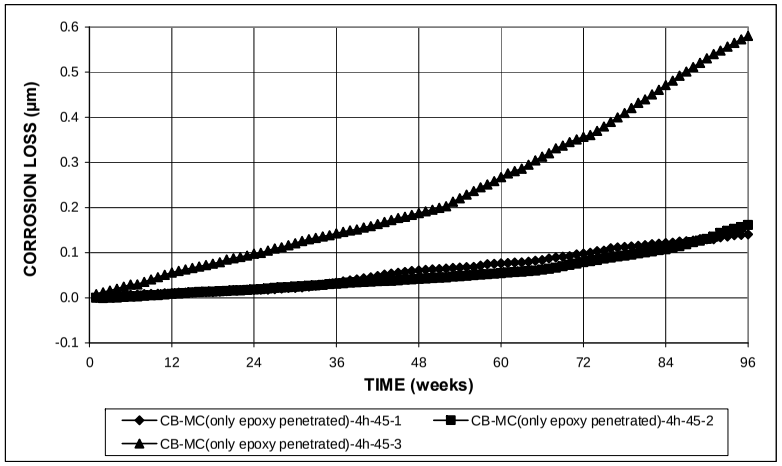

(b)

Figure A.101 – (a) Corrosion rates and (b) total corrosion loss based on total area of the bar in the Cracked Beam test for specimens with multiple coated bar (four 3-mm (1/8-in.) diameter holes, only epoxy penetrated), w/c = 0.45.

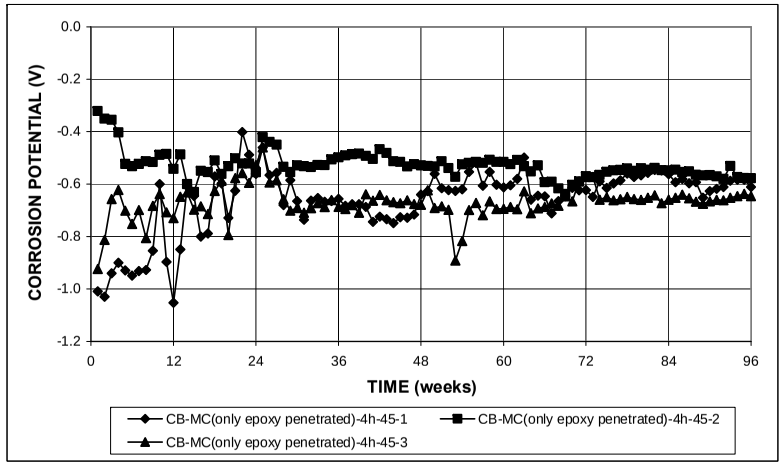

(a)

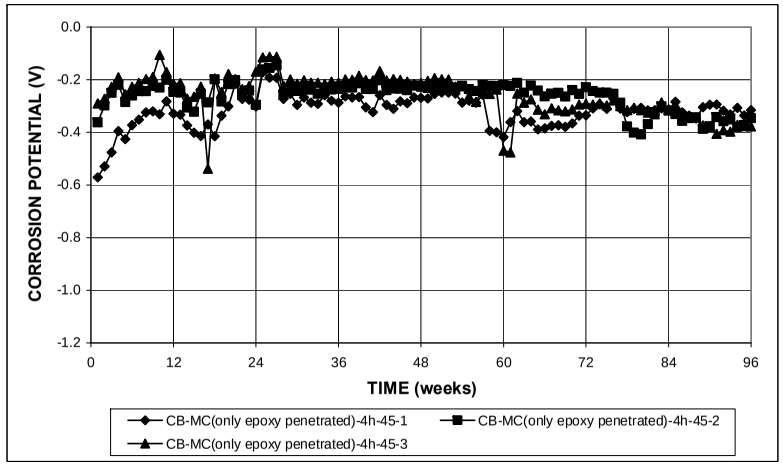

(b)

Figure A.102 – (a) Top mat corrosion potentials and (b) bottom mat corrosion potentials, with respect to the copper-copper sulfate electrode, in the Cracked Beam test for specimens with multiple coated bars (four 3-mm (1/8-in.) diameter holes, only epoxy penetrated), w/c = 0.45.

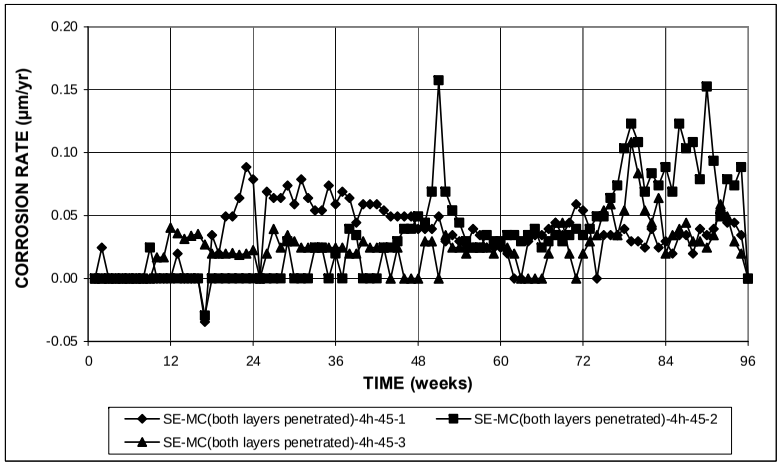

(a)

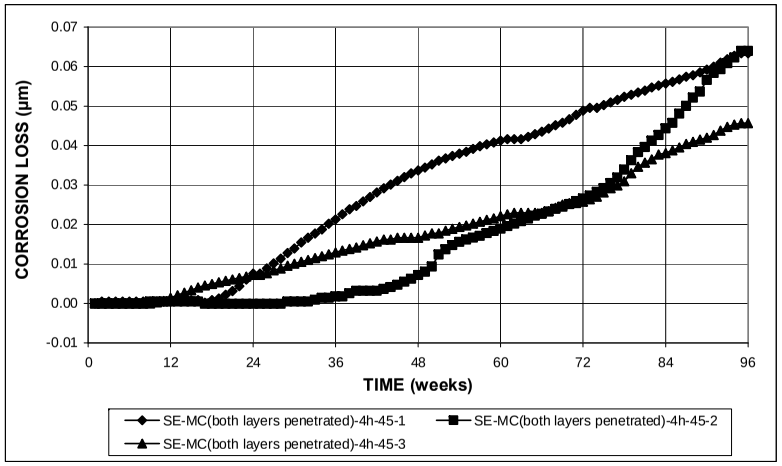

(b)

Figure A.103 – (a) Corrosion rates and (b) total corrosion loss based on total area of the bar in the Southern Exposure test for specimens with multiple coated bar (four 3-mm (1/8-in.) diameter holes, both layers penetrated), w/c = 0.45.

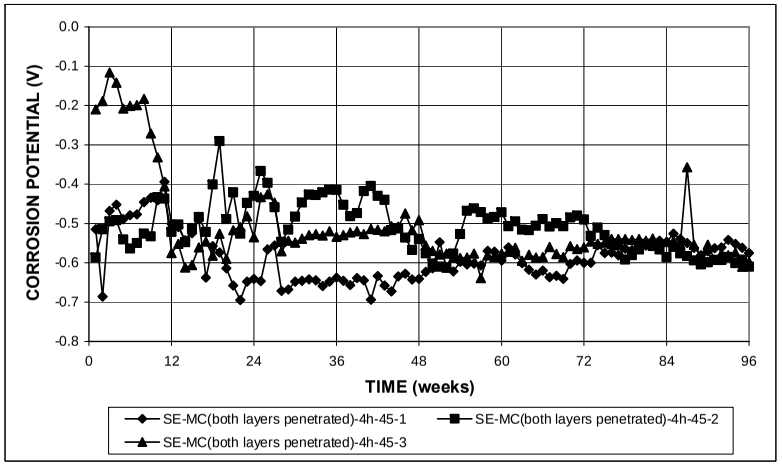

(a)

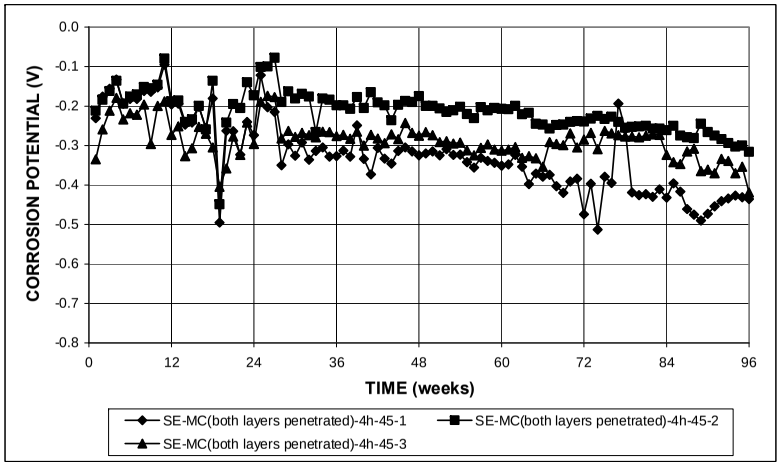

(b)

Figure A.104 – (a) Top mat corrosion potentials and (b) bottom mat corrosion potentials, with respect to the copper-copper sulfate electrode, in the Southern Exposure test for specimens with multiple coated bars (four 3-mm (1/8-in.) diameter holes, both layers penetrated), w/c = 0.45.

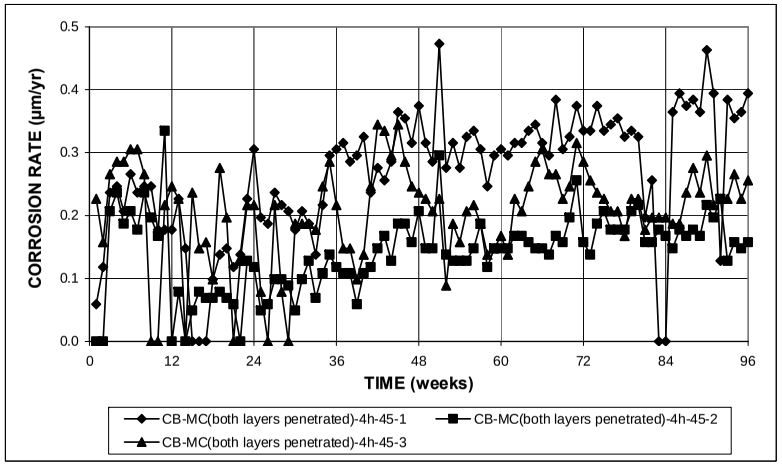

(a)

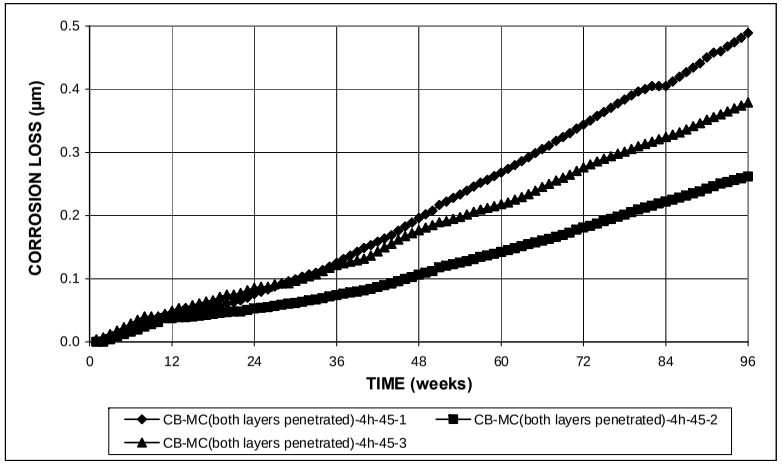

(b)

Figure A.105 – (a) Corrosion rates and (b) total corrosion loss based on total area of the bar in the Cracked Beam test for specimens with multiple coated bar (four 3-mm (1/8-in.) diameter holes, both layers penetrated), w/c = 0.45.

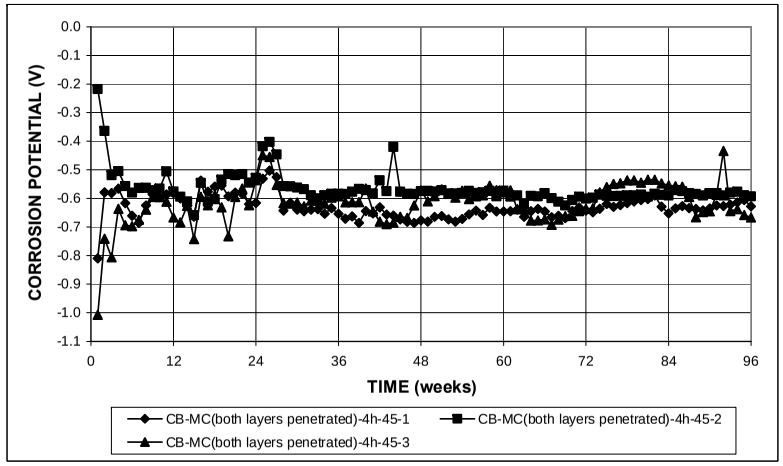

(a)

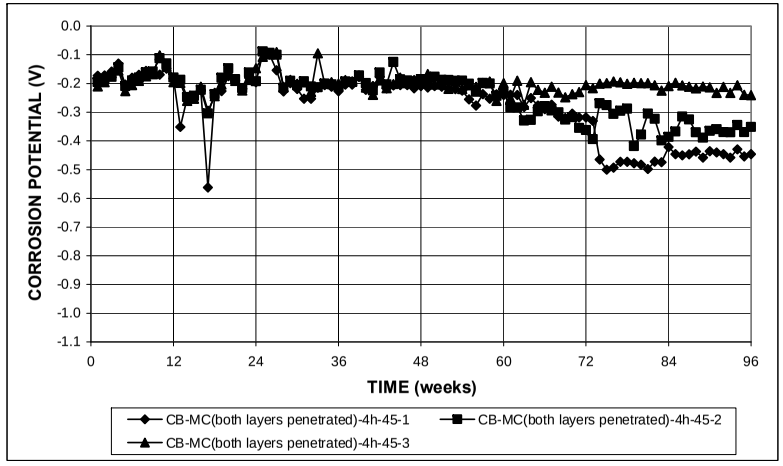

(b)

Figure A.106 – (a) Top mat corrosion potentials and (b) bottom mat corrosion potentials, with respect to the copper-copper sulfate electrode, in the Cracked Beam test for specimens with multiple coated bars (four 3-mm (1/8-in.) diameter holes, both layers penetrated), w/c = 0.45.

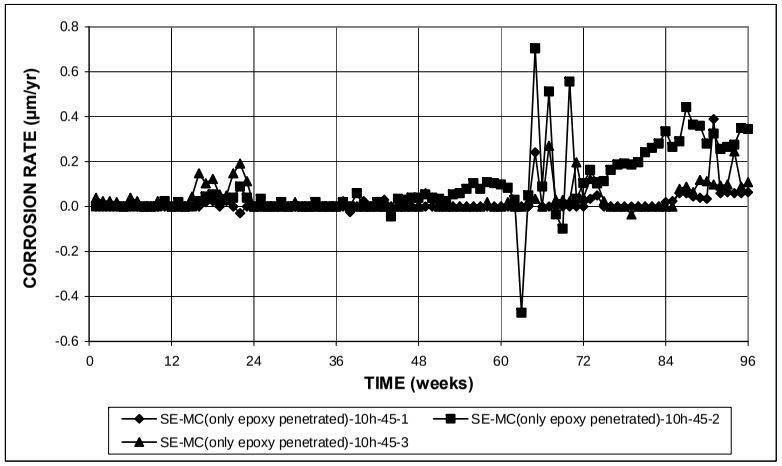

(a)

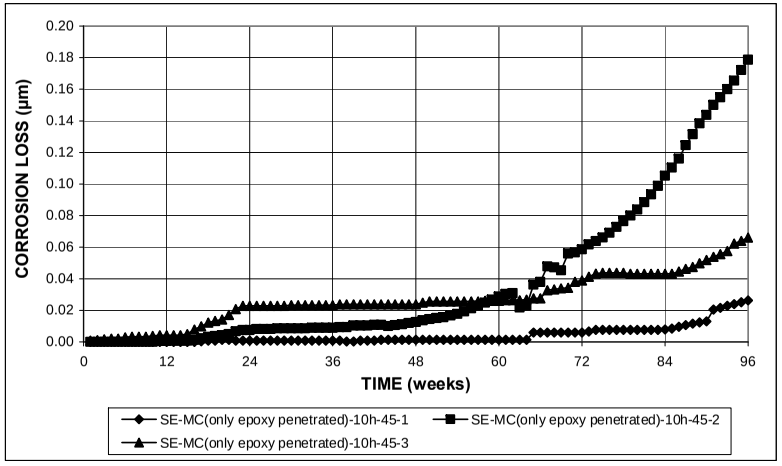

(b)

Figure A.107 – (a) Corrosion rates and (b) total corrosion loss based on total area of the bar in the Southern Exposure test for specimens with multiple coated bar (ten 3-mm (1/8-in.) diameter holes, only epoxy penetrated), w/c = 0.45.

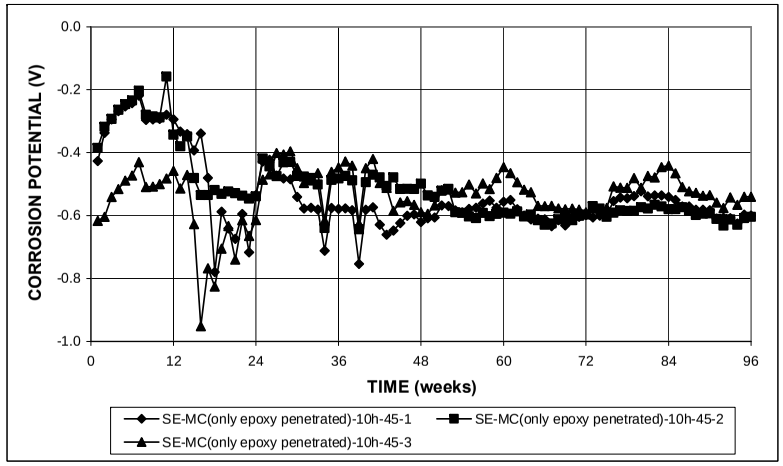

(a)

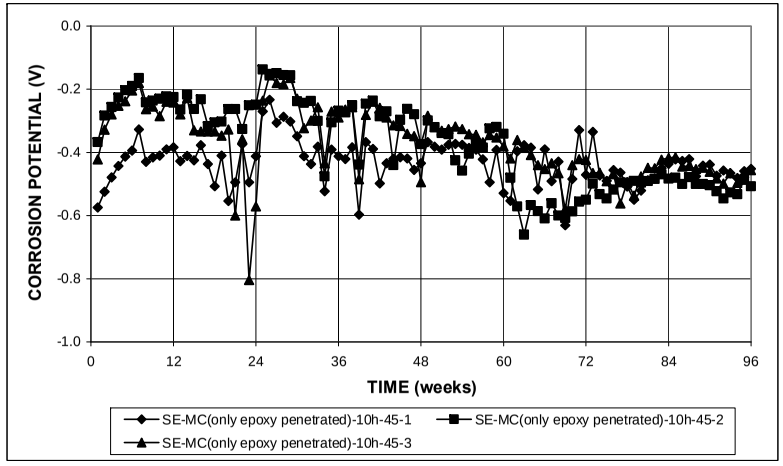

(b)

Figure A.108 – (a) Top mat corrosion potentials and (b) bottom mat corrosion potentials, with respect to the copper-copper sulfate electrode, in the Southern Exposure test for specimens with multiple coated bars (ten 3-mm (1/8-in.) diameter holes, only epoxy penetrated), w/c = 0.45.

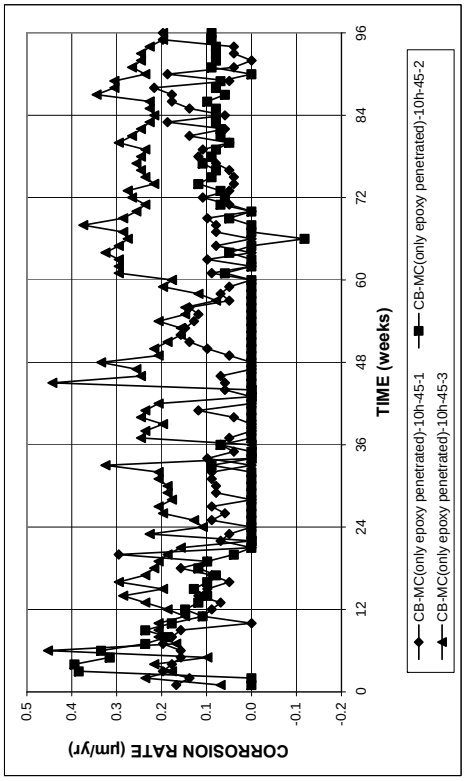

(a)

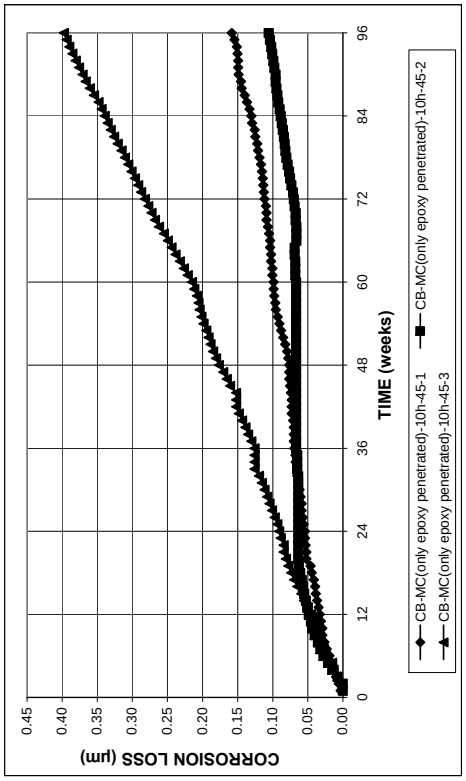

(b)

Figure A.109 – (a) Corrosion rates and (b) total corrosion loss based on total area of the bar in the Cracked Beam test for specimens with multiple coated bar (ten 3-mm (1/8-in.) diameter holes, only epoxy penetrated), w/c = 0.45.

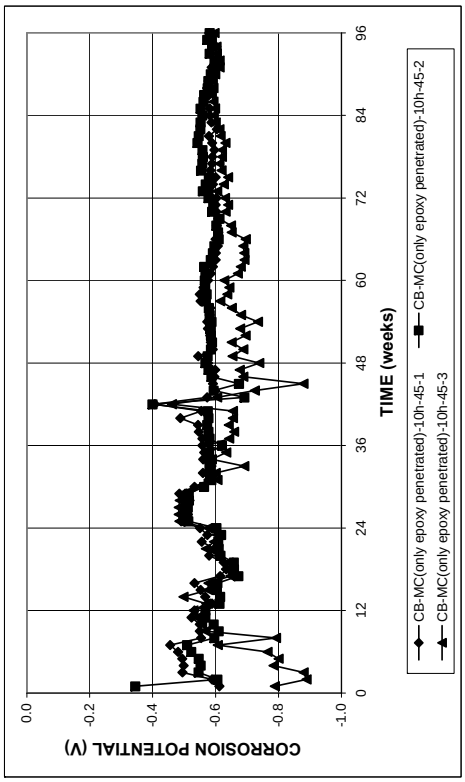

(a)

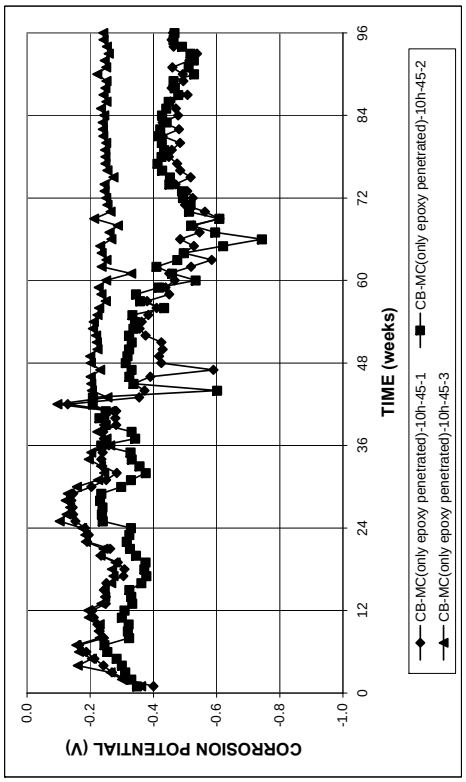

(b)

Figure A.110 – (a) Top mat corrosion potentials and (b) bottom mat corrosion potentials, with respect to the copper-copper sulfate electrode, in the Cracked Beam test for specimens with multiple coated bars (ten 3-mm (1/8-in.) diameter holes, only epoxy penetrated), w/c = 0.45.

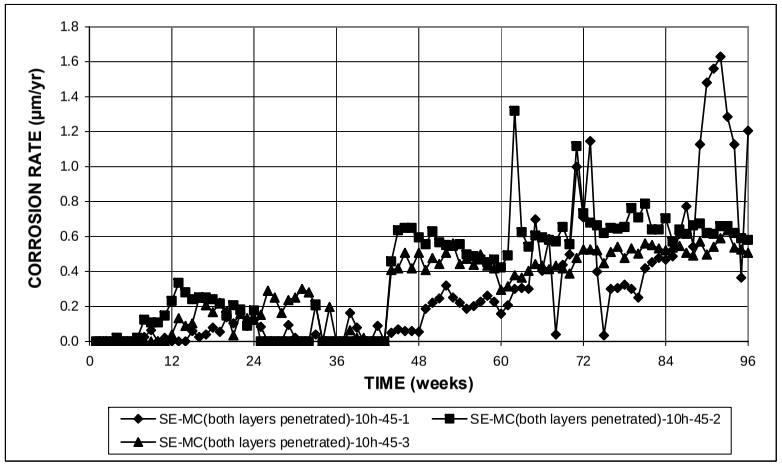

(a)

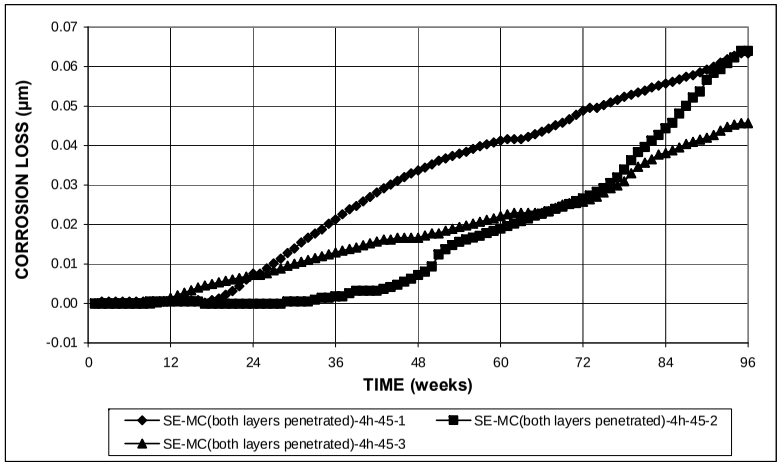

(b)

Figure A.111 – (a) Corrosion rates and (b) total corrosion loss based on total area of the bar in the Southern Exposure test for specimens with multiple coated bar (ten 3-mm (1/8-in.) diameter holes, both layers penetrated), w/c = 0.45.

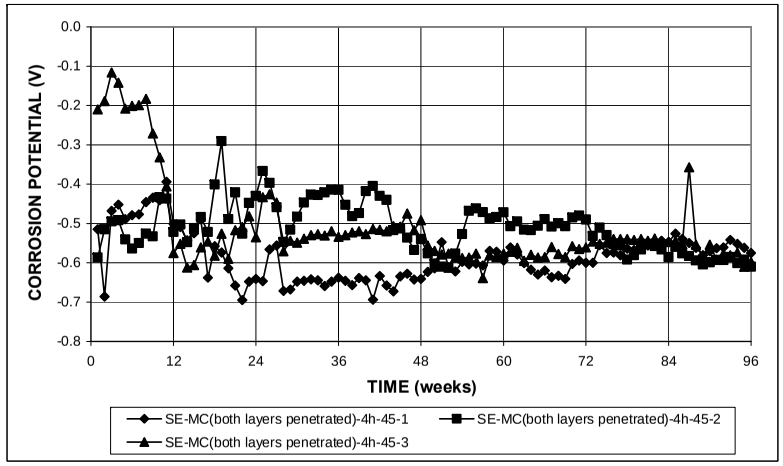

(a)

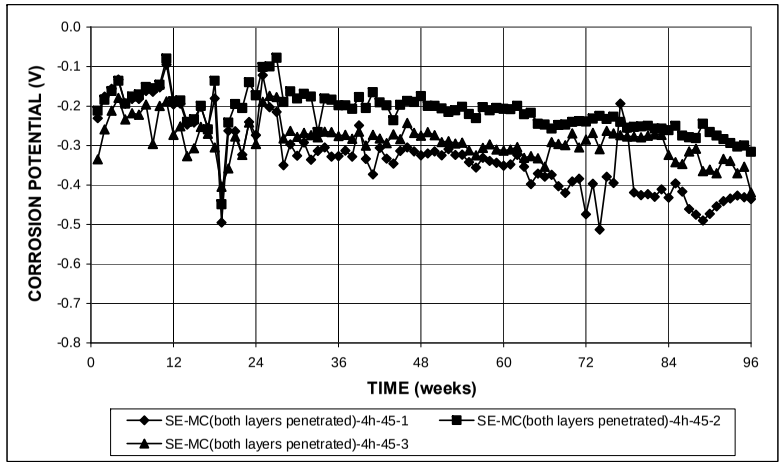

(b)

Figure A.112 – (a) Top mat corrosion potentials and (b) bottom mat corrosion potentials, with respect to the copper-copper sulfate electrode, in the Southern Exposure test for specimens with multiple coated bars (ten 3-mm (1/8-in.) diameter holes, both layers penetrated), w/c = 0.45.

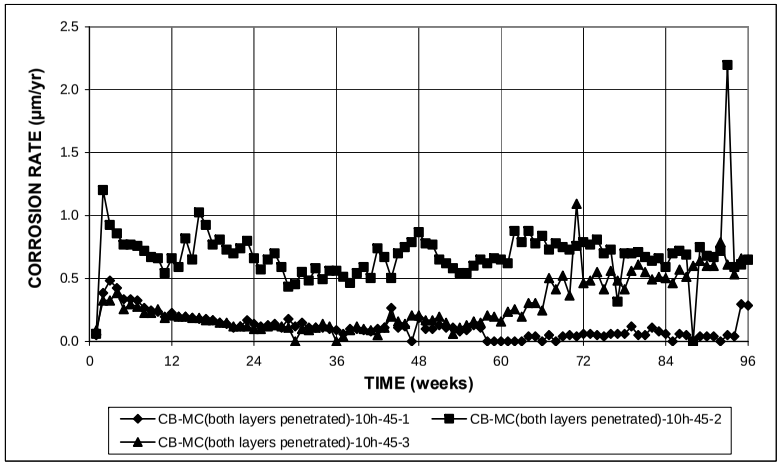

(a)

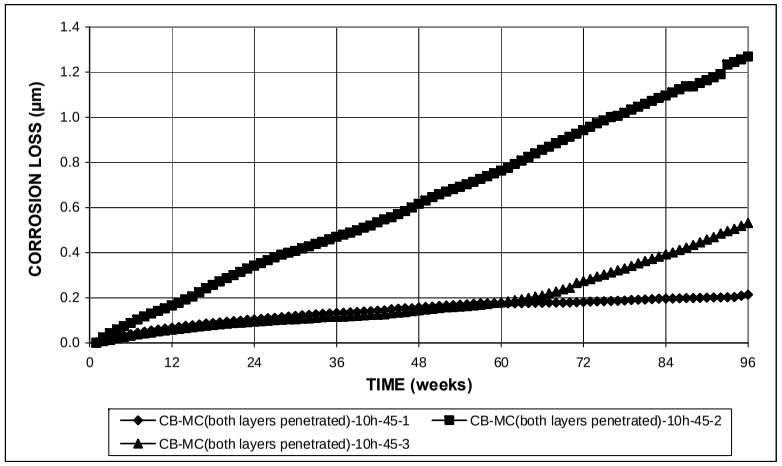

(b)

Figure A.113 – (a) Corrosion rates and (b) total corrosion loss based on total area of the bar in the Cracked Beam test for specimens with multiple coated bar (ten 3-mm (1/8-in.) diameter holes, both layers penetrated), w/c = 0.45.

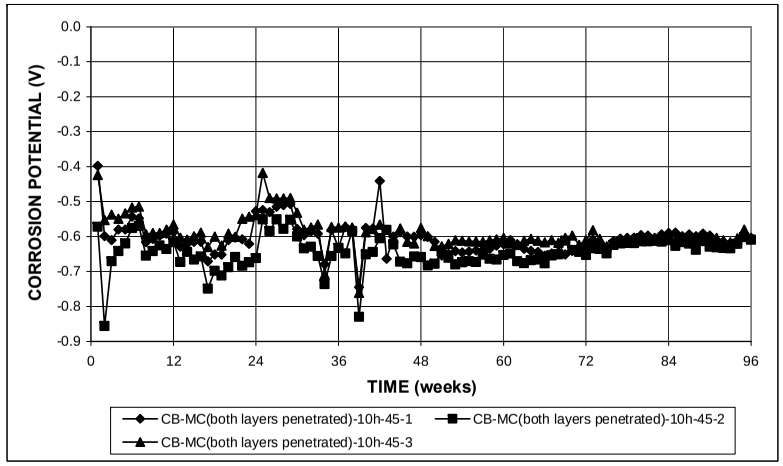

(a)

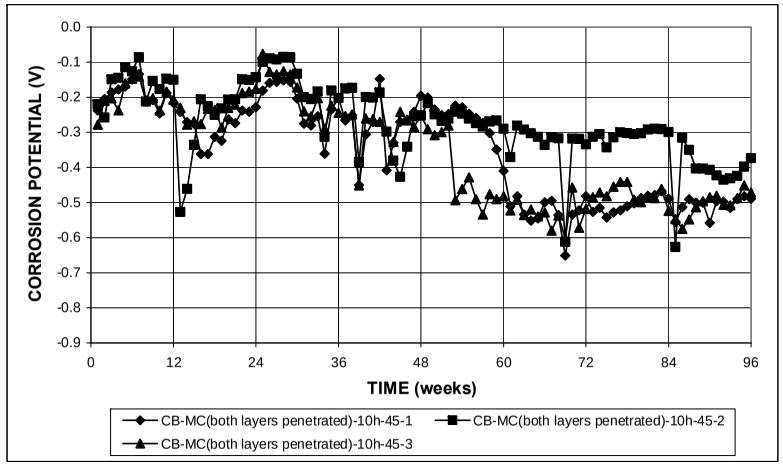

(b)

Figure A.114 – (a) Top mat corrosion potentials and (b) bottom mat corrosion potentials, with respect to the copper-copper sulfate electrode, in the Cracked Beam test for specimens with multiple coated bars (ten 3-mm (1/8-in.) diameter holes, both layers penetrated), w/c = 0.45.

APPENDIX B

MAT-TO-MAT RESISTANCES FOR INDIVIDUAL SPECIMENS

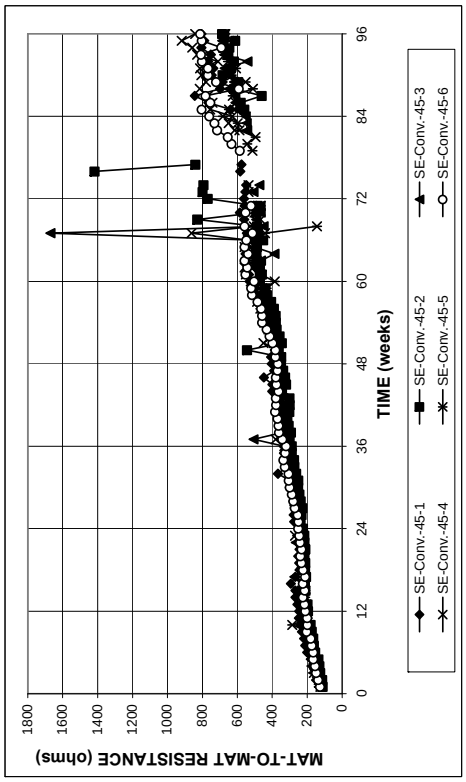

Figure B.1 – Mat-to-mat resistances for the Southern Exposure test specimens containing conventional steel, $w/c = 0.45$.

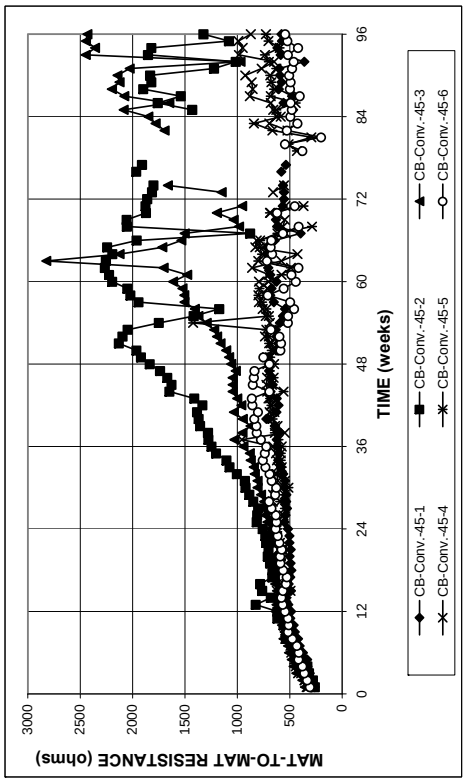

Figure B.2 – Mat-to-mat resistances for the cracked beam test specimens containing conventional steel, $w/c = 0.45$.

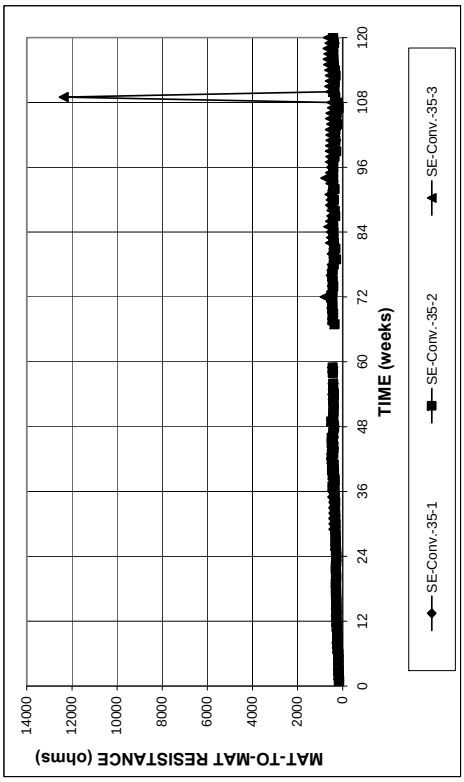

Figure B.3 – Mat-to-mat resistances for the Southern Exposure test specimens containing conventional steel, $w/c = 0.35$.

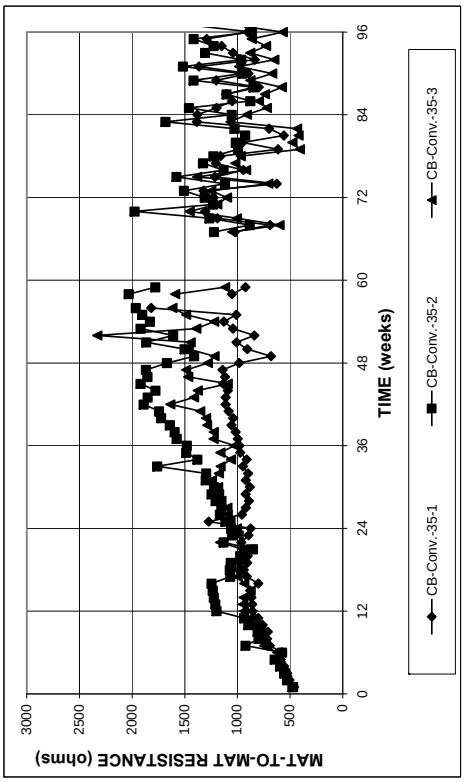

Figure B.4 – Mat-to-mat resistances for the cracked beam test specimens containing conventional steel, $w/c = 0.35$.

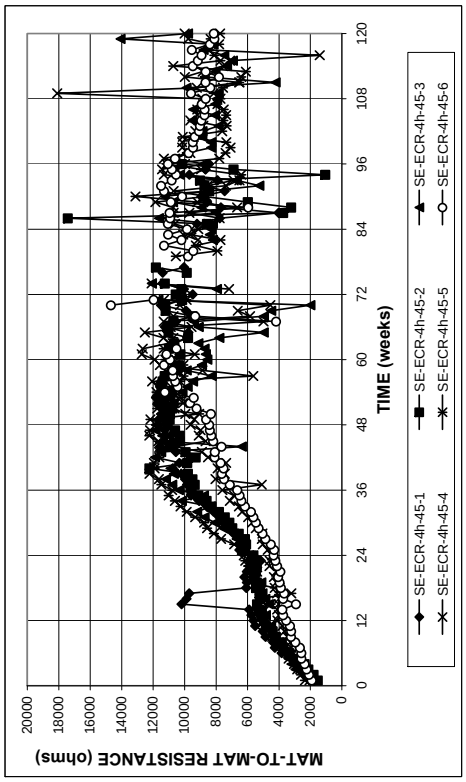

Figure B.5 – Mat-to-mat resistances for the Southern Exposure test specimens containing conventional epoxy-coated reinforcement with four holes through the epoxy, $w/c = 0.45$.

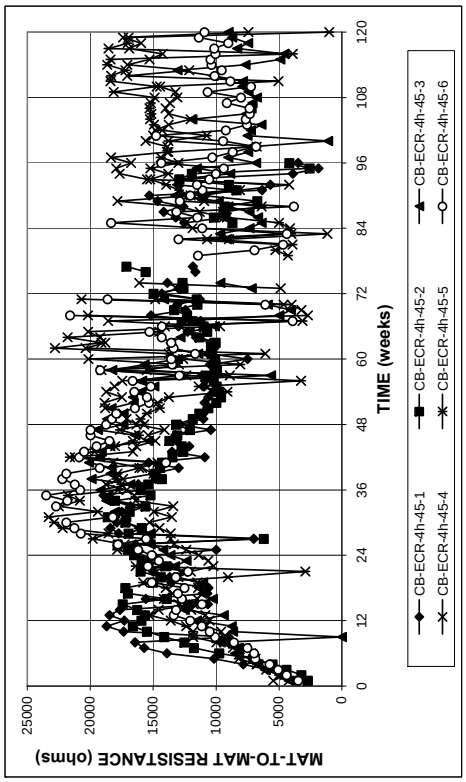

Figure B.6 – Mat-to-mat resistances for the cracked beam test specimens containing conventional epoxy-coated reinforcement with four holes through the epoxy, $w/c = 0.45$.

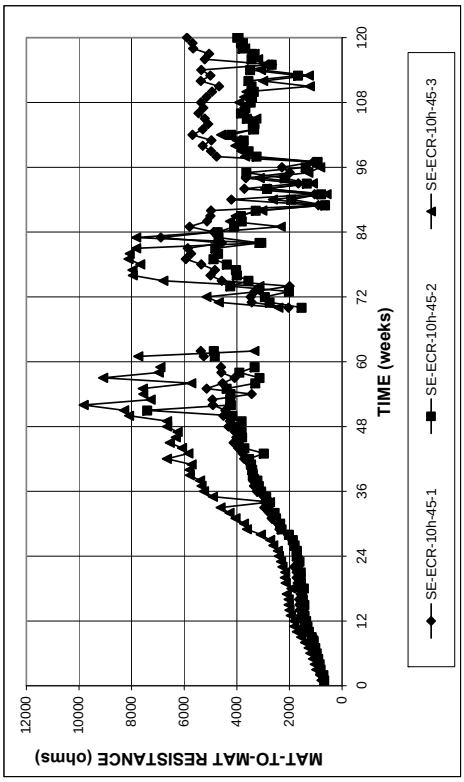

Figure B.7 – Mat-to-mat resistances for the Southern Exposure test specimens containing conventional epoxy-coated reinforcement with ten holes through the epoxy, $w/c = 0.45$.

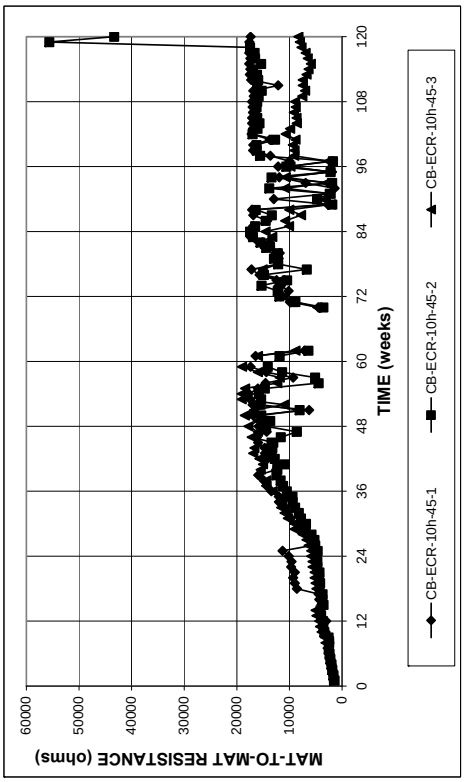

Figure B.8 – Mat-to-mat resistances for the cracked beam test specimens containing conventional epoxy-coated reinforcement with ten holes through the epoxy, $w/c = 0.45$.

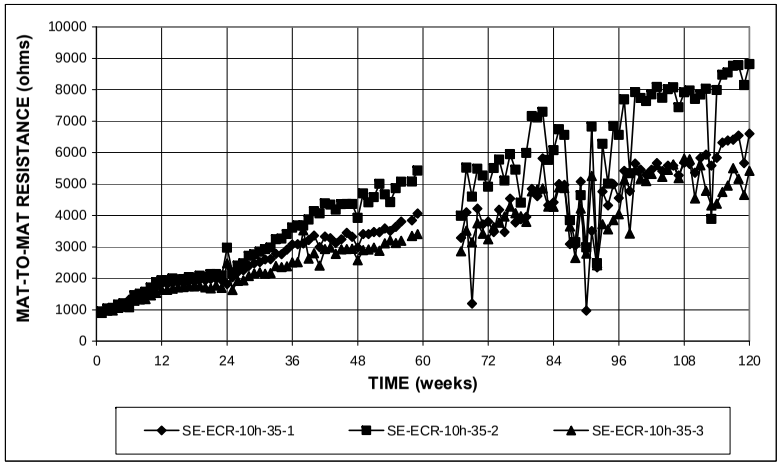

Figure B.9 – Mat-to-mat resistances for the Southern Exposure test specimens containing conventional epoxy-coated reinforcement with ten holes through the epoxy, $w/c = 0.35$.

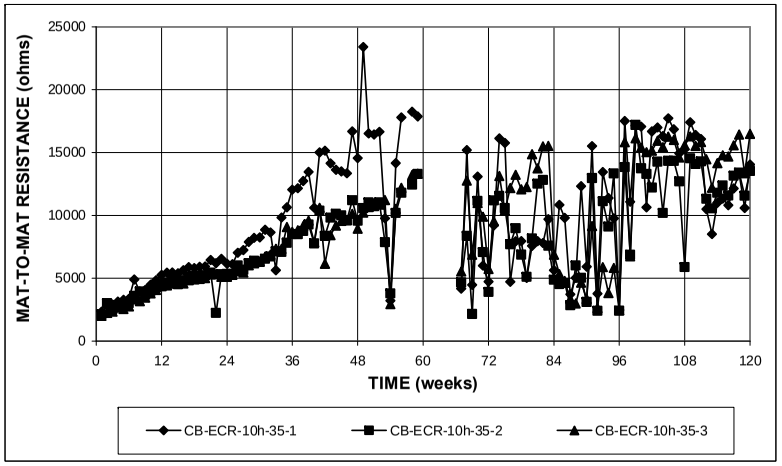

Figure B.10 – Mat-to-mat resistances for the cracked beam test specimens containing conventional epoxy-coated reinforcement with ten holes through the epoxy, $w/c = 0.35$.

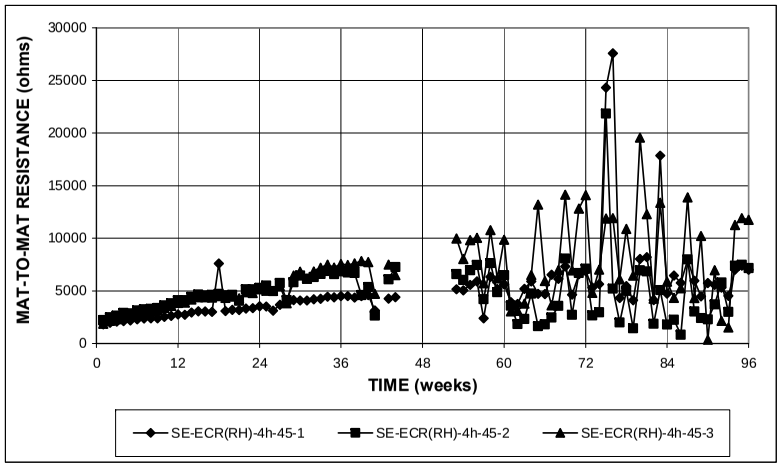

Figure B.11 – Mat-to-mat resistances for the Southern Exposure test specimens containing conventional epoxy-coated reinforcement with four holes through the epoxy in concrete containing Rheocrete corrosion inhibitor, $w/c = 0.45$.

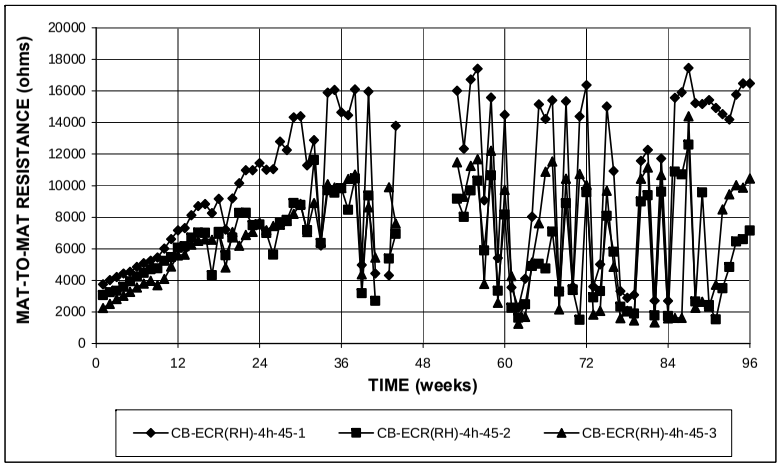

Figure B.12 – Mat-to-mat resistances for the cracked beam test specimens containing conventional epoxy-coated reinforcement with four holes through the epoxy in concrete containing Rheocrete corrosion inhibitor, $w/c = 0.45$.

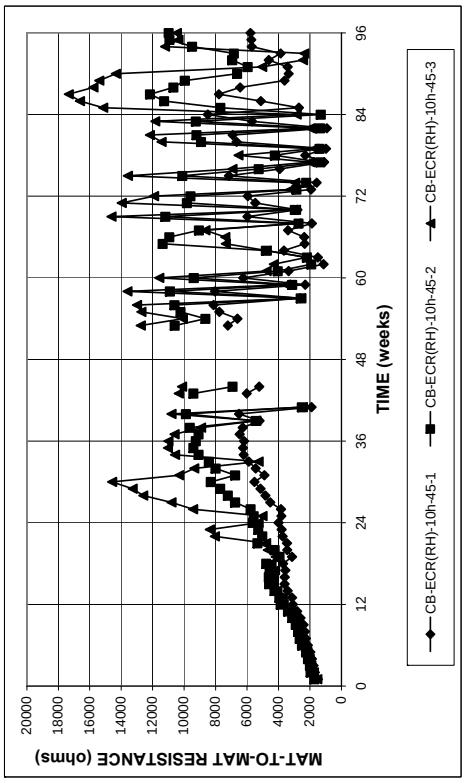

Figure B.14 – Mat-to-mat resistances for the cracked beam test specimens containing conventional epoxy-coated reinforcement with ten holes through the epoxy in concrete containing Rheocrete corrosion inhibitor, $w/c = 0.45$.

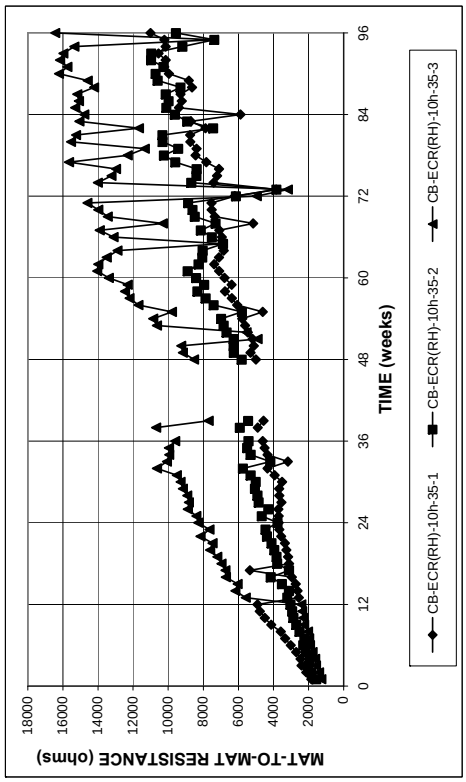

Figure B.16 – Mat-to-mat resistances for the cracked beam test specimens containing conventional epoxy-coated reinforcement with ten holes through the epoxy in concrete containing Rheocrete corrosion inhibitor, $w/c = 0.35$.

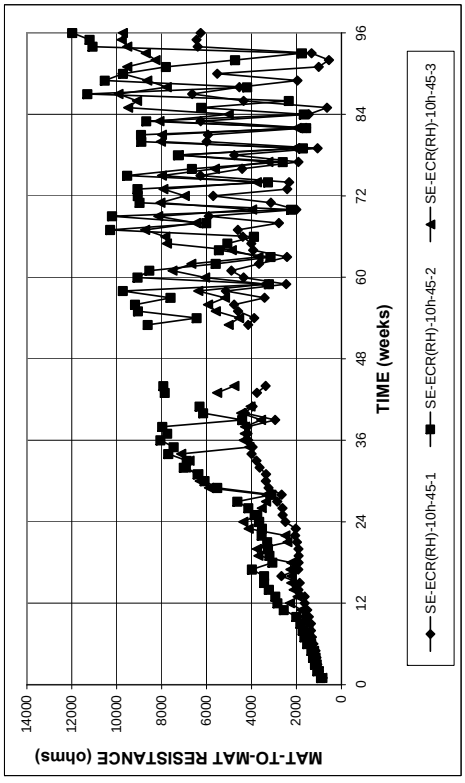

Figure B.13 – Mat-to-mat resistances for the Southern Exposure test specimens containing conventional epoxy-coated reinforcement with ten holes through the epoxy in concrete containing Rheocrete corrosion inhibitor, $w/c = 0.45$.

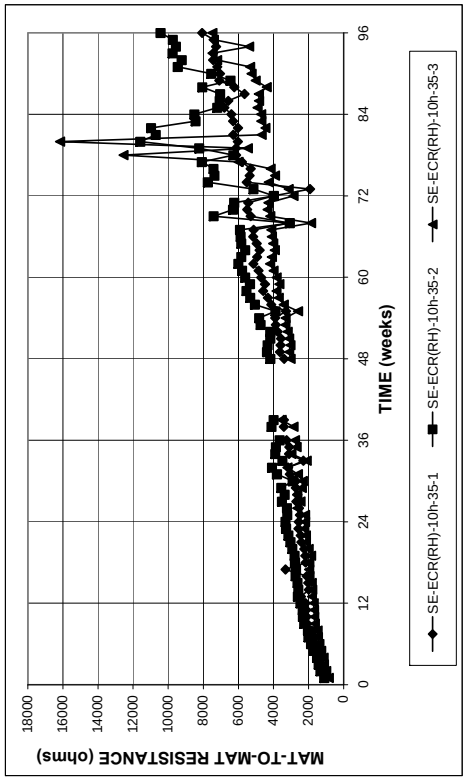

Figure B.15 – Mat-to-mat resistances for the Southern Exposure test specimens containing conventional epoxy-coated reinforcement with ten holes through the epoxy in concrete containing Rheocrete corrosion inhibitor, $w/c = 0.35$.

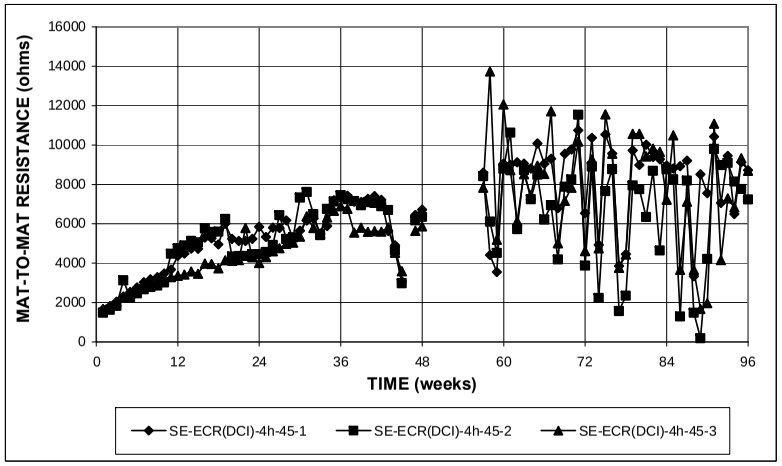

Figure B.17 – Mat-to-mat resistances for the Southern Exposure test specimens containing conventional epoxy-coated reinforcement with four holes through the epoxy in concrete containing DCI corrosion inhibitor, *w/c* = 0.45.

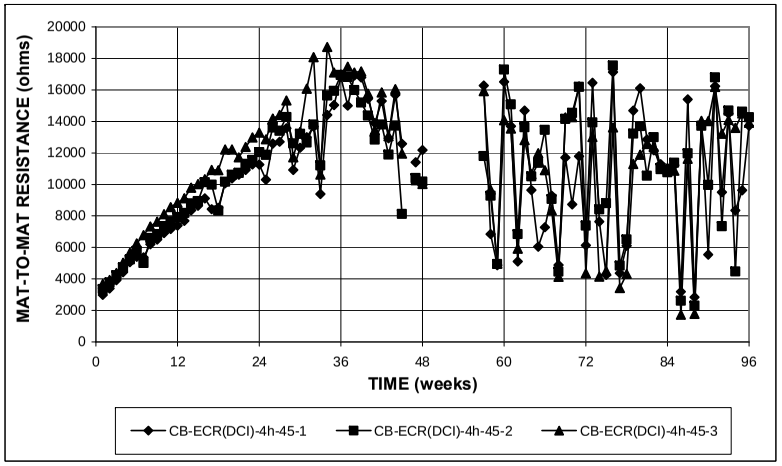

Figure B.18 – Mat-to-mat resistances for the cracked beam test specimens containing conventional epoxy-coated reinforcement with four holes through the epoxy in concrete containing DCI corrosion inhibitor, *w/c* = 0.45.

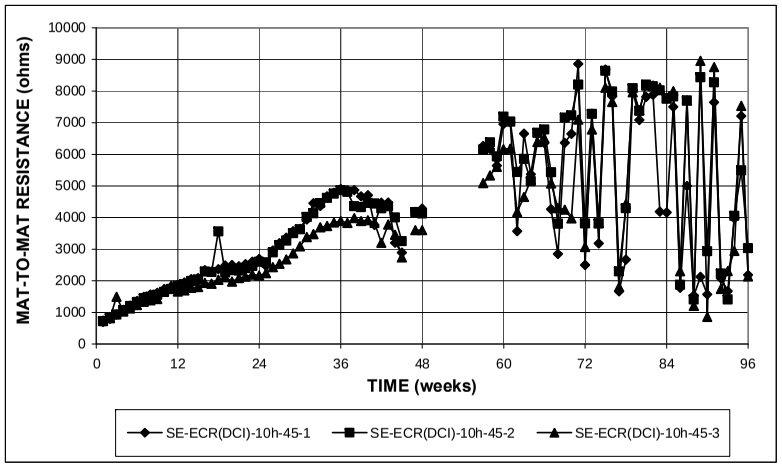

Figure B.19 – Mat-to-mat resistances for the Southern Exposure test specimens containing conventional epoxy-coated reinforcement with ten holes through the epoxy in concrete containing DCI corrosion inhibitor, *w/c* = 0.45.

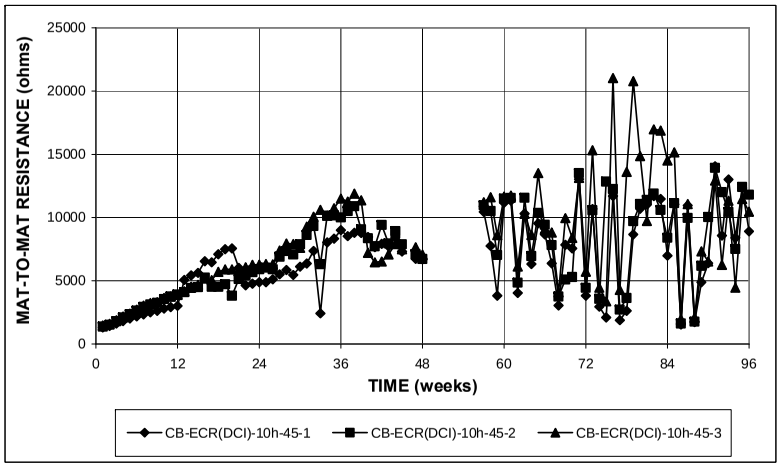

Figure B.20 – Mat-to-mat resistances for the cracked beam test specimens containing conventional epoxy-coated reinforcement with ten holes through the epoxy in concrete containing DCI corrosion inhibitor, *w/c* = 0.45.

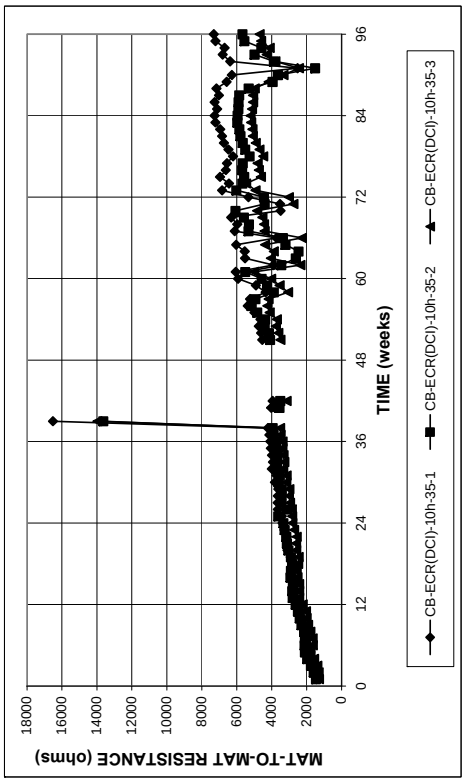

Figure B.22 – Mat-to-mat resistances for the cracked beam test specimens containing conventional epoxy-coated reinforcement with ten holes through the epoxy in concrete containing DCI corrosion inhibitor, $w/c = 0.35$.

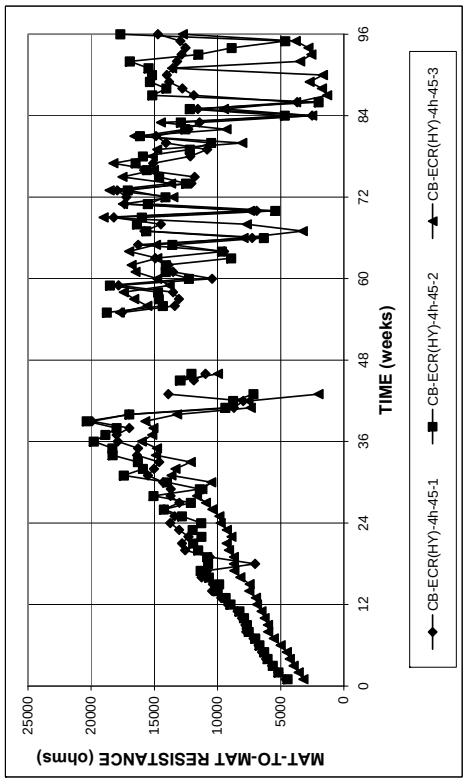

Figure B.24 – Mat-to-mat resistances for the cracked beam test specimens containing conventional epoxy-coated reinforcement with four holes through the epoxy in concrete containing Hycrete corrosion inhibitor, $w/c = 0.45$.

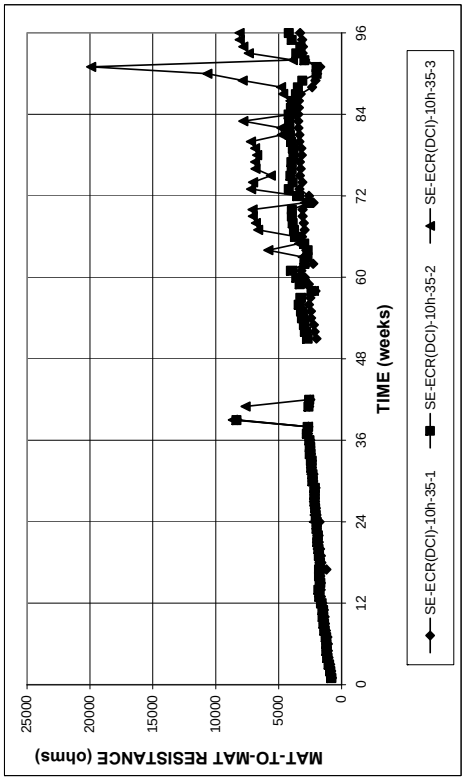

Figure B.21 – Mat-to-mat resistances for the Southern Exposure test specimens containing conventional epoxy-coated reinforcement with ten holes through the epoxy in concrete containing DCI corrosion inhibitor, $w/c = 0.35$.

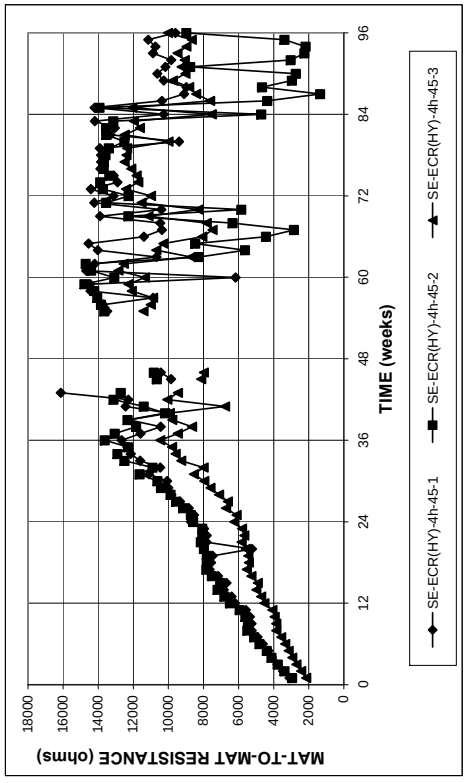

Figure B.23 – Mat-to-mat resistances for the Southern Exposure test specimens containing conventional epoxy-coated reinforcement with four holes through the epoxy in concrete containing Hycrete corrosion inhibitor, $w/c = 0.45$.

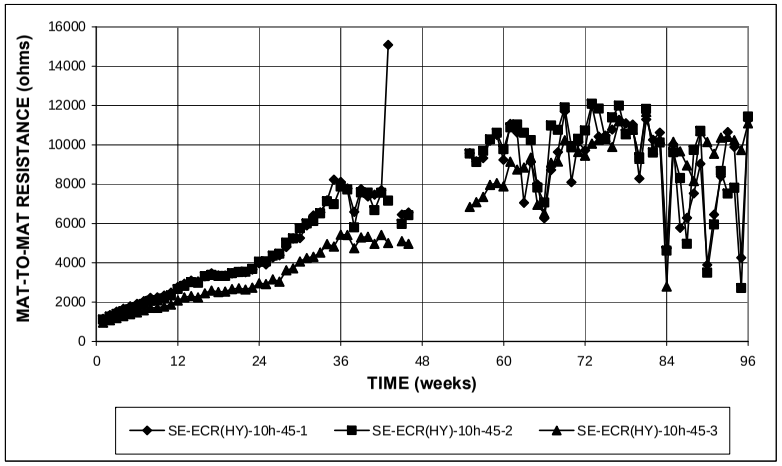

Figure B.25 – Mat-to-mat resistances for the Southern Exposure test specimens containing conventional epoxy-coated reinforcement with ten holes through the epoxy in concrete containing Hycrete corrosion inhibitor, $w/c = 0.45$.

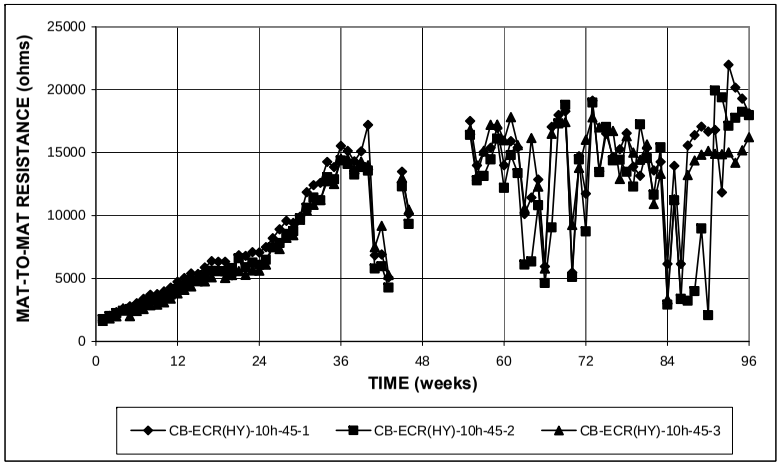

Figure B.26 – Mat-to-mat resistances for the cracked beam test specimens containing conventional epoxy-coated reinforcement with ten holes through the epoxy in concrete containing Hycrete corrosion inhibitor, $w/c = 0.45$.

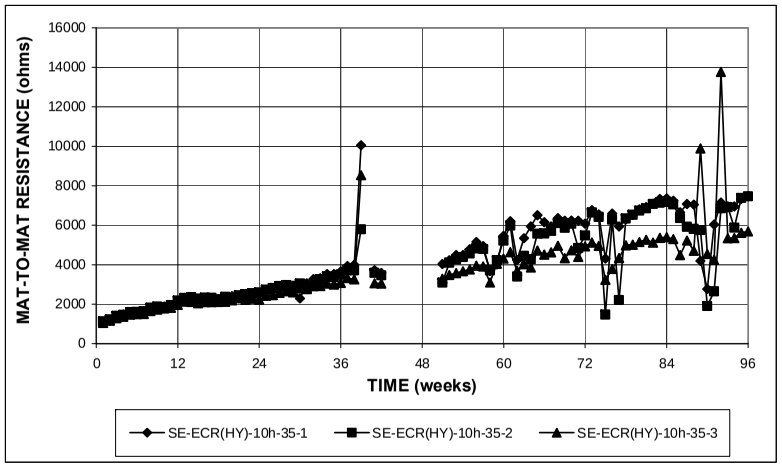

Figure B.27 – Mat-to-mat resistances for the Southern Exposure test specimens containing conventional epoxy-coated reinforcement with ten holes through the epoxy in concrete containing Hycrete corrosion inhibitor, $w/c = 0.35$.

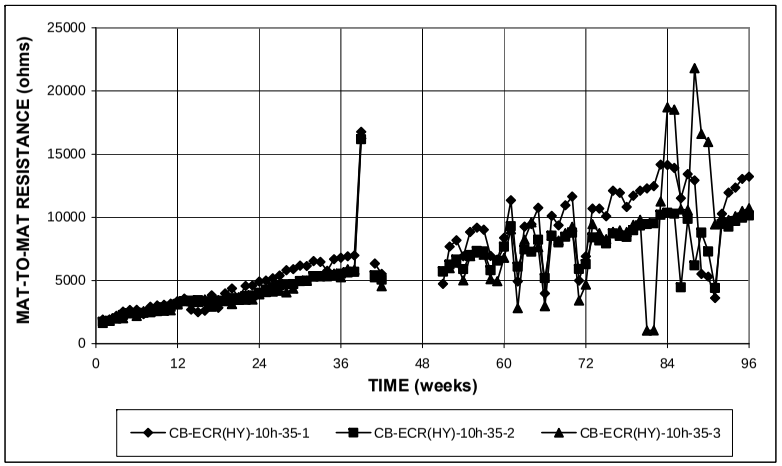

Figure B.28 – Mat-to-mat resistances for the cracked beam test specimens containing conventional epoxy-coated reinforcement with ten holes through the epoxy in concrete containing Hycrete corrosion inhibitor, $w/c = 0.35$.

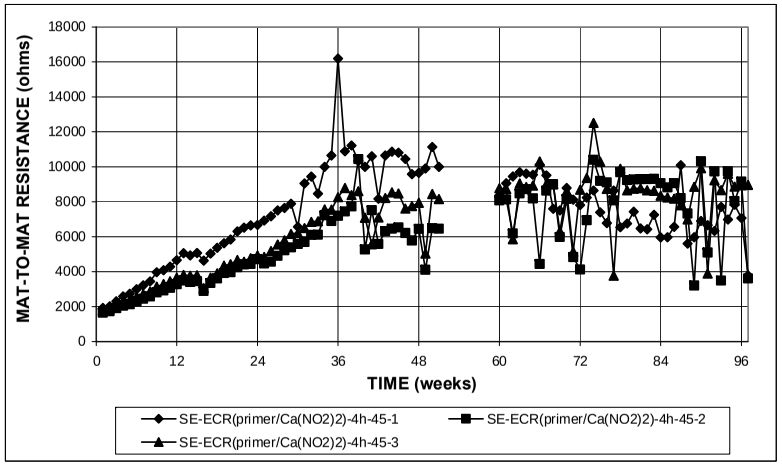

Figure B.29 – Mat-to-mat resistances for the Southern Exposure test specimens containing conventional epoxy-coated reinforcement with four holes through the epoxy with a calcium-nitrite primer, $w/c = 0.45$.

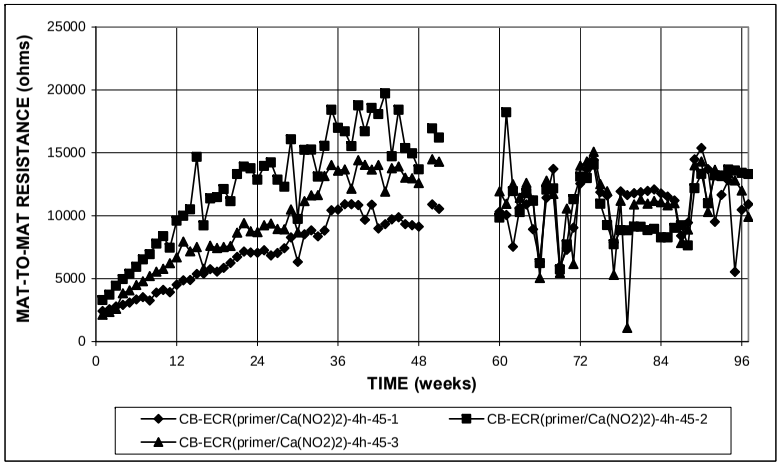

Figure B.30 – Mat-to-mat resistances for the cracked beam test specimens containing conventional epoxy-coated reinforcement with four holes through the epoxy with a calcium-nitrite primer, $w/c = 0.45$.

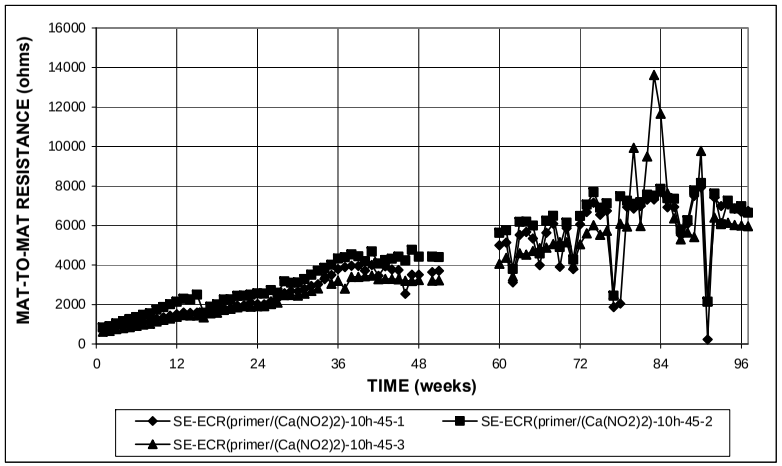

Figure B.31 – Mat-to-mat resistances for the Southern Exposure test specimens containing conventional epoxy-coated reinforcement with ten holes through the epoxy with a calcium-nitrite primer, $w/c = 0.45$.

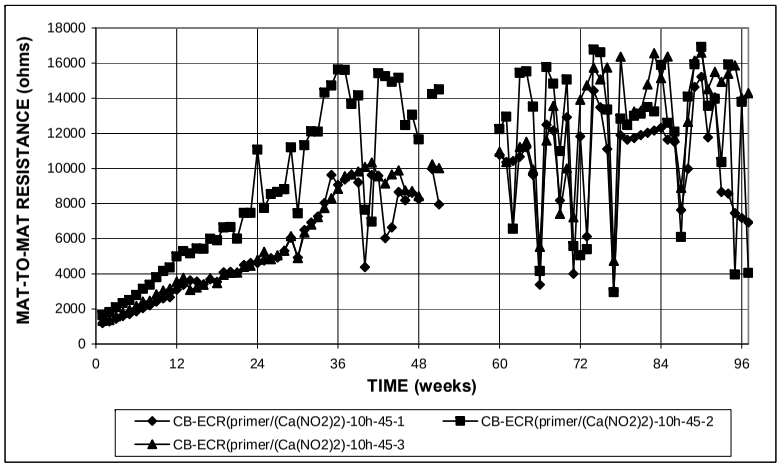

Figure B.32 – Mat-to-mat resistances for the cracked beam test specimens containing conventional epoxy-coated reinforcement with ten holes through the epoxy with a calcium-nitrite primer, $w/c = 0.45$.

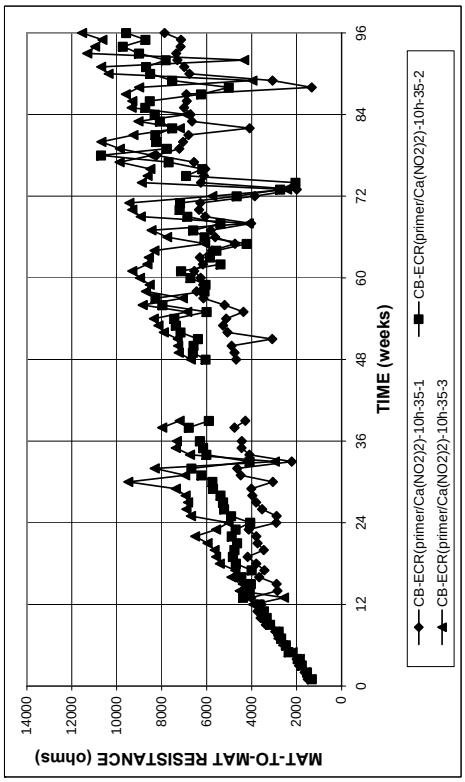

Figure B.34 – Mat-to-mat resistances for the cracked beam test specimens containing conventional epoxy-coated reinforcement with ten holes through the epoxy with a calcium-nitrite primer, $w/c = 0.35$.

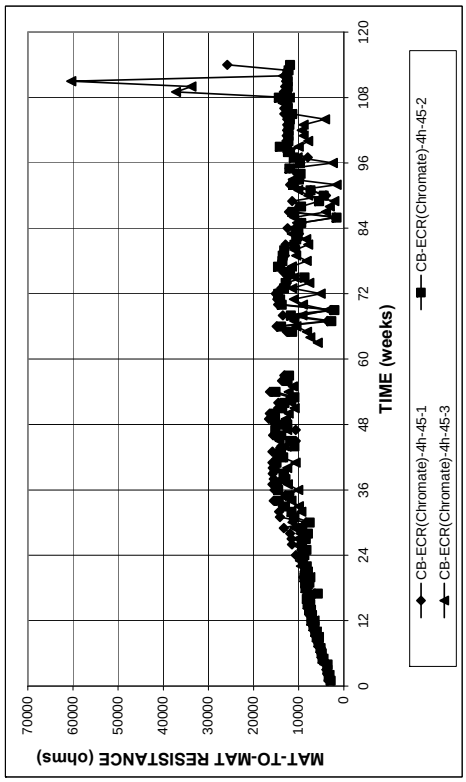

Figure B.36 – Mat-to-mat resistances for the cracked beam test specimens containing conventional epoxy-coated reinforcement with four holes through the epoxy with a chromate pretreatment, $w/c = 0.45$.

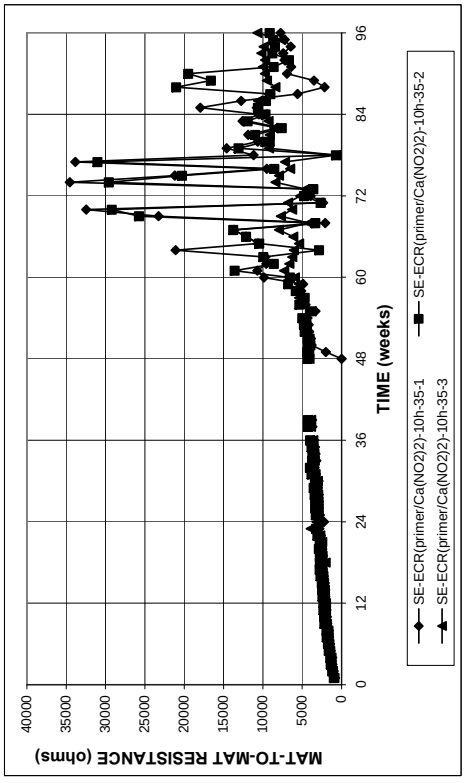

Figure B.33 – Mat-to-mat resistances for the Southern Exposure test specimens containing conventional epoxy-coated reinforcement with ten holes through the epoxy with a calcium-nitrite primer, $w/c = 0.35$.

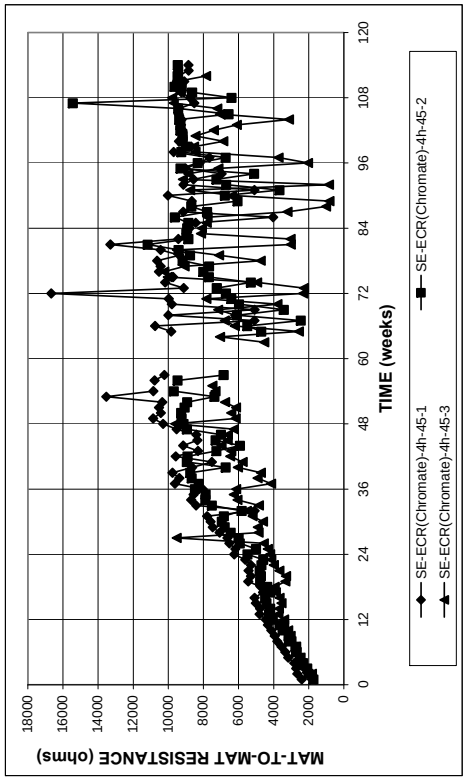

Figure B.35 – Mat-to-mat resistances for the Southern Exposure test specimens containing conventional epoxy-coated reinforcement with four holes through the epoxy with a chromate pretreatment, $w/c = 0.45$.

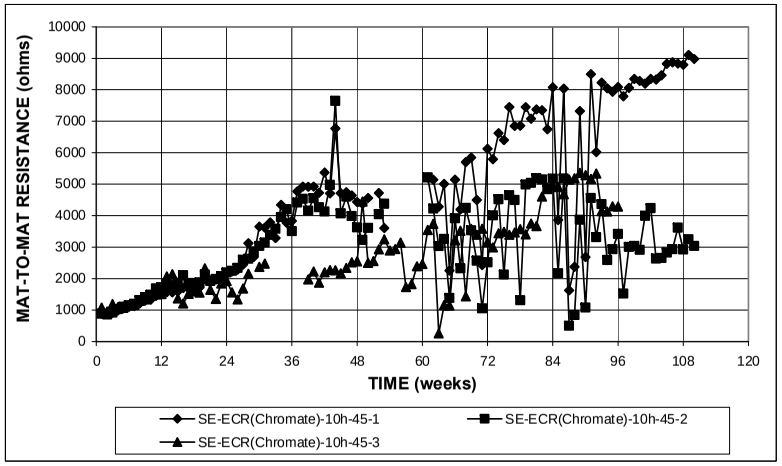

Figure B.37 – Mat-to-mat resistances for the Southern Exposure test specimens containing conventional epoxy-coated reinforcement with ten holes through the epoxy with a chromate pretreatment, *w/c* = 0.45.

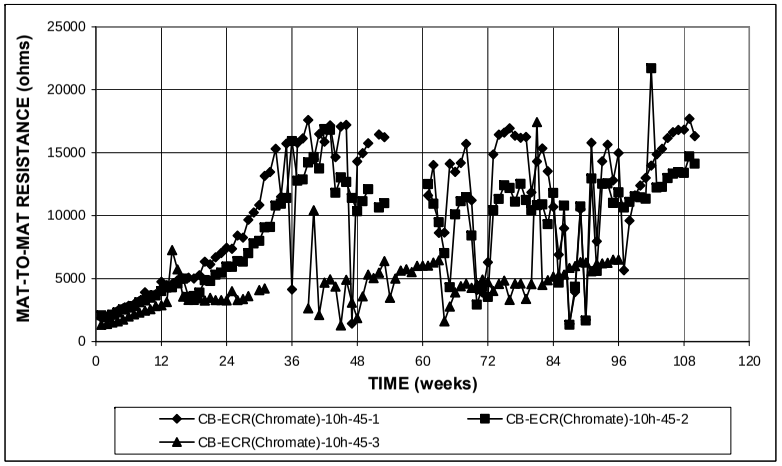

Figure B.38 – Mat-to-mat resistances for the cracked beam test specimens containing conventional epoxy-coated reinforcement with ten holes through the epoxy with a chromate pretreatment, *w/c* = 0.45.

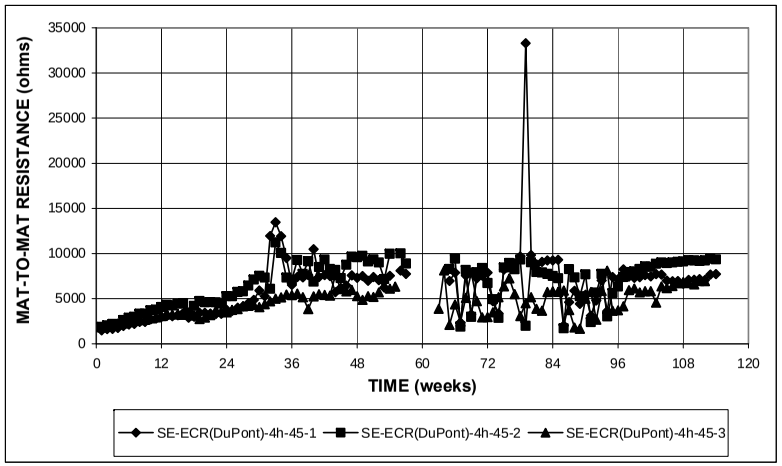

Figure B.39 – Mat-to-mat resistances for the Southern Exposure test specimens containing DuPont increased adhesion epoxy-coated reinforcement with four holes through the epoxy, *w/c* = 0.45.

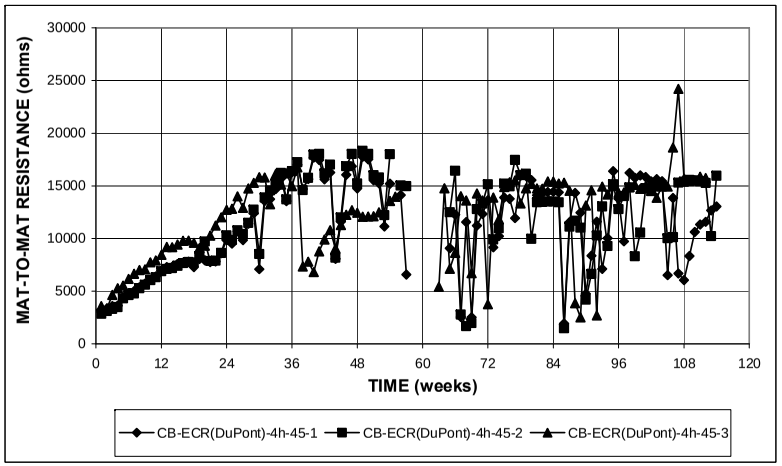

Figure B.40 – Mat-to-mat resistances for the cracked beam test specimens containing DuPont increased adhesion epoxy-coated reinforcement with four holes through the epoxy, *w/c* = 0.45.

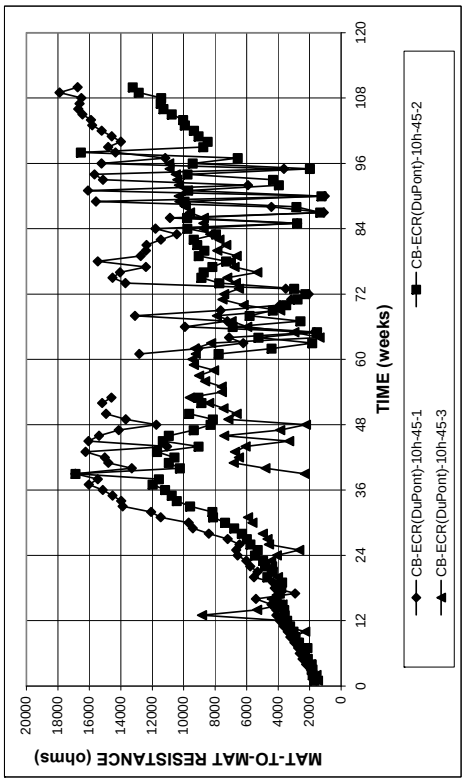

Figure B.42 – Mat-to-mat resistances for the cracked beam test specimens containing DuPont increased adhesion epoxy-coated reinforcement with ten holes through the epoxy, $w/c = 0.45$.

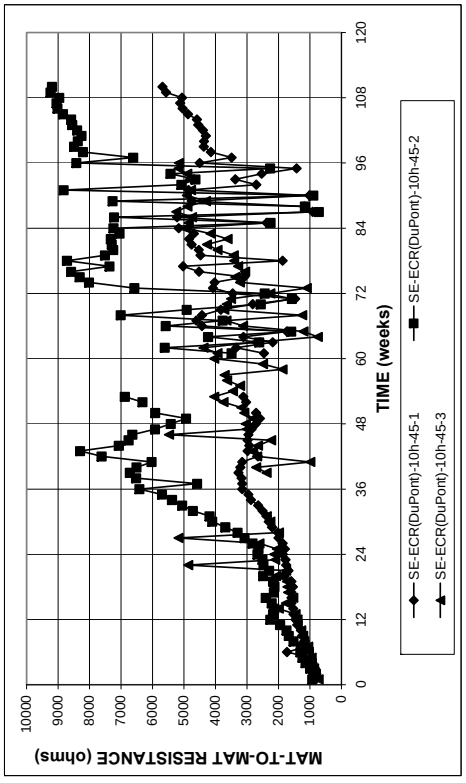

Figure B.41 – Mat-to-mat resistances for the Southern Exposure test specimens containing DuPont increased adhesion epoxy-coated reinforcement with ten holes through the epoxy, $w/c = 0.45$.

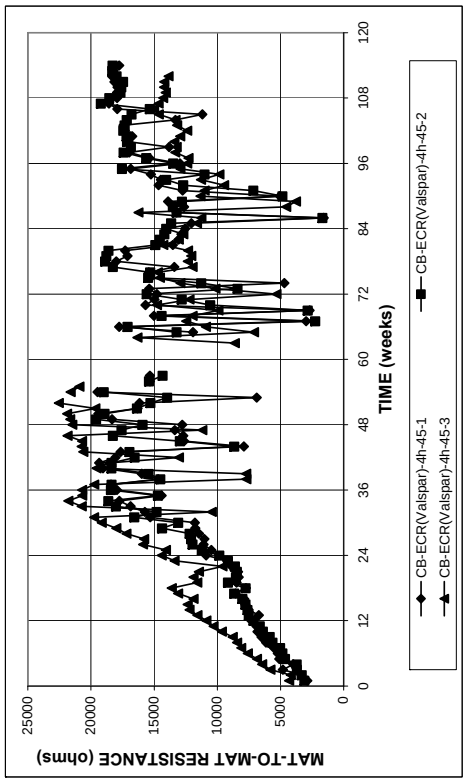

Figure B.44 – Mat-to-mat resistances for the cracked beam test specimens containing Valspar increased adhesion epoxy-coated reinforcement with four holes through the epoxy, $w/c = 0.45$.

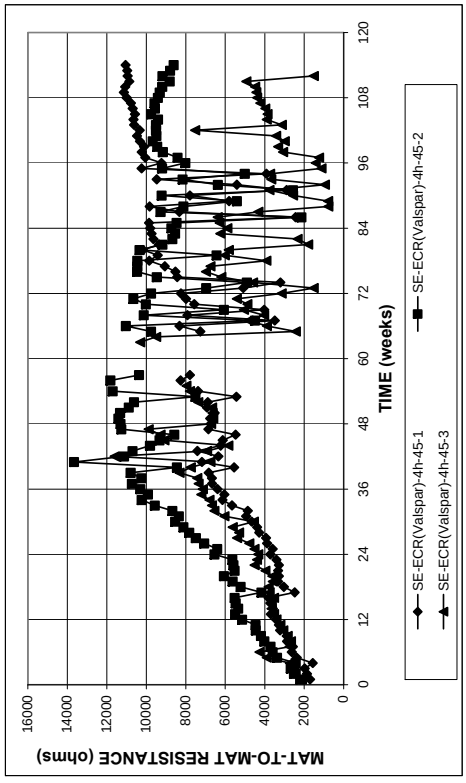

Figure B.43 – Mat-to-mat resistances for the Southern Exposure test specimens containing Valspar increased adhesion epoxy-coated reinforcement with four holes through the epoxy, $w/c = 0.45$.

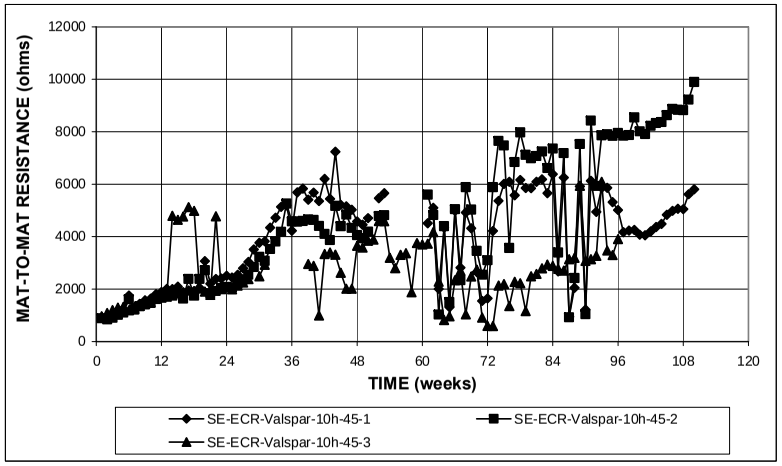

Figure B.45 – Mat-to-mat resistances for the Southern Exposure test specimens containing Valspar increased adhesion epoxy-coated reinforcement with tenq holes through the epoxy, *w/c* = 0.45.

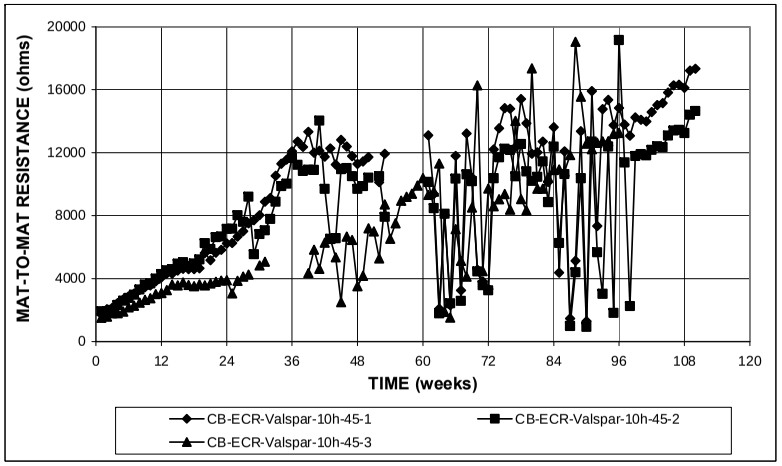

Figure B.46 – Mat-to-mat resistances for the cracked beam test specimens containing Valspar increased adhesion epoxy-coated reinforcement with ten holes through the epoxy, *w/c* = 0.45.

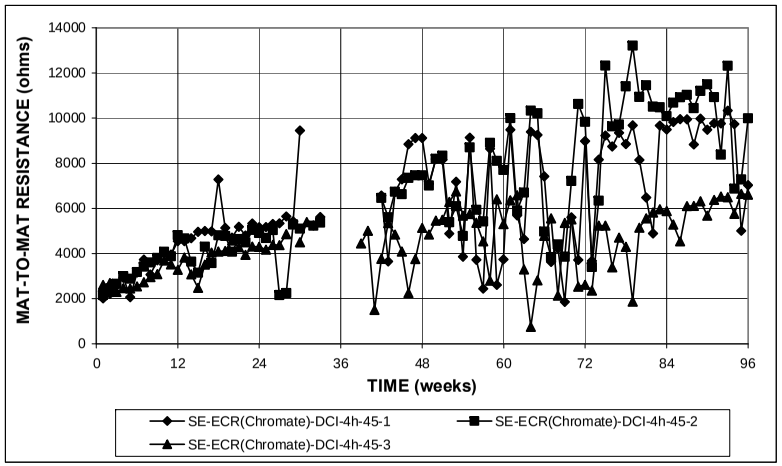

Figure B.47 – Mat-to-mat resistances for the Southern Exposure test specimens containing conventional epoxy-coated reinforcement with four holes through the epoxy with a chromate pretreatment in concrete containing DCI corrosion inhibitor, *w/c* = 0.45.

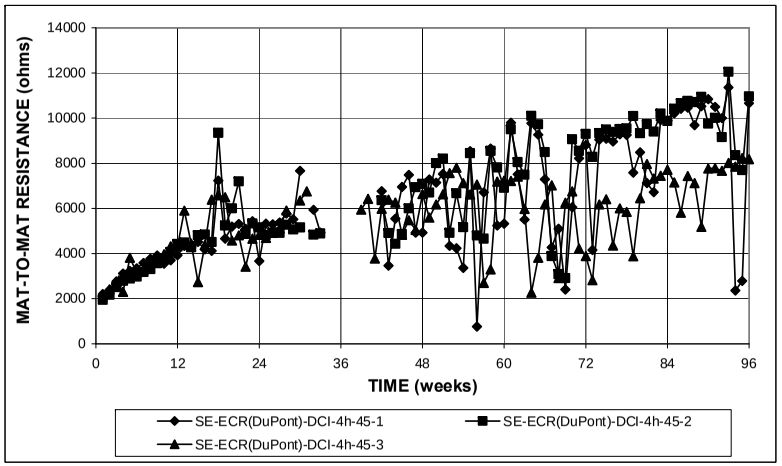

Figure B.48 – Mat-to-mat resistances for the Southern Exposure test specimens containing DuPont increased adhesion epoxy-coated reinforcement with four holes through the epoxy in concrete containing DCI corrosion inhibitor, *w/c* = 0.45.

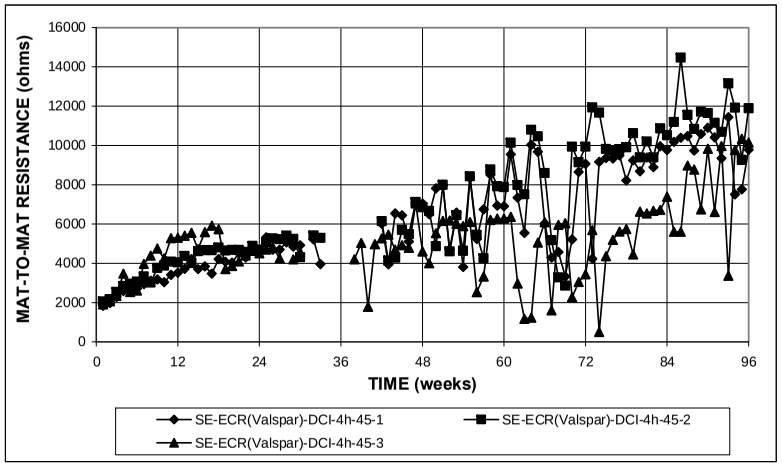

Figure B.49 – Mat-to-mat resistances for the Southern Exposure test specimens containing DuPont increased adhesion epoxy-coated reinforcement with four holes through the epoxy in concrete containing DCI corrosion inhibitor, *w/c* = 0.45.

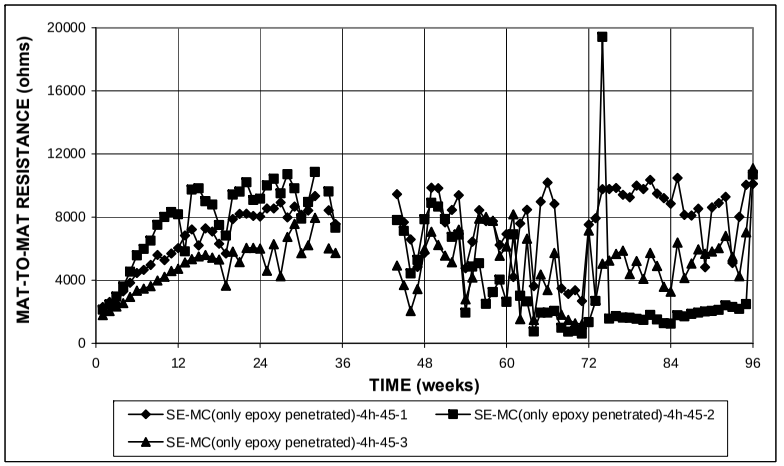

Figure B.50 – Mat-to-mat resistances for the Southern Exposure test specimens containing mulltiple coated reinforcement with four holes through the epoxy layer, *w/c* = 0.45.

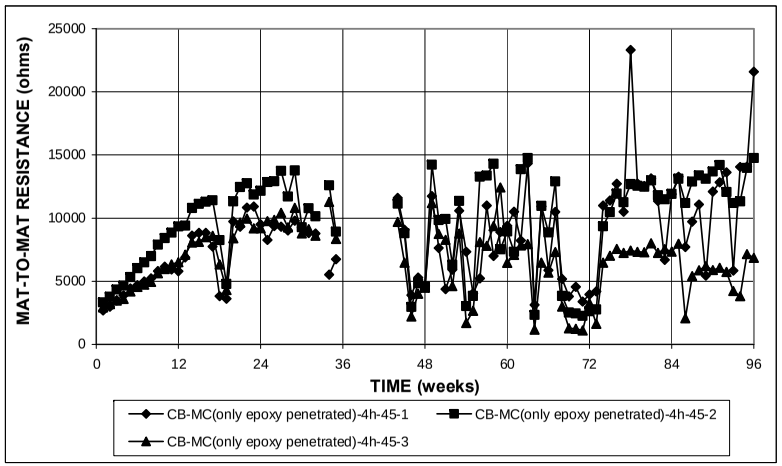

Figure B.51 – Mat-to-mat resistances for the cracked beam test specimens containing mulltiple coated reinforcement with four holes through the epoxy layer, *w/c* = 0.45.

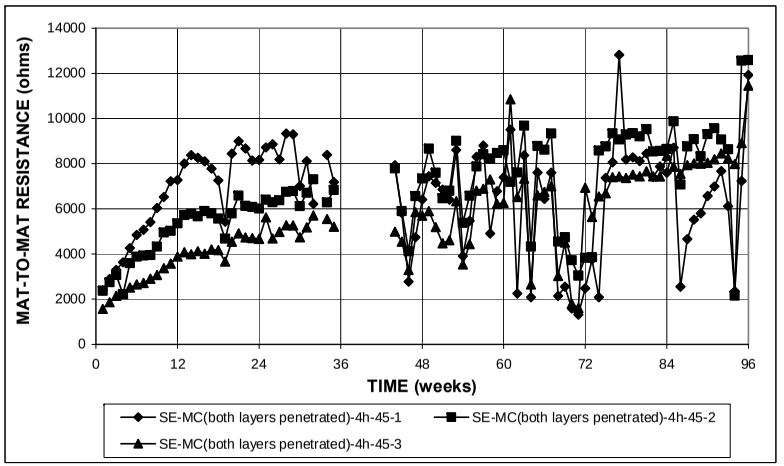

Figure B.52 – Mat-to-mat resistances for the Southern Exposure test specimens containing mulltiple coated reinforcement with four holes through the epoxy and zinc layers, *w/c* = 0.45.

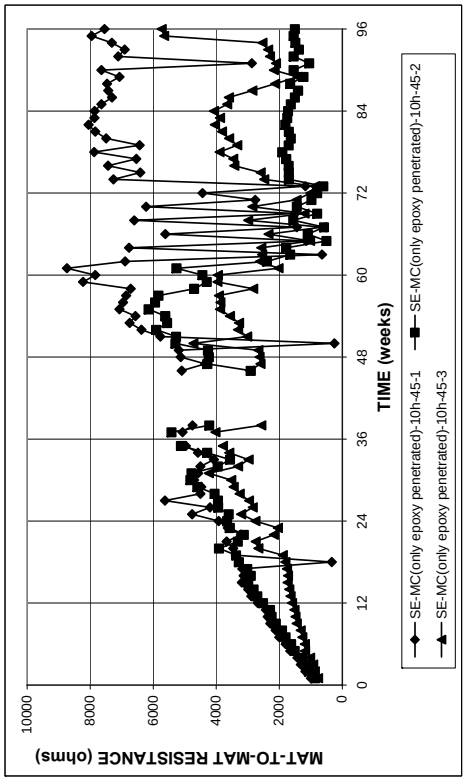

Figure B.54 – Mat-to-mat resistances for the Southern Exposure test specimens containing multiple coated reinforcement with ten holes through the epoxy layer, $w/c = 0.45$.

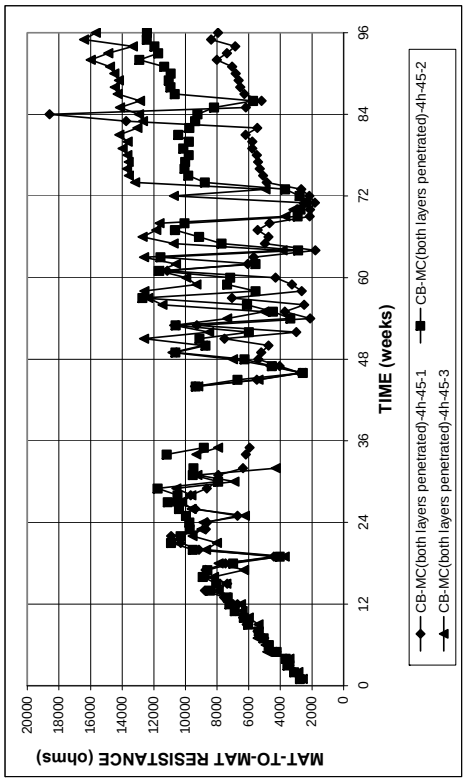

Figure B.53 – Mat-to-mat resistances for the cracked beam test specimens containing multiple reinforcement with four holes through the epoxy and zinc layers, $w/c = 0.45$.

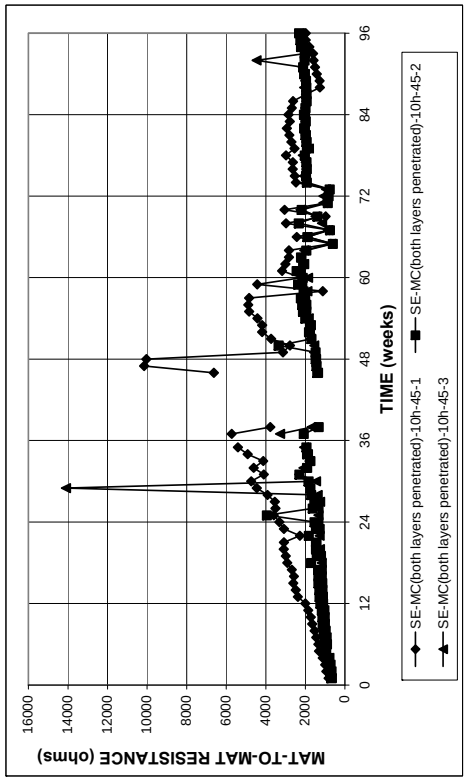

Figure B.56 – Mat-to-mat resistances for the Southern Exposure test specimens containing multiple coated reinforcement with ten holes through the epoxy and zinc layers, $w/c = 0.45$.

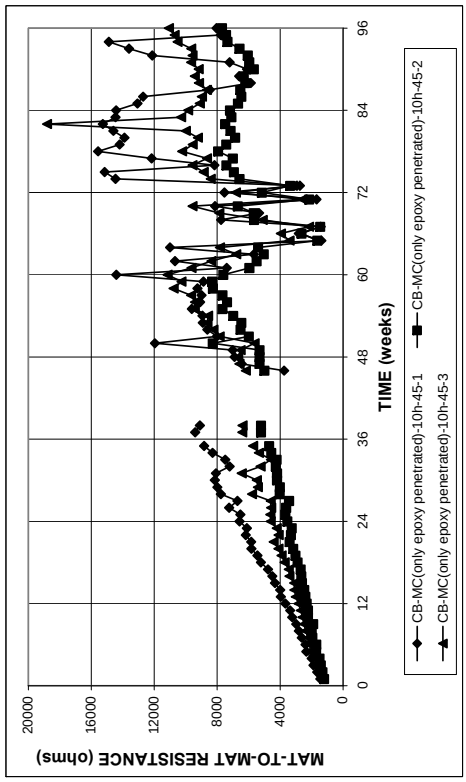

Figure B.55 – Mat-to-mat resistances for the cracked beam test specimens containing multiple coated reinforcement with ten holes through the epoxy layer, $w/c = 0.45$.

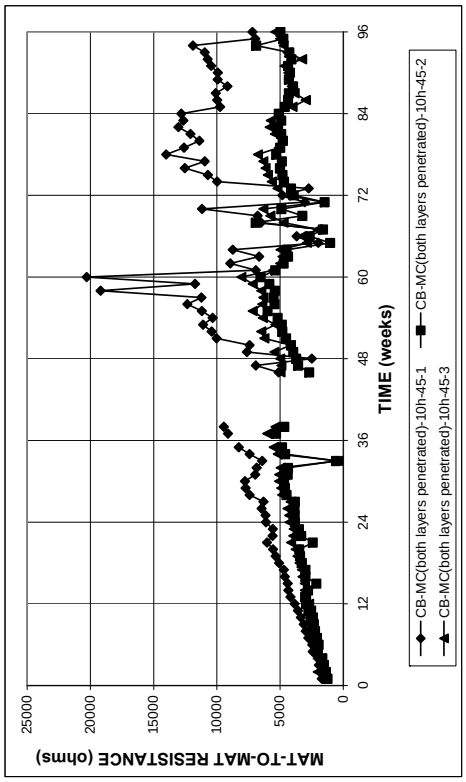

Figure B.57 – Mat-to-mat resistances for the cracked beam test specimens containing multiple reinforcement with ten holes through the epoxy and zinc layers, $w/c = 0.45$.

APPENDIX C

CHLORIDE CONCENTRATIONS AT 48 AND 96 WEEKS IN SOUTHERN EXPOSURE SPECIMENS

Table C.1 – Chloride ion concentrations measured at 48 weeks in Southern Exposure specimens containing conventional steel and epoxy-coated reinforcement

Specimen	Rate (µm/yr)	Top Mat Potential (V)	Water Soluble Cl^- (lb/yd^3) 1	2	3	4	5	6	Average (lb/yd^3)	SD[a]	COV[b]
Conv.-45-1	0.015	-0.193	7.98	†	†	†	†	†	7.98	†	†
Conv.-45-2	1.70	-0.498	7.32	†	†	†	†	†	7.32	†	†
Conv.-45-3	0.453	-0.354	3.96	†	†	†	†	†	3.96	†	†
Conv.-45-4	0.000	-0.410	†	†	†	†	†	†	†	†	†
Conv.-45-5	-0.495	-0.213	7.76	5.87	†	†	†	†	6.81	1.34	0.20
Conv.-45-6	0.743	-0.413	9.90	†	†	†	†	†	9.90	†	†
Conv.-35-1	0.000	-0.286	15.74	9.97	†	†	†	†	12.85	4.08	0.32
Conv.-35-2	0.263	-0.312	5.36	†	†	†	†	†	5.36	†	†
Conv.-35-3	0.286	-0.357	3.15	5.68	†	†	†	†	4.42	1.78	0.40
ECR-4h-45-1	0.000	-0.136	8.53	†	†	†	†	†	8.53	†	†
ECR-4h-45-2	0.000	-0.136	11.21	†	†	†	†	†	11.21	†	†
ECR-4h-45-3	0.000	-0.146	†	†	†	†	†	†	†	†	†
ECR-4h-45-4	0.000	-0.144	†	†	†	†	†	†	†	†	†
ECR-4h-45-5	0.000	-0.164	12.11	7.25	†	†	†	†	9.68	3.44	0.36
ECR-4h-45-6	0.000	-0.146	11.87	4.73	†	†	†	†	8.30	5.05	0.61
ECR-10h-45-1	0.000	-0.469	19.53	†	†	†	†	†	19.53	†	†
ECR-10h-45-2	0.000	-0.176	16.09	15.77	†	†	†	†	15.93	0.22	0.01
ECR-10h-45-3	0.000	-0.318	19.08	18.83	†	†	†	†	18.96	0.18	0.01
ECR-10h-35-1	0.000	-0.147	8.96	3.97	†	†	†	†	6.47	3.52	0.54
ECR-10h-35-2	0.000	-0.133	4.07	3.82	†	†	†	†	3.94	0.18	0.05
ECR-10h-35-3	0.000	-0.166	8.90	7.19	†	†	†	†	8.04	1.20	0.15

[a]Standard Deviation

[b]Coefficient of Variation

† Information not available

Table C.2 – Chloride ion concentrations measured at 48 weeks in Southern Exposure specimens containing epoxy-coated reinforcement cast in concrete containing corrosion inhibitors

Specimen	Rate (µm/yr)	Top Mat Potential (V)	Water Soluble Cl^- (lb/yd^3) 1	2	3	4	5	6	Average (lb/yd^3)	SD[a]	COV[b]
ECR(DCI)-4h-45-1	0.000	-0.099	13.00	17.54	9.53	10.76	14.76	18.61	14.03	3.63	0.26
ECR(DCI)-4h-45-2	0.023	-0.103	10.28	12.05	12.81	10.47	13.82	12.18	11.93	1.36	0.11
ECR(DCI)-4h-45-3	0.000	-0.168	11.86	13.06	11.36	12.81	9.97	15.58	12.44	1.90	0.15
ECR(DCI)-10h-45-1	0.027	-0.081	15.27	7.25	10.09	7.00	8.77	†	9.68	3.36	0.35
ECR(DCI)-10h-45-2	0.126	-0.104	12.08	9.72	12.49	15.39	13.44	†	12.62	2.07	0.16
ECR(DCI)-10h-45-3	0.015	-0.537	8.07	12.49	15.52	15.77	16.15	17.66	14.28	3.48	0.24
ECR(DCI)-10h-35-1	0.000	-0.175	2.02	0.76	2.46	4.61	4.42	7.76	3.67	2.48	0.68
ECR(DCI)-10h-35-2	0.000	-0.137	5.90	4.67	4.48	7.38	4.29	6.62	5.56	1.28	0.23
ECR(DCI)-10h-35-3	0.000	-0.146	4.54	4.64	7.81	6.50	6.62	7.70	6.30	1.43	0.23
ECR(RH)-4h-45-1	0.000	-0.200	7.82	6.50	7.00	8.20	7.44	7.07	7.34	0.61	0.08
ECR(RH)-4h-45-2	0.000	-0.139	19.46	9.18	10.85	7.89	6.06	7.32	10.13	4.86	0.48
ECR(RH)-4h-45-3	0.000	-0.245	10.16	10.47	8.14	8.07	8.01	†	8.97	1.23	0.14
ECR(RH)-10h-45-1	0.000	-0.475	7.32	7.00	9.78	9.15	8.96	9.21	8.57	1.13	0.13
ECR(RH)-10h-45-2	0.000	-0.134	6.06	4.48	4.92	8.14	5.93	3.28	5.47	1.66	0.30
ECR(RH)-10h-45-3	0.000	-0.171	10.28	6.06	7.44	10.60	8.26	10.98	8.94	1.99	0.22
ECR(RH)-10h-35-1	0.000	-0.234	2.59	4.35	†	†	†	†	3.47	1.25	0.36
ECR(RH)-10h-35-2	0.000	-0.213	4.35	5.05	5.84	†	†	†	5.08	0.74	0.15
ECR(RH)-10h-35-3	0.000	-0.242	0.82	4.22	3.47	†	†	†	2.84	1.79	0.63
ECR(HY)-4h-45-1	0.000	-0.117	6.18	1.07	0.47	8.83	3.66	0.88	3.52	3.39	0.96
ECR(HY)-4h-45-2	0.000	-0.136	1.17	2.30	3.38	2.33	3.44	†	2.52	0.93	0.37
ECR(HY)-4h-45-3	0.000	-0.096	11.29	3.70	5.77	5.27	6.12	†	6.43	2.87	0.45
ECR(HY)-10h-45-1	0.000	-0.251	7.44	3.60	2.77	6.72	†	†	5.13	2.29	0.45
ECR(HY)-10h-45-2	0.000	-0.114	4.10	6.84	5.49	3.60	†	†	5.01	1.46	0.29
ECR(HY)-10h-45-3	0.053	-0.544	8.33	4.29	6.25	7.82	7.33	†	6.80	1.60	0.24
ECR(HY)-10h-35-1	0.000	-0.191	4.26	5.24	2.43	3.09	5.84	†	4.17	1.42	0.34
ECR(HY)-10h-35-2	0.000	-0.135	2.78	2.84	2.08	2.27	3.47	2.71	2.69	0.49	0.18
ECR(HY)-10h-35-3	0.000	-0.178	0.63	2.21	9.05	4.61	2.02	2.65	3.53	3.00	0.85
ECR(primer/$Ca(NO_2)_2$)-4h-45-1	0.000	-0.314	11.79	†	†	†	†	†	11.79	†	†
ECR(primer/$Ca(NO_2)_2$)-4h-45-2	0.034	-0.540	13.57	12.49	†	†	†	†	13.03	0.77	0.06
ECR(primer/$Ca(NO_2)_2$)-4h-45-3	0.000	-0.305	12.62	14.83	†	†	†	†	13.72	1.56	0.11
ECR(primer/$Ca(NO_2)_2$)-10h-45-1	0.000	-0.563	22.40	14.57	15.33	15.14	14.01	13.37	15.80	3.31	0.21
ECR(primer/$Ca(NO_2)_2$)-10h-45-2	0.000	-0.320	10.91	17.85	17.92	14.70	16.40	†	15.56	2.91	0.19
ECR(primer/$Ca(NO_2)_2$)-10h-45-3	0.000	-0.139	9.84	10.72	15.33	15.96	17.79	16.61	14.38	3.29	0.23
ECR(primer/$Ca(NO_2)_2$)-10h-35-1	0.000	-0.118	1.32	3.97	0.63	3.03	2.65	2.02	2.27	1.21	0.53
ECR(primer/$Ca(NO_2)_2$)-10h-35-2	0.000	-0.230	7.13	4.10	5.24	2.97	0.95	1.58	3.66	2.32	0.63
ECR(primer/$Ca(NO_2)_2$)-10h-35-3	0.000	-0.120	2.14	0.88	1.83	2.78	3.03	4.61	2.54	1.26	0.50

[a]Standard Deviation

[b]Coefficient of Variation

† Information not available

Table C.3 – Chloride ion concentrations measured at 48 weeks in Southern Exposure specimens containing multiple-coated reinforcement

Specimen	Rate (µm/yr)	Top Mat Potential (V)	Water Soluble Cl^- (lb/yd^3) 1	2	3	4	5	6	Average (lb/yd^3)	SD[a]	COV[b]
MC(both layers penetrated)-4h-45-1	0.039	-0.641	15.87	17.47	14.19	16.94	13.63	14.95	15.51	1.52	0.10
MC(both layers penetrated)-4h-45-2	0.049	-0.540	11.80	11.54	11.92	17.60	17.41	17.35	14.60	3.12	0.21
MC(both layers penetrated)-4h-45-3	0.000	-0.492	9.90	19.49	16.40	10.85	10.72	11.23	13.10	3.90	0.30
MC(both layers penetrated)-10h-45-1	0.054	-0.569	21.83	21.89	15.96	15.33	17.10	14.76	17.81	3.23	0.18
MC(both layers penetrated)-10h-45-2	0.595	-0.583	17.10	17.03	14.95	23.03	17.98	18.67	18.13	2.71	0.15
MC(both layers penetrated)-10h-45-3	0.507	-0.572	16.65	16.53	16.40	15.90	22.08	19.05	17.77	2.38	0.13
MC(only epoxy penetrated)-4h-45-1	0.025	-0.521	12.55	11.48	9.27	16.02	22.52	17.03	14.81	4.75	0.32
MC(only epoxy penetrated)-4h-45-2	0.000	-0.506	20.31	17.44	17.98	15.71	12.36	7.82	15.27	4.51	0.30
MC(only epoxy penetrated)-4h-45-3	0.000	-0.536	13.82	18.36	10.91	12.30	15.20	17.47	14.68	2.91	0.20
MC(only epoxy penetrated)-10h-45-1	0.000	-0.621	16.50	17.19	12.77	16.62	15.65	15.87	15.77	1.57	0.10
MC(only epoxy penetrated)-10h-45-2	0.039	-0.499	16.84	13.50	12.21	20.03	12.81	24.54	16.65	4.86	0.29
MC(only epoxy penetrated)-10h-45-3	0.000	-0.589	21.35	22.36	18.42	16.97	15.08	16.65	18.47	2.85	0.15

[a]Standard Deviation

[b]Coefficient of Variation

Table C.4 – Chloride ion concentrations measured at 48 weeks in Southern Exposure specimens containing increased adhesion epoxy-coated reinforcement

Specimen	Rate (µm/yr)	Top Mat Potential (V)	Water Soluble Cl^- (lb/yd^3) 1	2	3	4	5	6	Average (lb/yd^3)	SD[a]	COV[b]
ECR(Chromate)-4h-45-1	0.000	-0.425	18.36	20.00	†	†	†	†	19.18	1.16	0.06
ECR(Chromate)-4h-45-2	0.000	-0.078	15.01	21.32	†	†	†	†	18.17	4.46	0.25
ECR(Chromate)-4h-45-3	0.015	-0.662	16.02	20.76	17.85	24.82	22.96	21.70	20.69	3.26	0.16
ECR(Chromate)-10h-45-1	0.000	-0.687	24.73	20.57	12.05	11.10	9.15	10.91	14.75	6.33	0.43
ECR(Chromate)-10h-45-2	0.015	-0.651	18.86	27.69	32.74	19.11	20.44	15.77	22.44	6.42	0.29
ECR(Chromate)-10h-45-3	0.141	-0.551	10.28	14.38	15.20	14.76	16.47	15.65	14.46	2.17	0.15
ECR(DuPont)-4h-45-1	0.000	-0.121	†	†	†	†	†	†	†	†	†
ECR(DuPont)-4h-45-2	0.000	-0.471	†	†	†	†	†	†	†	†	†
ECR(DuPont)-4h-45-3	-0.015	-0.504	17.98	18.55	19.11	20.94	23.15	18.93	19.78	1.93	0.10
ECR(DuPont)-10h-45-1	0.000	-0.569	14.07	20.44	19.18	17.47	17.85	13.56	17.10	2.75	0.16
ECR(DuPont)-10h-45-2	0.061	-0.677	19.94	20.38	17.98	31.16	21.64	25.61	22.78	4.83	0.21
ECR(DuPont)-10h-45-3	0.00	-0.464	18.11	16.15	16.02	20.31	17.85	15.39	17.31	1.82	0.11
ECR(Valspar)-4h-45-1	0.057	-0.494	12.65	19.87	†	†	†	†	16.26	5.11	0.31
ECR(Valspar)-4h-45-2	0.015	-0.573	19.18	20.31	†	†	†	†	19.75	0.80	0.04
ECR(Valspar)-4h-45-3	0.000	-0.560	21.32	27.25	25.68	16.78	17.73	10.91	19.95	6.08	0.30
ECR(Valspar)-10h-45-1	0.023	-0.565	23.50	6.25	24.32	19.65	19.49	20.19	18.90	6.53	0.35
ECR(Valspar)-10h-45-2	0.042	-0.631	18.93	23.97	18.55	23.91	26.18	20.38	21.99	3.13	0.14
ECR(Valspar)-10h-45-3	0.038	-0.541	10.54	16.78	13.06	17.41	13.44	21.01	15.37	3.75	0.24

[a]Standard Deviation

[b]Coefficient of Variation

† Information not available

Table C.5 – Chloride ion concentrations measured at 48 weeks in Southern Exposure specimens containing increased adhesion epoxy-coated reinforcement cast in concrete containing DCI

Specimen	Rate (µm/yr)	Top Mat Potential (V)	Water Soluble Cl^- (lb/yd^3) 1	2	3	4	5	6	Average (lb/yd^3)	SD[a]	COV[b]
ECR(Chromate/DCI)-4h-45-1	0.000	-0.133	6.47	7.25	8.77	9.84	9.53	12.74	9.10	2.21	0.24
ECR(Chromate/DCI)-4h-45-2	0.000	-0.142	6.84	7.07	7.79	9.94	6.25	10.03	7.99	1.62	0.20
ECR(Chromate/DCI)-4h-45-3	0.000	-0.150	10.25	11.28	13.33	†	†	†	11.62	1.57	0.13
ECR(DuPont/DCI)-4h-45-1	0.000	-0.194	8.90	12.68	5.49	11.04	9.15	7.25	9.08	2.57	0.28
ECR(DuPont/DCI)-4h-45-2	0.000	-0.178	5.87	6.12	6.50	6.81	10.85	10.43	7.76	2.25	0.29
ECR(DuPont/DCI)-4h-45-3	0.000	-0.202	15.90	15.83	18.23	20.12	17.79	10.85	16.45	3.18	0.19
ECR(Valspar/DCI)-4h-45-1	0.000	-0.148	11.54	5.49	7.25	8.33	9.27	11.10	8.83	2.31	0.26
ECR(Valspar/DCI)-4h-45-2	0.000	-0.277	8.36	8.52	6.31	10.22	6.75	9.78	8.32	1.57	0.19
ECR(Valspar/DCI)-4h-45-3	0.000	-0.230	9.75	9.78	9.65	17.95	12.24	†	11.87	3.57	0.30

[a]Standard Deviation

[b]Coefficient of Variation

[c]No corrosion initiation observed in specimen

† Information not available

Table C.6 – Chloride ion concentrations measured at 96 weeks in Southern Exposure specimens containing conventional steel and epoxy-coated reinforcement

Specimen	Rate (µm/yr)	Top Mat Potential (V)	Water Soluble Cl^- (lb/yd^3) 1	2	3	4	5	6	Average (lb/yd^3)	SD[a]	COV[b]
Conv.-45-1	0.107	-0.335	5.24	3.47	5.87	3.50	5.55	3.09	4.45	1.23	0.28
Conv.-45-2	1.551	-0.521	9.34	6.88	8.26	12.40	10.00	7.79	9.11	1.95	0.21
Conv.-45-3	3.025	-0.554	8.74	13.94	11.29	†	†	†	11.32	2.60	0.23
Conv.-45-4	2.408	-0.568	13.91	19.52	†	†	†	†	16.72	3.97	0.24
Conv.-45-5	2.755	-0.569	9.27	14.01	†	†	†	†	11.64	3.35	0.29
Conv.-45-6	1.417	-0.573	18.30	13.38	†	†	†	†	15.84	3.47	0.22
Conv.-35-1	10.679	-0.630	7.16	8.45	12.87	15.30	7.79	8.61	10.03	3.27	0.33
Conv.-35-2	12.805	-0.609	12.05	16.34	19.43	17.54	13.94	4.61	13.98	5.28	0.38
Conv.-35-3	2.057	-0.478	9.97	12.74	10.66	9.87	7.10	7.54	9.65	2.08	0.22
ECR-4h-45-1	0.000	-0.186	8.55	13.00	11.99	6.06	6.88	8.71	9.19	2.76	0.30
ECR-4h-45-2	0.000	-0.261	6.88	5.17	7.89	5.30	6.69	7.00	6.49	1.05	0.16
ECR-4h-45-3	0.000	-0.202	19.34	11.73	15.96	18.23	16.31	18.23	16.63	2.72	0.16
ECR-4h-45-4	0.000	-0.417	11.48	9.53	8.77	19.68	21.80	21.32	15.43	6.13	0.40
ECR-4h-45-5	0.000	-0.210	11.42	16.15	16.72	18.80	14.57	13.41	15.18	2.61	0.17
ECR-4h-45-6	0.000	-0.366	10.06	15.61	15.87	18.11	20.19	17.73	16.26	3.46	0.21
ECR-10h-45-1	0.034	-0.550	19.59	18.74	18.45	23.31	24.00	†	20.82	2.64	0.13
ECR-10h-45-2	0.122	-0.631	14.89	22.46	19.81	17.41	28.33	31.48	22.40	6.41	0.29
ECR-10h-45-3	0.450	-0.504	24.29	26.46	23.53	18.67	17.19	24.45	22.43	3.65	0.16
ECR-10h-35-1	0.000	-0.172	9.90	3.91	8.77	6.43	13.50	6.81	8.22	3.31	0.40
ECR-10h-35-2	0.000	-0.142	5.08	8.45	8.52	5.55	11.70	11.42	8.45	2.80	0.33
ECR-10h-35-3	0.023	-0.395	11.73	7.07	5.11	5.58	2.84	8.80	6.86	3.11	0.45

[a]Standard Deviation

[b]Coefficient of Variation

† Information not available

Table C.7 – Chloride ion concentrations measured at 96 weeks in Southern Exposure specimens containing epoxy-coated reinforcement cast in concrete containing corrosion inhibitors

Specimen	Rate (µm/yr)	Top Mat Potential (V)	Water Soluble Cl^- (lb/yd^3) 1	2	3	4	5	6	Average (lb/yd^3)	SD[a]	COV[b]
ECR(DCI)-4h-45-1	0.000	-0.357	†	†	†	†	†	†	†	†	†
ECR(DCI)-4h-45-2	0.015	-0.597	†	†	†	†	†	†	†	†	†
ECR(DCI)-4h-45-3	0.000	-0.303	†	†	†	†	†	†	†	†	†
ECR(DCI)-10h-45-1	0.000	-0.394	†	†	†	†	†	†	†	†	†
ECR(DCI)-10h-45-2	0.084	-0.569	†	†	†	†	†	†	†	†	†
ECR(DCI)-10h-45-3	0.141	-0.533	†	†	†	†	†	†	†	†	†
ECR(DCI)-10h-35-1	0.023	-0.505	5.33	4.10	12.30	23.91	9.65	25.11	13.40	9.10	0.68
ECR(DCI)-10h-35-2	0.000	-0.158	4.54	3.31	6.53	13.82	10.57	6.97	7.62	3.92	0.51
ECR(DCI)-10h-35-3	0.000	-0.172	4.72	2.14	5.49	†	†	†	4.12	1.75	0.43
ECR(RH)-4h-45-1	0.000	-0.513	6.43	8.39	8.01	4.48	4.16	†	6.30	1.95	0.31
ECR(RH)-4h-45-2	0.061	-0.514	10.22	14.70	16.40	10.98	14.64	11.36	13.05	2.52	0.19
ECR(RH)-4h-45-3	0.000	-0.254	10.72	11.29	11.99	10.41	9.27	5.68	9.89	2.26	0.23
ECR(RH)-10h-45-1	0.000	-0.345	12.62	12.55	7.82	17.54	16.40	11.17	13.02	3.54	0.27
ECR(RH)-10h-45-2	0.000	-0.171	4.97	9.43	10.59	8.30	10.03	7.03	8.39	2.11	0.25
ECR(RH)-10h-45-3	0.000	-0.286	6.69	7.03	6.84	14.83	19.37	10.72	10.91	5.22	0.48
ECR(RH)-10h-35-1	0.000	-0.173	1.58	1.20	4.45	3.19	2.71	†	2.62	1.30	0.50
ECR(RH)-10h-35-2	0.000	-0.333	4.79	1.61	10.47	4.79	7.44	0.54	4.94	3.67	0.74
ECR(RH)-10h-35-3	0.000	-0.218	6.97	9.68	6.37	3.09	5.24	†	6.27	2.41	0.39
ECR(HY)-4h-45-1	0.000	-0.231	4.23	12.11	4.98	0.69	1.77	4.04	4.64	4.01	0.86
ECR(HY)-4h-45-2	0.000	-0.232	8.71	6.56	2.71	6.25	1.32	†	5.11	3.02	0.59
ECR(HY)-4h-45-3	0.000	-0.223	9.43	7.63	9.59	4.79	8.64	7.76	7.98	1.76	0.22
ECR(HY)-10h-45-1	0.000	-0.266	0.95	2.90	0.57	2.21	4.73	6.62	3.00	2.32	0.77
ECR(HY)-10h-45-2	0.000	-0.188	9.02	2.65	4.07	3.34	5.80	4.29	4.86	2.30	0.47
ECR(HY)-10h-45-3	0.000	-0.198	4.92	2.27	6.18	14.76	6.94	2.59	6.28	4.56	0.73
ECR(HY)-10h-35-1	0.019	-0.398	0.95	1.77	0.76	0.88	0.88	2.27	1.25	0.62	0.49
ECR(HY)-10h-35-2	0.000	-0.146	1.89	3.09	1.32	1.07	6.06	2.84	2.71	1.82	0.67
ECR(HY)-10h-35-3	0.000	-0.148	7.00	3.91	1.48	1.10	6.25	2.78	3.75	2.45	0.65
ECR(primer/$Ca(NO_2)_2$)-4h-45-1	0.000	-0.422	16.28	14.32	7.32	24.92	15.46	15.08	15.56	5.62	0.36
ECR(primer/$Ca(NO_2)_2$)-4h-45-2	0.027	-0.509	19.30	16.43	11.17	12.87	20.53	19.90	16.70	3.93	0.24
ECR(primer/$Ca(NO_2)_2$)-4h-45-3	0.061	-0.568	19.62	20.76	20.44	8.45	15.01	19.18	17.24	4.78	0.28
ECR(primer/$Ca(NO_2)_2$)-10h-45-1	0.030	-0.520	14.83	14.32	13.63	22.65	18.61	15.14	16.53	3.46	0.21
ECR(primer/$Ca(NO_2)_2$)-10h-45-2	0.316	-0.547	23.40	14.89	12.24	13.18	13.00	16.06	15.46	4.13	0.27
ECR(primer/$Ca(NO_2)_2$)-10h-45-3	0.069	-0.630	21.39	23.15	20.82	20.25	12.43	18.36	19.40	3.75	0.19
ECR(primer/$Ca(NO_2)_2$)-10h-35-1	0.000	-0.142	2.14	1.70	5.24	2.46	4.35	1.20	2.85	1.59	0.56
ECR(primer/$Ca(NO_2)_2$)-10h-35-2	0.030	-0.518	3.66	4.86	1.39	5.24	8.83	4.35	4.72	2.43	0.52
ECR(primer/$Ca(NO_2)_2$)-10h-35-3	0.000	-0.140	5.99	4.73	3.79	6.25	4.83	1.92	4.58	1.58	0.35

[a]Standard Deviation

[b]Coefficient of Variation

† Information not available

Table C.8 – Chloride ion concentrations measured at 96 weeks in Southern Exposure specimens containing multiple-coated reinforcement

Specimen	Rate (µm/yr)	Top Mat Potential (V)	Water Soluble Cl^- (lb/yd^3) 1	2	3	4	5	6	Average (lb/yd^3)	SD[a]	COV[b]
MC(both layers penetrated)-4h-45-1	0.000	-0.575	22.36	25.01	24.19	18.64	8.61	13.53	18.73	6.51	0.35
MC(both layers penetrated)-4h-45-2	0.000	-0.610	17.25	14.01	22.11	21.07	15.93	12.81	17.20	3.75	0.22
MC(both layers penetrated)-4h-45-3	0.000	-0.598	20.53	21.26	21.23	20.31	20.12	15.27	19.79	2.26	0.11
MC(both layers penetrated)-10h-45-1	1.205	-0.638	22.90	21.83	17.22	22.21	19.05	25.55	21.46	2.94	0.14
MC(both layers penetrated)-10h-45-2	0.581	-0.601	22.30	19.37	17.35	20.38	25.17	22.21	21.13	2.71	0.13
MC(both layers penetrated)-10h-45-3	0.507	-0.595	20.31	21.26	17.63	20.88	25.93	23.03	21.51	2.78	0.13
MC(only epoxy penetrated)-4h-45-1	0.000	-0.562	17.82	9.97	13.09	20.16	15.33	12.93	14.88	3.68	0.25
MC(only epoxy penetrated)-4h-45-2	0.000	-0.628	37.35	33.91	26.87	19.11	19.56	18.36	25.86	8.24	0.32
MC(only epoxy penetrated)-4h-45-3	-0.025	-0.579	15.39	16.81	18.29	18.61	12.30	17.92	16.55	2.39	0.14
MC(only epoxy penetrated)-10h-45-1	0.064	-0.600	19.71	16.65	13.50	26.87	27.63	12.90	19.55	6.45	0.33
MC(only epoxy penetrated)-10h-45-2	0.344	-0.604	23.59	24.38	21.07	21.83	22.08	20.57	22.25	1.47	0.07
MC(only epoxy penetrated)-10h-45-3	0.108	-0.540	20.76	18.93	20.19	18.04	20.69	14.57	18.86	2.36	0.12

[a]Standard Deviation

[b]Coefficient of Variation

Table C.9 – Chloride ion concentrations measured at 96 weeks in Southern Exposure specimens containing increased adhesion epoxy-coated reinforcement

Specimen	Rate (µm/yr)	Top Mat Potential (V)	Water Soluble Cl^- (lb/yd^3) 1	2	3	4	5	6	Average (lb/yd^3)	SD[a]	COV[b]
ECR(Chromate)-4h-45-1	0.000	-0.347	27	24.5	16.02	21.39	20.19	23.40	22.10	3.82	0.17
ECR(Chromate)-4h-45-2	0.030	-0.501	29.3	32.6	22.7	20.00	29.71	26.87	26.88	4.73	0.18
ECR(Chromate)-4h-45-3	0.042	-0.486	23.8	19.8	29.21	21.64	21.07	†	23.11	3.70	0.16
ECR(Chromate)-10h-45-1	0.000	-0.396	31.8	22.3	18.55	12.36	12.11	17.25	19.07	7.35	0.39
ECR(Chromate)-10h-45-2	0.152	-0.605	39.5	35.7	23.34	28.39	33.50	36.34	32.79	5.91	0.18
ECR(Chromate)-10h-45-3	0.080	-0.496	12.36	18.42	14.67	11.26	22.02	14.47	15.53	4.01	0.26
ECR(DuPont)-4h-45-1	0.046	-0.492	23.4	19.9	19.05	22.71	20.06	24.22	21.56	2.15	0.10
ECR(DuPont)-4h-45-2	0.038	-0.609	30.5	28.7	26.81	25.11	32.17	33.15	29.42	3.12	0.11
ECR(DuPont)-4h-45-3	0.072	-0.57	12.8	17.6	24.57	24.13	17.29	14.35	18.46	4.91	0.27
ECR(DuPont)-10h-45-1	0.023	-0.534	21.2	18.2	16.43	29.90	35.90	†	24.33	8.29	0.34
ECR(DuPont)-10h-45-2	0.023	-0.58	23.8	27.9	27.28	26.18	26.37	†	26.31	1.53	0.06
ECR(DuPont)-10h-45-3	-0.03	-0.235	18.5	24.1	15.6	18.93	19.02	12.21	18.06	3.96	0.22
ECR(Valspar)-4h-45-1	0.019	-0.42	22.2	22.7	18.04	27.95	29.71	†	24.12	4.70	0.19
ECR(Valspar)-4h-45-2	0.019	-0.554	18.3	19.5	21.8	15.7	27.55	32.30	22.52	6.24	0.28
ECR(Valspar)-4h-45-3	0.248	-0.59	39.3	47.2	38.70	32.80	43.30	†	40.26	5.39	0.13
ECR(Valspar)-10h-45-1	0.053	-0.528	30.5	26.46	33.88	28.26	†	†	29.78	3.20	0.11
ECR(Valspar)-10h-45-2	0.034	-0.61	31.1	30.1	29.27	32.24	35.36	†	31.61	2.37	0.07
ECR(Valspar)-10h-45-3	0.175	-0.523	17.22	18.20	11.76	13.60	12.48	8.64	13.65	3.56	0.26

[a]Standard Deviation

[b]Coefficient of Variation

† Information not available

Table C.10 – Chloride ion concentrations measured at 96 weeks in Southern Exposure specimens containing increased adhesion epoxy-coated reinforcement cast in concrete containing DCI

Specimen	Rate (µm/yr)	Top Mat Potential (V)	Water Soluble Cl^- (lb/yd^3)						Average (lb/yd^3)	SD[a]	COV[b]
			1	2	3	4	5	6			
ECR(Chromate/DCI)-4h-45-1	0.000	-0.293	27.92	9.87	8.83	8.52	13.63	10.54	13.22	7.43	0.56
ECR(Chromate/DCI)-4h-45-2	0.000	-0.271	11.73	14.16	6.21	12.46	9.40	†	10.79	3.08	0.29
ECR(Chromate/DCI)-4h-45-3	0.069	-0.459	11.10	10.85	11.04	11.99	14.51	15.65	12.52	2.05	0.16
ECR(DuPont/DCI)-4h-45-1	0.000	-0.443	12.81	10.35	11.67	10.79	21.26	†	13.37	4.51	0.34
ECR(DuPont/DCI)-4h-45-2	0.000	-0.197	5.65	10.98	13.94	†	†	†	10.19	4.20	0.41
ECR(DuPont/DCI)-4h-45-3	0.000	-0.189	13.18	14.73	19.94	11.04	11.36	†	14.05	3.61	0.26
ECR(Valspar/DCI)-4h-45-1	0.000	-0.258	10.28	12.93	11.36	8.33	5.99	11.10	10.00	2.47	0.25
ECR(Valspar/DCI)-4h-45-2	0.000	-0.223	5.33	8.36	11.17	†	†	†	8.29	2.92	0.35
ECR(Valspar/DCI)-4h-45-3	0.000	-0.304	10.47	20.35	9.53	12.84	15.68	†	13.77	4.38	0.32

[a]Standard Deviation

[b]Coefficient of Variation

† Information not available

APPENDIX D

BOTTOM MAT CORROSION RATES BASED ON THE LINEAR POLARIZATION RESISTANCE TEST

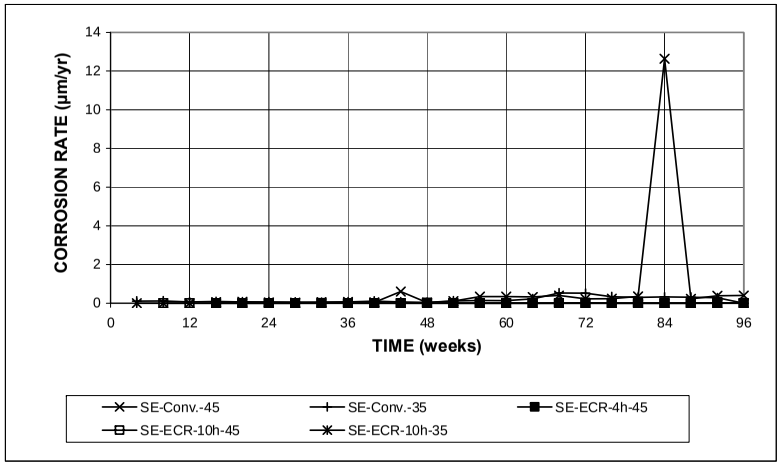

Figure D.1 – Microcell corrosion rates based on total area of the bar for the Southern Exposure specimens containing conventional steel and epoxy-coated reinforcement. 4h = four holes through epoxy, 10h = ten holes through epoxy, *w/c* = 0.45 and 0.35.

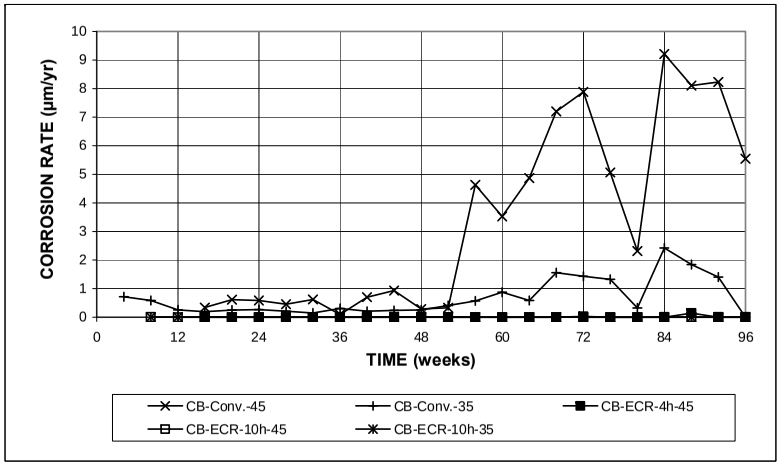

Figure D.2 – Microcell corrosion rates based on total area of the bar for the cracked beam specimens containing conventional steel and epoxy-coated reinforcement. 4h = four holes through epoxy, 10h = ten holes through epoxy, *w/c* = 0.45 and 0.35.

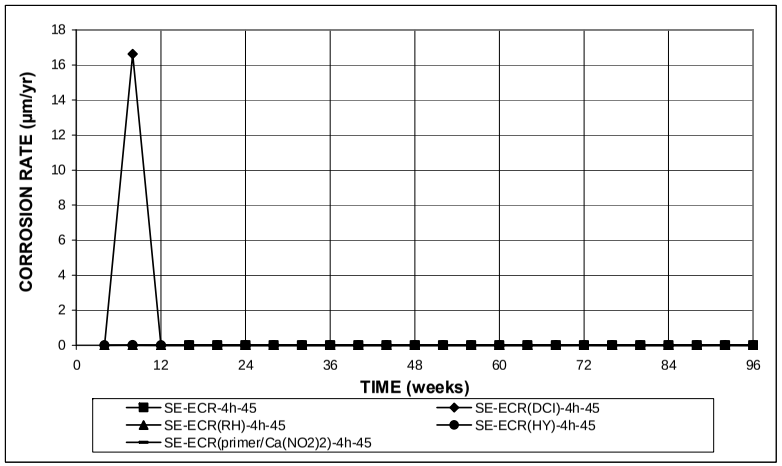

Figure D.3 – Microcell corrosion rates based on total area of the bar for the Southern Exposure specimens containing conventional ECR, ECR in concrete containing corrosion inhibitors, and ECR with a calcium nitrite primer, *w/c* = 0.45. Bars with four holes in epoxy coating.

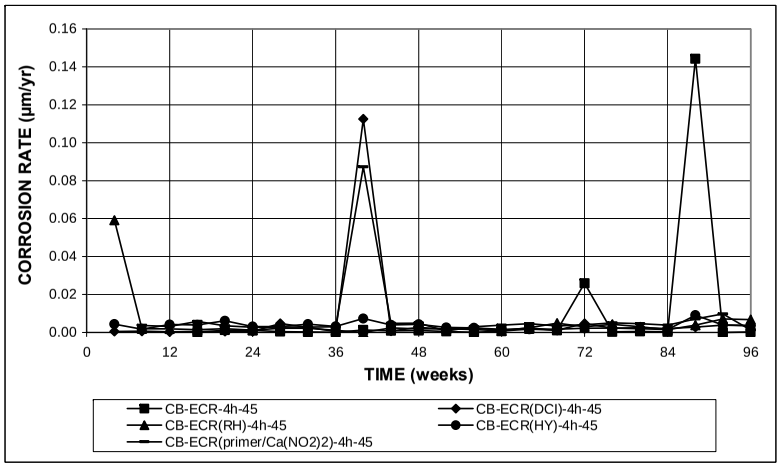

Figure D.4 – Microcell corrosion rates based on total area of the bar for the cracked beam specimens containing conventional ECR, ECR in concrete containing corrosion inhibitors, and ECR with a calcium nitrite primer, *w/c* = 0.45. Bars with four holes in epoxy coating.

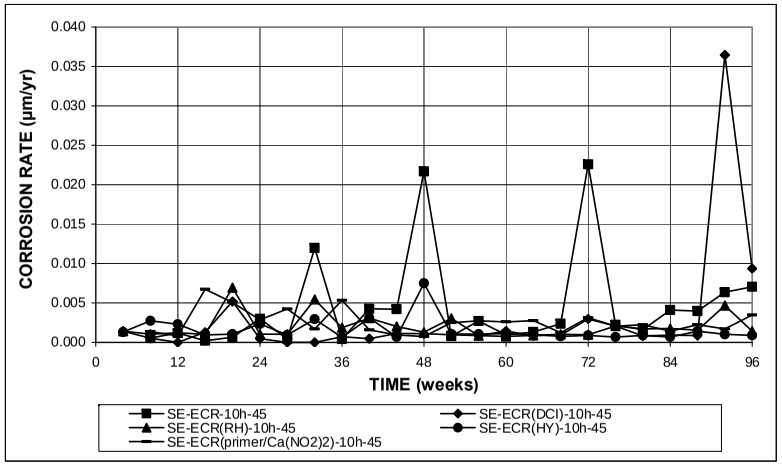

Figure D.5 – Microcell corrosion rates based on total area of the bar for the Southern Exposure specimens containing conventional ECR, ECR in concrete containing corrosion inhibitors, and ECR with a calcium nitrite primer, *w/c* = 0.45. Bars with ten holes in epoxy coating.

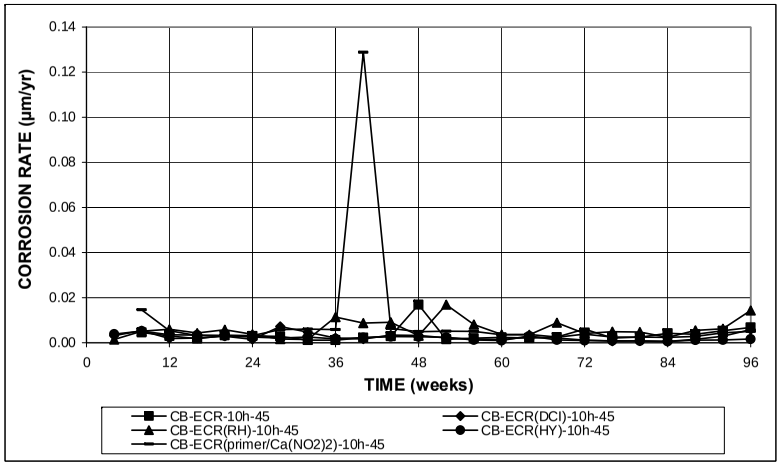

Figure D.6 – Microcell corrosion rates based on total area of the bar for the cracked beam specimens containing conventional ECR, ECR in concrete containing corrosion inhibitors, and ECR with a calcium nitrite primer, *w/c* = 0.45. Bars with ten holes in epoxy coating.

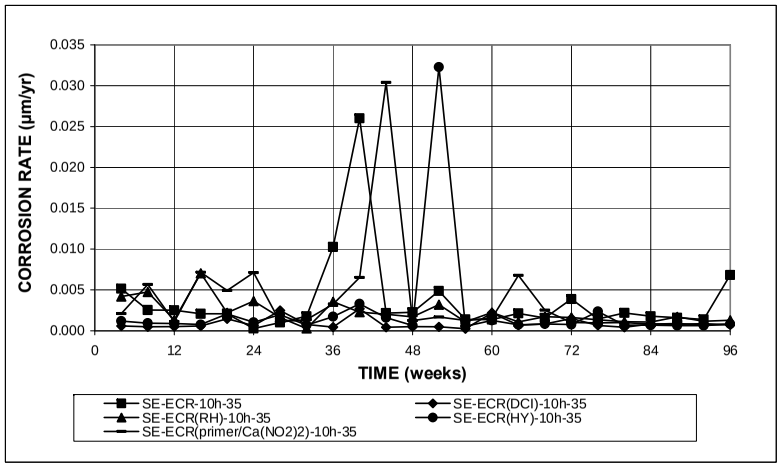

Figure D.7 – Microcell corrosion rates based on total area of the bar for the Southern Exposure specimens containing conventional ECR, ECR in concrete containing corrosion inhibitors, and ECR with a calcium nitrite primer, *w/c* = 0.35. Bars with ten holes in epoxy coating.

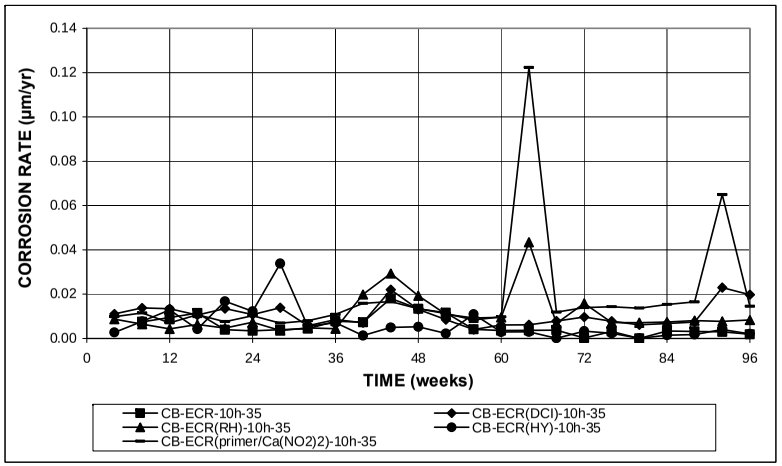

Figure D.8 – Microcell corrosion rates based on total area of the bar for the cracked beam specimens containing conventional ECR, ECR in concrete containing corrosion inhibitors, and ECR with a calcium nitrite primer, *w/c* = 0.35. Bars with ten holes in epoxy coating.

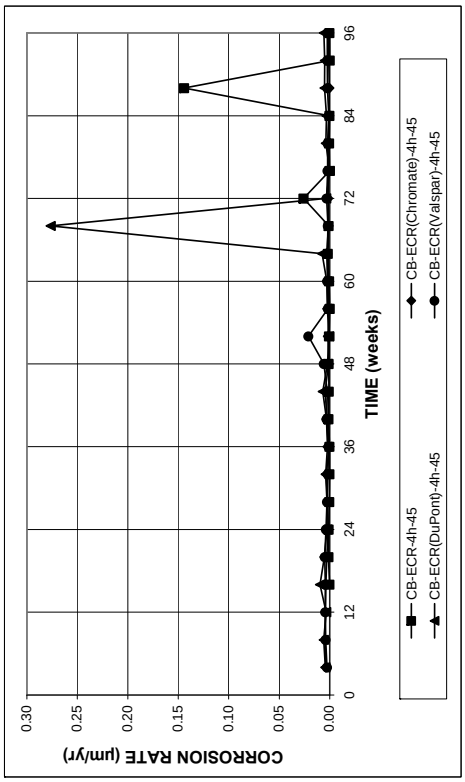

Figure D.10 – Microcell corrosion rates based on total area of the bar for the cracked beam specimens containing conventional ECR and ECR with increased adhesion, $w/c = 0.45$. Bars with four holes in epoxy coating.

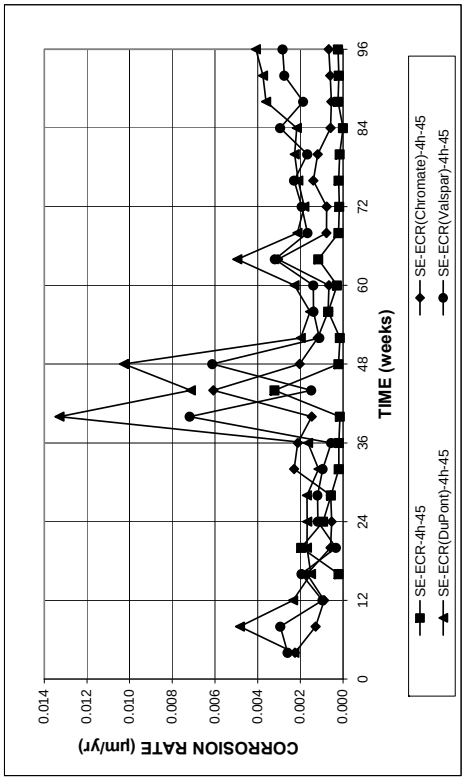

Figure D.9 – Microcell corrosion rates based on total area of the bar for the Southern Exposure specimens containing conventional ECR and ECR with increased adhesion, $w/c = 0.45$. Bars with four holes in epoxy coating.

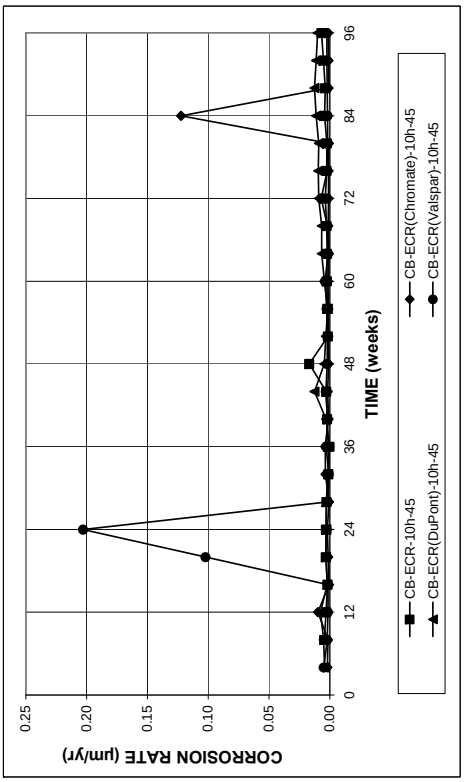

Figure D.12 – Microcell corrosion rates based on total area of the bar for the cracked beam specimens containing conventional ECR and ECR with increased adhesion, $w/c = 0.45$. Bars with ten holes in epoxy coating.

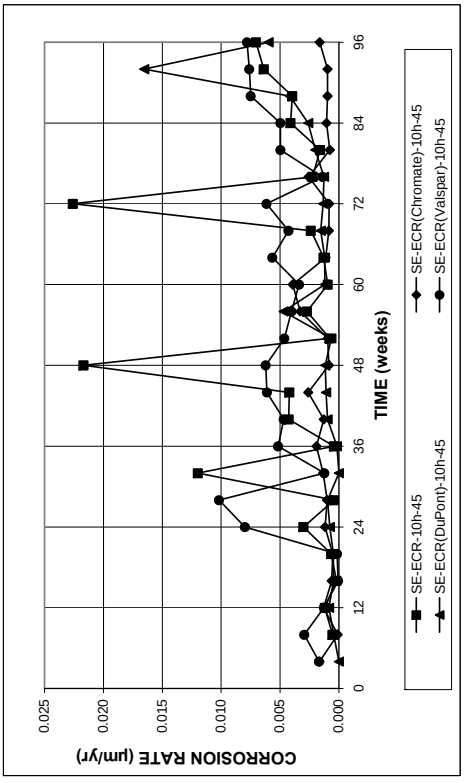

Figure D.11 – Microcell corrosion rates based on total area of the bar for the Southern Exposure specimens containing conventional ECR and ECR with increased adhesion, $w/c = 0.45$. Bars with ten holes in epoxy coating.

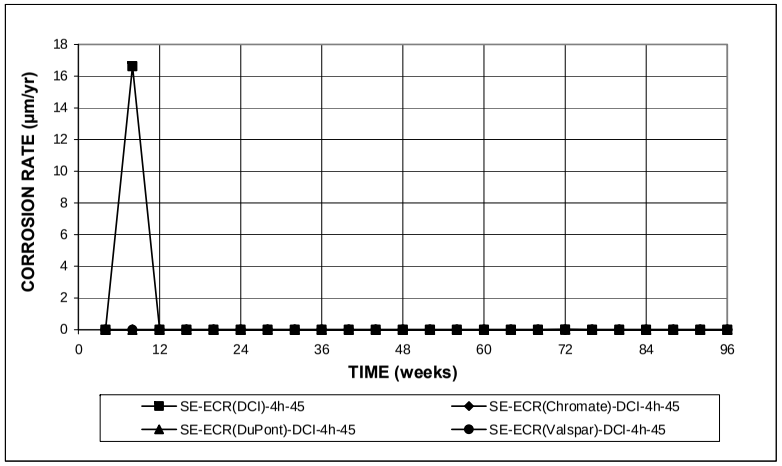

Figure D.13 – Microcell corrosion rates based on total area of the bar for the Southern Exposure specimens containing conventional ECR and ECR with increased adhesion, cast in concrete containing DCI corrosion inhibitor, w/c = 0.45. Bars with four holes in epoxy coating.

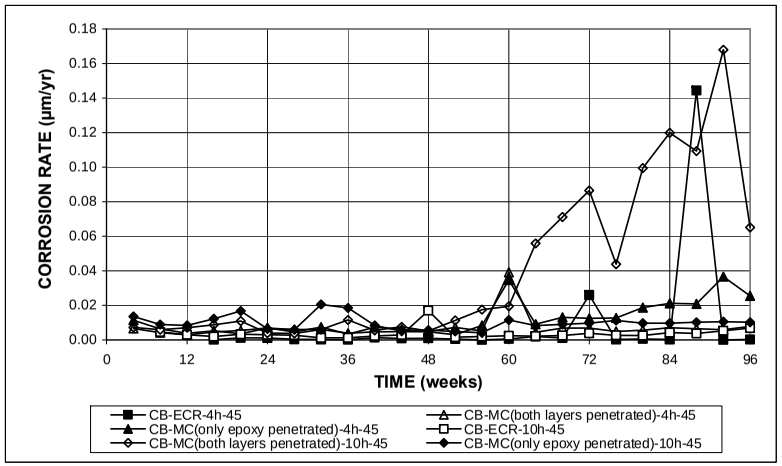

Figure D.15 – Microcell corrosion rates based on total area of the bar for the cracked beam specimens containing conventional ECR and multiple coated reinforcement, *w/c* = 0.45. 4h = four holes through the epoxy, 10h = ten holes through the epoxy.

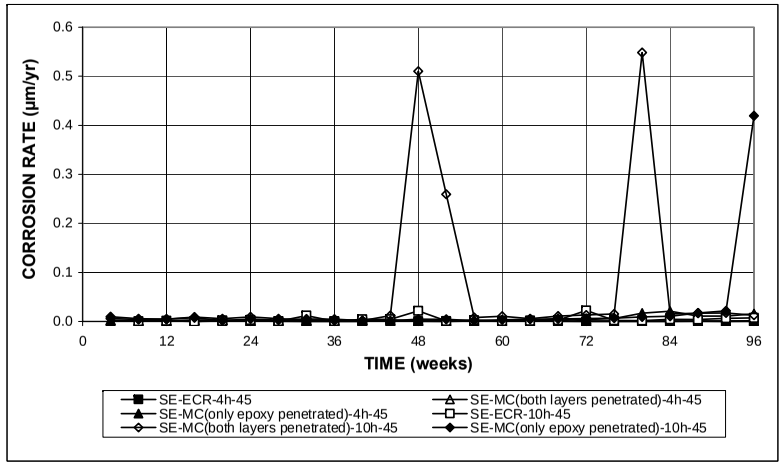

Figure D.14 – Microcell corrosion rates based on total area of the bar for the Southern Exposure specimens containing conventional ECR and multiple coated reinforcement, *w/c* = 0.45. 4h = four holes through the epoxy, 10h = ten holes through the epoxy.

APPENDIX E

INPUTS FOR THE STUDENT'S T-TEST FOR 96-WEEK MACROCELL CORROSION LOSSES IN SOUTHERN EXPOSURE AND CRACKED BEAM SPECIMENS

Table E.1 – Student's t-test inputs for Southern Exposure specimens

Test Specimen[a]	n[b]	$\overline{X}$[c]	s[d]
Conv.-45	6	1.75	1.08
Conv.-35	3	2.12	1.82
ECR-4h-45	6	0.003	0.001
ECR-10h-45	3	0.017	0.008
ECR-10h-35	3	0.008	0.004
ECR(DCI)-4h-45	3	0.004	0.003
ECR(DCI)-10h-45	3	0.012	0.012
ECR(DCI)-10h-35	3	0.007	0.006
ECR(RH)-4h-45	3	0.010	0.018
ECR(RH)-10h-45	3	-0.003	0.005
ECR(RH)-10h-35	3	0.003	0.001
ECR(HY)-4h-45	3	-0.002	0.001
ECR(HY)-10h-45	3	0.002	0.003
ECR(HY)-10h-35	3	0.001	0.004
ECR(primer/$Ca(NO_2)_2$)-4h-45	3	0.014	0.011
ECR(primer/$Ca(NO_2)_2$)-10h-45	3	0.064	0.064
ECR(primer/$Ca(NO_2)_2$)-10h-35	3	0.002	0.001
MC(both layers penetrated)-4h-45	3	0.058	0.010
MC(both layers penetrated)-10h-45	3	0.599	0.097
MC(only epoxy penetrated)-4h-45	3	0.033	0.017
MC(only epoxy penetrated)-10h-45	3	0.090	0.079
ECR(Chromate)-4h-45	3	0.018	0.016
ECR(Chromate)-10h-45	3	0.067	0.056
ECR(DuPont)-4h-45	3	0.026	0.008
ECR(DuPont)-10h-45	3	0.046	0.016
ECR(Valspar)-4h-45	3	0.032	0.016
ECR(Valspar)-10h-45	3	0.063	0.024
ECR(Chromate)-DCI-4h-45	3	0.007	0.010
ECR(DuPont)-DCI-4h-45	3	0.000	0.001
ECR(Valspar)-DCI-4h-45	3	0.012	0.019

[a] For explaination of of specimen nomenclature, see Table 2.3 in Chapter 2.

[b] n = number of samples

[c] $\overline{X}$ = mean macrocell corrosion loss of sample

[d] s = standard deviation

Table E.2 – Student's t-test inputs for cracked beam specimens

Test Specimen[a]	n[b]	$\overline{X}$[c]	s[d]
Conv.-45	6	13.1	4.15
Conv.-35	3	8.34	2.82
ECR-4h-45	6	0.041	0.024
ECR-10h-45	3	0.047	0.031
ECR-10h-35	3	0.139	0.020
ECR(DCI)-4h-45	3	0.026	0.021
ECR(DCI)-10h-45	3	0.079	0.065
ECR(DCI)-10h-35	3	0.223	0.197
ECR(RH)-4h-45	3	0.141	0.150
ECR(RH)-10h-45	3	0.171	0.060
ECR(RH)-10h-35	3	0.178	0.109
ECR(HY)-4h-45	3	0.036	0.049
ECR(HY)-10h-45	3	0.060	0.057
ECR(HY)-10h-35	3	0.194	0.073
ECR(primer/$Ca(NO_2)_2$)-4h-45	3	0.017	0.010
ECR(primer/$Ca(NO_2)_2$)-10h-45	3	0.098	0.048
ECR(primer/$Ca(NO_2)_2$)-10h-35	3	0.470	0.140
MC(both layers penetrated)-4h-45	3	0.377	0.114
MC(both layers penetrated)-10h-45	3	0.672	0.541
MC(only epoxy penetrated)-4h-45	3	0.294	0.248
MC(only epoxy penetrated)-10h-45	3	0.221	0.156
ECR(Chromate)-4h-45	3	0.074	0.022
ECR(Chromate)-10h-45	3	0.216	0.236
ECR(DuPont)-4h-45	3	0.105	0.045
ECR(DuPont)-10h-45	3	0.184	0.098
ECR(Valspar)-4h-45	3	0.084	0.082
ECR(Valspar)-10h-45	3	0.125	0.114

[a] For explaination of of specimen nomenclature, see Table 2.3 in Chapter 2.

[b] n = number of samples

[c] $\overline{X}$ = mean macrocell corrosion loss of sample

[d] s = standard deviation